Genetic modification of heavy metal resistant *Streptomyces* sp. strains

Dissertation

To Fulfill the Requirements for the Degree of
„doctor rerum naturalium“ (Dr. rer. nat.)

Submitted to the Council of the Faculty of Biological Sciences
of the Friedrich Schiller University Jena

by M.Sc. Brangsch, Hanka

born on 11.02.1988 in Berlin

Reviewer (Gutachter):

1. Prof. Dr. Erika Kothe, Jena

2. Prof. Dr. Christian Jogler, Jena

3. Prof. Dr. Beatrix Süß, Darmstadt

Day of public defense (Tag der öffentlichen Verteidigung):

10.09.2020

Contents

1. Introduction

1.1 Streptomycetes

Characteristics and ecological relevance

Soil is a habitat that is characterized by variable conditions regarding moisture, temperature, redox conditions and nutrient availability. Dry-wet alterations, climatic changes and anthropogenic perturbations demand a high level of flexibility and adaptation from the indigenous organisms. Nevertheless, a highly diverse bacterial community can be found dwelling in different niches. Actinobacteria, in particular *Streptomyces* sp., are the major members of this community that can even be found at highly contaminated sites (Li et al., 2016; Sandaa et al., 1999; Schmidt et al., 2005; Zhou et al., 2016). These Gram-positive bacteria are mostly recognized for their vast secondary metabolism that is the source of many of today's antibiotics. The number of predicted secreted proteins is exceptionally high in this genus and they serve as means for bacterial interaction, scavengers of nutrients and means of protection. Furthermore, being saprophytic organisms, streptomycetes possess a vast repertoire of enzymes for the degradation of organic compounds, e.g. cellulases and lignocellulases, that are commonly found in terrestrial habitats (Chater et al., 2010). Thus, they are an important group in the food web of the soil microbial community providing the basis for other bacteria by degradation of complex carbon sources (Flardh & Buttner, 2009).

Another characteristic trait of members of this genus is their morphological development, largely characterized by the formation of a thick mycelium. *Streptomyces* sp. undergo an elaborate life cycle that is built up of a succession of complex morphological differentiation steps. From a germinating spore, vegetative growth starts with the development of filamentous hyphae that branch and contain multiple copies of the genome in large compartments forming the mycelium. When nutrients get depleted, reproductive growth sets in with the production of aerial hyphae that ultimately divide into uninucleoid spores. Autolysis and programmed cell death of the vegetative mycelium serves as nutrient source for the reproductive growth (Chater, 1993; Chen et al., 2002).

The initiation of the reproductive growth stage is accompanied by the production of numerous secondary metabolites, like antibiotics and pigments, which not only serve as means of communication and defence, but also support the developmental process itself, as it was suggested for the melanin-producing enzyme tyrosinase (Endo et al., 2001).

The immense spectrum of degrading enzymes and their ability to endure harsh environmental periods as dormant spores enable *Streptomyces* sp. to prevail in habitats that only offer low nutrient concentrations and extreme conditions (Haferburg & Kothe, 2007). These facts also make them interesting objects for bioremediation purposes of soil.

Streptomyces sp. genomics

The size of bacterial chromosomes often correlates with their primary habitat and lifestyle, ranging between a few thousand base pairs, e.g. the 450 kb genome of the intracellular aphid symbiont *Buchnera* sp., to several million base pairs in free-living soil microorganisms like *Streptomyces* sp. which undergo a complex life cycle and produce numerous secondary metabolites (Chen et al., 2002; Gil et al., 2002). Streptomycete genomes usually constitute 8 to 10 million base pairs, are linear mole-

cules with a high GC content and code over 7000 genes, half of which being unique to the corresponding species (Ventura et al., 2007). Their linearity was discovered in *S. lividans* 66 for the first time (Lin et al., 1993) and since then observed in most other strains and species (Pandza et al., 1998; Ruckert et al., 2015; Zhou et al., 2016). However, the origin of this linearity is still an object of discussion (Chen et al., 2002; Volff & Altenbuchner, 2000).

In contrast to the appr. 6 Mbp central part of streptomycete genomes where most of the housekeeping genes are located, the terminal regions are more labile and prone to a frequent genetic flux (Chater et al., 2010; Chen et al., 2002; Choulet et al., 2006). The congruence of the conserved central core genome decreases with increasing phylogenetic distance of species and most of the strain-specific genes can be found in the terminal chromosomal regions. Additionally, genomic islands contribute to genetic diversity within this genus resulting in a highly compartmentalized chromosome (Choulet et al., 2006; Cruz-Morales et al., 2013).

Their linearity makes streptomycetes chromosomes typically unstable, because they can spontaneously circularize by fusion of the chromosome arms (Lin et al., 1993), which is accompanied by gene deletions. Furthermore, chromosomal deletions are commonly observed during sporulation with loss of over 10 % of the genome in more than 0.1 % of spores. Thereby, important phenotypic traits whose genetic determinants are mostly located at the chromosome ends, like secondary metabolite production or antibiotic resistance, can be lost (Chen et al., 2002; Cullum et al., 1986; Volff & Altenbuchner, 2000). A frequent phenomenon during the course of cultivation of streptomycetes is the appearance of colonies that are unable to produce aerial mycelium. This, so called, *bld* (bald) phenotype is ascribed to mutation in genes involved in aerial hyphae development (Willey et al., 1991).

Streptomyces sp. plasmids

The loss of phenotypic traits of a strain can also be the result of plasmid loss. There are many reports on *Streptomyces* sp. harbouring circular or linear plasmids, or even both (Bibb et al., 1977; Kendall & Cohen, 1988; Kieser et al., 1982; Zhang et al., 2008). While circular plasmids are known since the 1950s, their linear counterparts were firstly discovered in 1977 in maize (Pring et al., 1977) and two years later also in bacteria, namely in *Streptomyces rochei* (Hayakawa et al., 1979). Since then, linear plasmids have been reported repeatedly in eukaryotic and prokaryotic cells, especially in actinomycetes, like *Klebsiella* sp., *Streptomyces* sp., *Micrococcus* sp. and *Rhodococcus* sp., where they enable growth under heavy metal and antibiotic stress by providing the relevant resistance genes (Dib et al., 2010; Pandza et al., 1998; Ravel et al., 1998; Stoppel et al., 1995; Warren et al., 2004).

Giant linear plasmids have been shown to play an important role in secondary metabolism, antibiotic resistance, decomposition of aromatic compounds and phytopathogenicity (Chater & Kinashi, 2007; Dib et al., 2010; Hayakawa et al., 1979; Ravel et al., 1998). Many of them are self-transmissible and therefore drivers of horizontal gene transfer (Bibb et al., 1981; Chen et al., 1993a; Hosted et al., 2004). Their structure is similar to that of linear chromosomes with both having attached proteins at their 5'-termini and terminally repeated sequences (Keen et al., 1988; Ravel et al., 1998). This similarity makes an interaction of a plasmid with the chromosome more likely and accelerates genome evolution.

One consequence of such an interaction event is the integration of plasmid genes into the genome, which might bring advantages regarding the synchronization or modification of their expression and facilitates the transfer of traits to the next generation (Volff & Altenbuchner, 2000). Short common se-

quences suffice to allow the integration of plasmids into *Streptomyces* sp. chromosomes: in *S. rimosus* a plasmid integrated at a 4 bp common sequence by a single cross-over in a reiterated DNA sequence (Pandza et al., 1998). Additionally, transposons that are integrated in a genome might provide sites for recombination, owing to sequence homology.

Due to their similar structure, also recombination between plasmids is possible: Yang et al. (2011) found homologous regions on two *S. rochei* plasmids that hint at multiple recombination events. This was also observed in plasmids that originate from different strains, e.g. *S. lividans* and *S. parvulus* (Chen et al., 1993a).

Another way of plasmid-chromosome interaction is the exchange of ends, whereby chromosomal genes are mobilized (Pandza et al., 1998). This mobilization also takes place if a plasmid that integrated into the chromosome is excised again and transferred, taking adjacent chromosomal sections with it. In this way, entire chromosomal gene clusters can be co-transferred to a recipient cell during conjugation. Mobilization can be elicited by linear as well as circular plasmids (Bibb et al., 1981; Hu et al., 2000; Lee et al., 2011; Pettis & Cohen, 1994; 2000).

The main route of plasmid transfer between streptomycetes is the direct cell-cell contact during conjugation. Conjugation is an effective way for bacteria for exchanging genetic information that facilitates adaption and evolution (Aminov, 2011). It was observed in bacteria by Lederberg & Tatum (1946) for the first time. The exact mechanism of such a plasmid transfer between streptomycetes is not known and different modes have been postulated. There are possibly several mechanisms that also depend on plasmid topology (Lee et al., 2011; Thoma & Muth, 2015; Wang & Pettis, 2010).

Streptomyces mirabilis P16B-1 and *S. acidiscabies* E13

In the present study, two *Streptomyces* strains will serve as paradigm for the investigation of stress-related regulatory mechanisms in bacteria adapted to high heavy metal concentrations, namely *S. mirabilis* P16B-1 and *S. acidiscabies* E13 (hereafter called *S. mirabilis* and *S. acidiscabies*). Both strains were isolated from soil at a former uranium mining site near Ronneburg (Thuringia, Germany), a habitat characterised by scarce nutrient availability, high salt loads and a low pH, resulting in a low overall number of cultivable bacteria and low soil respiration (Amoroso et al., 2000; Schmidt et al., 2005). This site is representative for soils influenced by acid mine drainage (AMD) and demands a high degree of adaptability from the indigenous microbial community members. Especially cadmium, cobalt, nickel and zinc stand out as main contaminants in the mobile fraction in this soil (Schmidt et al., 2005).

Both strains were selected due to their resistance to high heavy metal concentrations. *S. mirabilis* exhibits a particularly high resistance to Ni^{2+}, tolerating upto 130 mM $NiSO_4$ on minimal medium, but also Zn^{2+}, Co^{2+}, Cu^{+} and Al^{3+} are tolerated at high levels (Schmidt et al., 2009). Its growth and survival in contaminated soil was shown in microcosm experiments, where it decreased the bioavailable heavy metal fraction (Schütze et al., 2014), which raised hopes on a potential utilization of this strain for bioremediation purposes. Furthermore, *S. mirabilis* exhibits traits which might be beneficial for plants and other soil organisms supporting their survival at the contaminated site, e.g. ammonification and the production of siderophores and pigments (Dimkpa et al., 2008; Schmidt et al., 2009; Schütze et al., 2015; Schütze et al., 2013).

The second investigated strain, *S. acidiscabies*, also shows multiple heavy metal resistances against Ni^{2+}, Cu^{+}, Cd^{2+}, Mn^{2+}, and Fe^{3+} (Amoroso et al., 2000; Schmidt et al., 2007), although to a lower level

than *S. mirabilis* (10 mM $NiCl_2$ on minimal medium). It was recognized for biomineralisation on solid and in liquid Ni^{2+} amended medium, where it led to the formation of Ni-struvite, a nickel phosphate mineral (Haferburg et al., 2008). Like *S. mirabilis*, this strain produces several metabolites, which could be beneficial for plant growth in bioremediation approaches, like auxins and three different hydroxamate siderophores, which were shown to promote plant growth at elevated Ni^{2+} concentrations (Dimkpa et al., 2008).

The preceding studies led to an increased interest in the molecular mechanisms that form the basis for the strain's high heavy metal resistance. Therefore, the genomes of both strains were sequenced (T. Kraußе, unpublished) and are now available for a detailed study of potential resistance determinants.

1.2 Heavy metals

Biological importance and threat

Depending on the applied scientific concept, the definition of heavy metals varies. However, in most microbiological works, they are defined as those elements having a higher density than 5 g/cm^3 (Nies, 1999). Accordingly, all transition metals from V to As, Zr to Sb, La to Po, the lanthanides and the actinides belong to the group of heavy metals, with exception of Sc, Ti and Y. Since this work will mostly focus on nickel and copper, this definition will suffice, as these elements meet most criteria for the classification as heavy metals.

In general, metals are essential for basic cell functions. They ensure stability and catalytic activity of proteins, establish charge and concentration gradients across the membrane as prerequisite for other important processes and enable electron transfer as well as the coordination of cofactors (Macomber & Hausinger, 2011). Which metals are used, is determined by several parameters: atomic size, ligand affinities, redox states and preferred coordination geometry (Kuchar & Hausinger, 2004).

Transition metals comprise the groups III to XII of the periodic table. Although these elements only account for 1-2 % of the total cell mass, they are nevertheless essential for cell functioning and for metalloproteins, which constitute appr. 30 % of all expressed proteins in a cell (Wackett et al., 2004). Essential heavy metals, like Mn, Fe, Ni, Co, Cu and Zn, are components of protein active centres or other biomolecules and serve as cofactors in several cellular processes (Ma et al., 2009c; Reyes-Caballero et al., 2011; Valls & de Lorenzo, 2002). Biological functions of Hg and Cd have only been rarely reported (Grégoire & Poulain, 2016; Park et al., 2007).

Despite their importance, metals, and in particular heavy metals, also pose a threat to the cells when available in excess, or even at low concentration, as it is the case for most heavy metals. Their toxicity can be mainly attributed to the generation of reactive oxygen species (ROS) like H_2O_2, hydroxyl radicals, superoxide, *via* the Fenton reaction that pose oxidative stress on the cell. Consequences are damage of lipids, DNA and proteins as well as inhibition of enzyme activity and interferences with gene expression (Cabiscol et al., 2000; Imlay, 2008; Macomber & Hausinger, 2011; Solioz et al., 2010).

However, the attraction of heavy metals to certain ligands, especially thiol groups, is also employed by cells to ensure specific binding of the metal to its target proteins, like responsive regulators. For in-

stance, copper responsive regulators exhibit ligand binding sites rich in cysteine, histidine and methionine that favour binding of the cognate Cu(I) ions (Cobine et al., 1999; Mills et al., 1993).

Environmental impact and distribution

In most habitats, the natural concentration of heavy metals is low, but the progressing industrialization causes the release of heavy metals from anthropogenic sources. Ross (1994) distinguishes five main groups of man-made metal contamination: agriculture, atmospheric deposition, waste disposal, industrial production and metalliferous mining/smelting. The latter activities lead to the exposition of rocks to oxygen, which were formerly isolated from air supply. The subsequent oxidation of metal-containing minerals (pyrite, arsenopyrite, marcasite etc.) generates sulphuric acids and acid mine drainage, which is characterized by a low pH and a high load of rare earth elements and heavy metals (Baker & Banfield, 2003; Banks et al., 1997; Kothe et al., 2005). This run-off is highly critical, as it can reach surface and groundwater reservoirs. However, habitats with high metal concentrations also occur naturally, e.g. in serpentine soils derived from ultramafic rock material (Vithanage et al., 2014).

In soil, free metal ions and metal complexes diffuse through the porous matrix with the water flow and can reach the groundwater or be taken up by plants, thereby entering the food chain (Sparks, 2005).

Whether a potentially toxic metal in the environment is problematic to a cell depends on its bioavailability which is controlled by different parameters. The main abiotic factors are the pH, the overall concentration, redox conditions and availability of sorption sites (Gadd, 1992; Nies, 2016; Sparks, 2005). Also microorganisms control metal availability due to their metabolic activity and cell properties, e.g. biosorption capacity (Gadd, 1992). Besides microorganisms, metals adsorb to soil organic matter and mineral surfaces, especially clay minerals, metal oxides and humic substances (Sparks, 2005). In contrast to most organic pollutants, heavy metals cannot be degraded and thus are one of the most persistent environmental contaminants.

Elevated heavy metal concentration not only has an impact on important ecosystem functions, e.g. by inhibiting nitrification, but also shapes the structure of the natural community (Kapoor et al., 2015). This became apparent in studies concerning microbial communities of heavy metal contaminated sites. On these sites bacteria prevail that are adapted to harsh conditions. Among them, Actinobacteria are often reported, but also *Pseudomonas* sp. and Acidobacteria (Amoroso et al., 1998; Mengoni et al., 2001; Mirete et al., 2007; Schmidt et al., 2005; Van Nostrand et al., 2007). Many isolates show enhanced resistances to the primary pollutant. Studies showed that there is a proportional connection between the number of metal resistant community members to the type and level of contamination: at highly contaminated sites, organisms with higher tolerance and also multiple resistances are isolated more frequently than from non-contaminates soils. This allows the assumption that enhanced metal loads act as selection pressure on the microbial community, consequently shaping their composition (Mengoni et al., 2001; Ryan et al., 2005; Van Nostrand et al., 2007).

1.3 Cellular heavy metal resistance mechanisms

Metal homeostasis and resistance

As stated above, elevated intracellular metal concentrations can have detrimental effects, wherefore every cell needs to control and maintain an optimal bioavailable metal concentration in the cytoplasm

that meets the metal needs of the cell but reduces harmfull effects to a minimum. This state of optimal balance is called homeostasis and contributing processes involve metal uptake and efflux, trafficking and storage mediated by specific complexes between metal and protein (Ma et al., 2009c). In this regard, metal resistance can be defined as the ability of a cell to sustain metal homeostasis even at high extracellular metal availability (Herzberg et al., 2016).

For most cations there are several transport systems coded on the bacterial chromosome, which are either low-affinity, high-capacity systems constitutively expressed or high-affinity, low-capacity systems that are regulated in response to nutrient concentration (Silver & Walderhaug, 1992). The substrate specificity of these transporters varies. Additionally to specific importers, heavy metals can enter the cell *via* constitutively expressed unspecific transport systems that cannot distinguish toxic metals from their cognate substrate due to similar structure and valence of the cations (Nies, 1999). For instance, transporters CorA or ZupT that serve as Mg^{2+} or Zn^{2+} importers, also transport Ni^{2+}, Co^{2+} and other metals (Grass et al., 2005; Herzberg et al., 2016; Kirsten et al., 2011). This unspecific uptake cannot be controlled or prohibited by the cell, which is why cells employ different strategies to protect themselves from metal stress.

Most of the heavy metal resistance mechanisms aim at the removal of metals from the cell by active efflux or the decrease of their toxicity by sequestration and detoxification by enzymes (Eitinger & Mandrand-Berthelot, 2000; Nies, 1999; Schmidt et al., 2007; Schmidt et al., 2009; Valls & de Lorenzo, 2002). In the cytosol, chaperones, storage protein, metallothioneins and metallocysteins serve as metal binding agents that reduce the concentration of free ions and can route them to their place of action (Schmidt et al., 2010).

For governing metal response, the cell has to sense elevated cytosolic concentrations in the first place. This prerequisite is met by metal sensors that regulate gene expression in accordance with metal availability inside the cell. Currently, there are ten families of metalloregulators known that bind one or more cognate metal ions and can be grouped according to their structure and functioning. Most of these sensors are transcriptional repressors that are released from the DNA in presence of their cognate metal, while others are only released in absence of their metals or change conformation when activated by metal binding but remain bound to operator allowing transcription. The high specificity of metalloregulatory proteins is effectuated by precise coordination chemistry and geometry of the binding site (Ma et al., 2009c).

In most cases, increasing metal concentrations induce the transcription of efflux transporters in order to restore metal homeostasis. Diverse efflux systems have been described (for review, see Nies (2003)). They belong to different classes of transporters, like P-type ATPases, the resistance-nodulation-cell division superfamily or transporters of the major facilitator superfamily. Cells usually possess several of these transporters, which exhibit different substrate specificities and affinities (Herzberg et al., 2016; Nies, 2003).

Metal homeostasis and resitance is very well studied in Gram-negative species, especially in *Cupriavidus metallidurans*. Strains of this species are commonly found in metal contaminated habitats all over the world (for overview, see Van Houdt et al. (2012)). Irrespective of the location and habitat type, *C. metallidurans* strains carry the same resistance determinants which suggests that these were acquired early during strain evolution (Van Houdt et al., 2012). The best studied strains of this species are *C. metallidurans* CH34 and 31A, which originate from a zinc factory and a metal-contaminated industrial site (Mergeay et al., 1985; Schmidt & Schlegel, 1989). Strain CH34 harbours at least seven

secondary metal uptake systems with low, overlapping substrate specificities. Also several heavy metal efflux transporters have been described in this species, that confer high-level metal resistance and whose corresponding genes are combined in highly efficient operons allowing synchronized transcription (Corbett et al., 2011; Herzberg et al., 2016; Nies, 2003; Odermatt & Solioz, 1995).
In *Streptomyces* sp., metal resistance mechanisms are less well investigated in dept, despite their frequent isolation from contaminated habitats. Therefore, the presented work aimed at transferring knowledge from well-investigated heavy metal resistant organisms to this genus.

Contribution of plasmids

Changing environmental conditions demand a high degree of flexibility, adaption and durability from microorganisms. Often, plasmids encode genes which are beneficial for adapting to those changing regimes. While in most cases genes that are necessary for basic metal homeostasis are coded on the genome, accessory genes, that confer resistance to a particular metal, are frequently found plasmids (Rensing et al., 1999). A role model for this structure, is *C. metallidurans* CH34 that harbours two plasmids, pMOL28 and pMOL30, which carry several clusters of resistance determinants for different heavy metals (Mergeay et al., 1985; Nies, 2016). However, resistance determinants can also be coded on the chromosome (Grass et al., 2000).
Besides *Cupriavidus* sp., plasmids coding genes for heavy metal resistance systems have been reported from many other species, like *Pseudomonas* sp., *Enterobacter* sp. and *Rhodococcus* sp. (Lee et al., 2006; Mills et al., 1993; Warren et al., 2004). Also in *Streptomyces* sp., isolated from estuary sediments, giant linear plasmids carrying mercury resistance genes are reported. The self-transmissible nature of these plasmids enable the spreading of resistance genes within the community (Ravel et al., 1998), which substantiates the importance of plasmids for adaption to environmental conditions.

Two examples: nickel and copper

Nickel is the 24th most abundant element in the earth's crust and an essential cofactor in several enzymes. Mulrooney & Hausinger (2003) reviewed the to date known nine known Ni-containing proteins, but recent studies of the bacterial metalloproteome suggest that there are more, yet unrecognized, proteins requiring Ni^{2+} or being involved in its trafficking (Cvetkovic et al., 2010; Robinson et al., 2018). Some examples of nickel enzymes are urease, NiFe hydrogenase, dioxygenases and some superoxide dismutases. The latter are especially found in *Streptomyces* sp., where they are primarily expressed in the exponential stage before being replaced by FeZnSOD (Orsaria et al., 1998). An example for a Ni-dependent dioxygenase in this genus is quercetinase QueD that uses Ni^{2+} and Co^{2+} as cofactors for the cleavage of the flavonol quercetin (Merkens et al., 2008).
For meeting the cell's Ni^{2+} requirement, there are specific Ni^{2+} uptake transporters, which will be examined in one of the following sections. However, these systems have a low capacity, which is why in contaminated habitats, the unspecific uptake of Ni^{2+} is more critical. The main unspecific influx path of this element is *via* the CorA system, which is actually responsible for Mg^{2+} uptake (Herzberg et al., 2016; Kirsten et al., 2011). Therefore, Ni^{2+} resistance mechanisms mainly depend on efflux to prevent metal accumulation. Well-studied examples for these resistance systems are *cnr*, *ncc* and *nre* resistance determinants of *Cupriavidus metallidurans* and homologous systems, as well as RcnA of *E. coli* and CznABC of *Helicobacter pylori* (García-Domínguez et al., 2000; Grass et al., 2001; Grass et al.,

2000; Liesegang et al., 1993; Rodrigue et al., 2005; Schmidt & Schlegel, 1994; Stahler et al., 2006). These systems often also confer cross-resistance to Co^{2+}.

Consequently, nickel resistant organisms have been isolated from different heavy metal polluted sites. Besides the already mentioned *C. metallidurans* strains, also *Klebsiella oxytoca*, *Hafnia alvei* and *Streptomyces* sp. are well-investigated bacteria from these sites (Mergeay et al., 1985; Park et al., 2003; Schmidt et al., 2009; Schmidt & Schlegel, 1989; Stoppel et al., 1995).

In comparison to nickel, copper is more frequently used in metallo-enzymes, being an important cofactor for essential enzymes, like cytochrome c oxidase, superoxide dismutases or tyrosinases (reviewed by Arguello et al. (2013) and Rensing & McDevitt (2013)). This bases upon the two highly reactive oxidation states of this element, that occurs either as Cu(II) or Cu(I). As copper rapidly oxidizes, copper ions are mainly found as Cu(II) in oxic environments. However, in the cytosol usually reducing conditions prevail, which is why Cu(I) is the main species that cells have to cope with and that has to be transported (Rensing et al., 1999). In both oxidation states, copper can bind to biomolecules.

Copper is not only highly toxic by inducing ROS generation, but also highly competitive for binding to metal sensors as non-cognate metal, whereby transcriptional responses to other stressors could be prevented (for a review, see Reyes-Caballero et al. (2011)). To circumvent deleterious intracellular effects, the Cu(I)-containing enzymes of many gram-negative bacteria are located in the periplasm or the cytoplasmatic membrane (Rademacher & Masepohl, 2012). However, several intracellular systems are known that either bind the copper ions or excrete excess ions to the extracellular space, on which Gram-positives depend. To prevent oxidative damage by highly reactive free copper, cells use intracellular chaperones that tightly bind this ion for copper trafficking (Arnesano et al., 2001; Dwarakanath et al., 2012; Robinson & Winge, 2010; Wimmer et al., 1999).

Anthropogenic copper sources are primarily mining activities and the application of copper-based pesticides in agriculture (Altimira et al., 2012; Dell'Amico et al., 2008). The resulting copper accumulation in soil negatively influences biological processes and soil quality (Altimira et al., 2012; Fernández-Calviño & Bååth, 2016). Also indirect effects of copper contamination, e.g. the induction of a decrease in soil pH have been reported (Fernández-Calviño & Bååth, 2016). Regarding the soil microbial community, an increased copper input initially leads to decreased bacterial respiration and growth and has a long-term effect on the community structure and diversity (Dell'Amico et al., 2008; Fernández-Calviño & Bååth, 2016). A subsequent decrease in substrate utilization or degradation, in turn, influences the soil's properties (Tsai & Chen, 2011).

In habitats with a high copper level the proportion of copper-tolerant bacteria is higher than in other soils and an enhanced spreading of Cu(I) resistance determinants on mobile genetic elements within the community can be observed (Altimira et al., 2012; Dell'Amico et al., 2008). One of the most common resistance systems is based on the efflux *via* metal ATPases, like CopA (Altimira et al., 2012).

1.4 Objectives of this study

The aim of this project was to identify genes responsible for heavy metal resistance the two streptomycete strains from a heavy metal contaminated site. Therefore, a transformation system for *in vivo* gene deletion had to be established. As first approach random transposon mutagenesis was chosen, in the course of which several heavy metal sensitive transformants could be isolated and first putative

target genes were identified. When the whole genome sequences of the investigated strains became available, this random approach was abandoned in favour of a directed knock-out method, that was on one hand applied for confirmation of the aforementioned putative resistance genes and on the other hand enabled deletion of genes that were predicted *in silico* to be potential heavy metal resistance genes based on sequence similarity to known resistance determinants.

Due to these dual approaches, in the course of this project, the focus broadened and besides heavy metals, also resistance to other stressors was examined, such as antibiotic and antimicrobial compounds, alkali metals and developmental barriers.

As these are diverse topics, the introduction shall give a broad overview over the addressed problems, while in the sections a detailed focus will be put on the examined object

2. Material and Methods

Bacterial strains and cultivation conditions

Bacterial strains and plasmid used in this study are listed in Table 1. *E. coli* KNabc was a gift from Prof. Dr. Etana Padan. *E. coli* ET12567 pUZ8002 and *E. coli* BW25113 pIJ790 as well as plasmids pSET152, pIJ773 and pKOSi were provided by Dr. Tina Netzker (Hans Knöll Institute, Jena, Germany). Media used in this study are given in Table 2. Suppliers of chemicals can be found in the electronic Supplemental material.

E. coli strains were routinely grown in StdI and *Streptomyces* sp. strains in TSB liquid medium. Cultures of *Streptomyces* sp. were incubated at 28°C and *E. coli* at 37°C, unless stated otherwise. If solid medium was used, 1.8 % agar was added to the medium. For cultivation of the sodium sensitive *E. coli* KNabc, LB medium was modified by substituting NaCl with 87 mM KCl (termed: LBK).

Table 1. Bacterial strains and plasmids used in this study with relevant characteristics.

Strain or plasmid	Properties	Source or reference
Strains		
S. mirabilis P16B-1		Schmidt et al. (2005)
S. acidiscabies E13		Amoroso et al. (2000)
S. mirabilis P16 489_3	*S. mirabilis* P16B-1 derivative lacking both endogenous plasmids; *Himar1* insertion in *P16nhaA1*	This study
S. lividans TK24	*str*-6, SLP2$^-$,SLP3$^-$	Hopwood et al. (1983)
S. violaceoruber A3(2) DSM 40783*		DSMZ, Germany
E. coli DH5α	*supE44* ∆*lacU169* (φ80 *lacZ*∆*M15*) *hsdR17 recA1 endA1 gyrA96 thi-1 relA1*	Sambrook (2001)
E. coli TransforMax EC100D™ pir-116	*F$^-$ mcrA Δ(mrr-hsdRMS-mcrBC) φ80dlacZΔM15 ΔlacX74 recA1 endA1 araD139 Δ(ara, leu)7697 galU galK λ- rpsL (Str^R) nupG pir-116(DHFR)*	Metcalf et al. (1994)
E. coli ET12567 pUZ8002	*dam$^-$ dcm$^-$ hsdS$^-$* Cm^r	MacNeil et al. (1992)
E. coli BW25113	K12 derivative: Δ*araBAD*, Δ*rhaBAD*	Datsenko & Wanner (2000)
E. coli KNabc	Δ*nha*A::Km^r, Δ*nha*B::Em^r, Δ*cha*A::Cm^r, *sup*E, *hsdΔ*5, *thi*, Δ (*lac-pro*AB)/F' (*traΔ*36, *pro*AB$^+$, *lacI*^{q}, *lac*ΔM15)	Nozaki et al. (1996)
Plasmids		
pSET152	*oriT (RK2) int attP(φC31) aac(3)IV*	Bierman et al. (1992)
pSEThph	Derivate of pSET152 with *hph* inserted at *Nhe*I site	This study
pIJ790	λ-RED (*gam, bet, exo*), *cat, araC, rep101*^{ts}	Gust et al. (2003)
pIJ773	*aac(3)IV* (Apra^R) *oriT*	Gust et al. (2003)
pTrc99A	Amp^r *trc*PO *lacI*^{q} ColE1*ori*	Amann et al. (1988)
pKOSi	Kan^r, pSG5*rep*	Netzker et al. (2016)
pUWL201	pUC18 *ori*, pIJ101*ori*, P*ermE**, Amp^r, Th^r	Doumith et al. (2000)
pTNM	*aac(3)IV*, *oriT*, *tipAp*, *tnp(a)*, pSG5*rep*, *hph* (Hyg^r), *oripMB1*, *R6Kγori*	Petzke & Luzhetskyy (2009)
pHTM	*aac(3)IV*, *oriT*, *tipAp*, *Himar1*, pSG5*rep*, *hph* (Hyg^r), *oripUC18*, *R6Kγori*	Bilyk et al. (2013)

* The strain was formerly designated *S. coelicolor* A3(2), but re-assigned. As the old designation is still commonly used in current literature, it will be named as *S. coelicolor* A3(2) in this work as well.

Where appropriate, antibiotics were added to the culture medium in the following final concentrations: ampicillin 50 µg/ml, apramycin 25 µg/ml, kanamycin 25 µg/ml, chloramphenicol 25 µg/ml, thiostrepton 12 µg/ml, hygromycin 25 µg/ml and nalidixic acid 25 µg/ml. For heavy metal amendment, metal stock solutions were filter-sterilised (0.22 µm Rotilabo PES filters, Carl Roth, Karlsruhe) and added prior to inoculation. For pH tolerance tests, the media were not autoclaved but filter-sterilized in order to avoid pH changes during the autoclaving process. pH was adjusted with NaOH, KOH or HCl.

Spore stocks for *Streptomyces* sp. strains were obtained from cultures grown on CSA plates and stored in 20 % (v/w) glycerol at -20 °C. Spore concentrations were determined by plating of a dilution series after one day of freezing. *E. coli* stocks were prepared from liquid culture and stored in 20 % glycerol, as before.

Table 2. Composition of media used in this study. Amounts are given per litre. All components were dissolved in *A. dest.*, except for MS medium, for which tap water was used instead. References: 1) Kieser et al. (2000); 2) Sambrook (2001); 3) Amoroso et al. (2000); 4) Carl Roth, Karlsruhe; 5) Hanahan (1983); 6) Elbing & Brent (2002); 7) DSMZ, Germany.

Mannitol soya medium[1] (MS)	**Casein starch medium (CSA)**	**Standard I [4] (Std I)**	**Tryptic soy broth[1] (TSB)**
20 g mannitol 20 g soya flour	10 g starch 1 g casein hydrolysate 0.5 g K_2HPO_4	25 g standard I	30 g tryptic soy broth
Glucose yeast medium[7] (GYM)	**Luria-Bertani broth[2] (LB)**	**2xTY[1]**	
10 g malt extract 4 g yeast extract 4 g glucose	5 g yeast extract 10 g tryptone 10 g NaCl	16 g tryptone 10 g yeast extract 5 g NaCl	
M9 medium[2]	**M63 medium[6], modified**	**SOB[5]**	**Minimal medium[3] (AM)**
<u>5x M9 salts</u>: 64 g Na_2HPO4 x $7H_2O$ 12 g KH_2PO_4 5 g NH_4Cl 2.5 g NaCl <u>Final medium</u>: 1x M9 salts 1 mM $MgSO_4$ 0.1 mM $CaCl_2$ 0.2 % glucose 0.025 % casamino aids 0.2 ‰ thiamine	<u>5x M63 salts</u>: 10 g $(NH_4)_2SO_4$ 68 g KH_2PO_4 2.5 mg $FeSO_4$ x 7 H_2O <u>Final medium</u>: 1x M69 salts 1 mM $MgSO_4$ 0.2 % glycerol 0.2 ‰ thiamine	5 g yeast extract 20 g tryptone 0.6 g NaCl 0.2 g KCl 10 mM $MgCl_2$ 10 mM $MgSO_4$	10 g glucose 0.5 g L-asparagine 0.5 g K_2HPO_4 0.2 g $MgSO_4$ x 7 H_2O 0.01 g $FeSO_4$ x $7H_2O$
NMMP[1], modified	**R2YE[1] (w/o succhrose)**		
2 g $(NH_4)_2SO_4$ 0.6 g $MgSO_4$ x 7 H_2O 1 ml minor elements solution 1.5 mM NaH_2PO_4/K_2HPO_4buffer (0.1 M, pH 6.8) Minor elements sol.: 1 g $ZnSO_4$ x 7 H_2O 1 g $FeSO_4$ x 7 H_2O 1 g $MnCl_2$ x 4 H_2O 1 g $CaCl_2$	103 g succhrose 0.25 g K_2SO_4 10.12 g $MgCl_2$ x 6 H_2O 10 g glucose 0.1 g casaminiacids 5 ml Difco yeast extract (10 %) 1 ml KH_2PO_4 (0.5 %) 8 ml $CaCl_2$ x 2 H_2O (3.68 %) 1.5 ml L-proline (20 %) 10 ml TES buffer (5.73 %, pH 7.2) 0.2 ml trace element solution 0.5 ml NaOH (1 N)	Trace element sol.: 40 mg $ZnCl_2$ 200 mg $FeCl_3$ x 6 H_2O 10 mg $CuCl_2$ x 2 H_2O 10 mg $MnCl_2$ x 4 H_2O 10 mg $Na_2B_4O_7$ x 10 H_2O 10 mg $(NH_4)_6Mo_7O_{24}$ x 4 H_2O	

Computational analysis

Gene identification and protein characterization

Similarity searches on gene and protein level were performed using BLAST (Altschul et al., 1990). For proteins the Swizzprot (The-UniProt-Consortium, 2017) and NCBI Reference Sequence (RefSeq) Database were browsed. With the help of NCBI's conserved domain database (Marchler-Bauer et al., 2015) conserved domains on protein level were identified and the Transporter Classification system (TCDB, Saier et al. (2016)) was consulted for the categorization of putative transporter proteins.

For protein characterization, their mass was predicted with the ExPASy online tool "Compute PI/Mw" (Gasteiger et al., 2005) and for some proteins hydropathy plots were calculated according to Kyte & Doolittle (1982) with "ProtScale", another ExPASy tool. When necessary, protein transmembrane domains were predicted by two online tools: HMMTOP (Tusnady & Simon, 1998) and Phobius (Kall et al., 2007). For charge plot generation, the EMBOSS online tool (http://www.bioinformatics.nl/cgi-bin/emboss/charge) (Rice et al., 2000) was used.

Phylogenetic trees and protein alignments

For multiple amino acid sequence alignments MAFFT online version 7 (Katoh et al., 2017) was used with the "Auto strategy" (BLOSUM62 scoring matrix, gap opening penalty: 1.53, offset value: 0.2). Where required, positions of uncertain alignment were removed using BioEdit (Hall, 1999). For bootstrapping and maximum likelihood calculation of phylogenetic trees RAxMLGUI 1.3.1 was used applying PROTGAMMA rate distribution and the DAYHOFF amino acid similarity matrix with 200 bootstrap repetitions (Silvestro & Michalak, 2012; Stamatakis, 2014). Trees were visualised using FigTree v1.4.3 (A. Rambaut, http://tree.bio.ed.ac.uk/software/figtree/) and graphically finalized using CorelDraw 11 (Corel Corporation, Ottawa, Canada). Figures displaying sequence alignments were compiled with the BoxShade online tool (https://embnet.vital-it.ch/software/BOX_form.htm). Residue shadings indicated the similarity of each residue to a hypothetical consensus sequence with black background indicating identity and gray background similarity with the consensus. Accession numbers of sequences used for generation of trees and allignemtns are listed in the electronic Supplementary Material (eS2, eS3)

Molecular methods

DNA isolation and PCR

Streptomyces sp. genomic DNA was isolated according to a modified salting-out procedure (Pospiech & Neumann, 1995) with an additional CTAB step for removal of polysaccharides (Kieser et al., 2000) after addition of 5 M NaCl. A detailed protocol can be found in the Supplemental material (S1). Concentration and purity of DNA, PCR products etc. was measured spectrophotometrically using a DS-11 Spectrophotometer (DeNovix, Wilmington, USA). Primers were designed using Vector NTI Advance 11.0 (Invitrogen Corporation, Carlsbad, USA) and subsequently checked with the online tools Oligo Calculator version 3.27 (http://biotools.nubic.northwestern.edu/OligoCalc.html) and Multiple Primer Analyzer (Thermo Fisher Scientific, Waltham, MA, USA) for ensuring the highest possible quality. Primers were synthesized by Eurofins Genomics (Ebersberg, Germany). Primer sequences are listed in the Supplemental material (S4 and eS1).

Depending on the purpose, different DNA polymerases were used in this study. Colony PCR was conducted using DreamTaq DNA polymerase (Thermo Fisher Scientific, Waltham, MA, USA), while DNA

amplification for cloning was conducted with either Phusion High-Fidelity DNA Polymerase (New England Biolabs, Ibswich, UK) or PrimeSTAR GXL DNA Polymerase (Takara Bio Inc., Kusatsu, Japan). Master mixes were prepared according to the manufacturer's instructions. When using Phusion polymerase, GC buffer was used and supplemented with 1 M betaine and 8 % DMSO to increase the polymerase performance on GC-rich templates. PCRs were run in TProfessional Standard Thermocycler gradient (Biometra, Göttingen, Germany) or T3 Thermocycler (Biometra, Göttingen, Germany) using two-step and three-step PCR programs.

For checking PCR product length, isolated DNA and plasmids, 0.8 % agarose gels were run at 100 V in 1X TAE buffer in a horizontal electrophoresis system (Biozym Scientific GmbH, Oldendorf, Germany). For band size estimation, *Pst*I-digested lambda DNA was used as marker, if not stated otherwise. Bands were visualised using the Transiluminator (pequlab Biotechnologie GmbH, Erlangen Germany) and Infinity Capture software (Teledyne Lumenera, Ottawa, Canada).

Sequencing of PCR products and plasmids was executed by GATC Biotech AG (Konstanz, Germany).

Plasmid construction and isolation

Purification steps necessary for vector construction were performed with the QIAquick PCR Purification Kit (QIAGEN N.V., Venlo, Netherlands). For ligation, T4 ligase (Thermo Fisher Scientific, Waltham, USA) was used according to manufacturer's instructions with incubation at 14 °C over night. Restriction digestion of DNA was performed with New England Biolabs (Ibswich, UK) enzymes, as recommended by the supplier. Plasmid isolation from *E. coli* cells was performed using the GeneJet Plasmid Miniprep Kit (Thermo Fisher Scientific, Waltham, USA).

Construction of pSEThph

Since the integrative *Streptomyces* sp.–*E. coli* shuttle vector pSET152 (Figure 1) carried the same apramycin resistance gene that was used for the generation of the *Streptomyces* sp. deletion transformants, the plasmid had to be modified in order to be applicable for genetic complementation experiments. Therefore, the hygromycin resistance gene (*hph*) of pHTM was chosen to be integrated in pSET152 downstream the *aac(3)IV* gene by blunt-end ligation into the *Nhe*I site. For this, pSET152 was digested with *Nhe*I (New England Biolabs, Ibswich) for linearization and the hygromycin resistance gene was cut out of pHTM using *Bsp*HI (New England Biolabs, Ibswich) at 37°C over night. The *hph* gene was subsequently purified using the GeneJet GelExtraction Kit (Thermo Fisher Scientific, Waltham) according to the manufacturer's protocol and the digested plasmid was purified using the QIAquick PCR Purification Kit. The ends of both, the purified *hph* fragment and the linearised pSET152, were blunted by treatment with the Klenow fragment of DNA polymerase I (Thermo Fisher Scientific, Waltham) for 15 min at 25°C in a total volume of 50 µl each as recommended by the producer. After inactivation of the enzyme by adding

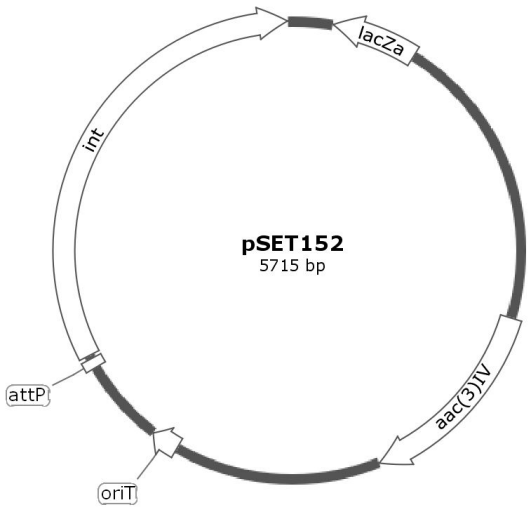

Figure 1. Vector map of the integrative *E. coli-Streptomyces* sp. shuttle vector pSET152 displaying the most important features: *attP* - φC31 phage attachment site; *aac(3)IV* – apramycin resistance gene; *int* – integrase gene, *oriT* – origin of Iransfer; *lacZa* – LacZ protein

1 µl 0.5 M EDTA, ligation of both fragments was conducted with T4 ligase at 16°C over night, yielding pSEThph, which was used for the transformation of *E. coli* TransforMax.

Transformation of E. coli

E. coli cells were made electrocompetent according to standard protocols (Hanahan, 1983; Sambrook, 2001). Transformation was conducted by electroporation (Sambrook, 2001) with a Gene-Pulser II (Bio-Rad Laboratories, Hercules, USA) at 25 µF und 2,5 kV. Transformed cells were subsequently recovered for one hour under non-selective conditions before plating on selective medium and incubation at 37° or 28°C over night.

Southern Blot

In order to verify the success of the knock-out procedure, DNA of *Streptomyces* sp. transformants was checked by Southern Blotting. This was done according to the standard procedures (Sambrook, 2001) and a detailed protocol can be found in the Supplemental material (S2). In short, 10 µg of *Streptomyces* genomic DNA was digested to completion over night with appropriate restriction enzymes and precipitated by ethanol precipitation. A 0.8 % agarose gel was run with the digested DNA for 1 h at 100 V, followed by documentation, as described above. Then, the gel was treated for 10 min with 250 mM HCl for depurination, followed by 10 min denaturation and neutralization steps, which were each repeated once. The DNA was transferred to an amphoteric nylon membrane (Porablot™ NY Amp, Macherey-Nagel, Düren, Germany) by downward capillary transfer over night and subsequently fixated by UV cross-linking.

For hybridization and detection the DIG labelling and detection system was used (Roche Diagnostics GmbH, Grenzach-Wyhlen, Germany), according to the manufacturers protocol. Hybridization with a probe was carried out in a mini-shaking oven (OV3, Biometra, Göttingen, Germany) for 18 h at high stringency conditions (68°C). The chemiluminescent signal was detected on X-ray film (Thermo Fisher Scientific, Waltham, USA). As probe PCR products were used, which were labelled with digoxigenin by random primed labelling after gel purification with the GeneJet Gel Extraction Kit (Thermo Fisher Scientific, Waltham, USA). For probe generation, 15 µl PCR product of the target sequence was denatured for 10 min at 95°C and immediately put on ice for 10 min. Then, 2 µl Hexanucleotide Mix (10 x), 2 µl DIG Labelling Mix (10 x) (Roche Diagnostics GmbH, Grenzach-Wyhlen, Germany) and 1 µl Klenow enzyme (Thermo Fisher Scientific, Waltham, USA) were added, mixed and incubated for 20 h at 37°C. The reaction was stopped by incubation at 65°C for 10 min. The labelled product was denatured as before and diluted in 5 ml standard hybridisation buffer and stored at -20°C until use.

In order to confirm the efficient labelling of the PCR product, the probe was tested using Dot Blot. Therefore, a dilution series of the unlabeled product in three steps was prepared, which was then de-

Table 3. Primers used for the generation of probes for Southern Blotting targeting central fragments of the native *Streptomyces* sp. plasmids.

Plasmid	Primer name	Primer sequence	Fragment length
P16 small plasmid (pI)	P16pI-F P16pI-R	ATGCGGCCTCCGAGCGAGAAGC TCACCCCGGACCGCGCAAAC	845 bp
P16 large plasmid (pII)	P16pII-F P16pII-R	ATGGGTAAGGCGCACTCTGC CCCTGGAACTTCGAGACGAGTG	757 bp
E13	E13-PlasmF E13-PlasmR	AGGAGGCGTCCGGCGTTCTT TTCGCCAACGGAGACCGCAC	817 bp

natured at 95°C for 10 min and subsequently cooled down on ice for 10 min. 1 µl of each dilution step and the original product was dropped on a nylon membrane and fixated by UV cross-linking. The hybridisation and detection was performed as described above.

Southern Blot analysis was also used to detect the native *Streptomyces* sp. plasmids in the heavy metal sensitive transposon transformants. As probes, fragments in the centre of each plasmid were amplified by PCR (Table 3) using PrimeSTAR GXL DNA Polymerase with 5 min 95°C initial denaturation and 30 cycles of 95°C 30s, 58°C 15s and 1 min 68°C, followed by 5 min 68°C and cooling at 8°C and labelled as described above.

Error-prone PCR

For introducing random base exchanges in *P16nhaA1* (see section 3.8), an error-prone PCR approach was chosen. By using DreamTaq polymerase that lacks proof-reading activity, at conditions that promote mis-incorporation of bases, gene mutations were promoted. The PCR mixture contained 0.4 µM per primer (Antip_pTrc_F & Antip_pTrc_R, Table 4), 1 mM dCTP/dTTP, 200 µM dATP/dGTP, 0.2 mM $MnCl_2$, 7 mM $MgCl_2$, 1x DreamTaq buffer, 5 U DreamTaq polymerase and 0.2 µg template per 50 µl. As template the plasmid pTrcnhaA1 was used, which carried the native *P16nhaA1*. The PCR program comprised 10 min denaturation at 95°C, followed by 40 cycles 1 min 95°C, 30 s 47°C, 2 min 72°C and subsequently 10 min 72°C final elongation with subsequent cooling at 12°C.

The PCR product was cleaned by gel purification using GeneJet Gel Extraction Kit according to the manufacturer's instructions. Subsequently, the product and vector pTrc99A were digested with *Xba*I and *Pst*I-HF for 4 h at 37°C, purified using the QIAquick PCR Purification Kit and ligated by T4 ligase at 14°C over night.

The ligation mixture was used for transformation of *E. coli* KNabc (Table 1), a Na^+ and Li^+ sensitive strain. The transformants were selected on LBK medium at pH 8.2 containing ampicillin, kanamycin, chloramphenicol and 1 mM LiCl. Plasmids from grown colonies were isolated, sequenced and used for the re-transformation of *E. coli* KNabc for excluding chromosomal mutations in the host strain that would have enabled growth under selective conditions.

Transformation of Streptomyces *sp.*

Interspecific conjugation for pSET152 introduction

For plasmid introduction in the investigated *Streptomyces* sp. strains a conjugation procedure according to Kieser et al. (2000) was followed, as this is widely used for different *Streptomyces sp.* strains. A detailed protocol for the conjugation procedure can be found in the Supplemental material (S3). In short, an over night liquid culture of *E. coli* ET12567 pUZ8002 carrying pSET152 (Figure 1) was used for the inoculation of fresh liquid medium containing chloramphenicol and kanamycin for the selection for the *dam* mutation and pUZ8002, and apramycin for selection for pSET152. When an OD_{600} of about 0.6 was reached, the culture was washed with 2xTY and resuspended in 250 µl 2xTY.

As recipient, *Streptomyces* sp. spores were used from a two week old plate (CSA medium). With a loop, spores from one single colony were picked and resuspended in 250 µl 2xTY. Subsequently, the spore suspension was incubated for 10 min at 50°C. This heat shock should initiate spore germination, as conjugation can only take place between actively growing mycelium and *E. coli* (Kieser et al., 2000). The solution was allowed to cool down for 10 min before mixing with the *E. coli* cell suspension. This mixture was then plated on MS agar containing 10 mM $MgCl_2$ for efficient transfer and incubated

over night at 28°C. The incubation temperature should not be raised, as the tested *Streptomyces* strains poorly grow at higher temperatures, e.g. 37°C.

After one night incubation, the plates were overlaid with 0.9 % sodium chloride solution containing nalidixic acid and apramycin, in order to prevent further growth of *E. coli* and select for *Streptomyces* transconjugants. After one week incubation, potential transconjugants were picked on CSA agar containing apramycin and nalidixic acid.

The integration of pSET152 into the *Streptomyces* chromosome was checked by Southern Blot analysis, as described above. As probe, the apramycin resistance gene *aac(3)IV* of pSET152 was amplified using primers ApraF and ApraR (see Supplemental material S4-1). The genomic DNA was digested using *Bam*HI.

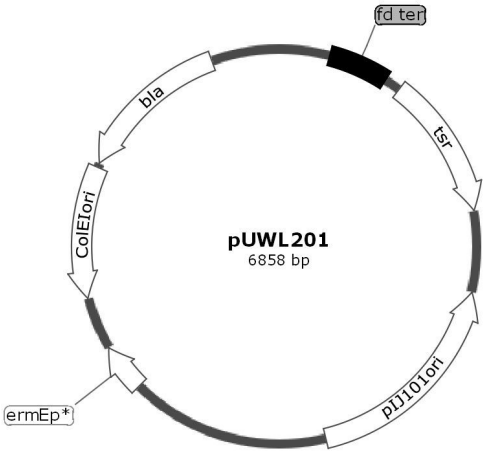

Figure 2. Vector map of pUWL201, used for gene overexpression in *Streptomyces* sp. Inserted genes were under transcriptional control of the *ermE* promoter (*ermEp**). For maintenance and selection in Streptomyces, thiostrepton resistance, encoded by *tsr*, was used.

Using the conjugation protocol decribed above also the vector pUWL201 (Figure 2) and its derivatives were introduced in *S. lividans*. For selection of transformants thiostrepton was used.

Transposon mutagenesis

Plasmids pTNM and pHTM (Table 1, Figure 3) served as delivery vectors for transposons of the Tn5 and *mariner* families. In both cases the transposon comprised the apramycin resistance gene *aac(3)IV* for transformant selection and the R6Kγ ori for replication in *E. coli* TransforMax required for downstream applications, all flanked by mosaic end sites (ME) that served as recognition sites for the transposase (Petzke & Luzhetskyy, 2009).

In a first approach, pTNM was delivered to the streptomycetes by conjugation. Two *S. mirabilis* and one *S. acidiscabies* transformants carrying the plasmid were chosen for further experiments. For transposition, these transformants were grown in liquid GYM medium, shaking for 5 d at 28°C. Transposition was initiated by addition of 1.25 µg/ml thiostrepton and the cultures were incubated as before for 1 h. Afterwards, the incubation temperature was raised to 39°C for eliminating the delivery vector and the cultures were shaken for one more night at this temperature.

After transposition, aliquots of the cultures were streaked on CSA agar plates containing apramycin and incubated for 5 d. The appearing colonies were picked in parallel on CSA agar containing apramycin, CSA agar containing hygromycin and AM medium containing 10 mM $NiSO_4$. Potential heavy metal sensitive transposon transformants were subjected to Southern Blot analysis using the same probe as for the pSET152 transformants.

In order to determine the transposon insertion site, rescue plasmids were generated as described by Bilyk et al. (2013). For this, 1 µg genomic DNA of the transformants was digested with *Pst*I and *Bam*HI in separate reactions over night, purified and diluted in 20 µl pure water each. The complete volume was subjected to self-circulation by adding T4 ligase and the appropriate buffer according to the supplier's protocol in order to create plasmid structures that can be used for *E. coli* transformation. The ligation reaction was stopped by incubation at 65°C for 10 min and 10 µl of the ligation mixture was

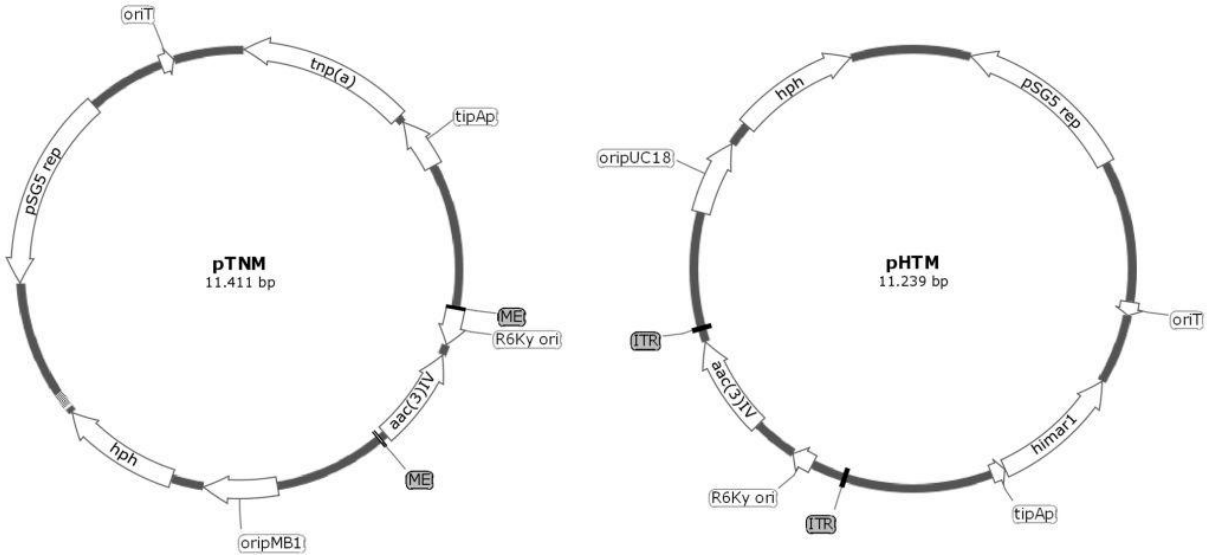

Figure 3. Vector maps of the transposon delivery vectors pTNM and pHTM. Plasmids either harboured the gene for a Tn5 family transposase (*tnp(a)*) or the mariner family *Himar1* (*himar1*), under control of a thiostrepton-inducible promoter (*tipAp*). Transposase recognition sequences (ME and ITR) flanked a gene encoding apramycin resistance (*aac(3)IV*) and a R6K type origin of replication (R6Kγ *ori*). As counterselection marker served hygromycin resistance, encoded by *hph* on the plasmid.

desalted by drop dialysis with a mixed cellulose esters membrane filter (0.025 µm, Merck KGaD, Darmstadt).

3 µl of desalted ligation mixture was used for the transformation of *E. coli* TransforMax EC100D pir-116. This strain harboured the *pir* gene, which encodes the Π protein that enabled the transcription from R6Kγ*ori* (Metcalf et al., 1994) that was located on the transposon, wherefore transformants carrying the DNA fragment containing the transposon could be selected for. Putative rescue plasmids were isolated and sent for sequencing (GATC Biotech AG, Konstanz, Germany) with sequencing primers pMODf and pMODr (Supplemental material S4-1, raw data of sequencing results: electronic Supplementary Material eS6) (Bilyk et al., 2013; Petzke & Luzhetskyy, 2009).

In a successive approach, the same transformation procedure was applied for transforming the investigated *Streptomyces* strains with a second transposon, *himar1*, which was delivered on plasmid pHTM (Figure 3) (Bilyk et al., 2013). As stated above, the main features of this plasmid were identical to pTNM, with exception of the transposase gene, which was in this case the synthetic *himar1*. As in pTNM, the transposon possessed an apramycin resistance as selection marker and a R6Kγ oriR for subsequent plasmid rescue. This transposon promised random, stable insertions even without selection pressure (Bilyk et al., 2013) and has already been used for random mutagenesis of different genera (Le Breton et al., 2006; Maier et al., 2006; Rubin et al., 1999).

PCR-targeted gene deletion in Streptomyces sp.

For gene deletion in *Streptomyces* sp. a PCR-targeted gene replacement method according to Gust et al. (2003) was chosen. A complete, detailed step-by-step protocol for the deletion of a gene of choice in *Streptomyces* sp. can be found in the Supplemental material (S3) and for visualisation of the principle see Figure 9. Primers used for all required PCR steps and all investigated genes in this approach are listed in the Supplemental material Table S4-2. Investigated gene and protein sequences are listed in the electronic supplement eS5.

In the following, the complete procedure is exemplified by one target gene, *P16nhaA1,* coding a putative Na^+/H^+ antiporter. Additionally, the procedures for genetic complementation and overexpression of the gene in *E. coli* are described in detail.

Directed knock-out of *P16nhaA1*

Cosmid construction

As cosmid backbone served the *Streptomyces sp.*-*E. coli* shuttle vector pKOSI (Netzker et al. 2016). Main features of this plasmid (Figure 4, Table 1) were the kanamycin resistance gene, the RSF origin of replication and the temperature-sensitive *Streptomyces* replicon pSG5 of pTNM, wherefore it is lost at incubation temperatures exceeding 34°C.

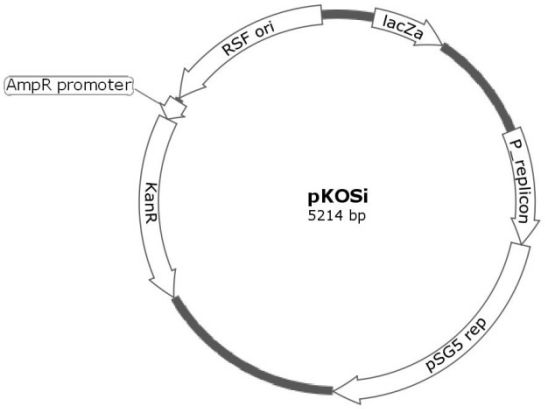

Figure 4. Vector map of pKOSi (Netzker et al., 2016), which was used as backbone for cosmid construction.

First, in a primary PCR a 4482 bp long fragment of *S. mirabilis* genomic DNA comprising *P16nhaA1* was amplified with the nAntipCon primer set (Table 4) using Phusion Polymerase with GC buffer and addition of 8 % DMSO and 1 M betaine in a two-step PCR protocol, where the primer annealing step was omitted: 10 min 98°C initial denaturation, followed by 35 cycles of 30s 98°C and 6 min at 72°C, 10 min 72°C and cooling at 8°C. The product was checked by agarose gel electrophoresis and used as template for the secondary (nested) PCR.

Nested PCR had to be used, as the amplification of large GC rich templates was difficult in most cases. The nested primers annealed to sites internal of the product of the primary PCR and had enzyme cutting sites attached to their 5' ends for subsequent ligation with the vector. For this PCR, AntipCosm primers were used and the 1:10 diluted product of the primary PCR served as template. Further conditions were identical to the primary PCR. The 4351 bp product was purified using the QIAquick PCR Purification Kit and eluted in 40 µl pure water.

The cosmid vector pKOSi and the secondary PCR product were digested with *Eco*RV and *Hind*III-HF at 37°C for 4 h, followed by a purification step as before and elution in 20 µl pure water each. Ligation was conducted using T4 ligase according to the supplier's protocol for 4 h at 22°C. After stopping the reaction (65°C, 10 min), the ligation mixture was used for transformation of *E. coli* TransforMax, from which cosmid, pKOSiAntipCosm, carrying the genomic antiporter region could be isolated and introduced in *E. coli* BW25113 pIJ790.

Resistance cassette generation

The resistance cassette was generated by PCR using plasmid pIJ773 as template. On this plasmid, an apramycin resistance gene and an *oriT* were flanked by priming sites complementary to the 3' ends of the primers (Table 4: Antip-ko primer sets, capital letters). For enabling recombination later, on each primer 39 bases had to be added to the 5' end that were complementary to the genomic DNA up- and downstream of the target (Table 4: Antip-ko primer sets, small letters). The PCR was conducted with PrimeSTAR GXL DNA Polymerase with 5 min 95°C initial denaturation and 30 cyles of 95°C 30s, 50°C 15s and 3 min 68°C, followed by 5 min 68°C and cooling at 8°C. The PCR product was sub-

jected to two consecutive rounds of gel purification with the GeneJet Gel Extraction Kit for eliminating the PCR template, which would otherwise give false-positives in the following knock-out procedure.

Homologous recombination in *E. coli*

Electrocompetent *E. coli* BW25113 pIJ790 pKOSiAntipCosm cells were prepared by inoculating 20 ml SOB supplemented with 10 mM L-arabinose with 1 ml over night culture. After 3 h incubation at 30°C shaking, cells were washed and resuspended in 60 µl 10 % glycerine. These cells were transformed with 300 ng resistance cassette by electroporation and plated on StdI agar containing 25 µg/ml apramycin and 25 µg/ml kanamycin for selection of cosmids with successful resistance cassette integration.

After incubation over night at 37°C, colony PCR was conducted with the grown colonies. DreamTaq Polymerase was used according to the manufacturer's protocol with primers ApraF and ApraR (Supplemental material S4-1), which targeted the *aac(3)IV* gene on the resistance cassette. The PCR program was as follows: 95°C 15 min for breaking of cells and denaturation, followed by 30 cycles of 95°C 30 s, 60°C 15 s and 1 min 72°C and subsequent 10 min 72°C and cooling at 8°C. Products were checked by gel electrophoresis, as before. Transformants that showed a band were cultured in liquid medium over night and plasmids were isolated, as before. The isolated plasmids were used as templates for a PCR with the same primers and conditions used for the colony PCR for confirmation of the

Table 4. Sequences of primers used for targeted replacement of *P16nhA1* in *S. mirabilis*, complementation and expression in heterologous hosts. Cutting sites for enzymes are underlined. Bases in small letters in Antip-ko primers are complementary to genomic DNA flanking the *P16nhA1* target gene.

Name	Sequence	Purpose
Cosmid construction and knock-out		
nAntipConF	AGCGGTTCCTCGACACGTAC	Primary PCR
nAntipConR	TGCGTCACTGTAGTCGTGCG	
AntipCosmF	AATAATAAGCTTGGGACGGGGCGAAGAAGGAC	Cloning in pKOSi
AntipCosmR	AATAATGATATCGGTAGGACAGGCGTTCCCGT	
Antip-koF	gccgtcagcaagcagccgtaacgacccggaggtcccgccATTCCGGGGATCCGTCGACC	Resistance cassette generation
Antip-koR	cggtcctgactgtccggttctgaccatccggttctgctcTGTAGGCTGGAGCTGCTTC	
Antip-ko-ctrR	GGGCTGATCTCTACGGTCTGGCTG	Deletion transformant selection
Antip-ko-SB_F	GCGGAGAACCGGGAGCTGGGG	Probe for Southern Blotting
Antip-ko-SB_R	ATGGGCGCCCGCGTGGACGT	
Complementation		
Antip2F	TTATTATCTAGAGGGCGGGCTCTCACAGGTCC	Cloning in pSEThph
Antip2R	TTATTAGCGGCCGCGGTTCTGCTCAGATCATGCC	
Ecol.nhaA-F	AATTTTCGATCGTCCTACACTATAATCTGATTTTAACG	Cloning in pSEThph
Ecol.nhaA-R	AATAGTGCGGCCGCTTGTAATTGATATGAGACAT	
Overexpression in *S. lividans*		
Antip_OvEx_F	AATAGTAAGCTTGTGGCCACGCCCAGTGCCAA	Cloning in pUWL201
Antip_OvEx_R	AATAAACTGCAGGCTCAGATCATGCCGGACCGTCGT	
Expression in *E. coli*		
Antip_pTrc_F	TTATTATCTAGAAGGGCGGGCTCTCACAGGTCC	Cloning in pTrc99A
Antip_pTrc_R	TTATTACTGCAGGGTTCTGCTCAGATCATGCC	
nhaA2-pTr-F	TTTTTTAAGCTTGATCTGTTCGAGGGCGCCCG	Cloning in pTrc99A
nhaA2-pTr-R	AATATTTCTAGATCCTTCCCCGGCATCGTTTCG	

recombination event, allowing the identification of a cosmid, where the native gene was successfully substituted, which was designated pKOSiAntipCosm-ko.

Conjugation and isolation of transformants

The cosmid carrying the gene deletion was used for transformation of *E. coli* ET12567 pUZ8002, which was subsequently used for conjugation with *S. mirabilis* on MS agar containing 10 mM $MgCl_2$, as described previously. After one night of incubation, the conjugation plates were overlain with 0.9 % NaCl containing nalidxic acid and apramycin and incubated for seven more days at 28°C. Then, putative transformants were picked on CSA agar with 25 µg/ml apramycin, incubated at 28°C for five days and then transferred to CSA agar plates without antibiotics, which were incubated 3 d at 37°C for promoting loss of the cosmid. Subsequently, the transformants were again transferred to selective agar plates.

After 5 d, colonies that showed growth were used for colony PCR. For this purpose, biomass from a single colony was resuspended in 50 µl pure water, incubated 20 min at 99°C and 450 rpm on a thermomixer (Eppendorf AG, Hamburg) and subsequently frozen over night at -20°C. Then, the biomass was shortly spun down and the supernatant used as template for the PCR, for which PrimeSTAR GXL DNA Polymerase was used, according to the supplier's protocol. The native *P16nhaA1* gene and the resistance cassette were nearly identical in size, which was why clean knock-out transformants could not be distinguished from the wildtype if the primers annealed up- and down-stream of the antiporter gene, which would be sufficient for other targets with a larger or smaller size than the resistance cassette (PCR product size would be an indicator for recombination). For the antiporter gene, a different strategy was applied by using a primer, which annealed downstream of the native gene (Antip-ko-ctrR) (Figure 14) and a second primer, which annealed to the *aac(3)IV* gene (ApraF). Clean deletion transformants would give a PCR product, while there should be no PCR product if the native gene was still in its place. For this PCR, the two step PCR approach was followed as mentioned above with elongation for 100 s. Transformants that yielded a correct PCR product were cultivated in TSB liquid medium and DNA was extracted. The genomic DNA was used as template in a PCR as described for the *Streptomyces* sp. colony PCR for confirming the presence of the resistance cassette.

Southern Blot analysis

As probe, a 731 bp DNA fragment located 140 to 871 bp upstream the antiporter gene (Figure 15) was amplified with PrimeSTAR GXL DNA Polymerase in a two step PCR with 60 s of elongation. By choosing a DNA stretch upstream the antiporter gene as hybridization target, band shifts in the Southern Blot with digested DNA allowed the identification of clean knock-outs. The PCR product was purified by gel purification, labelled as described before and tested by Dot Blot with a dilution series of unlabeled PCR product as targets.

For Southern Blot analysis, 10 µg of genomic transformant DNA was digested with *Pvu*I over night at 37°C and Blotting and hybridisation was conducted as described above. Wildtype DNA was used as control.

Complementation with the native gene and *E. coli nhaA*

pSEThphAntipor

For genetic complementation of the *S. mirabilis P16nhaA1* deletion strain vector pSEThph, a derivative of pSET152 carrying a gene for hygromycin resistance, was used. The antiporter gene was ampli-

fied from pKOSiAntipCosm using Phusion polymerase in GC buffer, supplemented with 1 M betaine and 8 % DMSO, and Antip2 primer set (Table 4). The PCR program was as follows: 10 min 95°C, followed by 30 cycles of 95°C 15 s, 15 s 47°C and 1 min 72°C with subsequent 5 min at 72°C and cooling at 8°C. The product was purified using the QIAquick PCR Purification Kit. Afterwards, the product and vector pSEThph were digested with *Xba*I and *Not*I-HF for 4 h at 37°C, purified as before and used for ligation with T4 ligase at 14°C over night, yielding pSEThphP16nhaA1. *E. coli* TransforMax was transformed with the ligation mixture and the plasmid was isolated, which was used for transformation of *E. coli* ET12567 pUZ8002. By conjugation of *S. mirabilis* Δ*nhaA1* with the latter, complemented strain P16 Δ*nhaA1* hphP16nhaA1 was constructed.

pSEThphEcolnhaA

Besides the native *S. mirabilis* antiporter gene, also *E. coli nhaA* was cloned in pSEThph. For this purpose, the gene was amplified from *E. coli* DH5α genomic DNA with primers Ecol.nhaA-F/R (Table 4) using PrimeSTAR GXL DNA Polymerase and the following PCR program: 95°C 10 min, followed by 30 cycles of 95°C 15 s, 55°C 15 s and 68°C 2 min and a final elongation for 5 min at 68°C with subsequent cooling at 8°C. The product was purified using the QIAquick PCR Purification Kit. The vector and the PCR product were digested with *Not*I-HF and *Pvu*I for 4 h at 37°C and then purified as before, followed by ligation using T4 ligase at 14°C over night, yielding pSEThphEcolnhaA. The ligation mixture was used for transformation of *E. coli* TransforMax, from which the plasmid was purified. For further transfer to *S. mirabilis*, the plasmid was introduced in *E. coli* ET12567 pUZ8002, which functioned as donor in the conjugation with the deletion strain Δ*nhaA1*, yielding strain P16 Δ*nhaA1* hphEcolnhaA.

Overexpression in *S. lividans* and *E. coli*

pUWLP16nhaA1

For heterologous *P16nhaA1* expression in *Streptomyces* sp. the gene was amplified with the Antip_OvEx primers (Table 4) with Phusion polymerase using the supplied GC buffer with additional 1 M betaine and 8 % DMSO and P16 genomic DNA as template. The PCR program was as follows: 5 min 95°C initial denaturation, followed by 35 cycles 95°C 15 s, 45°C 10 s and 2:30 min 72°C with subsequent 5 min 72°C and cooling at 8°C. The product was purified using the QIAquick PCR Purification Kit. PCR product and pUWL201 were digested with *Pst*I-HF and *Hind*III-HF for 5 h at 37°C and then purified as before. Ligation was conducted with T4 ligase over night at 14°C yielding pUWLP16nhaA1 and 1.5 µl ligation mixture was used for the transformation of *E. coli* TransforMax. The plasmid was then purified and used for transformation of *E. coli* ET12567 pUZ8002, which served as donor in a conjugation with *S. lividans* TK24, as described before, with the exception that in this case, thiostrepton was used for selection of *S.lividans* transformants, as the vector carried the *tsr* gene for resistance to this antibiotic.

pTrcP16nhaA1 and pTrcP16nhaA2

For overexpression of *P16nhaA1* as well as a second gene coding a putative NhaA transporter (*P16nhaA2*), both were cloned separately in the *E. coli* overexpression vector pTrc99A. The *P16haA1* gene was amplified with primers Antip_pTrc_F/R (Table 4) and purified in the same way as described for pSEThphAntipor. Then, the product and pTrc99A were digested with *Xba*I and *Pst*I-HF for 4 h at 37°C, purified as before and ligated using T4 polymerase over night at 4°C. *E. coli* TransforMax was transformed and plasmid pTrcP16nhaA1 was isolated.

For amplification of *P16nhaA2*, P16 genomic DNA was used as template in a PCR with GXL Polymerase using primers nhaA2-pTr-F/R (Table 4) in a two step PCR with 95°C 10 min initial denaturation, followed by 35 cycles of 95°C 30 s and 2 min 68°C, terminated with 5 min 68°C and cooling at 8°C. pTrc99A and the PCR product were digested with *Hind*III-HF and *Xba*I at 37°C over night and used for ligation with T4 polymerase at 14°C over night. Subsequently, *E. coli* DH5α was transformed and the resulting plasmid pTrcP16nhaA2 isolated.
Both plasmids carrying one of the antiporter genes, as well as the empty vector pTrc99A, were introduced in the *nhaAB* deficient strain *E. coli* KNabc by electroporation for further investigation.

Streptomyces sp. transformants tests

The *Streptomyces* sp. transformants and the wild types were tested in different assays for their resistance to heavy metals or other salts, antimicrobial compounds, hydrogen peroxide and pH. If not indicated otherwise, a spore stock solution from the glycerine stock was used for inoculation. Generally, resistance tests in liquid medium were performed in 24 well cell culture plates (CELLSTAR, Greiner Bio-One, Kremsmünster, Austria) in a volume of 2 ml per well. Each well was inoculated with 15 µl of a spore suspension containing 2 x 10^7 spores/ml.

Trench plates
In trench plate tests the resistance of the strains to different metals was tested. For these, square petri dishes (120 cm x 120 cm; Greiner Bio-One, Kremsmünster, Austria) were used, filled with AM, TSB or GYM medium. A trench of 1 x 10.5 cm was cut at one side of the plate, in which 3 ml of metal stock solution ($NiSO_4$/$NiCl_2$: 2 M, $CoSO_4$/$CoCl_2$: 0.5 M, $CuSO_4$/$CuCl_2$: 1 M, NaCl: 5 M, LiCl: 5 M) was added. The plates were left standing over night, in order for the metal to diffuse and establish a concentration gradient. Then, the plates were inoculated with a spore suspension starting from the trench and subsequently incubated for four weeks at room temperature.

Drop plates
In addition to the trench plate test, a drop plate assay was used for testing metal resistance. With this method, effects of differing spore concentrations shall be eliminated, since bacteria can also feed on dying biomass on the plate, which would be interpreted as growth, although they are not in direct contact with the medium.
Drop plate tests were conducted in petri dishes with different media, as indicated. A four step dilution series of spore suspension was prepared starting with 10^7 spores/ml. The suspensions were spotted on the plates in 2 µl aliquots. The plates were incubated for 1-4 weeks at 28°C.

Agar and disc diffusion assays
Disc diffusion assay were conducted on different media, as indicated in the respective sections. A spore suspension was spread on the plate and afterwards a cotton linter test disc (Ø 9 mm, Thermo Fisher Scientific, Waltham, USA) was placed in the middle of the plate. On this disc 40 µl of the chemical compound was added, as stated in the relevant section. Plates were incubated at 28°C for one week.
In agar diffusion assays, the resistance of some transformants to antimicrobial compounds was compared, For these, the plates containing the respective medium were pierced with a sterile pipette tip,

creating a 0.6 cm hole in the middle of the plate, in which 100 µl of a solution containing the compound to be tested, was added. Analogously to the trench plates, these plates were inoculated with a spore suspension starting from the hole. The plates were incubated for 7 d at 28°C.

Enzymatic assays

Cytochrome c oxidase activity

The activity of the cuproenzyme cytochrome c oxidase (CcO) was determined *in vivo* using N,N,N',N'-tetramethyl-p-phenylenediamine (TMPD) as substrate, according to Blundell et al. (2013). Spore suspensions of the strains were dropped in triplicates on square petri dishes (120 cm x 120 cm; Greiner Bio-One, Kremsmünster, Austria) containing TSB medium and incubated at 28°C for four days. The plates were overlain with 10 ml of 25 mM sodium phosphate (pH 7.4) solution containing 20 % ethanol, 0.6 % agarose, 1 % sodium deoxycholate and 10 mg TMPD. The colour development, which resulted from the conversion of TMPD to indophenol blue by CcO, was followed for 30 min by taking pictures every 5 min.

Urease activity

For determining the urease activity, liquid cultures in GYM and TSB medium were prepared and incubated for 5 d at 28°C on a shaker. The biomass was harvested and washed two times with 10 mM sodium phosphate buffer (pH 7.4) and resuspended in 300 µl of the same buffer per sample. For cell wall disruption, the mycelium was grinded in liquid nitrogen. After centrifugation at 14 000 rpm, 4°C for 20 min, the protein-containing solution was transferred to a new tube. The protein concentration was determined using Bradford Reagent (Sigma-Aldrich, St. Louis, USA), according to the manufacturer's instructions, measured in a 96 well plate (CELLSTAR, Greiner Bio-One, Kremsmünster, Austria) using a VERSAmax microplate reader (Molecular Devices, San Jose, CA, USA) with the corresponding software SoftMax Pro 4.8.

For the urease assay, the protein concentrations of the different samples were adjusted to the same level. The assay was performed with the help of the Urease Activity Assay Kit (Sigma-Aldrich, St. Louis, USA) according to the instructions. The samples were incubated with urea for one hour at 37°C. Triplicates were used for every measurement.

Mycelium attachment assay

For determining the ability of certain strains to attach to hydrophobic surfaces, an attachment assay according to de Jong et al. (2009) was conducted. The strains were cultured in a polystyrene 24 well plate (Greiner Bio-One, Kremsmünster, Austria) in 2 ml modified liquid NMMP medium per well, where PEG 600 and amino acids were omitted. As carbon sources glucose, mannitol or a combination of glucose and casaminoacids were provided (24 mM final concentration). Each strain was incubated in duplicate with every carbon source. The plate was cultivated as static culture at room temperature for 10 days.

After incubation, one well per duplicate was used for determining the total biomass produced, while in the other the attached fraction of the biomass was measured.

For determining the former, the complete biomass was removed from the wells into one reaction tube per sample. Then, 100 µl 0.5 % crystal violet was added and incubated for 30 min. After centrifugation for 10 min at 4°C (14 000 rpm) the liquid phase was discarded and the biomass was washed three times with tap water. For dissolving the crystal violet from the biomass, 1.5 ml 10 % SDS was added

to each tube and the samples were incubated on a shaker for 30 min. The OD_{570} of the resulting suspension was measured in 200 µl triplicates in a 96 well plate using a VERSAmax microplate reader with the corresponding software SoftMax Pro 4.8.
The attached biomass was determined by adding 100 µl 0.5 % crystal violet directly to the wells, incubating this solution for 10 min. The liquid and floating biomass were subsequently removed and discarded. After three times washing with tap water, whereby loose biomass and remaining crystal violet was removed, the plate was dried at 50°C for 45 min. Afterwards, 1.5 ml 10 % SDS was added to each well and the plate was shaken for 30 min. The OD_{570} of the resulting solution was measured as before.

Determination of biomass metal content
Bacterial strains were cultivated in liquid GYM medium with and without heavy metal amendment, as indicated, in baffled flasks at 28°C shaking with three biological replicates per strain and treatment. After incubation, the biomass was washed twice with *A. dest* and dried at 40°C before grinding. For analysis, heavy metals in the ground biomass were dissolved by microwave digestion using the Mars Xpress-System (CEM, Kamp-Lintfort, Germany) and subsequently measured by ICP-MS using a quadrupole-ICP-MS-spectrometer XSeries II (Thermo Scientific, Bremen, Germany) in three technical replicates. The hydrochemical analysis was conducted in the hydrochemical laboratory of the Applied Geology in the Institute of Geology, Friedrich-Schiller University, Jena (Germany). Raw data of the analysis can be found in the electronic Supplementary Material (eS8).

Interspecies plasmid transfer between *Streptomyces* sp.

Plasmid transfer from *S. mirabilis* P16B-1 to *S. lividans* TK24 was tested on plates and in sterile soil microcosms. In order to trace plasmid transfer, the large *S. mirabilis* plasmid was beforehand labelled by *in vivo* gene replacement with an apramycin resistance gene. Details of this procedure are given in section 3.2.
For plate matings spores of both strains were resuspended in 0.9 % saline solution and plated on CSA or MS agar containing 10 mM $MgCl_2$. After 7 d incubation the plates were overlayed with soft agar (12,5 g/l nutrient broth, 7 g/l agar), amended with 25 µg/ml apramycin and 12 µg/ml chloramphenicol for selection of successful transfer, as *S. lividans* is chloramphenicol resistant, while *S. mirabilis* is sensitive to this antibiotic. After four further days of incubation, arising colonies were isolated on CSA agar containing again both antibiotics. Plasmid transfer was confirmed by PCR with primers for the apramycin resistance gene (ApraF & ApraR) and by Southern Blotting.
Soil samples for sterile soil microcosms were taken in the Paradiespark, Jena (Germany), dried at 60°C and sieved (2 mm grain size). 17 g of soil were weight into 50 ml conical centrifuge tubes (Greiner Bio-One, Kremsmünster, Austria) and autoclaved. Subsequently, humidity was adjusted with sterile *A. dest* to 80 % and the microcosms were inoculated with 1 ml of a spore suspension, as before, in three replicates. The microcosms were incubated at 28°C in the dark. Re-isolation was carried out after six days by removing the upper 0.5 cm soil layer and resuspending it in 2 ml saline solution. For transconjugant selection, a dilution series of this suspension was plated on CSA agar containing chloramphenicol and apramycin, as before.

E. coli (over-)expression assays

For expression of *Streptomyces* sp. genes in *E. coli*, either pTrc99A or pSEThph were used as vectors (Table 1), as indicated. The assays were conducted in 96 well cell culture plates (CELLSTAR, Greiner Bio-One, Kremsmünster, Austria) in a total volume of 200 µl per well. As growth medium LB, LBK, M9 or M63 medium was used as it is indicated in the relevant sections, amended with the appropriate antibiotics. Cultures of the *E. coli* strains were adjusted to OD_{595} = 0.15 and 30 µl of this inoculum was added per well. When using pTrc99A and its derivatives 1.5 mM IPGT was added. Growth was monitored at A_{595} every hour for 24 h using a VERSAmax microplate reader (Molecular Devices, San Jose, CA, USA) with the corresponding software SoftMax Pro 4.8. The incubation temperature was set to 37 °C. Raw data can be found in the electronic Supplementary Material (eS7).

Microscopy

Biominerals and bacterial colonies were examined under a Stemi 2000-C stereo microscope (Carl Zeiss Microscopy GmbH, Jena, Germany) and pictures were taken with an Insight Spot Firewire 4 mega sample camera (model 14.2 color mosaic; Diagnostic Instruments Inc., Sterling Heights Michigan, USA).

For bright field and fluorescence microscopy an Axioplan 2 microscope with the Axiophot 2 Photo module (Carl Zeiss Microscopy GmbH, Jena, Germany) was used in connection with an Insight Spot Firewire 4 image sample camera (model 14.0 monochrome w/o IR Filter; Diagnostic Instruments Inc., Sterling Heights Michigan, USA).

The digitalization and processing of the pictures was carried out using Spot Software 5.1 and Spot Advanced Software 4.6 (Diagnostic Instruments Inc., Sterling Heights Michigan, USA).

3. Results

3.1 Molecular genetic tools for transformation of *Streptomyces* sp.

Introduction

Genetic modification of bacteria is a useful tool for several purposes. For one, gene functions can be studied in detail by targeted gene deletion or heterologous expression in order to understand the molecular basis of biological processes, but furthermore genetic modifications are of value for industrial applications, e.g. when synthesis gene clusters from a slowly growing organism are introduced in an easily cultivatable host for increasing the efficiency and yield of compound production (Comba et al., 2014).

The most commonly used host for gene cloning is *Escherichia coli*, as it is fast growing, easy to handle and readily transformable. In contrast to this Gram-negative organism, the transformation of Gram-positive bacteria is more difficult, mostly due to their different cell wall structure.

Being Gram-positives, the introduction of genetic material in *Streptomyces* sp. is not as easily realisable, but there are several methods available. The most commonly applied methods are conjugation, electrotransformation and polyethylene glycol-assisted protopolast transformation (Kieser et al., 2000). The latter method was used in the beginning of molecular manipulation of streptomycetes (Bibb et al., 1978). However, the conditions for formation and regeneration of protoplasts have to be adapted to every strain anew, which makes this method non-practical and often ineffective. A protocol for electroporation of *Streptomyces* sp. mycelium from 24 h-old cultures in a similar way to *E. coli* electrotransformation was established by Pigac & Schrempf (1995). However, this method, too, does not provide a reliable way of transformation.

One major obstacle for the introduction of foreign DNA in *Streptomyces* sp. is the methylation-dependent restriction system found in most *Streptomyces* sp. (MacNeil et al., 1992), which recognizes and degrades deviant DNA fragments. For overcoming this barrier, the application of conjugation is most suitable.

Conjugation between *Streptomyces* sp. and *E. coli* was first reported by Mazodier et al. (1989), who constructed *E. coli-Streptomyces* shuttle vectors and found the transfer to simply require an origin of transfer (*oriT*) and RP4 *tra* gene function. By using a nonmethylating *E. coli* strain (MacNeil et al., 1992) the methylation-dependent restriction system of *Streptomyces* sp. is circumvented, since otherwise the methylation patters of the strain of interest would have to be imitated to enable transformation (Flett et al., 1997; Suzuki, 2011). The transformation of *Streptomyces* sp. by conjugation with *E. coli* is by now an established and widely used method that has been employed for different species.

The plasmids for streptomycetes manipulation can be designed and constructed in *E. coli* before the transfer to the designated recipient, which makes the preparations convenient.

However, this method has its limitations and drawbacks as well. Interspecific conjugation depends on different parameters which have to be carefully chosen. There are several studies on the optimization of media and conjugation conditions for individual strains (Du et al., 2012; Kitani et al., 2000; Netzker et al., 2016; Sun et al., 2014; Wang & Jin, 2014). The composition of the medium used for conjugation has a major influence on the success (Du et al., 2012; Kim et al., 2008a; Sun et al., 2014), and most of

all the concentration of $MgCl_2$ or sometimes $CaCl_2$ has a decisive impact on conjugation frequency (Kim et al., 2008a; Wang & Jin, 2014). The optimization of these parameters can be laborious. Additionally, incubation times during the procedure, the donor-recipient ratio or the type of biomass employed in conjugation (*Streptomyces* sp. spores vs. mycelium) can vary between strains for optimal transfer (Du et al., 2012; Netzker et al., 2016; Sun et al., 2014; Wang & Jin, 2014). In most protocols *Streptomyces* sp. spores serve as recipients and the conjugation is conducted on medium containing 10 mM $MgCl_2$. Why and how the salt additive influences this process is not known, but reported in several studies as being an important factor.

This intergeneric conjugation with *E. coli* as donor can also be applied for other actinobacteria, like *Saccharopolyspora* sp., *Amycolatopsis* sp., *Arthrobacter* sp., *Nocardia* sp., *Micromonospora* sp., *Rhodococcus* sp. (Matsushima et al., 1994; Stegmann et al., 2001; Voeykova et al., 1998) and even for other phyla, e.g. *Pseudomonas* sp. (Bazire & Dufour, 2014).

As the transformation of *Streptomyces* sp. by intergeneric conjugation proved itself a reliable method in several studies and previous attempts of transformation using protoplasts were not successful, the aim of the present study was the establishment of a conjugation protocol for two heavy metal resistant *Streptomyces* sp. strains for enabling subsequent investigations of gene functions by random and targeted gene deletion.

Transposons are naturally mobile genetic elements that are composed of at least a gene for the transposase flanked by inverted repeats as recognition sequences, but may carry additional genes for phenotypic traits. Their more or less specific integration in DNA molecules is catalyzed by the transposase *via* different mechanisms, e.g. a cut and paste mode of Tn5 type transposons (Mahillon & Chandler, 1998). Integration of such an element in an ORF causes the disruption of the latter, whereby genes can be inactivated. This can be put to use for transformation of a strain.

The advantage of this transposon mutagenesis approach is that large random mutant libraries can be created and subsequently screened for a particular phenotypic change of interest. Knowledge about the exact genome sequence of the tested organism is not necessary, wherefore this method is also applicable to less well investigated strains.

As in the beginning of this project, the genome sequences of *S. mirabilis* and *S. acidiscabies* were not available this approached seemed suitable for addressing the question of genomic heavy metal resistance determinants. Random transposon mutagenesis has already been applied for the identification of heavy metal resistance genes in other species, like *Cupriavidus metallidurans* CH34 (Liesegang et al., 1993) or *Serratia marcescens* (Marrero et al., 2007). For *Streptomyces* sp. several transposon mutagenesis systems exist using either endogenous transposons from this genus (Irnich & Cullum, 1993; Weaden & Dyson, 1998) or mobile elements from other organisms (Bilyk et al., 2013; Petzke & Luzhetskyy, 2009). However, random mutagenesis has the crucial drawback that the search for transformants with the wanted phenotypic change can be tedious and might in the end be unsuccessful. Although, by this method new genes with functions connected to a phenotypic change can be detected, which were previously unknown.

A protocol for directed gene deletion in *Streptomyces* sp. has been developed by Gust et al. (2003). The target gene is replaced by a cassette carrying an antibiotic selection marker and an origin of transfer (*oriT*). As basis served the *E. coli* gene disruption assay by Datsenko & Wanner (2000), inwhich genes were deleted *via* recombination by the λ Red recombinase.

A schematic illustration of the procedure is given in Figure 9. The gene is firstly replaced on a cosmid comprising the target gene and at least 2.000 bases up- and downstream of the target by a PCR-generated resistance cassette. The latter was generated with primers for a resistance cassette located on a plasmid that was used as PCR template. Each primer had 39 bp of genomic sequence up- or downstream the target region attached to their 5' ends. Both, the cosmid and the generated cassette are introduced into *E. coli* BW 25113 that harbours plasmid pIJ790, which provides the λ Red recombination system that can be induced by arabinose addition and enables recombination between the cosmid and the PCR product (Datsenko & Wanner, 2000). The transformed cosmid is then introduced by conjugation as described above into the wildtype strain, where the native gene is replaced by homologous recombination (Gust et al., 2003).

Methodological approaches

Transformation of *Streptomyces* sp. *via* interspecific conjugation

For establishing a conjugation procedure for strains *S. mirabilis* and *S. acidiscabies*, pSET152 (Bierman et al., 1992) was chosen as vector that should be transferred to the streptomycetes, as this plasmid already proved in other studies to be easily transferred at a high frequency (Flett et al., 1997; Kuhstoss et al., 1991; Sun et al., 2014). The vector pSET152 is nonreplicative in *Streptomyces* sp., but carries the integrase gene and *attP* site of the φC31 phage, a *Streptomyces* sp. temperate phage (Bierman et al., 1992). Therefore, this vector can irreversibly integrate at *attB* sites in the *Streptomyces* sp. host chromosome. The φC31 integrase is a serine recombinase that needs no accessory factors for its activity and only requires small *attP* (39 bp) and *attB* (34 bp) sites (Groth et al., 2000). φC31 based vectors give high integration frequencies and are stably inherited (Kuhstoss et al., 1991).

The main integration site is an open reading frame coding for a pirin homologue involved in chromosome condensation (SCO3798 in *S. coelicolor* A3(2)), which is not essential under laboratory conditions. The integration does not influence the phenotype of the transformed strain (Combes et al., 2002; Sioud et al., 2009). However, pSET152 can have additional, secondary integration sites and may also integrate in tandem or persist extrachromosomally (Bilyk & Luzhetskyy, 2014; Combes et al., 2002; Kitani et al., 2000; Luzhetskii et al., 2001; Luzhetskyy et al., 2002; Ostash et al., 2009; Sioud et al., 2009). The transfer of this plasmid from *E. coli* to *Streptomyces* sp. is enabled by the origin of transfer (*oriT*) of the IncP plasmid RK2 on pSET152. The *E. coli* donor has to supply the necessary transfer functions for plasmid mobilization (Bierman et al., 1992).

As plasmid donor in the conjugation the methylation-deficient strain *E. coli* ET12567 (MacNeil et al., 1992) was chosen, which harboured the additional helper plasmid pUZ8002 (Kieser et al., 2000; Paget et al., 1999), that is necessary for plasmid mobilisation by enabling the transfer of *oriT*-carrying plasmids during the conjugation, but cannot be transferred itself.

Regarding the conjugation procedure, the protocol according to Kieser et al. (2000) was followed, as described in section 2. Potential *Streptomyces* sp. transconjugants carrying pSET152 were picked on CSA agar containing apramycin and nalidixic acid. The integration of the vector into their chromosomes was checked by Southern Blot analysis, using the apramycin resistance gene *aac(3)IV* of pSET152 as probe for hybridisation to genomic DNA digested with *Bam*HI, that cut once in the plasmid, in order to avoid exceedingly long DNA fragments that could not be properly separated.

Using the procedure given by Kieser et al. (2000) both strains, *S. mirabilis* and *S. acidiscabies*, could be successfully transformed. Therefore, no further modifications of the basic protocol were required. However, for some transconjugants the Southern Blot revealed multiple integrations of pSET152, as exemplified for *S. mirabilis* (Figure 5). Furthermore, in several *S. mirabilis* transconjugants phenotypic changes were detected regarding pigment production and heavy metal resistance. Some transconjugants lost the ability to form pigments and/ or became nickel sensitive, not tolerating 10 mM $NiSO_4$ on minimal medium, which was a significant reduction compared to the WT, which tolerated up to 130 mM.

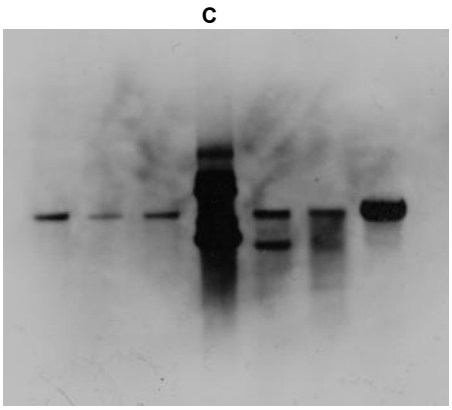

Figure 5. Southern Blot of *Bam*HI-digested DNA from six *S. mirabilis* P16 pSET152 transformants. The hybridisation probe targeted *aac(3)IV* encoded on pSET152. As control (C) the intact pSET152 plasmid was used.

This reduction in heavy metal resistance could either have resulted from the integration of the plasmid in a site that encoded a determinant connected to heavy metal resistance, or from secondary effects caused by the conjugation procedure itself, e.g. chromosome deletions or the loss of an endogenous plasmid. Despite several attempts using rescue plasmid generation, the location of the secondary integration site could not be determined.

When these experiments were conducted, the genome sequences of the tested strains were not available. However, after obtaining the genome sequence, several predictions could be made retrospectively using an *in silico* approach.

In studies of Combes et al. (2002) and Bilyk & Luzhetskyy (2014) the primary and secondary integration sites, termed pseudo-*attB*, of pSET152 were determined. Natural variations have been observed also for the primary *attB* site. The following primary integration site consensus sequence for several *Streptomyces* species can be inferred (Combes et al., 2002):

CGGTG(CG)GGGTGCCAGGG(CGA)GT(GT)CCCTT(GC)GGCTCNCC(GCT)G(GC)(GC)(GT)(GC)(GA)TA(GC)TCCACC.

S. mirabilis and *S. acidiscabies* each exhibited a single site matching this sequence, which was located on the genomes in ORFs encoding a pirin homologue (SMI3655 and E13_03935), in accordance with the primary integration site found in other species, as stated above. This integration site likely corresponded to the band in the Southern Blot (Figure 5) present in all transformants.

Regarding pseudo-*attB* sites, the consensus sequence as determined by Bilyk & Luzhetskyy (2014) was:

(GA)(GAT)(GA)(GT)(ATG)(GC)(CT)(AC)(GC)GGNG(AT)N(CAG)C(CGT)T(ATC)(CGT)(GA)(GTC)(CG)(AT)C(CGT)CC(GC).

In case of *S. mirabilis*, merely one site matched this consensus sequence, which was identical to the primary *attB* site. However, in *S. acidiscabies* a second matching site was detected on the chromosome, which was located within ORF E13_04194, encoding a putative dihydropteroate synthase. It was assumed, that this would be a preferred secondary integration site for pSET152.

Shaded in gray in the above sequence is the most conserved part of the consensus sequence (Bilyk & Luzhetskyy, 2014). When the *in silico* search was repeated using only this part of the consensus, several other putative integration sites were detected in both strains. In *S. mirabilis*, 13 sites were located on the chromosome and one on the large plasmid, while for *S. acidiscabies* ten additional matches on

the chromosome were identified. Hence, it was assumed that pSET152 could indeed integrate in other genomic locations, besides the usual primary *attB* site. Since the integration in these secondary sites is usually less efficient, they might not all be detected in the Southern Blot. Thus, it could not be excluded that pSET152 indeed integrated in several sites in the chromosomes of both strains, as Southern Blot analysis suggested for three transformants which displayed more than one band (Figure 5).

Random transposon mutagenesis

In a first approach, a Tn5 type transposon was used, delivered on plasmid pTNM (Petzke & Luzhetskyy, 2009). This plasmid harboured a gene for hygromycin resistance (*hph*), an origin of replication for replication in *E. coli* (*oripMB1*) and the temperature sensitive replicon pSG5 *rep*, which is inactive at temperatures above 34°C (Figure 3). The latter was needed for eliminating the plasmid backbone after the transposon jumped into the genome. The gene coding a synthetic hyperactive transposase (*tnp(a)*) was controlled by a thiostrepton inducible promoter (*tipAp*) and adapted for *Streptomyces* sp. codon usage. The plasmid pTNM was delivered by conjugation to the streptomycetes yielding two *S. mirabilis* and one *S. acidiscabies* transformants carrying the plasmid (Table 5). After transposition, the potential transformants had to be screened for transposon integration, loss of the delivery plasmid and heavy metal sensitivity, which was the phenotypic change of interest. Therefore, colonies were picked in parallel on CSA agar containing apramycin, CSA agar containing hygromycin and AM medium containing 10 mM $NiSO_4$. Potential heavy metal sensitive transposon transformants were subjected to Southern Blot analysis for confirming transposon integration as well as diversity of integration sites.

However, Southern Blot analysis revealed an identical integration site of the transposon for each transformant originating from one of the pTNM transformants (Figure 6). In *S. mirabilis* transformants, the transposon integrated in potential ORFs coding either a TetR family transcription regulator or an ECF family sigma factor. For *S. acidiscabies*, a single chromosomal integration site was determined in a phosphatase-coding ORF (Table 5).

These identical integration sites in the transformants lead to the conclusion that the transposition had been initiated in an early step of the streptomycete transformation process, probably after introduction of pTNM into the cells, wherefore every transconjugant already had the transposon integrated into the genome and the further procedure, e.g. addition of thiostrepton, had no influence anymore. This problem of early transposon jumping has already been observed by Bilyk et al. (2013) and Tina Netzker (personal communication). Bilyk et al. (2013) assigned this phenomenon to a lack of tight regulation of the expression of the transposase gene, which could be avoided by using a suicide vector for Tn delivery.

Therefore, another transposon and delivery plasmid were chosen. The second system utilized a *mariner* family transposon called *Himar1*, which was originally isolated from horn fly, but shows no host specificity or requirement of host-specific factors (Lampe et al., 1996).

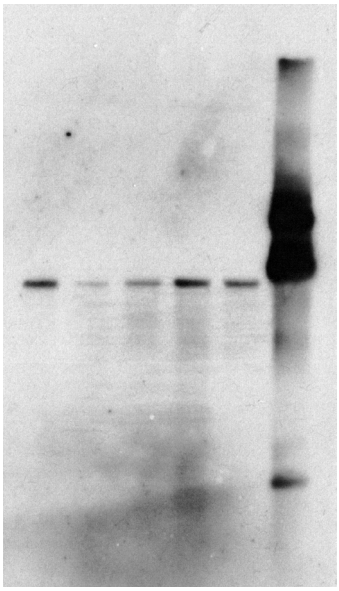

Figure 6. Southern Blot of five individual *S. mirabilis* transposon mutants (lanes 1-5) transformed with pTNM and plasmid pTNM (lane 6) as control. Labelled *aac(3)IV* was used as probe.

Table 5. Overview over transformants of *S. mirabilis* (P16) and *S. acidiscabies* (E13) generated by transposon mutagenesis using either Tn5-based pTNM or *Himar1*-carrying pHTM. Insertion sites [bp] were determined by plasmid rescue and ORFs subsequently analysed by BLAST search. Genomic location indicates site of transposon integration in nucleotides. ORFs which were not predicted in the annotations are indicated as "n.a.".

Strain	Tn-delivering plasmid	Trans-formant	Genomic location	Annotation number	Putative ORF
P16	pTNM	4	4 570 347	SMI4095	TetR-family transcriptional regulator
	pTNM	11	6 250 279	SMI5555	ECF-subfamily sigma factor
	pHTM	489_3	3 774 742	SMI3349	Na^+/H^+ antiporter
	pHTM	3_FK1	4 756 395	SMI4265	Lipoprotein
	pHTM	489_1	4 915 971	SMI4407	Phosphinothricin N-acetyltransferase
	pHTM	4_2	5 176 277	n.a.	Hypothetical protein
	pHTM	339_1	5 442 897	SMI4854	Glycosyl transferase
E13	pTNM	SK	664 817	E13_00584	Phosphoserine phosphatase
	pHTM	89_1	54 810*	E13_08014	Hydrolase

* Integration site was located on the host plasmid

Transposon delivery, initiation of transposition and selection of potential heavy metal sensitive transformants was conducted as before. In the Southern Blot analysis (Figure 7), transformants showed different integration sites, which were confirmed by plasmid rescue. Therefore, the pHTM plasmid and *Himar1* were better suited for the transformation of the tested *Streptomyces* strains.

Identity and characteristics of insertion sites

Using this method, several heavy metal sensitive transformants were obtained for *S. mirabilis* that exhibited integration sites in five different chromosomal loci, coding a transporter (Na^+/H^+ antiporter), two cell wall connected proteins (lipoprotein, glycosyl transferase), an antibiotic resistance enzyme (PPT N-acetyltransferase) and a protein of unknown function (Table 5). In contrast to *S. mirabilis*, in the single heavy metal sensitive *S. acidiscabies* transformant the *Himar1* transposon was found to be integrated on the host plasmid in an ORF encoding a hydrolase. As these transformants showed no growth on Ni^{2+} amended AM agar, these genes were considered suitable targets for further investigations.

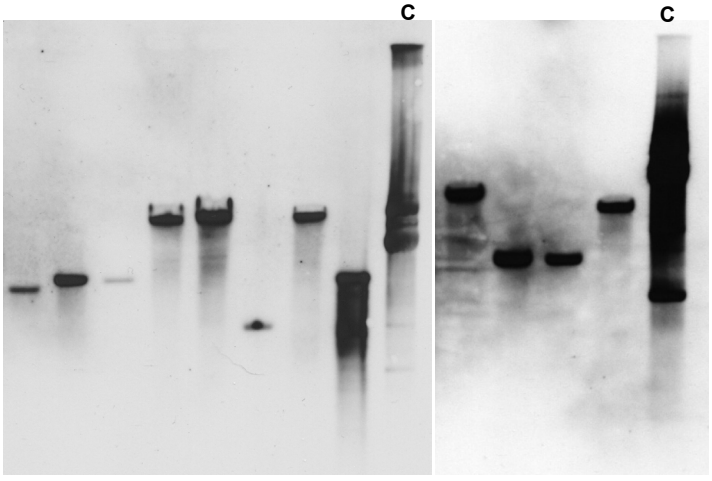

Figure 7. Southern Blot of individual *S. mirabilis* derivatives transformed by transposon mutagenesis using pHTM. The hybridisation probe targeted *aac(3)IV* encoded on the *Himar1* transposon. The original plasmid served as positive control (C). Left: *Kpn*I-digested DNA of eight transformants; right: *Apa*LI-digested DNA of four transformants.

The degree of preferences of transposons to integrate in a specific DNA sequence varies between different families. The two transposons utilized in this study should exhibit a low specificity (Lampe et al., 1998; Petzke & Luzhetskyy, 2009).

Analysis of the insertion sites of the Tn5 based transposon delivered by pTNM revealed the typical duplication of the five nucleotide target site sequence (Table 6) observed in all transposons of this type. The preference for integration in G/C pairs (Green et al., 2012; Lodge et al., 1988) can also be observed in these transformants, as they showed G/C pairs at both ends of the target duplication, which is a typical feature of Tn5 integration hotspots (Lodge et al., 1988). No other site specificities could be inferred, as there were only three Tn5-transposon transformants. It was hypothesized that DNA topology might additionally affect transposition (Lodge et al., 1988). However, Petzke & Luzhetskyy (2009) could not detect site preferences for integration of Tn5 in streptomycetes DNA, while Herron et al. (2004) reported a slight bias for sequences with a high GC content, which should not influence the transposition in *Streptomyces* sp. to a great extend, as their DNA is naturally GC rich.

Himar1 transposons only require a TA dinucleotide for integration and show a slight preference for TA-rich, as well as bent or bendable sequences (Lampe et al., 1996; Lampe et al., 1998; Le Breton et al., 2006; Maier et al., 2006; Rubin et al., 1999). Here, the insertion of *Himar1* occurred in all cases in TA nucleotides and was always accompanied by the duplication of this dinucleotide (Table 6), which is characteristic for *mariner* family transposons (Coates et al., 1998; Lampe et al., 1998; Le Breton et al., 2006). In five out of six cases the third position upstream of this dinucleotide was occupied by a T or A base. A comparable preference for *Himar1* to integrate in TA sites with T and A in 3rd position up- and downstream has been observed by Lampe et al. (1998), although the significance seemed to be low.

Despite the difficulties encountered using the Tn5 type transposon, it can be concluded that both transposons were applicable for the transformation of *Streptomyces* sp. strains and that the parallel usage of different transposon systems might help minimizing biases caused by integration site preferences. Establishing this system could not only offer the opportunity to inactivate genes randomly, but also contrarily to enhance the expression of genes, when the transposons are equipped with strong, outward-directed promoters, as shown by Horbal et al. (2013) for *S. globisporus*. Thus, for future studies the tested transposon systems can be of use for a variety of questions.

Table 6. Insertion sites of transposons in the genome of *S. mirabilis* P16 and *S. acidiscabies* E13 resulting from transposon mutagenesis approaches using the Tn5 type transposon or *Himar1*. Bold letters indicate characteristic duplications generated during integration flanking the insertion site.

Transformant	Insertion tag
P16 4	GGAGCG**GTCCGAAGC** <Tn5> **GTCCGAAGC**CGCGCT
P16 11	GGGGCT**GCGGTGTAC** <Tn5> **GCGGTGTAC**CTCGGC
E13 SK	CGCGGA**GGTCCTGGC** <Tn5> **GGTCCTGGC**CCACGA
P16 339_1	CCGGGGTG**TA** <*Himar1*> **TA**GACCGAGC
P16 3_FK1	GGTCCTCG**TA**<*Himar1*> **TA**GCGCCAGC
P16 4_2	TCGCCACC**TA**<*Himar1*> **TA**CGCCGAAC
P16 489_1	GGGCGAGG**TA** <*Himar1*> **TA**GATGGTGA
P16 489_3	GTACCACC**TA** <*Himar1*> **TA**CGGATGGC
E13 89_1	CAAGGTCG**TA** <*Himar1*> **TA**CAGGCGCC

PCR-targeted gene replacement

As in the course of this project the genome sequences of the test strains became available, the random mutagenesis approach was discontinued in favour of a directed knock out of genes that were beforehand identified as potential heavy metal determinants. Additionally, the role of the genes identified as potentially involved in metal resistance by the former approach should be confirmed by a clean deletion.

A PCR-targeted gene replacement method according to Gust et al. (2003) was established (Figure 9). This system was chosen for deleting potential heavy metal resistance genes in *S. acidiscabies* and *S. mirabilis*, as it has been successfully applied in many different *Streptomyces* sp. strains in other studies, e.g. for genes involved in the production of secondary metabolites like geosmine, cell division and development (*fts*KSC and *chp*) and metal homeostasis like the Cu(I) chaperone ScoC (Beites et al., 2011; Claessen et al., 2003; Fujimoto et al., 2012; Gust et al., 2003; Song et al., 2008; Thoma et al., 2016; Wang et al., 2007; Zuo et al., 2012).

One prerequisite for using this method was the availability of a cosmid that comprised the target gene as well as the adjacent genomic region. For well-investigated strains, like *S. coelicolor* A3(2), for which this method has been developed, cosmids are readily available. When working with molecularly less well characterised strains, like in the present study, cosmids have to be constructed beforehand for each target gene individually. This problem had been addressed by Netzker et al. (2016) who constructed the plasmid pKOSi that can be used as cosmid backbone.

All in all 24 genomic loci were chosen as promising targets (Table 7), three of which were promoter regions, while the rest coded putative membrane transporters, regulatory genes or proteins of unknown function. They were found suitable candidates potentially involved in metal resistance, stress response or metal homeostasis. Nine of these target genes were chosen, because they had previously been found to be disrupted in transposon mutants (Table 5) that exhibited reduced nickel resistance. Genes coding Ni superoxide dismutase (NiSOD) were chosen, since SodN was hypothesized to play an important role in metal resistance in these strains (Schmidt et al., 2007), as it is the case in other bacteria (Geslin et al., 2001). The remaining targets were determined by *in silico* analysis when searching for genes homologous to known heavy metal resistance determinants. Deletion of *tipA* genes and their promoters was conducted upon request of Thomas Kraußе who will characterise these transformants, wherefore they were not further investigated in the present study.

The *p(II)-ko* target has not been a direct choice, but a fortunate coincidence due to mispriming during PCR for cosmid construction, whereby a cosmid for this gene was generated and subsequently used for labelling of the large *S. mirabilis* plasmid. This will be explained in detail in section 3.2.

In the following chapters, most of these deletion mutants will be characterised and discussed in detail. However, a detailed study of all transformants would have exceeded the scope and workableness of this study. Transformants, which did not display a distinct phenotypic change (Δ*Phos*, Δ*tetR*, Δ*Lipo*, Δ*PutProt*) had to be neglected for the sake of the other target genes. Despite several attempt, three of the target genes could not be

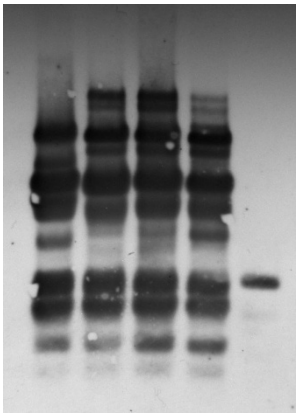

Figure 8. Southern Blot of *S. mirabilis* transformants generated in course of *P16sodN* deletion approach. WT DNA was used as control in the last lane.

deleted: *phox* of *S. mirabilis* and the *sodN* genes of both strains. For the latter, no clean knock-out transformant could be obtained, as the native gene was detected by Southern Blotting in the transformants even after several rounds of selection for the apramycin resistance (Figure 8).

Dupont et al. (2012) faced a similar problem, when trying to delete the Ni^{2+} transporter gene *sodT* and the NiSOD gene in *Synechococcus* sp. A knock-out could only be achieved by substituting either gene by the FeSOD-coding *sodB* gene. The authors attributed this to the essential role of these genes in the metal homeostasis of *Synechococcus* sp. A similar reason could be assumed for the failure in *sodN* deletion in the two *Streptomyces* sp. strains. Therefore, for further attempts, a new resistance cassette should be created that carries not only the resistance marker, but also a copy of the second *Streptomyces* sp. *sod* gene coding the iron-containing FeSOD (Schmidt et al., 2007).

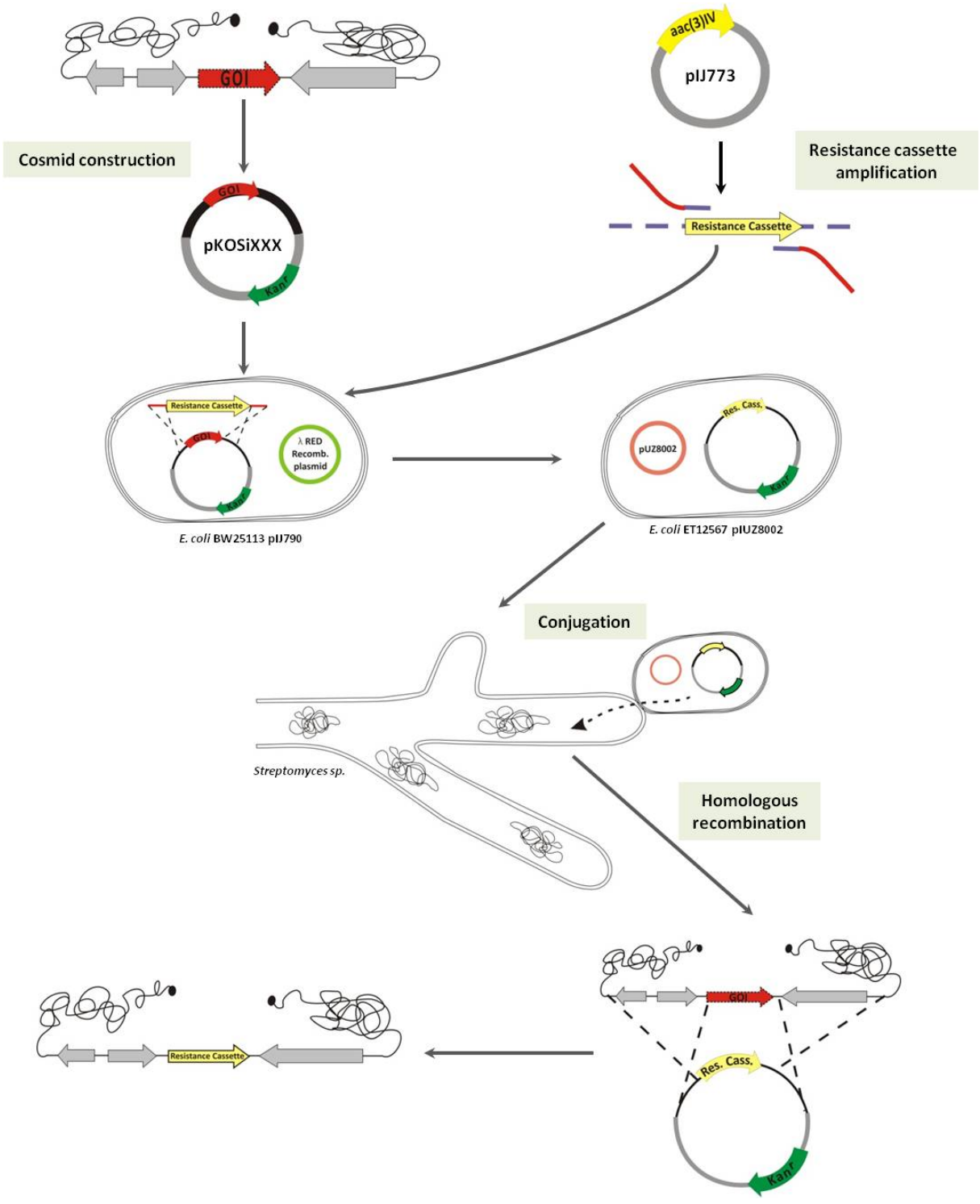

Figure 9. Schematic illustration of the knock-out procedure according to Gust et al. (2003).

The clean knock-out transformants were tested for their Ni^{2+} resistance, in order to confirm the results of the transposon mutagenesis. However, except for the *S. acidiscabies* E13 Δ*yjjG* strain none of the transformants with deletion of a target gene determined by transposon mutagenesis beforehand showed a reduction in heavy metal resistance. Therefore, the increased nickel sensitivity of the transposon mutant strains had to be caused by another factor.

One result of the genome sequencing of *S. mirabilis* and *S. acidiscabies* was the detection of two and one endogenous plasmids in the strains, respectively. *S. mirabilis* harboured two large linear molecules with a size of about 264 kb (pI) and 531 kb (pII), while the plasmid of *S. acidiscabies* had a size of about 112 kb (T. Kraußе, unpublished).

It had been hypothesized for *S. mirabilis* that an endogenous plasmid could be involved in the strain's exceptionally high heavy metal resistance (Schmidt et al., 2009). Indeed, none of the *S. mirabilis* transposon-transformed strains or the *S. acidiscabies* E13 SK strain showed a hybridization signal in the Southern Blot analysis, meaning that they all lost their native plasmids during the course of transformation. Therefore, it was concluded that the nickel sensitivity could rather be attributed to plasmid loss than integration of the transposon in these transformants. Furthermore, also the phenotypic changes in the pSET152 transformants, that exhibited reduced nickel resistance and/or pigment pro-

Table 7. Target genes for gene deletion experiments using targeted gene replacement. Plasmidal gene locations are listed as "p". ORFs which were not predicted in the annotations are indicated as "n.a.".

Strain	Target gene	Annotation	Presumed protein function
P16	*tetR*	SMI4095	HTH-type transcriptional repressor Bm3R1
	Lipo	SMI4265	Hypothetical protein
	Antip	SMI3349	Sodium/proton antiporter NhaA
	AceTra	SMI4407	Phosphinothricin N-acetyltransferase
	GlyTra	SMI4854	Cellulose synthase catalytic subunit [UDP-forming]
	PutProt	n.a.	Putative protein
	sodN	SMI2335	Superoxide dismutase [Ni] precursor
	tipA	SMI3293	HTH-type transcriptional activator TipA
	P_{tipA}	n.a.	Promoter of *tipA* gene
	SigFak	SMI5555	RNA polymerase sigma factor
	hoxN	SMI1158	High-affinity nickel transport protein
p(II)	*nreB*	SMI8362	H^+ Antiporter protein
	copY	SMI8181	Copper-sensitive operon repressor
	copZ	SMI8182	Zinc/cadmium/mercury/lead-transporting ATPase
	phoxN	SMI8194	High-affinity nickel transport protein
	p(II)-ko	SMI8460	PadR-family transcriptional regulator
p(I)	*melC2*	SMI8665	Tyrosinase
E13	*Phos*	E13_00584	stage II sporulation protein E
	hoxN	E13_00147	High-affinity nickel transport protein
	sodN	E13_05067	Superoxide dismutase [Ni] precursor
	tipA	E13_04179	HTH-type transcriptional activator TipA
	P_{tipA}	n.a.	Promoter of *tipA* gene
	$P_{tipA(alt)}$	n.a.	Alternative promoter of tipA gene
p	*yjjG*	E13_08014	Pyrimidine 5'-nucleotidase YjjG

duction, could then be explained by plasmid loss. Production of melanin-like pigments would be dependent on the activity of a tyrosinase encoded on the small *S. mirabilis* plasmid (pI), as concluded from the gene annotation.

However, curing strains from their plasmids could help distinguishing phenotypic traits that were imparted by the plasmids from chromosomal ones. Therefore, one of the cured *S. mirabilis* strains (489_3) was utilized in the further course of this study as plasmid-free *S. mirabilis* derivative, a reference strain for comparison with the wildtype and other transformants.

Complementation and overexpression

For confirming the function of a gene it is desirable to not only knock the gene out *in vivo*, but also to re-establish wildtype phenotypic traits, by re-introducing the deleted gene back into a deletion transformant. This complementation requires a suitable vector, in which the gene of interest can be cloned and transferred. In the present study, pSET152 was chosen as vector, as it proofed to be easily transferred to the *Streptomyces* strains and stably integrate into the genome in the previous experiments. Furthermore, this vector has already been applied for complementation and heterologous gene expression in *Streptomyces* strains by other studies (Beites et al., 2011; Malcolmson et al., 2013; McKenzie et al., 2010; Park et al., 2009), as well as in other genera (Ha et al., 2008; Li et al., 2003; Stinchi et al., 2003). The frequency and stability of pSET152 derivative integration remains specific even if they carry long DNA fragments (Ostash et al., 2009). Thus, vector pSEThph was created which carried an additional hygromycin resistance gene for enabling selection of complemented transformants.

For gene complementation, genome fragments carrying the gene of interest including the putative promoter site were cloned into the multiple cloning site of pSEThph and transferred by conjugation to the deletion strain, as described above. As pSET152 and its derivative did not possess a promoter that controlled the expression of the inserted genes, these were under control of their native promoters, which were included in the gene fragments introduced into these vectors.

However, for study of gene functions it can be of advantage to have the gene of interest under control of a known promoter for ensuring gene expression. If transcription from this promoter is initiated at high frequency, it is suitable for overexpression of the target protein. In the present study, the *E. coli-Streptomyces* sp. shuttle vector pUWL201 (Doumith et al., 2000) was used for overexpression of some of the target genes in *S. lividans* TK24. In contrast to pSET152 it did not integrate into the host chromosome. pUWL201 carried the *tsr* gene for thiostrepton resistance for selection in *Streptomyces* sp. and an ampicillin resistance gene (*bla*) for selection in *E. coli*. As in the other vectors used in this study, origins of replications in *E. coli* (ColEI) and *Streptomyces* sp. (pIJ101*ori*) enable maintenance of the vector in both generas (Wehmeier, 1995). The strong, constitutive promoter *ermEp** upstream of a multiple cloning site was the upregulated variant of *ermEp* of *Saccharopolyspora erythraea* (Bibb et al., 1985) and allowed permanent expression of a gene insert, additionally controlled by the transcription terminator from phage fd (*ter*) (Wehmeier, 1995).

Proof of concept: P16NhaA1 – the putative Na^+/H^+ antiporter of *S. mirabilis*

The genetic tools described above were used for the investigation of several *Streptomyces* sp. genes. In order to exemplify these methods, the procedure shall now be illustrated with an example, namely the putative sodium/proton antiporter coding SMI3349, designated *P16nhaA1*. In this section, exclusively the results of the transformation procedures itself are displayed. The phenotypic characterisation of the strains will be presented in section 3.8.

Directed knock-out of P16nhaA1

Cosmid construction

For the plasmid construction, two sets of primers were designed that would allow the amplification of the target gene region with additional 1200 and 1700 pb of the flanking genomic DNA (Figure 15). The primary PCR yielded several products, one of which had the correct size of 4482 bp (Figure 11 A, lane 3). A secondary (nested) PCR was conducted and the desired 4351 bp product (Figure 11 A, lane 2) carrying the genomic antiporter region was purified and used for cosmid construction. The resulting cosmid, named pKOSiAntipCosm (Figure 11 B) was used for transformation of *E. coli* BW25113 pIJ790, the host for recombination.

Homologous recombination in E. coli

In the next step, the native antiporter gene on pKOSiAntipCosm had to be exchanged by the resistance cassette, which was generated by PCR using plasmid pIJ773 as template. Therefore, *E. coli* BW25113 pIJ790 pKOSiAntipCosm was transformed with the resistance cassette and after incubation a colony PCR was conducted with the grown colonies using *aac(3)IV*-specific primers, as many false-positives can be expected, where the resistance cassette did not integrated into the cosmid. Transformants that yielded a PCR product (Figure 12) were cultured in liquid medium over night and plasmids were isolated. In case of the antiporter gene, the native gene had approximately the same size as the resistance cassette (approx. 1400 bp), wherefore cosmids with resistance cassette integration could not be distinguished from the original cosmid by their size (Figure 11 C). Therefore, the isolated plasmids were used as templates for a PCR with the same primers and conditions used for the colony PCR for confirmation of the recombination event (Figure 13 A). The cosmid, on which the native gene was successfully substituted, was then designated pKOSiAntipCosm-ko.

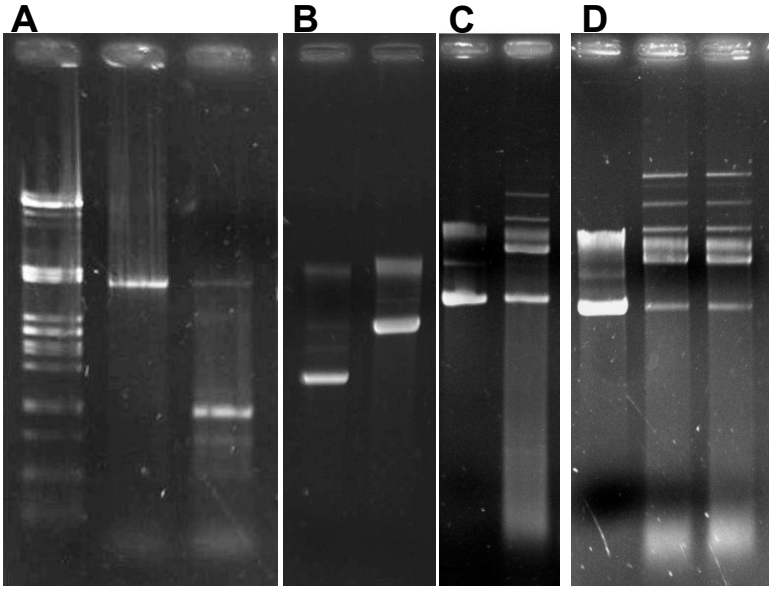

Figure 10. 0.8 % agarose gels depicting steps of cosmid construction for deletion of *P16nhaA1*. A) PCR products of primary PCR (lane 3) and nested PCR (lane 2) and *Pst*I-digested lambda DNA (lane 1); B) empty pKOSi (lane 1) and pKOSIAntipCosm with integrated genomic region of *P16nhaA1*; C) pKOSiAntipCosm (lane 1) and the cosmid after gene replacement in *E. coli* BW25113 (lane 2); D) pKOSi (lane 1) and two cosmid with *P16nhaA1* deletion isolated from *E. coli* ET12567 (lanes 2 and 3).

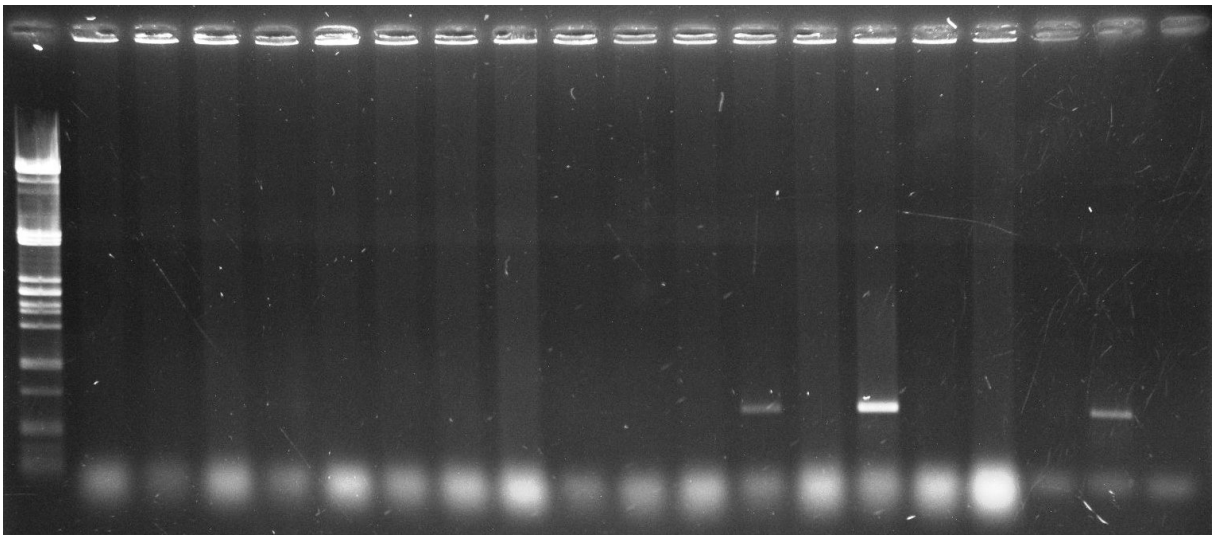

Figure 12. 0.8 % agarose gel of PCR products from *E. coli* colony PCR using *E. coli* BW25113 pKOSiAntip-Cosm after transformation with the resistance cassette for replacement of *P16nhaA1*. Strains in which the native gene was successfully replaced on the cosmid, should exhibit a product of approx. 700 bp. *Pst*I-digested lambda DNA (lane 1) served as ladder and pIJ773 was used as positive control (second to last lane).

Conjugation and isolation of transformants

One of these cosmids was used for the transformation of *E. coli* ET12567 pUZ8002, the strain required for conjugation. From two of the resulting transformants the cosmid was re-isolated for confirmation. Besides pKOSiAntipCosm-ko, also the accessory plasmid pUZ8002, which was necessary for plasmid mobilization, was visible in the subsequent agarose gel (Figure 11 D, three uppermost bands). *E. coli* ET12567 pUZ8002 pKOSiAntipCosm-ko was used for conjugation with *S. mirabilis*.

Putative *S. mirabilis* transformants were picked on selective CSA agar plates. After 5 d incubation, colonies that showed growth were used for colony PCR using a primer, which annealed downstream of the native gene (Antip-ko-ctrR) and a second primer, which annealed to the *aac(3)IV* gene (ApraF). Clean deletion transformants would give a PCR product, while there should be no PCR product if the native gene was still in its place. Four transformants that showed a band in the corresponding agarose gel (Figure 13 B) were chosen and subjected to colony PCR for confirming the presence of the resistance cassette. In the subsequent agarose gel, four transformants showed the expected band (Figure 13 C). Two of them were then subjected to Southern Blot analysis for proving the purity of the deletion transformant and the absence of copies of the native gene.

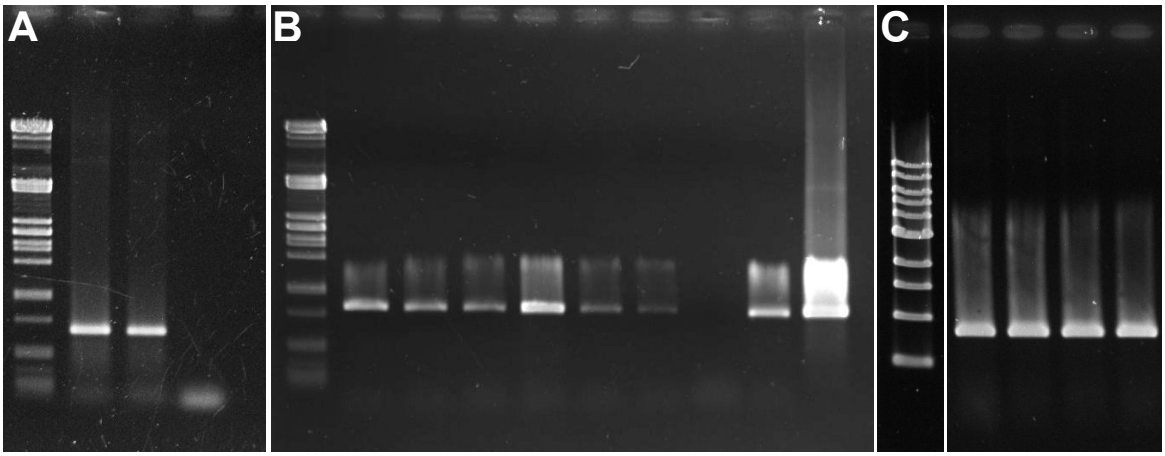

Figure 13. 0.8 % agarose gel of A) PCR with potential pKOSiAntipCosm-ko plasmids (isolated from *E. coli* BW25113) using primers for apramycin resistance cassette; B) *Streptomyces* colony PCR with putative *P16nhaA1* deletion strains and plasmid pKOSiAntipCosm-ko as positive control (last lane); C) control PCR for *P16nhaA1* deletion in P16 using genomic DNA from putative transformants (lanes 2-5) as template. Ladders were *Pst*I-digested lambda DNA (first lane in A and B) or 100 bp DNA ladder (New England Biolabs, Ibswich).

Southern Blotting and hybridization

As probe in the Southern Blot, a 731 bp DNA fragment located 140 to 871 bp upstream the antiporter gene (Figure 15) was used. By choosing a DNA stretch upstream the antiporter gene as hybridization target, band shifts in the Southern Blot allowed the identification of clean knock-outs. The probe labelling efficiency was tested by Dot Blot with a dilution series of unlabeled PCR product as targets (Figure 14 A).

For Southern Blot analysis, transformant DNA was digested with *Pvu*I. This enzyme was chosen, because there was a single cutting site in *P16nhaA1*, but none in the resistance cassette (Figure 15), meaning that transformants, where the antiporter gene was substituted by the resistance cassette would show a hybridization signal at a higher band size than the wildtype.

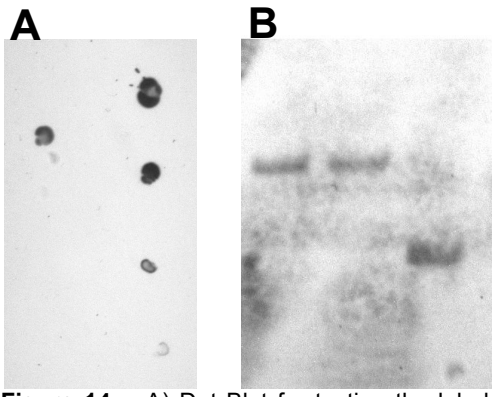

Figure 14. A) Dot Blot for testing the labelling of the probe for testing *P16nhaA1* deletion. A dilution series of non-labeled PR product served as target. B) Southern Blot with two *P16nhaA1* deletion strains (lanes1 and 2) and the WT DNA as control. Longer band size indicated successful replacement of the native gene by the resistance cassette.

Southern Blot analysis (Figure 14 B) revealed that in the two transformants the probe hybridized to a longer DNA band (3695 bp) than in the wildtype (1873 bp), which confirmed the absence of the native antiporter target gene in these *S. mirabilis* transformants. Therefore, they were designated ∆*nhaA1* and could be used for subsequent studies, whose results will be presented in section 3.8.

Complementation with the native gene and E. coli nhaA

pSEThphAntipor and pSEThphEcolnhaA

For confirmation of the function of P16NhaA1, deletion transformants should be complemented by reintroduction of the native gene. This was accomplished using the integrative *E. coli-Streptomyces* sp. shuttle vector pSEThph, a derivative of pSET152 carrying a gene for hygromycin resistance, as described above. The antiporter gene was amplified from pKOSIAntipCosm and used for ligation, yielding pSEThphP16nhaA1. *E. coli* TransforMax was transformed with the ligation mixture and the plasmid was isolated, which was used for transformation of *E. coli* ET12567 pUZ8002 and subsequently for transformation of ∆*nhaA1* by conjugation, yielding strain ∆*nhaA1* hphP16nhaA1.

Besides the native *S. mirabilis* antiporter gene, also *E. coli nhaA* was cloned in pSEThph and transferred to *S. mirabilis*, yielding strain ∆ *nhaA1* hphEcolnhaA.

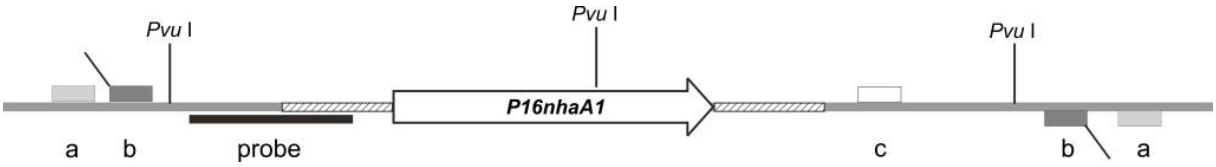

Figure 15. Schematic representation of the *P16nhaA1* genomic region and primer positions, as well as enzyme cutting sites used for digestion and the probe position for Southern Blotting. a and b represent primers for primary and secondary cosmid PCR. c represents position of Antip-ko-ctrR for control of successful recombination between chromosome and resistance cassette. The hatched regions indicate recognition sites for homologous recombination, which were also synthesized to the 5' ends of primers for the resistance cassette.

Overexpression in S. lividans *and* E. coli

In order to test the effect of P16NhaA1 in a heterologous *Streptomyces* sp. host, the coding gene was cloned in the *Streptomyces* sp. overexpression vector pUWL201. The plasmid was then purified and used for transformation of *E. coli* ET12567 pUZ8002, which served as donor in a conjugation with *S. lividans* TK24, as described before, with the exception that in this case, thiostrepton was used for selection of *S. lividans* transformants, as the vector carried the *tsr* gene for resistance to this antibiotic.

For overexpression of *P16nhaA1* as well as a second *S. mirabilis* gene coding a putative NhaA transporter (*P16nhaA2*) in *E. coli* both were cloned separately in the *E. coli* overexpression vector pTrc99A. Both plasmids carrying one of the antiporter genes, as well as the empty vector pTrc99A, were introduced in the *nhaAB* deficient strain *E. coli* KNabc for further investigation.

Conclusion

The *Streptomyces* sp. transformation methods presented in this section provided the basis for all following investigations in this study. It was important to firstly establish a system for introducing plasmids in the strains of interest, which was achieved by interspecies conjugation with *E. coli*, which proved to be an easy and reliable method for both strains. Subsequently, random and directed mutagenesis could be applied for gene deletion and other modifications.

The introduction of vectors basing on an *attB/attP* system was a convenient method of genetic manipulation, since even large constructs like cosmids with a size over 35 kb can be integrated into the genome of a strain by this system (Bilyk & Luzhetskyy, 2014). Therefore, the described methods for transformation of *Streptomyces* strains would open up the possibility to better understand the genetic mechanisms underlying important traits, like heavy metal resistance.

However, genetic modifications of a strain can have unwanted side-effects, as seen for both strains, that lost their endogenous plasmids due to stress during the conjugation and transposition procedure. Random transposon mutagenesis results should therefore always be confirmed by direct knock-out of the gene of interest for excluding other, unknown factors that interfere with test results, as seen in the here presented transformants.

Another conclusion that could be drawn from the results was that the application of random transposon mutagenesis was problematic, when the tested strain harbours one or more plasmids which potentially code for desired phenotypic traits, as they might get lost during the process.

However, when the transposition was successful, genes can be detected that might otherwise would not have been considered primary targets for heavy metal resistance, like the hydrolase-coding gene of *S. acidiscabies*, which seemed to be involved in nickel resistance and will be investigated in detail in section 3.5. Transposon mutagenesis also proved in other studies a suitable method for detecting genes that have not been recognized yet specifically for their involvement in Ni^{2+} resistance, e.g. in *Serratia marcescens* (Marrero et al., 2007)

Lastly, the presented results substantiated the notion that native plasmids played a major role in the heavy metal resistome of *S. mirabilis* P16B-1 and *S. acidiscabies* E13.

3.2 Transferability of the *S. mirabilis* plasmids and investigation on their impact on phenotypic traits

Introduction

The spread of antibiotic resistance genes to pathogens first drew the spotlight on the importance of horizontal gene transfer between bacteria. Now, this process is recognized as a major driving force for bacterial evolution (Heuer & Smalla, 2007; Ochman et al., 2000) and indicators for the acquisition of genes from foreign genomes were identified in many bacterial chromosomes by remnants of mobile genetic element (MGE) sequences (Bordeleau et al., 2012; Ochman et al., 2000). Gene transfer is considered an important mean for competing successfully for survival in an ecological niche within a bacterial community, whereby the adaptability and diversity of bacteria in a habitat is modulated (reviewed by Heuer & Smalla (2007)). Plasmids, phages and transposons can serve as vectors for gene transfer. Their introduction into new hosts cannot only provide beneficial genetic material, e.g. resistance systems (Silver & Misra, 1988), but also change the dynamic of chromosomal evolution, as multiple integration of the same MGE into one genome provides sites for recombination, because of sequence homology.

As stated above, streptomycetes often harbour one or in many cases several plasmids, which are mostly large, linear and transferable with terminal inverted repeats. In *S. rochei*, three linear plasmids were detected (Kinashi et al., 1994), one of which is 113 kb long with 352 bp inverted repeats at the termini and carries genes for self-defence (Yang et al., 2011). Early after the first reports on *Streptomyces* sp. plasmids (Hayakawa et al., 1979; Okanishi et al., 1970), the transferability of these elements to other *Streptomyces* species was reported (Bibb & Hopwood, 1981).

In members of the Actinomycetales a conjugative mechanism that is different from that of other Gram-positive bacteria has evolved (Bordeleau et al., 2012; Grohmann et al., 2003). Furthermore, the transfer mechanisms for linear and circular elements differ (Wang & Pettis, 2010). Whereas the determinants employed by the latter have been well investigated, little is known about the transfer determinants for linear *Streptomyces* sp. plasmids.

The transfer of circular elements only requires a small number of genes, namely a single plasmid-encoded ATPase, TraB, which is homologous to SpoIIIE/FtsK family motor proteins, an integral part of the machinery needed for processing of DNA during bacterial cell division and spore formation (Pettis & Cohen, 1994; Reuther et al., 2006; Vogelmann et al., 2011). TraB is responsible for the translocation of double-stranded circular DNA to the recipient by forming a hexameric ring structure in the lipid bilayer and pumping the plasmid through the so-formed pore. For enabling this process, TraB recognises a specific non-coding plasmid region, termed *clt* (“cis-acting locus of transfer”) that exhibits 8 bp TRS (TraB Recognition Sequence) repeats serving as binding site. These two components, TraB and *clt*, possibly present the minimal module necessary for plasmid transfer in *Streptomyces* sp. (Grohmann et al., 2003; Pettis & Cohen, 1994; 2000; Reuther et al., 2006; Vogelmann et al., 2011).

Once the plasmid has entered the recipient cell, its spreading in the mycelium is ensured by Spd proteins, which are small hydrophobic molecules that form oligomers and interact with TraB (Thoma et al., 2016; Tiffert et al., 2007). The spreading process can be observed by naked eye on agar plates by the formation of growth retardation zones, called pocks (Bibb & Hopwood, 1981).

In *Streptomyces* sp. the genetic variability apparently is particularly high, even within one and the same strain, which can be attributed to the linearity of most *Streptomyces* sp. chromosomes providing a basis for several recombination events. Linear chromosomes and plasmids may circularize accompanied by large chromosomal deletions (Kinashi et al., 1994; Wang & Pettis, 2010; Yang et al., 2011). Furthermore, crossover events between two copies of a chromosome/ plasmid or between plasmids and genome were frequently reported, which is reflected by high homologies between plasmids and chromosomes, providing again sites for follow-up recombinations. Integration of plasmids into the host chromosome can lead to the mobilization of chromosomal genes upon re-excision of the plasmid (Chen et al., 1993a; Huang et al., 2003; Lin et al., 1993; Pandza et al., 1998; Yamasaki & Kinashi, 2004; Yang et al., 2011).

This potential of genetic remodelling in *Streptomyces* sp. is most probably an important factor for the evolution of these bacteria, as it facilitates gene exchange and adaption, allowing *Streptomyces* sp. the survival in the highly diverse soil environment. Accordingly, multiple unrelated conjugative elements were frequently found in actinomycete genomes (Bordeleau et al., 2012).

When looking on the gene flux in nature, transfer from Gram-positive to Gram-negative species occurs extensively, especially with this polarity (Courvalin, 1994) and the transfer of plasmids in soil has been reported repeatedly (De Rore et al., 1994; Ravel et al., 2000; Wellington et al., 1990). Under laboratory conditions, *Streptomyces* sp. plasmids could be transferred to other genera, e.g. *Mycobacterium smegmatis*, *Micromonospora*, *Thermomonospora*, *Saccharopolyspora* and *Amycolatopsis* (Bhatt et al., 2001; Kojic et al., 1991; Marsh & Wellington, 1994). However, since all of these organisms are actinobacteria, the likeliness of transfer is comparably high, but little is known about the transfer to more distantly related species, as there are several restrictions to the genetic exchange: The expression of foreign genes is not always effective or even prevented due to genus- or species-specific barriers. In the case of *Streptomyces* sp., most promoters of Gram-negative as well as Gram-positive bacteria can be recognized by streptomycete RNA polymerases, while in the opposite way it only works in a few cases and with little efficiency (Bibb & Cohen, 1982). Even promiscuous plasmids, e.g. of the incompatibility group IncP-1, have limits to their host range (Heuer et al., 2007). However, the presence of stressors, like antibiotics or metals, can modulate the plasmid transfer frequency and avoid loss of genetic elements within a community (Altimira et al., 2012; Heuer & Smalla, 2007; Sandaa et al., 2001), wherefore a more frequent plasmid transfer can be assumed for heavy metal contaminated habitats.

For the investigated strain *S. mirabilis* P16B-1, the presence of at least one plasmid was demonstrated in a previous study (Schmidt et al., 2009) and the existence of even two large linear elements was proven by genome sequencing (T. Kraußе, unplublished data). A characteristic trait of this strain is the production of a melanin-like pigment, which seems to be less well regulated than in other species, as the strain cannot down-regulate the production during heavy metal treatments for saving costs for the activation of its resistance machinery (Schmidt et al., 2009). This lead to the early hypothesis, that the tyrosinase-coding gene might be located on a plasmid.

The production of melanin-like compound is a common trait in *Streptomyces* sp. (Hintermann et al., 1985; Huber et al., 1985; Ikeda et al., 1996; Schrempf, 1983). The enzyme providing the precursor for the pigment synthesis is a copper-containing monooxygenase, called tyrosinase. It catalyzes the oxidation of tyrosine to dopaquinone, which is then oxidized forming melanin upon polymerization (Endo et al., 2001; Matoba et al., 2006; Riley, 1997). In *Streptomyces* sp. the tyrosinase operon usually

comprises a gene coding a copper chaperone protein (*melC1*), besides the actual tyrosinase gene (*melC2*). Both are required for melanin synthesis at low copper levels (Chen et al., 1993b; Hintermann et al., 1985; Ikeda et al., 1996).

There is a close connection between morphological differentiation and melanogenesis in *Streptomyses* sp. Melanin-negative mutants of *S. griseus* showed a delayed development of aerial mycelium and reduced antibiotic production. The overproduction of tyrosinase in *S. lividans*, on the other hand, accelerated the production of aerial mycelium, proving a stimulatory effect of this enzyme on bacterial development (Endo et al., 2001).

It is commonly assumed that melanin-like compounds have a protective function against several stressors, like UV radiation and heavy metals (García-Rivera & Casadevall, 2001; Saxena et al., 2002). Due to their polymeric structure they potentially can bind heavy metals and might be one metal resistance mean of *S. mirabilis* P16B-1.

Results

Computational prediction of plasmid transfer genes

Several genes are known to participate in the transfer of plasmid DNA to a recipient cell. In actinomycetes, mostly *tra* and *spd* genes are required for conjugational transfer and plasmid maintenance. In order to predict the likeliness of pI and pII of *S. mirabilis* to be transferred to other bacteria, the plasmids and chromosome were screened for genes coding proteins homologous to known transfer proteins. However, there are indicators that the transfer mechanisms employed by circular and linear extrachromosomal molecules differ (Wang & Pettis, 2010). Three main transfer mechanisms have been postulated for *Streptomyces* sp. plasmids up to now: two for circular plasmids and another for linear molecules. The transfer of the latter was hypothesized to be more complex with more genes involved (Wang & Pettis, 2010; Xu et al., 2006). Furthermore, distinctions have to be made between double- and single-stranded DNA transfer.

In contrast to the well-studied transfer determinants for circular plasmids, the mechanisms involved in transfer of linear plasmids are not well understood (Huang et al., 2003). Therefore, both plasmid transfer modes will be considered in this study.

Several annotated ORFs encoding putative transfer machineries were identified by similarity search using BLAST with components of transfer proteins from other *Streptomyces* sp. plasmids as query. However, for some *Streptomyces* sp. plasmids it has been observed, that other conjugative molecules are able to promote the transfer of non-transmissible plasmids (Kataoka et al., 1991). Similar transfer promotion functions could be assumed for chromosomally encoded proteins, wherefore also the *S. mirabilis* chromosome was searched for proteins with a putative transfer function.

On the chromosome, three loci were annotated as coding conjugal transfer proteins: SMI1025 coded a predicted TraG protein of the TraG-D_C family (pfam 12696), while SMI2574 and SMI3341 encoded homologues of the mycobacterial conjugal transfer ATPase MT3759 of the CpaF family. Furthermore, genes for the type IV secretion system for DNA transfer were annotated: VirD4, TraC, VirB4 (SMI4014, SMI4015, SMI4016). The latter genes belonged to a different secretion system than TraB. However, both systems for DNA transfer are known to be utilized by *Streptomyces* sp. (Ghinet et al., 2011).

Merely one predicted protein of the *S. mirabilis* genome showed a significant similarity to genuine TraB proteins of various other species, e.g. to the Tra protein of the *S. lividans* plasmid pIJ101 (P22409.1), namely SMI8630, located on the smaller plasmid pI. This ORF was annotated as coding a septum-associated FtsK-like DNA translocase (pfam01580), which was in agreement with the TraB homology, as it resembled the proteins for chromosome segregation, from which they might have evolved (Vogelmann et al., 2011). TraB mediates the transfer of dsDNA during conjugation (Reuther et al., 2006; Tiffert et al., 2007). However, the *tra* locus appears to exclusively promote transfer of circular DNA (Wang & Pettis, 2010). Therefore it remained questionable whether the gene product of SMI8630 would promote the transfer of the linear pI plasmid or even pII. This locus could be a hint that pI had been a circular molecule that linearised over time with TraB being a remnant of the former employed transfer machinery.

On the large *S. mirabilis* plasmid pII, none of the predicted proteins could be identified as TraB homologues, however three loci encoded proteins which could be part of an operon for a plasmid transfer machinery (Figure 16). SMI8066 showed 54 % similarity to *S. coelicolor* A3(2) SCP1.146, a conjugative protein. Conserved domain search classified the protein as ATP/GTP-binding with an AAA-like domain (pfam12846), which is a feature of several conjugative proteins in this superfamily (cl26287).

The downstream located SMI8063 encoded a predicted conjugative transposon protein TcpC (pfam12642), which is known from the *Clostridium perfringens* conjugation machinery for single-stranded DNA (Goessweiner-Mohr et al., 2014). Lastly, SMI8058 showed 30 % homology to TraR of *Streptomyces* sp. 14R-10 (YP_008998135.1), a GntR-type transcriptional repressor, which controls *tra* gene transcription for preventing uncontrolled expression (Grohmann et al., 2003).

For the linear *S. lividans* plasmid SLP2 it has been shown that the plasmid-encoded helicase TtrA was required for transfer, probably by helping strand displacement during transfer (Huang et al., 2003). On *S. mirabilis* plasmid pII a TtrA homologue was identified (SMI8532) showing 33 % identity to the *S. lividans* protein (AAO61192.1). Like in *S. lividans*, the coding gene was terminally located. Therefore, this putative TtrA protein could constitute a part of the pII transfer machinery.

This analysis showed that, in principle, the *S. mirabilis* plasmids had the necessary genes for transfer. The fact that only one ORF showed a significant similarity to TraB proteins of other *Streptomyces* sp. can be attributed to the existence of six groups of Tra proteins, whose members only share low sequence identity (Bordeleau et al., 2012), which makes the prediction hard. Furthermore, also in the NCBI databases proteins with homology to known TraB proteins were solely annotated as hypothetical proteins, which impeded the assignment of function of homologues in *S. mirabilis*. Therefore, it is likely that additional *tra* genes existed, also on pII. The involvement of chromosomally encoded genes could not be excluded, as it is known that large linear plasmid may also recruit chromosomally encoded proteins for vital functions, like replication (Xu et al., 2006).

Likewise, the *clt* locus, that is required for binding of the plasmid to TraB for transfer remained obscure for the *S. mirabilis* plasmids. A possible reason might be high sequence variability in this locus between plasmids, as every TraB only recognizes its cognate *clt* locus (Thoma & Muth, 2015; Vogelmann et al., 2011). Besides, for linear plasmids it is not known whether the *clt* locus is involved in transfer, as these plasmids possess other unique features.

Plasmids could rely to a certain extend on a conjugal machinery for mobilisation encoded in *trans* (Thoma & Muth, 2012), but genes for spreading functions should be located on the plasmid, as its distribution within the new host has to be ensured.

The best investigated *Streptomyces* sp. proteins with plasmid spreading functions are termed Spd. These hydrophobic proteins, which are often co-transcribed, show no sequence conservation to other proteins and act in a cooperative manner (Grohmann et al., 2003; Kataoka et al., 1991; Servin-Gonzalez et al., 1995; Tiffert et al., 2007). Tiffert et al. (2007) proposed that Spd proteins form a channel in septal cross-walls, with which TraB interacts pumping dsDNA to the neighbouring compartment. The loss of one or more *spd* genes does not necessarily prevent plasmid spreading, as the product can be substituted by remaining Spd proteins (Servin-Gonzalez et al., 1995). In contrast to Tra proteins, the Spd proteins might even be required for linear plasmids, as homologues were found on *S. lividans* SLP2 (Huang et al., 2003).

However, no *spd* genes or corresponding products could be detected in the *S. mirabilis* genomic content. Possibly the sequence variation between Spd proteins was too high in order to find significant similarities. Likewise, the lack of similarity to functionally characterized proteins (Thoma & Muth, 2012) impeded their identification.

The last genetic determinant which should be considered here, determines the maintenance of the plasmids in a new host: terminal proteins (Tpg). They are attached to the end of linear DNA molecules and essential for maintenance and propagation of linear plasmids and chromosomes in *Streptomyces* sp., as they are required for DNA replication (Bao & Cohen, 2001). If the *S. mirabilis* plasmids did not carry genes encoding Tpg proteins, they might still recruit chromosomally encoded proteins, as Tpg were found to be interchangeable even between *Streptomyces* species (Bao & Cohen, 2001; Chen, 1996). However, this would restrict the host range of the *S. mirabilis* plasmids to organisms that possess the coding genes, as in other organisms plasmid replication would be prevented.

The similarity search with known Tpg sequences did not yield a result for the annotated proteins of pI, but on pII SMI8531 showed high similarity to several Tpg proteins. SMI8531 exhibited 88.5 % identity to the terminal protein TpgA1 of *Streptomyces* sp. WAC02707 (WP_125774744.1) and 41.1 % identity to the plasmidal Tpg protein of *S. clavuligerus* ATCC 27064 (EFG04331.1).

Interestingly, this Tpg-coding ORF was located directly upstream the TtrA coding SMI8532, which was a further hint for the involvement of this helicase in plasmid transfer and maintenance.

Considering the results of the *in silico* analysis, particularly pII exhibited many determinants required for plasmid transfer and maintenance in heterologous hosts. Therefore, it was hypothesized that this plasmid could be transferred to other organisms, which was then tested in the following mating experiments.

The fact that for pI not as many transfer and maintenance traits were identified could be explained by the high variability of transfer functions between plasmids, even when they apply the same mechanism (Servin-Gonzalez et al., 1995). Genetic determinants which were found to be important for plasmid transfer in one *Streptomyces* species, can be absent on conjugative plasmids of others (Huang et al., 2003), which complicates the identification of candidate genes.

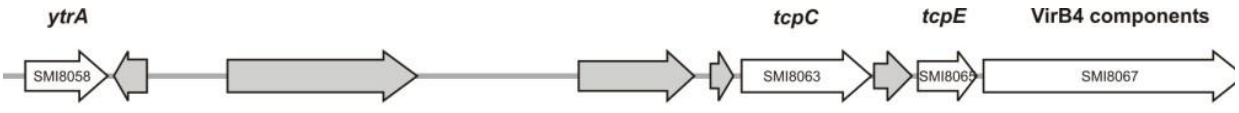

Figure 16. Schematic to scale representation of the *S. mirabilis* plasmid pII section encompassing loci SMI8058 to SMI8067, some of which are encoding putative proteins with plasmid transfer functions. Predicted names of coding sequences are given above, if allocatable. ORFs without deducible function are shaded grey.

Table 8. Primers used for the generation of the resistance cassette in the knock-out of SMI8460 on the large plasmid of *S. mirabilis* (pII). Primer parts complementary to pIJ773 are underlined.

Name	Sequence
K.o.-P16pII-F	GCGTATGGACATCGGTGCGTCATCCTGCCCTGCCGTATGATTCCGGGGATCCGTCGACC
K.o.-P16pII-R	GGACGGTGTGGACCAGCGGTGACCGCAAGCGTGGCCTCATGTAGGCTGGAGCTGCTTC

Plasmid labelling

In order to be able to detect the transfer of the large *S. mirabilis* plasmid (pII) to a recipient, the plasmid had to be labelled with a selectable marker. This was achieved by substituting a gene on the plasmid with an apramycin resistance cassette by PCR-targeted gene replacement used for creating deletion strains. As betokened in section 3.1 the choice of gene was not deliberate, but due to erroneous priming in a PCR, whereby a fragment of the plasmid was amplified instead of the intended target. The primer pair used in this PCR (sodNconF: TTGGTATCATGATGGGACTCGCCTTCCATCTC, sodNconR: TTGGTATCATGAAGTTGAAGATCGTGTCGGGC) was originally designed for the amplification of a *S. mirabilis* genomic DNA fragment comprising *sodN* for subsequent cosmid construction. PCR was conducted using Phusion polymerase with GC buffer and addition of 8 % DMSO with *S. mirabilis* genomic DNA as template. The PCR program comprised two parts: first, initial denaturation for 5 min at 95°C, followed by 10 cycles of 95°C 30 s, 40°C 15 s and 2 min 72°C with subsequent 25 cycles, where the annealing temperature was raised to 50°C, terminated by 5 min 72°C and cooling at 8°C. The product was purified by gel purification. As the direct cloning of the PCR product in pKOSi was not successful, it was subcloned into pDrive using the QIAGEN PCR Cloning Kit according to the manufacturer's protocol, but an extended incubation for ligation at 14°C over night. *E. coli* TransforMax was transformed with the ligation mixture and the resulting plasmid pDrivesodcon could be isolated. The desired fragment was excised from this vector with *Xba*I and *Bam*HI-HF and gel purified. The recipient vector pKOSi was treated in the same way. Vector and DNA fragment were ligated with T4 ligase at 22°C for 1 h and used for transformation of *E. coli* TransforMax, yielding vector pKOSisodcon, which was subsequently introduced in *E. coli* BW25113 pIJ790.

For confirmation of the insert, the cosmid was sequenced and from the evaluation of these results it was reasoned, that not the desired fragment containing the *S. mirabilis sodN* gene, but a fragment of the large plasmid had been amplified. Furthermore, it could be determined that this was caused by misbinding of the primer sodNconR to sequences on the plasmid in complementary directions, enabling the amplification of a 2068 bp fragment.

Figure 18 shows the junctions between genomic DNA, pKOSi and pDrive on both sides of the insert, as they were determined by sequencing of the vector. Below each vector sequence the stretch of genomic DNA to which sodconR inexactly annealed is displayed. A high level of sequence identity between primer and the demonic DNA could be observed (underlined in Figure 18). Particularly the CGGGC sequence at the 3' end probably promoted primer binding.

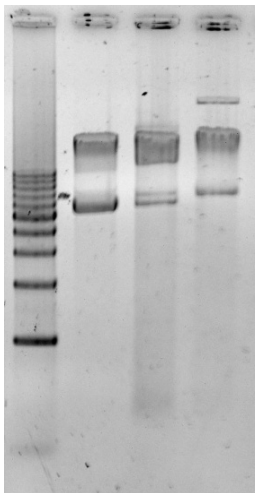

Figure 17. 0.8 % agarose gel of the cosmid for SMI8460 deletion, isolated in different steps of the knock-out procedure. Lane 1: 1 kb ladder; lane 2: original cosmid; lane 3: after transformation with the resistance cassette; lane 4: isolation from *E. coli* ET12567 pUZ8002

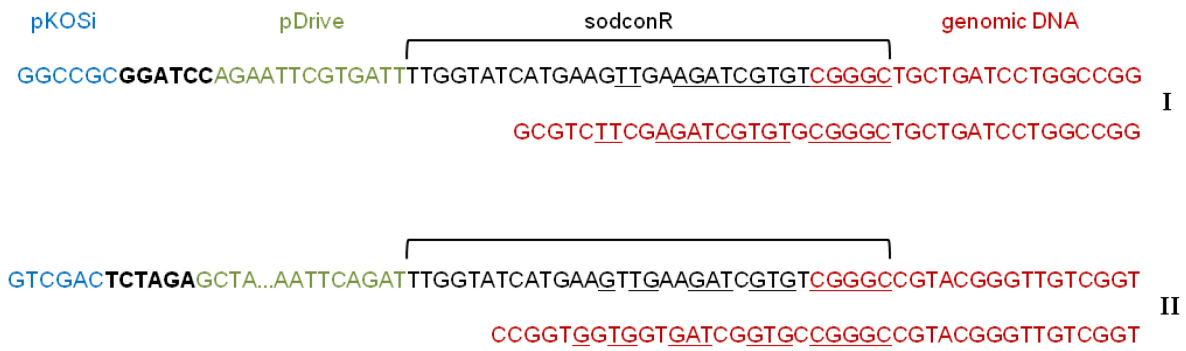

Figure 18. Junction sites between the cosmid vector backbone pKOSi (blue) and the *S. mirabilis* genomic DNA (red). Sequences in green result from subcloning in pDrive. Enzyme restriction sites used for ligation with pKOSi are indicated in bold. Underlined bases show putative annealing sites between primer sodconR and the *Streptomyces* genomic DNA, which were responsible for mispriming.

After detection of this PCR error, it was decided to put the constructed cosmid to use for introducing the *aac(3)IV* gene in an ORF that potentially would not interfere with plasmid transfer or heavy metal resistance, in order to see the influence of pII on heavy metal resistance in a heterologous host.

As target, a 450 bp gene coding a putative PadR family transcriptional regulator (SMI8460) was chosen. The resistance cassette was generated using primer set K.o.-P16pII (Table 8) and the gene deletion and recombination in *S. mirabilis* was conducted as described in section 2.

In the agarose gel shown in Figure 17 the steps of the introduction of the gene deletion on the cosmid can be nicely followed due to the app. 1000 bp larger size of the resistance cassette compared to the native gene. In lane 3 the cosmid was isolated from *E. coli* BW25113 after transformation with the resistance cassette. It is often observed that in this step the *E. coli* cell harbours copies of the original cosmid, as well as those with the integrated cassette, resulting in two bands. The original cosmid is lost after transformation of *E. coli* ET12567 pUZ8002 with this plasmid mixture, due to the selection on apramycin containing agar, resulting in a single cosmid band matching the deletion cosmid (lane 4).

The resulting transformant was named P16 pII-ko and the labelled plasmid pP16pII-ko, accordingly.

Streptomyces conjugation on plates and in soil microcosms

For assessing plasmid transfer from *S. mirabilis* P16B-1 to other bacteria, the heavy metal sensitive *S. lividans* TK24 was chosen as recipient. This strain is a plasmid-free very well investigated model organism (Hopwood et al., 1983; Ruckert et al., 2015), which shows an inherent chloramphenicol resistance that allowed its selection against *S. mirabilis*.

First, interspecific transfer was tested by plate mating, as described in section 2. Different media were used, as previous studies showed that medium composition has a crucial influence on the transfer frequency (Bibb et al., 1981; Kim et al., 2008a). The spores of both strains were mixed in a 1:10 ratio of donor and recipient, to enable the development of a mycelium lawn, as conjugal transfer requires direct cell-cell contact (Thoma et al., 2016). The development of growth retardation zones, so-called pocks, was the first indicator for plasmid transfer (Figure 19). In these areas the growth of recipient cells that receive the plasmid is transiently slowed (Bibb & Hopwood, 1981). Furthermore, the development of a blue pigment could be observed on MS agar amended with 10 mM $MgCl_2$. The nature of this pigment could not be determined, but as *S. lividans* is known for its production of various pig-

mented antibiotics, e.g. actinorhodin (Ruckert et al., 2015), it is most probably the producer, maybe as a reaction to the rapid nutrient depletion caused by synchronous growth of *S. mirabilis* and *S. lividans*.

Figure 19 shows mating plates after 7 d of incubation with the soft agar overlay. *S. lividans* colonies showing chloramphenicol and apramycin resistance could be observed on every tested medium, although in different numbers. However, the transfer frequency could not be determined due to development of a thick lawn of colonies on the soft agar, which was uncountable. Colonies were picked from this soft agar and further investigated for proving the plasmid transfer from *S. mirabilis* to *S. lividans*.

In order to test if this plasmid transfer could be of significance in natural systems, the mating experiments were repeated in sterile soil microcosms (Figure 19). Two types of soil were chosen: the low heavy metal containing Paradies Park soil (Jena, Germany) and an acidic, highly heavy metal contaminated soil from Kanigsberg (Ronneburg, Germay). The latter was used to assess if an enhanced heavy metal pressure promoted plasmid transfer, like it was observed in other studies (De Rore et al., 1994). The soil moisture was stably maintained to promote mycelium growth, as plasmid transfer can only take place between actively growing cells.

From the microcosms with Paradies Park soil, colonies could be re-isolated at all tested time points and on every medium, meaning CSA containing either apramycin or chloramphenicol or a combination of both. Only cells of *S. lividans* harbouring the *S. mirabilis* plasmid should be able to grow on the latter, while the other plates allowed growth of the parental strains, but also transconjugants. Therefore, the transfer frequency could not be determined by this method. No colonies could be re-isolated from Kanigsberg soil microcosms, probably due to the harsh conditions in this soil, in which the strains could not produce mycelium or died after inoculation.

These experiments showed that the plasmid could indeed be transferred to other bacteria also in soil environments. Therefore, it is likely that it could spread within a natural community.

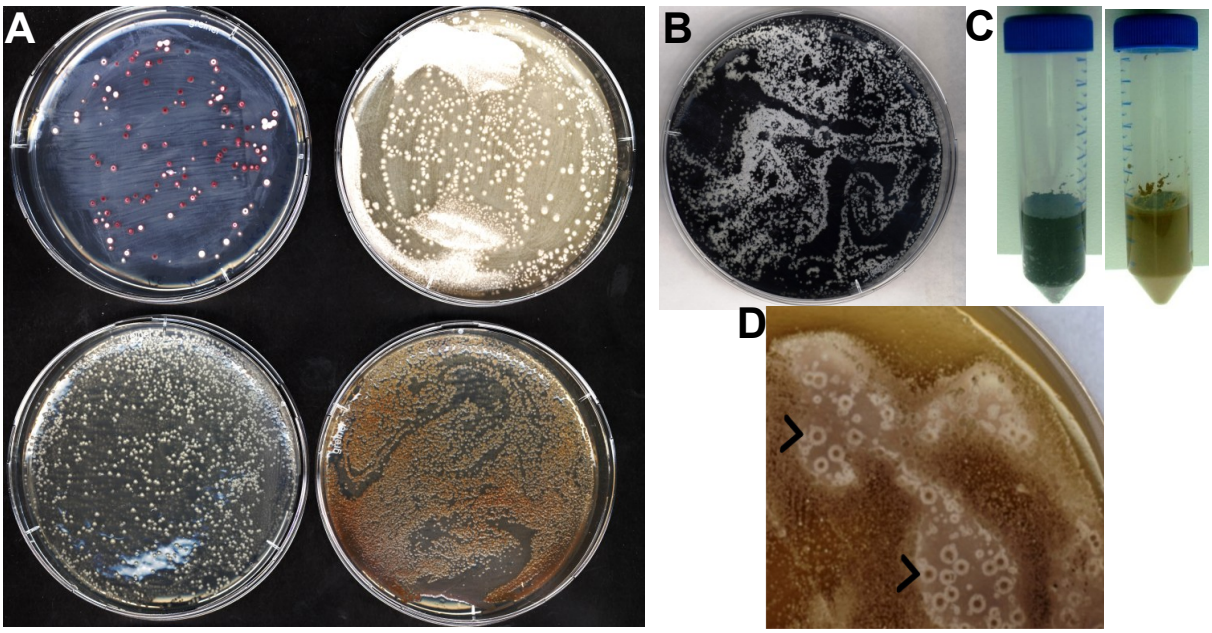

Figure 19. Intergeneric conjugation of *S. mirabilis* and *S. lividans* TK24. A) Growth of putative *S. lividans* transconjugants on conjugation plates with different media after softagar overlay containing apramycin and chloramphenicol; B) production of a blue pigment during conjugation on MS + 10 mM $MgCl_2$; C) microcosms with soil from Paradiespark (left) and Kanigsberg (right); D) pock formation (arrows) on a conjugation plate indicating plasmid spreading in the new host .

Intergeneric plasmid transfer to soil isolates

Plasmids can have different host ranges and of course a soil community consists of various species. In other studies, the transfer of streptomycete plasmids to other genera has been observed (Marsh & Wellington, 1994), although this was not necessarily the result of conjugation. Bhatt et al. (2001) observed the transfer to *Mycobacterium smegmatis*. This propagation was DNAse I sensitive, which hints at the release of DNA from the streptomycete followed by an uptake by *Mycobacterium* sp. In that case the plasmidal transfer functions were non-relevant and the plasmid suffered deletions, probably during uptake. To the author's knowledge, there is no reliable proof of conjugative plasmid transfer from *Streptomyces* sp. to other bacterial species, up to now.

For determining the probability of pII to spread within a community, also the transfer to other bacterial genera should be considered. This was investigated in the same plate setup as described for the mating with *S. lividans*. Several different genera were tested, all isolated from a former uranium mining site near the original isolation point of *S. mirabilis* (Gessenwiese, Ronneburg, Jena, Germany): *Pseudomonas sp., Stenotrophomonas sp., Sphingobacterium sp., Pedobacter sp., Kribbella sp., Bacillus sp., Virgibacillus sp., Oerskovia sp.* The strains were isolated and identified in the course of a master's thesis (Waqas, 2018), in which also the plasmid transfer from *S. mirabilis* to these strains was tested. As the latter experiments were of limited success and for reasons of brevity, the reader is directed to this thesis for further details.

The isolates were chosen to cover a wide variety of bacteria and different Gram types. The likeliness of plasmid transfer decreases with phylogenetic distance, as there are several barriers. For example, some genes cannot be transcribed in other species due to inefficient promoter recognition, or foreign DNA is degraded by an intrinsic methylation dependent restriction system (Bibb & Cohen, 1982; Mazodier et al., 1989). Nevertheless, also heterogramic transfer has been reported (Bertram et al., 1991) and should therefore be tested.

Despite several attempts, no viable transconjugants could be obtained in the intergeneric transfer experiments in the present study, except for *Kribbella* sp. Co-cultivation of *Kribbella* sp. with *S. mirabilis* yielded *Kribbella* sp. transconjugants, which showed apramycin resistance, hinting at the presence of pII. The identity of the transconjugants as *Kribbella* sp. was confirmed by amplification

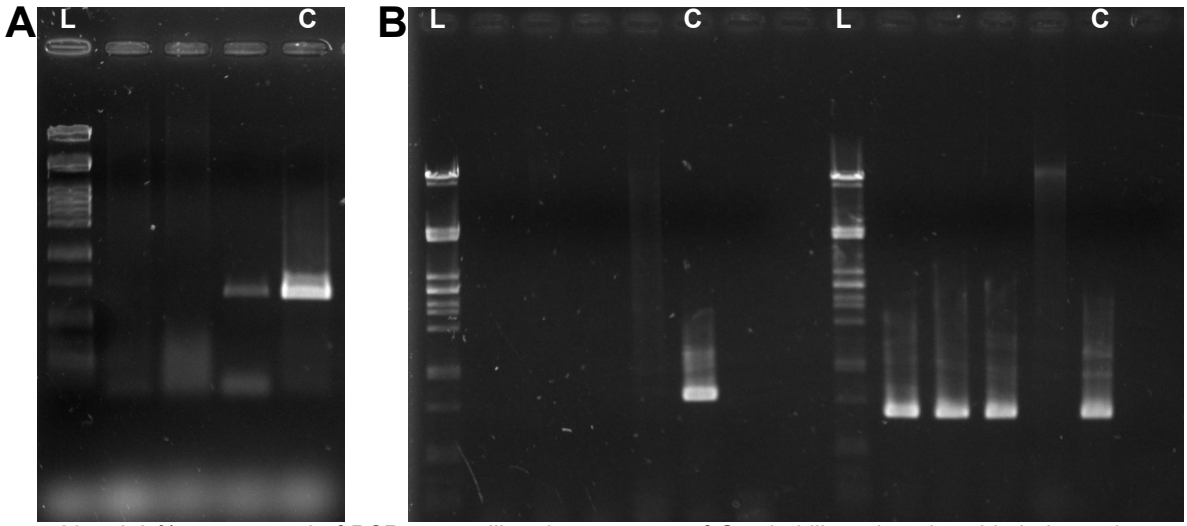

Figure 20. 0.8 % agarose gel of PCRs controlling the presence of *S. mirabilis* native plasmids in heterologous hosts. A) Confirmation of pII in *Kribbella* sp. with three DNA dilutions as PCR template (lanes 2-4); B) Detection of pI (left) and pII (right) in four putative *S. lividans* TK24 transconjugants. In both gels *Pst*I-digested lamda DNA served as ladder (L) and *S. mirabilis* WT DNA as positive control (C).

and sequencing of the 16S rDNA. Also a PCR using primers P16pII-F and P16pII-R (Table 3), which were specific for pII yielded a product of the correct size (Figure 20 A). Therefore, it was assumed that *Kribbella* sp. had acquired the plasmid. Whether this was the result of conjugation or uptake of plasmid DNA after lysis of *Streptomyces* sp. cells, remained obscure. However, the transconjugants grew poorly on medium containing apramycin and in corresponding liquid culture. No viable conserves could be obtained and also the biomass produced in liquid culture did not suffice for isolating sufficient DNA for a Southern Blot analysis. It was concluded, that *Kribbella* sp. could not efficiently maintain pII, which would be in line with the *in silico* analysis, in which several genes for plasmid spreading (*spd*) and replication (*tpg*) were not detected on pII. Therefore, the host spectrum of pII might be restricted to species which chromosomally encode the required determinants for maintenance. Of course, it cannot be excluded that maintenance genes of pII were simply not efficiently expressed in *Kribbella* sp.

Furthermore, the transfer of pII to the tested bacteria or other organisms might still be possible in nature, as laboratory conditions differ from natural soil and other factors might enable plasmid transfer, which were not considered here.

Characterisation of transconjugant strains

Confirmation of plasmid transfer

Three putative *S. lividans* transconjugants harbouring pII (designated TK24 pP16pII) were chosen for further studies and verification of plasmid transfer. First, the presence of pII in all transconjugants was verified by PCR using primers P16pII-F and P16pII-R (Table 3) (Figure 20 B). The small *S. mirabilis* plasmid pI could not be detected by PCR with primers specific for pI (P16pI-F and P16pI-R (Table 3)), confirming that only the large *S. mirabilis* plasmid was transferred and maintained in *S. lividans* under the tested conditions.

Heavy metal resistance

As it was assumed that pII carried determinants for heavy metal resistance, the transconjugants were tested for their resistance to nickel, copper and cobalt in trench plate tests and liquid culture. TSB and GYM were used as complex media, while AM served as defined minimal medium for comparing the impact of media composition and minimize effects caused by carbon sources or complexation of metals, since other studies showed that media composition has a major influence on metal concentrations tolerated by bacteria (Schmidt et al., 2009; Umeda et al., 1984).

Out of the tested heavy metals, plasmid pII had the strongest impact on the resistance of *S. lividans* to nickel, as shown by the trench plate tests (Figure 21). *S. lividans* WT was markedly less resistant to Ni^{2+} than the strains harbouring pII, especially on AM medium. However, *S. mirabilis* WT was still more resistant than the transconjugants, which suggested the presence of additional resistance determinants encoded on the chromosome of this strain. Likewise, the resistance to Co^{2+} and Cu^{+} was increased in TK24 pP16pII strains, although to a lesser extent than to Ni^{2+}, while *S. mirabilis* WT was again the most resistant strain. Furthermore, differences in resistance were most apparent on the defined AM medium and partly poorly visible on GYM, which underlined the importance of testing different media types in these assays.

For quantification of resistance differences, the strains were cultured on plates and in liquid medium amended with $NiSO_4$ and $CuSO_4$ (Table 9, Table 10). The results were in accordance with the obser

vations made using trench plates. *S. lividans* was markedly more sensitive to Ni^{2+} than the transconjugant or *S. mirabilis*.

The difference was most pronounced on AM medium, where *S. lividans* growth was impaired by 2.5 mM $NiSO_4$, while *S. mirabilis* tolerated 130 mM (Table 9). The same applied for liquid medium (Table 10).The pII carrying transconjugant, though, showed an increased tolerance to Ni^{2+}, e.g. 30 mM $NiSO_4$ on AM plates, but could not reach the same resistance level as *S. mirabilis*, which again hinted at additional chromosomally encoded resistance determinants in *S. mirabilis*.

Regarding copper, the differences between the wild types was not as high as for Ni^{2+}, probably due to the essential nature of this element, which plays an important role in the streptomycete life cycle.

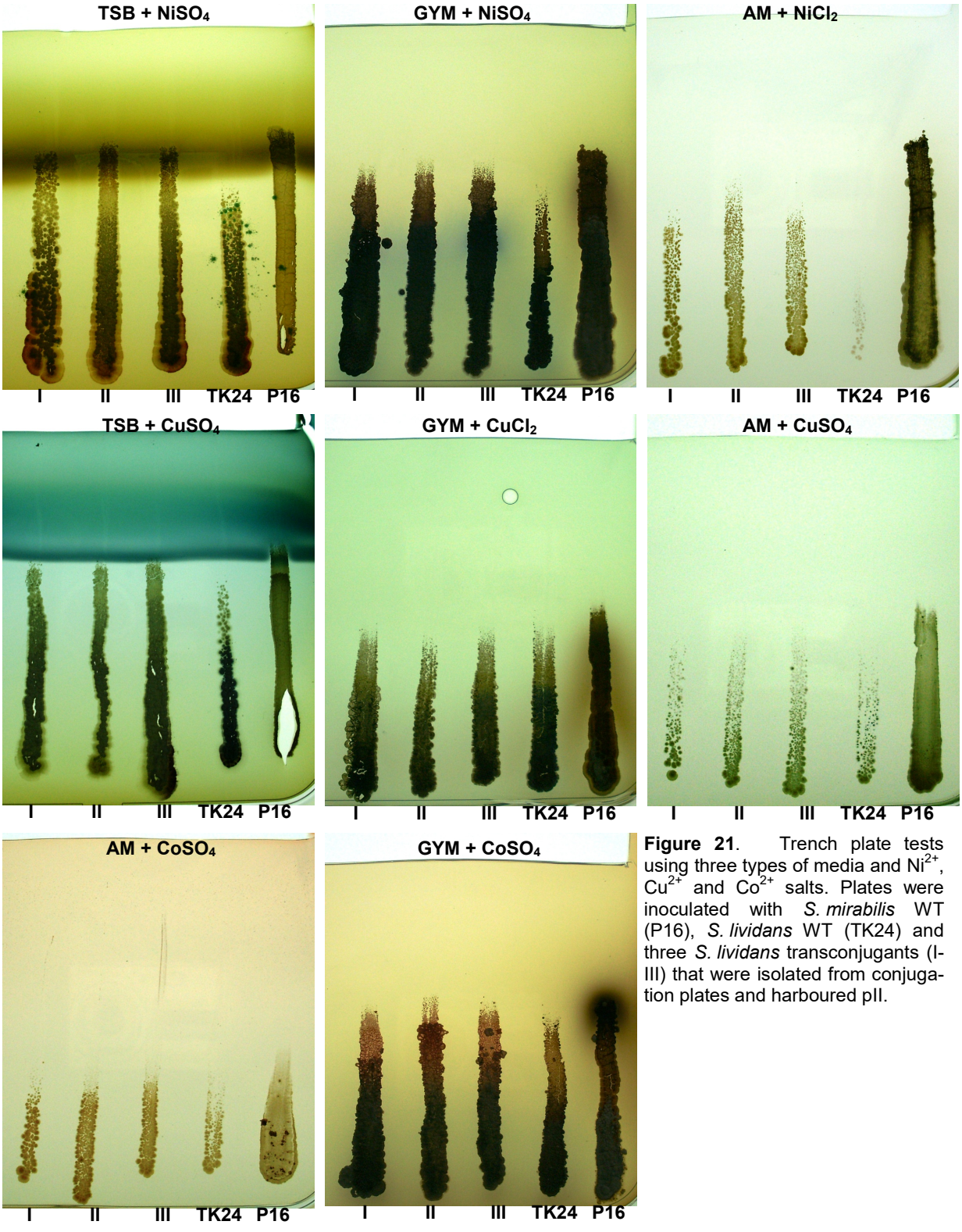

Figure 21. Trench plate tests using three types of media and Ni^{2+}, Cu^{2+} and Co^{2+} salts. Plates were inoculated with *S. mirabilis* WT (P16), *S. lividans* WT (TK24) and three *S. lividans* transconjugants (I-III) that were isolated from conjugation plates and harboured pII.

Table 9. Maximal concentrations of heavy metal salts [mM] tolerated by *S. mirabilis* WT (P16), plasmid-free P16 489_3, *S. lividans* WT (TK24) and the *S. mirabilis* plasmid pII carrying TK24 pP16pII on complex and minimal media agar plates. Growth was evaluated after four weeks incubation.

	$NiSO_4$		$CuSO_4$	
	TSB	**AM**	**TSB**	**AM**
P16	35	130	15	2.5
489_3	7.5	2.5	5	1
TK24	10	< 2.5	10	1
TK24 pP16pII	30	30	12.5	1

However, the introduction of the large *S. mirabilis* plasmid could raise the maximally tolerated Cu^+ concentration of *S. lividans* in complex TSB medium from 9 mM to 10 mM $CuSO_4$ (Table 10).

In liquid culture also the resistance to $CoSO_4$ was tested (Table 10), as it was often found that Ni^{2+} and Co^{2+} resistance co-occur (Schmidt & Schlegel, 1994; Stoppel & Schlegel, 1995). Like in the case of Cu^+, *S. lividans* was more sensitive to Co^{2+}, but could tolerate slightly higher concentrations when carrying pII, although the level of *S. mirabilis* was not reached.

Taken together, it was concluded that the *S. mirabilis* plasmid pII carried resistance determinants for Ni^{2+}, Cu^+ and Co^{2+}, which could be expressed in *S. lividans*. However, the *S. lividans* transconjugant did not tolerate the same metal concentrations as *S. mirabilis*, which lead to the conclusion that additional resistance determinants in *S. mirabilis* must exist and/or an interplay between pII and chromosomally encoded mechanisms promoted metal tolerance in this strain.

Metal content in biomass and tolerance of oxidative stress

In order to test, whether the increased metal resistance of TK24 pP16pII was the result of an increased metal efflux, the transconjugant and the wild type strain were cultivated in liquid GYM medium, amended with 0.25 mM $NiSO_4$ and the metal content of the biomass was determined (Table 12). The concentration of Ni^{2+} was slightly lower in TK24 pP16pII, while the Cu^+ concentration was slightly elevated. However, the difference was not statistically relevant. Possibly, the resistance mechanisms were not fully activated at this low Ni^{2+} concentrations or the resistance was not mainly based on efflux, but sequestration mechanisms.

Table 11. Maximally tolerated concentration of H_2O_2 [ppm] in TSB liquid medium.

	H_2O_2
P16	42
489_3	30
TK24	30
TK24 pP16pII	12

Since metal stress and oxidative stress are connected, it was tested whether pII would provide means for increasing the tolerance to H_2O_2. However, in contrast to the increased metal resistance, TK24 pP16pII tolerated merely 12 ppm H_2O_2, while *S. lividans* could grow upto 30 mM (Table 11).

Table 10. Maximal concentrations of heavy metal salts [mM] tolerated by *S. mirabilis* (P16), plasmid-free P16 489_3, *S. lividans* WT (TK24) and the *S. mirabilis* plasmid pII carrying TK24 pP16pII in liquid media. Growth was evaluated after two weeks incubation.

	$NiSO_4$			$CuSO_4$			$CoSO_4$	
	TSB	**GYM**	**AM**	**TSB**	**GYM**	**AM**	**TSB**	**GYM**
P16	35	12.5	45	11	2.5	1.25	5	1.2
489_3	9	1	13	11	2.5	1.4	2.5	0.8
TK24	5	0.8	0.75	9	2.5	0.8	3	1
TK24 pP16pII	25	4.5	10	10	2.5	1	5	1.4

Apparently, the expression of pII proteins elevated the intracellular oxidative stress. A possible reason could be the expression of transcriptional regulators, which could interfere with the expression of *S. lividans* native oxidative stress response machinery.

Table 12. Ni^{2+}, Co^{2+} and Cu^{+} concentration [µg/g] in the biomass of *S. lividans* WT (TK24) and pII carrying TK24 pP16pII grown in GYM with 0.25 mM $NiSO_4$ for 5 d at 28°C. Given are the means of three biological replicates with standard deviation.

	Ni^{2+}	Co^{2+}	Cu^{+}
TK24	776 ± 103	0.73 ± 0.04	3.02 ± 0.44
TK24 pP16pII	676 ± 46	0.75 ± 0.17	3.37 ± 0.39

Formation of biominerals

In former studies, the formation of struvite minerals and nickel hydrogen phosphates in the vicinity of *S. mirabilis* colonies was observed, when the strain was cultivated on TSB agar with different metals (Schütze et al., 2013). The nickel mineral was identified as Ni-struvite ($Ni(NH_4)(PO_4)$ x 6 H_2O,), whose formation was probably the result of passive mineralization rather than of active processes. It was firstly described as biomineral formed by *S. acidiscabies* E13 (Haferburg et al., 2008).

The formation of green crystals was also observed in this study, when the tested strains were cultivated on Ni-containing TSB agar plates, but not on AM or GYM. The minerals were formed directly below the colonies and in the near vicinity. They exhibited a hemimorphic habit and were mostly rosette shaped with a size ranging from a few 100 µm to 2 mm (Figure 22), similar to crystals observed by Haferburg et al. (2008). Their green colour indicated a nickel mineral and the investigations using Raman spectroscopy identified them as Ni-struvite (Falko Langenhorst, personal communication). Therefore, their formation was attributed to the high phosphate content of TSB as compared to the less complex media. Interestingly, the formation of Ni-struvite was also observed around *S. lividans* WT colonies, as visible on the trench plates (Figure 21). Therefore, this process did not seem to be connected to the *S. mirabilis* inherent Ni^{2+} resistance mechanisms. On plates inoculated with TK24 pP16pII Ni-struvite formation was even accelerated as compared to *S. mirabilis*, possibly by quicker growth of the transconjugant promoted by pII.

The mineral formation was thus regarded as passive process, which was not controlled by any of the strains. However, as no minerals were detected on plates inoculated with dead biomass (Haferburg et al., 2008), the Ni-struvite formation had to be connected to cell processes. Possibly, the increased nickel stress activated the expression of efflux pumps that transported Ni^{2+} from the cytosol into the surrounding medium. Therefore, an increased Ni^{2+} concentration in the vicinity of the colonies could be assumed, that enabled the mineral precipitation. This would account for the lack of biomineral formation in liquid culture, as no gradient could be established when the flasks were shaken.

A further hint, that this process was not a directed mineralization of nickel minerals, was the fact that also on TSB plates amended with $CoSO_4$ small wedge-shaped crystals with a hemimorphic habit were observed, although their size was comparably small (Figure 22). Again, this could be the result of the increased metal efflux, possibly driven by partly the same transporters as for Ni^{2+}, since some transporters transport both metals as substrates.

When the strains were tested on TSB amended with $CuSO_4$, no mineral formation was detected. Either, the Cu^{+} concentration was not sufficiently high to enable mineral precipitation or other conditions required for copper phosphate mineral precipitation were not met.

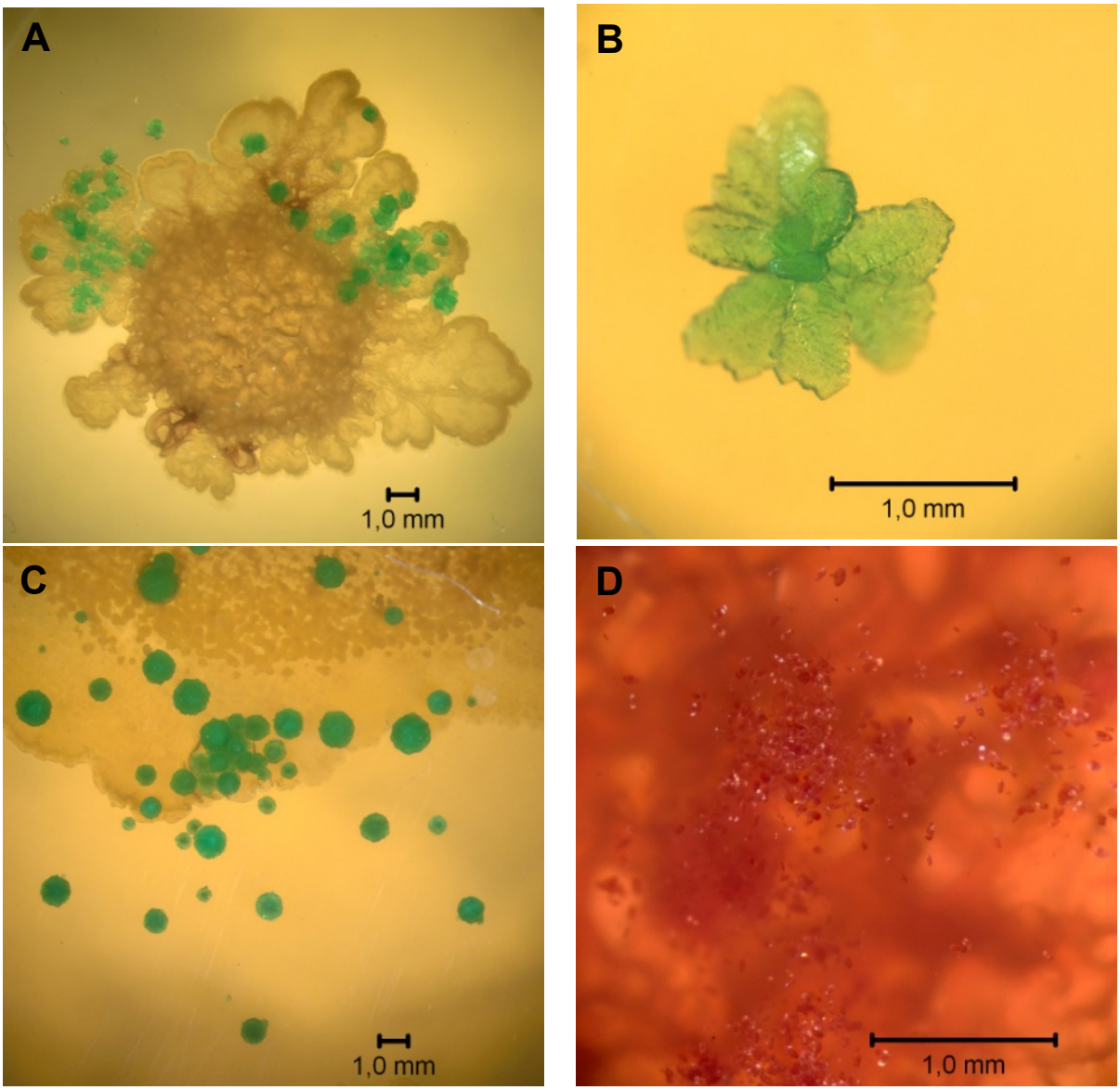

Figure 22. Formation of struvite minerals below and near colonies of *S. lividans* TK24 pP16-pII, cultivated on TSB amended with either 10 mM $NiSO_4$ (A, B), 20 mM $NiSO_4$ (C) or 9 mM $CoSO_4$ (D).

The phenomenon of struvite formation by bacteria is known for a long time, although these mostly have been magnesium phosphate minerals. It has been observed for Gram-negative and Gram-positive bacteria and was attributed to a change of media characteristics in the near vicinity of the colony creating a microenvironment as a result of bacterial metabolic activity, which supplies PO_4^{3-} and NH_4^+. It was hypothesized that the adsorption of Mg^{2+} and PO_4^{3-}, together with the NH_4^+ release would enable struvite formation (Rivadeneyra et al., 2014; Rivadeneyra et al., 1992). Furthermore, the importance of pH has been acknowledged, with an optimum between 7 and 8 for mineral precipitation (Pérez-García et al., 1989; Simoes et al., 2018).

Thus, it was assumed that the metabolic activity of the streptomycetes investigated in this study changed the conditions in the surrounding medium in a similar manner. Since Ni^{2+} was present in higher concentrations, Ni-struvite was formed instead of the more common Mg^{2+} containing form. To the author's knowledge, there are no reports on the formation of struvite where Mg^{2+} was substituted by copper. Studies on Cu^{2+}-containing waste water showed that induction of struvite formation by addition of magnesium, ammonia and phosphate did not result in Cu-struvite, but the precipitation of Mg-struvite to which $Cu(OH)_2$ could bind (Hutnik et al., 2013; Peng et al., 2017).

Metal efflux as promoter for biomineralisation has already been observed in the highly metal resistant *Cupriavidus metalidurans* CH34. Under heterotrophic conditions at elevated metal concentrations plasmid-encoded efflux pumps enabled the precipitation of minerals (Diels et al., 1995). This process was dependent on the carbon source, which could partly explain the lack of mineral formation on AM and GYM.

Since bioprecipitation prevents the re-entry of metals into the cell once they have been expelled, it can be considered a metal resistance factor (Diels et al., 1995).

Characterisation of a cured *S. mirabilis* strain and reintroduction of plasmid fragments

The above described tests using the *S. lividans* transconjugant showed that the large *S. mirabilis* plasmid pII harboured metal resistance-conferring genes. For determining what impact the loss of this plasmid would have on the wildtype strain, a cured *S. mirabilis* strain, designated 489_3, which was isolated in the course of the transposon mutagenesis experiments (see section 3.1) was tested for heavy metal resistance and H_2O_2 tolerance.

The maximally tolerated concentration of all tested metals was predominantly reduced in 489_3. The largest difference appeared on AM medium with $NiSO_4$: while *S. mirabilis* WT could grow upto 130 mM $NiSO_4$, growth of 489_3 ceased above 2.5 mM (Table 9). However, in liquid culture it showed that 489_3 still tolerated higher Ni^{2+} levels than *S. lividans* (Table 10), suggesting chromosomally encoded resistance mechanisms. Correspondingly to nickel, the sensitivity to cobalt was decreased in the cured strain, although to a lesser extent. Regarding copper, there was no strong change in liquid culture, where 489_3 again tolerated higher levels than *S. lividans*, but on plates a reduction of Cu^{+} resistance of a third was observed (Table 9).

In contrast to the *S. lividans* transconjugant, in which the presence of pII decreased the sensitivity to H_2O_2, the loss of pII in *S. mirabilis* did not promote H_2O_2 tolerance, but a decrease from 42 ppm to 30 ppm was recorded (Table 11), meaning the presence of pII increased the tolerance of oxidative stress in this strain. Apparently, there were host-dependent processes which would negatively affect *S. lividans*, while *S. mirabilis* benefitted from pII with regard to oxidative stress tolerance.

It should be noted that 489_3 also lacked the small plasmid pI and it could not be excluded that this plasmid as well would influence *S. mirabilis* resistance to metals and oxidative stress.

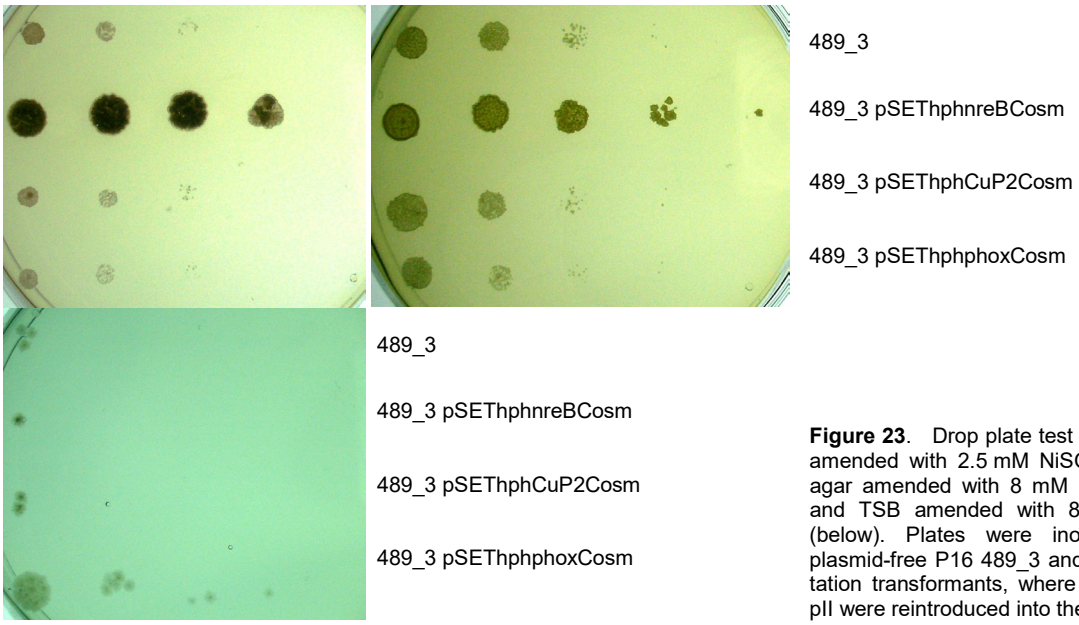

Figure 23. Drop plate test on GYM agar amended with 2.5 mM $NiSO_4$ (left), TSB agar amended with 8 mM $NiSO_4$ (right), and TSB amended with 8 mM $CuSO_4$ (below). Plates were inoculated with plasmid-free P16 489_3 and complementation transformants, where fragments of pII were reintroduced into the strain.

After obtaining a first impression on the metal resistance potential conferred by pII, the question arose which genes or gene clusters would be involved. Therefore, using an *in silico* approach, potential metal resistance genes known from other bacteria were identified on pII and used as targets for gene deletion. For the deletion procedure cosmids had to be created, which contained 3400 to 5700 bp fragments of pII. Taken together, three pII parts were amplified, comprising genes encoding either a putative Ni^{2+} efflux pump (*nreB*), a Ni^{2+} transporter of the NiCoT family (*phox*) or two copper resistance determinants (*copZ*, *copY*). Details on the predicted functions will be given in the following sections. In order to see if these fragments would also confer metal resistance independently, these pII parts used for cosmid constructions were inserted in pSEThph and separately introduced in 489_3, yielding strains 489_3 pSEThphnreBCosm (comprising *nreB*), 489_3 pSEThpgCuP2Cosm (comprising *copZ* and *copY*) and 489_3 pSEThphphoxCosm (comprising *phox*). Subsequently, the strains were tested in drop plate tests for their resistance to Ni^{2+} and Cu^{+} (Figure 23).

When 489_3 carried the plasmid fragment containing *nreB*, the resistance to Ni^{2+} strongly increased and enabled growth on TSB amended with 30 mM $NiSO_4$ and AM with 5 mM $NiSO_4$, on which 489_3 would not grow (data not shown). In contrast, pSEThphphoxCosm had a slightly negative effect on Ni^{2+} resistance. However, this strain showed better growth on TSB amended with $CuSO_4$ while pSEThphCuP2Cosm did not affect Ni^{2+} or Cu^{+} resistance under the tested conditions. No conclusive change in Co^{2+} resistance was determined for the complemented 489_3 strains, indicating that other parts of the plasmid were involved in resistance to this metal.

These results confirmed the assumption that the *nreB* carrying plasmid fragment would be involved in nickel resistance and encouraged the further investigation of this plasmid fragment.

Tyrosinase deletion transformants

Melanin production is a phenotypic trait often found in *Streptomyces* sp. (Schrempf, 1983). Frequently, tyrosinase activity is lost during cultivation cycles, which was first thought to be due to loss of a putative extrachromosomal DNA molecule carrying the tyrosinase-coding *mel* operon, as it is the case for *S. scabies* (Gregory & Huang, 1964). However, in many cases the melanin synthesis cluster was found to be located on the chromosome and melanine negative mutants were often observed nevertheless (Crameri et al., 1982; Schrempf, 1983).

Melanin synthesis was of interest in this work, as *S. mirabilis* produced a brownish pigment on complex media. It was hypothesized that this process is not optimally regulated by *S. mirabilis*, which resulted in a reduced heavy metal resistance on complex TSB agar as compared to minimal medium, where tyrosinase is probably not expressed (Schmidt et al., 2009). Furthermore, genome sequencing revealed that the *S. mirabilis mel* operon was coded on the small plasmid pI, whereby the investigation of this operon would additionally be a first step in the characterisation of this plasmid.

Computational analysis of P16melC2 *and its gene product*

A 825 bp long putative tyrosinase encoding gene (SMI8665) was annotated on *S. mirabilis* plasmid pI, which exhibited a high homology to *Streptomyces* sp. tyrosinase coding genes, as it was commonly observed for this enzyme in streptomycetes (Hintermann et al., 1985; Schrempf, 1983).

The gene product was predicted to be a 274 aa protein of 31.1 kDa possessing a central domain characteristic for tyrosinases (pfam00264), which was in accordance with other *Streptomyces* sp. tyrosinases regarding protein size and mass (Bernan et al., 1985; Huber et al., 1985; Lerch & Ettinger,

1972). On amino acid sequence level it was highly identical (> 80 % identity) to several *Streptomyces* sp. monophenol monooxygenases, e.g. sharing 89 % identity with the *S. antibioticus* tyrosinase (P07524.2). Therefore, the protein was termed P16MelC2.

Details regarding the protein crystal structure and catalytic mechanism of streptomycete tyrosinases were determined in a study by Matoba et al. (2006) on *S. castanaeoglobisporus* MelC2.

Upstream of *P16melC2*, a 393 bp ORF was annotated as tyrosinase co-factor MelC1 (SMI8666). The two ORFs probably constituted an operon, as this gene organization is conserved among *Streptomyces* sp. (Bernan et al., 1985; Hintermann et al., 1985). In other species, MelC1, termed “caddie protein” (Matoba et al., 2006), was found to be an accessory protein forming a complex with the tyrosinase protein, which is required for expression of the fully catalytically active tyrosinase (della-Cioppa et al., 1990; Ikeda et al., 1996). It has dual functions: firstly, delivering cupric iron for tyrosinase maturation as copper chaperone (Chen et al., 1993b; Matoba et al., 2006) and secondly, serving as secretion accessory (Leu et al., 1992).

Until 2009, *Streptomyces* sp. tyrosinases were always thought to be excreted. However, Yang & Chen (2009) reported a second, intracellular tyrosinase-like protein (MelD2) in several *Streptomyces* species and found that *S. coelicolor* MelD2 exhibited a narrow substrate spectrum and oxidized mono-and di-phenolic compounds. They postulated a role for MelD2 in detoxification of intracellular phenolic compounds, which might also be generated by the activity of MelC2.

Regarding its amino acid sequence, P16MelC2 was more similar to the excreted tyrosinase MelC2 than the intracellular MelD2 of *S. avermitilis* (Figure 24), wherefore it could be expected that P16MelC2 was indeed responsible for the extracellular melanin production in *S. mirabilis*. Also, no homologue of MelD proteins was detected in the *S. mirabilis* genome, wherefore the strain lacked this detoxification system for intracellular phenolics. Hence, P16MelC2 was the only candidate protein for tyrosinase activity.

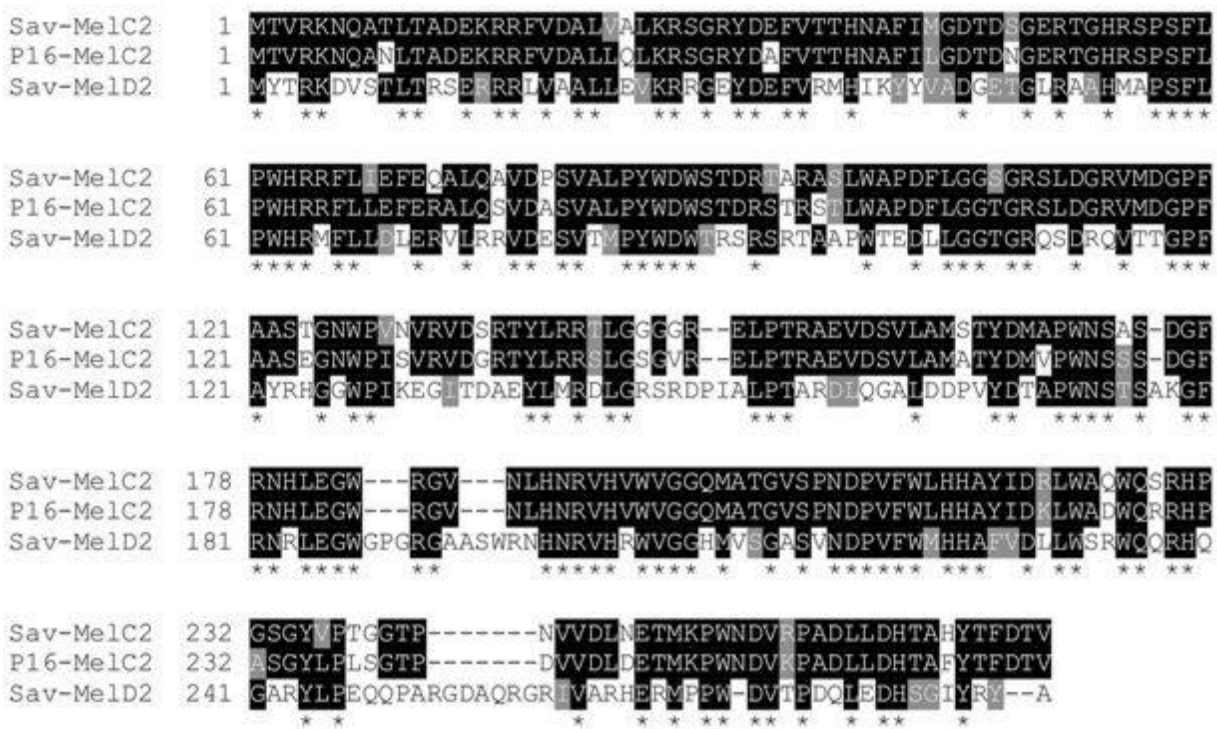

Figure 24. Alignment of the amino acid sequence of P16MelC2 and the extracellular MelC1 and intracellular MelD2 tyrosinases of *S. avermitilis*. Asterisks indicate residues identical in all sequences.

Phenotypic changes in a P16melC2 *deletion strain: pigmentation and heavy metal sensitivity*

For verification of P16MelC2 tyrosinase activity and a possible connection to heavy metal sensitivity on complex medium, *P16melC2* was deleted by targeted gene replacement as described above. The deletion strain, ΔTyr, was defective in production of the brownish pigment on complex medium (Figure 26), which proved the success of the deletion and that P16MelC2 was solely responsible for melanin production by the strain.

It was observed that *P16melC2* deletion accelerated the morphological development of *S. mirabilis* on minimal medium (Figure 25). The production of aerial mycelium and spores was enhanced at an early time point. This could be a reason for the frequent observation of *mel*⁻ mutants in this strain, when cultivated on plates for several successive cycles. Natural mutants which are defective in melanogenesis, possibly by loss of pI, would sporulate earlier and inadvertently be selected for re-plating.

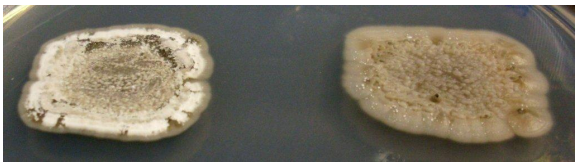

Figure 25. Development of aerial mycelium of *S. mirabilis* WT (right) and *melC2* deletion strain (left) on AM agar.

A connection between tyrosinase activity and morphological development in *Streptomyces* sp. has been frequently reported. However, in contrast to *S. mirabilis*, other melanin negative mutants were found to be impaired in spore formation, due to the down-regulation of sporulation-related genes, especially under increased osmotic stress (Beausejour & Beaulieu, 2004; Endo et al., 2001; Pandey et al., 2018). In *S. mirabilis*, the presence of tyrosinase slowed down development. The contrasting consequence of *P16melC2* deletion might be connected to the location of the gene on a plasmid, while in *S. avermitilis melC2* is chromosomally encoded, possibly leading to differences in transcriptional control.

Melanin formation requires the enzyme's substrate tyrosine, copper as co-factor and inducer amino acids. Lack of copper would reduce the expression of the apoprotein and abolish tyrosinase activity

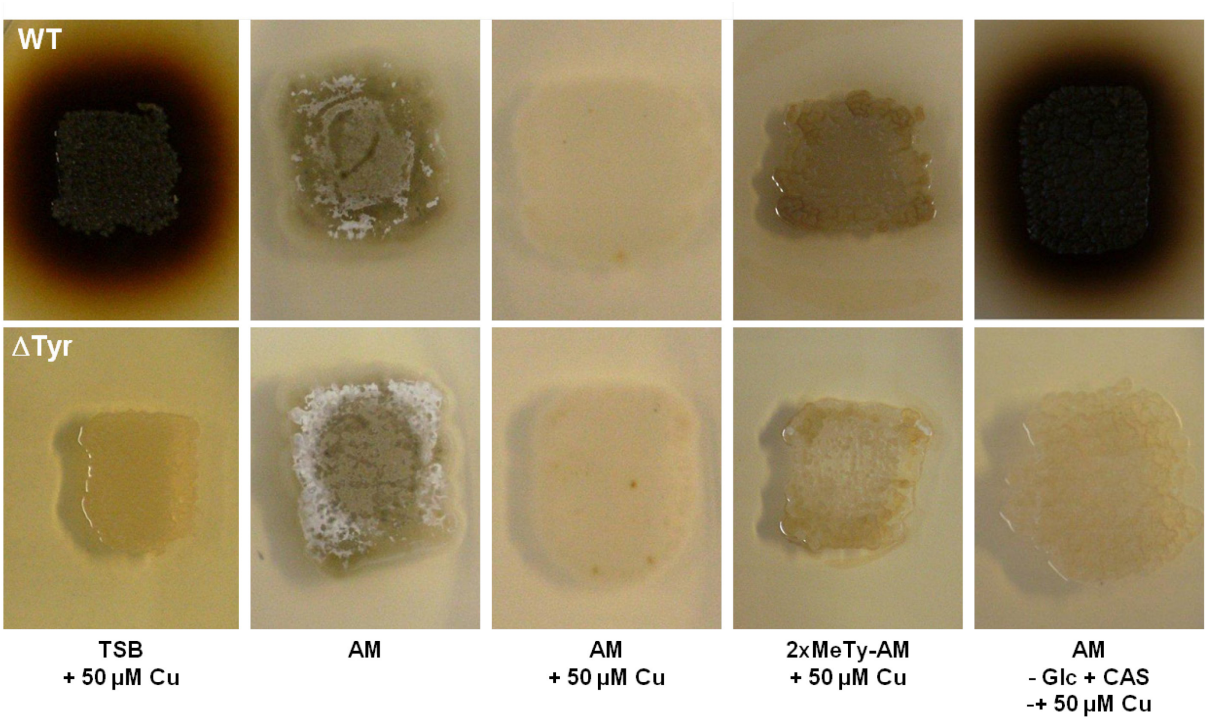

Figure 26. Comparison of growth and pigment production between *S. mirabilis* WT (upper row) and *melC2* deletion strain ΔTyr (below) on different media. Some media were supplemented with 50 µM $CuSO_4$ to promote tyrosinase maturation, as indicated.

Table 14. Maximally tolerated $NiSO_4$ concentrations [mM] on agar plates using different media. Growth was evaluated after four weeks incubation.

	P16	ΔTyr
TSB	45	50
TSB-Cu	35	45
AM	80	80
AM-Cu	50	50
2xMeTy-AM-Cu	60	60
CAS-AM-Cu	40	50

(Betancourt et al., 1992; della-Cioppa et al., 1990). Which additional amino acids are necessary for tyrosinase induction varies between strains (Crameri et al., 1982). In *S. antibioticus* and *S. glaucescens*, tyrosinase activity would be induced by methionine and analogous substances in a concentration-dependent manner, while lack of methionine would abolish tyrosinase activity even on tyrosine-containing medium (Betancourt et al., 1992; Hintermann et al., 1985).

In order to test the necessary compounds for P16MelC2 activity AM minimal medium was amended with either 50 µM $CuSO_4$ or 0.2 g/l methionine and tyrosine (2xMeTy-AM) and 50 µM $CuSO_4$. Additionally, AM medium was modified by substituting glucose with the same amount casamino acids and adding copper as in the other modifications. When the deletion strain and *S. mirabilis* were tested on these media, no phenotypic difference was observed on AM and AM + 50 µM $CuSO_4$ (Figure 26).

When tyrosine and methionine were present, *S. mirabilis* WT produced a light brownish pigment, which was excreted and the colony appeared darker than ΔTyr. The strongest pigment production by *S. mirabilis* WT could be observed when casamino acids were provided. This lead to the conclusion that methionine and tyrosine were not sufficient for full expression, maturation or functioning of P16MelC2. In further experiments this finding was utilized for investigating the influence of tyrosinase production on resistance to different stressors.

As stated at the beginning, P16MelC2 expression was hypothesized to reduce the heavy metal resistance of *S. mirabilis* on complex medium (Schmidt et al., 2009). Usually, the complex melanin molecules are thought to protect organisms from metals due to their numerous functional groups serving as metal binding sites, as it is known from fungal melanin (Fogarty & Tobin, 1996). In *S. scabies*, loss of melanogenesis was accompanied by a higher heavy metal sensitivity, particularly to copper (Beausejour & Beaulieu, 2004).

Deletion of *P16melC2* resulted in a slight increase in copper resistance in liquid medium, but reduced resistance to Ni^{2+} in all tested liquid media (Table 13). This was surprising, as in AM and GYM tyrosinase expression was expected to be low in the wildtype, wherefore the difference in resistance between ΔTyr and *S. mirabilis* WT should be neglectable in these media. The results for Ni^{2+} resistance on plates (Table 14) were contrasting the tests in liquid culture. Firstly, a connection between Ni^{2+} resistance and the provided carbon source became apparent, when modified AM medium was used.

With glucose as carbon source, both strains showed a similar high resistance (upto 80 mM $NiSO_4$), while amino acids increased Ni^{2+} sensitivity. Furthermore the test showed that indeed expression of tyrosinase reduced the heavy metal resistance of *S. mirabilis*, as on CAS-AM-Cu where melanin formation was high ΔTyr tolerated 50 mM $NiSO_4$ and the wild type grew upto 40 mM. Copper amendment

Table 13. Maximally tolerated concentrations of $CuSO_4$ and $NiSO_4$ [mM] and H_2O_2 [ppm] in liquid culture using different media. H_2O_2 tolerance was determined in TSB medium. Cultures were grown for two weeks.

	$CuSO_4$			$NiSO_4$			H_2O_2
	TSB	GYM	AM	TSB	GYM	AM	
P16 WT	11	2.5	1.25	35	12.5	45	42
ΔTyr	11	3.5	1.5	25	3	30	21

increased the strain's sensitivity to Ni^{2+} on AM in general, probably by increasing intracellular oxidative stress. In contrast to AM, on TSB copper addition even slightly promoted Ni^{2+} resistance. As observed for CAS-AM-Cu, ΔTyr tolerated higher $NiSO_4$ concentrations on complex TSB medium than the WT, although the difference was not as high (appr. 5-10 mM).

These findings confirmed the hypothesis of Schmidt et al. (2009). Since P16MelC2 was encoded on the plasmid, it was conceivable that its expression is less well regulated than that of chromosomal encoded proteins. It seemed that the costs for melanin formation exceeded the protective benefit that metal binding by the molecule would offer. However, different, pleiotropic effects could not be excluded.

Beside metals, melanin was found to protect cells from other environmental stressors and also oxidative stress. Deletion of the tyrosinase encoding *melA* in *Rhizobium etli* reduced the strain's H_2O_2 tolerance and the same has been observed for *S. scabies* (Beausejour & Beaulieu, 2004; Pinero et al., 2007). In *S. mirabilis*, deletion of *melC2* also resulted in a decreased H_2O_2 tolerance from 42 ppm in the wild type to 21 ppm in ΔTyr (Table 13). Tyrosinase activity contributed to the reduction of intracellular oxidative stress, which might explain the increased nickel sensitivity in ΔTyr in liquid medium, as heavy metals induce oxidative stress. However, copper sensitivity did not increase, although this element is particularly known for generating ROS in cells (see section 3.4).

Sensitivity to phenolic compounds and UV radiation

Extracellular *Streptomyces* sp. tyrosinases are known to oxidize phenol and various related compounds, like catechol, 4-methylcatechol, gallic acid, caffeic acid, o-aminophenols and salicylic acid with varying specificities (Crameri et al., 1982; Faccio et al., 2012; Lerch & Ettinger, 1972; Pandey et al., 2018; Yang & Chen, 2009). For assessing the substrate spectrum of P16MelC2, the parental and deletion strain were tested for their sensitivity to phenol and the phenolic compounds catechol and syringic acid on different media which promoted different level of melanin production by the WT.

The sensitivity to phenol was markedly increased in ΔTyr on TSB-Cu and CAS-AM-Cu (Figure 27), where melanin could be produced, while there was no difference between wildtype and ΔTyr on media where tyrosinase expression was expected to be redundant. The same was observed for sensitivity to catechol and syringic acid (Figure 28), although for the latter, sensitivity of ΔTyr was higher even on AM and MeTy-AM-Cu.

Taken together, it was shown that P16MelC2 participated also in the detoxification of phenolic compounds, which was in accordance with findings that MelA of *Rh. etli* caused resistance to p-hydroxybenzoic, vanillinic, syringic acids when expressed in *E. coli* (Pinero et al., 2007). However, contrasting findings have been made for MelC2 of *S. avermitilis* and *S. antibioticus*: melanogenesis defective mutants of these strains were more resistant

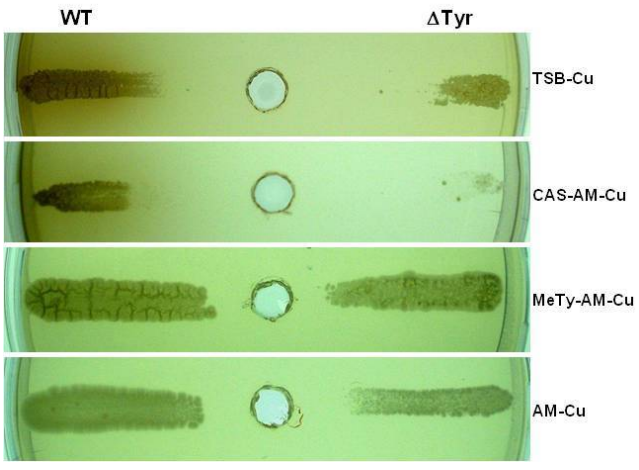

Figure 27. Agar diffusion assay for comparing the sensitivity of *S. mirabilis* (WT) and ΔTyr to phenol. Different media were used allowing different levels of melanin production. 10 µl phenol was applied per plate.

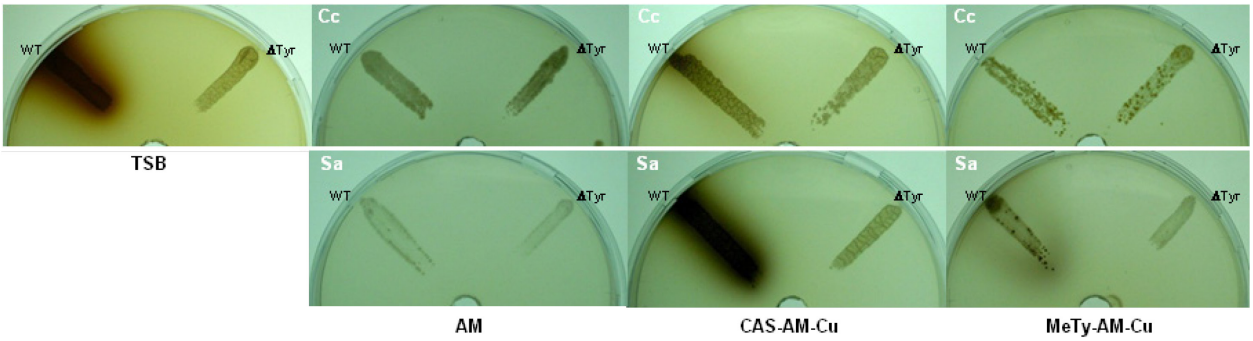

Figure 28. Agar diffusion assay for comparing the sensitivity of *S. mirabilis* (WT) and ΔTyr to phenolic compounds catechol (Cc) and syringic acid (Sa) (both dissolved in NaOH). Different media were used allowing different levels of melanin production. 100 µl solution were applied per plate.

to phenols, which was thought to be due to the conversion of these compounds to quinones by MelC2, which are hydrophobic and more membrane-permeable, thereby increasing intracellular stress (Yang & Chen, 2009). This observation has lead the authors to the hypothesis on cooperative action of extracellular MelC2 and intracellular MelD2 in *Streptomyces* sp., mentioned above, where MelC2 produces phenolic compounds, which enter the cell, where they can be detoxified by MelD2. This would give streptomycetes a fitness advantage in soil over organisms which do not harbour the *melD* detoxification system. This model did not fit the observation made for *S. mirabilis*, contradicting Yang & Chen (2009) hypothesis that MelD2-like tyrosinases are universal in *Streptomyces* sp. It is noteworthy that P16MelC2 was encoded on a plasmid, while in *S. avermitilis* and *S. antibioticus* both *mel* operons are located on the chromosome. Maybe, the model of Yang & Chen (2009) preferably accounts for strains with chromosomal *mel* operons. However, it was not tested if P16MelC2 was mainly excreted and it cannot be excluded that this tyrosinase also acted intracellularly, which would make a MelD2 protein redundant.

By acting on phenolic compounds, P16MelC2 might help in lignin degradation or make other carbon sources accessible and participate in the detoxification of compounds from other organism's defence systems (Bhattacharya et al., 2010; Lanoue et al., 2010). This tyrosinase activity might be one feature that promoted maintenance of pI in *S. mirabilis*, as it was found that cured mutants of *S. mirabilis* were also more sensitive to phenolic compounds (data not shown).

It is often assumed that melanin protects cells from UV radiation (Sies, 1997; Toledo et al., 2017), although this effect is still under debate. Therefore, it was determined if the melanin negative *S. mirabilis* strain was more sensitive to UV radiation. A dilution series of spore suspensions of the WT and ΔTyr was plated on TSB medium containing 50 µM $CuSO_4$ and incubated for 24 h to allow germination and tyrosinase activity. Then, half of the plates were exposed to UV light for 5 min. After incubation for three further days, CFUs were counted. The experiment was performed in triplicates per treatment.

The survival rates differed between the tested strains. While 56.5 % of the germinated WT spores survived, only 23 % persisted in case of ΔTyr. Apparently, the loss of melanin production reduced the sensitivity to UV light, contradicting a statement of Yang & Chen (2009), who did not observe a protective effect of melanin in *Streptomyces* sp. on plates. However, in case of *S. mirabilis* the tyrosinase provided some protection from UV radiation.

Conclusion

One main finding of this study was the capability of the large *S. mirabilis* plasmid pII to be transferred to and maintained in other *Streptomyces* species and potentially also other actinobacteria.

In the new host pII conferred resistance to Ni^{2+}, Co^{2+} and Cu^{+}, although the level of resistance was below that of *S. mirabilis*, which indicated additional heavy metal resistance determinants encoded on the *S. mirabilis* chromosome. In any case, pII could promote the adaption of a *Streptomyces* sp. community to metal contamination, as its transfer was also shown in soil microcosms. However, its host range might have been restricted to this genus, as no genetic determinants for spreading and maintenance were detected on the plasmid. A more thorough investigation of the transport mechanisms of pII might provide insight into the potential host range. Thus, pII was another example for a mobile genetic element that might spread within the actinomycete soil community enabling growth of inherently metal sensitive organisms.

It is often found in strains from contaminated sites that metal resistance mechanisms are located on transferrable plasmids. A role model for this case is *Cupriavidus metallidurans* CH34, which was isolated from a tank of a zinc factory. This strain harbours the conjugative plasmids pMOL28 and pMOL30, encoding resistances to several metals, e.g. Ni^{2+}, Hg^{2+} and Zn^{2+}. The resistance genes are mostly arranged in putative genomic islands, probably originating from recent horizontal gene transfer and gene duplication (Mergeay et al., 2009; Mergeay et al., 1985; von Rozycki & Nies, 2009). Whether the same accounted for pII could not be stated. However, further experiments were conducted in this study for identifying putative resistance determinants, which will be discussed in the following chapters.

In contrast to pII, no transfer of pI was observed, although this plasmid carried the only genuine *traB* homologue. It was assumed that this plasmid could lack other functions, which either promote transfer or the spreading and maintenance of the plasmid in the new host. There is one report of a similar case, where the maintenance of the small plasmid of *S. rochei* depended on the strain's chromosome and another plasmid, whereby it could not be transferred separately (Bao & Cohen, 2001; Kinashi et al., 1994). Since, up to now, TraB was shown to exclusively transfer circular molecules, it could be hypothesized that pI had been circular once. After a linearization event, this transfer machinery would have become inactive.

However, this plasmid apparently increased the strain's fitness in competition with other microbes, e.g. by harbouring self-defence genes like the *mel* operon, which might have been the reason for plasmid maintenance. Melanognesis was one reason for the reduced metal resistance of *S. mirabilis* on complex medium as compared to minimal medium. This might have resulted from the plasmidal location of the *mel* operon. For substantiating this hypothesis a comparison to a strain, where the tyrosinase is chromosomally encoded, would be desirable, e.g. by deleting *melC2* in *S. acidiscabies* E13.

On the other hand, tyrosinase activity protected *S. mirabilis* from phenolic compounds and UV radiation. Thus, a task sharing was observed for both plasmids in dealing with different kinds of stressors.

The formation of the biomineral Ni-struvite was no *S. mirabilis* specific trait, but also observed in the heavy metal sensitive *S. lividans*. Thus, this was most likely the result of basic cellular processes, possibly increased export of Ni^{2+} under metal stress. However, since *S. mirabilis* tolerated higher Ni^{2+} concentrations, this process might be employed for nickel removal from waste waters by bioprecipitation, as it was shown for *Cupriavidus metallidurans* (Diels et al., 1995).

3.3 The plasmid-encoded Ni^{2+} exporter P16NreB

Introduction

Highly specialized transporters have evolved for conferring metal resistance to cells. For nickel, these exporters predominantly belong to three classes: the resistance-nodulation-cell division superfamily, NiCoT family transporters and the major facilitator family (MFS). The latter is the largest group of secondary active transporters comprising at least 74 families found in all domains of life. Many of these proteins display a 12 TMD (transmembrane domain) topology and function as uniporter, symporter or antiporter for different substrates (Reddy et al., 2012).

These resistance determinants are commonly found in naturally as well as anthropogenically polluted ecosystems, regardless of the contamination source. Stoppel & Schlegel (1995) found in hybridization experiments with strains from sites with high Ni^{2+} concentrations that the most abundant types of Ni^{2+} resistance determinants are *cnr*, *ncc* and *nre* homologues. The former two, cobalt-nickel (*cnr*) and nickel-cobalt-cadmium (*ncc*) resistance loci confer resistance to multiple metals, while *nre* was found to be specific for Ni^{2+} upto now (Schmidt & Schlegel, 1994; Sensfuss & Schlegel, 1988).

NreB, the eponymous member of the latter class, was first described in *Cupriavidus metallidurans* 31A where it is responsible for low-level nickel resistance (Schmidt & Schlegel, 1994). This transporter belongs to the MFS family functioning as Ni^{2+}/H^{+} antiporter and there are several homologues known, like *Klebsiella oxytoca* NirA, *Hafnia alvei* NcrA and *Synechocystis sp.* NrsD (García-Domínguez et al., 2000; Park et al., 2004; Park et al., 2008). The transcription of all these transporters is induced by Ni^{2+} and in some cases also by Co^{2+}.

Results

Computational analysis

Identification of an nre *homologue in* S. mirabilis

In the previous section it was shown that the large *S. mirabilis* plasmid conferred resistance to several heavy metals. This raised the question, which genes might be involved in the resistome, in particular in nickel resistance.

A sequence similarity search on DNA-level for homologues of known nickel resistance determinants on the large plasmid of *S. mirabilis* yielded a locus (SMI8362) with significant similarity to the chromosomal *nre* (nickel-resistance) operon of *Achromobacter xylosoxidans* (AHC47869). No similarly homologous region was detected on the chromosome or on the second plasmid of this strain.

Plasmids with *nre*-like Ni^{2+} resistance determinants are known from several species, e.g. *Cupriavidus metallidurans*, *Sinorhizobium meliloti* and *Enterobacter* sp., many of which are transferrable (Lee et al., 2006; Mergeay et al., 1985; Pini et al., 2014; Schmidt & Schlegel, 1994).

This type of nickel resistance determinant is mainly studied in Gram-negative species, where the coding operons comprise several ORFs, like *ncrBACD* of *Synechocystis* sp. (García-Domínguez et al., 2000) or *ncrABCY* of *Leptospirillum ferriphilum* (Tian et al., 2007). In contrast to these, *P16nreB* did not appear to be part of any operon (Figure 29). This could be attributed to *Streptomyces* sp. being Gram-positive, which is why there is no necessity for transporters that translocate metals from the periplasm through the outer membrane to the extracellular environment. However, upstream of

P16nreB, a transcriptional regulator of the ArsR family, KmtR, was located, which is often found in association with *nreB*-like genes in Actinobacteria (Pini et al., 2014). Members of the ArsR-SmtB transcriptional repressor family regulate metal transport and detoxification in response to elevated intracellular metal concentrations (Campbell et al., 2007). KmtR was found to regulate the transcription of a cation diffusion facilitator family metal transporter in *Mycobacterium tuberculosis* responding to Ni^{2+} and Co^{2+} (Campbell et al., 2007). Downstream of *P16nreB* a second regulator of this family was identified (NmtR), together with a gene for a putative Cd^{2+} translocating P-type ATPase (NmtA). A similar arrangement is found in *S. coelicolor*, where NmtR functions as transcriptional repressor for the Ni^{2+}/Co^{2+} exporter NmtA contributing to tolerance to these metals (Kim et al., 2015). KmtR and NmtR exhibit different affinities and consequently differing sensitivities for their cognate metals, Co^{2+} and Ni^{2+}, depending on the type of medium used for cultivation: KmtR repression is alleviated in complex medium, while NmtR remains bound to DNA and is only released in minimal medium or medium supplemented with Ni^{2+} or Co^{2+} (Campbell et al., 2007; Cavet et al., 2002).
It seemed likely, that *nreB* transcription in *S. mirabilis* was regulated by one or both of these regulators, taking their genomic association into account.

P16NreB protein characteristics

The predicted *P16nreB* gene product was a 444 aa protein with a mass of 46.6 kDa. This was in accordance with other known NreB-type transporters, e.g. *C. metallidurans* NreB (436 aa, 46.2 kDa) or *Serratia marcescens* NcrA (432 aa, 46,9 kDa). Based on BLASTP amino acid alignments, P16NreB was classified as major facilitator superfamily (pfam07690) member, functioning as H^+ antiporter protein (TIGR00900). The conserved domain search furthermore identified a putative substrate translocation pore. A metal/H^+ antiport function was assumed for NreB-like transporters (Pini et al., 2014), although, to the author's knowledge, this has not been substantiated yet.
The predicted protein displayed the highest similarity (> 80 %) to other *Streptomyces* sp. MFS transporters, found in soil isolates from China and India. Notable was the sequence identity of 82 % with a *Streptomyces* sp. CdTB01 MFS transporter (WP_07907823), as this isolate comes from a heavy metal contaminated soil and exhibits a high level of metal resistance (Zhou et al., 2016). The similarity of P16NreB to non-actinobacterial MFS family transporters was comparably high as well: 58 % to *C. metallidurans* (WP_029309659), 55 % to *K. oxytoca* (WP_103815562) and 24 % to *H. alvei* (WP_004091410).
NreB-like transporters differ in their topology. While some were found to exhibit 12 TMDs (*Synechocystis* sp. NrsD (SyNrsD), *C. metallidurans* NreB (CmNreB) (García-Domínguez et al., 2000; Grass et al., 2001)), others only posses 10 TMDs (*Leptospirillum ferriphilum* (LfNcrA) (Tian et al., 2007)) or even less (six predicted TMDs for *E. coli* NreB (EcNreB)). P16NreB was predicted to have a 12 TMD topology. However, these predictions cannot be substantiated, as none of these transporters has been crystallized upto now.

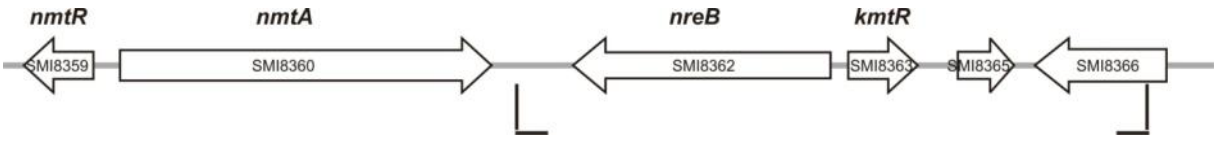

Figure 29. Schematic to scale representation of the *S. mirabilis* plasmid pII fragment encompassing loci SMI8359 to SMI8366. Predicted names of coding sequences are given above, if allocatable. Black bars indicate genomic segment used for construction of vector pSEThphnreBCosm.

Amino acid sequence alignment

This high level of congruence also showed when P16NreB was aligned with well-investigates transporters of the NreB-type (Figure 30). The alignment illustrated the high sequence similarity of these homologous proteins, despite the phylogenetic distance of the species.

Not all NreB-like transporters have the same substrate spectrum: while some exclusively transport Ni^{2+}, others also transport Co^{2+}. From the alignment it could be seen that the Ni^{2+} and Co^{2+} transporting SmNcrA and HaNcrA shared more identical residues with each other than with the exclusively Ni^{2+} transporting CmNreB. In P16NreB, residues that were present in the former two transporters could be found, which were substituted in CmNreB (e.g. A110, R127, V169), which hinted at P16NreB transporting Ni^{2+} as well as Co^{2+}. However, also the opposite case could be observed, where P16NreB

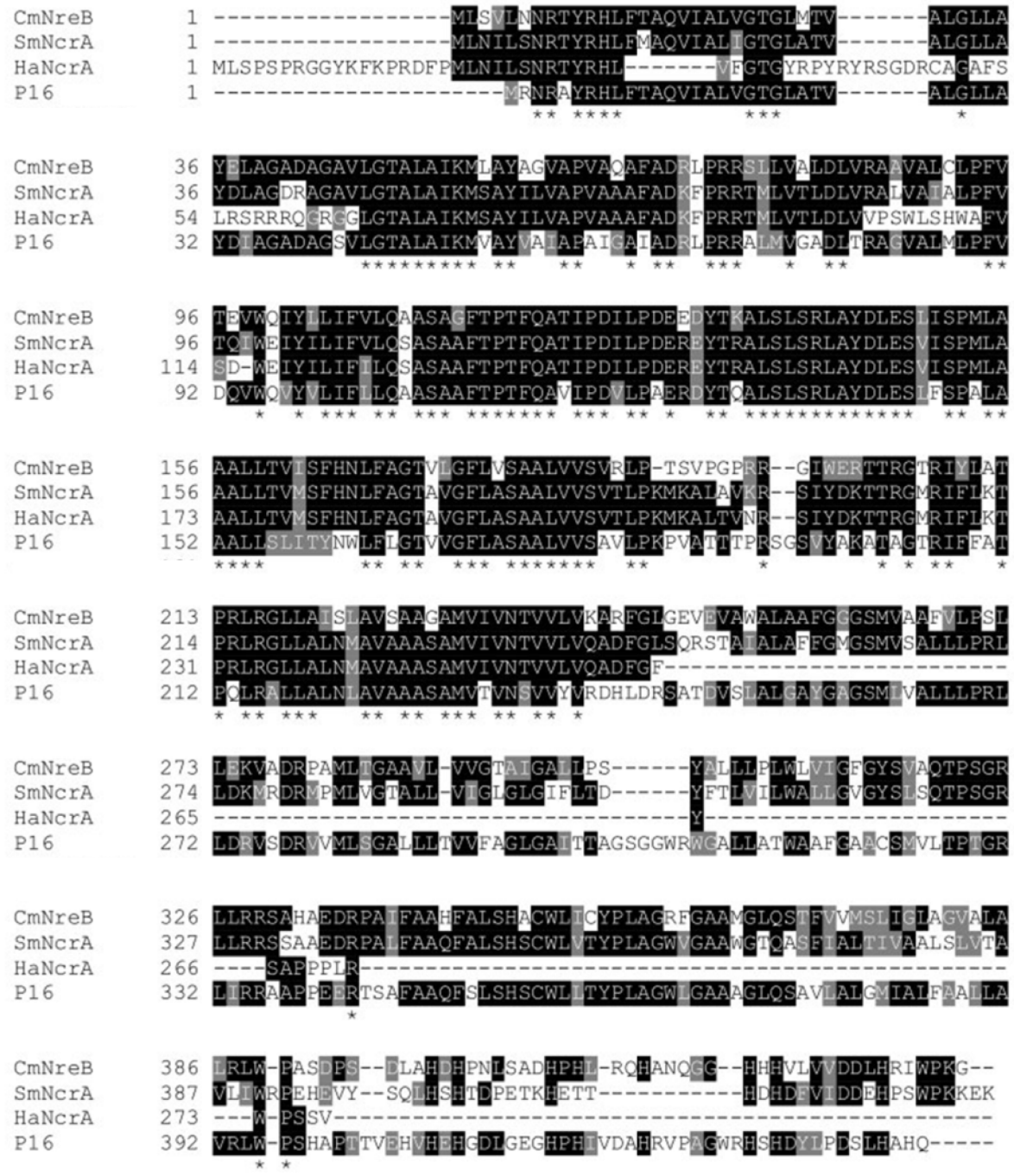

Figure 30. Amino acid sequence comparison between P16NreB (P16) and the NreB homologues of *C. metallidurans* (CmNreB), *Se. marcescens* (SmNcrA) and *Hafnia alvei* NcrA (HaNcrA). Residues which were identical in all sequences were marked with an asterisk.

residues solely matched those of CmNreB (e.g. R67, L73, A106) or residues, which were conserved in CmNreB, SmNcrA and HaNcrA, but substituted in P16NreB (e.g. A77, T80, V118). As it is not known, which residues determine the substrate spectrum of NreB-like transporters, no definite statement about the substrate spectrum of P16NreB could be made based on this alignment.

In accordance with other NreB-like transporters, the putative Ni^{2+} binding motif (HX_4DH) of other types of Ni^{2+} transporters, like HoxN, was not present in P16NreB. Also, the (MX)CXXC motif, which is found in other metal binding and transporting proteins, e.g. CPx-ATPases (Nies, 2003; Radford et al., 2003), was absent in the examined transporters, suggesting that other motifs were essential for metal transport.

A feature, which P16NreB shared with several other transporters of this type, was a strongly hydrophilic C-terminal part with high histidine content: 11 out of 52 C-terminal positions were occupied by His. The similarly histidine rich C-terminus of SyNrsD and CmNreB displayed a low specificity in metal binding and were found not to be essential for functioning of the transporters, as deletion of this end in CmNreB did not interfere with Ni^{2+} resistance. It was concluded that this putative metal binding domain serves as metal storage (García-Domínguez et al., 2000; Grass et al., 2001). This might be the case in P16NreB as well. The comparably low sequence identity between the transporters in this part seemed therefore negligible, as it should not interfere with the metal transport.

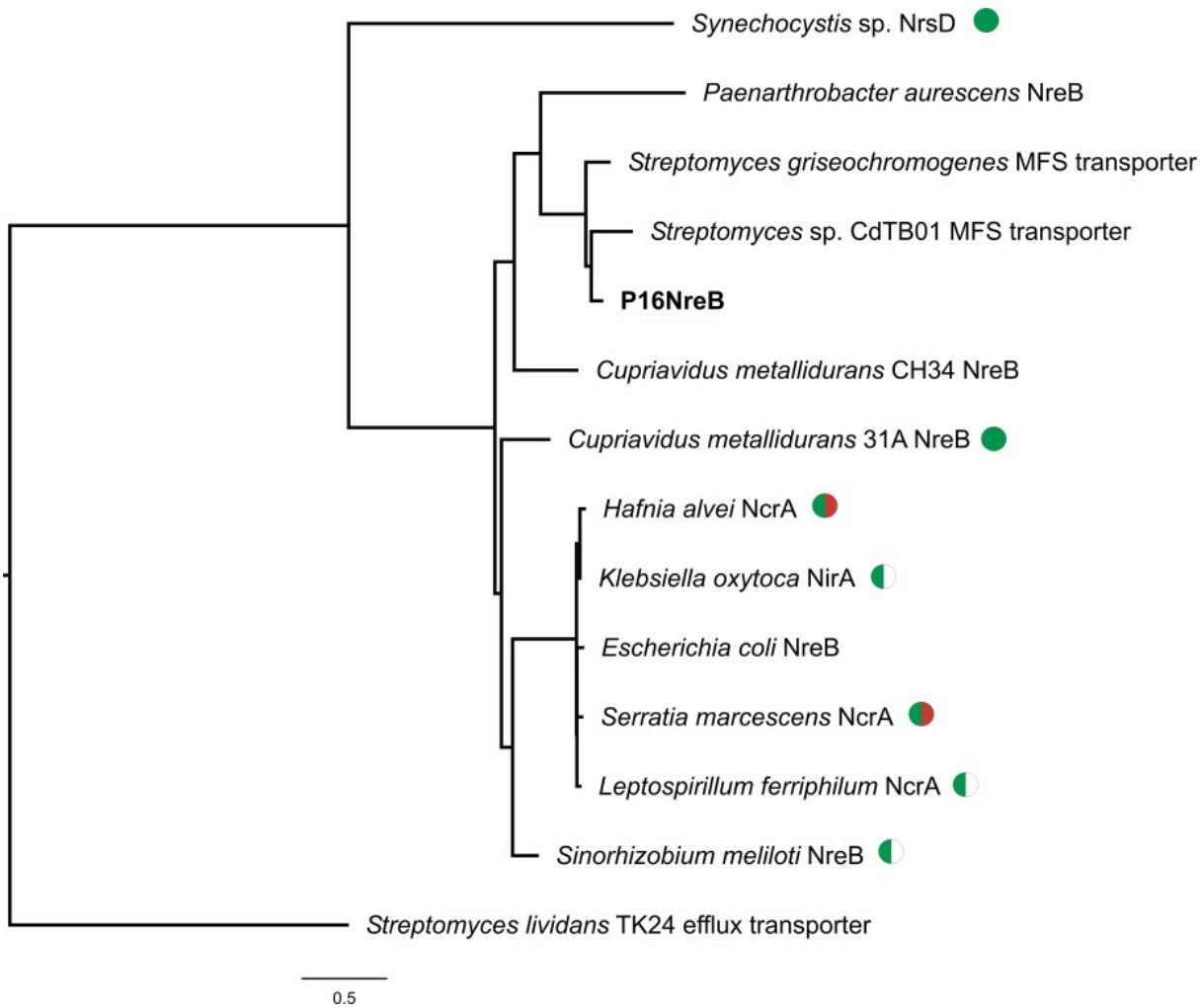

Figure 31. Phylogenetic tree of NreB-like transporters. Circles indicate known transported metals determined in other studies (see text). Transporters may exclusively transport Ni^{2+} (full green circle) or Ni^{2+} and Co^{2+} (green and red circle). If the transporter has been shown to transport Ni^{2+}, but Co^{2+} transport was not determined, one half of the circle was left empty.

Phylogenetic distance to other NreB-like proteins

Regarding the distribution of *nre* resistance determinants in terms of the origin of the strains and their phylogenetic affiliation, it became apparent that they were identified mostly in species from contaminated habitats. The strains were isolated from mining areas (*Le. ferriphilum* (Tian et al., 2007)), tanks with mineral oil and from a zinc factory (*K. oxytoca* (Stoppel et al., 1995), *C. metallidurans* CH34 (Mergeay et al., 1985)) and serpentine deposits (*Se. marcescens* (Marrero et al., 2007)). Despite their spatial separation and affiliation to different phyla and classes, the sequence similarity of NreB-like transporters on amino acid level was high. Seven out of the eleven homologous transporters displayed in the phylogenetic tree (Figure 31) were found to be located on plasmids, which could be transferred to other species. This might be one reason for the apparently broad distribution of this resistance determinant and the high homology. Pini et al. (2014) suggested the propagation *via* horizontal gene transfer, as they also observed a high level of homology among these transporters with little correlation to phylogeny in a more expansive computational comparison.

As stated above, NreB-like transporters differ with respect to their substrate metals. As the Ni^{2+} and Co^{2+} transporting SemNcrA and HaNcrA can be found in the same cluster of highly similar transporters, it is probable that all of these transport both metals. However, reports on these solely tested for Ni^{2+} transfer and no statement was made concerning Co^{2+} transport (Park et al., 2003; Pini et al., 2014; Tian et al., 2007). The transporters of *C. metalliduans* 31A and *Synechocystis* sp. exclusively translocate Ni^{2+} (García-Domínguez et al., 2000; Grass et al., 2001). From this, it was hard to make a statement about the substrate specificity of P16NreB regarding the transport of Co^{2+}. P16NreB would most probably function as Ni^{2+} transporter, but the Co^{2+} transporting activity would have to be tested.

Deletion of *P16nreB* and heterologous expression in *S. lividans*

Although they appeared to be widely distributed in *Streptomyces* sp., to the author's knowledge, NreB-like transporters have never been investigated regarding their role in heavy metal resistance in this genus. In other bacteria, their function as nickel exporters whose expression is enhanced under Ni^{2+} stress is well documented (Grass et al., 2001; Pini et al., 2014). Furthermore, *nre* determinants located on large plasmids which are involved in Ni^{2+} resistance have been reported (Park et al., 2003; Stoppel et al., 1995). In the symbiotic nitrogen fixing *Sinorhizobium meliloti* a gene coding NreB located on a megaplasmid was found relevant for response to multiple stressors, like Ni^{2+}, urea and Cu^{+} (Pini et al., 2014). These reports and the results of the computational analysis made *P16nreB* a likely candidate for a resistance determinant against Ni^{2+} and possibly Co^{2+}. For confirming this hypothesis, the gene was deleted by targeted gene replacement, yielding strain Δ*nreB*. One deletion transformant was subsequently genetically complemented for further confirmation of gene functioning, using vector pSEThphMFS. The change of metal resistance in these strains was tested in different approaches.

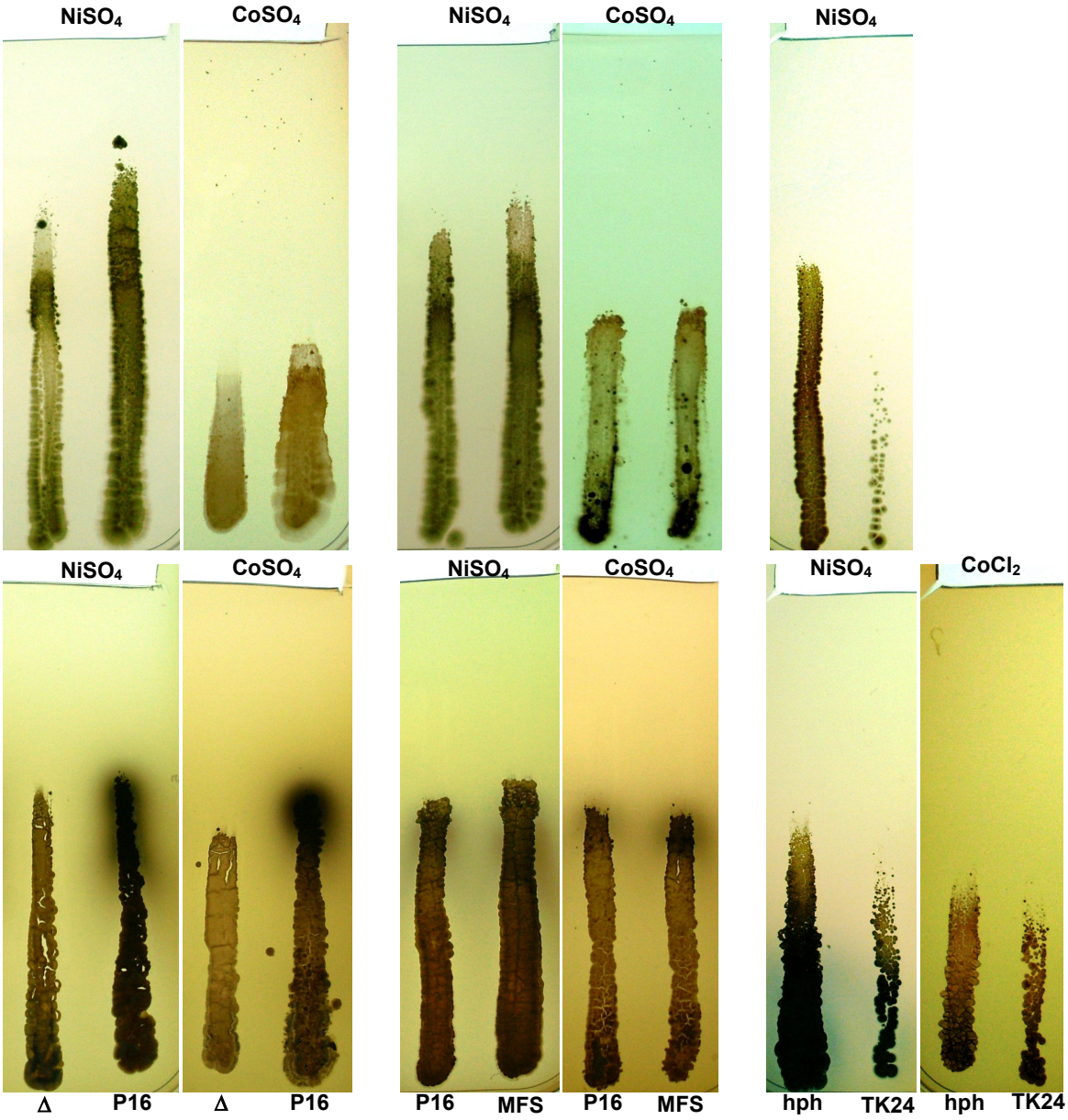

Figure 32. Trench plate tests on AM agar (upper row) and GYM agar (lower row) with Ni^{2+} and Co^{2+} salts. Plates were inoculated with wiltype *S. mirabilis* and *P16nreB* deletion transformant (Δ) (left), or P16 pSEThphMFS (MFS) in which an additional copy of *P16nreB* was integrated (middle), or wildtype *S. lividans* TK24 and TK24 pSEThphMFS (hph) carrying the *P16nreB* gene (right).

Heavy metal resistance tests

For roughly assessing the level of resistance reduction, trench plate tests were conducted comparing the resistance of the wildtype to that of the deletion strain Δ*nreB* on AM and GYM medium (Figure 32). On both media Δ*nreB* showed a higher sensitivity to Ni^{2+} and Co^{2+}, whereby the Ni^{2+} tolerance was markedly more reduced.

In plate tests with defined Ni^{2+} concentrations the wildtype tolerated upto 60 mM $NiSO_4$ on TSB agar, while deletion of *P16nreB* allowed growth upto 40 mM. Similarly, in liquid culture the Ni^{2+} resistance was reduced in complex and minimal media (Table 15). The Ni^{2+} concentrations tolerated by Δ*nreB* were approximately half of the amount tolerated by the WT. Complementation did increase the nickel resistance of the deletion strain, but could not fully re-establish WT level in TSB and GYM medium. However, the tolerated Ni^{2+} level in minimal medium increased to 47.5 mM, while *S. mirabilis* WT tolerated 45 mM.

Table 15. Maximally tolerated $NiSO_4$ and $CoSO_4$ concentrations [mM] in liquid cultures. Growth was evaluated after 14 d.

	$NiSO_4$			$CoSO_4$	
	TSB	**GYM**	**AM**	**TSB**	**GYM**
P16	35	12.5	45	5	1.2
Δ*nreB*	17.5	6	27.5	2	0.6
Δ*nreB* pSEThphMFS	25	10	47.5	4	1
P16 pSEThphMFS	40	15	45	4	1
TK24	5	0.8	0.75	3	1
TK24 pSEThphMFS	20	3	5	5	1.8
TK24 pP16pII	25	4.5	10	5	1.4
TK24 pP16pIIΔnreB	20	3.5	2.5	4	1.2

This effect could also be observed in drop plate assays (Figure 33). In these tests, Ni^{2+} markedly impaired the growth of the deletion strain. On TSB, the complemented strain showed similar growth as the WT, but higher sensitivity on GYM (data not shown) and AM (Figure 33), although growth was still enhanced as compared to Δ*nreB*. This could be due to either methodological or functional factors. Firstly, the methods used for genetic manipulation of *S. mirabilis* itself could have several unwanted consequences. The insertion of the resistance cassette might influence the transcription of downstream genes. As resistance genes often cluster together, a negative effect on other resistance determinants cannot be excluded. Furthermore, for complementation *P16nreB* was not introduced in its original, plasmidal location, but at the chromosomal *attB* site of φC31 (see section 3.1), whereby its transcription could be differentially regulated, especially if *P16nreB* was part of a larger operon.

Furthermore, *nre* resistance determinants typically confer only a low level of Ni^{2+} resistance (Schmidt & Schlegel, 1994; Schmidt et al., 1991; Taghavi et al., 2001), which implied that at higher bioavailable Ni^{2+} concentrations the transport capacity of P16NreB might be saturated. This would explain the reduced growth of the complemented strain on AM containing 50 mM $NiSO_4$ (Figure 32), where less metal is chelated and thus a higher bioavailability can be expected. However, also on AM agar amended with 5 mM $NiSO_4$, Δ*nreB* pSEThphMFS growth was reduced as compared to the WT.

Regarding the media composition, also the carbon source or the availability of other compounds might influence Ni^{2+} transport. NreB-like proteins are thought to function as antiporters driven by the proton motive force (Nies, 2003; Pini et al., 2014). However, to the author's knowledge, this has never been investigated in detail. If the Ni^{2+} transport by P16NreB was dependent on the antiport or symport of a different substrate, media composition should strongly impact its capacity, resulting in a higher activity in more complex media like TSB.

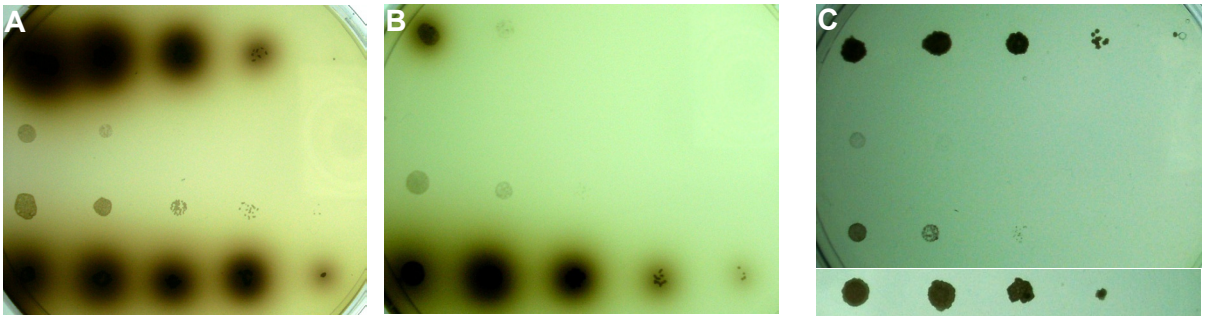

Figure 33. Drop plate assays with *S. mirabilis* (first row), Δ*nreB* (second row), Δ*nreB* pSEThphMFS (third row), P16 pSEThphMFS (last row) on TSB + 20 mM $NiSO_4$ (A), TSB + 25 mM $NiSO_4$ (B) and AM + 50 mM $NiSO_4$ (C).

Lastly, secondary, unintended changes on the genetic level that were induced by the knock-out procedure cannot be excluded. One definite side effect was the loss of the small *S. mirabilis* plasmid pI. As visible on the TSB plates (Figure 33), Δ*nreB* had lost the ability to produce the melanine-like component, which was attributed to pI loss. Potential Ni^{2+} resistance determinants coded on this plasmid might therefore be lost as well in the transformant additionally reducing its overall fitness, which could not be rescued by *P16nreB* re-introduction.

The increased sensitivity of Δ*nreB* to Ni^{2+} and also Co^{2+} (data not shown) was in accordance with other studies and the hypothesis that this transporter acts as Ni^{2+} and Co^{2+} efflux pump. Deletion of *nreB* in *Si. meliloti* slightly increased its sensitivity to $NiCl_2$ and $CuCl_2$ (Pini et al., 2014). The latter effect could not be observed in case of Δ*nreB*.

Tolerance of hydrogen peroxide and urease activity

Deletion of *P16nreB* additionally increased the strain's sensitivity to hydrogen peroxide. While the WT tolerated 30 ppm H_2O_2 in TSB liquid medium, the deletion strain only grew upto 15 ppm. As metal resistance and oxidative stress response are closely connected (Nies, 1999), the reduced Ni^{2+} efflux might enhance intracellular oxidative stress in Δ*nreB* rendering the strain more sensitive to oxidative agents. Since nickel serves as co-factor for several enzymes, the activity of the Ni-containing urease was tested in two assays. Firstly, the strain's sensitivity to urea was determined. In Δ*nreB* the tolerance to urea in liquid AM medium was reduced (450 mM) compared to the wild type (500 mM), while genetic complementation re-established WT level. Secondly, the urease activity in the protein extract of *S. mirabilis* WT and Δ*nreB* grown in TSB and GYM liquid medium for 4 d at 28°C was compared in a colorimetric assay (see section 2). In accordance with the urea sensitivity test, urease activity in the deletion strain was reduced by 40 % compared to the WT in both media tested.

These findings were contrary to effects caused by the deletion of *nreB* in *Si. meliloti* reported by Pini et al. (2014). An *nreB* deficient strain was more tolerant to urea due to increased urease activity, which was not caused by enhanced transcription of the enzyme, but most probably by a higher Ni^{2+} availability (Pini et al., 2014) as consequence of reduced metal efflux. Also in *Helicobacter pylori*, the deletion of the Ni^{2+} efflux transporters CznA and CznC resulted in an enhanced urease activity (Stahler et al., 2006), contrasting the obtained results for the P16NreB deficient strain.

Effect of a second P16nreB *copy in* S. mirabilis *WT*

In order to assess the contribution of P16NreB to the metal resistance of *S. mirabilis*, a second copy of *P16nreB* was introduced into the WT strain, identical to the complementation procedure used for the knock-out strain, yielding strain P16 pSEThphMFS. A slight increase of Ni^{2+} resistance was observed in liquid culture (Table 15) and also in trench plate tests on all tested media (Figure 32). The resistance to Co^{2+} only increased on AM and TSB medium, but not visibly on GYM. However, the gaining in metal resistance caused by a second NreB transporter gene was less pronounced than the resistance reduction in Δ*nreB*, which substantiated the hypothesis of secondary effects caused by the resistance cassette integration and/or the loss of pI. In drop plate tests *S. mirabilis* benefited from the additional *P16nreB* copy on TSB and GYM medium (Figure 33), but not on AM with 50 mM $NiSO_4$. P16 pSEThphMFS furthermore tolerated higher urea concentrations (550 ppm) than the WT (500 ppm), which was in accordance with the reverse effect caused by the deletion of *P16nreB*.

Biomass nickel content

The above described results were partly contradictory. On the one hand, deletion of *P16nreB* reduced the strain's resistance to Ni^{2+} and other stressors, leading to the assumption of an increased Ni^{2+} accumulation in the cytosol, but on the other hand urease activity was reduced, which would account for a reduced Ni^{2+} availability in the cell. Therefore, the Ni^{2+} content in the biomass of the wild type and Δ*nreB* grown in liquid GYM amended with $NiSO_4$ was determined.

Surprisingly, the Ni^{2+} content in the deletion strains was reduced (Figure 34). At 2 mM $NiSO_4$ the difference was statistically significant, while at higher Ni^{2+} concentration (2.5 mM), the deletion had less impact on the nickel content. There was no significant difference in the Co^{2+} content under both conditions (data not shown).

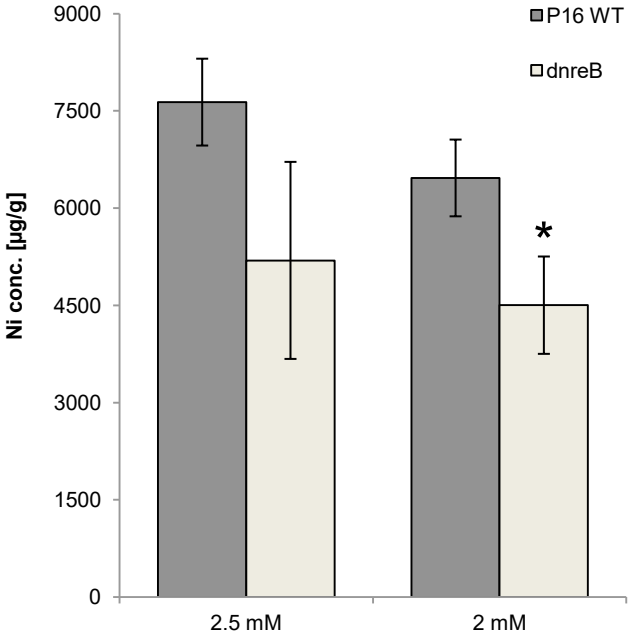

Figure 34. Nickel concentration in the biomass of *S. mirabilis* and Δ*nreB* when grown in liquid GYM supplemented with 2 mM or 2.5 mM $NiSO_4$ for 4 d at 28°C. Asterisk indicates significant difference (P=95 %). Bars show standard deviations derived from three biological replicates.

The reduced Ni^{2+} content in Δ*nreB* would account for the reduced urease activity. However, it was contradicting the reduced Ni^{2+} tolerance, as deletion of an efflux transporter should increase the metal concentration in the cytosol. For instance, for *Se. marcescens* NcrA it was shown that the overexpression of this NreB-like transporter in *E. coli* reduced Ni^{2+} and Co^{2+} accumulation (Marrero et al., 2007).

It was conceivable that the reduced cytosolic Ni^{2+} content in Δ*nreB* resulted from an increased activation of other Ni^{2+} efflux systems compensating P16NreB loss in this strain. The Ni^{2+} concentration in the liquid cultures used for biomass analysis was far below the tolerated limit to avoid growth stage-dependent differences between WT and the deletion strain. NreB-type transporters are known to confer a comparably low nickel resistance in other bacteria (Schmidt & Schlegel, 1994; Schmidt et al., 1991; Taghavi et al., 2001). Thus, P16NreB could be assumed a first line of defence against cytosolic Ni^{2+} stress, being active at low Ni^{2+} concentrations. Therefore, its loss had a stronger impact at low Ni^{2+} stress inducing activation of Ni^{2+} exporters with higher activity sooner, which would account for the statistically significant difference at lower $NiSO_4$ concentrations.

The absence of P16NreB would increase the intracellular Ni^{2+} content first, wherefore more Ni^{2+} could bind to nickel-specific transcriptional regulators which resulted in a higher expression of other, possibly more active Ni^{2+} efflux pumps, as compared to the WT, resulting in the observed lower Ni^{2+} content in Δ*nreB*. However, when the extracellular Ni^{2+} concentration and consequently also the cytosolic Ni^{2+} pool would reach a threshold, where all binding sites and transport capacity were saturated and no further activation could take place, the loss of P16NreB would negatively affect the growth of the deletion strain, resulting in an increased Ni^{2+} sensitivity, which showed in the resistance tests.

For substantiating this model, further biomass analysis would have to be conducted using different amounts of Ni^{2+} in the cultivation medium.

Effect of P16NreB expression on Ni-sensitive Streptomyces *sp. hosts*

For testing the function of P16NreB independently from potential *S. mirabilis*-specific biases, e.g. loss of pI, the transporter was heterologously expressed in the Ni^{2+} sensitive model strain *S. lividans* TK24. When delivered on an overexpression vector, P16NreB increased the resistance to Ni^{2+} and Co^{2+} (Figure 35). However, it was observed that *S. lividans* when harbouring pUWL201 and its derivative, showed in general reduced growth compared to the wildtype. Therefore, for further testing, P16NreB was introduced into *S. lividans* using pSEThph as vector, similarly to the above mentioned complementation approach. Since this vector had no promoter for insert expression, it offered the chance to test if transcription of *P16nreB* could also be initiated from its native promoter in a heterologous host.

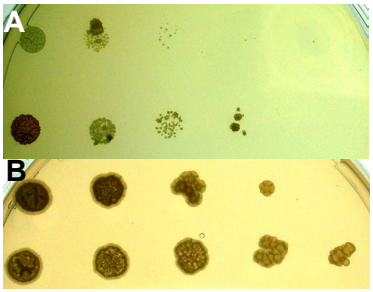

Figure 35. Drop plate assays on TSB containing 5 mM $NiSO_4$ (A) or 4 mM $CoSO_4$ (B) inoculated with TK24 pUWL201 (top) and TK24 pUWLMFS (below), with the later vector being a derivative of pUWL201 with *P16nreB* inserted.

Integration of *P16nreB* resulted in an increase in Ni^{2+} and Co^{2+} resistance in *S. lividans*, as observed in trench plate tests (Figure 32). Accordingly, the resistance in liquid medium strongly increased (Table 15). While the WT could only grew upto 0.75 mM $NiSO_4$ in AM medium, the transformant tolerated more than five times the amount of the metal (5 mM). In accordance with the above described results for *S. mirabilis*, *S. lividans* benefited most in minimal medium from the integration of the transporter regarding Ni^{2+} tolerance.

Comparing the Ni^{2+} resistance gaining in liquid culture between *S. mirabilis* and *S. lividans* when transformed with pSEThphMFS, the increase in resistance was more pronounced in *S. lividans* (Table 15). A difference of resistance level conferred by the same genetic determinant might be due to a differential regulation in both organisms, as regulatory functions govern gene expression (Liesegang et al., 1993). Schmidt et al. (1991) observed that when fragments of megaplasmids of *Ralstonia eutropha* strains 31A and KTO2 carrying Ni^{2+} resistance determinants were cloned into a metal sensitive *R. eutropha* strains, the level of resistance they conferred varied between strains. As *S. lividans* pSEThphMFS did not possess the complete pII plasmid, potential plasmidal regulatory genes did not influence *P16nreB* transcription. The fact that single plasmidal resistance determinants can be more effective when introduced in a heterologous host on their own, has been observed before (Schmidt et al., 1991).

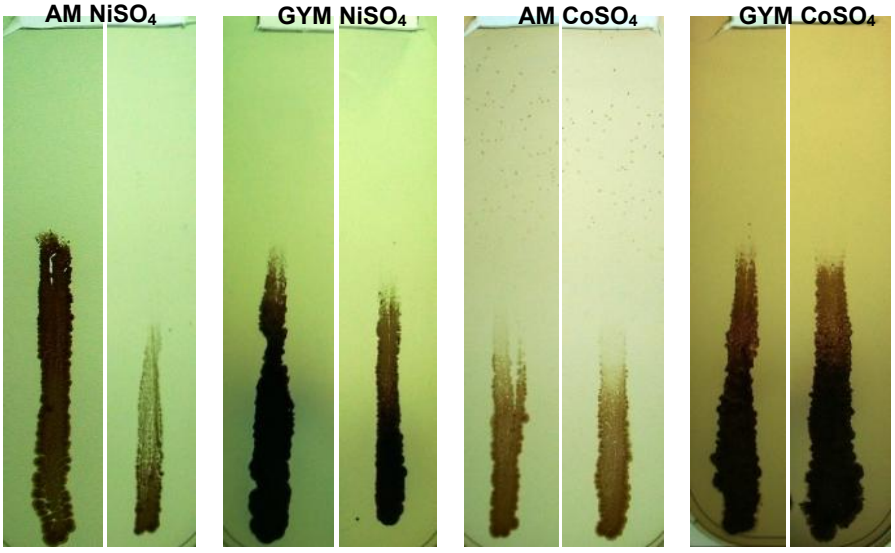

Figure 36. Trench plate assays with strains *S. lividans* (right) and transformant TK24 pSEThphnreBCosm (left) carrying a *S. mirabilis* plasmid pII fragment on which *P16nreB* was located. Plates were inoculated with 1 M metal stock solutions. Growth was evaluated after four weeks incubation.

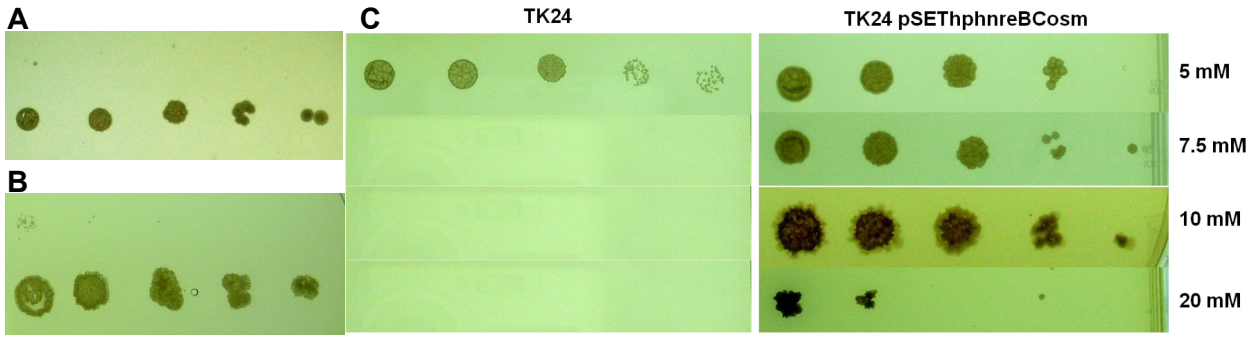

Figure 37. Left: Drop plate assays with *S. mirabilis* derivatives 489_3 (top) and 489_3 pSEThphnreBCosm (below) on GYM with 2,5 mM $NiSO_4$ (A) and TSB with 9 mM $NiSO_4$ (B). Right (C): Drop plate assay with *S. lividans* and *S. lividans* carrying the pII fragment nreBCosm on TSB medium containing different amounts of $NiSO_4$.

S. lividans and the plasmid-free *S. mirabilis* derivative 489_3 (see section 3.2) were furthermore transformed with a 3400 bp fragment of pII carrying *P16nreB* (nreBCosm; Figure 29) including the upstream located predicted transcriptional regulator KmtR using vector pSEThph for further confirmation of the importance of this plasmid fragment for the Ni^{2+} resistance conferred by pII. In both strains Ni^{2+} resistance markedly increased upon integration of this fragment. *S. lividans* pSEThphnreBCosm tolerated higher $NiSO_4$ concentrations on minimal and complex media in trench plate tests and could grow on TSB amended with 20 mM $NiSO_4$, while growth of the WT was omitted by 7.5 mM (Figure 37). Likewise 489_3, which was metal sensitive due to the loss of both native plasmids, showed markedly better growth in drop plate tests on different media when nreBCosm was integrated (Figure 37). Therefore, this plasmid section was considered a part of the *S. mirabilis* Ni^{2+} resistance machinery. Resistance to Co^{2+} was only slightly increased (Figure 36).

In section 3.2 it was shown that *S. mirabilis* plasmid pII, on which *P16nreB* was located, could be transferred to *S. lividans* rendering the strain more resistant to Ni^{2+}, Co^{2+} and Cu^{+}. In order to answer the question to what extend P16NreB contributed to the Ni^{2+} resistance conferred by pII, the complete *S. mirabilis* plasmid pII carrying the *P16nreB* deletion, was transferred to *S. lividans* by conjugation. Therefore, TK24 pP16pII and TK24 pP16pIIΔnreB could be directly compared, independent from the genetic background of the native host.

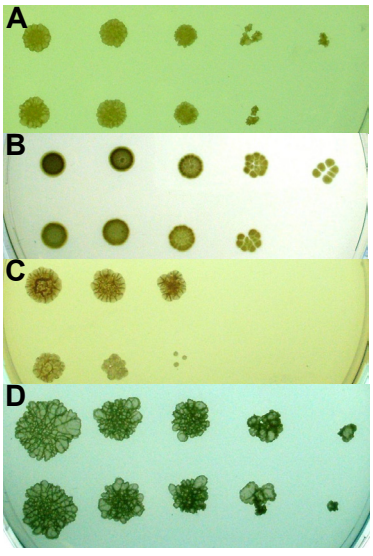

Figure 38. *S. lividans* carrying either pP16pII (top) or pP16pIIΔnreB (below) in drop plate assays on GYM + 2.5 mM $NiSO_4$ (A), AM + 1 mM $NiSO_4$ (B), TSB + 6 mM $CoSO_4$ (C) and 10 mM $CuSO_4$ (D)

Deletion of *P16nreB* decreased the Ni^{2+} resistance in liquid culture in different dimensions (Table 15). Particularly in AM medium resistance was reduced to a quarter (2.5 mM) of that of the strain harbouring the intact plasmid (10 mM), but was still higher than that of *S. lividans* WT (0.75 mM). Furthermore, *P16nreB* deletion slightly reduced the maximally tolerated Co^{2+} concentration (Table 15).

In drop plate tests a slight reduction in resistance to Co^{2+} and Ni^{2+} was observed in the transformant with *P16nreB* deletion, while Cu^{+} resistance was unaffected (Figure 37). This supported the hypothesis that P16NreB, like other *nre* homologues (Schmidt & Schlegel, 1994; Schmidt et al., 1991), was responsible for a low level of Ni^{2+} resistance. Furthermore, additional resistance deter-

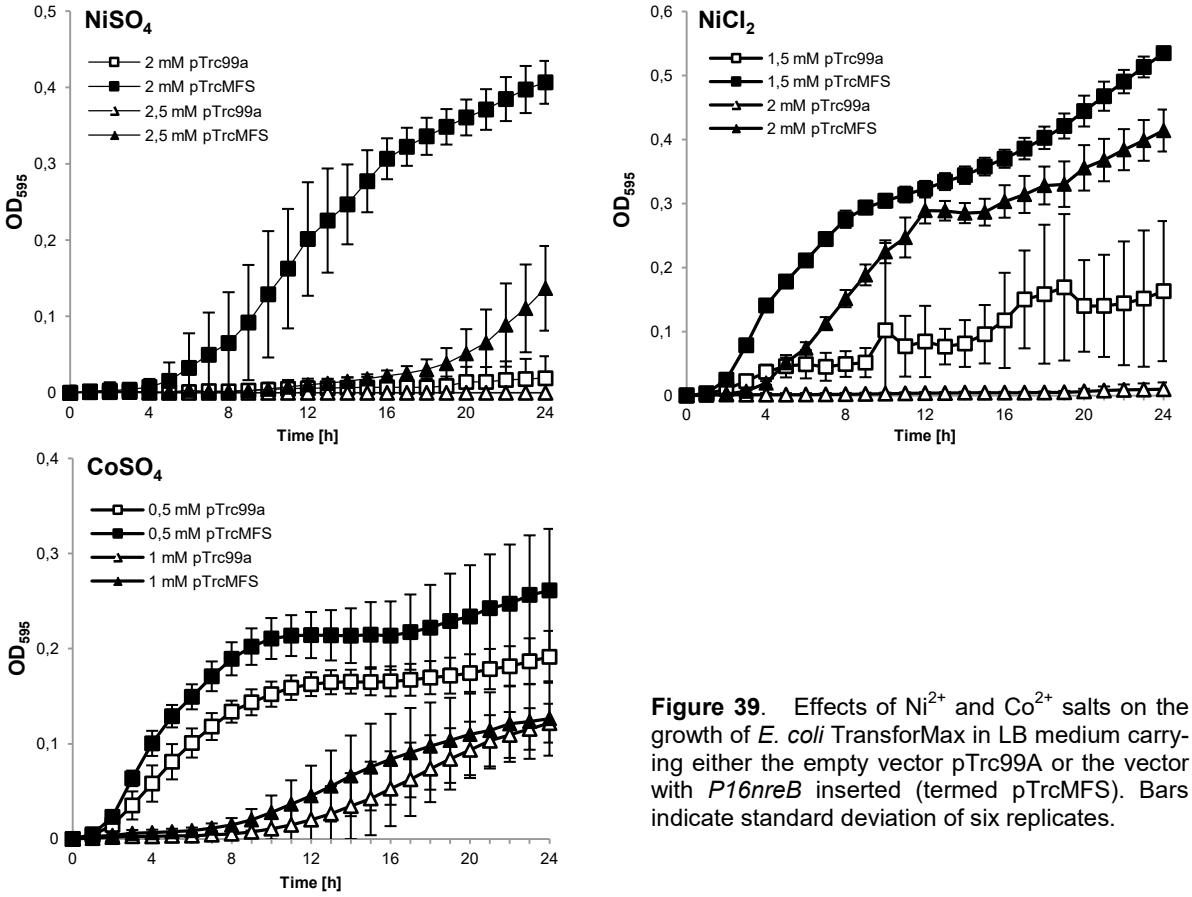

Figure 39. Effects of Ni^{2+} and Co^{2+} salts on the growth of *E. coli* TransforMax in LB medium carrying either the empty vector pTrc99A or the vector with *P16nreB* inserted (termed pTrcMFS). Bars indicate standard deviation of six replicates.

minants were expected on pII, since TK24 pP16pIIΔnreB still showed a markedly increased Ni^{2+} resistance compared to the WT.

Overexpression of P16NreB and the corresponding plasmid fragment in *E. coli*

P16NreB was introduced in *E. coli* for determining the substrate spectrum more in detail and demonstrating the functionality in a heterologous host other than *Streptomyces* sp. Expression of P16NreB delivered on pTrcMFS increased the resistance to Ni^{2+} and enabled growth at 2.5 mM $NiSO_4$ and 2 mM $NiCl_2$, where the empty vector control (pTrc99A) did not show growth (Figure 39). This growth range was well in accordance with other studies: NirA, the NreB homologue of *K. oxytoca*, enabled growth upto 3 mM $NiCl_2$ when expressed in *E. coli* (Park et al., 2008).

Regarding cobalt, P16NreB expression improved growth only slightly. For Cu^{+} no beneficial effect of P16NreB expression could be observed (data not shown). Therefore, P16NreB could be considered as mainly Ni^{2+}-transporting pump with a low affinity for cobalt.

After showing that P16NreB could be expressed in *E. coli*, the next step was to test whether it could also be transcribed from its native promoter, similar to the above described experiment for *S. lividans*. Promoter recognition in more distantly related species would be a prerequisite for conferring resistance to a larger variety of members of a natural community after transfer of the plasmid. Therefore, *E. coli* was transformed with pSEThphnreBCosm and growth under Ni^{2+} and Co^{2+} stress was tested. Figure 40 shows the growth curve of the empty vector control (pSEThph) and the plasmid fragment carrying strain in LB medium amended with either 1.25 mM $NiSO_4$ or 0.75 mM $CoSO_4$.

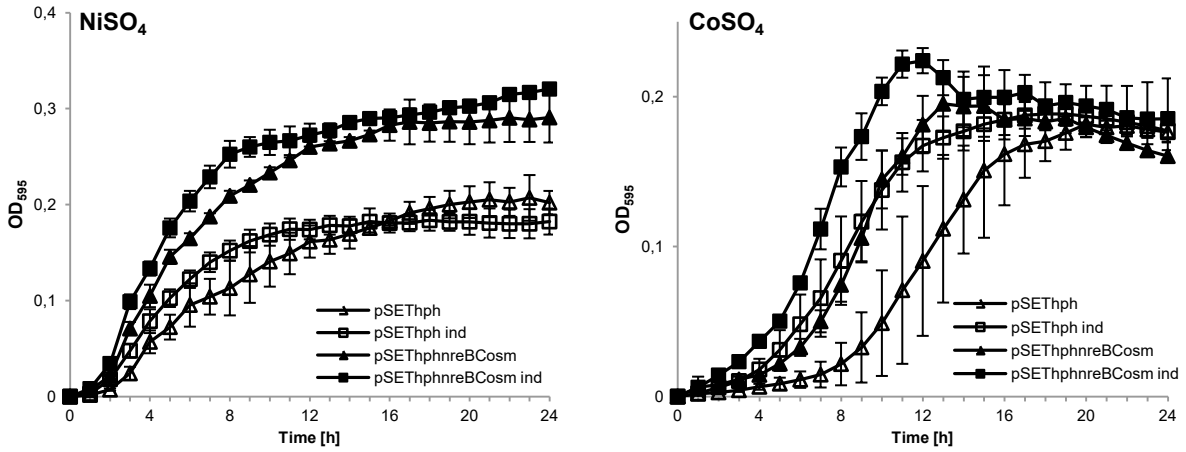

Figure 40. Growth curves of *E. coli* TransforMax in LB medium amended with either 1.25 mM $NiSO_4$ or 0.75 mM $CoSO_4$. Strains carried the empty vector pSEThph or this vector containing a fragment of *S. mirabilis* plasmid pII with the *nre* loci (nreBCosm). Pre-cultures were cultured in LB medium or LB medium containing 0.5 mM $NiSO_4$ ("ind"). Bars indicate standard deviation of six replicates.

The enhanced growth of *E. coli* pSEThphnreBCosm proved that *P16nreB* was indeed transcribed from its native promoter improving the tolerance to both tested metals. Therefore, this transporter should be functional in several genera and phyla.

The capability of transfer and expression of *nre*-type resistance determinants from one genus to another has already been observed (Schmidt & Schlegel, 1994; Stoppel et al., 1995; Taghavi et al., 2001), ascribing them a broad host range, which was in consent with the results of the present study. Due to this characteristic, the *nre* resistance determinant of *C. metallidurans* 31A has already been utilised for the construction of mini transposons and successfully applied in transformation of different bacteria, e.g. endophytic *Burkholderia* sp. and *Herbaspirillum* sp. (Lodewyckx et al., 2001; Taghavi et al., 2001). However, transcription of *P16nreB* was less effective from its native promoter, as the resistance level conferred was lower than in the pTrcMFS transformant.

Former studies of NreB homologues showed that their expression is inducible by Ni^{2+} (García-Domínguez et al., 2000; Grass et al., 2001; Park et al., 2003). For demonstrating a similar activation mechanism for *P16nreB* transcription, cultures of *E. coli* pSEThphnreBCosm and the control strain were pre-incubated over night in LB medium amended with 0.5 mM $NiSO_4$ and subsequently used in growth experiments as before. Pre-incubation with nickel slightly enhanced growth in the first 12 h of incubation in both strains to a comparable level (Figure 40). Therefore, this could be rather attributed to the activation of inherent *E. coli* resistance systems, like the Ni^{2+} and Co^{2+} efflux pump RcnA (Rodrigue et al., 2005) than P16NreB activation. However, since pSEThphnreBCosm only carried a small fragment of pII, regulatory elements might be coded in different loci on the plasmid. Ni^{2+}-dependent transcription activation could therefore not be excluded in the native plasmid.

Conclusion

The presented results substantiated that the plasmid encoded P16NreB was an exporter for Ni^{2+} with lower affinity for Co^{2+}, which conferred a low level of resistance to these metals. Nickel sensitive organisms benefitted from the presence of this transporter, which enabled growth at slightly elevated Ni^{2+} concentrations. However, its loss did not equivalently impaired growth of the *P16nreB* deletion strain, but merely resulted in a low decrease in Ni^{2+} and Co^{2+} resistance.

Transport and/or transcriptional regulation was clearly influenced by media composition. Either, P16NreB activity depended on the presence of other substrates, e.g. carbon sources, or the coding gene was under regulation of KmtR or NmtR, whose activities were shown in *M. tuberculosis* to be strongly dependent on the complexity of the medium used (Campbell et al., 2007). Hence, a control of *P16nreB* transcription by plasmidal encoded transcriptional regulators could be assumed.

P16NreB proved to be one Ni^{2+}/Co^{2+} resistance determinant of the *S. mirabilis* plasmid pII, among others. The fact that it could be expressed also in distantly related species made it a candidate for mediating heavy metal resistance in a variety of organisms within a natural community in case of spreading of pII, thus potentially impacting the community composition.

3.4 Plasmid-encoded components of the *S. mirabilis* copper resistome

Introduction

Copper is an essential micronutrient needed as structural element and for redox reactions, e.g. during respiration and electron transport. Its ability to cycle between the oxidation state Cu(I) and Cu(II) makes it an important cofactor in cuproenzymes, like laccases superoxide dismutases, cytochrome c oxidases and tyrosinases. Many cuproproteins are further involved in the homeostasis and storage of the element itself (Arguello et al., 2013; Rensing & McDevitt, 2013).

In *Streptomyces* sp., copper was found to be essential for the morphologic development, especially during the transition from vegetative to reproductive growth where it probably serves the developmental switch between growth stages (Fujimoto et al., 2012; Ueda et al., 1997).

Although copper is indispensable for a cell, free Cu(I) ions are highly reactive and have multiple detrimental effects if freely available in the cytoplasm. Copper can bind to free protein thiol groups and competes with other metals for protein binding sites, whereby proteins can be disrupted and inactivated. Furthermore, it damages phospholipids and nucleic acids (Ramirez et al., 2005; Yoshida et al., 1993). The improper binding of Cu(I) to iron-sulfur clusters not only interferes with important processes like amino acid synthesis, but also indirectly exerts oxidative stress due to the displacement and release of iron ions (Macomber & Imlay, 2009). In humans, an imbalance of copper homeostasis can cause serious diseases, like Menkes syndrome and Wilson's disease (Gupta & Lutsenko, 2009).

Due to these deleterious effects, bacterial cells have evolved numerous systems for tightly controlling the cytosolic copper concentration, thereby reducing its toxicity. The copper homeostasis machinery controls every step of copper trafficking in the cell and comprises Cu(I)-transporters that interact with Cu(I)-binding chaperones, metallothioneins and copper-dependent transcription factors (Arguello et al., 2007; Dwarakanath et al., 2012; Ma et al., 2009c; Solioz et al., 2010). Several of these systems have been characterized (for a review see Arguello et al. (2013)) and often bacteria possess several copper homeostasis systems. In *E. coli* three systems have been identified, called *cop*, *cue* and *cus* (Outten et al., 2001; Rensing et al., 2000).

A common and well characterized copper homeostasis system is the *cop* complex, e.g. described in *Enterococcus hirae* (Strausak & Solioz, 1997) *Pseudomonas* sp. (Lim & Cooksey, 1993), *Xanthomonas* sp. (Teixeira et al., 2008), *E. coli* (Rensing et al., 2000), *Lactococcus lactis* (Magnani et al., 2008) and *Listeria monocytogenes* (Corbett et al., 2011). The *Ent. hirae copYZAB* operon comprises four genes coding two copper ATPases (CopA, CopB), a copper responsive repressor (CopY) and a copper chaperone (CopZ) (Cobine et al., 1999; Odermatt et al., 1993; Strausak & Solioz, 1997). There has been some controversy regarding the function of CopB. While it was originally described as Cu(I) importer (Odermatt et al., 1993), later studies support the theory of CopB acting as exporter, but with a lower activity than CopA (Arguello et al., 2013; Lubben et al., 2009).

In any case, an integral part of the copper resistance machinery is the energy-dependent efflux of the metal *via* metal ATPases, which belong to the P_{1B}-type subgroup of the P-type ATPases superfamily. These couple the unidirectional efflux of Cu(I) to ATP hydrolysis for maintaining a stable Cu(I) level in the cytosol (Arguello et al., 2007; Solioz et al., 2010). Their expression is induced by elevated copper concentrations and cells lacking genes for these transporters show an increased copper sensitivity

(Macomber et al., 2007; Rensing et al., 2000). Besides Cu(I), Ag(I) was found to induce CopA and CopB expression in *E. coli* and *Ent. hirae*, which lead to the hypothesis that also this metal was transported (Odermatt et al., 1993; Rensing et al., 2000).

For directing copper ions to the appropriate ATPases or their point of use in the cell, specific copper chaperones are needed that bind their cognate metal tightly and escort it, whereby damage of the cell by free metal ions is prevented. In case of the *cop* operon, this task is accomplished by CopZ, a member of a family of copper chaperones that is highly conserved on Prokaryotes and Eukaryotes. It exhibits a characteristic MXCXXC metal binding motif that is responsible for transferring and exchanging Cu(I) with the transcriptional repressor CopY (Cobine et al., 1999; Cobine et al., 2002).

CopY is a copper-responsive transcriptional repressor controlling the transcription of *copA* and *copB* in *Ent. hirae*. It is released from the target DNA upon reception of two Cu(I) ions from CopZ, which displace two Zn(II) from the allosteric site (Cobine et al., 1999; Strausak & Solioz, 1997). Similar regulators are also found in *Lactococcus* sp., *Streptococcus* sp. and other bacteria. Rademacher & Masepohl (2012) distinguish nine classes of copper-sensing transcriptional regulators, three of which can be found in Gram-positive bacteria: CopY, YcnK and CsoR. The latter has also been investigated in *Streptomyces lividans*, where it represses the transcription of *copZA* and its own gene, *csoR* (Dwarakanath et al., 2012). CsoR was firstly described in *Mycobacterium tuberculosis*, where it is essential for the bacterium's fitness during host infection, and since then found in several other species. It probably competes with CopZ for Cu(I) and is known to regulate the transcription of different genes (Baker et al., 2011; Chillappagari et al., 2009; Corbett et al., 2011; Dwarakanath et al., 2012; Marcus et al., 2016).

Results

Computational analysis

Gene identification and location

In section 3.2 it was shown that the large *S. mirabilis* plasmid not only conferred resistance to nickel, but also to copper, although at a lower level. Therefore, the aim of the present section is to determine, which plasmidal genes might be involved in copper resistance.

In order to determine candidate genes, a search for homologues to known copper resistance determinants of the *cop* system was performed based on their DNA sequence, as this operon is commonly found in different bacterial and eukaryotic species (reviewed in Arguello et al. (2013)). In this way, several ORFs coding putative copper chaperones, copper transporting P-type ATPases and copper-sensitive operon repressors were identified on pII. In contrast to other known copper resistance determinants, e.g. from *Streptomyces lividans* 66 (Cruz-Morales et al., 2013) or *Pseudomonas syringae* (Feil et al., 2005), these genes were not organized in a single genomic island, but scattered all over the *S. mirabilis* plasmid.

Usually, genes of the *cop* operon are organized in the same operon allowing concerted transcription in response to elevated Cu(I) concentrations, although the organization of the genes varies between species. Exemplary *cop* operon structures are *csoR-copAZ* of *Listeria moncytogenes* (Corbett et al., 2011), *copSR-copABCD* of *Cupriavidus metallidurans* (Mergeay et al., 2003), *copRZA* of *Lactococcus lactis* (Magnani et al., 2008) and the *Deinococcus radiodurans csoR-copZ-copA*, where *copZ* and *copA* are arranged in opposing reading directions (Zhao et al., 2014).

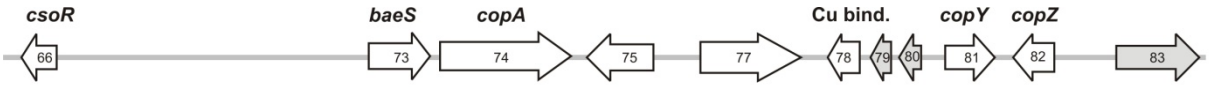

Figure 41. Gene location of putative copper resistance determinants on the large *S. mirabilis* plasmid. Genes of unknown function are shaded gray. Numbers indicate locus tags (SMI8166-SMI8183). For clearness, several genes, for which no function could be predicted, are not displayed.

Comparable gene arrangements were not found for most putative *cop* genes on the *S. mirabilis* plasmid, which were predominantly separated from each other by several thousand bases. Only in one case, *copZ* was located directly upstream of a gene for a Cu(I) exporting ATPase (SMI8202, SMI8203), as it is found in *Bacillus subtilis*, *Ent. hirae* and other organisms (Kihlken et al., 2002; Magnani et al., 2008; Odermatt et al., 1993). However, for closer examination of copper resistance genes, a loci with a more unusual organization was chosen, where the putative *copY* and *copZ* genes (SMI8181 and SMI8182) exhibited an antipodal reading direction, without a directly associated gene coding an ATPase (Figure 41). This arrangement is rarely found and similar to a *cop* operon present in *Streptomyces* sp. CdTB01 (ALV33142, ALV33143), a strain isolated from a metal contaminated site which exhibits high metal resistance (Zhou et al., 2016). Therefore, it was hypothesized that these genes may play a key role in regulation of copper homeostasis in *S. mirabilis*.

Protein characteristics

SMI8182 encoded a 97 aa CopZ-like protein with a mass of 9.3 kDa (Table 16) containing a heavy-metal associated domain (pfam00403), which is conserved in proteins for heavy metal transport and detoxification (cd00371). The protein exhibited 41 % identity to copper chaperones of *Listeria* sp. (WP_003762991), 36 % identity to *Bacillus subtilis* CopZ (O32221.1) and 29 % to *Staphylococcus aureus* CopZ (Q6GDP0.1). Compared to other well-investigated copper chaperones, that often have a size of around 70 aa and mass of about 8 kDa (Arnesano et al., 2001; Odermatt & Solioz, 1995; Radford et al., 2003), P16CopZ was slightly larger.

The highest identity on amino acid level (71 %) was observed with a heavy-metal-associated domain-containing protein *Streptomyces* sp. CdTB01 (WP_058922818). In the well-investigated copper homeostasis systems of *B. subtilis* and *L. monocytogenes*, CopZ binds intracellular Cu(I) and shuttles it to copper transporting P-type ATPases as well as transcriptional regulators, like CopY (Corbett et al., 2011; Radford et al., 2003), thereby serving detoxification of the cell. Accordingly, *copZ* is highly up-regulated after copper exposure (Zhao et al., 2014). The transfer of copper from these chaperones to the transcriptional regulator CopY has been investigated in detail in *Ent. hirae* (Cobine et al., 2002). By interacting with this transcriptional regulator, CopZ is directly involved in the regulation of copper homeostasis.

Table 16. Predicted characteristics of *P16copY*, *P16copZ* and their gene products.

	P16CopY	**P16CopZ**
Annotation	SMI8181	SMI8182
Gene size	309 bp	291 bp
GC content	66 %	68 %
Protein size	102 aa	97 aa
Mass	11.2 kDa	9.3 kDa
Pfam	pfam02583	pfam00403
COG	-	COG2608

CopY of *Ent. hirae* is the founding member of one out of two families of copper-sensing transcriptional regulators found in Gram-positive bacteria, known so far (Ma et al., 2009c; Odermatt & Solioz, 1995). The other family being CsoR-like regulators, which have been identified in *M. tuberculosis*, *B. subtilis*, *D. radiodurans* and others (Liu et al., 2007; Smaldone & Helmann, 2007; Zhao et al.,

2014). Both families comprise transcriptional repressors that regulate the expression of proteins of the *cop* operon and other loci, whose products are often of unknown function (Festa et al., 2011; Rademacher & Masepohl, 2012).

The predicted gene product of *P16copY* was a 102 aa protein of 11.2 kDa (Table 16) that was classified as metal-sensitive transcriptional regulator CopY of the homonymous family whose members are involved in the regulation of genes for Cu(I) homeostasis by derepression of transcription upon binding of the cognate metal (pfam02583). However, also a conserved domain of CsoR-family proteins was detected (cd10148). P16CopY shared the highest amino acid level identity with CsoR-family members: 62 % with the copper-sensing transcriptional repressor RicR (62 %) of *Mycobacterium tuberculosis* (O07434.1), CsoR (48 %) of *B. subtilis* (O32222.1) and RcnR (36 %) of *Salmonella enterica* (A9MRK3.1).

RicR (regulated in copper repressor) is a paralogue of CsoR in *M. tuberculosis* and the second transcriptional repressor described in this bacterium that releases from its target DNA at elevated Cu(I) concentration. It regulates the transcription of five loci, some of which are of unknown function (Festa et al., 2011).

Taken together, the analysis of the predicted protein sequences of P16CopZ and P16CopY confirmed the results of the DNA-level search for *cop* operon homologues, classifying the proteins as copper chaperone and Cu-dependent transcriptional regulator, although on amino acid level P16CopY showed no significant similarity to other CopY-family proteins but rather CsoR-family repressors.

For both proteins, significant similarity to *B. subtilis* proteins was observed, which belong to the same operon of *B. subtilis*, *copZA*, under control of CsoR (NC_000964.3), the only known Cu(I) efflux system in this species (Gaballa et al., 2003). This operon comprises the minimal number of constituents necessary for copper resistance in Gram-positive bacteria: a chaperone (CopZ), the transcriptional regulator (CsoR) and an efflux ATPases (CopA).

Alignment – P16CopZ

The overall sequence variability of bacterial copper chaperones was found to be high, but the degree of sequence conservation usually increases around the metal binding site (Arnesano et al., 2002). An alignment of the amino acid sequence of P16CopZ with other CopZ-like chaperones revealed a region of high congruence between residues 31 and 38 which contained the metal-binding residues M32, T33, C34 and C37 (Figure 42). These were part of the characteristic metal binding motif MXCXXC found in chaperones and metal-transporting ATPases (Arnesano et al., 2002; Cobine et al., 2002; Drees et al., 2015; Radford et al., 2003). Thus, they were mostly conserved in all considered CopZ proteins, being an important requisite for functioning as a chaperone. The importance of the Cys residues in this motif for copper transport has been shown for the *Saccharomyces cerevisiae* copper chaperone Atx1 and *B. subtilis* CopZ (BsCopZ), as Cu(I) is bound between these residues, wherefore substitution by Ser reduces the capacity for metal binding (Arnesano et al., 2001; Kihlken et al., 2002).

From the alignment, an expanded consensus for the displayed bacterial CopZ proteins could be inferred distinguishing these proteins from eukaryotic and archaean CopZ: GM(T/S)CXHC. The fact that this complete sequence was not conserved in non-bacterial chaperones should not differentiate the proteins regarding their capacity for metal binding as the Met residue in the second position was shown to be dispensable for copper binding, but probably required for the stabilization of the metal

binding loop during hydrophobic interactions (Arnesano et al., 2002). Thus, the CXXC motif is the minimal consensus for metal binding (Pufahl et al., 1997; Sazinsky et al., 2007; Wimmer et al., 1999).

The presence of this metal binding motif in P16CopZ was most probably the reason for the incorrect initial annotation of this protein as metal-transporting ATPase, since metal chaperones as well as ATPases have metal-binding domains with high homology, as observed for the *Archaeoglobus fulgidus* chaperone (AfCopZ) and the corresponding CopA (Gonzalez-Guerrero & Arguello, 2008). The CopA protein of *E. coli* comprises two metal-binding domains, one of which is functioning analogously to metallochaperones by binding and shuttling Cu(I) to the ATPase (Drees et al., 2015).

The overall sequence identity of P16CopZ was highest with *Streptomyces* sp. CdTB01 CopZ (SsCopZ) (Figure 42), as was expected considering their close phylogenetic distance. Both proteins shared an N-terminal tail of 21 residues which was not found in the other bacterial CopZ. This tail might be a feature specific to actinomycete CopZ proteins, as BLASTP search for this particular amino acid stretch solely yielded similar sequences in *Streptomyces* sp., *Kitasatospora* sp. and *Rhodococcus* sp.

The only CopZ homologue for which an N-terminal tail has been reported is AfCopZ (Sazinsky et al., 2007). However, this tail is longer (115 aa) and showed no homology to the *Streptomyces* sp. proteins, wherefore it is not completely displayed in the alignment. This tail enables AfCopZ to bind an additional copper ion, as it is rich in Cys and contains a [2Fe-2S] cluster (Gonzalez-Guerrero & Arguello, 2008; Sazinsky et al., 2007). Furthermore the iron-sulfur cluster is redox-active and can reduce Cu(II) to Cu(I), an activity that has not been found in other copper chaperones (Sazinsky et al., 2007).

The additional N-terminual sequence of the *Streptomyces* sp. proteins contained likewise a high number of potentially metal binding residues (Cys, His, Asp), but no [2Fe-2S] cluster was identified. It is possible, that this tail increases the affinity for metal binding or may stabilize a bound Cu(I) ion.

For delivering Cu(I) to the ATPases, copper chaperones interact with CopA proteins. This interaction

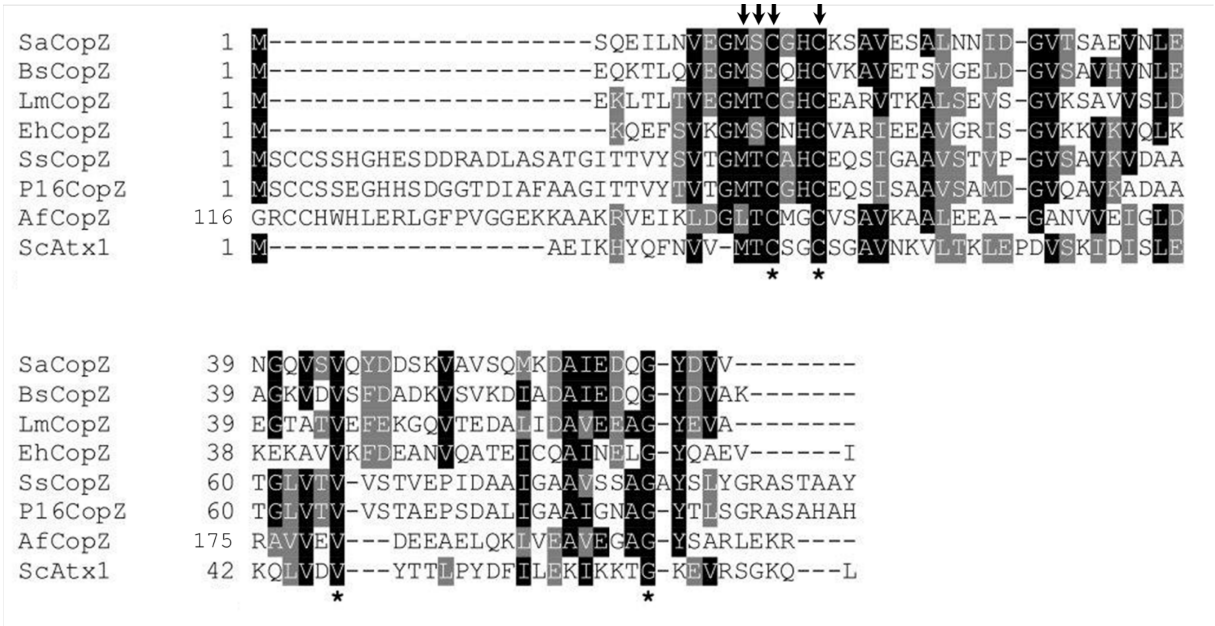

Figure 42. Amino acid sequence alignment of the plasmidal P16CopZ and other bacterial CopZ proteins (from , as well as the eukaryotic ScAxt1 and archeal AfCopZ. Arrows indicate residues responsible for metal binding and asterisks mark residues which are identical in all sequences. (Sa - *Staphylococcus aureus*, Bs - *Bacillus subtilis*, Lm - *Listeria monocytogenes*, Eh - *Enterococcus hirae*, Ss - *Streptomyces s*p. CdTB01, Af - *Archaeoglobus fulgidus*, Sc - *Saccharomyces cerevisiae*)

has been characterized for several systems, e.g. in *B. subtilis* and *A. fugidus* (Gonzalez-Guerrero & Arguello, 2008; Radford et al., 2003). In the latter, CopZ directly transfers Cu(I) to the transmembrane metal-binding site of CopA. The recognition and metal transfer between both proteins is enabled by hydrogen bonding, as well as electrostatic and hydrophobic interactions (Arnesano et al., 2002).

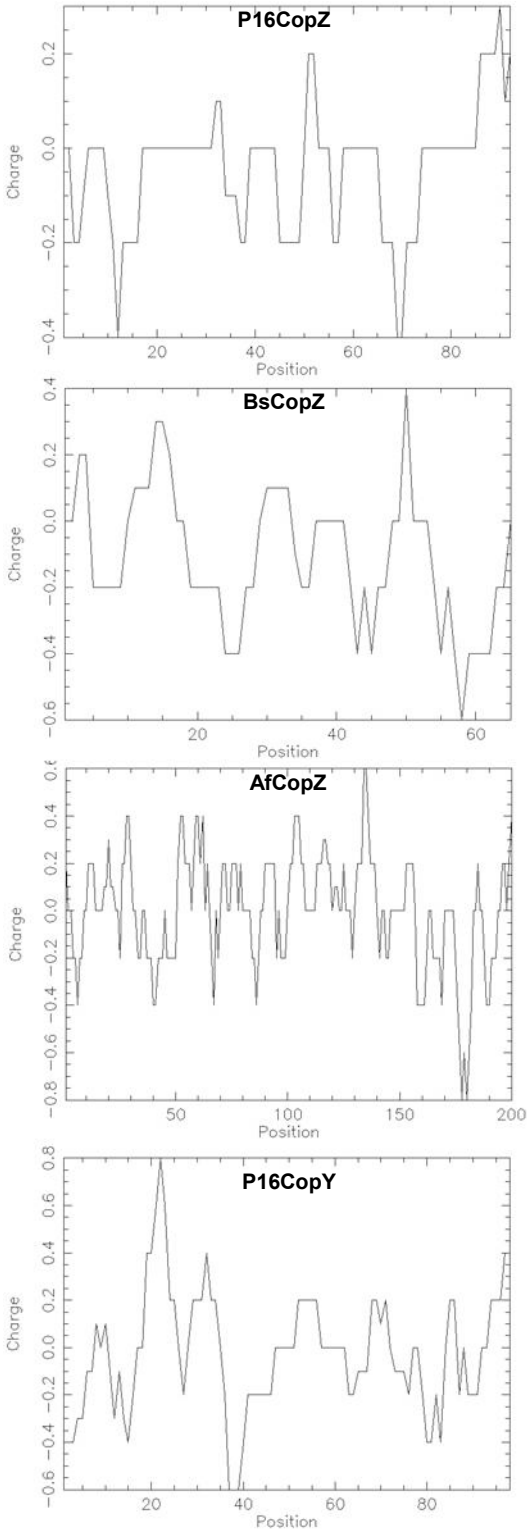

Figure 43. Charge plots of bacterial copper chaperones and the putative copper-dependent regulator P16CopY.

For this interaction, charged residues on the chaperone surface were found to be important. Wimmer et al. (1999) hypothesized that the uneven distribution of charges on the EhCopZ surface might serve as recognition site for other proteins. These polar residues were not conserved in any herein considered protein, but as the overall charge is important, amino acid identity would not be required. For better comparability of the charge distribution, charge plots were generated for P16CopZ, BsCopZ and AfCopZ (Figure 43). Here, it became apparent that the charge distribution as well as the level of charge differed between these proteins. P16CopZ had less charged regions than the other two proteins, while AfCopZ showed more and higher peaks, indicating an uneven strong charge distribution, which might be important for protein interactions.

Most CopZ homologues exhibited a negatively charged C-terminus, which showed in the alignment and the charge plots. Although the residue positions were not well conserved, the overall tendency for negatively charged residues (Asp, Glu) was apparent in all proteins, but the two *Streptomyces* sp. CopZ proteins P16CopZ and SsCopZ (Figure 41). While in these two proteins only two negative C-terminal residues were present, the other CopZ had five to seven in the corresponding amino acid stretch. It is conceivable that the negative C-terminus plays an important role in the interaction of the chaperone with Cu(I) transporters or transcriptional regulators, like CopY (Wimmer et al., 1999). In AfCopZ the negative residues of the C-terminal platform interact with positive residues of CopA (Padilla-Benavides et al., 2013). Mutation of residues in one of the negatively charged AfCopZ surface patches prevented this interaction, abolishing transfer of Cu(I) to the ATPase (Padilla-Benavides et al., 2013). A similar role for interaction could be assumed for the C-terminal end of P16CopZ, although with different charge distributions than for the mentioned examples, as it was hypothesized for the differently charged BsCopZ and yeast Atx1 (Arnesano et al., 2002).

Regarding the protein's tertiary shape, solution structures of several CopZ proteins are known, which all share a "ferrodoxin-like" fold with four beta-strands and two alpha-helices connected by loops (Arnesano et al., 2002; Arnesano et al., 2001; Wimmer et al., 1999). A detailed computational comparison of chaperone structures can be found in Arnesano et al. (2002). The studies revealed that CopZ assembly varies between species. EhCopZ and BsCopZ associate into homodimers upon Cu(I) binding (Kihlken et al., 2002; Wimmer et al., 1999). A similar assembly could be assumed for P16CopZ.

Alignment – P16CopY

From the alignment of P16CopY with CsoR family proteins (Figure 44) it became obvious that P16CopY was more similar to CsoR-like regulators, especially *Mycobacterium tuberculosis* RicR (MtRicR) which was expectable regarding the closer phylogenetic relationship.

The task of metalloregulators is the modulation of transcription of an operon in response to metal concentration. Therefore, two sites are of utmost importance for proper functioning of these proteins: a site for the recognition of the cognate metal and residues that control the consequential allosteric switching that leads to the derepression of transcription. In P16CopY both of these essential sites could be identified by conserved domain search: The metal-binding motif comprised residues C44, H69 and C73, which were also conserved in other CsoR-like regulators in the alignment, as they are responsible for Cu(I) coordination. Substitution experiments with *Listeria monocytogenes* CsoR, MtRicR and MtCsoR with residues corresponding to C44 and H69 in P16CopY rendered the regulators unable to sense Cu(I) and thereby abolished the Cu(I)-dependent regulation (Corbett et al., 2011; Liu et al., 2007; Shi et al., 2014).

The His residue in position 69 of P16CopY was a multifunctional residue that was also involved in the control of the allosteric switching (Liu et al., 2007; Ma et al., 2009b), besides Y43 and E90. From studies of MtCsoR and *B. subtilit* CsoR (BsCsoR) it is known that these residues are necessary for the modulation of the DNA-binding region of the regulator (Liu et al., 2007; Ma et al., 2009a; Smaldone & Helmann, 2007). Accordingly, substitution of the Glu residue of this motif by Ala abolished the Cu(I)-dependent release of the repressor from the operator (Ma et al., 2009a).

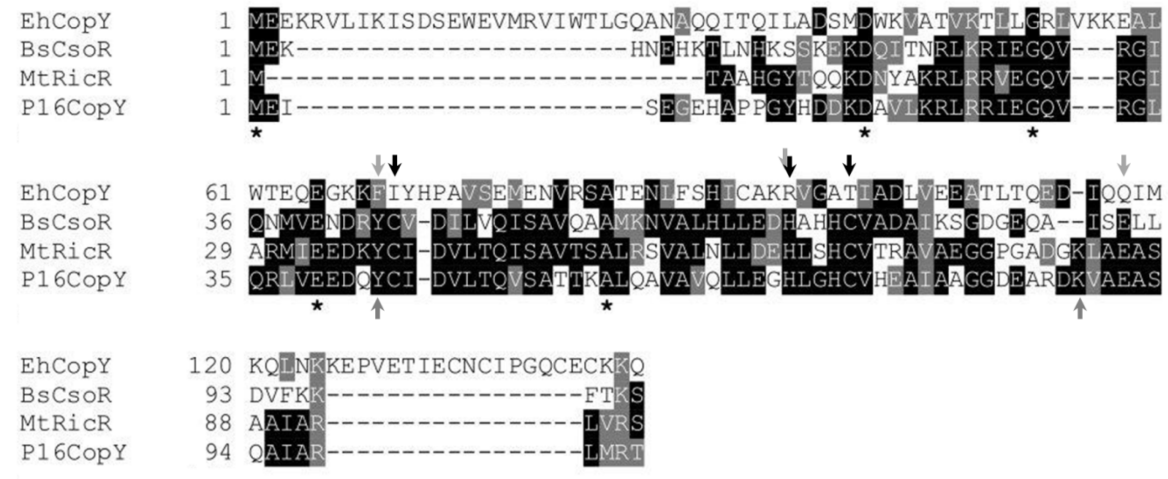

Figure 44. Amino acid sequence comparison of bacterial Cu(I)-responsive regulators. Black arrows indicate residues of the metal binding motif and gray arrows above the sequences indicate residues involved in allosteric switching of CsoR-like proteins. Arrows below sequences indicate second coordination shell residues. Asterisk mark residues that are identical in all sequences. (Bs - *Bacillus subtilis*, Eh - *Enterococcus hirae*, Mt - *Mycobacterium tuberculosis*)

These characteristic metal-binding and allosteric switch controlling motifs were not present in EhCopY, which supported the hypothesis that P16CopY rather belonged to the CsoR family of metalloregulators. The metal binding site of EhCopY is a CXCXXXXCXC motif located at the C-terminus of the protein, similar to that of metallothioneins (Cobine et al., 2002; Odermatt & Solioz, 1995), which was absent in the CsoR-type regulators. Hence, it was expected that for P16CopY metal binding as well as DNA binding and release would work similarly to the mentioned CsoR regulators.

Phylogenetic affiliation of P16CopY

As the alignment suggested that P16CopY was a CsoR-like transcriptional repressor a phylogenetic comparison of this protein with other members of this family was conducted. CsoR homologues can be divided in seven major clades, which are found in many species and also include non-copper-sensing regulators, e.g. RcnR and InrS (Chang et al., 2014). Proteins from all groups share the metal-binding motif, which was in accordance with the above describe alignment result. However, they can be distinguished by features outside this motif, e.g. N- and C-terminal extensions and specific conserved residues that determine clade-specific interactions (Chang et al., 2014).

P16CopY clustered with other *Streptomyces* sp. CsoR-like proteins (*S. coelicolor* and *S. lividans* CsoR) in group III of the regulator family, which was in accordance with the high sequence similarity to MtRicR seen in the alignment. All group III members in this analysis shared a Lys residue as the second out of two second coordination shell residues (K88 in P16CopY, Figure 44), a position occupied by a Glu residue in other CsoR-like proteins (Chang et al., 2014).

MtRicR is the best investigated regulator of this group. Genes belonging to the RicR regulon in *M. tuberculosis* are exclusively found in pathogenic mycobacteria, except for the regulator gene itself. They are important for copper tolerance, although the exact mechanisms are yet unknown (Shi et al., 2014).

It was hypothesized that the groups probably have differences in pathways of allosteric communication, as amino acid substitutions of corresponding residues in MtCsoR (group I) and LmCsoR (group IV) had different effects (Corbett et al., 2011; Guerra & Giedroc, 2012; Ma et al., 2009b). The phylogenetic analysis therefore showed that deductions for P16CopY regulatory mechanisms could hardly be drawn from MtCsoR or BsCsoR, as they belonged to other clades.

P16CopY structure

CopY- and CsoR-like regulators do not only differ in regard to their metal binding motif, but also in their tertiary structure and binding specificity: while CopY adopts a winged helix conformation and is Cu(I) specific, CsoR forms an alpha-helical bundle and can also bind other heavy metals, like Ni^{2+}, Co^{2+} and Zn^{2+}, although this binding does not result in transcriptional derepression (Ma et al., 2009a; Ma et al., 2009c). It seemed likely that also P16CopY would show the characteristics of the latter group, as the helix-turn-helix domain of EhCopY was not identified in P16CopY.

P16CopY was expected to be a putative interaction partner of P16CopZ, since the genes for both proteins seemed to be associated. The exchange of Cu(I) between a chaperone and a transcriptional regulator has been already demonstrated in *Ent. hirae* (Cobine et al., 1999). As stated above, surface charges were proposed to be essential for this interaction. In order to identify putative complementary charged sites in P16CopY to P16CopZ, a charge plot was generated (Figure 43). The charge distribu-

tion in P16CopY was more uneven than in P16CopZ with more positive residues near the N-terminus, followed by a negative peak around the predicted metal binding site, which was required for binding of electropositive copper ions. The steep charge difference in the N-terminal part of P16CopY might enable an electrostatic interaction with the C-terminus of P16CopZ, where a more negative amino acid stretch is followed by a positive region.

Of course, the primary amino acid sequence only provides limited insight into the charge distribution, as the tertiary protein structure is of utmost importance in this regard for enabling protein interactions, which could not be inferred from the charge plot. However, for *S. lividans* CsoR (SlCsoR), which was highly similar to P16CopY (Figure 45), an electropositive surface area running diagonally across the regulator was identified as contact site with the DNA (Tan et al., 2014). As the charge plot of SlCsoR (data not shown) was very similar to that of P16CopY, a similar charge distribution and accordingly identical DNA binding characteristics were assumed.

CsoR of *B. subtilis* was shown to adopt a tetrameric structure (Ma et al., 2009a), while MtCsoR forms homodimers, where each monomer can bind one molar equivalent of Cu(I) (Liu et al., 2007). Also for SlCsoR a dimerization was observed (Tan et al., 2014), wherefore P16CopY likely adapted this conformation as well.

Effect of *P16copY* and *P16copZ* deletion on heavy metal resistance and copper accumulation

For studying the role of P16CopY and P16CopZ in the copper resistance system in *S. mirabilis*, the corresponding genes were deleted individually by targeted gene replacement, yielding strains Δ*copY* and Δ*copZ*. Subsequently, the heavy metal resistance of the deletion strains was tested on plates and

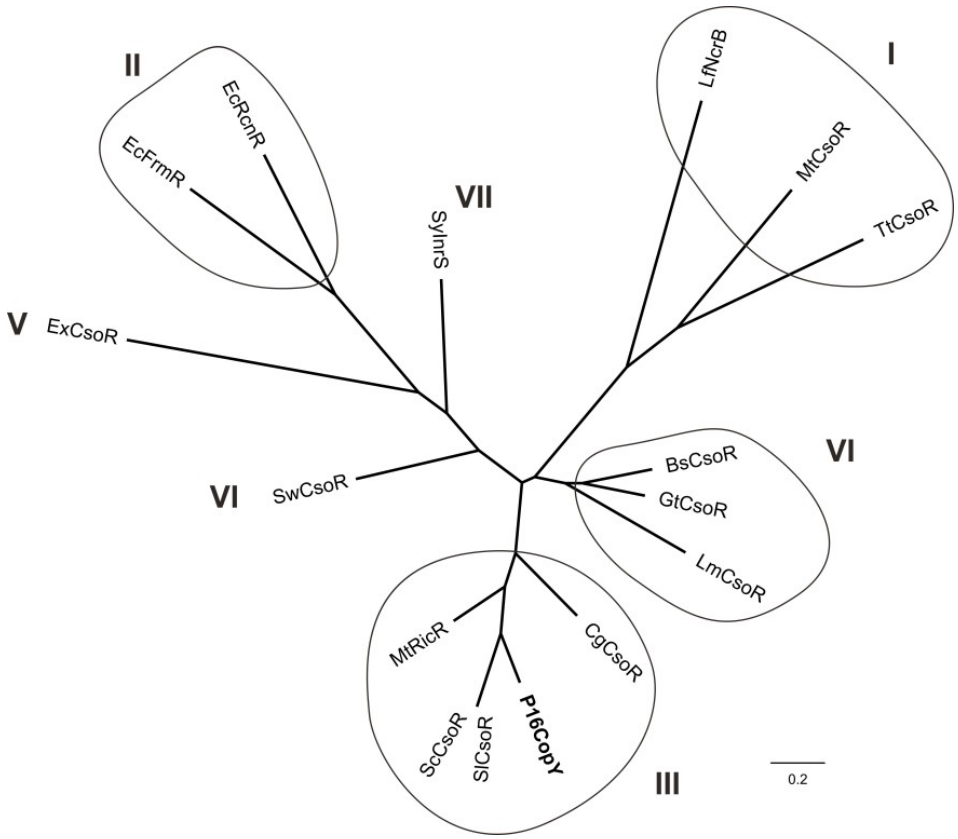

Figure 45. Unrooted phylogenetic tree of CsoR-like family proteins and two putative CsoR-like regulators of *S. mirabilis* with group affiliations (I-VII) according to Chang et al. (2014).

in liquid culture using different media. Besides copper, nickel resistance has been used to evaluate the general response to heavy metal stress. This might furthermore give hints on (i) potential cross-regulation of other metal resistance genes by P16CopY and (ii) the potential binding of metals other than Cu(I) by P16CopZ.

P16CopY

S. mirabilis Δ*copY* showed no apparent change in resistance to Cu(I) or Ni^{2+} on plates (Figure 46). However, in liquid culture the resistance to Cu(I) increased, particularly in AM and GYM, where the deletion strain tolerated almost double the amount of $CuSO_4$ than the WT (Table 17), and more biomass was produced (evaluation by eye). The increase in tolerance in TSB was not as high, probably due to the high $CuSO_4$ concentrations already tolerated by the WT. The increased resistance was comparable to that observed in *Mycobacterium tuberculosis* upon deletion of either MtRicR or MtCsoR (Festa et al., 2011; Marcus et al., 2016), where in the later case, the bacterium tolerated double the amount of Cu(I) in the growth medium as compared to the WT (Marcus et al., 2016).

On the contrary, resistance to nickel decreased in liquid culture (Table 17). To the author's knowledge, there is no study testing changes of resistance to nickel in *csoR* deletion strains or on how nickel influences the CsoR-dependent copper resistance machinery.

The mechanisms underlying the CopY-dependent regulation are well investigated (Cobine et al., 1999; Portmann et al., 2004; Solioz et al., 2010): in the DNA-bound state Zn^{2+} is bound to the repressor. At elevated Cu(I) levels, the Zn^{2+} is replaced by Cu(I), whereby the DNA affinity of the regulator is reduced causing the dissociation of the CopY-DNA complex (Solioz et al., 2010). However, the functioning of CsoR family repressors is less well investigated. These regulators probably apply a mechanism different from that of the CopY-type proteins, as in the later a Zn atom is bound to the C-terminal metal-binding motif, which is absent in CsoR (Cobine et al., 1999; Strausak & Solioz, 1997). In how far other metals may play a role in CsoR-dependent regulation can thus hardly be predicted. Evaluating the role of nickel or other heavy metals in this system could therefore help understanding the underlying mechanisms.

The deletion strain accumulated less copper than the wildtype when grown in liquid GYM amended with 1 mM $CuSO_4$ (Figure 47). This was in accordance with the hypothesis of P16CopY being a transcriptional repressor of operon(s) involved in Cu(I) efflux, as *P16copY* deletion should result in a constitutive expression of these operons, whereby Cu(I) accumulation is reduced and resistance increased. Similar findings were reported when *copY* was deleted in *Ent. hirae* and *csoR* in *B. subtilis*. In both cases the according *cop* operon (*copAB* and *copZA*) was constitutively expressed leading to a tolerance of higher copper levels (Odermatt & Solioz, 1995; Smaldone & Helmann, 2007). Therefore, a similar role for P16CopY in the strain's copper resistome can be

Table 17. Maximally tolerated $CuSO_4$ concentration [mM] in liquid culture using different media. Growth was determined after 14 d.

	TSB	**GYM**	**AM**
S. mirabilis P16	11	2.5	1.25
Δ*copY*	13	4	2
Δ*copZ*	10	2	1
S. lividans TK24	9	2.5	0.5
TK24 pSEThphCuP2Cosm	8	2	0.5
TK24 pUWL201	8	1.2	0.8
TK24 pUWLCopZ	8	0.6	0.8
489_3	11	2.5	1.4
489_3 pSEThphCuP2Cosm	10	2	1.3

assumed.

The comparably small increase in copper resistance hinted on other CsoR-family repressors encoded either on the genome or the plasmids of *S. mirabilis* substituting for the loss of P16CopY. However, while the copper content in the Δ*copY* biomass did not decrease in a statistically significant level, a significant difference was seen for Ni^{2+} (Figure 47). Although nickel resistance was reduced in Δ*copY* (Table 18), the deletion strain accumulated less Ni^{2+} than the WT.

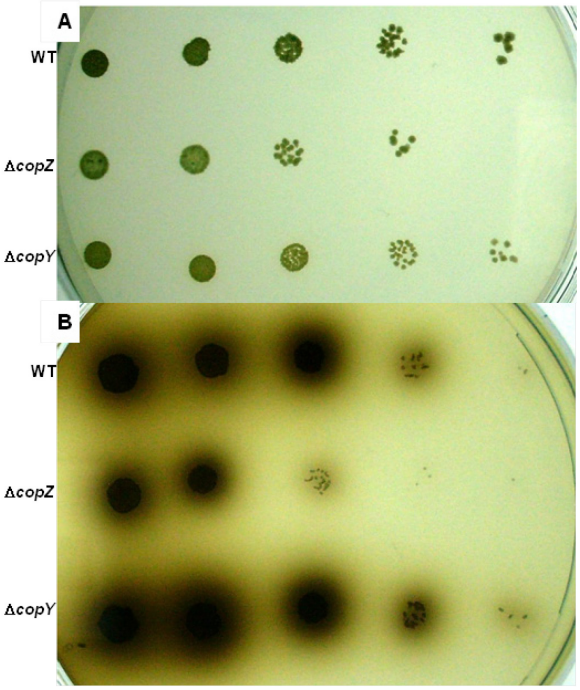

Figure 46. Drop plate tests of *S. mirabilis* WT and deletion strains on AM with 1 mM $CuSO_4$ (A) and TSB with 20 mM $NiSO_4$ (B).

P16CopZ

In contrast to *P16copY*, deletion of the gene encoding the copper chaperone P16CopZ resulted in an increased sensitivity to Cu(I) and Ni^{2+} on plates and in liquid culture (Figure 46, Table 17). Regarding copper, this effect could be mostly attributed to the loss of the buffering capacity of the chaperone. Incoming Cu(I) remained freely in the cytosol and was less efficiently transported to CopA or other places of action. For BsCopZ it was shown that the chaperone itself contributes to copper tolerance, although the metal buffering capacity of the protein is redundant (Drees et al., 2015; Radford et al., 2003). Odermatt & Solioz (1995) found that in *Ent. hirae* the disruption of *copZ* suppressed the expression of CopA and CopB, leading to an increased copper sensitivity. Therefore, P16CopZ might also affect the expression of efflux pumps, wherefore the sensitivity to this metal increased, possibly because Cu(I) was less efficiently transported to the transcription repressors, e.g. P16CopY.

Interestingly, the copper content in the biomass of the deletion strain decreased in a level comparable to the Δ*copY* strain (Figure 47). This first seemed contradictory, since a lower intracellular metal content should lead to a higher tolerance of copper, which was not the case (Table 17). However, this finding was in line with other studies, as in *B. subtilis*, the deletion of *copZ* lead to a slight decrease in resistance and a significantly lower number of Cu(I) atoms per cell (Radford et al., 2003). These observations could be explained with the binding and sequestration of Cu(I) by the chaperone in the wild type, as soon as Cu(I) entered the cell with less harmful effects than when remaining in solution. Thereby, intracellular copper levels were increased, but in the CopZ-bound state copper was less reactive, allowing a longer retention time of the ions in the cell. The loss of P16CopZ left Cu(I) in an unbound state, where it was highly reactive inducing oxidative stress and damage. Therefore, even lower intracellular copper content exerted a higher toxicity in the deletion strain. Thus, the loss of the sequestering function of P16CopZ reduced the storage of Cu(I) in the cell.

Table 18. Maximally tolerated $NiSO_4$ concentration [mM] in liquid culture. Growth was determined after 14 d.

	TSB	GYM	AM
S. mirabilis P16	35	12.5	45
Δ*copY*	25	9	22.5
Δ*copZ*	25	10	27.5
TK24 pUWL201	6	0.65	0.75
TK24 pUWLCopZ	5	0.5	0.6

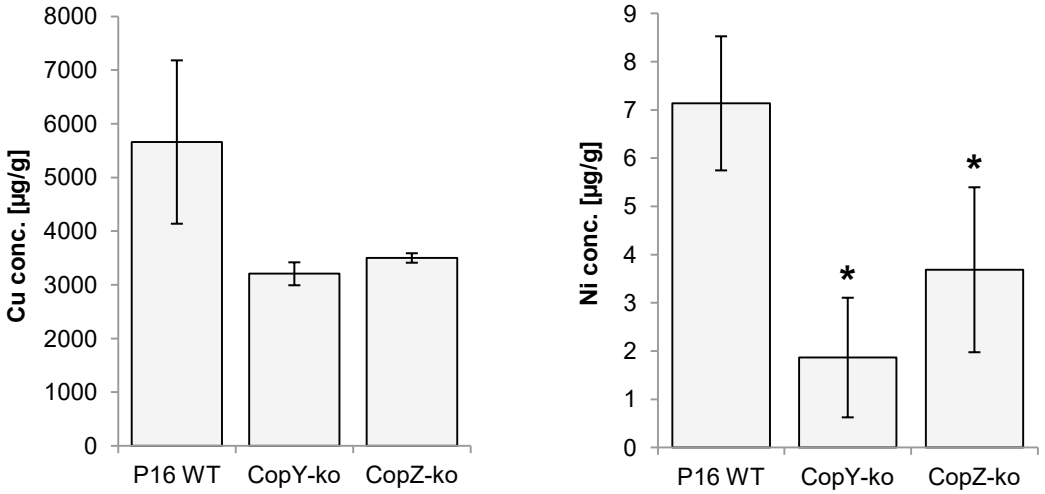

Figure 47. Copper and nickel content in the biomass of *S. mirabilis* (P16 WT), Δ*copY* (CopY-ko) and Δ*copZ* (CopZ-ko) after growth in liquid GYM supplemented with 1 mM $CuSO_4$ for 5 d at 28°C. Bars indicate standard deviation derived from three parallels. Asterisk indicate a statistically significant difference to the WT (CopY-ko: P= 99 %; CopZ-ko: P= 95 %).

Besides copper tolerance, also the tolerance to Ni^{2+} was negatively affected by *P16copZ* deletion (Table 18), although the strain accumulated significantly less nickel (Figure 47). Particularly in AM medium the tolerated concentration of $NiSO_4$ decreased from 45 mM in the WT to 27.5 mM. It could not be excluded that P16CopZ might also bind metals other than Cu(I), since the CXXC motif is not specific for copper, but a general metal binding motif, also found in the nickel chaperone HypA of *Helicobacter pylori* (Xia et al., 2009). Furthermore, the copper chaperone Cox17 of eukaryotes was found to also bind Zn^{2+} (Palumaa et al., 2004). P16CopZ could therefore also exhibit buffering capacities for Ni^{2+}. The strong decrease in Ni^{2+} tolerance could also be caused by a general imbalance in the oxidative stress resistance, caused by the loss of the chaperone, which would be further increased under metal stress.

Heterologous P16CopZ overexpression

When *P16copZ* was introduced in *S. lividans* TK24 on the overexpression plasmid pUWL201 (yielding strain TK24 pUWLCopZ), growth of the transformant strain visibly decreased compared to the empty vector control, even without metal amendment. However, in TSB and AM liquid medium no change in resistance to copper was detected (Table 17), indicating that P16CopZ alone did not confer resistance to the metal, analogous to results for BsCopZ (Drees et al., 2015). On the contrary, in GYM Cu(I) resistance even deceased in TK24 pUWLCopZ.

A study on the expression of CopZ in *Ent. hirae* (Lu & Solioz, 2001) revealed that *copZ* is merely transcribed at slightly elevated copper concentrations (upto 0.5 mM), while the protein was not detected at higher concentration (5 mM). Under these conditions, the protein is more labile and prone to proteolysis. The authors concluded that high concentrations of copper-bound CopZ might be toxic, because the metal is still exposed to the cytoplasm and able to participate in Fenton-type reactions and radical generation (Cobine et al., 1999; Lu & Solioz, 2001). Owing to this effect, *S. lividans* overexpressing CopZ was more sensitive to Cu(I).

The poor growth of TK24 pUWLCopZ even in medium without copper addition could be attributed to the fact that copper chaperones not only receive Cu(I) from importers but are also involved in recycling of endogenous intracellular Cu(I) from metalloproteins or weaker copper binding sites (Tottey et al.,

2002). In conjunction with the fact that this copper bound to CopZ then becomes solvent-exposed, oxidative stress could be assumed to increase even under normal growth conditions.

Ni^{2+} sensitivity was slightly increased in the CopZ overexpression strain (Table 18), which was either the result of the generally higher oxidative stress level in this transformant, or the binding of Ni^{2+} by CopZ, whereby the metal would remain solvent-exposed in the cytosol inducing more oxidative stress, as it was discussed for Cu(I). Further studies for determining the metal binding capacities of P16CopZ were required for definitely explaining this effect.

copYZ-*carrying plasmid fragment introduction in* S. lividans *and a cured* S. mirabilis *strain*

In order to assess the effect of *copYZ* independently from other Cu(I) homeostasis genes present on pII, the fragment of pII carrying *copYZ* (Figure 41) was introduced in *S. lividans* TK24 and the cured P16 489_3 on the integrative vector pSEThph (pSEThphCuP2Cosm). This complementation slightly decreased both strain's resistance to $CuSO_4$ (Table 17).

The adversary effect on Cu(I) resistance could be caused firstly by the expression of P16CopZ, which increased intracellular oxidative stress, as seen in TK24 pUWLCopZ, and secondly also by the action of P16CopY. Being a transcriptional repressor P16CopY could potentially reduce the expression of *copA* genes by binding to the promoter, wherefore a higher intracellular Cu(I) concentration would be required for reaching a threshold at which sufficient Cu(I)-CopY complexes are formed for allowing transcription. However, which of these effects dominated and if there was a difference between the native host *S. mirabilis* and the heterologous host *S. lividans*, could not be stated.

Sensitivity of transformants to oxidative stress

The general decrease of Ni^{2+} resistance in the deletion strains could be a result of several factors. On the one hand, both proteins might be somehow involved in the homeostasis of several heavy metals, either by regulating the expression of resistance genes or by binding metals other than Cu(I), thereby sequestering them from the cytosol. On the other hand, the sensitivity could arise from an increased sensitivity to oxidative stress. Copper homeostasis and oxidative stress are tightly connected. By deleting a component of the copper resistome, also the balance of the system reacting to oxidative stress could be upset, whereby the cell is rendered more sensitive to ROS formation induced by metals.

Therefore, the tolerance of the transformed strains to the oxidant H_2O_2 was evaluated. The sensitivity of Δ*copY* and Δ*copZ* to H_2O_2 corresponded to the change in Cu(I) resistance with higher levels tolerated by the former (39 ppm) and lower concentrations (21 ppm) by the latter strain (Table 19). In the disc diffusion assay the increase in tolerance of Δ*copY* was particularly visible on minimal and complex medium (Figure 48). Additionally, this assay visualized the strong impact that CopZ overexpression had on *S. lividans*, whose H_2O_2 tolerance more than halved from 30 ppm to 12 ppm (Table 19).

Table 19. Maximally tolerated H_2O_2 concentration [ppm] in TSB liquid culture. Growth was evaluated after 5 d.

	H_2O_2
S. mirabilis P16	30
Δ*copY*	39
Δ*copZ*	21
TK24 pUWL201	30
TK24 pUWLCopZ	12
489_3	30
489_3 pSEThphCuP2Cosm	30
S. lividans TK24	30
TK24 pSEThphCuP2Cosm	12

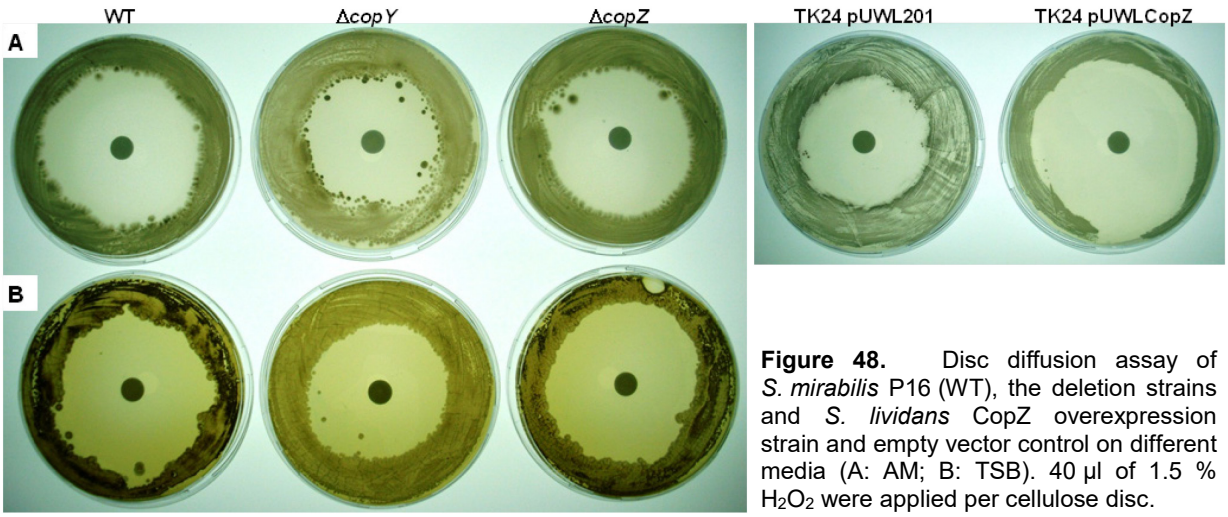

Figure 48. Disc diffusion assay of *S. mirabilis* P16 (WT), the deletion strains and *S. lividans* CopZ overexpression strain and empty vector control on different media (A: AM; B: TSB). 40 µl of 1.5 % H_2O_2 were applied per cellulose disc.

These results supported the hypothesis that the *S. mirabilis* copper resistance machinery influenced the response to oxidative stress. However, this does not seem to be the case in all bacteria, as the deletion of *copZ* in *Deinococcus radiodurans* did not alter its H_2O_2 sensitivity (Zhao et al., 2014). The CopZ overexpression indeed strongly affected the oxidative stress response of *S. lividans*, probably due to the reasons stated above.

The introduction of the *copYZ*-carrying plasmid fragment in *S. lividans* reduced H_2O_2 tolerance to the same level as CopZ overexpression, wherefore it can be assumed that the higher sensitivity was mainly the result of CopZ expression.

Activity of the cuproezyme cytochrome c oxidase

Copper is an important structural element for several enzymes, wherefore a change in copper homeostasis affects the functioning of these. As one important representative of cuproenzymes in aerobic bacteria, cytochrome c oxidase (CcO) was chosen for investigating the impact of *P16copY* and *P16copZ* deletion on enzyme activity. In an *in vivo* colorimetric assay using TMPD (see section 2) the CcO activity of colonies spotted on nutrient agar with and without metal amendment was assessed qualitatively.

An accelerated blue colour development indicating TMPD oxidation was observed for Δ*copY*, and to a lesser extend also for Δ*copZ* (Figure 49), hinting at a higher CcO activity in these strains. The amendment of the growth medium with low concentrations of copper or nickel did not have an effect on the CcO activity in any strain (data not shown)

An increase of CcO activity upon deletion of a CsoR-type transcriptional regulator was also observed in a study on *S. lividans* (Dwarakanath et al., 2012). The authors attributed this effect to a more efficient Cu(I) incorporation in the cuproenzyme. For *S. mirabilis*, the increase in CcO activity might have been connected to the derepression of *copA* transcription in Δ*copY*, since, contrariwise, CopA loss can reduce CcO activity: Mutation of the copper exporting ATPase CopA2 in *Pseudomonas aeruginosa* reduced CcO activity (Gonzalez-Guerrero et al., 2010) and the opposite effect could be assumed for a constitutive CopA expression. Therefore, it could be assumed that P16CopY not only controls the expression of CopA transporters that confer Cu(I) resistance, but also controls those connected to CcO functioning. Whether in *S. mirabilis* the same CopA protein was serving both pur-

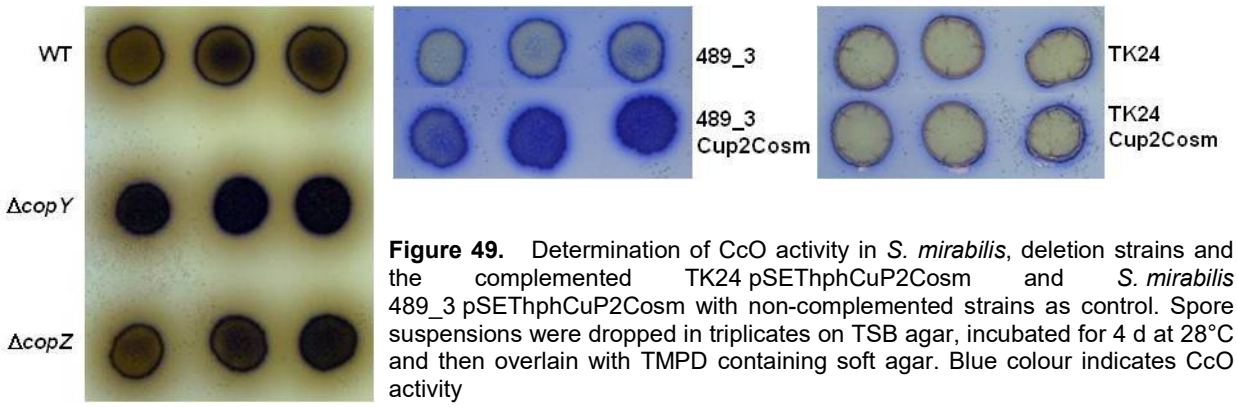

Figure 49. Determination of CcO activity in *S. mirabilis*, deletion strains and the complemented TK24 pSEThphCuP2Cosm and *S. mirabilis* 489_3 pSEThphCuP2Cosm with non-complemented strains as control. Spore suspensions were dropped in triplicates on TSB agar, incubated for 4 d at 28°C and then overlain with TMPD containing soft agar. Blue colour indicates CcO activity

poses, or if different CopA ATPases were required for either tasks, like it is the case in *P. aeruginosa* (Gonzalez-Guerrero et al., 2010), remained elusive.

The deletion of copper chaperones or storage proteins in different bacteria had differing effects on CcO activity depending on the organism in question (Blundell et al., 2013; Fujimoto et al., 2012; Radford et al., 2003; Straw et al., 2018; Tottey et al., 2002). In *Streptomyces* sp., the deletion of the cytosolic copper storage protein Ccsp increased the CcO activity, while deletion of the extracellular copper chaperone Sco reduced the enzyme's activity, as this protein delivers Cu(I) for CcO maturation (Blundell et al., 2013; Fujimoto et al., 2012; Straw et al., 2018). A similar role for P16CopZ in CcO maturation could therefore be excluded. The slight increase of CcO activity in Δ*copZ* is best comparable to a *B. subtilis copZ* deletion strain, in which CcO activity also slightly increased (Radford et al., 2003). Therefore, BsCopZ and P16CopZ probably have similar roles in copper homeostasis serving intracellular copper trafficking to exporters and transcriptional regulators.

The introduction of the *copYZ*-carrying pII fragment in the cured *S. mirabilis* 489_3 and the heterologous host *S. lividans* resulted in an increased CcO activity in *S. mirabilis*, but had no apparent influence on *S. lividans* (Figure 49). This was a further hint at a potential interaction between P16CopY and/ or P16CopZ with *S. mirabilis*-specific chromosomal copper homeostasis determinants.

Implications for the role of P16CopY and P16CopZ in the strain's copper resistome

Putative operons regulated by P16CopY

The best-known promoter for binding of copper-responsive regulators is the so-called „*cop*-box", which is recognized by members of both families, CsoR- and CopY-type proteins (Magnani et al., 2008; Zhao et al., 2014). Accordingly, genes under control of this promoter are transcribed at elevated copper levels. In order to identify putative operons controlled by P16CopY and similar regulators, the consensus promoter sequence (TACAnnTGTA) was searched in the genome of *S. mirabilis*. On the large plasmid, where *P16copY* was located, no *cop*-box could be identified, but five matching sequences were found on the chromosome. This number was comparably low, as in the *Lactococcus lactis* genome 28 *cop*-boxes were detected (Magnani et al., 2008). However, only for seven of these sequences an interaction with the CopY-like regulator CopR could be shown.

The five putative promoter sequences identified in *S. mirabilis* were located within predicted ORFs. Hence, an actual involvement of these loci in transcription regulation was unlikely. Apparently, promoters recognized by Cu(I) responsive regulators in *Streptomyces* sp. extended beyond the *cop*-box sequence.

Accordingly, CsoR-family members are known to target other promoters as well (Dwarakanath et al., 2012; Zhao et al., 2014). Dwarakanath et al. (2012) investigated the binding of *Streptomyces lividans* CsoR (SlCsoR, Figure 45) and could identify another consensus sequence: ATA-TACCCCTNAGGGGTATAT (underlined are the most conserved residues). Since this regulator clustered together with P16CopY in the phylogenetic tree, it seemed highly likely, that also the *S. mirabilis* regulator would target this sequence.

In the *S. lividans* chromosome, three consensus-like operator sequences where identified (Dwarakanath et al., 2012), while in *S. mirabilis* altogether five promoters were found, when the most conserved part of this operator was used as target (ATACCCX_5GGGTAT). Two operators were located on the genome upstream of genes coding either a putative copper chaperone (SMI4977) or a copper sensitive repressor (SMI4031). The other three sites were found on the large plasmid: one within the ORF of *P16copZ* and the second upstream of another putative *copZ* gene (SMI8203), which was followed by *copA*. In contrast to the latter two matches, the third operator was located upstream of a gene coding a hypothetical protein without known conserved domains (SMI8205). A copper-dependent transcription of most of these genes seemed reasonable, as they were important for copper trafficking, wherefore P16CopY might be involved in their regulation. Analogically, the regulation of genes, to which no function could be attributed, yet, has been shown already for MtRicR (Festa et al., 2011).

Of course, it could not be excluded that P16CopY also recognized other promoters, as the selectivity might not only depend on the promoter sequence, but also the DNA conformation resulting from dyad symmetry of the promoter (Tan et al., 2014).

In silico prediction of additional CopZ and CsoR homologues

For many bacteria it is known that they possess multiple copies of components for copper resistance systems and that these act in concert for ensuring copper homeostasis (Arguello et al., 2013). There-

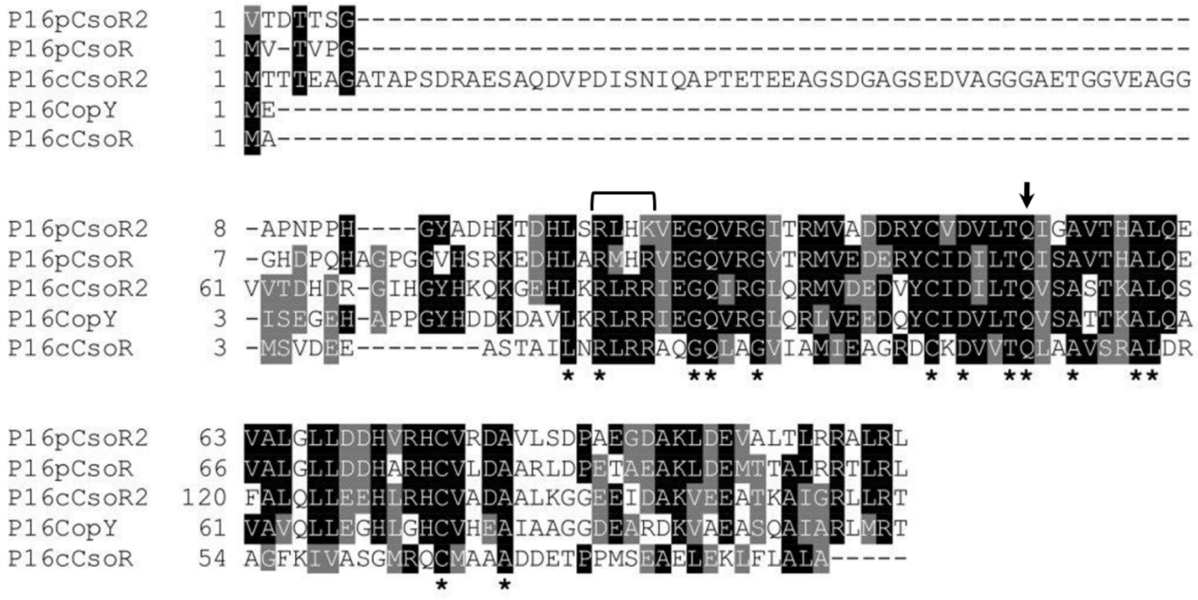

Figure 50. Amino acid sequence alignment of *in silico* identified CsoR family transcriptional repressors of *S. mirabilis*. Arrow marks the Gln residue found important for binding to DNA in SlCsoR. The bracket indicates the RLXR motif that determines SlCsoR binding to the operator site (Tan et al., 2014). Asterisks mark matching residues in all compared sequences.

fore, another *in silico* analysis was conducted for identifying other putative CsoR and CopZ protein-coding genes in the genome and the large plasmid of *S. mirabilis*, as these would likely influence the above presented results.

In the gene annotation, four more CsoR homologues were predicted and confirmed in a search for conserved domains, two of which were on the chromosome (SMI0140 – P16cCsoR, SMI4031 – P16cCsoR2) and the other two on the plasmid pII (SMI8166 – P16pCsoR, SMI8235 – P16pCsoR2). For comparing these proteins, they were aligned to P16CopY (Figure 50).

Tan et al. (2014) found that in SlCsoR, the RLXR motif together with a Gln residue (Q81) form a high-affinity operator binding region, which is crucial for binding of the regulator to the DNA. These features were also present in the two chromosomal CsoR homologues of *S. mirabilis*, as well as the plasmidal encoded P16CopY. In the other two plasmidal CsoR proteins, substitutions occurred in the RLXR motif. When considering the essential residues for metal binding and allosteric switching, which were discussed above, P16cCsoR showed the most differences to the other regulators. In this protein, all residues for allosteric switching in P16CopY (Y43, H69, E90) and the second coordination shell residues (Y43, K88), as well as one residue for metal binding (H69) were substituted, which could be a hint on a different derepression mode as compared to the other *S. mirabilis* CsoR-like regulators.

For better visualizing the sequence similarities, another phylogenetic tree was generated including all *S. mirabilis* CsoR-like proteins (Figure 52). Here, it became clear, that P16cCsoR belonged to another group of CsoR-like proteins (group V), while all other homologues clustered with group III proteins. The potential of CsoR family regulators to substitute each other was found to be restricted to members of the same group, due to the differences in protein structure between the groups, e.g. the RicR regulon (group III) is not regulated by CsoR (group I) in *M. tuberculosis* (Festa et al., 2011).

From the phylogenetic tree it was concluded that the *S. mirabilis* CsoR group III regulators might share the same DNA binding and derepression mechanisms as SlCsoR. The latter forms dimers, which exhibit an electropositive surface area running diagonally across the CsoR complex serving as contact site with the DNA (Tan et al., 2014). Four positively charged Lys and Arg residues in the third alpha helix of SlCsoR contribute to this electropositive tract. The same number of these amino acids was present in the C-terminus of the *S. mirabilis* group III CsoR proteins. Therefore, it was highly likely, that these regulators could bind to the same operators and may substitute each other.

For the identification of other putative CopZ-like proteins, the consensus sequence of the metal binding motif (GM(TS)CXHC) inferred from the above presented alignment (Figure 51) was used as query. In that way, one putative copper chaperone was found on the chromosome (SMI4977) and one more on the large plasmid (SMI8203). All shared a high degree of sequence similarity (Figure 51). However the chromosomal P16cCopZ was more similar to the plasmidal P16pCopZ2. Charge differences were

Figure 51. Amino acid sequence alignment of *in silico* identified CopZ-like copper chaperones of *S. mirabilis*. Asterisks mark identical residues in all compared sequences

more pronounced in these proteins (data not shown), which could hint at different interaction partners than for P16CopZ, implying that P16CopZ loss could only be partially compensated by these chaperones.

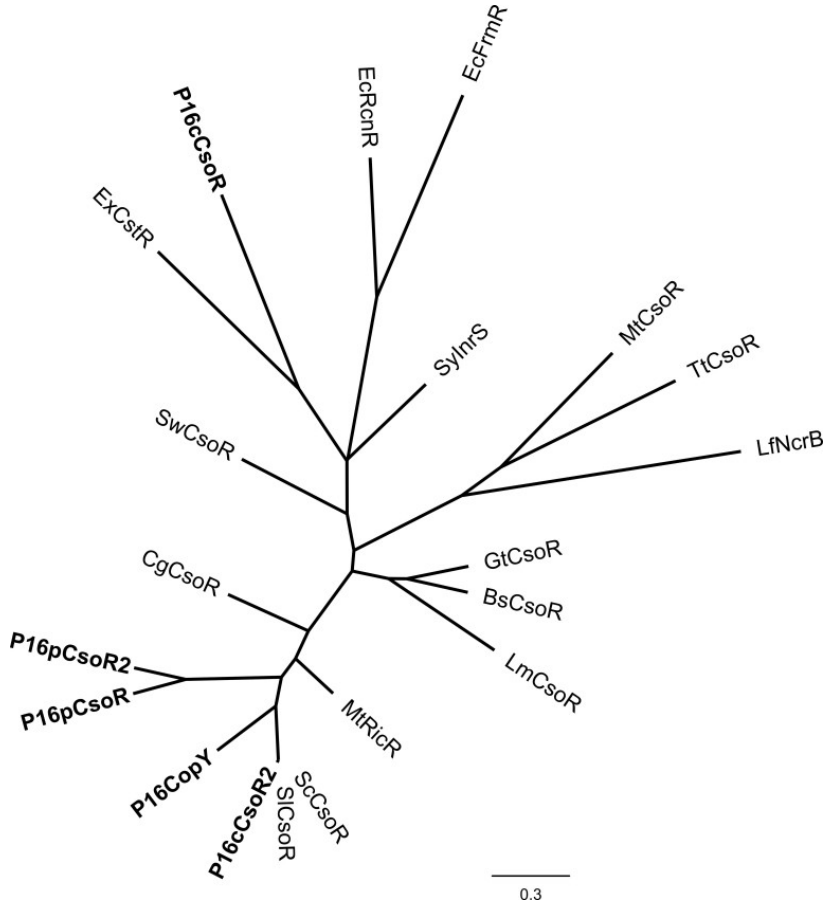

Figure 52. Phylogenetic tree of CsoR family members including *in silico* predicted CsoR family proteins of *S. mirabilis*.

Expression in *E. coli*

The same pII plasmid fragment carrying *P16copY* and *P16copZ*, which was used for the transformation of P16 489_3 and *S. lividans*, was introduced in *E. coli* on pSEThph. The plasmid backbone had no promoter controlling insert expression, wherefore the genes were under control of their native promoters. When the *E. coli* transformant was challenged with $CuSO_4$ in liquid culture, the strain carrying the insert initially had an advantage and showed stronger growth in the first six hours (Figure 53), which might have resulted from the expression of P16CopZ that exerted a buffering effect by binding intracellular Cu(I). However, it is likely that the interaction between *E. coli* copper efflux pumps and the *Streptomyces* sp. chaperone was not ideal or even prevented regarding the phylogenetic distance between these organisms, resulting in elevated levels of CopZ-bound copper in the cell. Although copper chaperones were shown to exhibit a certain level of promiscuity regarding their interaction with CopA, e.g. BsCopZ with *E. coli* CopA (Drees et al., 2015), the above described analysis of the charge plot (Figure 43) showed differences between different BsCopZ and P16CopZ that might hinder the interaction with the same exporter.

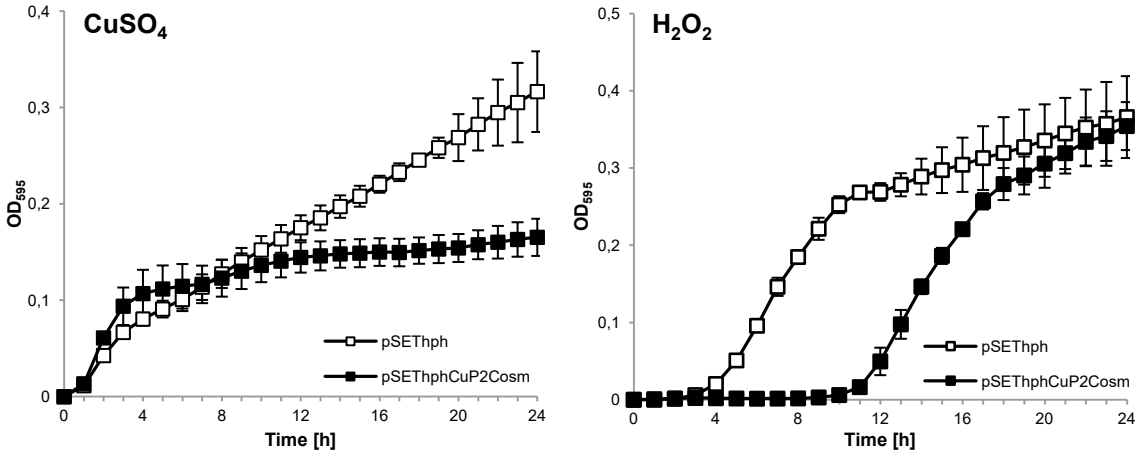

Figure 53. Growth of *E. coli* carrying the copYZ-containing *S. mirabilis* pII fragment (CuP2Cosm) or the empty vector pSEThph in LB medium supplemented with 2.5 mM $CuSO_4$ or 45 ppm H_2O_2.Bars show standard deviation derived from five replicates.

In the same manner that CopZ overexpression reduced *S. lividans* growth, the CopZ-bound copper would then engage in the formation of ROS when accumulating during the course of incubation, which would explain the growth reduction upon further incubation.

An involvement of P16CopY in the resistance change of the *E. coli* strain was less likely. Even if the gene was transcribed in *E. coli*, the protein only might have had a buffering effect by binding copper, but the probability of a streptomycete transcriptional regulator to recognize a promoter sequence in *E. coli* was unlikely.

Besides a reduction in copper resistance, the pII fragment also increased the sensitivity of *E. coli* to oxidative stress (Figure 53), which could also be a consequence of P16CopZ expression, as a similar effect had been observed in TK24 pUWLCopZ. The growth of *E. coli* was delayed as it took the bacterium longer to overcome the imbalance in the oxidative stress level induced by P16CopZ.

Conclusion

Taken together, the results of this study confirmed that the plasmidal *S. mirabilis* genes designated *P16copY* and *P16copZ* encoded a CsoR family transcriptional regulator and a chaperone protein, respectively, both of which were involved in copper homeostasis of the organism. However, these proteins were merely two components of a complex network of probably interacting regulators, trafficking proteins and efflux pumps, as could be inferred from *in silico* analysis. Their localisation on pII substantiated the notion that this plasmid impacted copper homeostasis in its host.

The initial assumption that the unusual arrangement of *P16copZ* and *P16copY* in head-on orientation would make them interesting targets for further investigation proved to be correct, as deletion of these genes had major impacts on the copper resistance of *S. mirabilis*, although several homologues were detected in the genome, which could potentially substitute their loss. Merrikh & Merrikh (2018) found that head-on orientated resistance genes show an accelerated rate of evolution due to an increased mutation rate, making gene inversion a driver of evolution, from which the strain benefits. This might also apply for the *cop* genes investigated in this study. The *copY-copZ* arrangement could have resulted from gene inversion, whereby the operon was under positive selection enabling the strain to adapt to higher copper concentrations.

The *cop* operon was not the only copper responsive network operating in *S. mirabilis*, as also genes encoding additional copper responsive systems, e.g. *cueR* and *cutRS*, could be identified. It was assumed that several layers of reaction to copper stress existed in *S. mirabilis*, like it has already been suggested for *S. lividans* (Straw et al., 2018). Marcus et al. (2016) hypothesized that in *M. tuberculosis* CsoR is not the only regulator responsible for induction of its target operons, but that a second regulator was required for complete induction, hinting on a hierarchy of Cu(I)-dependent regulation. Similarly, in other bacteria it was observed that the *cop* operon could also be controlled by other global regulators, CueR or indirectly by multidrug efflux systems (Gaballa et al., 2003; Torres et al., 2014). Therefore, a collaboration of multiple systems, either directly or indirectly connected to Cu(I) homeostasis, seemed likely and most probably also influenced the results of this study. Losses of components could be either compensated by homologous proteins or by increased activity of other Cu(I) homeostasis systems.

Transcription of putative *copA* genes or other regulating systems has not been investigated in the present study, as several potential operons exist and this could not have been realized within given time. However, the author believes that transcriptional studies would provide a deeper insight into the influence of P16CopY and P16CopZ on the regulation of *cop* operon transcription and therefore metal response. This would additionally help the identification of a putative cross-regulation of metal resistance determinants and the copper homeostasis systems, also in response to other heavy metals, such as Ni^{2+}, as nickel resistance was affected by *P16copZ* deletion.

3.5 The plasmid-encoded house-keeping hydrolase E13YjjG

Introduction

Protecting the integrity of its genomic information is of utmost importance for every living cell. There are numerous causes for DNA lesions, whether it is spontaneous depurination and base misincorporation or caused by an exogenous source, like reactive oxygen species (ROS), radiation or chemicals. The attack of ROS on DNA leads to modified base or sugar moieties, which can interfere with DNA replication and stability. Oxidation of nucleotides increases the intracellular pool of noncanonical nucleotides (Haghdoost et al., 2006; Kamiya, 2003; Rai, 2010). When incorporated into the DNA, these nucleotides cause mispairing or inhibition of DNA replication, thereby increasing the mutation rate (Hizi et al., 1997; Kamiya, 2003). These lesions are repaired by cellular enzymes of the cell's DNA repair machinery, but moreover DNA damage by noncaonical dNTPs can be prevented by intercepting and hydrolyzing such compounds (Akiyama et al., 1989; Michaels et al., 1992; Proudfoot et al., 2004).
Nucleotide phosphatases, also called nucleotidases, recognize and detoxify nucleobase derivatives (Galperin et al., 2006). The first identified, so-called "house-cleaning" enzyme is MutT of *E. coli*: a low-specificity phosphatase that hydrolyzes oxidized dGTP and other dNTPs (Akiyama et al., 1989; Bhatnagar & Bessman, 1988) and thereby prevents the incorporation of noncanonical nucleotides into the DNA. This hydrolase is a member of the haloacid dehydrogenase (HAD)-like superfamily, a large family of small molecule phosphatases that exhibit diverse activities from amino acid biosynthesis to detoxification. Due to their large variability, they only show little protein sequence similarity, whereby substrate specificity is hardly predictable *in silico* (Allen & Dunaway-Mariano, 2004; Koonin & Tatusov, 1994; Kuznetsova et al., 2006).
Some HAD-like hydrolases act on antimetabolites, like fluoropyrimidines, that inhibit biosynthetic processes and can be incorporated in DNA and RNA, whereby they inhibit the normal functioning of these molecules (Longley et al., 2003). 5-Fluorouracil (5-Fu) is an antimetabolite drug often used in cancer treatment (An et al., 2007). It is an uracil analogue with a fluorine at the C-5 position (Figure 54). When entering the cell, it exhibits toxic effects that directly and indirectly impair DNA integrity. 5-Fu is converted into several active metabolites, like 5-fluorouridine (5-Fd) and fluoridine triphosphates that are misincorporated into DNA and inhibit the thymidylate synthase, which methylates dUMP to dTMP. Since the latter is a precursor for dTTP, the blockage of *de novo* dTMP synthesis results in dTTP depletion and accumulation of the reactant dUMP. The dNTP pool is thereby pertubated which impairs DNA synthesis and repair (An et al., 2007; Harada et al., 2006; Longley et al., 2003; Santi et al., 1974). Moreover, the relatively elevated dUTP content in the dNTP pool leads to misincorporation of dUTP in DNA, which triggers a uracil-DNA glycosylase attack that may cause double-strand breaks and damages DNA (Kouzminova & Kuzminov, 2004).

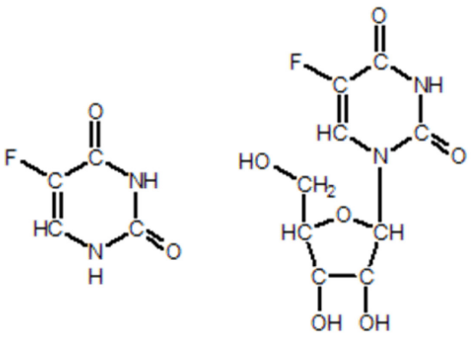

Figure 54. Chemical structures of pyrimidine analogues and abbreviations used in this study.

Results

Gene identification and location

As described in section 3.1 the first approach for the identification of putative heavy metal resistance genes was the application of random transposon mutagenesis. In one of the transformants of *S. acidiscabies* E13 which showed a reduced resistance after transposon integration, it was found that the transposon integrated into a 642 bp long ORF (E13_08014) on the strain's plasmid, which was annotated as pyrimidine 5'-nucleotidase YjjG coding gene. Interestingly, this gene showed the highest sequence identity to plasmidal sequences from other *Streptomyces* sp. strains, namely *S. rochei* 7434AN4 (Yang et al., 2011) and *S. violaceoruber* (Spatz et al., 2002), whose plasmids pSLA2-M and pSV2 are known to harbour self-defence genes. On these plasmids, the putative *yjjG* was associated with a downstream NAD(P)-binding protein of unknown function (DUF1932, pfam09130), which was identical to the gene organization in *S. acidiscabies* (Figure 55).

Table 20. Predicted properties of *E13yjjG* and its gene product.

	E13YjjG
Annotation	E13_08014
Gene size	642 bp
GC content	67 %
Protein size	214 aa
Mass	23.4 kDa
Pfam	13419
COG	1011

Protein characteristics

The product of *E13yjjG* was predicted a 214 aa protein of 23.4 kDa (Table 20). On the basis of conserved domains found in the protein sequence, the protein was identified as a hydrolase of the haloacid dehalogenase-like (HAD) superfamily (pfam13419), specifically a member of the orthologous group of YigB-like phosphatases (COG1011). Members of the HAD superfamily are ubiquitously found and relatively small molecules of 200-250 aa (Koonin & Tatusov, 1994), which was in accordance with E13YjjG. They serve mainly as defense system by detoxification of metabolic by-products and xenobiotics. However, the sequence identity between proteins of this superfamily is low and they are only identified by four characteristic motifs (Koonin & Tatusov, 1994), which will be examined below.

Accordingly, E13YjjG merely showed a low sequence congruence with proteins of the Swizzprot Database. It shared 35 % identity with the *E. coli* pyrimidine 5'-nucleotidase YjjG (P0A8Y1) and 28 % with a glyceraldehyde 3-phosphate phosphatase of *Pyrococcus horikoshi* (O59346), which catalyses the dephosphorylation of D,L-glyceraldehyde 3-phosphate. *E. coli* YjjG is one of the few characterized bacterial enzymes of the HAD superfamily acting as intracellular nucleotidase with a narrow substrate specificity (5'-dTMP, 5'-dUMP, 5'-UMP) (Proudfoot et al., 2004).

However, the homology to *Streptomyces* sp. proteins of the NCBI Reference Sequence Database was found to be exceptionally high, with often more than 90 % amino acid identity. These were mostly predicted HAD family hydrolases that were not characterized, e.g. a putative YigB of *Streptomy-*

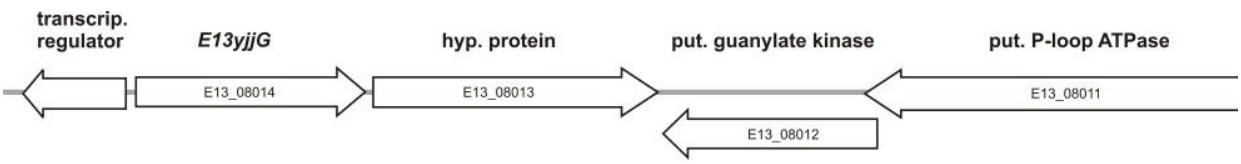

Figure 55. Schematic representation of the genomic location of *E13yjjG* on the endogenous plasmid of *S. acidiscabies*. Annotation numbers are given within the arrows. Above, predicted gene product characteristics are given. The predicted transcriptional regulator upstream *E13yjjG* has not been identified in the genome annotation, but retrospectively by BLAST search.

ces sp. M41 (WP_081224635), which showed 94 % identity to E13YjjG. Hence, this protein was well conserved among members of this species.

The high sequence variability within the HAD members, also showed when the sequences were subjected to a phylogenetic comparison (Figure 56). E13YjjG clustered with other *Streptomyces* sp. hydrolases of unknown function. Moreover, the similarity to a predicted noncanonical pyridine nucleotidase of a spirochaetes strain, which was isolated from a costal soil sample (Shivani et al., 2016), was high. Most of the bacterial proteins displayed in the tree have not been characterized. However, the above mentioned *E. coli* nucleotidase YjjG clustered comparably close with E13YjjG.

One reaction catalysed by *E. coli* YjjG is the dephosphorylation of deoxyuridine monophosphate to deoxyuridine (Weiss, 2007). The sequence similarity to E13YjjG led to the assumption that a similar intracellular function as house-cleaning enzyme could be expected for the *Streptomyces* sp. protein. The likewise well investigated *E. coli* MutT, which also acts as nucleotidase by hydrolysing 8-oxo-dGTP (Maki & Sekiguchi, 1992), was not included in the tree, as it showed comparably little sequence homology to the members of the HAD family (see below).

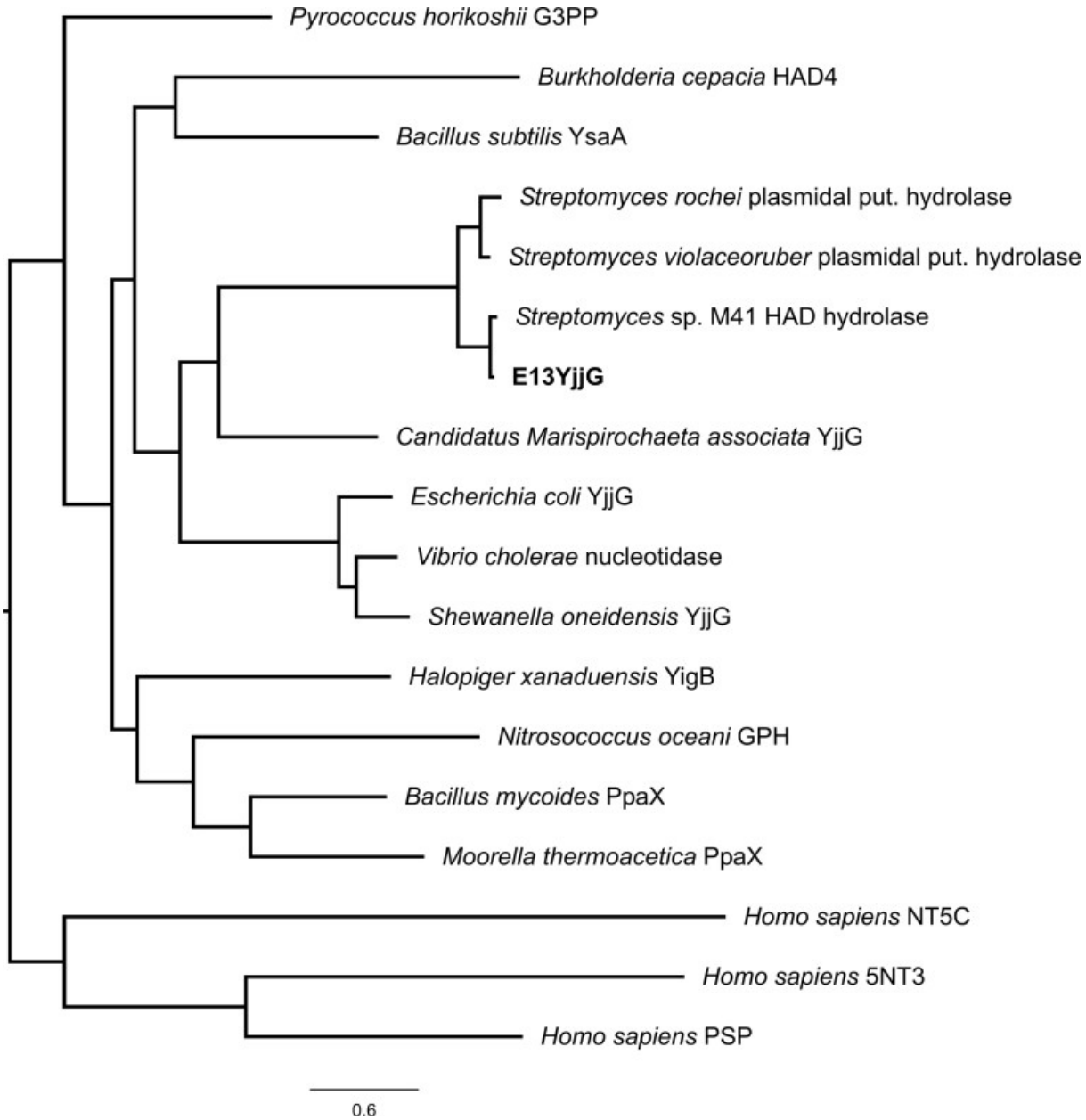

Figure 56. Phylogenetic tree of HAD family proteins.

The presumption of a similar enzymatic activity of *E. coli* YjjG and E13YjjG was substantiated by the fact that in the tree the clusters were on the one side in accordance with the phylogenetic relation between the organisms, with clusters of *Streptomyces* sp., Gammaproteobacteria and human proteins, but also showed a separation according to protein function and substrate spectrum.
The more distantly related *Burkholderia cepacia* HAD4 was a (S)-2-haloacid dehalogenase acting on small 2-haloalkanoic acids with a chain length of C(2)-C(4) (Q51645.3).
Separated from these enzymes was a cluster of phosphatases exhibiting a diverse substrate spectrum of pyrophosphate, riboflavin-5′-phosphate and 2-phosphoglycolate comprising predicted PpaX proteins, the *Halopiger xanaduensis* YigB and *Nitrosococcus oceani* GPH. Thus, these enzymes participated in different biosynthetic and metabolic pathways, but would not act on pyrimidine compounds. Likewise, *Pyrococcus horikoshii* G3PP, a glyceraldehyde 3-phosphate phosphatase, would be involved in cellular metabolic pathways.
Although their substrate spectrum and tasks within the cell would mostly resemble that of *E. coli* YjjG, the human pyrimidine nucleotidases 5NT3 and NT5C were separated in this tree from the bacterial an archaeal proteins. They have been recognized as resistance determinants against antimetabolites and a deficiency in these enzymes can cause serious diseases (Seifried et al., 2013).
In summary, the phylogenetic comparison of HAD family proteins indicated a functioning of E13YjjG as nucleotidase similar to the activity of *E. coli* YjjG.

Alignment

As stated above, HAD family members exhibit a low over-all amino acid sequence homology (< 29 %), but share four conserved signature core motifs (Koonin & Tatusov, 1994; Proudfoot et al., 2004; Ridder & Dijkstra, 1999). In order to check the presence of these motifs in E13YjjG, its protein sequence was aligned to two proteins of the same superfamily (the *Homo sapiens* phosphoserine phosphatase (HsPSP), *E. coli* pyrimidine 5'-nucleotidase YjjG (EcYjjG)) and MutT of *E. coli*, which belongs to another protein family (Nudix hydrolase superfamily, pfam00293), but acts as nucleoside triphosphatase hydrolysing dGTP and dGMP (Akiyama et al., 1989; Bhatnagar & Bessman, 1988), thereby serving the same purpose as EcYjjG. HsPSP on the other hand catalyzes the hydrolysis of L-phosphoserine, the last step in L-serine formation, and has no nucleotidase activity (NP_004568.2). Comparing these enzymes in an alignment should help to identify putative motifs determining catalytic activity and substrate specificity.
All four motifs of the HAD superfamily were identified in E13YjjG in consensus with the other two HAD family proteins, which was evident, as mutations in these motifs decrease or even abolish the activity, as has been shown for HsPSP (Collet et al., 1999).
The first motif (DXDX(T/V)) was located at the N-terminus and contained the catalytic core residues D7, D9 and T11. It was found that the consensus sequence of this motif could be extended to hhhDXDX(T/V)(L/V)h, with “h” being any hydrophobic residue (cd04305) (Ridder & Dijkstra, 1999). This extended motif was identified in all three considered phosphatases (Figure 57). The first Asp residue in this motif (D7) was the essential nucleophile that catalyses the nucleophilic attack on the substrate, as has been shown in homologous proteins (Allegrini et al., 2001; Allen & Dunaway-Mariano, 2004; Collet et al., 1999; Koonin & Tatusov, 1994).

The second motif was a conserved Thr or Ser residue in the centre of the protein sequence (T105 in E13YjjG), that is necessary for the substrate orientation by forming a hydrogen bond. It was found that for this purpose the hydroxyl-group in this position was essential, as only these two amino acids are tolerated, while substitution by Ala lead to inactivation in mutation experiments with HsPSP (Collet et al., 1999).

The same effect was observed when the third motif, a conserved Lys (K138), was exchanged by Ala in the same experimental setup (Collet et al., 1999). This residue is important for the charge stabilization during the catalytic reaction and was therefore conserved in all displayed HAD family proteins, although in the alignment HsPSP K159 was not aligned with the other two sequences, which could be attributed to the high sequence variability between the proteins.

The fourth and last HAD motif is less conserved and tolerates a higher degree of variation: (G/S)(D/S)X_{3-4}(D/E)hhhh (Seifried et al., 2013). The sequence identity in this motif was higher between E13YjjG and EcYjjG than to HsPSP with G163, D164 and D169 being the essential residues in E13YjjG. Substitutions of residues in this position would decrease or abolish the enzyme activity, depending on the type of substituted amino acid, as it is essential for the coordination of the metal cofactor, wherefore the charges of the amino acids were found to be crucial (Collet et al., 1999). EcYjjG manly uses Mg^{2+} as cofactor but also Mn^{2+} and Co^{2+} are tolerated, although at a lower affinity (Proudfoot et al., 2004). Regarding the high sequence similarity to E13YjjG in this motif, it was likely that also these metals are suitable cofactors for the latter enzyme.

Being a member of the Nudix hydrolase superfamily, the addressed motifs were not present in EcMutT, as expected. However it was hoped for, that residues essential for substrate binding might be

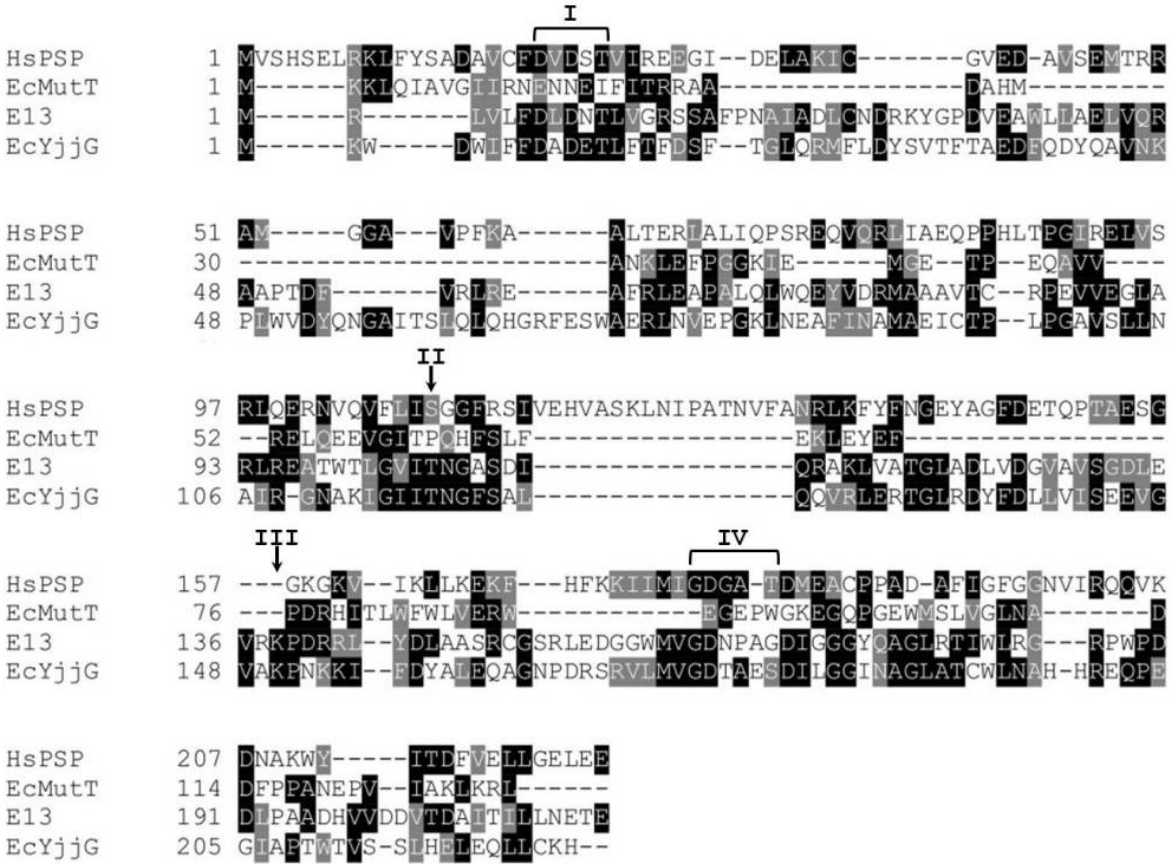

Figure 57. Amino acid sequence comparison between E13YjjG (E13) and other HAD family proteins (HsPSP – human phosphoserine phosphatase; EcYjjG – E. coli pyrimidine 5'-nucleotidaseYjjG) and the 8-oxo-dGTP diphosphatase MutT of E. coli (EcMutT). Arrows and bars indicate conserved signature core motifs of members of the HAD family.

homologous to EcYjjG, as both enzymes act as nucleotidases. Although some of the residues known to be important for binding of 8-oxo-dGMP in EcMutT were conserved in EcYjjG and E13YjjG, no substantial conclusion could be drawn from this comparison, as the identity to HsPSP was comparable.
From the alignment was concluded that E13YjjG would use the same catalytic mechanism as HsPSP and EcYjjG, meaning phosphorylation of a substrate using preferably Mg^{2+} as cofactor, as all motifs necessary for this catalysis were found in the protein sequence. Regarding the substrate spectrum, it could only be assumed that E13YjjG might function as nucleotidase, as the sequence identity to the *E. coli* enzyme was higher than to the human phosphoserine phosphatase.

Deletion and complementation of *E13yjjG*

For determining the function of E13YjjG, the coding gene was deleted using targeted gene replacement, yielding strain Δ*yjjG*. Additionally, a deletion strain was genetically complemented by reintroducing *E13yjjG* using the integrative vector pSEThph. The resulting transformant was named hphyjjG.
Δ*yjjG* did not show any apparent growth defect compared to the WT strain, which was in accordance with studies of hydrolase deletion strains of other species. Most house-cleaning genes are not essential, wherefore growth of knock-out mutants is not impaired, but the genome mutation rate is elevated (Bacon & Treffers, 1961; Gerdes et al., 2003; Maki & Sekiguchi, 1992). The deletion of *mutT* in *E. coli*, for example, increased the A:T → C:G transversion rate (Maki & Sekiguchi, 1992). Due to time limitation, the mutation rate was not compared between *S. acidiscabies* WT and Δ*yjjG* in the present work. However, for further studies this would be a feasible starting point for a more thorough determination of E13YjjG tasks.
However, *E13yjjG* was chosen as target gene for deletion, because the corresponding transposon mutant (see section 3.1) showed a reduced resistance to Ni^{2+}. Thus, it was hypothesized that this enzyme might be involved in stress response. From the amino acid sequence similarity to EcYjjG, it was inferred that E13YjjG could use 5-Fd and 5-Fu as substrates. Thus, the sensitivity of the WT and deletion strain to these antimetabolites was tested.

Sensitivity to 5-Fd and 5-Fu

When cultivated in liquid CSA, *S. acidiscabies* WT tolerated up to 600 µg 5-Fd/ml, while the tolerance of the deletion strain was reduced to 500 µg/ml. The change of tolerance in AM medium was more apparent, with a reduction by more than halve (*S. acidiscabies* WT: > 600 µg 5-Fd/ml; Δ*yjjG*: 300 µg 5-

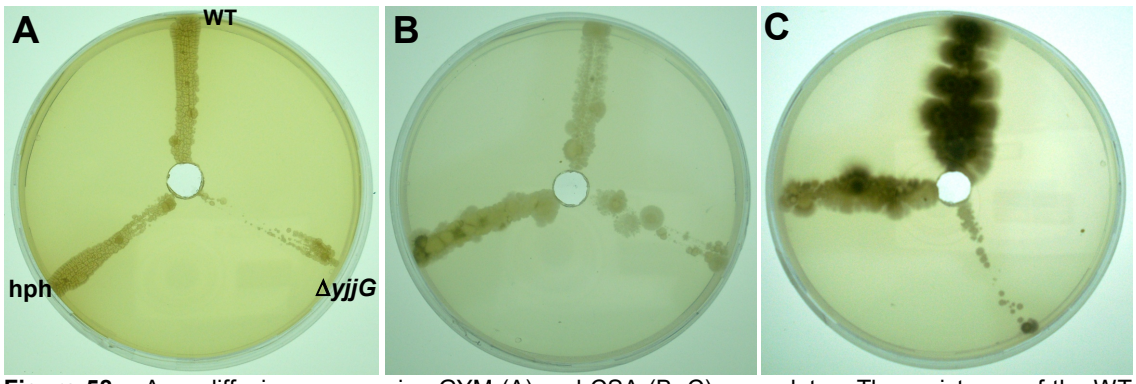

Figure 58. Agar diffusion assay using GYM (A) and CSA (B, C) agar plates. The resistance of the WT, Δ*yjjG* and the complemented strain hphyjjG (hph) against 5-Fu (A, B) and 5-Fd (C) was tested.

Fd/ml). Likewise, the sensitivity to 5-Fu increased from 500 µg/ml in the WT to 100 µg/ml in the deletion strain in AM medium. The higher sensitivity of Δ*yjjG* to these two antimetabolites also showed in agar diffusion assays using different media (Figure 58). Here, also the complemented deletion strain was tested. The genetic complementation re-established growth at elevated 5-Fu and 5-Fd concentrations confirming the role of the *E13yjjG* gene product in the detoxification of these compounds.

Compared to *E. coli*, the *E13yjjG* deletion strain still resisted high concentrations of 5-Fu and 5-Fd, as growth of an *E. coli* strain lacking the corresponding gene was strongly impaired by 5 µM 5-Fd and 50 µM 5-Fu (Titz et al., 2007). The limits for E13 Δ*yjjG* were 11 mM and 770 µM, respectively. However, *yjjG* deletion in *E. coli* did not increase the sensitivity to all nucleosides, indicating a primary activity against 5-fluoropyrimidine derivatives (Titz et al., 2007). The same could apply for E13YjjG, although more compounds have to be tested. The generally lower sensitivity of the streptomycete strains to these compounds could be either attributed to a reduced uptake in the cell, or the possession of additional defence mechanisms.

The toxicity of antimetabolites is a result of several mechanisms. On the one hand, they can directly integrate in DNA and RNA, disturbing DNA synthesis, transcription and translation, but they also compete with other substrates in enzymatic reactions, blocking the binding sites (Harada et al., 2006; Longley et al., 2003). For example, thymidylate synthase is inhibited by 5-Fu, thereby DNA metabolism is hindered and mutation rates increase. Furthermore, the compound induces the SOS response in *E. coli* (Oda, 1987). It would be interesting to see whether similar effects are induced by 5-Fu in *Streptomyces* sp. and whether they are enhanced in Δ*yjjG*.

Sensitivity to heavy metals

As the *E13yjjG* transposon mutant exhibited increased nickel sensitivity, Δ*yjjG* was tested for its sensitivity to heavy metals. For a preliminary assessment, trench plate tests were performed with Ni^{2+} salts (Figure 59). The resistance of the deletion strain was markedly reduced, but genetic complementation did not fully re-establish WT levels. The same was observed in liquid culture when testing $NiSO_4$ resistance in different media (Table 21). The decrease in Ni^{2+} resistance was most pronounced in TSB medium, where *S. acidiscabies* WT tolerated up to 20 mM, while Δ*yjjG* could grow up to 6 mM, but also the complemented strain merely tolerated 8 mM of the nickel salt. In contrast, the resistance to copper was not affected by *E13yjjG* deletion (Table 21), although this metal is known for its strong ability to induce oxidative stress, which could result in a higher proportion of oxidised nucleotides and thus a disturbance in the nucleotide pool (Haghdoost et al., 2006; Kasprzak, 2011; Rai, 2010).

These results indicated that E13YjjG was not generally involved in the stress response to heavy metals. It could not be stated whether the increase in nickel sensitivity in the deletion strain was directly connected to the loss of *E13yjjG*, or whether the insertion of the resistance cassette in this genomic

Table 21. Growth of *S. acidiscabies* (WT), Δ*yjjG* (Δ) and complemented mutant Δ*yjjG* pSEThphyjjG (hphyjjG) in liquid medium amended with different stressors. Given are the maximally tolerated concentrations of $CuSO_4$ and $NiSO_4$ [mM] and H_2O_2 [ppm]. H_2O_2 tolerance was determined in TSB medium. Cultures were grown for two weeks.

	$CuSO_4$			$NiSO_4$			H_2O_2
	TSB	**GYM**	**AM**	**TSB**	**GYM**	**AM**	
WT	8	1.5	0.8	20	5	4	39
Δ	8	1.5	0.8	6	2	2	21
hphyjjG	9	1.5	0.8	8	2.5	2.5	39

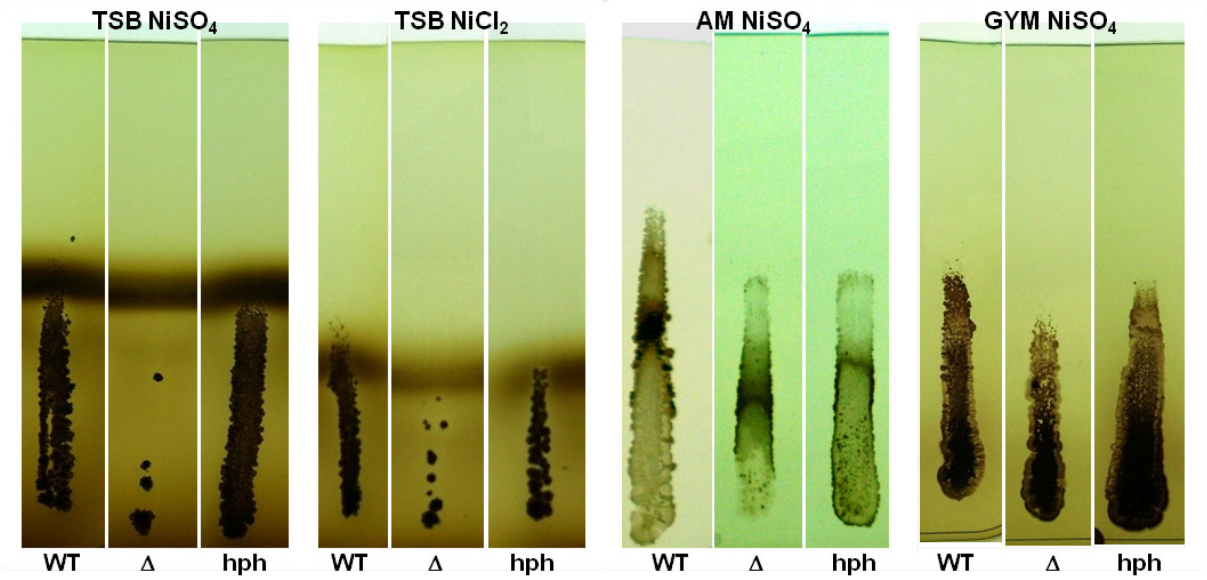

Figure 59. Trench plate tests on TSB, AM and GYM agar using different Ni^{2+} salts. Plates were inoculated with *S. acidiscabies* (WT), Δ*yjjG* (Δ) and complemented strain E13 Δ*yjjG* pSEThphyjjG (hph). Growth was evaluated after four weeks of incubation.

locus induced changes in the transcription of genes located up- or downstream. The latter effect would account for the inability of the genetic complementation to re-establish WT resistance levels. In the near vicinity of *E13yjjG* there were no annotated genes for which a direct connection to nickel homeostasis could be drawn at first sight (Figure 55). The product of the gene located downstream *E13yjjG* showed high similarity to streptomycete NAD(P)-dependent oxidoreductases and contained a domain of the MmsB superfamily (COG2084). Thus, it could be involved in lipid transport and metabolism. However, a loss of this enzyme function would more likely affect heavy metal resistance in general and it was considered unlikely to only be involved in Ni^{2+} resistance.

The predicted transcriptional regulator encoded upstream *E13yjjG* would be a more conceivable candidate. This protein was rarely found in *Streptomyces* sp. and did not exhibit conserved domains characteristic for any regulator family. Also on DNA level no significant similarity to many other streptomycete gene was identified. Possibly, this regulator was involved in the transcriptional regulation on Ni^{2+} resistance genes in *S. acidiscabies*.

Of course, the inability of the genetic complementation of Δ*yjjG* to re-establish Ni^{2+} resistance levels of the WT could also result from the different genomic location, in which the gene has been inserted. The disadvantage of using pSEThph as delivery vector for complementation was that the gene was not inserted at its original position, but at an *attB* site on the chromosome (see section 3.1). Thus, the transcription efficiency might be changed or transcriptional regulation abolished.

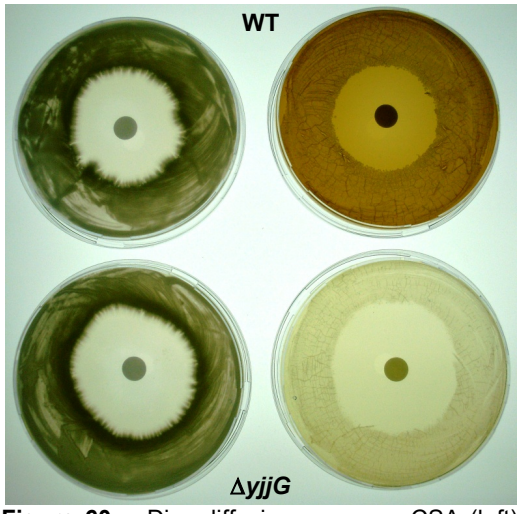

Figure 60. Disc diffusion assay on CSA (left) and TSB (right) medium using 1.5 % H_2O_2.

Tolerance of H_2O_2

As oxidative stress would potentially increase the number of oxidised nucleotides in the pool, which nuleotidases could use as substrates, the sensitivity of Δ*yjjG* to H_2O_2 was tested. In disc diffusion assays, growth of

Δ*yjjG* was stronger impaired by H_2O_2 than that of the WT (Figure 60). Also in liquid TSB medium the tolerance decreased from 39 ppm for the WT to 21 ppm in the deletion strain. In contrast to Ni^{2+} resistance, genetic complementation successfully enabled the deletion strain to resist again 39 ppm H_2O_2 (Table 21). This substantiated the hypothesis that the increase in Ni^{2+} sensitivity was a secondary effect of *E13yjjG* deletion and not due to a change in gene transcription in a different genomic location.

Overexpression of E13YjjG in *E. coli*

The results presented so far indicated that there might be other genes affected by *E13yjjG* deletion. Thus, for separating these effects from E13YjjG activity, the coding gene was introduced in *E. coli* using pTrc99A. The strain was challenged with 5-Fd, 5-Fu and $NiSO_4$ and compared to a control strain carrying the empty vector (EVC). Both antimetabolites impaired growth of the strain carrying *E13yjjG* stronger than that of the EVC (Figure 61). The activity of E13YjjG could possibly lead to an accumulation of reaction products, which could be toxic to the cell. Additionally, the action of another nucleotidase, besides the inherent *E. coli* enzymes, would result in a change of the cell's nucleotide pool, which is known to result in misincorporations and increased mutation rates (Richards et al., 1984). If E13YjjG catalysed the same reactions as EcYjjG, it would also convert dUMP to deoxyuridine. The latter can be incorporated in the DNA as dU/A base pairs and exert mutagenic and inhibitory effects on the transcription by RNA polymerases (Cui et al., 2019).

Determining the number of uracil residues in the DNA would be a convenient method for substantiating this hypothesis. Several methods could be applied, like GC/MS or the use of labelled nucleotides (Blount & Ames, 1994; Goulian et al., 1980), but also indirect methods like the excision of uracil from DNA using uracil-DNA glycosylase and subsequent HPLC-tandem mass spectrometry (Ren et al.,

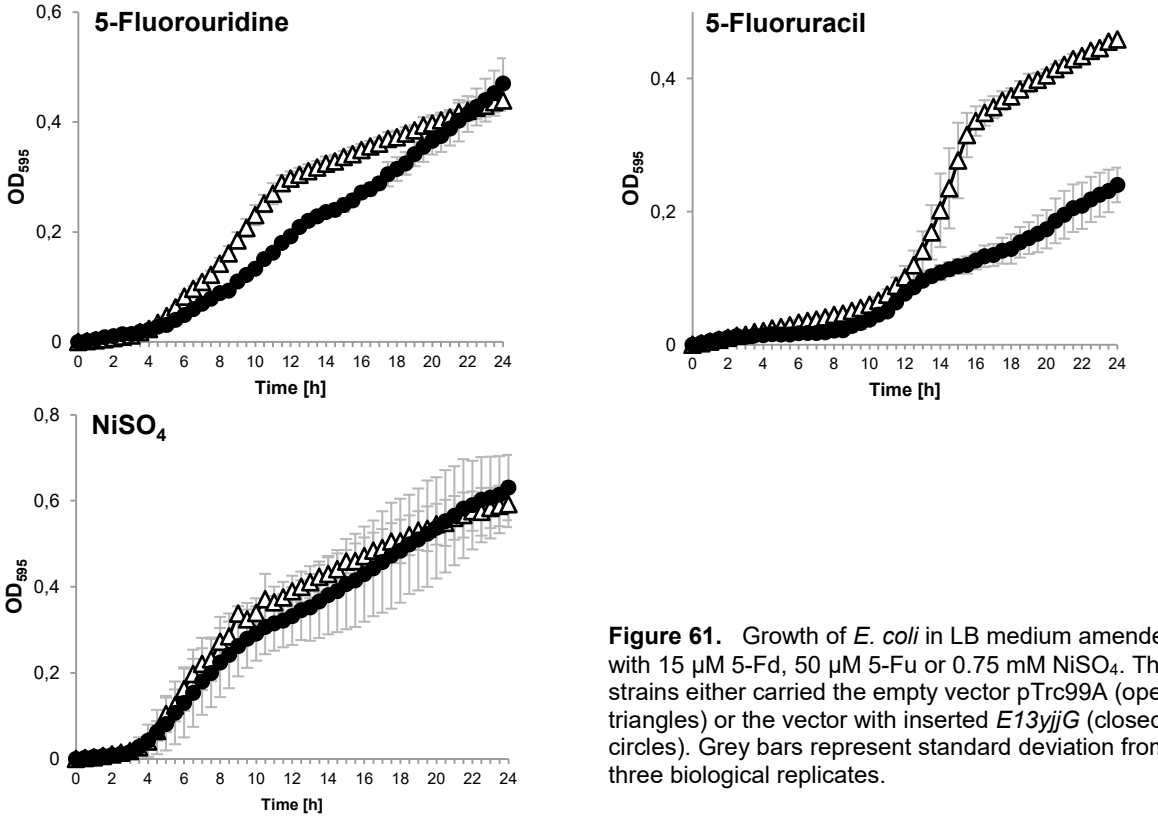

Figure 61. Growth of *E. coli* in LB medium amended with 15 µM 5-Fd, 50 µM 5-Fu or 0.75 mM $NiSO_4$. The strains either carried the empty vector pTrc99A (open triangles) or the vector with inserted *E13yjjG* (closed circles). Grey bars represent standard deviation from three biological replicates.

2002).

The overexpressio of E13YjjG also confirmed that the enzyme was not directly involved in resistance to Ni^{2+}, as there was no difference between the *E13yjjG* carrying strain and the EVC (Figure 61).

Conclusion

The presented results suggested that E13YjjG was a nucleotidase of the haloacid dehalogenase-like (HAD) superfamily acting on pyrimidine analogues, e.g. 5-Fd and 5-Fu. Deletion of the coding gene had no apparent impact on phenotypic traits. However, it could be expected that the mutation rate was elevated, as in other studies the knock-out of nucleotide hydrolases did also not result in a distinct phenotypic change, but merely slightly elevated mutation rates (Zhang & Inouye, 2002). By using a BrdU incorporation assay, a changed incorporation rate of nucleotide analogues in the DNA of *S. acidiscabies* and Δ*yjjG* could be assessed, as an *E. coli yjjG* deletion strain exhibited a strongly increased amount of BrdU containing DNA (Titz et al., 2007).

It could not be excluded that *E13yjjG* deletion had other effects on the strain's properties, as antimetabolites were shown to influence several cellular processes. In some bacteria, like *E. coli*, 5-Fu decreases biofilm formation and changes the expression of other virulence genes by inducing the expression of repressing proteins, e.g. of the global transcriptional regulator AriR, which impacts biofilm formation, cell motility and acid stress tolerance (Attila et al., 2009). In *Streptomyces antibioticus* a treatment with 5-Fu stimulated the production of pheoxazinone synthase which is involved in actinomycin biosynthesis (Jones, 1985). Hence, these effects could be reinforced in Δ*yjjG*. Studying changes in the transcriptome of the deletion strain would surely reveal further changes in cellular processes.

The increase in Ni^{2+} sensitivity in Δ*yjjG* and the corresponding transposon mutant most probably resulted from polar effects on other genetic determinants rather than from the loss of E13YjjG. Again, transcriptomic studies might help approaching this question. However, these results underlined the importance of genetic complementation and heterologous overexpression for studying gene functions and preventing false conclusions.

The hydrolase E13YjjG can thus be considered a player in stress response in streptomycetes, although not to heavy metals, but other compounds which pose a threat to DNA integrity.

3.6 Ni^{2+} influx – the other side of nickel homeostasis

Introduction

High-affinity uptake systems for essential elements are especially needed in environments with low metal availability. For nickel, such a system was first reported in *Cupriavidus necator* H16 (Tabillion & Kaltwasser, 1977). In general, Ni^{2+} uptake in cells is mediated by two high-affinity systems (Eitinger & Mandrand-Berthelot, 2000): ABC transporters, like NikA-E of *E. coli*, or transition metal permeases. The latter constitute the NiCoT superfamily, a family of integral membrane transporters found in all domains of life (Eitinger et al., 2000; Eitinger et al., 1997; Komeda et al., 1997; Wolfram & Bauerfeind, 2002). The first and best described member of this family is HoxN of *C. necator*, which is also the first Ni^{2+}-specific transporter that was analyzed at a molecular level (Eitinger & Friedrich, 1991). Examples for homologous proteins are *Helicobacter pylori* NixA (Wolfram & Bauerfeind, 2002), *Schizosaccharomyces pombe* Nic1p (Eitinger et al., 2000), *Rhodococcus rhodochrous* NhlF (Degen et al., 1999), *Bradyrhizobium japonicum* HupN (Fu et al., 1994) and *Bacillus sp*. UreH (Maeda et al., 1994). On the basis of their substrate specificity they can be grouped into three different classes displaying (i) a specificity for Ni^{2+}, (ii) a preference for Co^{2+}, but also transport Ni^{2+}, and (iii) a preference for Ni^{2+}, but Co^{2+} is a substrate as well (Hebbeln & Eitinger, 2004). HoxN and NixA belong to the first group (Eitinger et al., 1997; Fischer et al., 2016), while the Co^{2+} transporter NhlF is a member of the second. This transporter was originally identified as exclusive Co^{2+} transporter in *Rhodococcus rhodochrous* (Komeda et al., 1997) and was later shown to transport Ni^{2+} as well (Degen et al., 1999). These three transporters are paradigms of NiCoT proteins showing a characteristic eight transmembrane domain topology and an energy-dependent high-affinity, low-capacity transport mode (Eitinger et al., 1997; Fulkerson et al., 1998; Komeda et al., 1997; Wolfram et al., 1995).

According to the TCDB the NiCoT superfamily (TC# 2.A.52) is divided in two subfamilies. One of them

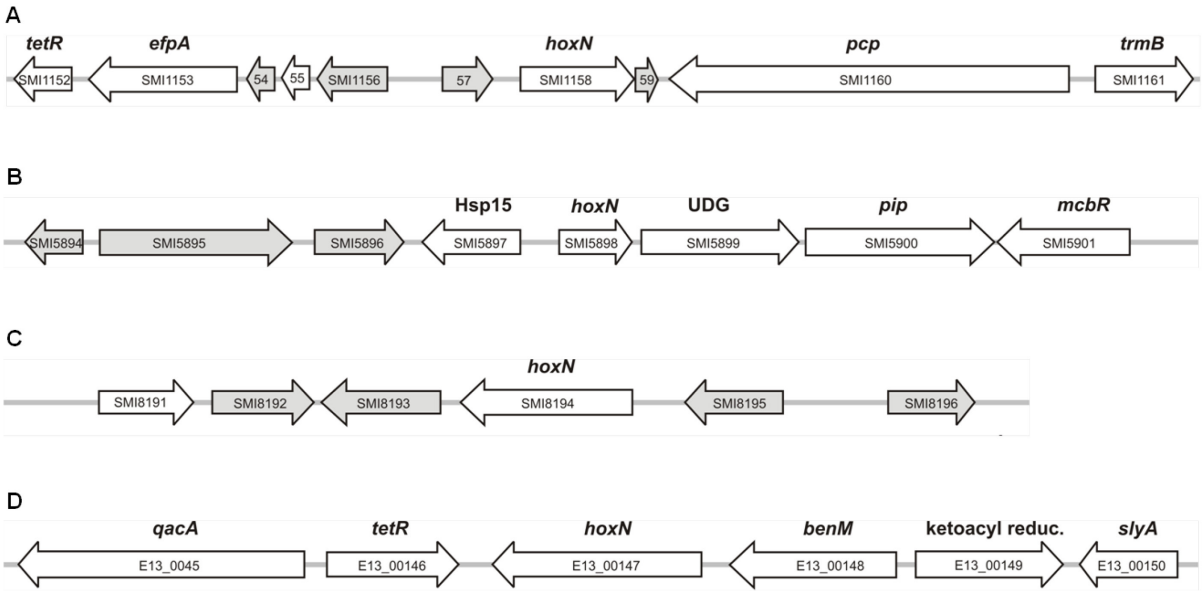

Figure 62. Genomic locations of putative *hoxN* genes in *S. mirabilis* and *S. acidiscabies*: A) *P16hoxN*; B) *P16hoxN2*; C) *P16phoxN*; D) E13*hoxN*. Numbers in arrows indicate annotation ID and predicted gene functions are given above. If no function was predicted, arrows are shaded grey.

comprises the well-investigated transporters mentioned above, while the other mainly consists of putative proteins, some of which are predicted to export Ni^{2+} and Co^{2+} from the cytoplasm (Saier et al., 2016). The latter are shorter and possess six to seven TM helices.

Regarding their amino acid sequence, NiCoT proteins share several conserved motifs that are essential for transport functioning and substrate affinity. The motifs (R/K)HAXDADH(I/L) in TMD II and $GX_2FX_2GH(S/T)(S/T)(V/I)$ in TMD III are crucial for transporter functioning (Eitinger et al., 2000; Saier et al., 1999). Amino acid exchanges in these motifs were shown to completely abolish Ni^{2+} transport in HoxN and NixA (Eitinger et al., 1997; Wolfram & Bauerfeind, 2002).

To the best of the author's knowledge, all hitherto investigated NiCoT family proteins function as metal importers for supplying the cell with essential metals for enzyme functioning. Their role in metal homeostasis in *Streptomyces* sp. has not been determined yet.

Results

Computational analysis

Protein characteristics

Comparison of the *hoxN* sequence of *Cupriavidus necator* H16 (AY305378.1:21335-22390) with the genomic sequences of *S. mirabilis* P16 and *S. acidiscabies* E13 yielded four ORFs exhibiting sufficient sequence similarity: one in the genome of *S. acidiscabies*, two in the *S. mirabilis* genome and the fourth on the large plasmid of *S. mirabilis* (Table 22). They were predicted to code for high-affinity nickel transport proteins and were therefore chosen for further analysis.

On protein level the high sequence similarity to other high affinity nickel transporters of the NiCoT family was confirmed, as conserved motifs of this family (pfam03824) were identified in all four putative streptomycete HoxN proteins. From swizzprot database entries, the highest sequence identity (44-53 %) and query coverage (79-90 %) for all four proteins was observed with *C. necator* HoxN (P23516; CnHoxN). Also the similarity to *Helicobacter pylori* NixA (Q48262; HpNixA), *Rhodococcus rhodochrous* NhlF (P96454; RrNhlF) and *Bradyrhizobium diazoefficiens* HupN (Q45247) was comparably high with at least 32 % sequence identity and 74 % query coverage. From this, it was concluded that the streptomycete transporters belonged to the group of high-affinity Ni^{2+} permeases (COG3376).

The predicted protein sizes of about 380 aa and 41 kDa (Table 22) were slightly higher, but still in

Table 22. Characteristics of putative HoxN proteins of *S. mirabilis* and *S. acidiscabies*, as well as location of the corresponding genes. For comparison, features of the well-investigated *C. necator* H16 HoxN (CnHoxN) and *R. rhodochrous* (RrNhlF) are displayed.

	P16HoxN	P16HoxN2	P16pHoxN	E13HoxN	CnHoxN*	RrNhlF*
Gene location	chromosome	chromosome	plasmid	chromosome	plasmid	chromosome
Annotation	SMI1158	SMI5898	SMI8194	E13_00147	P23516	P96454
Amino acids	378	121	375	383	351	352
Mass	41.1 kDa	13.4 kDa	40.8 kDa	41.9 kDa	38.8 kDa	37.2 kDa
Predicted TMD	8	2-3	7-8	7-8	8	8

*Data were taken from NCBI database entries.

accordance with published NiCoT members (Saier et al., 1999), except for P16HoxN2, which was markedly shorter (121 aa) and its product was presumably truncated. Therefore, this gene was excluded from further, more thorough analysis.

CnHoxN, HpNixA and RrNhlF exhibit eight TM helices (Eitinger et al., 1997; Fulkerson & Mobley, 2000; Komeda et al., 1997). The same topology was predicted for P16HoxN (Table 22), while the topology analysis for the other two proteins differed, depending on the deployed tool, ranging from seven to eight helices. Following the positive-inside rule (von Heijne, 1992), it was concluded that an eight TMD topology was more likely for P16pHoxN and E13HoxN with both protein termini facing the cytoplasm.

One main task of metal importers is to provide ions for enzyme maturation, which is why they are often found to be co-transcribed in the same operon as the respective enzyme to ensure enzyme functioning (Maeda et al., 1994; Sebbane et al., 2002). *In silico* analysis of the up- and down-stream regions adjacent to the *hoxN* in *S. mirabilis* and *S. acidiscabies* did not identify such potential operons (Figure 62). Therefore, these transporters might be transcribed independently from specific enzyme-coding genes. Known Ni^{2+}-dependent enzymes in *Streptomyces* sp. are for example urease and NiSOD, for which coding genes were also found in the genome of both investigated strains. Thus, the strains should have a requirement for Ni^{2+} for basic cellular functions.

Protein sequence comparison

NiCoT family proteins feature four clusters of essential amino acids as conserved motifs which are crucial for metal transport (Degen & Eitinger, 2002; Wolfram & Bauerfeind, 2002):

(R/K)HAXDADH(I/L)
GXXFXXGH(S/T)(S/T)(V/I)
LGX(D/E)T(A/S)(T/S)E
GMXXXD(T/S)XD.

These recognition sequences are located within the TMDs, which are the most conserved parts of the transporters in prokaryotic as well as eukaryotic HoxN-like proteins (Eitinger et al., 2000; Saier et al., 1999). Even single amino acid exchanges in these motifs by similar amino acids were shown to abolish Ni^{2+} transport (Eitinger et al., 1997; Fulkerson et al., 1998; Wolfram & Bauerfeind, 2002).

In an alignment of the *Streptomyces* sp. HoxN sequences with the three best characterized HoxN-like transporters (Figure 63), all four recognition sequences of the family were identified. The motifs were conserved, with one exception in P16pHoxN, where the last Glu residue of motif III was replaced by Gln (Q224).

TMDs IV and V of all aligned proteins were connected by a large hydrophilic loop, a feature shared by all NiCoT proteins, which stood out by a high number of charged amino acids (10-14 residues out of about 45).

HoxN-like permeases exhibit different ion selectivities. While some are highly selective for Ni^{2+}, others also transport Co^{2+} (reviewed in Eitinger & Mandrand-Berthelot (2000)), which is mainly determined by residues in the first two TM helices and the interaction of these domains (Degen & Eitinger, 2002). For predicting the substrate specificity, the streptomycete transporters were therefore aligned with CnHoxN and HpNixA, which exclusively transport Ni^{2+}, and the Co^{2+} and Ni^{2+} transporting RrNhlF (Degen et al., 1999; Fischer et al., 2016) (Figure 63).

Degen & Eitinger (2002) proved, that the substrate specificity is mainly determined by TMD I and II, as replacement of TMD I of CnHoxN by the corresponding RrNhlF domain, enabled Co^{2+} transport. In these TMDs the sequence similarity of the *Streptomyces* sp. HoxN was higher to RrNhlF than to CnHoxN.

In studies of CnHoxN and HpNixA, the importance of specific amino acids for transport was investi-

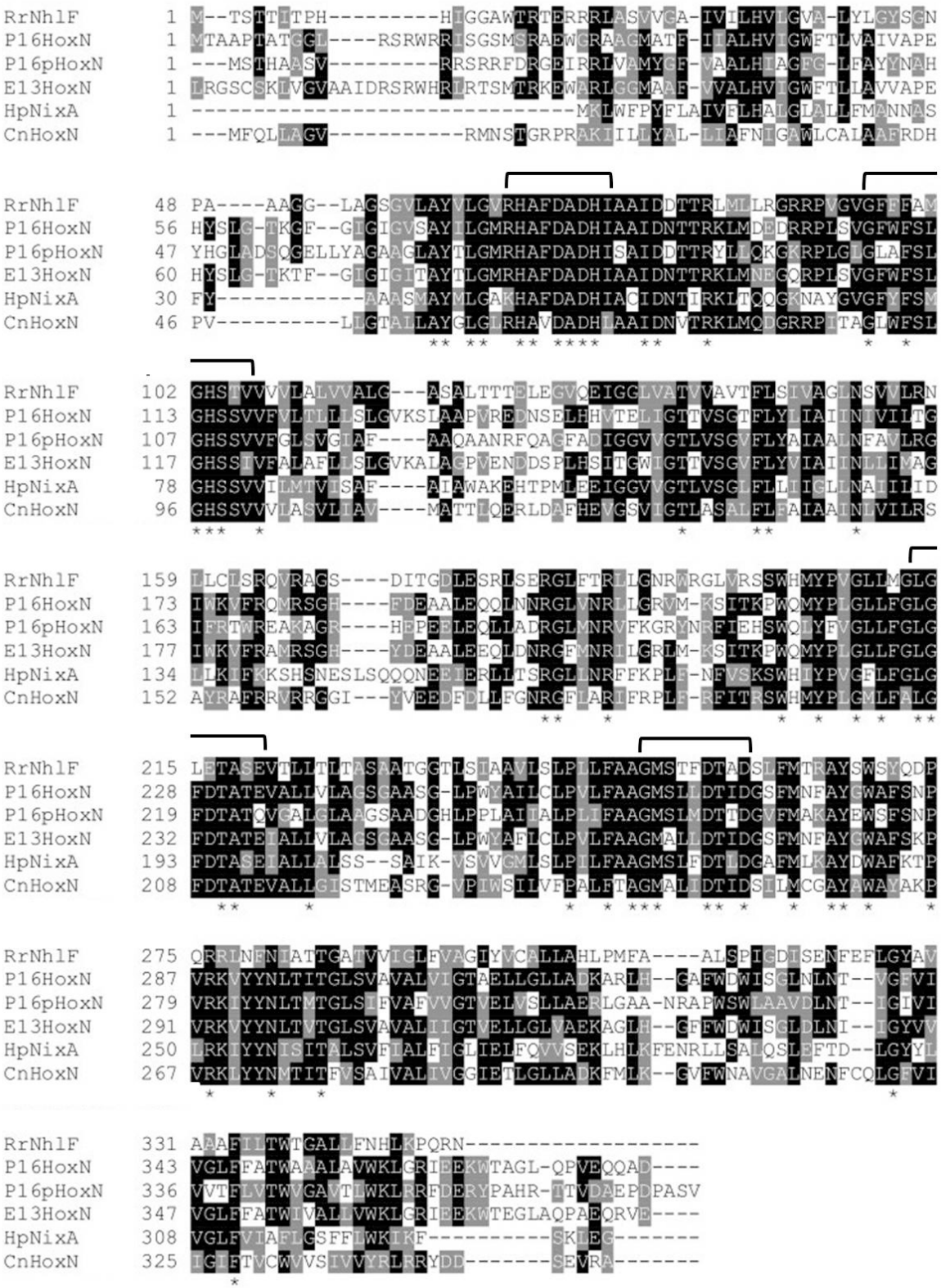

Figure 63. Alignment of amino acid sequences of putative streptomycete HoxN-like proteins with *H. pylori* HoxN (HpHoxN) and well-investigated homologues. Brackets indicate recognition sequences of HoxN-like proteins. Asterisks mark identical residues in all compared sequences.

gated by single-side exchanges (Eitinger et al., 1997; Fulkerson et al., 1998; Wolfram & Bauerfeind, 2002). All residues that were shown in these experiments to be important for Ni^{2+} transport were mostly conserved in the *Streptomyces* sp. transporters as well. In HpNixA, Wolfram & Bauerfeind (2002) could determine single residues, whose exchanges strongly affect Ni^{2+} uptake. Two of these exchanges were observed in the *Streptomyces* sp. transporters. Firstly, HpNixA V82 was replaced by Ile in E13HoxN and secondly, H181 was exchanged by Gln in all streptomycete HoxN proteins. Similarly, C331 of CnHoxN was substituted in all *Streptomyces* sp. HoxN, as well as RrNhlF, by Thr. Replacement of these residues in HpNixA and CnHoxN significantly reduced Ni^{2+} uptake (Eitinger et al., 1997; Wolfram & Bauerfeind, 2002).

V64 in TMD II of CnHoxN, which had been shown to play an important role in CnHoxN substrate specificity (Degen & Eitinger, 2002), was replaced by Phe in the other transporters. This exchange was shown to enable the transport of Co^{2+} and enhance Ni^{2+} transport in CnHoxN (Degen & Eitinger, 2002). The same applied for F30 and N31 of CnHoxN, which were replaced by Leu and His in RrNhlF as well as the *Streptomyces* sp. HoxN, but also HpNixA. The VXLHVLGXAL signature in TMDI of RrNhlF, where these two residues were located, was hypothesized to be a main determinant of substrate specificity, as it can also be found in other Co^{2+} transporters (Degen & Eitinger, 2002; Degen et al., 1999; Komeda et al., 1997). Regarding their sequence similarity to RrNhlF, it was highly likely that the streptomycetes HoxN proteins would transport Ni^{2+} as well as Co^{2+}.

Phylogenetic comparison

As the sequence identities to other NiCoT family proteins were high, a phylogenetic tree was generated for a broader comparison, where also less well-investigated proteins were included (Figure 64). In accordance with their phylogenetic affiliation, the *S. mirabilis* and *S. acidiscabies* transporters clustered with other transporters of the order Actinomycetales, with highest similarity to *Streptomyces* sp. proteins. However, a differentiation between the chromosomally encoded HoxN proteins and P16pHoxN, which was coded on the *S. mirabilis* plasmid, became apparent. The latter was more similar to transporters from two *Streptomyces* strains isolated from Chinese soil, one of which exhibit high heavy metal resistance (Zhou et al., 2016). These proteins also cluster with the *R. rhodochrous* NhlF, a protein that was first recognized as Co^{2+} transporter and later shown to transport Ni^{2+} as well (Degen & Eitinger, 2002; Degen et al., 1999).

The cluster containing the chromosomal *S. mirabilis* and *S. acidiscabies* encoded HoxN proteins on the other hand, did not comprise well-investigated NiCoT family proteins and the transporters with the highest similarity originated from strains which are not known particularly for their metal resistance.

Therefore, the phylogenetic tree did not allow prediction of the substrate specificity of the transporters regarding Co^{2+} transport, but the separation of P16pHoxN from the other *S. mirabilis* HoxN proteins might indicate an extrinsic origin of this transporter instead of a strain-internal gene duplication.

Deletion of chromosomal *hoxN* genes and genetic complementation

The *in silico* analysis substantiated the assumption that the streptomycete HoxN homologues might be involved in Ni^{2+} homeostasis. In order to confirm this hypothesis, the chromosomal *hoxN* genes were deleted by targeted gene replacement, yielding strains P16 Δ*hoxN* and E13 Δ*hoxN*. Despite several attempts, the plasmidal *S. mirabilis hoxN* gene (*P16phoxN*) could not be deleted and had to be dismissed as potential deletion strain from the following experiments due to time limitations. However, the clean knock-out transformants were further genetically complemented by introducing *E13hoxN*, *P16hoxN* or *P16phoxN* separately in P16 Δ*hoxN* and E13 Δ*hoxN* for investigating the capability of each *hoxN* gene to impact the phenotype of the deletion strain and re-establish WT characteristics. The integrative plasmid pSEThph was used as delivery vector for complementation.

In order to roughly assess the change in heavy metal resistance in the thus modified strains, trench plate tests were performed on minimal medium (AM) and the more complex medium GYM, using Ni^{2+}

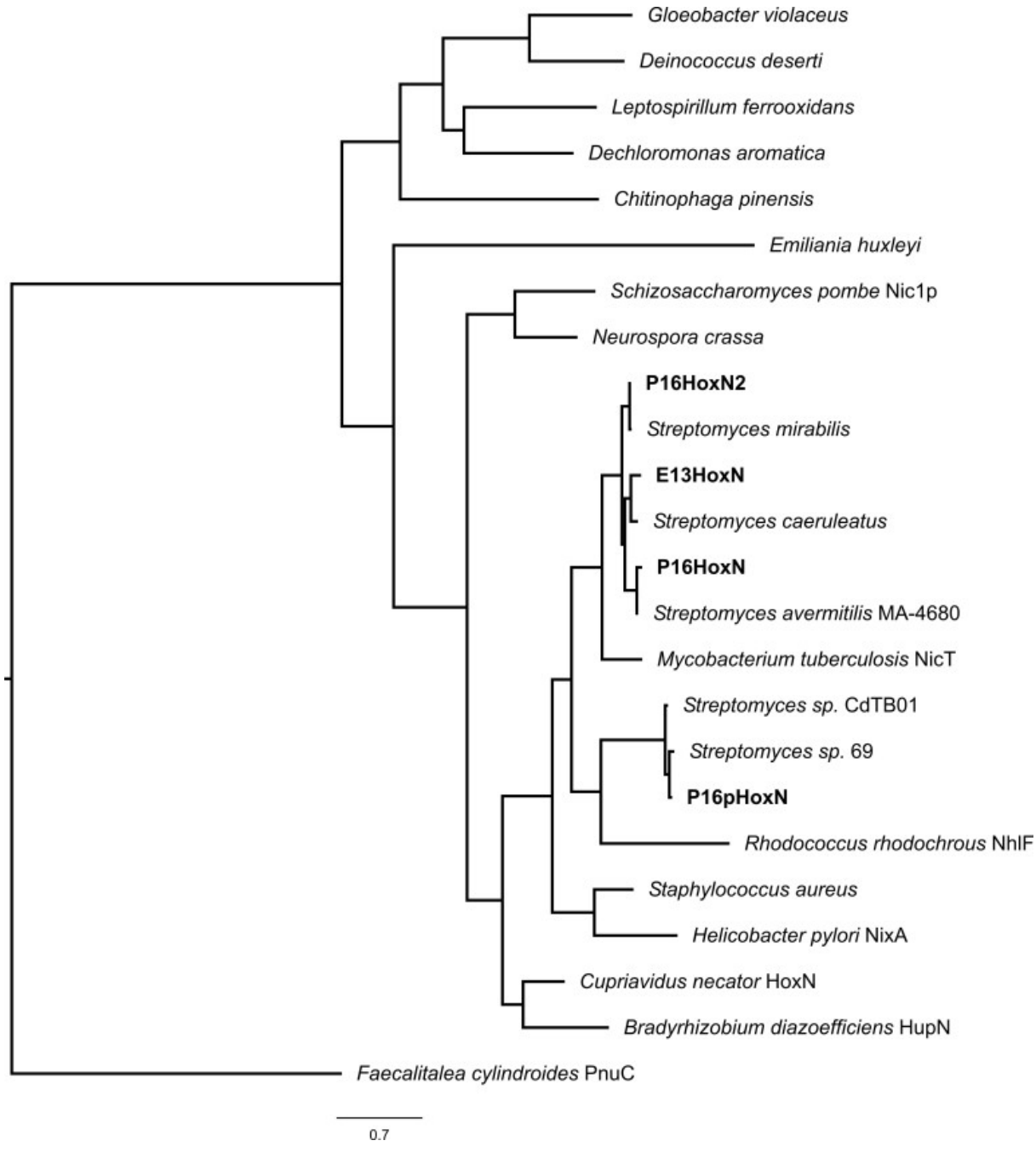

Figure 64. Phylogenetic tree of HoxN homologues.

and Co^{2+} salts (Figure 65). In *S. mirabilis*, *hoxN* deletion increased the resistance to Ni^{2+}, particularly on minimal medium, while complementation with *P16hoxN* reduced resistance to WT level. This was in accordance with other studies of HoxN homologues. For instance, the inactivation of HpNixA increases nickel tolerance, as the transporter is responsible for Ni^{2+} influx, wherefore its absence would decrease intracellular Ni^{2+} levels (Fischer et al., 2016).

In contrast, *hoxN* deletion in *S. acidiscabies* strongly reduced Ni^{2+} resistance and also the genetically complemented strain would be more sensitive to this metal. Again, the change was most pronounced on minimal medium. This result was unexpected and suggested a different role for E13HoxN in the nickel homeostasis of this streptomycete. Usually, an increase in sensitivity indicates a function as metal exporter, e.g. as observed in section 3.3 for P16NreB.

The strains complemented with the respective heterologous chromosomal *hoxN* or *P16phoxN* exhibited mostly growth differing from the strain complemented with the homologous gene. Especially for *S. mirabilis* this effect was most prominent. On AM medium the integration of *E13hoxN* or *P16phoxN* in P16 Δ*hoxN* did not impact the Ni^{2+} sensitivity to a high degree. These complemented strains still

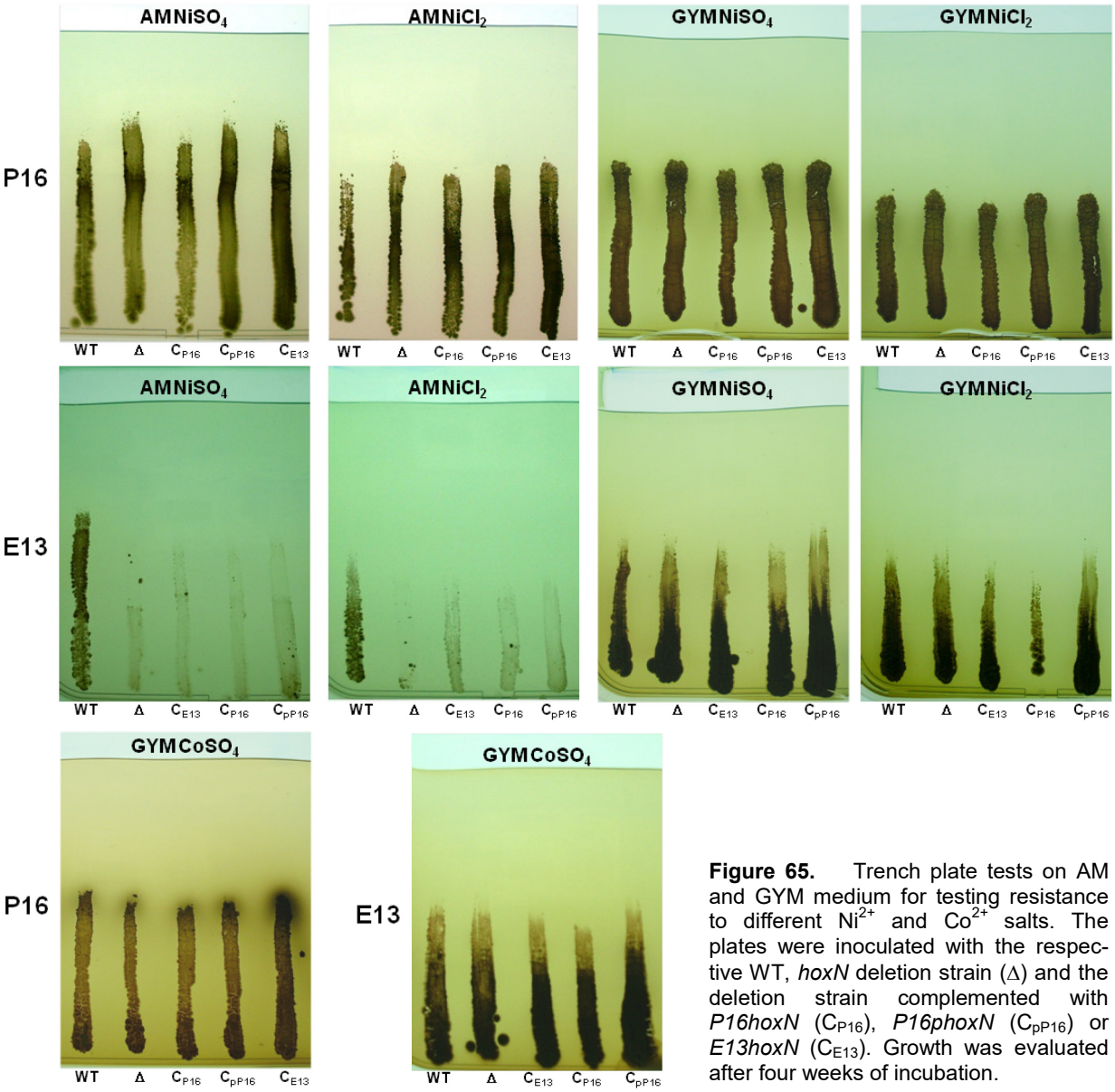

Figure 65. Trench plate tests on AM and GYM medium for testing resistance to different Ni^{2+} and Co^{2+} salts. The plates were inoculated with the respective WT, *hoxN* deletion strain (Δ) and the deletion strain complemented with *P16hoxN* (C_{P16}), *P16phoxN* (C_{pP16}) or *E13hoxN* (C_{E13}). Growth was evaluated after four weeks of incubation.

showed higher Ni^{2+} resistance than *S. mirabilis* WT, which was another hint that E13HoxN function might differ from that of P16HoxN and the same applied for P16pHoxN.

In E13 Δ*hoxN*, the complementation with the heterologous transporters resulted in a decrease of Ni^{2+} resistance in case of *P16hoxN* and better growth with Ni^{2+} in case of *P16phoxN*, both on GYM medium. The former observation was in line with the findings for P16 Δ*hoxN*, meaning that the expression of an additional Ni^{2+} influx pump would lead to higher Ni^{2+} levels in the cell, subsequently decreasing Ni^{2+} resistance. In E13 Δ*hoxN* hphP16phoxN Ni^{2+} resistance appeared to be slightly increased as compare to the deletion strain. Thus, the transport direction might be rather directed to the extracellular space. However, this could not be inferred for certain from these tests, as it could not be ensured that the Ni^{2+} gradient established in the trench plates was homogenous.

Regarding Co^{2+}, the trench plate test gave no conclusive result. Either, the change of sensitivity was too subtle to be detected, or the deletion had no influence on resistance to this metal. Thus, for obtaining a more detailed insight in the change of metal sensitivity, the deletion strains and their respective complemented strain were tested in liquid medium.

The Ni^{2+} resistance limits obtained in liquid culture were partly contradicting the growth observed on solid medium (Table 23). Whether deletion of *hoxN* impacted Ni^{2+} resistance in liquid medium appeared to be strongly dependent on the medium type, as for *S. mirabilis* in AM no change was observed, while in GYM the resistance decreased by 2.5 mM in Δ*hoxN* whereas in TSB *hoxN* deletion increased Ni^{2+} resistance from 35 mM in the WT to 40 mM in P16 Δ*hoxN*. The complementation with *P16hoxN* reduced Ni^{2+} resistance in all media below WT levels.

In *S. acidiscabies*, a reduced Ni^{2+} resistance was observed for the *hoxN* deletion strain in all tested media, which was in accordance with the results from the trench plate tests. E13 Δ*hoxN* tolerated roughly half of the amount of Ni^{2+}. Genetic complementation, further decreased resistance in AM to 1.25 mM and TSB to 10 mM, but increased resistance in GYM from 1.5 mM in E13 Δ*hoxN* to 2.25 mM, which was still below WT level (5 mM).

Interestingly, cobalt resistance changed contrariwise in both deletion strains, with a slight reduction for P16 Δ*hoxN* and an increase in E13 Δ*hoxN*. For the latter strain, genetic complementation nearly re-established WT levels, while no change was observed in the complemented P16 Δ*hoxN* strain.

Taken together, the results from the heavy metal resistance were partly contradictory and did not allow for definite conclusions. It could be assumed that there were differences in either the transport capacity or directions of the HoxN proteins. In particular, the strong increase in Ni^{2+} resistance in E13 Δ*hoxN*

Table 23. Maximally tolerated concentrations of $NiSO_4$ [mM] and $CoSO_4$ [mM] in liquid media. Growth was evaluated after two weeks incubation.

	NiSO4			CoSO4	
	AM	**GYM**	**TSB**	**GYM**	**TSB**
P16 WT	45	12.5	35	1.2	5
P16 Δ*hoxN*	45	10	40	0.8	4
P16 Δ*hoxN* hphP16*hoxN*	40	7	27.5	0.8	4
E13 WT	4	5	20	0.2	1
E13 Δ*hoxN*	2	1.5	11	0.3	1.8
E13 Δ*hoxN* hphE13*hoxN*	1.25	2.25	10	0.1	1

was surprising. However, since this defect could not be rescued by re-introducing the native gene, it could be suspected that this effect was the result of other, unexpected changes in the Ni^{2+} resistome of the strain. Since E13HoxN was the only predicted transporter of this type in *S. acidiscabies*, the loss might affect the streptomycete more than loss of P16HoxN in *S. mirabilis*, as this strain still disposed of a second putative HoxN homologue, P16pHoxN.

Moreover, the differences observed between different media suggested the presence of other transporters whose activity might depend on media composition, e.g. availability of a certain carbon source, wherefore they could only compensate the loss of HoxN activity under certain conditions, which accounted for the plasticity of the metal transportome.

Sensitivity to NTA, EDTA and H_2O_2

Since the results of the heavy metal resistance test did not gave a definite picture of the transport functions of the streptomycete HoxN proteins, the sensitivity of the strains to other compounds, which could be indirectly connected to Ni^{2+} transport, was tested.

Table 24. Maximally tolerated concentrations [mM] of NTA and EDTA in liquid culture using TSB or GYM medium. Growth was evaluated after 14 d incubation.

	NTA	EDTA	
	TSB	TSB	AM
P16	17	0.4	0.2
P16 Δ*hoxN*	16	0.2	0.05
E13	14	0.5	0.2
E13 Δ*hoxN*	12	0.4	0.05

In *Streptomyces* sp., nickel is required for different cellular processes, which enable growth of the bacterium. Thus, the cells are depending on the availability of this element. By using metal chelating compounds like NTA and EDTA, nickel availability in the medium can be reduced. Thereby, unspecific Ni^{2+} uptake in the cell is inhibited which necessitates the ability to efficiently sequester remaining Ni^{2+} ions from the surrounding. Thus, the loss of Ni^{2+} influx transporters should result in reduced growth under Ni^{2+} limiting conditions (Eitinger et al., 2000; Eitinger et al., 1997). Hence, the WT and *hoxN* deletion strains were tested for their sensitivity to NTA and EDTA. Both deletion strains tolerated less of these agents in liquid culture (Table 24). The higher difference between *S. acidiscabies* WT and E13 Δ*hoxN* as compared to *S. mirabilis* and its deletion strain and the generally higher tolerance of *S. mirabilis* to NTA, probably reflected the ability of P16pHoxN to partly compensate the loss of the chromosomal *hoxN* gene.

Additionally, the sensitivity to oxidative stress was assessed by testing H_2O_2 sensitivity (Table 25). Both deletion strains tolerated less H_2O_2 than their wildtypes, indicating a lower tolerance to oxidative stress. Possibly, the increase in sensitivity resulted from a disturbance in the oxidative stress response system of the cells, due to reduced NiSOD activity, whose expression is regulated by Ni^{2+} and which additionally requires Ni^{2+} for activity (Kim et al., 1998; Youn et al., 1996).

Table 25. Maximally tolerated concentrations of urea [mM] in liquid AM and of H_2O_2 [ppm] in liquid TSB medium. Growth was evaluated after 5 d incubation.

	P16	P16 Δ*hoxN*	P16 Δ*hoxN* hphP16hoxN	E13	E13 Δ*hoxN*	E13 Δ*hoxN* hphE13hoxN
Urea	500	400	450	550	550	550
H_2O_2	42	36	42	39	36	39

Ureas activity

In order to confirm a change in the activity of a Ni^{2+}-containing enzyme in the deletion strains, the urease activity was determined. In many studies on the functioning of HoxN and homologous proteins, monitoring the urease activity served as indirect reporter for intracellular Ni^{2+} levels (Fischer et al., 2016; Fulkerson et al., 1998; Mobley et al., 1995; Wolfram & Bauerfeind, 2002). The urease activity of *S. mirabilis*, *S. acidiscabies* and the deletion strains was measured in biomass from liquid cultures in two different media, TSB and GYM. E13 Δ*hoxN* exhibited 72 % of the urease activity of the WT in TSB and 85 % when cultured in GYM medium. The same was observed for P16 Δ*hoxN*, in which the urease activity was reduced to 71 % in TSB and 68 % in GYM medium. The reduced activity matched the assumption of the HoxN proteins being Ni^{2+} importers, as reduced Ni^{2+} import interfered with protein maturation (Eitinger et al., 1997; Fulkerson et al., 1998). Concordantly, deletion of HoxN homologues in *Schizosacchromyces pombe* and *H. pylori* decrease urease activity in these organisms (Fulkerson et al., 1998; Mobley et al., 1995).

The reduced urease activity in P16 Δ*hoxN* also showed when the strains were tested for urea tolerance in liquid culture (Table 25). While the deletion strain tolerated 400 mM, the WT could grow with up to 500 mM urea. Re-introduction of *P16hoxN* only partly complemented tolerance to urea. Interestingly, in *S. acidiscabies* deletion of *E13hoxN* did not impact urea tolerance.

Biomass nickel content

Despite being partly contradictory, the results of the tests described so far indicated a change in intracellular nickel concentrations resulting from loss of HoxN function. Thus, the Ni^{2+} content in the biomass of the wildtypes and deletion strains from liquid GYM cultures was determined (Figure 66).

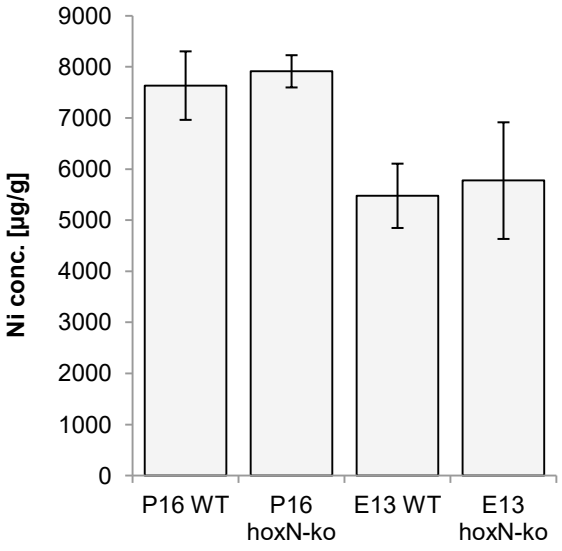

Figure 66. Nickel content in biomass from 4 d old liquid cultures. The strains were cultivated in GYM medium amended with either 2.5 mM (P16, P16 Δ*hoxN*) or 1 mM NiSO4 (E13, E13 Δ*hoxN*).

There was a slight increase in the biomass Ni^{2+} concentration in both deletion strains, but without statistical significance. Again, this was an unexpected result, being contrary to reports on other *hoxN* deletion strains, which showed a reduced intracellular Ni^{2+} content (Fischer et al., 2016; Herzberg et al., 2016). Deletion of a chromosomal *hoxN* gene in *C. metallidurans* also impacted copper accumulation in the cells, increasing the Cu(I) concentration. In P16 Δ*hoxN* and E13 Δ*hoxN* copper content was slightly reduced, but not in a significant level.

For *S. acidiscabies*, the slight increase in Ni^{2+} accumulation was in accordance with the reduced Ni^{2+} resistance of the strain. However, the activity of the Ni^{2+}-containing urease was found to be reduced nevertheless.

One could only speculate about the reasons for this discrepancy. Firstly, the liquid cultures used for biomass analysis were amended with $NiSO_4$, as it was hoped for that Ni^{2+} amendment would increase

any differences. However, at elevated Ni^{2+} concentrations HoxN expression or activity might be down-regulated and thus be insignificant, which would explain the lack of difference between WT and deletion strains. In general, the expression of HoxN-like transporters is found to be differentially regulated in organisms. While in *C. metallidurans* HoxN expression is independent from Ni^{2+} availability, *nixA* of *H. pylori* is under transcriptional control of NikR, that represses NixA synthesis at elevated Ni^{2+} levels (Herzberg et al., 2016; Wolfram et al., 2006). How *hoxN* was regulated in *Streptomyces* sp. remained to be determined.

Secondly, the incubation time for the liquid cultures of 4 d might have been too short, as HoxN transport activity is usually low, wherefore differences between the strains might only have shown after prolonged incubation.

Overexpression of *Streptomyces sp.* HoxN in *E. coli*

The *in vivo* gene deletion experiments did not yield conclusive evidence on the activity of the streptomycete HoxN homologues. One possible reason might be the interference of other intrinsic Ni^{2+} homeostasis systems that were affected by HoxN loss and changed their activity accordingly. Thus, to minimize these interferences the *Streptomyces* sp. HoxN proteins were expressed in *E. coli* using vector pTrc99A. If the investigated transporters import Ni^{2+}, rather than export it, the *E. coli* transformants should be impaired in growth when challenged with Ni^{2+}.

In Figure 67 the growth of the strains in LB medium amended with 1 mM $NiSO_4$ is shown. In all cases *E. coli* growth benefitted from *hoxN* compared to the empty vector. This was in contrast to findings for NixA, which increased Ni^{2+} sensitivity when expressed in *E. coli* (Mobley et al., 1995). Although, without Ni^{2+} amendment *E. coli* growth likewise was increased in transformants carrying *nixA* (Mobley et al., 1995). Under aerobic conditions, *E. coli* does not require much Ni^{2+}, wherefore it was hardly explainable why increased Ni^{2+} influx would result in increased growth. These results rather suggested a Ni^{2+} export function for the HoxN homologues, similarly to P16NreB.

However, already other authors acknowledged the limited validity of HoxN expression tests in *E. coli* regarding changes in growth. This was attributed to the high affinity, but low capacity of these per-

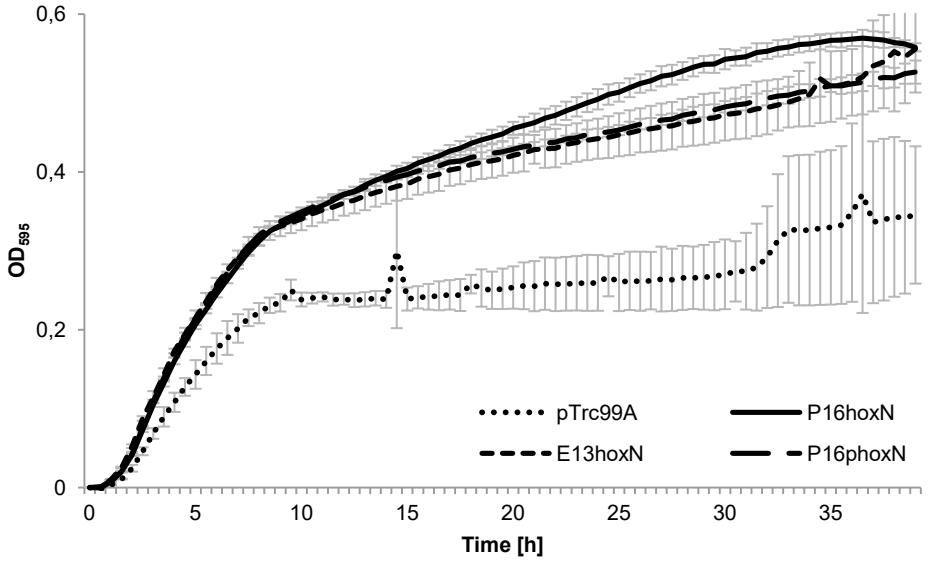

Figure 67. Growth of *E. coli* in LB medium amended with 1 mM $NiSO_4$. The strains carried either one of the streptomycete *hoxN* genes or the empty vector pTrc99A. Bars indicate standard deviation from three biological replicates.

meases. Hence, in other studies nickel isotope accumulation was used for confirming the function of these transporters and only in this way NhlF was recognized to not only transport Co^{2+}, but Ni^{2+} as well (Degen et al., 1999; Wolfram et al., 1995).

Another way of circumventing this limitation was the expression of reporter genes simultaneously to the putative Ni^{2+} transporters. Often, urease was used for these experiments and a higher urease activity served as indicator for increased Ni^{2+} influx in the cell, mediated by HoxN homologues (Degen et al., 1999; Fulkerson et al., 1998; Mobley et al., 1995). As *E. coli* DH5α was devoid of measurable Ni-containing enzyme activity, a Ni-dependent *Streptomyces* sp. enzyme had to be expressed for a similar approach. Due to difficulties in the amplification of the *S. mirabilis* urease cluster, it was decided to use the better investigated *sodN* gene of *S. coelicolor* A3(2), which encodes the NiSOD. Kim et al. (1998) found that for expression of an active NiSOD enzyme in *E. coli* the *sodN* gene had to be truncated, as this bacterium lacked the machinery for post-translational modification, during which the 14 N-terminal amino acids are cleaved off the precursor polypeptide yielding the functional NiSOD enzyme. Thus, primers for *sodN* amplification were chosen according to Kim et al. (1998) and the gene was integrated in pSET152 and used for transformation of *E. coli*. Growth of this transformant was compared to an empty vector control in LB medium containing 25 µM $NiSO_4$ amended with $CuSO_4$, H_2O_2 or $NiSO_4$ (Figure 68). In all cases, *E. coli* growth was reduced when NiSOD was expressed.

The *sodN* carrying *E. coli* strain was subsequently transformed with pTrc99A carrying either *Streptomyces* sp. *hoxN*. Growth was monitored as before in LB medium amended with 25 µM $NiSO_4$ for ensuring Ni^{2+} supply for SOD activity (Figure 69). At elevated copper concentrations, that would potentially increase intracellular oxidative stress which could be diminished by NiSOD activity, the transformant carrying *P16phoxN* performed best and also at high Ni^{2+} concentration this strain showed particularly good growth, which could result from higher NiSOD activity resulting from better Ni^{2+} supply. Another notable change was observed for the *E13hoxN* carrying strain when treated with H_2O_2, which strongly impaired growth. However, in the $NiSO_4$ treatment also growth of this strain was better than that of the empty vector control.

Hence, also the co-expression of NiSOD and the *Streptomyces* sp. HoxN did not allow decisive conclusions on the nature of these transporters. Probably NiSOD expressed in *E. coli* was not fully active

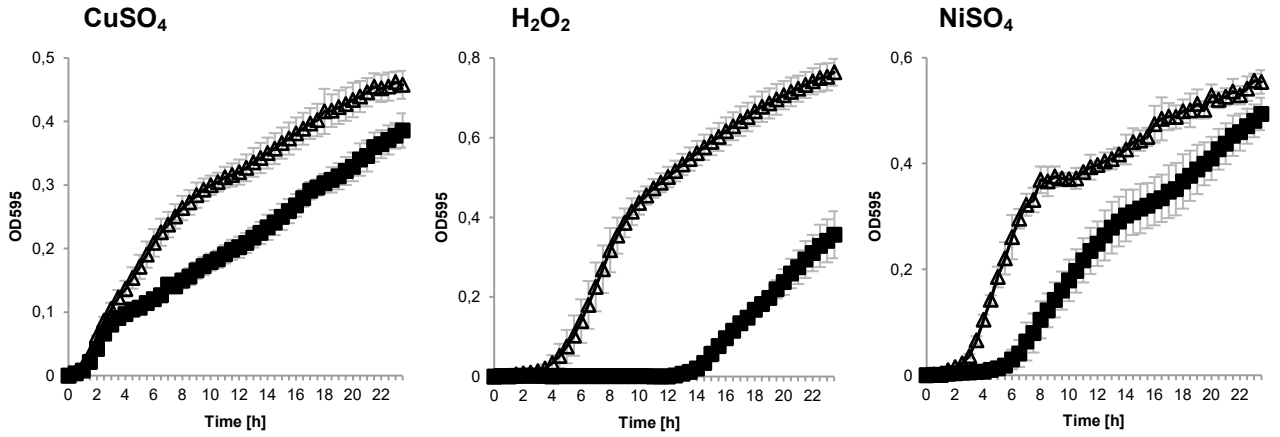

Figure 68. Growth of *E. coli* in LB medium amended with 25 µM $NiSO_4$. The strains carried the NiSOD encoding gene *sodN* of *S. coelicolor* A3(2) (closed squares) or the empty vector pSET152 (open triangles). In the treatments the strains were challenged with 1.5 mM $CuSO_4$, 60 ppm H_2O_2 or 1 mM $NiSO_4$. Bars indicate standard deviation from three biological replicates.

– a problem that has been encountered by Kim et al. (1998) as well, even for the truncated enzyme. Thus, the experiment should be repeated using a different Ni-dependent enzyme as reporter.

Conclusion

In this section, potential members of the NiCoT family were investigated regarding their role in Ni^{2+} homeostasis in *S. mirabilis* and *S. acidiscabies*. The presence of these transporters in the streptomycetes was in accordance with the wide distribution of NiCoT proteins among many bacterial taxonomic groups, as they constitute an old group of transporters with high functional diversity that has probably developed early in evolution (Zhang et al., 2009).

HoxN homologues usually display a high affinity, but low capacity, which complicates the determination of the transport functions of these proteins (Herzberg et al., 2016). This might have been one reason for the problems encountered in the present study. Deletion of *hoxN* homologues increased nickel

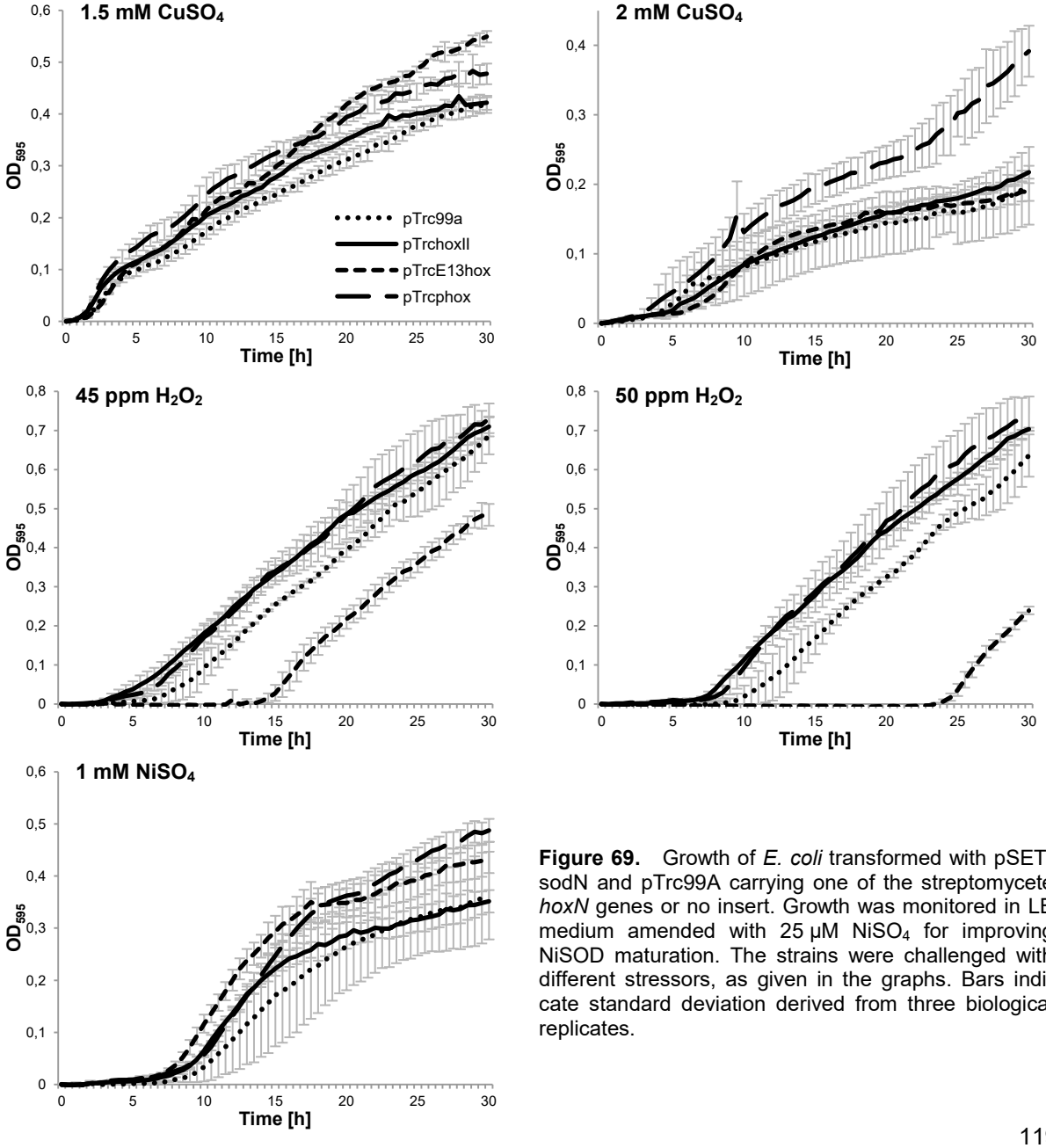

Figure 69. Growth of *E. coli* transformed with pSET-sodN and pTrc99A carrying one of the streptomycete *hoxN* genes or no insert. Growth was monitored in LB medium amended with 25 µM $NiSO_4$ for improving NiSOD maturation. The strains were challenged with different stressors, as given in the graphs. Bars indicate standard deviation derived from three biological replicates.

resistance in *S. mirabilis*, as can be expected if P16HoxN was a Ni^{2+} importer, while Ni^{2+} resistance was strongly decreased in *S. acidiscabies*, pointing to a contrary role of E13HoxN as compared to P16HoxN. However, as urease activity decreased and NTA and EDTA sensitivity increased in E13 Δ*hoxN*, as it did in P16 Δ*hoxN*, similar functions of both HoxN homologues could be assumed.

One possible explanation for the lack of a strong, unambiguous phenotypic change was that the loss of HoxN could be compensated by other transporters with low selectivity. Ni^{2+} can also enter the cell *via* unspecific uptake systems like magnesium transporters or as phosphate complexes (Herzberg et al., 2016; Kirsten et al., 2011) and Co^{2+} can be taken up by Zn^{2+} transporters (Grass et al., 2005). In *C. metallidurans* the deletion of seven secondary metal import systems reduced the fitness of the bacterium, but the strain was still able to maintain its cellular metal content, proving the high import capacity *via* unspecific uptake (Herzberg et al., 2016). Thus, it was expected that also in *Streptomyces* sp. the investigation of metal importers was strongly affected by this unspecific metal uptake, obscuring the actual effects of *hoxN* deletion.

Hence, for substantiating the function of the streptomycete HoxN homologues as Ni^{2+}, and possibly Co^{2+}, transporters, further studies were required, possibly by using nickel and cobalt isotopes. A first assessment could be the analysis of Ni^{2+} content in *E. coli* cells expressing the HoxN proteins, although it could be expected that also inherent *E. coli* Ni^{2+} transporters would impact the results.

3.7 Genes with impact on *Streptomyces* sp. development

Introduction

Mechanisms involved in actinobacterial development are complex and partly unique to these organisms. In the following, a short overview of the processes governing *Streptomyces* sp. morphological development will be given with focus on the important aspects for this chapter. More detailed descriptions of the underlying processes can be found in several review papers and references within, e.g. Chater (1993); Chater (1998); Claessen et al. (2006); Flardh & Buttner (2009).

The streptomycete life cycle starts when a spore encounters favourable conditions and geminates. A dense network of branching hyphae develops, the vegetative mycelium, which grows across surfaces and into substrates allowing colonization of the surrounding habitat and exploitation of available resources (Flardh & Buttner, 2009). Hyphal growth occurs apically by tip extension and branching. The assembly of new cell-wall material is strongly dependent on the polarity determinant DivIVA, which is mainly located at growing tips. This coiled-coil protein is involved in remodelling and synthesis of the streptomycete's cell wall peptidoglycan (Hempel et al., 2008).

Nutrient depletion as well as other factors demand the transition into the next growth stage, the reproductive growth, which is characterised by the formation of protruding aerial hyphae. This requires the formation of mycelium with the ability to break the barrier between the aqueous substrate environment and the air. Currently, at least three pathways are known to be involved in the development and maturation of aerial mycelium (Claessen et al., 2006): the initiation of aerial *Streptomyces* sp. growth is under control of the *bld* cascade, while the expression of signalling molecules after crossing the liquid-air barrier is controlled by the so-called "sky pathway", followed by spore formation which is directed by *whi* genes. This complex succession of regulatory pathways is necessary, as several factors have to be faced for aerial growth, like the medium-air interface, the regime change from aqueous to airy environment and change in tugor pressure for extension into air (Chater, 1998). Therefore, numerous genetic loci are involved in the morphological development (Claessen et al., 2006).

A hydrophobic, protective layer around the hyphae enables overcoming the surface tension of aqueous surroundings allowing aerial growth (Claessen et al., 2003). Depending on the media composition, different compounds are required for this process when *Streptomyces* sp. is grown on an agar plate under laboratory conditions. On complex media, a surfactant peptide, SapB, which is related to lantibiotics, is compulsory for aerial growth, while other hydrophobic molecules merely play a supportive role (Flardh & Buttner, 2009; Willey et al., 1991). However, on minimal media a SapB-independent pathway mediated by chaplins and rodlins exists. There are different types of these surface-active molecules with distinct functions. Their ability to self-assemble into amyloid-like filaments enables the creation of a protective coat around the hyphal cell (Claessen et al., 2003; Flardh & Buttner, 2009). Although all of these compounds have been investigated in numerous studies, the signalling pathways for the production of hydrophobic surface proteins is still poorly understood in *Streptomyces* sp. (Flardh & Buttner, 2009).

The production of extracellular matrix polymers does not only provide the hyphae with a hydrophobic layer, but also enables attachment to hydrophobic surfaces and the formation of pellets in liquid cultures (Petrus & Claessen, 2014). De Jong et al. (2009) found that cellulose fibrils produced by

S. coelicolor serve as anchoring platform for the assembly of chaplin proteins and subsequent fimbriae formation. These cellulose polymers are produced by the cellulose-synthase-like protein CslA, which is mostly located at the hyphal tip, as it is important for maintaining the tip integrity during growth synthesising β-glucan-containing polysaccharides (de Jong et al., 2009; Xu et al., 2008). An association between DivIVA and CslA has been hypothesised, in which CslA is integrated in the cell membrane and interacts with DivIVA, thereby locating the latter at the tip and enabling the synthesis of polysaccharides at the correct position (Xu et al., 2008). However, CslA is not restricted to the hyhal tip as it is important for hyphae attachment as well (de Jong et al., 2009).

The onset of the reproductive growth phase can be easily recognised on agar plates by the appearance of fluffy, often whitish mycelium. Mutations in genes involved in the above mentioned pathways may impair the production of aerial hyphae, wherefore such mutant colonies remain smooth and are called “bald”. Accordingly, genes whose deletion or mutation causes this phenotype, e.g. the SapB-coding *ramS*, are called *bld* genes (Claessen et al., 2006; Willey et al., 1991). Most of them encode transcription factors and have no obvious role in the morphologic development, but rather indirectly influence this process (Flardh & Buttner, 2009).

The production of aerial mycelium is accompanied by the lysis of the vegetative mycelium and partial self-cannibalization, as this process provides nutrients for reproductive growth (Chater, 1998). Several growth and cell-cycle processes are reorganised resulting in the differentiation in spore chains by synchronous, multiple cell division (Flardh & Buttner, 2009). Sporulation is controlled by *whi* genes whose mutation impairs spore formation, whereby colonies remain whitish (Chater, 1998). In the last step of the *Streptomyces* sp. life cycle, the spores undergo a maturation process by developing a thick, lysozyme-resistant wall, which enables the persistence under unfavourable conditions and allows dispersal (Flardh & Buttner, 2009).

The timing of gene transcription of the different pathways has to be accurately controlled for ensuring the correct sequence of processes. This can be achieved by employing alternative sigma factors, which control the specificity of promoter recognition by RNA polymerases, as activity depends on the association of the polymerase core enzyme with a sigma subunit (Paget et al., 2002). Therefore, sigma factors are transcribed differently under different growth conditions and growth stages for adjusting cellular processes to the current needs (Kang et al., 1997; Marcos et al., 1995). Numerous sigma factors connected to morphological development have been identified, which are active at different life cycle stages, e.g. *whiG* and *sigF* that code alternative sigma factors for the production and maturation of spores (Chater, 1998; Cho et al., 2001; Kelemen et al., 1996; Lee et al., 2005; Mao et al., 2009; Westpheling et al., 1985).

Results

Two transformants that arose in the preliminary transposon mutagenesis experiments, showed either a delay or a complete inhibition of aerial mycelium formation. In these strains, the transposon was found to be integrated into ORFs coding a cellulose synthase catalytic subunit (SMI4854) or a RNA polymerase sigma factor (SMI5555), respectively. As these genes both seemed to be involved in the morphological development of *S. mirabilis*, they will be examined together in this section.

Computational analysis

Identification of P16CslA

The 1998 bp long ORF SMI4854 coded a 665 aa protein with a mass of 73.9 kDa (Table 26) displaying conserved domains of the cellulose synthase superfamily, specifically the glycosyl transferase family (pfam13506). The protein only showed a low level of amino acid sequence identity to proteins of the swizzprot database and interestingly exclusively to Eukaryotes. The highest identity (32 %) was found to an UDP-forming cellulose synthase catalytic subunit of the soil-living amoeba *Dictyostelium discoideum* (Q9U720.1), which polymerizes uridine 5'-diphosphate glucose to cellulose as protection for emerging stalks of the cell (Blanton et al., 2000). Next best match (27 %) was with a cellulose synthase-like protein of *Oryza sativa* (Q7PC76) with glucomannan mannan synthase activities.

When the search was extended to the NCBI Reference Sequence database, the homology to other *Streptomyces* sp. proteins was surprisingly high, exceeding 90 % of identity in several cases with a query coverage of 100 %. All of these proteins were annotated as glycosyl transferases. The highest identity of the *S. mirabilis* protein was observed with a glycosyl transferase of *Streptomyces* sp. OK885 (WP_101404976). Among these proteins, the best characterized was a protein coded by SCO2836 in *S. coelicolor* A3(2) (WP_011028608.1), which was 84 % identical to the *S. mirabilis* protein and known as the cellulose synthase-like protein CslA (Xu et al., 2008). Because of the high identity between the two proteins, the *S. mirabilis* protein was designated P16CslA.

In *S. coelicolor*, CslA is the only protein of this type and it is proposed to be located in the cell membrane at hyphael tips, where it is important for the deposition of β-linked glucan by interacting with DivIVA (Xu et al., 2008). Also the above mentioned proteins of *D. discoideum* and rice exhibit transmembrane domains. Accordingly, for P16CslA six transmembrane domains were predicted, which is typical for these glycosyltransferases (cd06421).

Regarding putative catalytic sites of the predicted protein, two function-determining domains were identified by conserved domain search: firstly, a QXXRW domain, which is often found in processiv glycosyltransferases, like the *D. discoideum* protein, and proposed to be necessary for holding the glycan chain in the active site (Saxena et al., 2001) and secondly, two Asp residues in a DXD motif (D259, D261) at the N-terminal part of P16CslA, that served as catalytic site and were probably involved in the binding of a metal ion required for phosphate coordination in the active site (Roberts & Bushoven, 2007).

These findings suggested that P16CslA was indeed a glycosyltransferase integrated into the membrane which was involved in the formation of cell wall components like glucan.

In *S. coelicolor* the *cslA* gene is located upstream of a gene called *glxA* that codes a putative galactose oxidase which is also involved in aerial mycelium development (Liman et al., 2013). Liman et al. (2013) hypothesize that the *cslA*-*glxA* locus in streptomycetes could have been acquired by lateral gene transfer. The authors argue that this locus exhibits a lower GC content than the average genome and homologues of CslA and GlxA are absent in closely relates actinobacteria, e.g. *Mycobacterium* sp. Likewise, *P16cslA*

Table 26. Characteristics of *P16cslA*, *P16sfECF* and their predicted products.

	P16CslA	**P16SfECF**
Annotation	SMI4854	SMI5555
Gene size	1998 bp	1044 bp
GC content	67 %	75 %
Protein size	665 aa	347 aa
Mass	73.9 kDa	36.9 kDa
Pfam	13506	04542
COG	1215	1595

was associated with a downstream gene coding a putative galactose oxidase (SMI4853), although in the annotation of the genome the ORF was not named accordingly. Therefore, the annotation for this ORF should be changed to *glxA*. Regarding the GC content of this DNA region, a similar situation as in *S. coelicolor* could be found: *cslA* and *glxA* exhibit a lower GC content (67 % and 65 % respectively) than the overall genome (70.2 %). The proposed horizontal gene transfer must have taken place during the early differentiation of the genus *Streptomyces* sp. from related genera.

Identification of P16SfECF

In contrast to *P16cslA,* the GC content of the gene coded by SMI5555 was higher than that of the average genome (75 %) (Table 26). According to the annotation this 1044 bp long ORF coded a RNA polymerase sigma factor. The gene product was predicted to exhibit 347 aa, a mass of 36.9 kDa and several putative DNA-binding residues. A search of the Pfam database revealed that it showed conserved domains of σ^{70} proteins region 2 (pfam04542) and region 4 (cd06171) with a helix-turn-helix motif (smart00421). σ^{70} is the principle sigma factor in *E. coli* encoded by *rpoD*, which is responsible for many housekeeping functions (Helmann & Chamberlin, 1988).

Strohl (1992) found that approx. 20 % of the at that time 139 identified streptomycete promoters showed sequence similarity to those recognized by σ^{70} in *E. coli*, implying that the transcription of the downstream genes was connected to sigma factors of this family.

For a more detailed identification of this sigma factor, a search for homologous proteins was conducted. The *S. mirabilis* protein showed 31 % identity to a probable *Mycobacterium tuberculosis* σ^{70} factor family protein of the ECF subfamily (P9WGH2) deposited in the swizzprot database. When uncharacterized proteins were included in the search, a significantly higher similarity was found (often > 90 %) to numerous putative *Streptomyces sp.* RNA polymerase subunit sigma factors, which were not further characterized, e.g. 98 % identity to a sigma subunit of *Streptomyces* sp. 94 (WP_099922976).

The results lead to the conclusion that the protein coded by SMI5555 was a σ^{70} type sigma factor of the ECF subfamily, which is widely found in *Streptomyces* sp. and therefore might be important for essential cell functions. In *S. coelicolor* A3(2) 51 out of the 65 so-far known sigma factors in this species belong to the ECF family (Mao et al., 2009; Paget et al., 2002). Hence, they are involved in the transcriptional regulation of numerous cellular processes and only a few are characterized in detail.

For small regulons, it is known that ECF sigma factor genes often cluster together with the genes they regulate (Paget, 2015). *P16sfECF* lay within a cluster of genes connected to cell wall biogenesis and stability maintenance, which is highly conserved among actinobacteria: the entire cluster shown in Figure 70 exhibited 94.9 % identity on DNA level to the *S. avermitilis mce* cluster (BA000030.4) with a query coverage of 99 %. Downstream, three genes were located that coded proteins for the maintenance of outer membrane lipid asymmetry (MlaF, MlaE1, MlaE2) (Figure 70). The ORF upstream of *P16sfECF* coded a protein with conserved domains of the MltB superfamily (COG2951), whose members are involved in cell wall biogenesis. As these proteins are involved in membrane structure-related processes, P16SfECF might play a role in coordinating the cellular structure and development.

Examination of P16sfECF *gene location and the* S. mirabilis mce *cluster*

In the description of *P16sfECF* given above it was already stated that this sigma factor coding ORF is located adjacent to genes connected to cell wall biogenesis and properties. In order to determine if the

sigma factor in deed regulated the transcription of these genes, a more detailed look on the putative functions of the predicted gene products was required for choosing further tests.

Genetic clusters comprising genes for mammalian cell entry (*mce*) are ubiquitous among pathogenic and non-pathogenic actinobacterial species, like *Streptomyces* sp. and *Mycobacterium* sp. (Casali & Riley, 2007). They are hypothesized to be involved in virulence and survival in the environment by governing different cell surface properties and carbon source utilization (Clark et al., 2013; Klepp et al., 2012). In Gram-negative bacteria paralogous can be found, termed *mla*, whose gene products ensure the maintenance of the outer membrane lipid asymmetry by transporting phospholipids from the outer to the inner membrane (Malinverni & Silhavy, 2009; Thong et al., 2016).

Mycobacteria often harbour several *mce* clusters, e.g. four in *M. tuberculosis* and six in *M. smegmatis*, which usually comprise eight genes arranged in a similar pattern (Casali & Riley, 2007; Klepp et al., 2012): two *yrbE* genes (*yrbEAB*) are followed by six *mce* genes (*mceABCDEF*). This typical gene arrangement was also found in *S. mirabilis* (Figure 70). These *mce* clusters encode transport systems involved in lipid translocation, whereby YrbE are putative permeases and Mce proteins are hypothesized to have substrate-binding functions (Casali & Riley, 2007; Forrellad et al., 2014; Pandey & Sassetti, 2008).

The predicted gene products of the *S. mirabilis mce* cluster showed the highest similarity to *M. tuberculosis* Mce4 proteins, which constitute an import system for cholesterol required for the persistence of the bacterium in the host during infections (Pandey & Sassetti, 2008). The cluster is well conserved among Actinobacteria and also present in *S. coelicolor* (Clark et al., 2013), wherefore it was hypothesized that it is a reminiscent of a common actinobacterial ancestor (Casali & Riley, 2007). In *S. coelicolor* and *S. mirabilis* the *mce4* homologues were the only *mce* clusters.

Regulators for the transcription of *mce* clusters are usually located upstream the operons, but not conserved between the different clusters. In *Mycobacterium* sp., transcriptional regulators of the TetR and GntR family were found to regulate *mce* transcription (Casali et al., 2006; Kendall et al., 2010; Santangelo et al., 2008). In *S. coelicolor mce* genes were not preceded by a sigma factor or other transcriptional regulator (Clark et al., 2013). Interestingly, no P16SfECF homologue was identified in this species. *P16sfECF* homologues in others strains, e.g. *S. avermitilis*, were exclusively found in association with *mce* clusters. Therefore, it was highly likely that P16SfECF indeed would play a role in the transcription of this cluster. However, this sigma factor did not seem not to be essential.

The deletion of all six *mce* clusters in *M. smegmatis* impacted carbon source utilization and cell surface properties, which was recognisable in a change in colony morphology, aggregation in liquid culture, biofilm formation and a reduction in cholesterol uptake (Klepp et al., 2012). Therefore, the following experiments were carried out to see if *P16sfECF* deletion would have an impact on some of these properties, although it was not certain that the *mce* cluster in *S. mirabilis* was involved in the same biological processes.

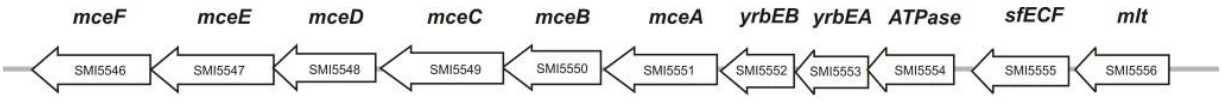

Figure 70. Gene location of SMI5555 encoding the putative sigma factor P16SfECF. Up- and downstream genes encoding Mce proteins were designated according to the gene annotation of a homologous cluster in *S. coelicolor* (Clark et al., 2013).

Characterization of *cslA* and *sfECF* deletion strains

Colony morphology changes on agar plates and in liquid culture

The morphological development of *Streptomyces* sp. is strongly impacted by the culture medium used, especially with regard to the provided carbon source. The aerial hyphae production of some strains that show a *bld* phenotype on complex medium may be restored by cultivating them on minimal medium with sugars like mannitol or arabinose as sole carbon source, but there are also other mutants, which remain *bld* (Chater, 1998; O'Connor et al., 2002; van Keulen et al., 2003; Willey et al., 1991). Hence, the potential of rescuing *bld* mutants depends on which developmental pathway is blocked: usually, on complex medium aerial hyphae development depends on the production of an additional surfactant, SapB, which is redundant on minimal medium, where amphipathic proteins, termed chaplins, are sufficient for protruding the solid-air interface (reviewed in Chater et al. (2010)).

For investigating the role of *P16cslA* and *P16sfECF* in the developmental pathways of *S. mirabilis*, strains carrying a deletion of either gene were created and characterized.

On minimal medium, both deletion strains were strongly delayed in their morphological development. Δ*sfECF* was more severely impaired as production of aerial mycelium was completely abolished on AM and CSA, while for Δ*cslA* sporadic aerial mycelium could be observed (Figure 71).

However, on complex medium, neither the deletion strains, nor the wild type did produce aerial mycelium. Even after two months of incubation the wild type remained bald when observed by naked eye and only at closer examination singular colonies with a light cover of hyphae were detected (Figure 81). In contrast, other streptomycetes, like *S. coelicolor* and *S. lividans,* are able to sporulate also on complex media and deletion of *cslA* in these strains delays the aerial mycelium development on complex media, but not on the minimal medium MS (Chaplin et al., 2015; Liman et al., 2013; Xu et al., 2008). Therefore, the results for *P16cslA* are in general accordance with studies of other strains, that

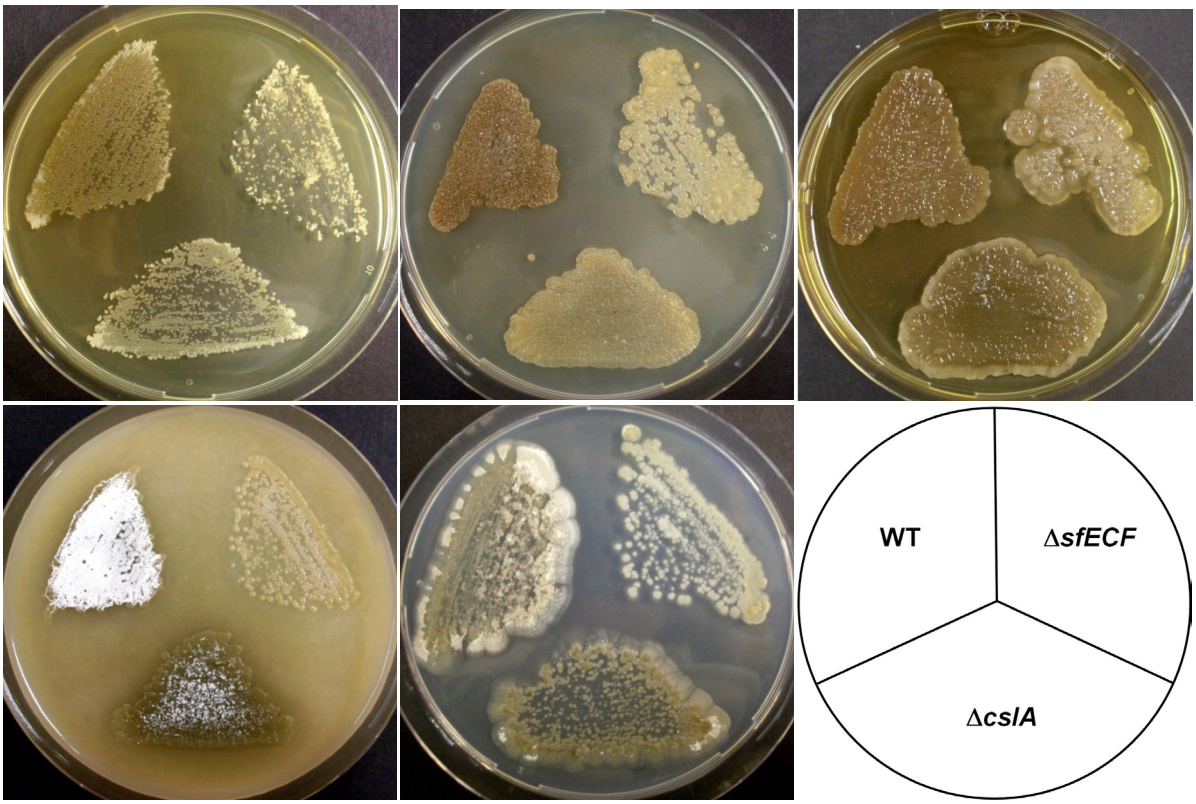

Figure 71. Comparison of growth of *S. mirabilis* wild type and the deletion strains Δ*cslA* and Δ*sfECF* on different media. Upper row: TSB, R2YE without saccharose, R2YE with 10.3 % saccharose; below: MS10, AM.

its deletion caused a delay in development. However, differences to other *Streptomyces* species became apparent for the wild type strain.

The involvement of *P16sfECF* in the strain's morphological development, as it was inferred from its location in the genome, was confirmed by the plate tests. The contribution of numerous sigma factors in governing the *bld* cascade has been acknowledged in several studies (Bibb et al., 2000; Kelemen et al., 1996; Mao et al., 2009). As *P16sfECF* is developmentally impaired on both media types, this sigma factor should be important in an early step of the cascade before the SapB- and chaplin-dependent pathway would be activated.

It was further observed that the colonies of Δ*sfECF* on R2YE appeared more bulky and turgid as compared to the other tested strains (Figure 72), accounting for an increased stress level when growing on complex medium, since a similar colony morphology is usually observed in *S. mirabilis* when grown under stress conditions, e.g. with heavy metals. Increased stress on complex medium might result from a higher osmotic pressure. A cross-regulation of morphological development and osmoprotection by P16SfECF as it was observed for σ^B in *S. coelicolor* (Lee et al., 2005) could be assumed.

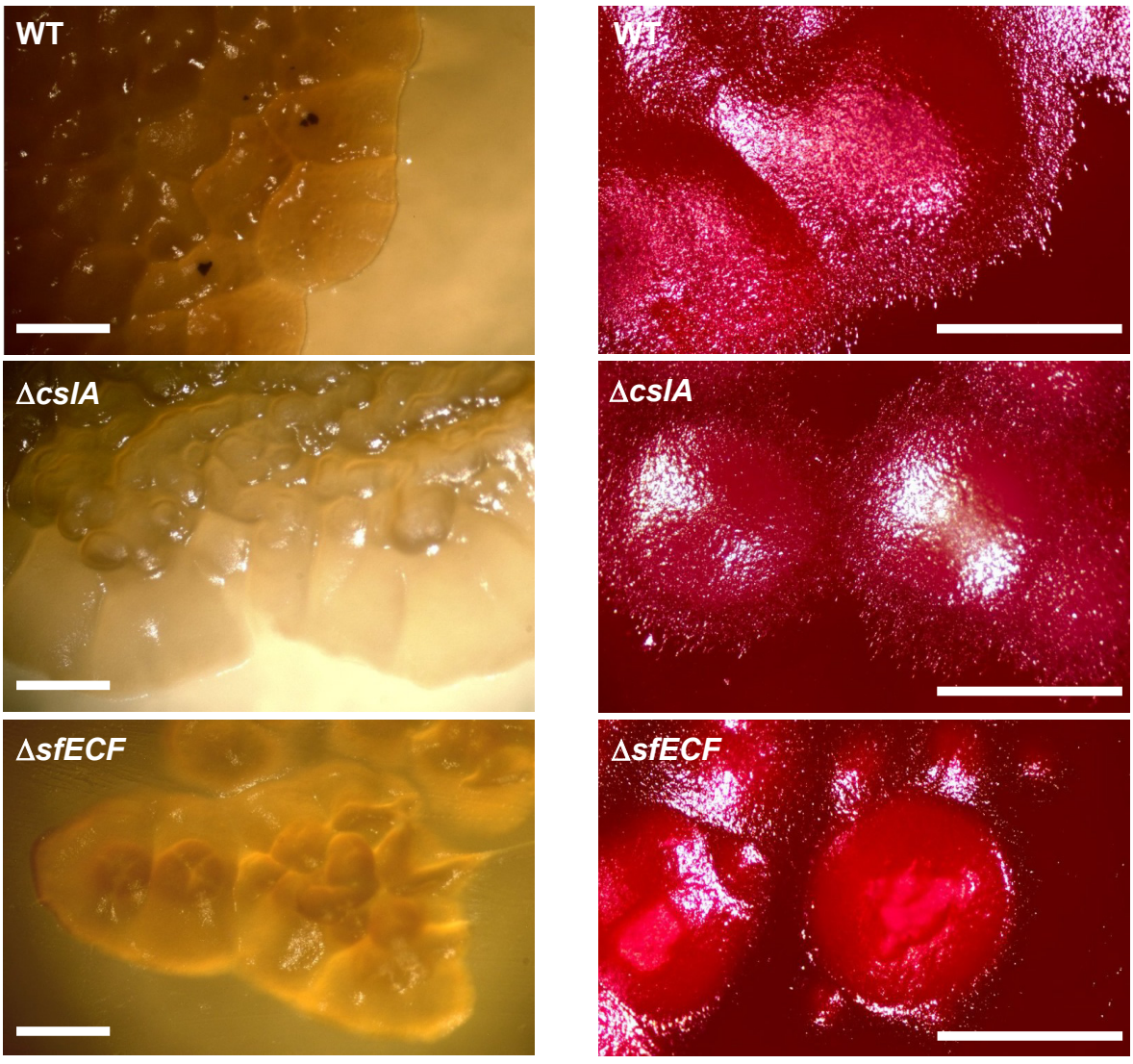

Figure 72. Colony morphology of *S. mirabilis* wild type and the deletion strains Δ*cslA* and Δ*sfECF* on R2YE without saccharose (left) and CSA supplemented with 0.01 % Congo Red (right). White bar: 1 mm.

Figure 73. Comparison of growth of *S. mirabilis* wild type (upper left), deletion strain (upper right) and genetically complemented deletion strain (below) on CSA agar. Left picture: *P16cslA* deletion strain, right picture: *P16sfECF* deletion strain.

The difference in colony morphology on minimal medium only became visible when plates were supplemented with 0.01 % Congo red (Figure 72). Δ*sfECF* colonies on CSA were more elevated, shiny and lighter in colour, which indicated a change in cell envelope properties . This observation lead to a closer examination of colony morphology on media supplemented with Congo red. The results will be described later in this section.

The normal wild type phenotype could be re-established in both deletion strains by re-introducing the deleted gene on the vector pSEThph (Figure 73). An extracellular complementation by growing the transformant in vicinity to the wild type strain was not successful for both deletion strains (Figure 74). Therefore, the *bld* phenotype of the deletion strains cannot be complemented by diffusible compounds from the wild type that would re-activate the signalling cascade, as it is the case for some *bld* mutants (Capstick et al., 2007; Chater, 1998; Willey et al., 1991). In *S. coelicolor* the addition of highly concentrated chaplin and rodlin proteins to a *cslA* mutant enabled the strain to produce aerial hyphae (Xu et al., 2008). However, in case of *S. mirabilis*, the concentration of these proteins diffusing from the wild type seemed to be insufficient for exerting any effect.

Streptomyces sp. development in liquid culture is different from morphological differentiation on solid medium and less well investigated. The formation and integrity of mycelium aggregates is depending on extracellular glycan synthesis (Petrus & Claessen, 2014; Xu et al., 2008). A role for CslA in pellet architecture in liquid culture has been postulated following the observation that *cslA* deletion mutants showed strongly reduced aggregate size (Chaplin et al., 2015; Mangiameli, 2014; Xu et al., 2008). However, the deletion of *P16cslA* did not reduce the pellet size in any of tested media (TSB, GYM, AM, NMMP), but impaired the formation of floating, sporulating colonies in static cultures with minimal medium when casamino acids were provided (Figure 75). In NMMP with glucose and casamino acids,

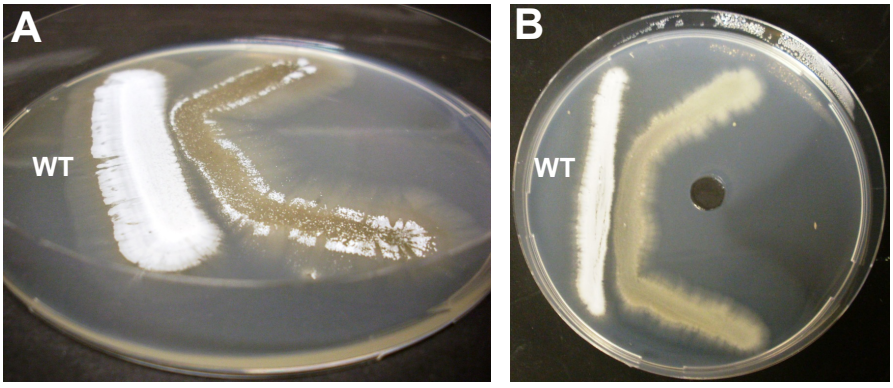

Figure 74. Extracellular complementation assay on CSA medium. Deletion strains Δ*cslA* (A) and Δ*sfECF* (B) were grown next to *S. mirabilis* (WT) for screening for re-establishment of aerial mycelium development.

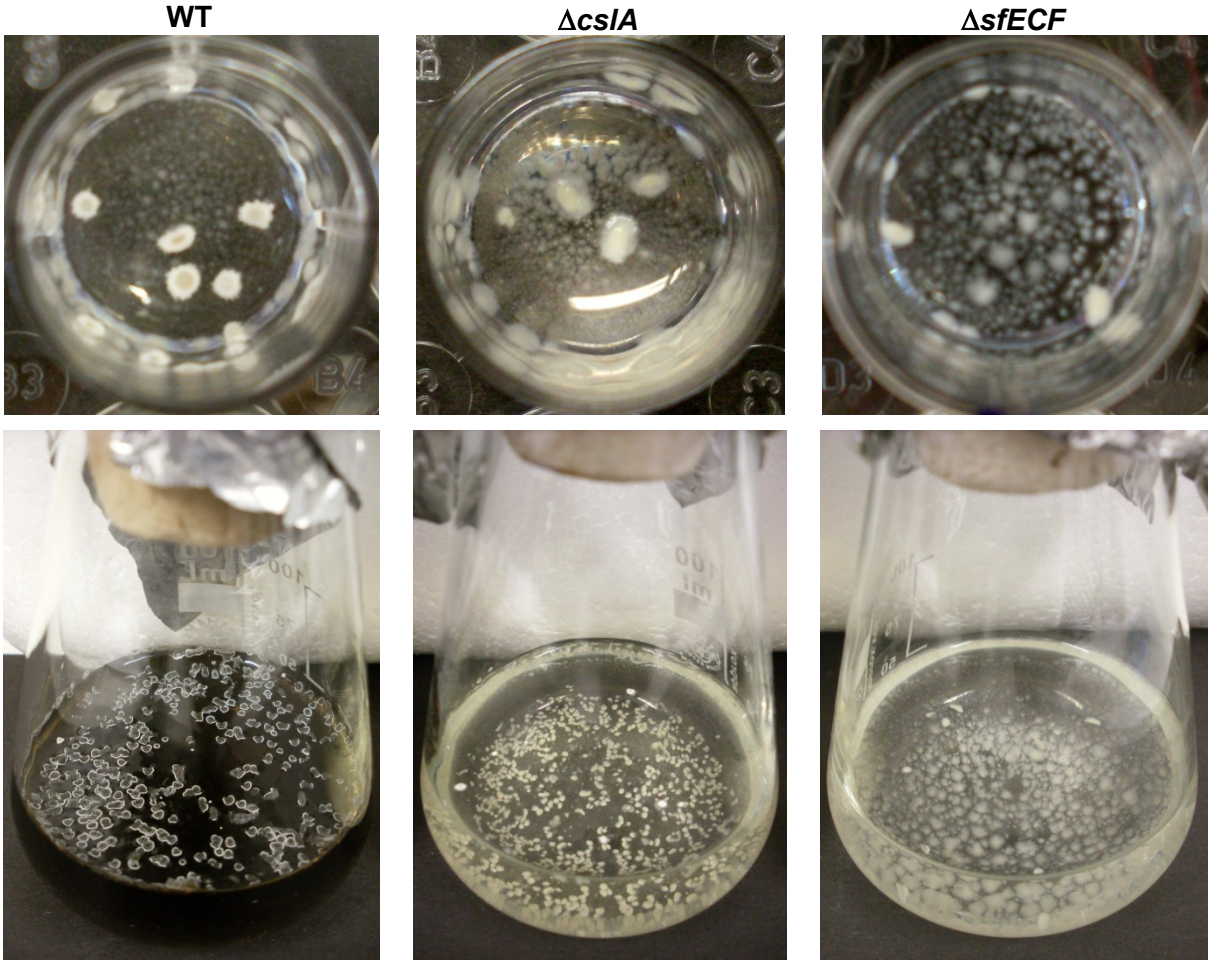

Figure 75. Comparison of growth of *S. mirabilis* (WT) and both deletion strains in static liquid cultures using NMMP with glucose and casamino acids (upper row) and AM medium without glucose but casamino acids as carbon source (below). The cultures were grown for two weeks at room temperature.

Δ*cslA* could form floating colonies, but no aerial mycelium was produced, which again hinted on an impediment for the strain's hyphae to cross the liquid-air barrier.

Δ*sfECF* showed an even stronger phenotypic change under these conditions. Only sporadic floating colonies were produced and the pellets appeared fuzzier and less compact. Possibly, this could be the result of a change in cell surface properties, which are responsible for promoting pellet formation.

The inability of both mutant strains to produce the brownish pigment in AM with casamino acids (Figure 75) was caused by the loss of the small plasmid pI, on which the tyrosinase was encoded (see section 3.2).

Microscopy

Light microscopy

The hyphal morphology in different media was checked by light microscopy. No change could be observed in complex or minimal medium. Solely in YEME liquid medium Δ*cslA* showed more frequent splitting and apical branching of the hyphae (Figure 76), which was in accordance with findings for a *cslA* deletion strain of *S. coelicolor*, where branching appeared in closer intervals than in the WT when cultivated on complex medium (Xu et al., 2008).

The connection between CslA and branching of hyphae is indirect, as CslA is not responsible for emergence of new branches, but probably involved in the positioning of the tip organizing centre com-

prising DivIVA and two other proteins (Holmes et al., 2013). Being an integral membrane protein, CslA is hypothesized to interact with DivIVA, thereby locating it at the tip and along the hyphae (Xu et al., 2008). This interaction is supported by the affinity of DivIVA to cellulose (Soderholm et al., 2018). DivIVA, in turn, serves as marker of cell wall assembly sites for lateral branching and recruits the necessary components that determine the hyphal growth direction (Hempel et al., 2008; Holmes et al., 2013). Due to these interactions, deletion of *P16cslA* might have led to incorrect localization of DivIVA and other cell wall assembly components resulting in a phenotype resembling *cslA* and *scy* deletion strains which showed apical branching close to the hyphal tip or tip splitting and irregular branching, especially in complex medium (Flärdh, 2003; Holmes et al., 2013). Therefore, it can be hypothesized, that also P16CslA interacted with DivIVA and was indirectly involved in branching.

It was somewhat surprising that no phenotypic change was visible in Δ*sfECF*. If P16SfECF was involved in governing the lipid composition of the cell membrane, it could potentially also indirectly influence DivIVA positioning: DivIVA was shown to recognize membrane curvature and exhibit a preference for bent and slightly curved membranes, especially for negative curvature (Hempel et al., 2008; Lenarcic et al., 2009; Ramamurthi & Losick, 2009). Membrane curvature, in turn, is controlled by several parameters, one being the lipid composition and asymmetry (reviewed by McMahon & Boucrot (2015)). In that way, deletion of *P16sfECF* might impact membrane bending and DivIVA positioning. However, the absence of phenotypic change in Δ*sfECF* did not substantiate such a connection.

Fluorescence microscopy

As CslA is responsible for the synthesis of cellulose-like fibrils, staining with calcofluor white was conducted. Calcofluor white is a fluorescent dye binding to β-(1,4)-linked polysaccharides, e.g. chitin and cellulose (Herth & Schnepf, 1980). In several studies with *S. coelicolor* and *S. lividans*, *cslA* deletion mutants showed no fluorescence when grown on MS plates or in NMMP with mannitol as carbon source (Chaplin et al., 2015; Mangiameli, 2014; Xu et al., 2008). To screen for a corresponding phenotypic change, *S. mirabilis* and the deletion strains were cultivated in different complex and minimal media in liquid culture and on plates.

When grown in liquid TSB medium, all strains showed a similar high level of fluorescence along the hyphae (data not shown). Also in the WT no enhanced signal intensity was detected at hyphal tips or branching sites, like it was reported for *S. coelicolor* (Xu et al., 2008). Hence, it was conluded that the excretion of cellulose-like compounds occurred almost all-over the hyphae of *S. mirabilis* under these conditions.

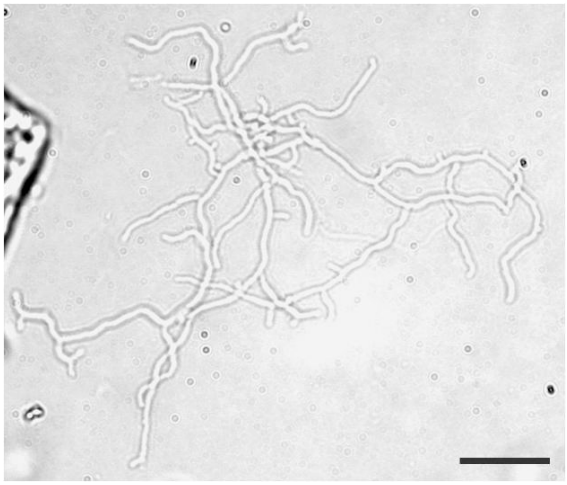

Figure 76. Hyphae of Δ*cslA* grown in liquid YEME medium amended with 100 mM KCl. Bar indicates 10 µm.

In contrast, differences became apparent when the strains were cultured in liquid NMMP with glucose or mannitol as carbon source. After 24 h incubation, the fluorescence level was low in all strains, but after 5 d incubation, differences became apparent (Figure 77). The WT strain showed a high fluorescence signal with both carbon sources,

which was stronger when cultivated with mannitol. For Δ*sfECF* a similar level of fluorescence could be observed, although the pellets were less dense and compact than for the WT, which was in accordance with the fluffy pellets formed in liquid culture (Figure 75).

A marked change was observed for Δ*cslA*. When glucose was provided as carbon source, no fluorescence signal was detected. However, in medium with mannitol the fluorescence showed, although at a

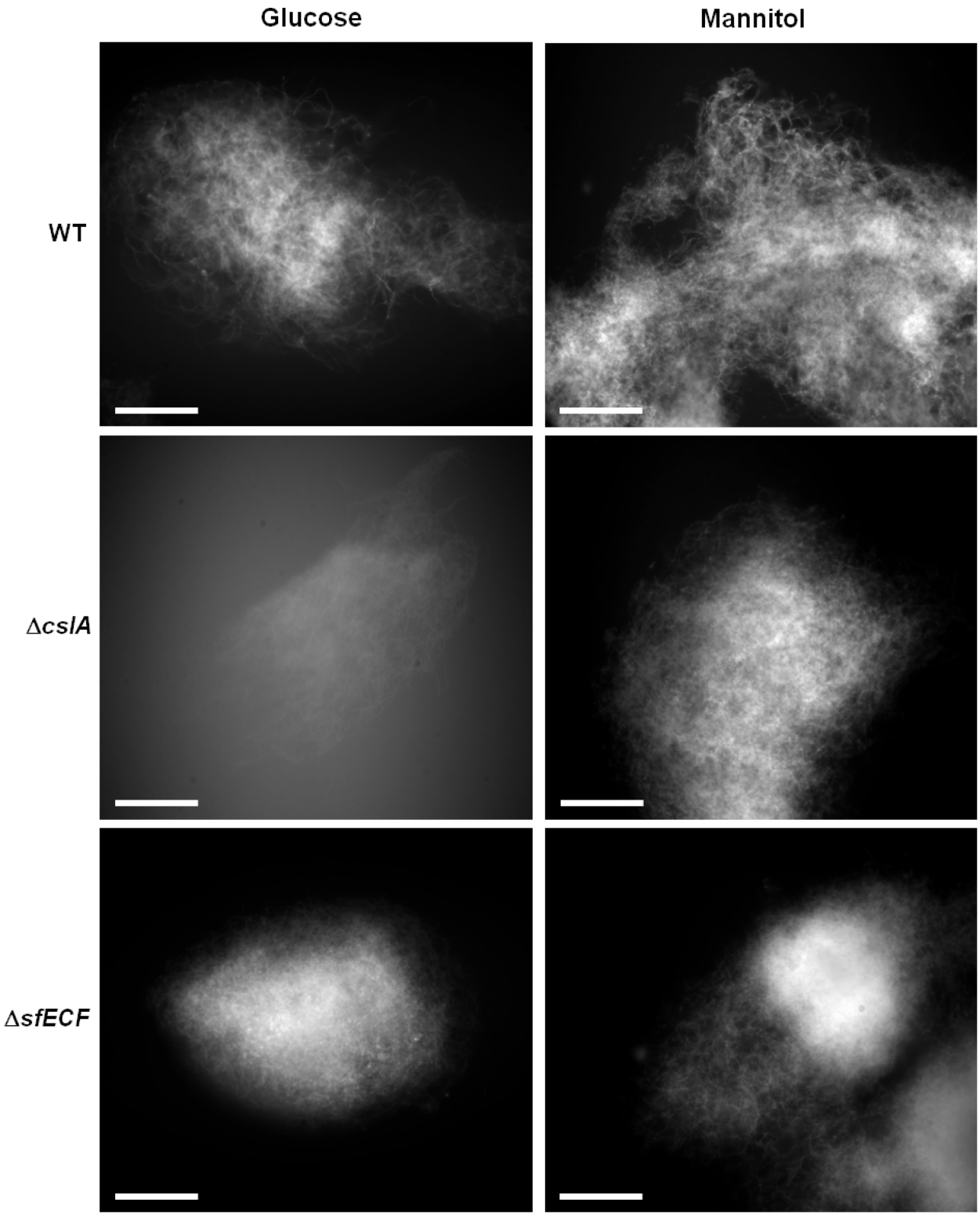

Figure 77. Calcofluor white staining of mycelium from static liquid cultures using NMMP with either glucose or mannitol as carbon source. Pictures were taken after 5 d incubation at 28°C. White bar represents 100 µm.

lower level than for the WT and fluffy presumably cellulose-containing clumps appeared along the hyphae. This could hint at a loss of control over the localization of cellulose extrusion, due to the deletion of *P16cslA*. Interestingly, the fluorescence signal of *S. coelicolor* A3(2) in the same media was stronger than for *S. mirabilis* wild-type (data not shown).

In order to investigate differences between growth in liquid and solid medium, the strains were cultivated on plates (TSB, MS10 or AM medium) with cover slides stuck slanted in the inoculation site for allowing the hyphae to grow on the slides. After 24 h (for TSB and MS10) or 48 h (AM) the slides were removed, stained with calcofluor white and observed under the microscope (Figure 78).

Independent from the growth medium used, a strong fluorescence signal was observed for all strains. As in the liquid cultures, the signal was not restricted to the tips and branching sites of the hyphae, but all-over the hyphae resulting in a dotted pattern (Figure 78). On MS10, there was slightly stronger fluorescence at hyphal tips, which was not as strong in Δ*cslA*. However, on AM medium there was no apparent difference, although glucose was provided as carbon source, which lead to strong differences in liquid NMMP.

These findings were different from fluorescence pattern usually reported for *S. coelicolor*, where spots

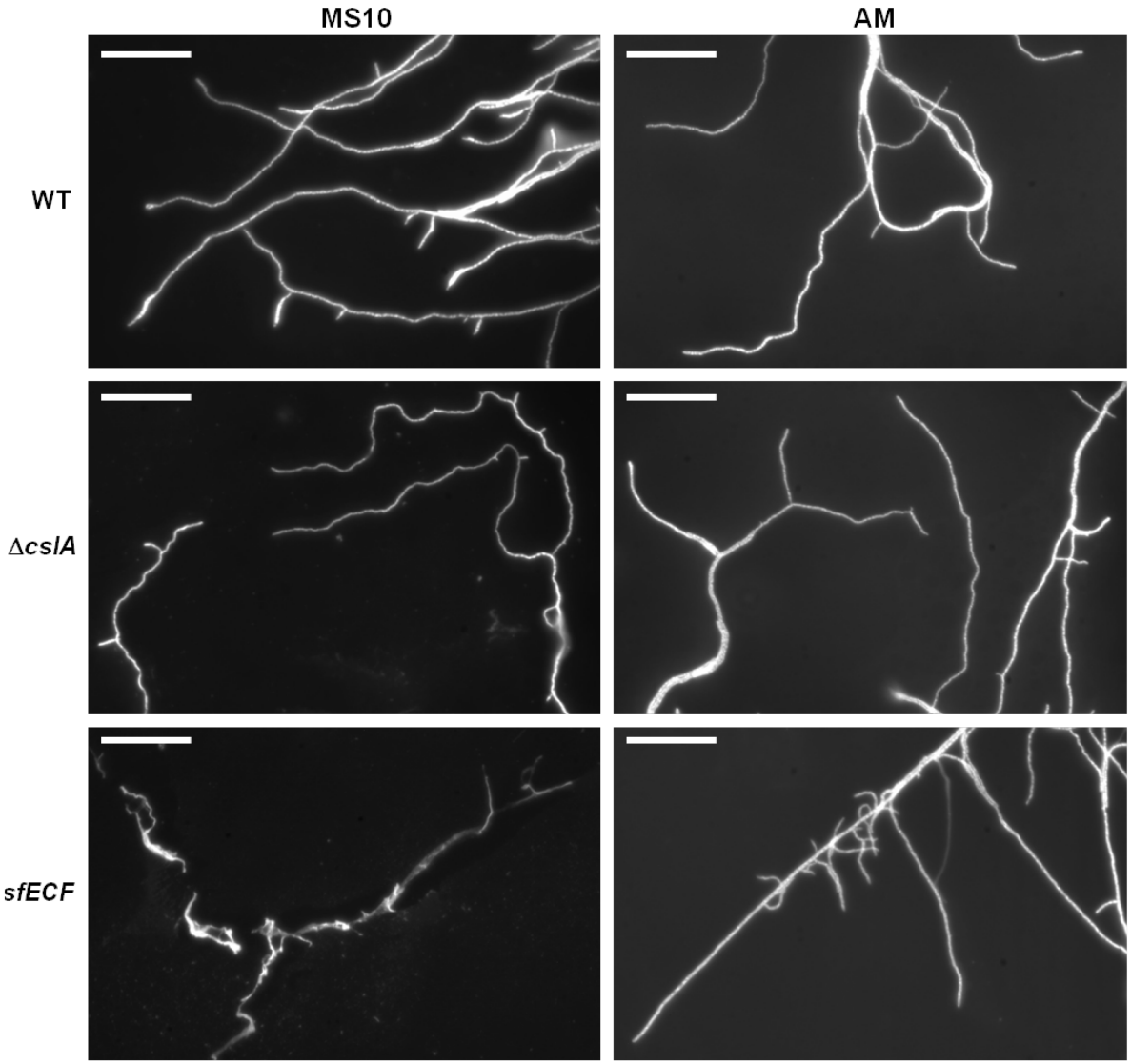

Figure 78. Fluorescence staining of mycelium grown on cover slides from either MS10 or AM agar plates using calcofluor white. Slides were examined after 24 h (MS10) or 48 h (AM) incubation at 28°C. White bar represents 20 µm.

of strong fluorescence appeared primarily at tips and branches (Chaplin et al., 2015; Chater et al., 2010; Holmes et al., 2013; Xu et al., 2008). However, in a report by Soderholm et al. (2018), fluorescence pictures of a *S. coelicolor cslA* deletion strain also showed fluorescence along the hyphae, besides single spots. The pattern observed in *S. mirabilis* could therefore be a strain-specific difference in the production of cellulose-like compounds or the result of differing cultivation conditions.

The evaluation of fluorescence in Δ*sfECF* in this plate set-up was hardly possible, as only very little hyphae attached to the cover slide, which pointed at a reduced ability of the strain to adhere to the glass surface, especially when cultivated on TSB medium. From the latter, no hyphae were detected on the slide after 24 h and 48 h. However, the few hyphae observed on AM and MS10 gave a fluorescence signal similar to the WT (Figure 78).

The attachment of Δ*cslA* was comparable to that of the WT, which showed that P16CslA was not required for attaching to this surface, as it was shown for *S. lividans* (van Dissel et al., 2018). Therefore, additional systems for the production of exopolysaccharides (EPS) had to be present in *S. mirabilis*, which were responsible for the attachment to different types of surfaces.

Attachment assay

The ability of *Streptomyces* sp. to attach to surfaces is an important prerequisite for adhering to soil particles and colonizing soil habitats. Changes in cell surface properties might interfere with this ability. For CslA it was shown that the protein produces cellulose-like fibrils (de Jong et al., 2009; Xu et al., 2008), which serve as anchoring platform for chaplin amyloids forming fimbriae that allow attachment to hydrophobic surfaces (Petrus & Claessen, 2014). Therefore, CslA provides the basis for attachment.

In static liquid cultures with minimal medium, hyphae attach to polystyrene surfaces and the expression of CslA is stronger than in shaken cultures (de Jong et al., 2009; van Keulen et al., 2003). Therefore, *S. mirabilis* WT and the deletion strains were cultured in static liquid cultures using modified NMMP supplemented with glucose, mannitol or glucose and casamino acids in polystyrene 24 well plates. After 11 d attachment of the hyphae was measured, as studies showed that the maximum of attached hyphae is usually reached after 7 to 10 days (van Keulen et al., 2003).

Under these conditions, the percentage of hyphae attached to the polystyrene was reduced in both deletion mutants independent from the carbon source (Table 27), e.g by 10 % in Δ*cslA* and by 20 % Δ*sfECF*. The generally lower attachment in glucose containing NMMP was in agreement with results from a similar assay with *S. coelicolor* (de Jong et al., 2009). This effect was attributed to the in-

Table 27. Attachment assay in NMMP with different carbon sources (mannitol, glucose or combination of glucose and casamino acids (CAS)). Given are the percentages of biomass attached to polystyrene wells with standard deviation derived from three separate experiments.

	Glucose	Glucose + CAS	Mannitol
P16 WT	59.6 ± 24.9	66.0 ± 23.0	78.5 ± 7.2
Δ*cslA*	50.2 ± 6.4	53.8 ± 2.6	67.3 ± 3.8
Δ*sfECF*	38.7 ± 7.5	18.1 ± 3.4	38.4 ± 11.7

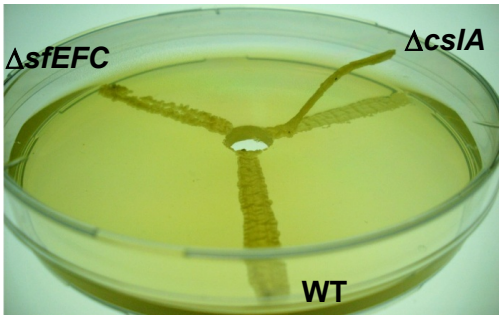

Figure 79. Plate with TSB medium for LiCl agar diffusion assay. Plate was stored upside down.

creased formation of extracellular matrix mainly consisting of fimbriae in medium containing mannitol. Since the cellulose fibres produced by CslA serve as anchoring platform for chaplin proteins, that form fimbriae (Petrus & Claessen, 2014), the deletion of this protein should interfere with fimbriae formation, thereby decreasing the attachment. This connection explained the observed reduction in attached biomass for Δ*cslA*. Although fimbriae formation is expected to be impeded in *cslA* deletion strains, de Jong et al. (2009) found that the appearance of fimbrae of *S. coelicolor* Δ*cslA* was indistinguishable from that of the wild type. It would be worthwhile to compare fimbrae structure between *S. mirabilis* WT and Δ*cslA.*

However, the difference between *S. mirabilis* WT and Δ*cslA* attachment was not as high as it has been observed for *S. coelicolor* M145, in which deletion of *cslA* reduced the attachment in NMMP with mannitol by 40-50 % (de Jong et al., 2009). This could account for species-specific differences in the composition of the extracellular matrix, since *S. mirabilis* WT also showed a lower attachment level than *S. coelicolor*.

The reduction in attachment was more pronounced in the *sfECF* deletion strain (Table 27), accounting for a change in cell surface properties, which was in accordance with the above described results. De Jong et al. (2009) likewise found a drastic decrease in attachment when deleting the ECF sigma factor BldN in *S. coelicolor* M145, a sigma factor that is involved in aerial hyphae production by controlling *chp* and *rdl* transcription (Bibb et al., 2012; Bibb et al., 2000). If P16SfECF was also involved in the transcription of these genes cannot be stated, as also Mce proteins would impact the cell surface structure.

Regarding surface attachment to agar plates, on none of the test plates a difference between the deletion mutants and *S. mirabilis* WT was observed. Solely in one case, when the strains were streaked on TSB for testing LiCl resistance and the plate was stored upside down, the upper layer of Δ*cslA* biomass could not adhere to the surface (Figure 79). In contrast, for a *S. lividans cslA* deletion strain it was reported, that it lost its ability to attach to agar surfaces completely (Mangiameli, 2014).

Comparison of *S. mirabilis* P16B-1 and *S. coelicolor* A3(2) growth

While studying the deletion strains, it became apparent, that already *S. mirabilis* showed phenotypic characteristics, which were typical for *bld* mutants of other *Streptomyces* species, like *S. coeli-*

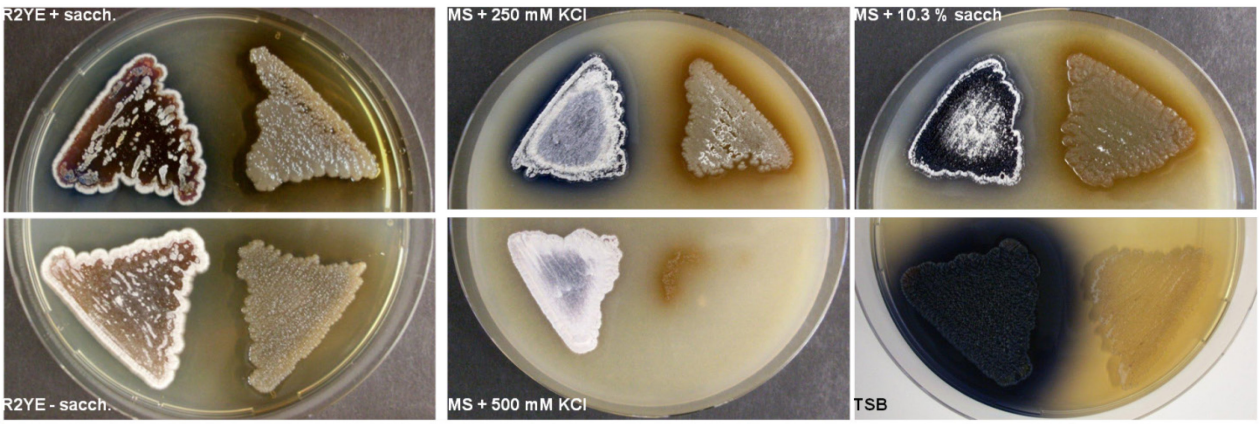

Figure 80. Comparison of colony morphology between *S. coelicolor* A3(2) (left) and *S. mirabilis* WT (right) on different media. Plates were incubated for 5 d at 28°C. KCl and saccharose (sacch.) were added to some plates for increasing osmotic pressure.

color A3(2) (de Jong et al., 2012). This raised the question, whether *S. mirabilis* lacked one or more genes responsible for one pathway of morphological differentiation.

In direct comparison to *S. coelicolor* A3(2) the impairment of aerial mycelium production by *S. mirabilis* on R2YE became unambigous (Figure 80). While for the former strain aerial hyphae could be observed after three days of incubation, *S. mirabilis* only sparsely produced aerial mycelium after two months incubation. The addition of 10.3 % saccharose completely abolished aerial mycelium development in *S. mirabilis* on complex (R2YE) and minimal (MS) medium. Furthermore, supplementation of MS medium with KCl inhibited the morphological development of *S. mirabilis* and the strain's growth nearly ceased at 500 mM KCl, while *S. coelicolor* A3(2) was unaffected.

Figure 81. Growth of *S. mirabilis* on R2YE without saccharose. After four weeks incubation slight aerial mycelium was observed. White bar: 0.5 mm.

These growth defects of *S. mirabilis* corresponded to the phenotype observed in SapB-deficient *S. coelicolor* mutants (Capstick et al., 2007; de Jong et al., 2012). SapB is a small (usually 41-45 aa) hydrophobic protein acting as surfactant by aggregating at the air-water interface thereby reducing the surface tension and enabling the erection of aerial mycelium on complex media (Tillotson et al., 1998; Willey et al., 1991). On minimal medium, SapB is produced, but not required for aerial morphogenesis, wherefore SapB-deficient mutants can produce aerial mycelium on MS plates (Capstick et al., 2007). Therefore, it was hypothesized that *S. mirabilis* was either naturally deficient of the genes encoding SapB and associated proteins, or that there must be another defect in the SapB-dependent developmental pathway.

The 'rapid aerial mycelium formation' gene cluster (*ramCSABR*) encodes and controls SapB production, whose precursor is the gene product of *ramS* (Capstick et al., 2007; Kodani et al., 2004; O'Connor et al., 2002; Willey et al., 1991). In some *Streptomyces* strains, homologues of SapB carry out analogous functions, e.g. AmfA of *S. griseus* (Ueda et al., 2002).

In the gene annotation of *S. mirabilis*, none of the listed proteins was designated a SapB-related protein. As the overall gene organization of the *ram* cluster and its homologues seemed to be conserved among different species, an *in silico* search on protein and DNA level using BLAST was carried out for identifying putative *ram* genes in *S. mirabilis*. Although *ram* members from different species were used as query, no significant similarity to any annotated protein or gene of *S. mirabilis* was found.

For ensuring that the inability to find a SapB homologue was not due to a methodical problem, the same search was conducted with the genome and protein annotation of *S. acidiscabies* E13. In this strain, a SapB homologue was already annotated (E13_06913: Spore-associated protein B). The coding ORF showed a high similarity on DNA level to SapB of *Streptomyces* sp. ADI95-16 (AYV31285.1). Also, the protein sequence seemed to be highly conserved, as E13SapB identity to those from other *Streptomyces* species was over 90 % for several species and even 100 % for a group of SapB/AmfS family lantipeptide proteins (WP_058940762.1) annotated in several *Streptomyces* sp. genomes.

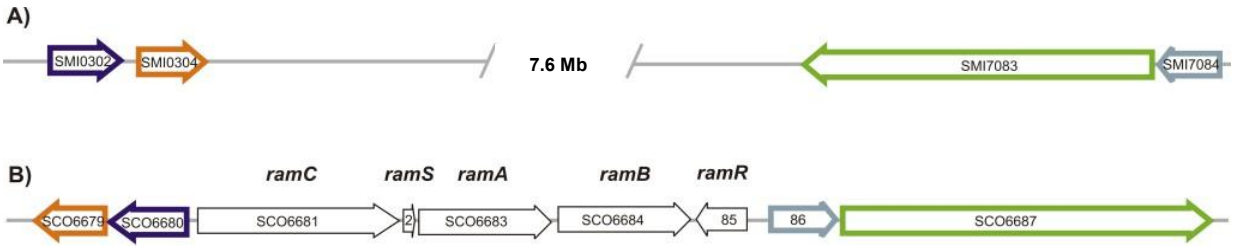

Figure 82. Comparison of the *S. coelicolor* A3(2) *ram* cluster organization including up- and downstream genes (B) with genomic locations of homologous genes (marked in same colour) in *S. mirabilis* (A). In *S. mirabilis*, the *ram* cluster flanking genes in *S. coelicolor* A3(2) were located at opposite ends of the chromosome in reversed orientation.

Therefore, it was concluded that the strong impairment of aerial mycelium production of *S. mirabilis* on complex medium was the result of the absence of the complete *ram* cluster and not only a single deletion. Homologues of proteins encoded up- and downstream the *ram* cluster in *S. coelicolor* A3(2) were present in *S. mirabilis*, but located on opposite ends of the genome (Figure 82) in reading directions which would suggest that a *ram* cluster, which once could have been located between these ORFs, had been deleted.

Since *S. mirabilis* could produce aerial hyphae and spores on minimal medium, it was concluded that only the SapB-dependent developmental pathway was affected, while genes encoding chaplins and rodlins, which are required under these conditions (Bibb et al., 2012; Capstick et al., 2007; de Jong et al., 2012; Elliot et al., 2003), should be present. These proteins were probably responsible for the residual aerial mycelium formation observed on R2YE (Figure 81).

Using protein similarity search, out of eight chaplin proteins found in *S. coelicolor* A3(2) (Elliot et al., 2003), six homologues were identified in *S. mirabilis*: two long and four short chaplins (Figure 83), although none were annotated as Chp protein. Furthermore, one additional *chp* gene which was annotated as SMI4997 with a length of 618 bp, was found to actually be part of a longer 933 bp ORF (position 5617883-18815) coding a long chaplin corresponding to ChpA of *S. coelicolor* A3(2), as the protein was predicted to possess two chaplin domains, characteristic for these proteins (Elliot et al., 2003).

Also the gene organization was similar to that in other streptomycetes: *chp* genes were not organized in one cluster, but scattered on the genome and *chpDA* was adjacent to the rodlin coding *rdlAB* (Figure 83). That *S. mirabilis* was lacking one chaplin protein present in *S. coelicolor* A3(2) should not have a strong impact on its development, as only ChpCEH are found to be conserved in all *Streptomyces* sp. (Bibb et al., 2012) and chaplin proteins can substitute each other to a certain degree (Elliot et al., 2003).

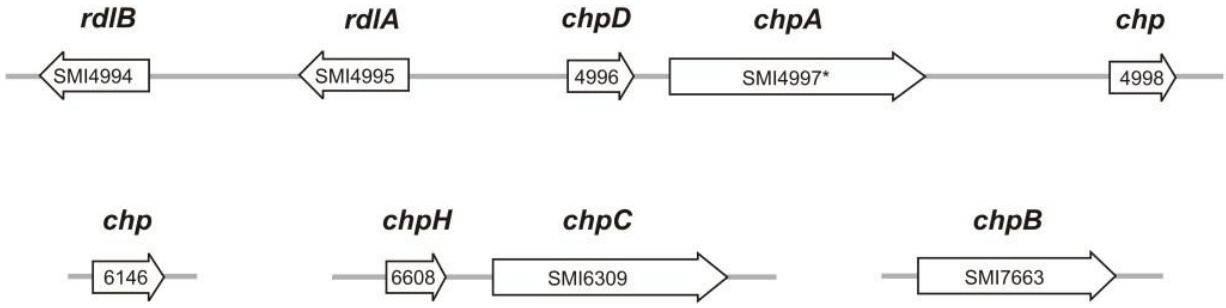

Figure 83. Predicted genes encoding chaplin and rodlin proteins in *S. mirabilis*. Gene designations were inferred from *S. coelicolor* A3(2) annotation (Elliot et al., 2003), when possible.

These results lead to the conclusion that *S. mirabilis* would mainly depend on chaplin and rodlin proteins for reducing the water/medium surface tension in order to escape an aqueous environment. However, it cannot be excluded that also other, yet unknown pathways contributed to this developmental step, as it was found that regulators of morphological development can differ even between closely related *Streptomyces* species (Keijser et al., 2000).

Detection of differences in EPS production of *S. mirabilis* and the deletion strains

Congo Red plate assay

The results presented so far pointed at changes of extracellular matrix components or cell envelope properties in the deletion strains. For better visualising this change, a colorimetric approach using Congo red (CR) was chosen. This azo dye binds strongly to cellulose and other bacterial amyloids. It is widely used for the detection of biofilm formation, EPS production, colony morphology and curli production in bacteria and eukaryotes, e.g. *E. coli*, *Staphylococcus* sp. and *Saccharomyces* sp. (Freeman et al., 1989; Ignatova-Ivanova, 2017; Linder, 2018; Reichhardt et al., 2015; Reichhardt et al., 2016). Arciola et al. (2002) established a scale for colony colouration, as different *Staphylococcus* strains formed 'very black' to 'very red' colonies on agar amended with CR, depending on their ability to produce EPS. Here, the change of the dye from red to black indicates EPS production. In *Staphylococcus epidermidis* it was found that slime production and black colony colouration is connected to the presence of *ica* and *atl* operons, the former encoding the synthesis machinery of β-1,6-linked glucosaminglycans (Arciola et al., 2002; Ferreira et al., 2014).

As it is known that EPS production depends on cultivation conditions (Ferreira et al., 2014), the strains were streaked on different media containing 0.01% CR. On TSB and CSA all tested strains showed a similar red colour with no differences between the WT and the deletion strains (data not shown), hinting at a general lack or strongly reduced production of cellulose-containing compounds on these media. On MS10 medium the colonies also remained red. However, differences between the WT and deletion trains became visible. While *S. mirabilis* developed hairy colonies, Δ*cslA* remained smooth and slightly darker red spots appeared on the colonies of Δ*sfECF* (Figure 85), probably due to changed cell envelope properties.

The strongest difference was observed on AM medium. *S. mirabilis* and Δ*sfECF* were severely impaired in growth, whereas Δ*cslA* growth was promoted, accompanied by a strong colour change to

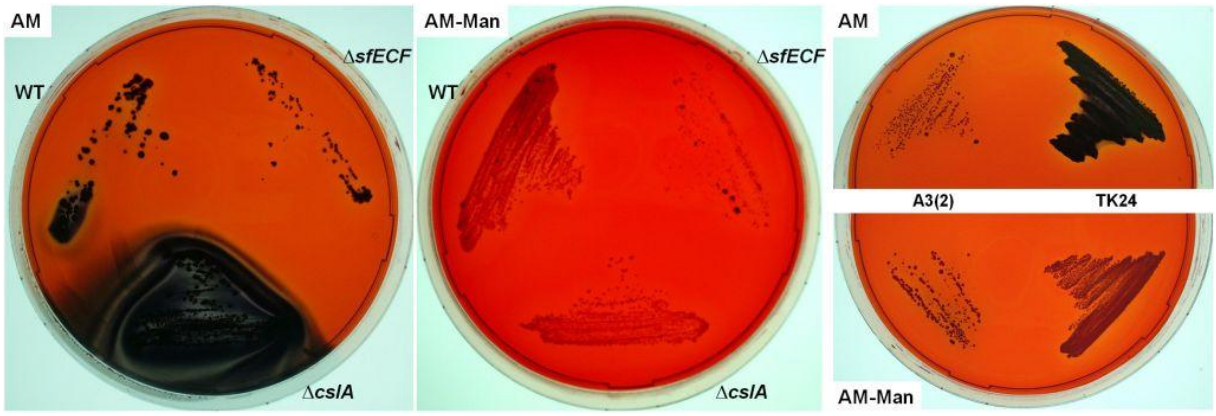

Figure 84. Agar plates of AM medium with either glucose (AM) or mannitol (AM-Man) as carbon source, amended with 0.01 % Congo red. Pictures were taken after 5 d incubation at 28°C.

black, which was not restricted to the colonies, but faned out to the surrounding medium in a wide range (Figure 84). Upon prolonged incubation and growth (appr. 14 d), black halos also appeared around the colonies of the other strains. A closer look at the colonies after 4 d incubation showed that in the centre of WT colonies a slide change to black started, while Δ*cslA* colonies were completely stained. On Δ*sfECF* singe black spots were detected (Figure 85).

This colour change of CR indicated the production of EPS on AM medium, comprising cellulose-containing compounds. The absence of P16CslA, which is responsible for covering the hyphae in cellulose fibres, was a distinct growth advantage. The inhibiting effect CR had on the WT, probably by binding to the amyloid fibres, was repealed in Δ*cslA*. The black colouration of its colonies could either result from the diffusion of cellulose compounds in the medium, which were unable to adhere to the hyphae due to the lack of anchoring fibres, or it could be the result of an increased production of other EPS compounds *via* a different pathway for compensating the loss of the cellulose fibres, like poly-β-1,6-N-acetylglucosamine (PNAG) by the Mat system (van Dissel et al., 2018).

In several microorganisms, CR does not inhibit growth, although different sensitivities have been re-

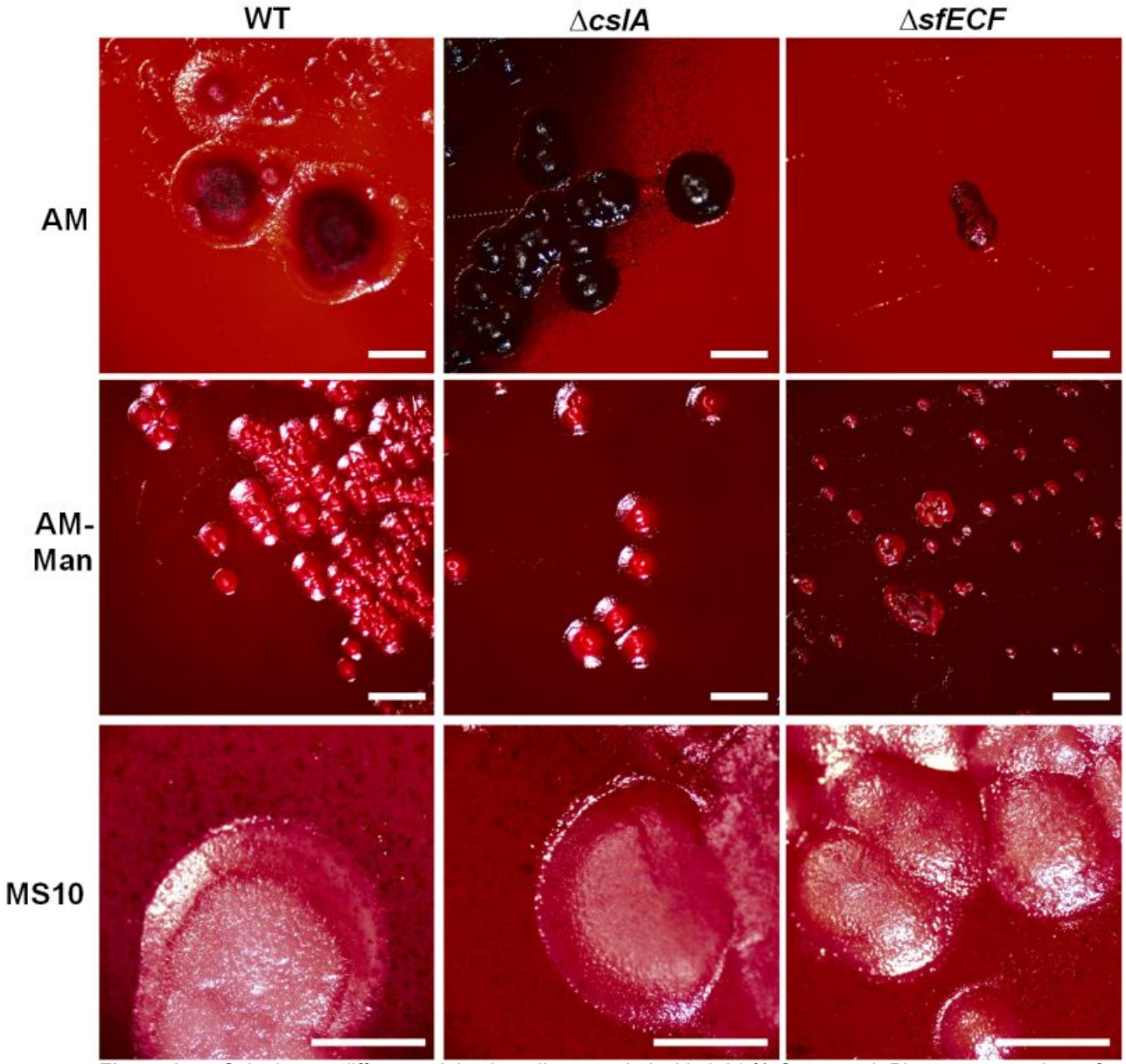

Figure 85. Colonies on different minimal media amended with 0.01 % Congo red. Pictures were taken after 4 d incubation at 28°C. White bar represents 1 mm.

ported (Arciola et al., 2002; Ferreira et al., 2014; Linder, 2018; Reichhardt et al., 2015). However, the dye can act intracellularly as cell poison (Colvin & Witter, 1983) at elevated concentrations and might interfere with cellulose formation and cell wall morphogenesis by forming complexes with the synthesized polysaccharides (Colvin & Witter, 1983; Linder, 2018).

For *E. coli* it was reported that the colony morphology changed in presence of CR and the cellulose fibres were more dense and compact, possibly due to the precipitation by CR (Reichhardt et al., 2016). A similar situation could be assumed for *S. mirabilis*. The binding of the dye to the glucan chains would prevent polymerisation, impeding further growth due to the CR-cellulose precipitate around the hyphae. In Δ*cslA*, on the other hand, the cellulose compounds would not be strongly attached to the hyphae, whereby precipitation would not be restricted to the near vicinity of the hyphae.

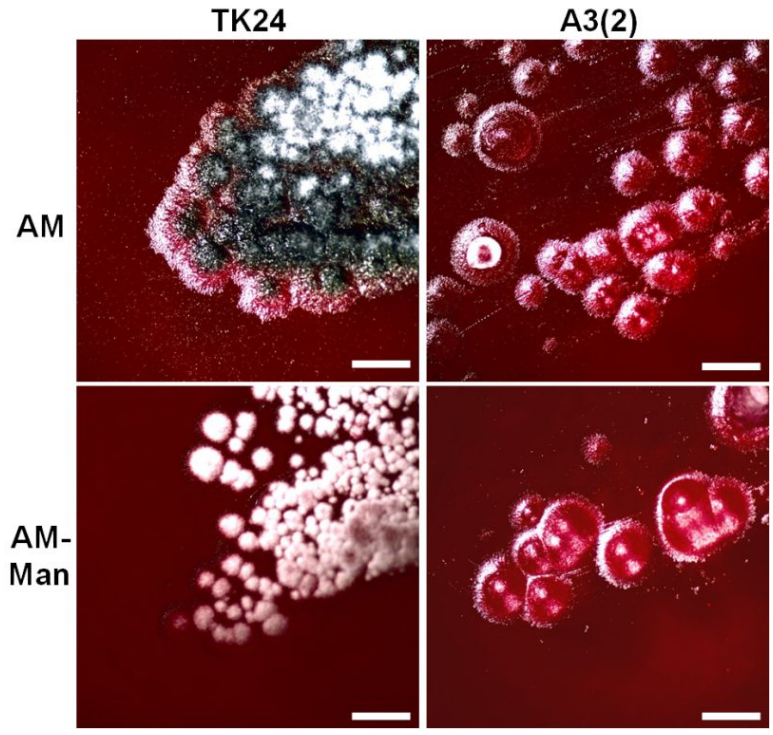

Figure 86. Colonies of *S. lividans* TK24 and *S. coelicolor* A3(2) on AM medium with either glucose or mannitol as carbon source, amended with 0.01 % Congo red. Pictures were taken after 4 d incubation at 28°C. White bar represents 1 mm.

In order to test if the EPS production was connected to the availability of glucose, the strains were cultivated on AM-Man medium, where glucose was substitute by mannitol (Figure 85). Indeed, no colour change of CR was observed, which proofed that cellulose-containing EPS production was dependent on glucose availability. The colony morphology of Δ*sfECF* changed compared to the WT, showing a shiny, bright red and more bulky phenotype (Figure 85).

In order to test, if the difference in colouration depending on the carbon source was a strain-specific trait of *S. mirabilis*, *S. coelicolor* A3(2) and *S. lividans* TK24 were tested in the same manner (Figure 84, Figure 86). None of the strains were impaired in growth on both media. *S. lividans* TK24 rapidly produced aerial mycelium and spores. Whether the black colouration of this strain on AM was due to the production of a pigment or a colour change of CR, cannot be stated with certainty. However, the difference on AM to *S. mirabilis* was apparent, as no dark black halos were produced. Thus, the EPS production of *S. mirabilis* was different from these strains and might constitute an additional metal resistance mechanism of *S. mirabilis*. As these EPS were only produced on AM medium and not TSB, they could be one cause for the increased metal resistance of *S. mirabilis* on minimal medium compared to complex TSB medium.

Liquid medium amended with Congo red

For gaining a better understanding of the nature of the macroscopically observed growth impairment caused by CR, the strains were cultured in liquid NMMP with glucose or mannitol as carbon source,

supplemented with 100 µg/ml CR. It is known that in liquid culture CR interferes with fimbrae formation in *Streptomyces* sp. (de Jong et al., 2009). The polymerization of glucan is prevented, resulting in the formation of short microfibrils. Furthermore, growth defects were observed when fungi were grown in

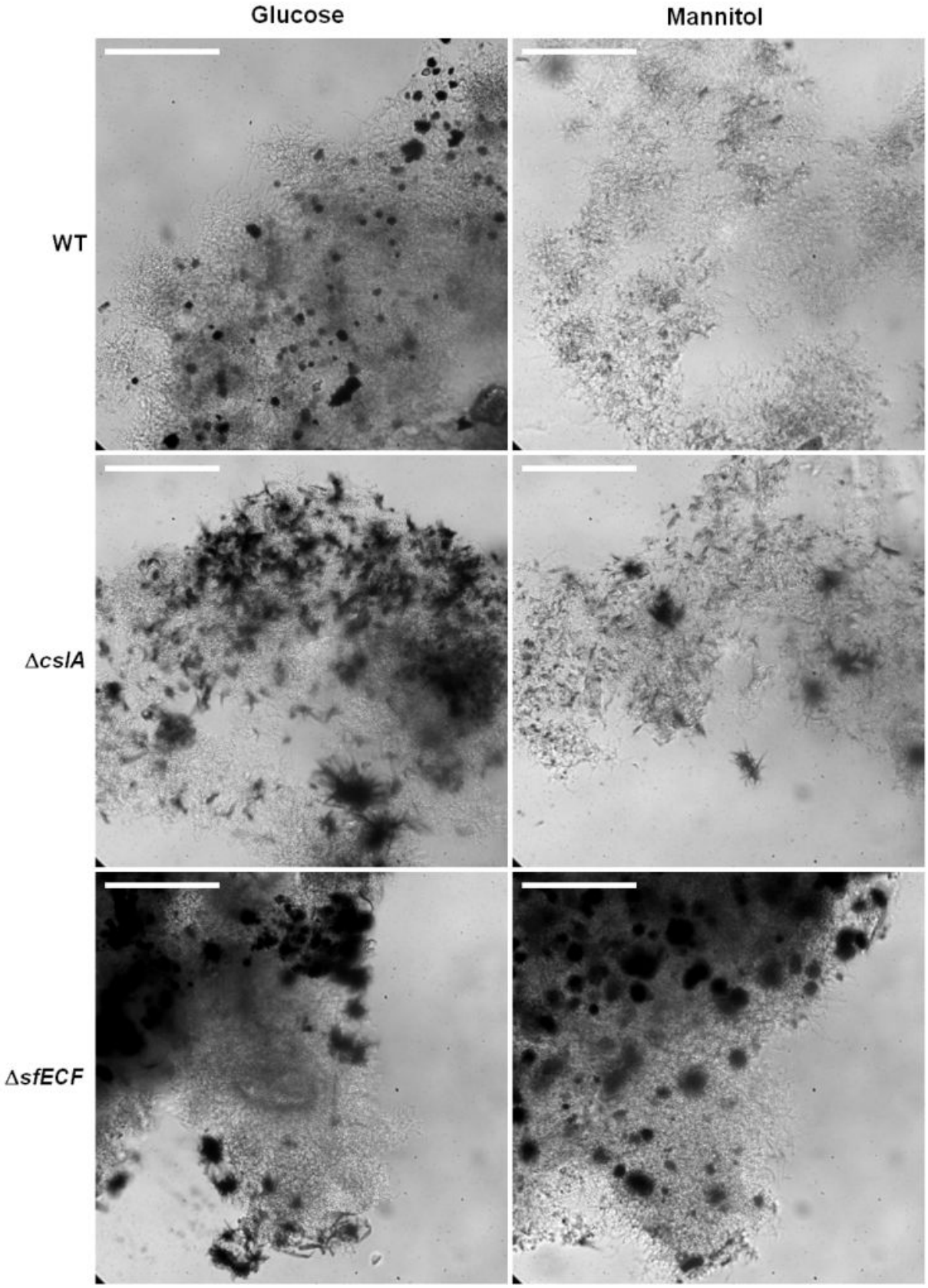

Figure 87. Microscopy pictures of mycelium from static liquid cultures in NMMP with glucose or mannitol, supplemented with 100 µg/ml Congo red. Cultures were grown for 4 d at 28°C. White bar: 200 µm.

presence of CR, e.g. swollen and lysed hyphal tips and loss of tip polarity (Nodet et al., 1990; Roncero & Duran, 1985).

In *S. mirabilis* and the deletion strains, no such effect was observed in the tested media, probably because the cell wall structure differed from that of fungi regarding the structure and composition of cellulose-like compounds.

However, differences were observed between *S. mirabilis* and the deletion strains. Firstly, Δ*cslA* produced markedly more biomass than *S. mirabilis* and Δ*sfECF* and secondly, there was a difference in the formation of dark violet aggregates. In Δ*cslA* and Δ*sfECF* these aggregates were observed in association with the mycelium pellets (Figure 87), especially when glucose was provided as carbon source. These aggregates did not show fluorescence, although they were probably the result of CR binding to cellulose compounds. For the wild type strain, these aggregates were only observed in glucose-containing NMMP, but to a lesser extent.

The strains also differed in the coloration within the mycelium pellets. *S. mirabilis* and Δ*sfECF* showed a strong red colouration of the centre of the pellets, especially when glucose was the carbon source.

As reference strain, *S. coelicolor* A3(2) was cultivated in the same manner. This strain did not produce dark aggregates, but showed a similar red centre of the pellets regardless of the carbon source, like *S. mirabilis* (data not shown).

The pellets of Δ*cslA* were merely light red, indicating a reduced amount of cellulose material compared to the other strains. These results substantiated the reduced level of cellulose material produced in Δ*cslA* remaining associated with the hyphae. The increase in growth in comparison to the WT fitted to an observation for the fungi *Geotrichum lactis*, whose protoplasts showed a higher resistance to CR than the mycelium, due to the lack of a cellulose layer (Roncero & Duran, 1985),

The nature of the dark aggregates remained elusive. They might have been cellulose material which precipitated with CR. Since in Δ*cslA* the cellulose-like compounds possibly diffused more freely, this would explain the higher number of dark aggregates in the pellets. However, also in Δ*sfECF* these aggregates were observed, although it was assumed that there was no change in the fimbriae formation. For further investigation of this phenomenon, it would be expedient to determine the nature of the black aggregates.

The experiments using Congo red showed that the deletion of *P16sfECF* changed cell envelope properties, but probably did not interfere with the production of EPS directly. Δ*cslA*, on the other hand, benefitted from the reduced attachment of cellulose-like material, whose precipitation in close vicinity to the hyphae was most probably the reason for growth inhibition in the WT. Again, the carbon source was shown to play a major role in the developmental processes of the streptomycete.

Carbon source utilisation and sensitivity to different stressors

Like the WT, both deletion strains were able to use different carbon sources (glucose, arabinose, xylose, maltose, mannitol, sorbit, galactose, saccharose, casamino acids) when cultivated in liquid minimal medium (AM w/o Glc, NMMP). However, different phenotypes in pellet morphology were observed, when cultivated with casamino acids, as described above. As Mce4 is likely a cholesterol import system that enables growth on sterols as carbon source (Mohn et al., 2008; Pandey & Sassetti, 2008), the strains were also checked on AM medium with cholesterol.

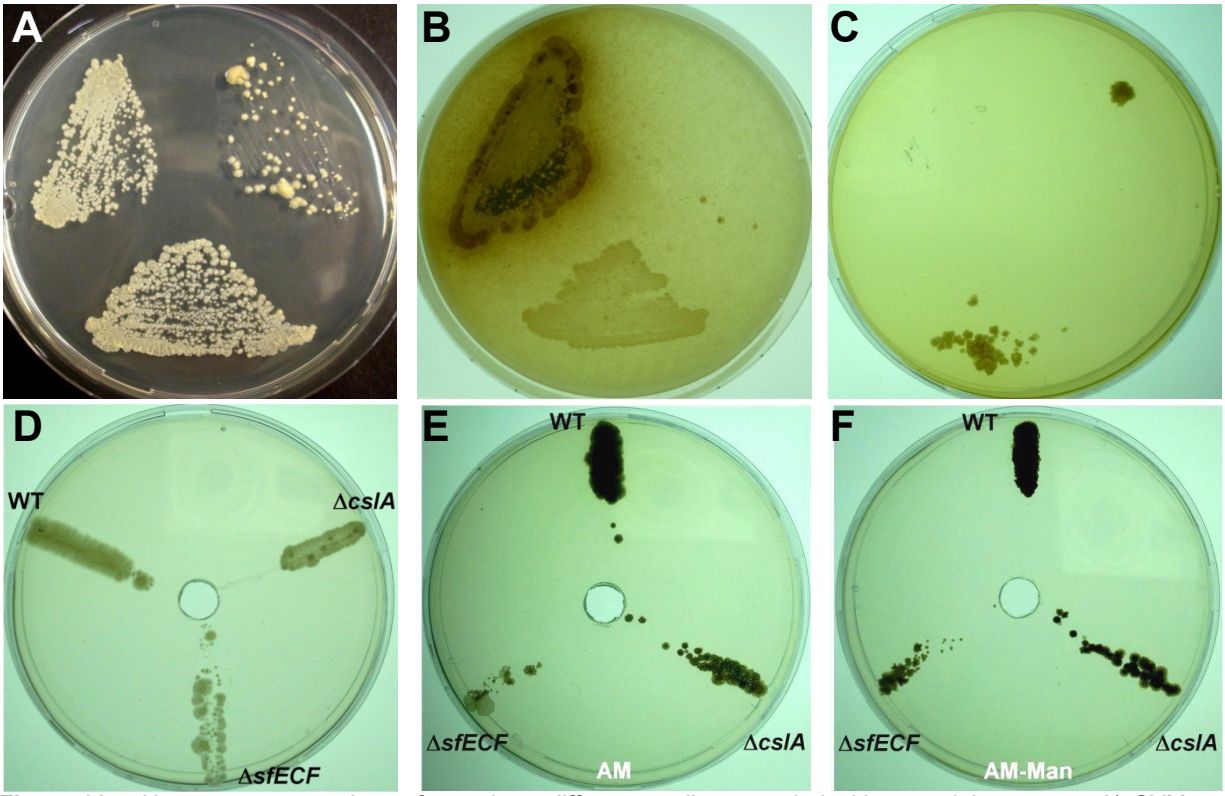

Figure 88. Upper row: comparison of growth on different media, amended with potential stressors: A) GYM + 600 mM KCl; B) MS + 300 mM KCl; C) TSB + 550 ppm SDS. Plates were inoculated as in Figure 71 with *S. mirabilis* left, Δ*sfECF* right and Δ*cslA* below. Lower row: agar diffusion assays on AM medium testing resistance to ampicillin (D, using 100 µl of 25 mg/ml stock solution) and $NiSO_4$ (E-F using 150 µl 2 M stock solution on AM or AM-Man medium)

However, growth was very weak in all strains and not different from that on AM without carbon source, probably due to the utilisation of agarose by the strains. Therefore, no definite conclusion could be drawn regarding cholesterol utilisation. The test could not be conducted in liquid culture due to the low water solubility of cholesterol.

It was further tested, if the hypothesized changes of the cell envelope in the deletion strains affected the sensitivity to osmotic stress, since osmoadaption and the ability to erect aerial mycelium are known to be connected in *Streptomyces* sp. (Bishop et al., 2004; Cho et al., 2001). *S. mirabilis* and Δ*cslA* showed similar good growth on MS amended with KCl up to a concentration of 0.5 M, while Δ*sfECF* was more sensitive and growth was markedly impaired by 0.2 M KCl and ceased at 0.3 M KCl (Figure 88). Possibly, a change in turgor pressure in Δ*sfECF* prevented growth at higher KCl concentrations, which indicated a direct or indirect role of this sigma factor in osmoadaption.

Besides osmotically active compounds, antibiotics may pose stress to bacterial cells. Therefore, the strain's resistance to ampicillin was tested (Figure 88). Deletion of *P16cslA* rendered the strain more susceptible to ampicillin, while Δ*sfECF* was more resistant. In case of Δ*cslA* the loss of the glucan layer probably facilitated the access of the antibiotic to the cell, leading to an increased uptake. The amyloid layer seemed to shield the WT hyphal to a certain degree – an effect which is known for EPS from other bacteria (Anderl et al., 2000; Izano et al., 2007). The increased resistance of Δ*sfECF* might be the result of a lower number of cell membrane-crossing channels, through which ampicillin would enter the cell, if this sigma factor indeed regulated the Mce4 cluster, which partly encodes channel proteins (Casali & Riley, 2007).

Changes in the cell envelope may also impact the resistance to other toxic compounds, which directly attack the cell membrane, like EDTA and SDS (Malinverni & Silhavy, 2009). The resistance to these compounds was tested on TSB plates. All strains tolerated EDTA to a similar level, growing up to 0.5 mM EDTA. Apparently, the amyloid fibres did not protect the hyphal cells from this compound. However, a difference in SDS sensitivity was observed (Figure 88). Both deletion strains tolerated up to 0.005 %, while *S. mirabilis* showed growth up to 0.003 % SDS. The main point of action of SDS are membrane-associated proteins, which are unfolded and released, thereby fragmenting and destabilizing the cell membrane. ATPases are preferably extracted by SDS, before lipids are solubilised (Kragh-Hansen et al., 1998). A reduction of cell wall proteins would therefore increase SDS resistance, which could be the reason for increased resistance of the deletion strain, since Mce proteins, as well as β-glycosyl transferases are localised in the cell membrane (Casali & Riley, 2007; Forrellad et al., 2014; Saxena et al., 1995). Therefore, the loss of these proteins would reduce the number of primary attacking sites for SDS. A similar increased SDS resistance was observed in a *mce* deletion mutant of *S. coelicolor*, which also showed no difference in the ability of utilization of different carbon sources (Clark et al., 2013). These findings supported a role for P16SfECF in transcriptional control of the *S. mirabilis mce* cluster.

If the cellulose cover of hyphae was considered to have similar functions in *Streptomyces* sp. as biofilm formation in other bacteria, they might also be a mean for protection against heavy metals. Although the metal adsorption capacity of unmodified cellulose is low (O'Connell et al., 2008), *Streptomyces* sp. EPS compounds were shown to have metal chelating functions, probably due to binding to negatively charged functional groups (Elnahas et al., 2017; Manivasagan et al., 2013). Thus, the sensitivity of the deletion strains to $NiSO_4$ was tested in plate diffusion assays (Figure 88) using minimal medium with either glucose or mannitol as carbon source. Both deletion strains exhibited a higher resistance to Ni^{2+} on both media. In particular, nickel resistance was increased in Δ*cslA*, which was unexpected. Apparently, the cover of the hyphae by cellulose-like fibres might affect the WT strain negatively, as they might provide sites of metal accumulation, or in the deletion strains other EPS production systems were up-regulated, which were more effective in sequestering metals, thereby promoting growth of the streptomycete.

Potential genomic basis for *S. mirabilis* EPS production

The results presented so far in this section indicated that there might be several systems in *S. mirabilis* that were involved in the production of extracellular matrix components, which enabled the streptomycete to adhere to various surfaces and might serve as resistance mechanism against different stresses. Strain-specific differences were observed, which might also be connected to environmental stressor resistance.

The fact that different EPS production systems act in concert in *Streptomyces* sp. is very well known (van Dissel et al., 2018) and also for *S. mirabilis* CslA-independent systems could be assumed. Accordingly, the composition of *Streptomyces* sp. EPS can vary between strains, but often sugar acids, glucose and mannose were found as components (Elnahas et al., 2017; Manivasagan et al., 2013; Selim et al., 2018). If, indeed, EPS were involved in the metal resistance of *S. mirabilis*, the strain

might possess either several clusters connected to EPS production, or the genes might be differentially regulated as compared to metal sensitive *Streptomyces* sp. strains.

For addressing at least the first question, genes which are known from other species to regulate EPS production, were searched in the *S. mirabilis* genome and several putative homologues could be identified. .

Besides cellulose, poly-β-1,6-N-acetylglucosamine (PNAG) often constitute a bacterial extracellular matrix component. In numerous bacteria, different clusters for the production of PNAG were identified, e.g. *pga* and *ica* genes of *Aggregatibacter* sp. and *Staphylococcus* sp. (Ferreira et al., 2014; Izano et al., 2008). In *Streptomyces* sp., this compound is synthesized by MatAB, a paralogue of the *Staphylococcus epidermidis ica* system, connected to slime production in the latter (Arciola et al., 2002). The *matAB* gene products are connected to pellet formation and attachment to hydrophilic surfaces (van Dissel et al., 2015; van Dissel et al., 2018).

Five ORFs of *S. mirabilis* were annotated as poly-β-1,6-N-acetyl-D-glucosamine synthase-encoding genes (SMI3098, SMI3592, SMI3912, SMI2625, SMI4718). The products of SMI3098 and SMI4718 showed high sequence similarity to *S. coelicolor* SCO2962 (45.8 %, 50.5 %), a paralogue of IcaC of *St. epidermidis*. Except for SMI3912, the predicted proteins furthermore were similar to PgaC of *Actinobacillus* sp. (24-35 % similarity with query coverage > 50 %), which is a PNAG-specific enzyme of the cellulose synthase superfamily (cd06423) involved in EPS formation (Izano et al., 2007). In *S. coelicolor* A3(2), for comparison, the search for PgaC homologues yielded only two results: besides the mentioned IcaC paralogue SCO2962, SCO4554 exhibited a significant similarity (> 30 %, with query coverage > 50 %). SCO4554 was annotated as possible bi-functional transferase/deacetylase.

The product of SMI3912 was similar to the probable glycosyl transferase SCO4022 (84.4 % identity) of *S. coelicolor* A3(2), which showed no homology to PgaC. Hence, the annotation of SMI3912 as PNAG synthase was questionable.

The higher number of IcaC and PgaC homologues in *S. mirabilis* could explain the ability of the *cslA* deletion strain to form pellets, while in a *S. coelicolor cslA* deletion strain pellet formation was prevented (Xu et al., 2008). Besides *cslA*, also the *matAB* locus for PNAG production is responsible for pellet formation. Van Dissel et al. (2018) found that introduction of a second copy of *matAB* in a *cslA* deficient *S. lividans* strain restored pellet formation. Therefore, the additional loci encoding PNAG synthases in *S. mirabilis* would very likely be sufficient for pellet formation also in the Δ*cslA* strain. Likewise, a higher PNGA production could explain the high fluorescence level of Δ*cslA* hyphae observed when grown on agar plates, while for *S. coelicolor cslA* deletion strains it was reported that no fluorescence could be observed.

Another cluster for EPS production found in *Streptomyces* sp. is the *ste* locus, which was firstly described in *Streptomyces* sp. 139. The cluster (AY131229.2) comprises 22 ORFs, including a priming glycosyltransferase gene (*ste5*). These genes are also present in *S. coelicolor* A3(2), but *ste1-ste4* are separated from the others forming an individual cluster (Wang et al., 2003). The same situation was found for *S. mirabilis ste* genes. SMI2367-SMI2364 were homologous to *ste1-ste4*, while SMI1604 was identified as *ste5* with the other *ste* genes located downstream. The *ste* locus is not well investigated, wherefore no statement could be made about its possible contribution to *S. mirabilis* EPS production. However, since the operon was similar to that of *S. coelicolor* A3(2), it was assumed that they

might participate in a similar way and would not account for the increased metal resistance of *S. mirabilis*.

Lastly, an example for indirect regulation of EPS production shall be given. The production of extracellular matrix in *S. coelicolor* also involves the diguanylate cyclase CdgB (SCO4281), which is controlled by BldD. It exerts an indirect effect on EPS production by producing c-di-GMP, which leads to an increased EPS production. CdgB overexpression resulted in an increased surface attachment (Tran et al., 2011). Two *S. mirabilis* ORFs showed a high similarity to SCO4281: SMI4165 (83 % identity, 100 % coverage) and SMI0176 (69 % identity, 98 % coverage). Both were annotated as putative diguanylate cyclase YeaP. Similar to the higher number of PgaC homologues, two copies of CdgB proteins might increase the EPS production by *S. mirabilis* enhancing stress resistance.

Conclusion

The presented results substantiated that *S. mirabilis* was inherently bald on complex medium, caused by the lack of the *ram* cluster. It could be hypothesised that this was an adaption to its original habitat, a contaminated soil, in which the costs for the production of potentially redundant proteins might negatively impact functionality of the resistance machinery. For confirming this assumption, further studies are required. Potential setups could either involve the introduction of another strain's *ram* cluster in *S. mirabilis*, or deletion of this cluster in a heavy metal resistant streptomycete, like *S. acidiscabies* E13, and investing the impact on heavy metal resistance.

Morphological differentiation and environmental stresses necessitate the ability to remodel the cell membrane, e.g. by the synthesis of lipids *via* various pathways (Sandoval-Calderon et al., 2017). Whether P16SfECF was involved in the regulation of membrane lipid content, namely the *mce* cluster, could not be said for certain. However, the test results obtained here, hinted at a change in the cell envelope, which might be connected to a down-regulation of *mce* transcription. In particular, the increased resistance of the *P16sfECF* deletion strain to SDS indicated a reduction of cell wall-associated proteins, which could result from a loss of the membrane-spanning Mce transporter. Furthermore, the reduced attachment and loose pellet structure of this strain accounted for a direct or indirect effect of P16SfECF on cell wall composition. That these effects were founded by changes other than the loss of EPS production was proven by fluorescence microscopy. This set Δ*sfECF* apart from the second developmentally delayed transformant, Δ*cslA*. However, P16SfECFmight also be involved in the transcriptional regulation of genes connected to morphological development other than the *mce* cluster, since a *S. coelicolor mce* mutant strain was not impaired in spore production, although surface changes were observed (Clark et al., 2013).

In *S. mirabilis*, CslA played a similar role for attachment and cellulose fibre production as in other streptomycetes. However, the loss of the coding gene was partially compensated by other systems regarding pellet structure and attachment. Thus, *S. mirabilis* harbored numerous systems enabling the attachment to surfaces, which prevented negative effects of *cslA* deletion observed in *S. lividans* or *S. coelicolor*.

The diffusion of EPS compounds in Δ*cslA* indicated by the Congo red plate assay implied that cellulose fibres produced by P16CslA not only served as anchoring sited for Chp and Rdl proteins, but also directly or indirectly for other EPS compounds.

The results obtained in this study furthermore emphasised the importance of the cell envelope and EPS production on heavy metal resistance of *S. mirabilis*. However, it was unexpected that deletion of *P16cslA* increased resistance to Ni^{2+}, as the cover of hyphae by cellulose fibres could be considered a protective layer, which would sequester metals, as it has been observed for EPS in *Enterobacter* sp. (Naik et al., 2012). However, it could not be excluded that *P16cslA* deletion led to an increased production of other EPS compounds, which sequestered metals more efficiently.

Lastly, the importance of media composition, particularly regarding the carbon source, was shown. Mannitol apparently induced or increased EPS production that improved attachment and caused a high calcofluor white fluorescence, also in Δ*cslA*. Likewise, nickel resistance was increased. For gaining a deeper understanding of the underlying machinery, gene transcription should be investigated with regard to different cultivation conditions. Differences to heavy metal sensitive species could be expected.

In how far these results had implication for the *Streptomyces* sp. ecology, could not be stated for certain. Since cellulose components were shown to be important in other bacteria for the attachment to plant roots, a similar role could be assumed in *Streptomyces* sp. (Wheatley & Poole, 2018). However, this has not been established yet. Further investigations of the membrane composition of *S. mirabilis*, e.g. the lipid profile, and its EPS composition might help understanding their impact on survival in a contaminated habitat

3.8 Maintenance of cytosolic pH and essential metal homeostasis

Introduction

In most habitats, sodium and hydrogen are common ions and both are highly important for the proper functioning of the cell and its proteins. However, when concentrations exceed a certain threshold, also these essential elements can become cytotoxic. The most common sodium salt, NaCl, inhibits metabolism and DNA repair and poses osmotic and ionic strength related stress on the cell (Dmitrieva & Burg, 2005; Mittova et al., 2002). Therefore, cells have to regulate intracellular Na^+ and H^+ concentrations as tightly as for other elements. For ensuring proper cell functioning, the intracellular pH has to be kept ideally at a constant level, which is often close to neutral, regardless of external pH changes (Padan & Schuldiner, 1986; Shimamoto et al., 1994).

One way for metal homeostasis regulation is the employment of monovalent cation/H^+ antiporters. These transporters are located in the cell membrane and exchange H^+ for cations in a process that is driven by the proton electrochemical gradient generated by primary proton pumps of the respiratory chain etc. As the proton concentration in the surrounding of a cell is often higher than in the cytoplasm, usually the antiporters transport protons into the cell while removing the substrate from the cytoplasm. Antiporters are indispensible for maintaining the cellular ion homeostasis by sensing environmental signals of their cognate ions and adjusting their activity accordingly (Padan et al., 2004; Padan et al., 2001).

Na^+/H^+ antiporters constitute one large family of transporters (TC# 2.A.33) whose members are found in all domains of life. They are responsible for establishing an electrochemical potential and a sodium gradient across the cell membrane, which is the basis for several other H^+- and Na^+-coupled processes, e.g. Na^+/solute transport (Guffanti et al., 1981; Padan et al., 1989). Furthermore, they protect the cell from toxic effects of sodium and lithium by extruding these ions and regulate intracellular pH under alkaline conditions and during pH shift (Hunte et al., 2005; Inaba et al., 1994; Padan & Schuldiner, 1994; Pinner et al., 1992; Taglicht et al., 1993). Also their contribution to cell volume regulation has been recognized (Grinstein et al., 1992).

The first described Na^+/H^+ antiporter is NhaA of *E. coli* (West & Mitchell, 1974), a Na^+, Li^+/H^+ antiporter, which became the paradigm for this family of transporters and is very well investigated. NhaA exhibits a high turnover rate with a stoichiometry of 2 H^+ to 1 Na^+ ions and works in a pH-dependent manner (Maes et al., 2012; Padan et al., 1989; Taglicht et al., 1991). Also the crystal structure is known (Hunte et al., 2005). The direction of cation exchange is determined by the electrochemical potential difference of the substrate, relative to that of the protons (Padan, 2008).

NhaA of *E coli* is part of the NhaA/NhaB salt extrusion system of this bacterium. Although both transporters belong to the same family, they differ regarding their substrate specificity and activity. NhaB exhibits a lower affinity to Li^+ and works independently of pH. Furthermore, NhaB only confers limited tolerance against Na^+, although it can compensate a lack of NhaA activity to a certain degree (Inaba et al., 1994; Pinner et al., 1992). Deletion of both transporters in *E. coli* renders the cells highly sensitive to Li^+ and Na^+ (Pinner et al., 1993).

Numerous homologous of *E. coli* NhaA have been characterized, e.g. *Salmonella enterica* NhaA (Lentes et al., 2014), *Vibrio parahaemolyticus* NhaAB (Radchenko et al., 2006) and *Bacillus subtilis*

ShaA (Kosono et al., 2000). Disruption of the latter not only increased the sensitivity to Na^+, but also impaired sporulation of *Bacillus subtilis*, which was ascribed to the increased Na^+ level in the cells affecting σ^H, a sigma factor involved in sporulation (Kosono et al., 2000). Indirect effects of antiporter activity on cell functions were also observed in *Streptomyces* sp., where it stimulated the secondary metabolite production (Park et al., 2009).

As more members of the Na^+/H^+ antiporter family have been characterized, it became apparent that they can be divided, according to their transport characteristics, into three main groups, CPA1, CPA2 and NaT-DC, which again contain several subgroups (Brett et al., 2005). While CPA1 transporters are electroneutral and exchange one proton per sodium ion, CPA2 members work in an electrogenic mode exchanging multiple protons per substrate ion, e.g. *E. coli* NhaA (Saier et al., 2016; Taglicht et al., 1991; 1993). However, all of these transporters function according to the alternating excess model (Mager et al., 2011), implying that the substrate binding site is sequentially exposed to one side of the membrane or the other by changing conformation, whereby the accessibility alternates (Jardetzky, 1966). This change is induced by binding of the substrate. NhaA antiporters can thus function in both directions, pumping protons out or into the cell, as sodium and H^+ compete for the same binding site. Therefore, at high H^+ concentrations, Na^+ cannot effectively bind to the substrate site and sodium transport is inhibited, while at higher pH, meaning lower proton concentrations, the turnover increases (Arkin et al., 2007; Maes et al., 2012; Mager et al., 2011). This determines the pH-dependency of these transporters.

Results

Computational analysis

In silico *identification of putative Na^+/H^+ antiporters and their characteristics*

Gene annotation predicted several transporters for alkali metals coded in the *S. mirabilis* genome. One of these genes, SMI3349, that encoded a putative Na^+/H^+ antiporter turned up as candidate gene in the random mutagenesis experiment when Ni^{2+} sensitive transformants were selected for. Due to this, the antiporter was firstly considered to be involved in heavy metal resistance of *S. mirabilis* and was therefore chosen for further investigation. Screening the annotated *S. mirabilis* proteins for homologous transporters, a second ORF, SMI7074, was found that was predicted to encode a sodium/proton antiporter. The coding genes were accordingly named *P16nhA1* and *P16nhaA2*, respectively. They differed in size as well as GC content (Table 28). *P16nhaA1* was located in the core segment of the genome comprising 1398 bp with a GC content of 68.5 %. In contrast, *P16nhA2* was found near the chromosomal end and was about 500 bp longer than *P16nhaA1* with a higher GC content (71.4 %). The size and mass of the predicted gene products differed accordingly, but lay in the range typically found for antiporters of the NhaA family (TC# 2.A.33).

The affiliation of P16NhaA1 and P16NhaA2 to this family was confirmed by searching the Pfam database, which identified the conserved domain Pfam06965 in the two proteins, which is characteristic for a family of integral membrane transporters that exchange Na^+ and H^+ in a pH-dependent manner.

P16NhaA1 showed high amino acid level similarity to other *Streptomyces* sp. NhaA proteins, e.g. 86 % with S. *avermitilis* MA-4680 NhaA (Q82EL6) and 81 % with *S. antibioticus* NhaA (Q93F90), which suggested a high degree of conservation in this genus. In contrast, P16NhaA2 seemed to be

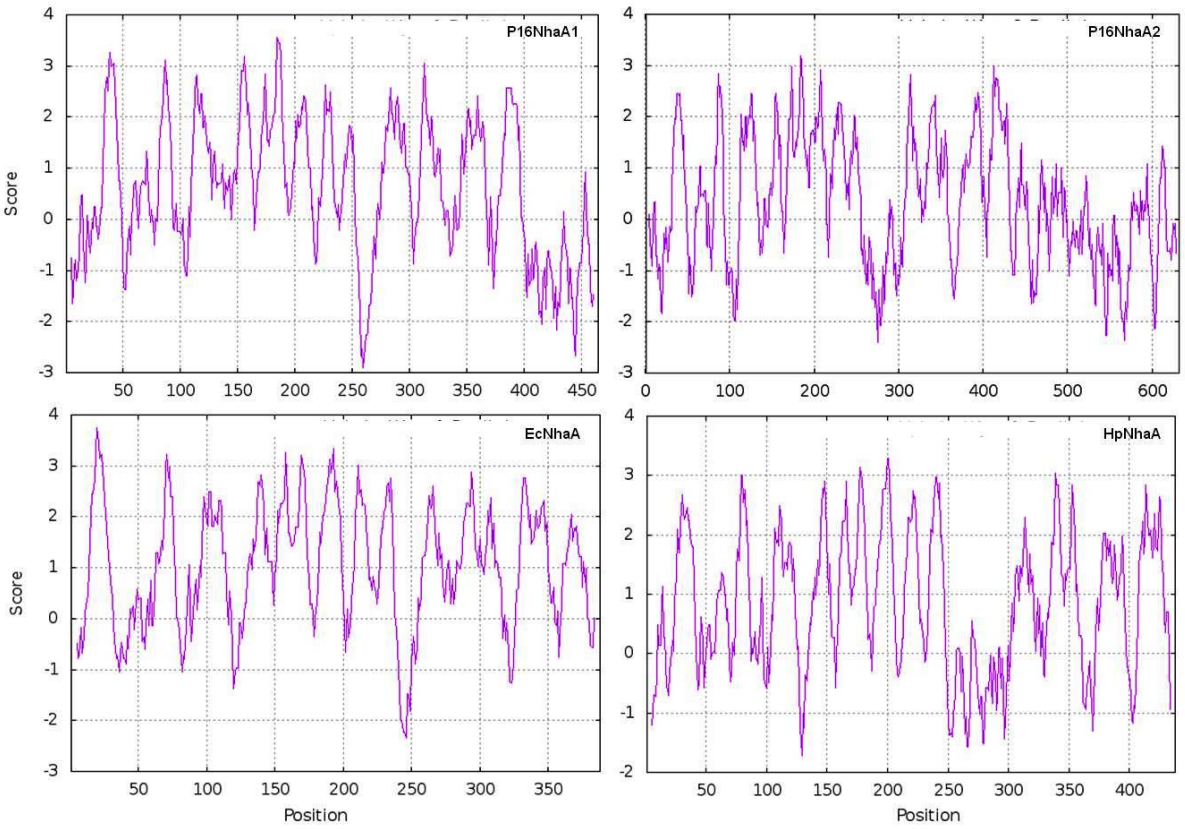

Figure 89. Hydrophobicity plots of the putative Na^+/H^+ antiporters P16NhaA1 and P16NhaA2 of *S. mirabilis* and the model antiporters of *E. coli* (EcNhaA) and *H. pylori* (HpNhaA).

less conserved, exhibiting 62 % identity to *S. coelicolor* NhaA2 (Q9S2C8). The similarity to *Salinispora arenicola* NhaA1 (A8LVS8) and *Salinispora tropica* NhaA3 (A4X5I0) to P16NhaA2 was comparably high (61 % and 59 %). Both *Salinispora* strains were marine actinomycetes adapted to high salt conditions.

As the paradigm of the NhaA family is the *E. coli* NhaA protein, the amino acid sequence of both *Streptomyces* sp. transporters was additionally compared to strains of this genus. As expected, the sequence similarity was lower than to the actinomycete transporters, but still significant with around 40 % for P16NhaA1 and 35 % for P16NhaA2 (*E. coli* CFT073 NhaA (Q8FLC1)).

Transporters of the NhaA family typically exhibit ten to twelve transmembrane domains, which was in agreement with the prediction for both *Streptomyces sp.* transporters. Online tools gave different predictions for P16NhaA1, varying between ten to twelve TMD, but regarding the hydropathy plot (Figure 89), a twelve TDM topology had to be favoured, as the similarity to the homologous *E. coli* NhaA, which possesses twelve TMDs (Rothman et al., 1996) was sufficiently high.

Comparing the hydropathy plots of P16NhaA1 and P16NhaA2 with well characterized homologous antiporters of *E. coli* (EcNhaA) and *Helicobacter pylori* (HpNhaA), a higher similarity of P16NhaA1 to EcNhaA and P16NhaA2 with HpNhaA was observed. The latter two shared a characteristic stretch of low hydropathy between residues 250 and 300, while the others exhibited a negative peak in this region. This could be taken as a first hint on difference in function of the

Table 28. Predicted *S. mirabilis* Na^+/H^+ antiporter genes and characteristics of their products.

	P16NhaA1	**P16NhaA2**
Annotation	SMI3349	SMI7074
Gene size	1398 bp	1899 bp
GC content	68.5 %	71.4 %
Protein size	465 aa	632 aa
Mass	48.9 kDa	67.6 kDa
TMD	12	12

Streptomyces sp. transporters, as EcNhaA and HpNhaA display different activities, which will be discussed in more detail below.

Phylogenetic comparison

Na^+/H^+ antiporters are included in the Cation:Proton Antiporter superfamily (CPA), which comprises four families of mostly secondary active transporters. The two largest of these are CPA1 (TC# 2.A.36) and CPA2 (TC# 2.A.37), which exhibit high homology and can furthermore be divided in several subfamilies (Chen et al., 2011; Saier et al., 1999). For the electrogenic transporters of CPA2, two subfamilies, NHA and CHX, have been identified (Brett et al., 2005). A single cell normally possess several CPA transporters, often from one as well as numerous of these families (Padan et al., 2005), wherefore the existence of two NHA family transporters in *S. mirabilis* was not surprising.

The separation of CPA1 and CPA2 as well as both CPA2 subfamilies clearly showed in a phylogenetic tree based on the amino acid sequences of CPA members (Figure 90).

Within the NHA subfamily, the NhaA and NhaB groups of transporters could be distinguished. Regarding their functioning, NhaA-type transporters differentiate from NhaB by their strongly pH-dependent activity and a 1 $Na^+(Li^+)/2\ H^+$ stochiometry (Lentes et al., 2014; Saier et al., 2016). As both *S. mirabilis* transporters clustered within the NhaA group, a corresponding activity could be assumed.

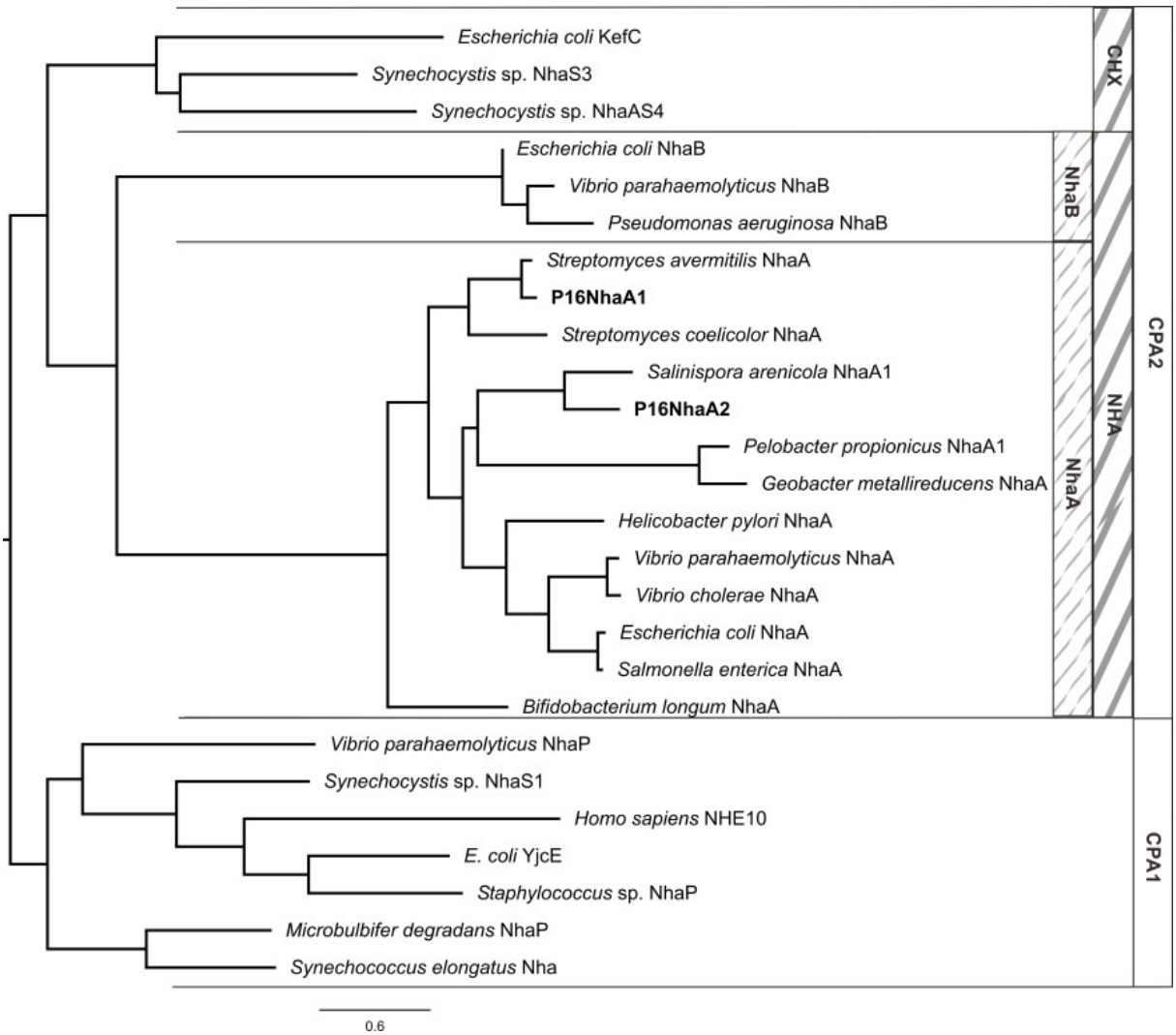

Figure 90. Phylogenetic tree of members of the Cation:Proton Antiporter superfamily (CPA) including the putative Na^+/H^+ antiporters of *S. mirabilis*. Group assignment according to Brett et al. (2005).

Furthermore, in the tree an apparent correlation of the regarded transporters with the usual habitat of their host could be observed. There was a cluster of potential human pathogens inhabiting the gastrointestinal tract, e.g. *E. coli* and *H. pylori*, which was distinct from environmental isolates. Activity profiles of Na^+/H^+ antiporters can differ, especially regarding the pH dependency, and seem to be adapted to the conditions found in the habitat. Accordingly, NhaA of *H. pylori* has a high activity at lower pH values than *E. coli* NhaA, as *H. pylori* dwells under acidic conditions in the human stomach (Inoue et al., 1999). All of these transporters are necessary for survival at high NaCl and LiCl concentrations (Billini et al., 2008; Inoue et al., 1999; Kuroda et al., 2005; Lentes et al., 2014).

P16NhaA1 and P16NhaA2 belonged to different clusters. While the latter shared a higher similarity to homologues of bacteria isolated from marine and freshwater habitats, P16NhaA1 clustered with well investigated soil isolates. Concluding from the clustering of the *Streptomyces* sp. transporters in the tree and the fact that transporter function is related to environmental conditions, P16NhaA2 might be specifically responsible for coping with elevated salt concentrations, similar to that found in marine environments, while P16NhaA1 could be necessary for the basic Na^+, Li^+ and H^+ homeostasis. Similar task sharing of transporters has been observed in organisms that are challenged with high osmotic pressure and therefore depend on the collective activity of several efflux pumps, like *Vibrio parahaemolyticus*, which possesses 12 Na^+/H^+ antiporters (Radchenko et al., 2006) or the alcaliphilic cyanobaterium *Synechococcus elongatus*, which posseses seven *nha* genes that code putative Na^+/H^+ antiporters belonging to CPA1 and CPA2 (Billini et al., 2008).

Sequence alignment

In site-directed mutagenesis experiments, several residues have been identified that influence the substrate transport and pH activity profile of Na^+/H^+ antiporters. To check the presence of these residues in the examined *Streptomyces* sp. transporters, the amino acid sequences of P16NhaA1 and P16NhaA2 were aligned to other well characterized NhaA proteins of *E. coli* (EcNhaA) and *H. pylori* (HpNhaA), that differ in their pH sensing, as well as to *E. coli* NhaB (EcNhaB). While EcNhaA is functional at pH 7.5-8.5 (Taglicht et al., 1991), HpNhaA exhibits a broader pH activity range of 6.0-8.5 (Inoue et al., 1999). Besides, these antiporters exhibit pH-dependent changes of Li^+/H^+ and Na^+/H^+ transport activities. The transport of Li^+ by EcNhaA increases between pH 7.5 to 8.0 and Na^+ is preferably transported at pH 8.0 to 8.5. HpNhaA merely exhibits an increase of Li^+ transport at pH 7.0 to 8.6, while Na^+ transport is constant over the entire pH range (Inoue et al., 2001). EcNhaB has a lower but constitutive activity at all pH values and is therefore considered pH-independent (Thelen et al., 1991).

The size, sterospecificity and charge of some residues govern the activity and pH profile of antiporters (Tzubery et al., 2004). Due to these different aspects to NhaA functioning, mutations exert different effects: either the pH activity profile, the transport capacity/specificity for one or all substrate ions and the integrity of the protein are changed or there is no observable effect at all (Galili et al., 2002; Gerchman et al., 1993; Gerchman et al., 1999; Kuwabara et al., 2006; Noumi et al., 1997; Rimon et al., 1998; Tzubery et al., 2004).

The pH response of Na^+/H^+ antiporters is determined by residues in both loops and TMDs. Especially the structure formed by the interaction of TMDs IV, V, X and XI determines the pH range (Inoue et al.,

2001; Tsuboi et al., 2003). A high degree of congruence was observed in these regions, especially for HpNhaA, EcNhaA and P16NhaA (Figure 91).

All in all, the sequence similarity between the considered NhaA transporters was high and several

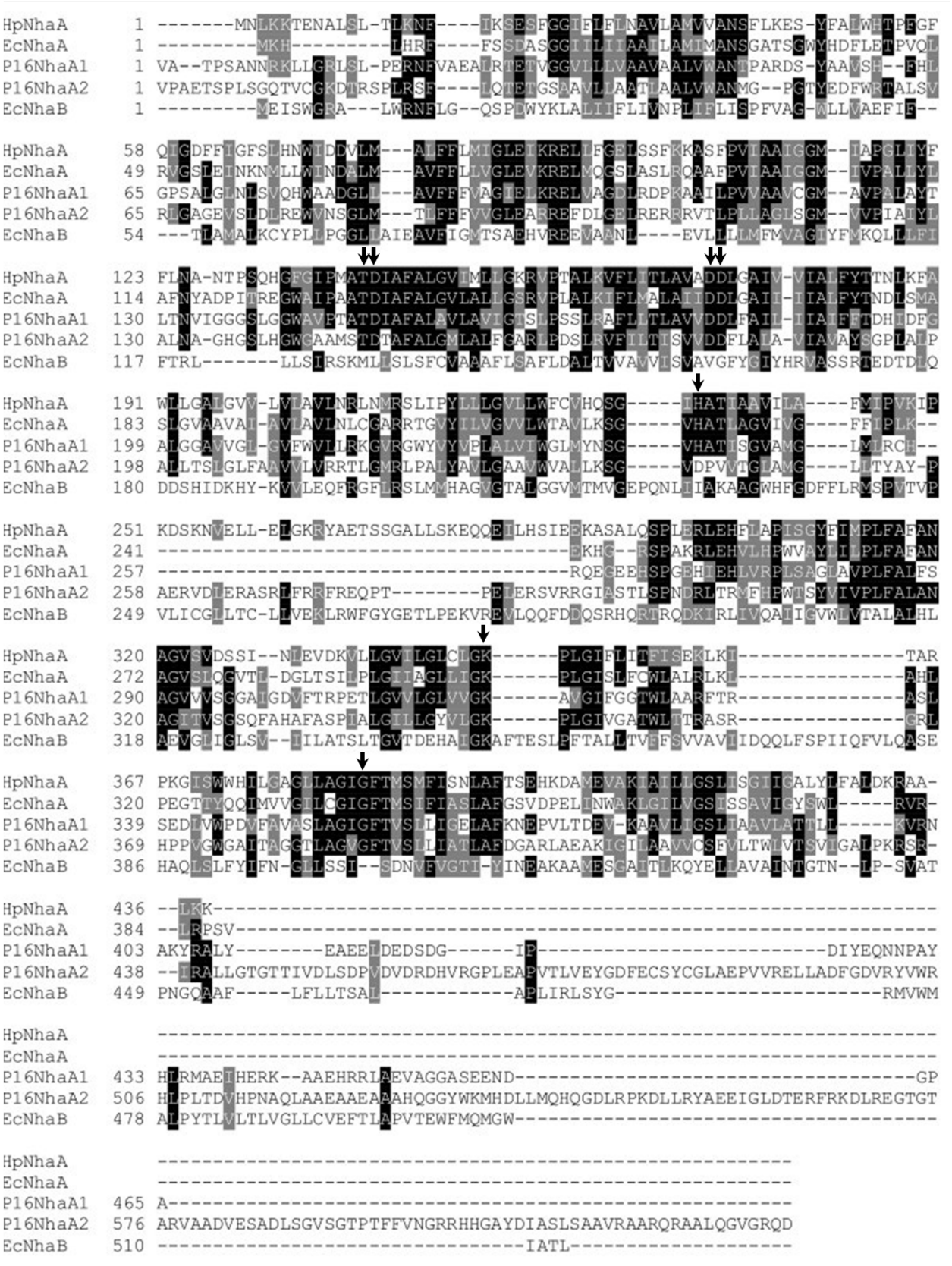

Figure 91. Alignment of *H. pylori* NhaA (HpNhaA), *E. coli* NhaA and NhaB (EcNhaA, EcNhaB) and the putative *S. mirabilis* Na^+/H^+ antiporters P16NhaA1 and NhaA2. Arrows indicate essential residues for substrate transport and pH control.

residues that were found to be essential for transport activity and pH dependency were conserved. For instance, three asparate residues in TMD IV and V that are essential for substrate transport in EcNhaA (D133, D163, D164) and HpNhaA (Inoue et al., 1995; Kuwabara et al., 2006), were also conserved in the *S. mirabilis* transporters, but not EcNhaB. Mutations of theses residues would impair substrate transport, as they enable transport of the ion along the transporter and regulate conformational switching (Arkin et al., 2007; Gerchman et al., 2001; Inoue et al., 1995).

A substitution in TMD IV that indicated differing pH profiles of the two *Streptomyces* sp. transporters was M145 of P16NhaA2, which was occupied by Thr in P16NhaA1 and Ala in EcNhaA, while the corresponding residue in HpNhaA was also Met (M138). Mutation of this position in HpNhaA resulted in a lower activity at acidic pH and higher activity at alkaline conditions (Tsuboi et al., 2003). This might be taken as a clue that P16NhaA2 had a broader pH activity range, similar to that of HpNhaA (pH 6-8.5). This assumption was further substantiated by another residue in the same TMD that was shown to influence the pH response of EcNhaA, namely A127 (Galili et al., 2002). This position was also occupied by Ala in P16NhaA1, but by Gly in both HpNhaA and P16NhaA2.

Regarding residues determining the substrate affinity in TMD IV, one potentially significant substitution was observed for P16NhaA2: the Pro that occupied this position in the other NhaA transporters (P129 in EcNhaA) was substituted by Ala. A P129L mutation in EcNhaA was shown to increase the substrate affinity of the transporter, but also shift the activity profile towards alkaline pH (Galili et al., 2002; Rimon et al., 1998).

Besides the Asp residues, G338 of EcNhaA (TMD XI) was conserved in all considered NhaA transporters, but not EcNhaB. This residue is crucial for inducing a conformational change in response to pH. When a mutation was introduced at this position (G338S) in EcNhaA, the pH control was alleviated and cells became sensitive to alkaline pH in presence of Na^+ (Rimon et al., 1998). Accordingly, the *Streptomyces* sp. transporters were expected to exhibit a pH-dependent activity.

Two amino acid changes in TMD V and the following loop that might influence the *Streptomyces* sp. transporters' pH regulatory system were at HpNhaA positions 168 and 183, the mutation of which caused an activity shift to the alkaline range (Kuwabara et al., 2006). In P16NhaA2 the HpNhaA A168 was exchanged by Ser. This could influence substrate preference in dependence on pH as well, since an A168C substitution impaired Li^+ binding, while for Na^+ merely the pH range of activity changed (Kuwabara et al., 2006).

A further substitution that possibly influenced the transport activity with regard to the pH was observed at position 241 of P16NhaA2. In *E. coli* the corresponding His residue (H225) was found to be the only His essential for transport activity and pH sensitivity (Gerchman et al., 1993). When this residue was exchanged by the acidic polar amino acid Asp, as it was the case in P16NhaA2, the threshold for pH-dependent activation shifted towards alkaline pH while transport efficiency remained constant (Rimon et al., 1995). In NhaB the corresponding amino acid was occupied by Ile (I227), a non-polar amino acid. A substitution of EcNhaA H225 with the non-polar alanine resulted in a low constant activity, independent from pH (Gerchman et al., 1993), which fits the character of NhaB antiporter activity and further emphasises the importance of this residue. Rimon et al. (1995) suggested that hydrogen bonding, polarity and/or charge of the residue at this position might be important for the pH-sensitivity of a transporter.

A noticeable feature that P16NhaA2 shared with HpNhaA and EcNhaB was the large loop between two TMD (TMD VIII and IX in HpNhaA), which was not present in EcNhaA and P16NhaA1. It was hypothesised that this amino acid stretch might be responsible for the altered pH response of HpNhaA compared to EcNhaA (Inoue et al., 1999; Tsuboi et al., 2003). However, deletion of this loop did not alter pH dependency of HpNhaA, but decreased Li^+ transport at alkaline pH, which could be a result of an indirect destabilization of the ion pathway (Inoue et al., 2001). In any case, the fact that EcNhaB and HpNhaA both display a more constant activity profile at a broader pH range than EcNhaA, might be connected to this loop or the resulting interaction between the transporter halves, implicating a similar pH-dependent activity for P16NhaA2. Mutations in the corresponding EcNhaA loop impacted the pH profile and substrate affinity, possibly by influencing interactions of residues (Gerchman et al., 1999; Tzubery et al., 2004).

One residue of EcNhaA which is involved in this interaction is K249 (Tzubery et al., 2004), which was substituted in both *Streptomyces* sp. transporters. In P16NhaA1 it was exchanged for Glu as in HpNhaA, and in P16NhaA2 the position was occupied by Asp, as in EcNhaB. Accordingly, differences to EcNhaA activity were assumed.

However, single amino acid substitutions can merely give limited clues about the actual activity of the transporters. From their mutation studies of HpNhA Tsuboi et al. (2003) concluded that pH sensing of this transporter is rather dependent on the structure formed by the interaction of TM I-VIII and TM IX-XII than determined solely by a single residue or loop 8. This was manifested by experiments with chimeric antiporters composed of EcNhaA and HpNhaA N-terminal and C-terminal halves, which exhibited an intermediate pH-dependent activity (Inoue et al., 2001). The interplay between amino acids within the transporter structure is more important than the residues themselves, implying that the replacement of a single amino acid by a similar one might not change the activity or can be compensated by others.

Lastly, on the basis of the alignment, predictions could be made about the structure of the two *Streptomyces* sp. antiporters. In the membrane, EcNhaA is composed of oligomers formed by physically and functionally interacting monomers (Gerchman et al., 2001) creating two funnels in an hourglass-like structure that lead from both sides of the membrane to D164 (Hunte et al., 2005). Likewise, in HpNhaA this Asp residue was suggested to protrude into the funnel, being accessible from the cytoplasm and the periplasm (Kuwabara et al., 2006). Since this residue was conserved in the *Streptomyces* sp. transporters as well (D180 and D179 in P16NhaA1 and P16NhaA2, respectively), a similar positioning of this residue was assumed.

In a simulation study of EcNhaA, Alhadeff & Warshel (2015) found that protons and the substrates compete for the same binding sites at D163 and D164. At the side of the membrane with a lower pH, unbinding of Na^+ occurs, followed by a conformational change and the release of protons and binding of Na^+ at the side with more basic conditions. In P16NhaA1 and P16NhaA2 this would involve D179/D180 and D178/D179, respectively.

Solely Na^+ and Li^+ can induce transport activity of EcNhaA, although D164 is a promiscuous binding site, where several alkali ions can bind (Alhadeff et al., 2011). Whether in the *Streptomyces* sp. transporters also other ions would undergo such a functional binding, remained to be determined.

All in all, the alignment of *S. mirabilis* Na^+/H^+ antiporters with homologous proteins lead to the conclusion that they might have different pH profiles, with P16NhaA1 being more similar to EcNhaA and

P16NhaA2 more similar to HpNhaA with a higher activity also at acidic conditions and a broader pH range.

However, as discussed above, single residue exchanges might be redundant for the overall activity of the transporter, as they can be offset by exchanges in a second position. For instance, second-site mutations in EcNhaA were shown to restore WT characteristics of transporter (Rimon et al., 1998). Also, *Vibrio parahaemolyticus* possesses a transporter that shows high sequence similarity to EcNhaB, but displays an activity profile that rather resembles that of EcNhaA with no activity at pH 7 (Nozaki et al., 1996). Therefore, the actual activity of the *Streptomyces* sp. transporters had to be determined *in vivo*.

Impact of *P16nhaA1* deletion on salt and pH tolerance and growth

Salt tolerance on solid medium

In order to determine the substrate spectrum of P16NhaA1, a *P16nhaA1* deletion strain was created using targeted gene replacement. The *P16nhaA1* deficient mutant was genetically complemented by re-introducing the native gene on the integrative vector pSEThph, yielding strain hphnhaA1. Furthermore it was tested if also the *E. coli* NhaA transporter could re-establish WT levels by complementing Δ*nhaA1* with the *E. coli nhaA* gene using pSEThph. Additionally, *P16nhaA1* was introduced in *S. lividans* TK24 on the vector pUWL201.

Trench plate tests using NaCl and LiCl gave a first impression on the reduction of tolerance (Figure 92). Growth of Δ*nhaA1* was markedly impaired by LiCl and to a lesser extend also by NaCl. WT level was almost re-established in the complemented hphnhaA1 strain on GYM (Figure 92 A + B). On the AM trench plate (Figure 92 C), additionally the transposon mutant 489_3 and its complementation transformant (489_3 pSEThphnhaA1) were tested. Both showed growth similar to the directed knock-out strain and the respective complemented strain, which confirmed the insertion of the *Himar1* transposon in *P16nhaA1*. Thus, also random transposon mutagenesis could be useful for identifying determinant of specific phenotypic traits.

On AM medium, the overexpression of *P16nhaA1* in *S. lividans* increased the strain's LiCl tolerance.

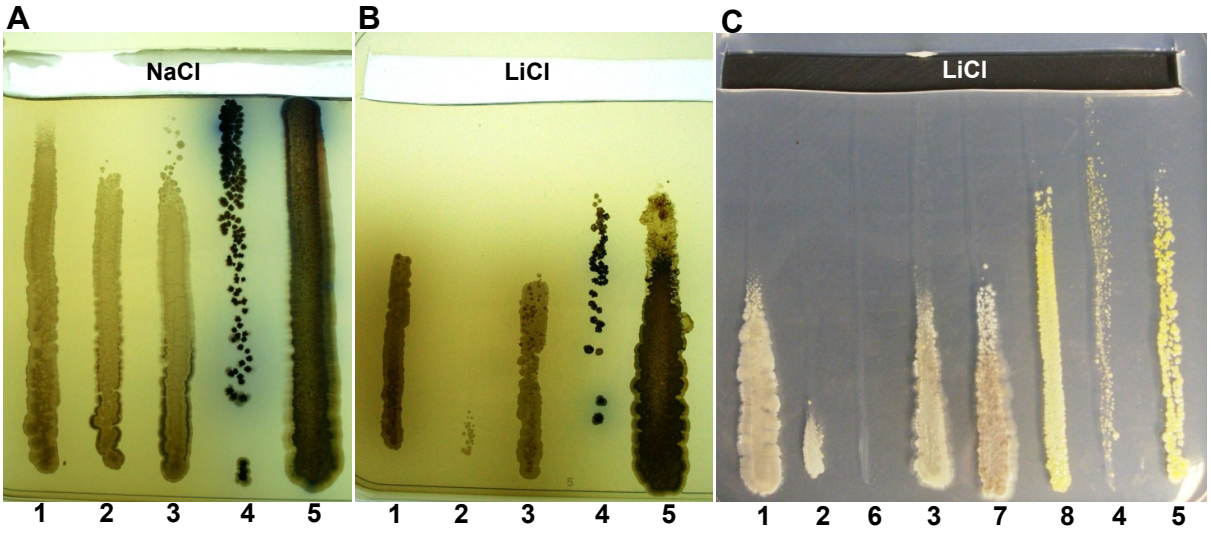

Figure 92. Trench plate test on GYM (A+B) and AM (C), inoculated with: 1 - *S. mirabilis* WT, 2 - Δ*nhaA*1, 3 - Δ*nhaA*1 pSEThphnhaA1, 4 - TK24 pUWLP16nhaA1, 5 – *S. lividans* TK24 WT, 6 - *S. mirabilis* P16 489_3, 7 - *S. mirabilis* P16 489_3 pSEThphnhaA1, 8 - *S. lividans* TK24 pSEThphnhaA1.

The reduced biomass production and enhanced pigment production in TK24 pUWLP16nhaA1 could be attributed to the vector used, as strains carrying pUWL201 and derivatives thereof showed growth reduction in all experiments in this project.

When KCl was used, all strains grew up to the trench (data not shown). It was not possible to establish a concentration gradient high enough to reveal putative growth defects, possibly due to the lower toxicity of potassium, as compared to other salts.

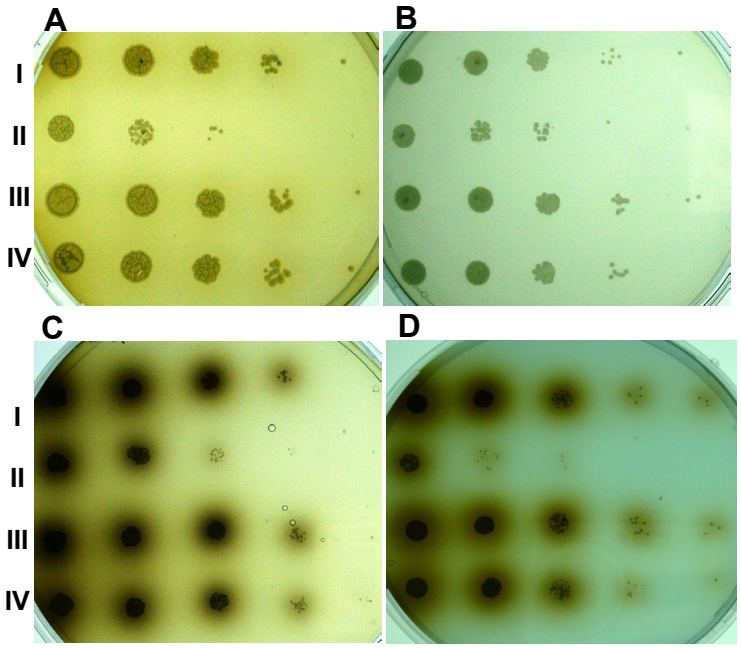

Figure 93. Drop plate tests for sensitivity of *S. mirabilis*, Δ*nhaA1* and the complementation strains hphnhaA1 and hphEcnhaA to different salts: A) GYM + 5 mM LiCl, B) AM + 100 mM NaCl C) TSB + 20 mM $NiSO_4$ and D) TSB + 10 mM $CuSO_4$.

For better visualizing differences between the knock-out, complemented and WT strains, drop plate tests were performed (Figure 93). In accordance with the results of the trench plate test, Δ*nhaA1* growth was impaired on LiCl and NaCl containing medium, while complementation re-established WT level. Furthermore, the sensitivity of the deletion strain to Ni^+ and Cu^{2+} was increased (Figure 93).

The differently strong increase of Na^+ and Li^+ sensitivity caused by *P16nhaA* deletion indicated a selectivity of this transporter, where Li^+ is preferred over Na^+, similar to EcNhaA, in which the selectivity of $Li^+ > Na^+ >> K^+$ is determined by the binding capacity of the substrate binding site (Arkin et al., 2007; Padan et al., 1989).

P16NhaA1 was required for the survival at high NaCl and LiCl concentrations, but dispensable at low concentrations of these salts. A similar importance of NhaA transporters has been shown for many other species, like *E. coli* and *Vibrio parahaemolyticus* (Kuroda et al., 2005; Padan et al., 2005). At low salt conditions, other systemy might be sufficient for homeostasis or able to substitute the loss of P16NhaA1. In *S. coelicolor* eight putative Na^+/H^+ antiporter genes (*sha*) (Kim et al., 2011) have been identified, which are induced under different conditions (Park et al., 2009) and the same might apply to *S. mirabilis*.

Connection between pH and salt sensitivity

It is well known that due to their pH-dependent activity, Na^+/H^+ antiporters respond differently to pH levels (Inaba et al., 1994; Liu et al., 2005; Padan et al., 1989; Padan et al., 2004).

Studies with purified EcNhaA in proteoliposomes showed, that the antiporter is directly responsible for pH response, typifying a regulation on protein level, because the pH shift causes a conformational change (Alhadeff & Warshel, 2015; Taglicht et al., 1991). A similar connection between transport activity and pH was assumed for P16NhaA1, wherefore the sensitivity of the strains to salts at different pH values was assessed.

On solid agar medium, the influence of pH on Na^+ and Li^+ sensitivity could not be tested. Hence, additional tests in liquid GYM were performed, in which the pH was adjusted with KCl and the medium was sterile filtered in order to prevent pH changes caused by autoclaving.

Without the addition of salts, Δ*nhaA1* could grow at the same pH range as the WT (pH 4 to 10.5 in GYM), although growth was reduced at alkaline pH. Thus, under low-salt conditions other systems were sufficient for maintaining the electrochemical gradient across the membrane. Also for *E. coli*, *nhaA* deficient mutants were viable at high pH levels, mostly due to the activity of NhaB, a low-capacity transporter whose activity decreases with increasing pH (Padan et al., 1989; Pinner et al., 1993), MdfA, a transporter with multi-drug/H^+ and $K^+(Na^+)/H^+$ antiport capacity (Lewinson et al., 2004) and the Ca^+/H^+ antiporter ChaA (Ivey et al., 1993). As biomass production of Δ*nhaA1* was reduced at high pH, it was expected that the activity of P16NhaA1 would be similar to that of EcNhaA. Like in other bacteria, P16NhaA1 was assumed to promote growth under alkaline conditions by ensuring acidification of the cytoplasm relative to the cell's environment (Padan et al., 2005). However, the transporter was dispensable, as other systems apparently participated in pH homeostasis.

In general it was observed for all strains that their sensitivity to salts increased at more alkaline conditions (Table 29). That metal toxicity strongly depends on the pH is a phenomenon very well known from other studies which could result from an additional alkali stress and disturbance of pH homeostasis, impeding a stable cytosolic pH, which is the prerequisite for functioning of many proteins (Krulwich et al., 2011).

In liquid culture Δ*nhaA* tolerated slightly less NaCl, while the sensitivity to Li^+ was markedly increased (Table 29). At acidic and neutral pH the differences between WT and deletion strain was highest for LiC with Δ*nhaA1* not being able to tolerate at tenth of the amount of metal. The difference between the strains was not as high at pH 10, where the reduction of tolerance was comparable between NaCl and LiCl.

As tolerance of KCl did not change strongly in Δ*nhaA1* (only at pH 5), the inhibitory effect of NaCl and LiCl had to be the result of metal toxicity, probably due to Na^+ and Li^+ accumulation, and not of an increased sensitivity of the deletion strain to osmotic stress. Similarly, KCl had no negative effect on the growth of Na^+/H^+ antiporter deficient *E. coli* or *V. parahaemolyticus* (Kuroda et al., 2005; Padan et al., 1989).

From the increased sensitivity of Δ*nhaA1* to Li^+ and Na^+ it was concluded, that both metals would be transported by P16NhaA1. However, which metal was the preferred substrate could hardly be inferred from these tests, due to different cytotoxicity levels of the metals. Random mutagenesis approaches of *E. coli nhaA* showed that in most mutants with overall reduced antiporter activity, the sensitivity to Li^+

Table 29. Growth of *S. mirabilis* (WT), *nhaA1* deletion strain and complemented transformants in GYM medium supplemented with different salts at three pH levels. Given are the maximal concentrations [mM] where growth was observed after two weeks of incubation.

Salt	**NaCl**			**KCl**			**LiCl**			**$NiCl_2$**		
pH	**5**	**7**	**10**	**5**	**7**	**10**	**5**	**7**	**10**	**5**	**7**	**10**
WT	725	750	9	750	850	75	>100	80	10	6	8	10
Δ*nhaA*1	700	625	1	650	850	75	10	6	2	6	8	10
hphnhaA1	750	750	9	600	575	75	>100	80	10	6	8	10
hphEcnhaA	725	675	3	600	575	75	60	50	5	6	8	10

increased more strongly that that to Na^+ (Noumi et al., 1997), which was attributed to the higher cytotoxicity of Li^+. Even the partial loss of EcNhaA activity impacted metal homeostasis causing an imbalance, where Li^+ affected the cells stronger. Regarding the strong increase in LiCl sensitivity in Δ*nhaA1* particularly at pH 5 and 7, it could be hypothesized that P16NhaA1 would be more active at low pH transporting preferably Li^+. With increasing pH the specificity of transport might change and Li^+ and Na^+ could be equally transported, resulting in a similar sensitivity to both metals at pH 10 in the deletion strain. Likewise, in EcNhaA substrate affinity is pH-dependent, as Li^+ transport can be observed starting from pH 7.5, while sodium is transported at pH 8 and above (Inoue et al., 2001).

The test in liquid culture also revealed differences between the complemented strains. While complementation with the native gene re-established WT levels of Li^+ and Na^+ tolerance, complementation with *E. coli nhaA* could not fully complement *P16nhaA1* loss (Table 29). At alkaline pH and for LiCl the differences were most apparent (Table 29). EcNhaA either exhibited a different pH profile or transport capacity than P16NhaA1 or the coding gene was inefficiently transcribed, as it was under control of its native promoter. EcNhaA translation is initiated from a GUG codon, which is unusual for *E. coli* (Taglicht et al., 1991), but more frequently found in *Streptomyces* sp. Still, the GC content of *EcnhaA* (51 %) was below that of *P16nhaA1* (68 %) and the average genomic GC content of streptomycetes.

Regarding metal transport, EcNhaA is inactive at pH 6.5 and exhibits the highest activity at high pH (≥ 8.5) (Inaba et al., 1994; Padan et al., 1989; Taglicht et al., 1991; Thelen et al., 1991), which would account for the inability of hphEcnhaA to grow at high salt concentrations at pH 5 and 7 tolerated by *S. mirabilis* WT. Possibly, the activity profile of P16NhaA1 would more correspond to that of HpNhaA, which exhibits its main activity at acidic to neutral pH (Inoue et al., 1999), although sequence similarity to EcNhaA is high, as it was the case for P16NhaA1.

However, the actual activity of P16NhaA1 could hardly be assessed in these experiments, as other transporters of *S. mirabilis* might compensate the loss of this antiporter. Transporters similar to NhaB of *E. coli* (Pinner et al., 1993), which has a high affinity but low capacity, could confer a basic resistance to Na^+ and Li^+ and might ensure a stable intracellular pH. Additionally, transporters for symport of metals and other substrates participate in homeostasis, as observed for *E. coli* and *Bacillus alcalophilus* (Deguchi et al., 1990; Guffanti et al., 1981).

A putative candidate for compensating P16NhaA1 loss was the above mentioned P16NhaA2. A cooperative action of both transporters could be assumed. In *Synechococcus elongates*, two out of seven putative antiporters were found responsible for pH and salt tolerance, while the other transporters played minor roles, probably supporting the main transporters (Billini et al., 2008). In *S. mirabilis*, P16NhaA1 could be assigned a major role in Na^+ and Li^+ homeostasis. Whether P16NhaA2 equally participated in metal homeostasis, but possibly at a different pH range, remained to be determined.

Morphological changes resulting from P16nhaA1 deletion

Salt stress is a consequence of multiple factors. Not only the toxic effects of the metals themselves, but also the desiccation caused by osmolarity and ionic strength pose a threat to the cells. Therefore, it is believed that Na^+/H^+ antiporters participate in cell volume regulation and maintaining cell integrity (Demaurex & Grinstein, 1994; Grinstein et al., 1992).

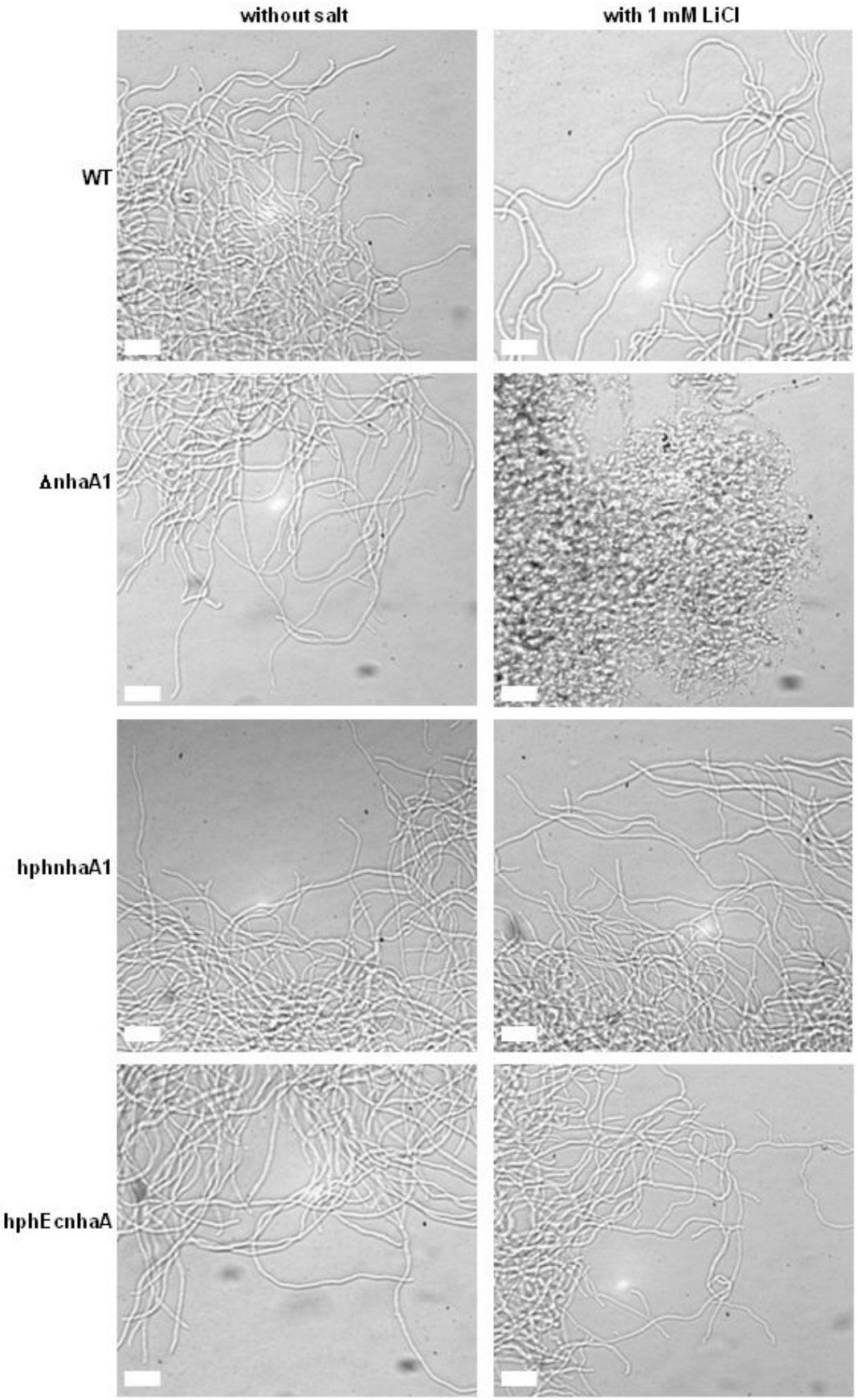

Figure 94. Light microscopy of *S. mirabilis* WT, Δ*nhaA1*, and the complemented strains hphnhA1 and hphEcnhaA grown in GYM liquid medium at pH 7.5 without (left) and with 1 mM LiCl amendment. White bar represents 5 µm.

In *S. mirabilis*, deletion of *nhaA1* drastically changed the cell morphology (Figure 94), even when the salt concentration was below the tolerated limit. Without salt addition, the WT and deletion strain hyphae showed no differences at any tested pH. However, the addition of LiCl resulted in crimped, short hyphae in Δ*nhaA1*. This growth defect was cured in the complemented strains, which had the same appearance as the WT.

The absence of apparent morphological changes in Δ*nhaA1* under no-salt conditions over the entire pH range proved, that P16NhaA1 was dispensable for maintaining the cell shape with regard to pH changes. However, the addition of salt necessitated the action of the antiporter for properly regulating the cell volume preventing desiccation.

Overexpression of both P16NhaA transporters in *E coli*

As discussed above, other transporters and systems of *S. mirabilis* might have substituted the loss of *P16nhaA1*, e.g. *P16NhaA2*. In order to obtain a better understanding of the transport activity of P16NhaA1 with regard to substrates and pH profile, the coding gene was cloned in the *E. coli* overexpression vector pTrc99A. For comparison, also *P16nhaA2* was used for cloning. As expression host served the *nhaA* deficient *E. coli* KNabc, which lacked *nhaA*, *nhaB* and *chaA* (Nozaki et al., 1996), a kind gift of E. Padan. Due to the deletion of the specific Na^+/Li^+ antiporters NhaAB and the unspecific transporter ChaA *E. coli* KNabc would grow on non-selective medium with low sodium content, but not at elevated Na^+ or Li^+ concentrations (Padan et al., 2004). Therefore, this strain has been used in numerous studies for testing the impact of Na^+/H^+ antiporter expression of different species on the growth profile of an antiporter deficient strain (Kurz et al., 2006; Liu et al., 2005; Tsuboi et al., 2003).

The complemented strains and an empty vector control were grown at three pH levels (6.5, 7.5 and 8.5) with NaCl or LiCl in complex medium (LBK) or minimal medium (M63) for assessing the influence of several factors on the capability of the transporters to support growth.

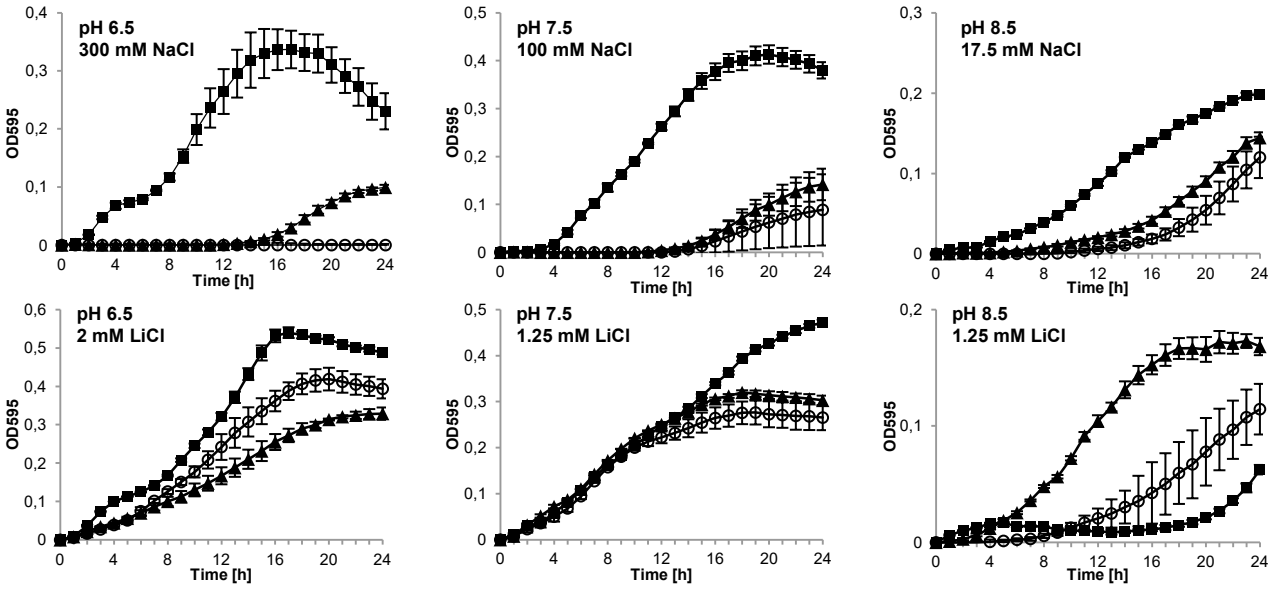

Figure 95. Growth of *E. coli* KNabc in LBK medium amended with NaCl or LiCl. Strains carried pTrc99A either with *P16nhaA1* (squares) or *P16nhaA2* (triangles) inserted, or the empty vector (open circles). Bars represent standard deviation of three replicates.

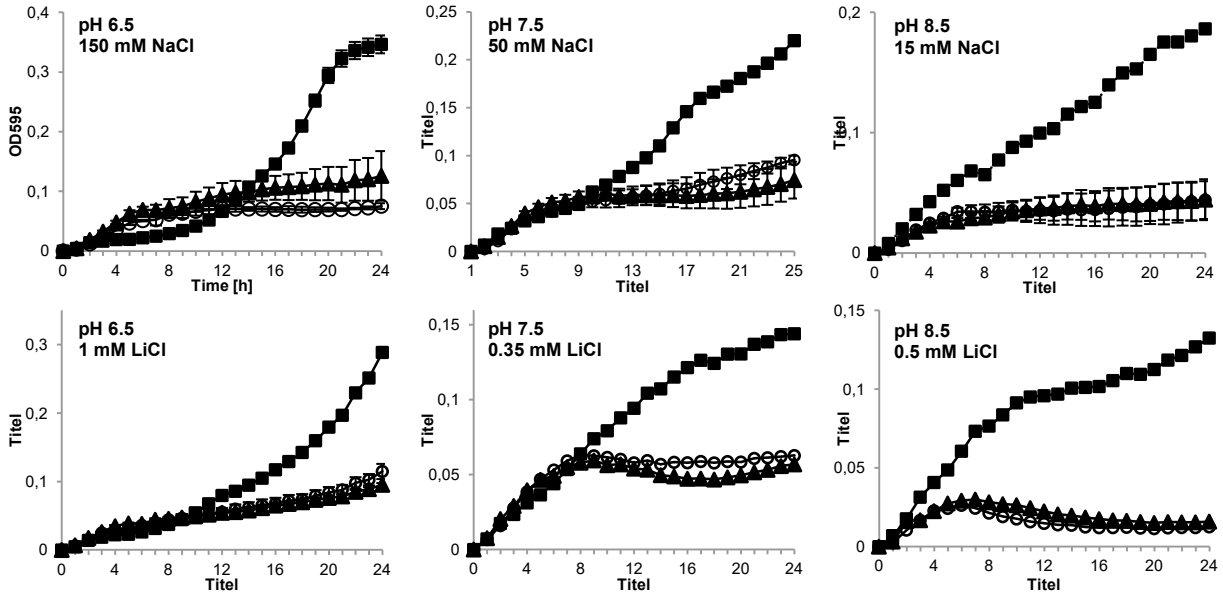

Figure 96. Growth of *E. coli* KNabc in M63 medium amended with NaCl or LiCl. Strains carried pTrc99A either with *P16nhaA1* (squares) or *P16nhaA2* (triangles) inserted, or the empty vector (open circles). Bars represent standard deviation of three replicates.

In LBK medium both *S. mirabilis* Na^+/H^+ antiporters increased the growth of *E. coli* KNabc when NaCl was added (Figure 95). Especially at slightly acidic and neutral pH P16NhaA1 enabled growth, while the difference was not as strong at pH 8.5. Likewise, *E. coli* benefitted from P16NhaA1 expression at lower pH when LiCl was increased. However, interestingly at pH 8.5 expression of P16NhaA1 increased growth only in the first five hours of incubation and then the strain showed less growth than the empty vector control, while P16NhaA2 expression markedly increased the growth of *E. coli*. Thus, it was concluded that P16NhaA1 and P16NhaA2 exhibited different pH-dependent activities and specificities. P16NhaA1 seemed to be mainly active at acidic and neutral pH, transporting Na^+ and Li^+, while P16NhaA2 expression promoted growth mostly at alkaline pH when LiCl was added. Therefore, it was assumed that both transporters could only partly substitute each other under these conditions.

However, carbon sources and the medium composition in general can have major influences on the growth of bacteria. Therefore, the tests were repeated in minimal medium (M63) (Figure 96). The results obtained from these experiments differed greatly from the growth observed in LB medium. In M63, P16NhaA1 improved *E. coli* growth mostly at alkaline pH with both metal salts. The strain complemented with *P16nhaA2*, on the other hand, showed a growth similar to the empty vector control. It could be hypothesized, that either one or both *S. mirabilis* antiporters might transport other substrates as well, wherefore their activity would also depend on other medium components. A lack of the second substrate in minimal medium would explain the apparent loss of activity of P16NhaA2. These results emphasised the importance of testing conditions for comparability of results. However, it could be concluded that P16NhaA1 would indeed transport Li^+ and Na^+ and was active over the entire tested pH range, which was different from *E. coli* NhaA, which is inactive at acidic pH (Taglicht et al., 1991; Thelen et al., 1991). P16NhaA2 might partially substitute P16NhaA1, but most likely other systems would participate as well, as transport activity of both transporters varied.

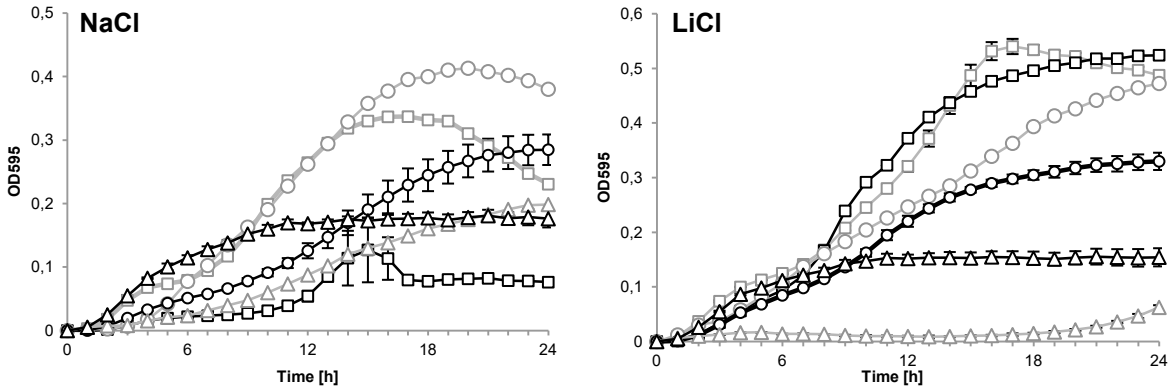

Figure 97. Comparison of growth of *E. coli* KNabc carrying pTrc99A with either WT *P16nhaA1* (gray) or mutated *P16nhaA1** (black) inserted. Growth was monitored in LBK medium at different pH values (squares: pH 6.5, circles: pH 7.5, triangles: pH 8.5). The medium was amended with the same concentrations of NaCl or LiCl, as given in Figure 95. Bars represent standard deviation of three replicates.

Random mutagenesis of P16nhaA1

For studying antiporter properties more in detail, single base pair substitutions can be introduced that potentially change the transporter's activity. Using this method, past studies could identify multiple residues that impact NhaA transport capacity or substrate specificity.

In the present study, error-prone PCR was applied for introducing random base mutations in *P16nhaA1*. The aim was the identification of residues responsible for the low activity of the transporter at alkaline pH in complex medium amended with LiCl, as it was observed in the growth tests described above. The generated, potentially mutated PCR products were cloned in pTrc99A and directly used for transformation of *E. coli* KNabc. Subsequently the transformants were selected on LBK medium (pH 8.2) containing 1 mM LiCl. Under these conditions growth of strains expressing a mutated P16NhaA1 with improved Li^+ transport activity at alkaline pH would be promoted. By this method, one transformant was isolated that showed fast growth at the selective medium. Sequencing of the vector insert showed, that the error-prone PCR introduced four single base substitutions (C103T, C144T, A264C, A667C) which resulted in amino acid changes (A6V, R20W, S60R, H194P).

Growth of *E. coli* Knabc with the native and the mutated *P16nhaA1* gene (*P16nhaA1**) was compared in LBK medium as before (Figure 97). The mutation apparently changed the pH profile of the transporter shifting it to a more alkaline range, as the strain carrying *P16nhaA1** showed enhanced growth at pH 8.5 with both, Na^+ and Li^+. However, growth was reduced at acidic and neutral pH, except for pH 6.5 with LiCl, where the native and the mutated transporter supported comparable growth. Therefore, the mutations caused a convergence of P16NhaA1 activity to that of EcNhaA at alkaline pH, although P16NhaA1* was still active over the complete tested pH range.

All mutations were located outside of predicted TMDs of P16NhaA1. It was assumed that the H194P substitution was mostly responsible for the observed change in transport activity. This residue was predicted to be part of a short spacer region between TMD V and VI. Amino acid exchanges in HpNhaA in this region (Y183C, T184C) were shown to influence the pH regulatory system and the binding capacity of the two Asp residues D171 and D172 (Kuwabara et al., 2006). A Y183C substitution in HpNhaA shifted the activity of the transporter to a more alkaline range, which was in accordance with the change observed for P16NhaA1*.

However, it was surprising that none of mutations was located within TMDs, as these parts of the proteins has been recognized for mainly determining the pH profile, substrate specificity and transport capacity. The amino acid substitutions in the N-terminal part of P16NhaA1 might have been of little

consequence, although yet unknown interactions between this part of the protein and the TMDs could be assumed.

Conclusion

In the presented study it was shown that P16NhaA1 was a major NhaA-type transporter for Li^+ and Na^+ in *S. mirabilis* P16B-1, whose activity was dependent on pH and apparently reached a maximum at neutral pH. Thus, the pH profile differed from that of the paradigm NhaA protein of *E. coli* and possibly reflected the predominant habitat condition in acid mine drainage influenced soil. However, the loss of *P16nhaA1* could be compensated under low-salt conditions by other transporters, like the second NhaA-type transporter encoded in the *S. mirabilis* genome, P16NhaA2, or unspecific transporters, as observed in other studies (Cheng et al., 1994; Pinner et al., 1993). The importance of the P16NhaA1 for maintaining the hyphal shape already at slightly raised salt concentrations was shown.

The expression of P16NhaA1 and P16NhaA2 in the *nhaAB* deficient strain *E. coli* KNabc could be regarded as first step for determining the pH profile. However, the delivery of the coding genes on an overexpression vector might obscure the actual activity in the native host, as was the case in a study by Thelen et al. (1991) with *E. coli* NhaA, substantiating that these experiments have limited validity. Thus, for examining the pH-dependency more in detail, the transporters should be studied in right-side-out or everted membrane vesicle systems (Guffanti et al., 1981; Mager et al., 2011).

Furthermore, the regulation of P16nhaA1 transcription would be interesting for investigating the reaction of *S. mirabilis* to pH and salt stress, which could also influence heavy metal resistance systems, as metal toxicity is closely connected to environmental and intracellular pH. Secondary metabolism has been shown to be induced or enhanced by pH shifts (Kim et al., 2008b). Hence, the regulation of *P16nhaA* genes by a regulator, like NhaR that positively regulates *nhaA* transcription in *E. coli* (Dover et al 96), was very likely.

3.9 The phosphinothricin N-acetyltransferase P16Pat1

Introduction

Streptomycetes are well known for their vast secondary metabolism. They are one of the most important sources for antibiotic compounds which are not only used for medical purposes, but also in agriculture as herbicides. Basta™ (Bayer Crop Science) and Herbiace™ (Meiji Seika Kaisha) are two herbicides whose essential element is the antibiotic phosphinothricyl-alanyl-alanine (PTT), known as bialaphos, that is naturally produced by two *Streptomyces* species, *S. hygroscopicus* and *S. viridochromogenes* (Bayer et al., 1972; Kondo et al., 1973). The compound is enzymatically activated by the removal of both alanine residues by intracellular peptidases, releasing phosphinothricin (PPT). This glutamate analogue can bind irreversibly to the substrate pocket of glutamine synthase, whereby the enzyme is blocked (Bayer et al., 1972; Gill & Eisenberg, 2001). The result is a rapid depletion in glutamine and accumulation of ammonia and glutamate in the cell leading to cell death (Evstigneeva et al., 2003). PPT thereby interferes with the nitrogen metabolism of bacterial and eukaryotic cells (Bayer et al., 1972; Wu et al., 2014). Due to this activity, phosphinothricin is of economic importance as herbicide (Evstigneeva et al., 2003).

When bacteria produce antibiotics, they have to protect themselves from the harmful effects of autotoxicity. Therefore, genes conferring antibiotic resistance are often found in clusters with the respective antibiotic synthesis genes, as observed in microcin C producing *E. coli* strains (Kazakov et al., 2014). In the case of PTT, a single enzyme from the biosynthetic pathway of this compound also confers resistance: a PPT N-acetyltransferase catalyzes the N-acetylation of the free NH_2 group of PPT, thereby impeding binding to glutamine synthase (Murakami et al., 1986). The corresponding genes are called *pat* and *bar* in *S. viridochromogenes* and *S. hydroscopicus*, respectively (Murakami et al., 1986; Strauch et al., 1988). Expression of these genes in other bacteria and plants, like *Arabidopsis*, confers high level resistance to bialaphos (Strauch et al., 1988; Wohlleben et al., 1988; Yun et al., 2009).

PPT N-acetyltransferases belong to the Gcn5-related N-acetyltransferases (GNAT) superfamily whose members are present in all domains of life (VanDrisse et al., 2016). They protect cells from various stressors by transferring acetyl-CoA to proteins and small molecules (Davies et al., 2007; Davies et

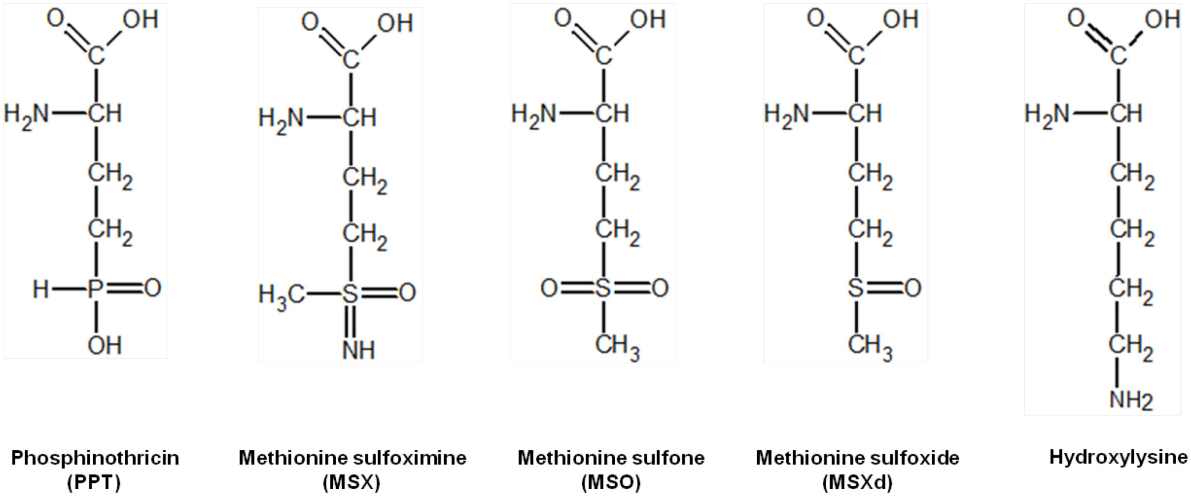

Figure 98. Chemical structures of methionine analogues.

al., 2009; Hentchel & Escalante-Semerena, 2015; VanDrisse et al., 2016). Homologues of Pat and Bar can be found in bialaphos non-producers, e.g. *S. coelicolor* (Bedford et al., 1991), and they are also widespread among other bacterial genera (Davies et al., 2007; Davies et al., 2009; VanDrisse et al., 2016; Wu et al., 2014; Yun et al., 2009). However, these homologous proteins can exhibit different substrate specificities. Besides PPT, some N-acetyltransferases are found to act additionally or exclusively on other glutamate analogues (Figure 98), like oxidized forms of methionine that also inhibit glutamine synthesis (Davies et al., 2007; Hentchel & Escalante-Semerena, 2015; Ronzio et al., 1969; Wu et al., 2014). Since oxidation of methionine is a result of oxidative stress which aerobically growing cells have to face constantly, acetyltransferases are one integral part of cellular stress response.

Results

Computational analysis

Identification of putative PPT N-acetyltransferase-coding genes

In the course of the transposon mutagenesis approach, an ORF coding a putative phosphinothricin N-acetyltransferase (SMI4407) was identified in the *S. mirabilis* genome. The genome annotation predicted a second ORF coding a similar protein (SMI5667). Therefore, both putative PPT acetyltransferases were chosen for further analysis to address the question, why an organism should retain two seemingly homologous proteins. Based on their annotation, SMI4407 and SMI5667 were designated *P16pat1* and *P16pat2*.

S. mirabilis is not a producer of bialaphos, which is why both genes were not part of the PTT biosynthesis gene cluster, as it is the case in *S. viridochromogenes* (AY632421, Blodgett et al. (2005)). The genomic location of *P16pat1* was found to be similar to that of *S. coelicolor* and *S. griseus pat* genes (Bedford et al., 1991; Marcos et al., 1995) with an upstream located ORF encoding an Hrd sigma factor in opposed orientation.

P16pat1 encoded a 180 aa protein of 20.1 kDa (Table 30) that showed 29 % identity with *S. viridochromogenes* Pat (Q57146.1) and 28 % identity with *S. hygroscopicus* Bar (P16426) on protein level. The highest homology (77 %), however, was observed with *S. coelicolor* Pat (P21861.2), a protein that was shown to confer bialaphos resistance (Bedford et al., 1991). Likewise, the amino acid identity to a putative N-acetyltransferase coded by the *nat* gene in *S. griseus* (Q54225.1) was high (65 %). This also displayed in the phylogenetic tree (Figure 99). Concerning similarities to proteins of other bacterial phyla, P16Pat1 exhibited an identity of 31 % to *Pseudomonas aeruginosa* MddA (Q9HUU7.1), 28 % to *E. coli* MnaT (P76112.1) and 31 % to *Bacillus subtilis* YwnH (P71043.1). MddA and YncA are reported to acetylate L-methionine and its derivatives, but not PPT (Davies et al., 2007; Sevin et al., 2017).

Accordingly, P16Pat1 was classified a COG1247 protein belonging to the acetyltransferase superfamily 4 (Pfam13402) (Table 30).

Table 30. Characteristics of putative PPT N-acetyltransferase coding genes of *S. mirabilis* P16B-1 and their products

	P16Pat1	**P16Pat2**
Annotation	SMI4407	SMI5667
Gene size	540 bp	489 bp
GC content	67,2 %	71, 0 %
Protein size	180 aa	163 aa
Mass	20.1 kDa	18.1 kDa
Pfam	13420	00583
COG	1247 *E. coli* YncA	0456 *E. coli* RimI

In contrast, the *P16pat2* gene product possessed conserved domains of the acetyltransferase superfamily 10 (Pfam00583) and could be grouped with COG0456, that comprises ribosomal-protein-alanine N-acetyltransferases similar to *E. coli* RimI (Table 30). P16Pat2 had a shorter amino acid sequence and lower mass than P16Pat1 and did not show a significant similarity to either PPT N-acetyltransferases of *S. hygroscopicus* or *S. viridochromogenes*. Surprisingly, in the UniProt database (The-UniProt-Consortium, 2017) only one related protein sequence could be found in members of the Actinobacteria phylum: a mycothiol acetyltransferase of *Beutenbergia cavernae* (C5C246.1) displayed 39 % similarity, but with a low query coverage (48 %). A higher homology was observed with the *E. coli* L-methionine N-acetyltransferase AaaT/YhhY (P46854.1) (34 %), a protein that catylzes the N-acetylation of L-phenylalanin, L-methionine and several nonhydrolyzable aminoacyl adenylates (Kazakov et al., 2014; Sevin et al., 2017). Like P16Pat1, P16Pat2 showed homology to the putative PPT acetyltransferase YwnH of *Bacillus subtilis* (P71043.1), but with a higher sequence similarity (35 %). YwnH acetylates PPT and the two methionine compounds L-methionine sulfone (MSO) and L-methionine sulfoximine (MSX) (VanDrisse et al., 2016).

Phylogenetic comparison

A phylogenetic comparison of P16Pat1 and P16Pat2 protein sequences with the most homologous, characterised N-acetyltransferases from other reports (Figure 99) underlined the differences of the two *S. mirabilis* acetyltransferases. P16Pat1 clustered with other PPT-acetyltating *Streptomyces* sp. proteins, while P16Pat2 belonged to a cluster of enzymes, which are not known to function on PPT or other glutamate analogues.

In several reports, PPT N-acetyltransferases were characterized regarding their activity on oxidized forms of L-methionine, mainly L-methionine sulfone (MSO) and L-methionine sulfoximine (MSX). For some enzymes, also information about acetylation of hydroxylysine and methionine sulfoxide (MSXd) is available. The inhibitory effect of these glutamate analogues is similar to that of PPT, meaning an mostly irreversible binding and inactivation of glutamine synthetase (Evstigneeva et al., 2003).

Except for *Streptomyces* sp. Pat proteins, there was no apparent correlation between phylogenetic relationship and protein sequence identity. Within the larger group of PPT N-acetyltransferases, smaller clusters could be differentiated that partly differ in substrate specificity. However, not in all cases all putative substrates were tested in the corresponding studies. Particularly for the closest relatives of P16Pat1 no information on their activity on MSO and MSX were available. Of the *Streptomyces* sp. PPT acetyltrasferases clustering with P16Pat1, merely *S. coelicolor* Bar has been investigated more in detail. This enzyme confers low level resistance to bialaphos (< 2 µg/ml). Solely, when it is expressed using an overexpression vector, higher resistance levels can be reached (500 µg/ml) (Bedford et al., 1991), indicating the importance of transcriptional control and expression efficiency for the level of antibiotic resistance.

Notably, the cluster formed by *Pseudomonas aeruginosa* MddA, *E. coli* MnaT, *Sa. enterica* MddA and *Pseudomonas putida* PhoN2 exclusively comprised enzymes that do not act on PPT, in contrast to the others (Davies et al., 2007; Hentchel & Escalante-Semerena, 2015; Paez-Espino et al., 2015; Sevin et al., 2017; VanDrisse et al., 2016).

The higher similarity of the *P. putida* enzyme PhoN1 to *Streptomyces* sp. acetyltransferases was in accordance with the author's theory that this gene has been recently acquired by horizontal gene

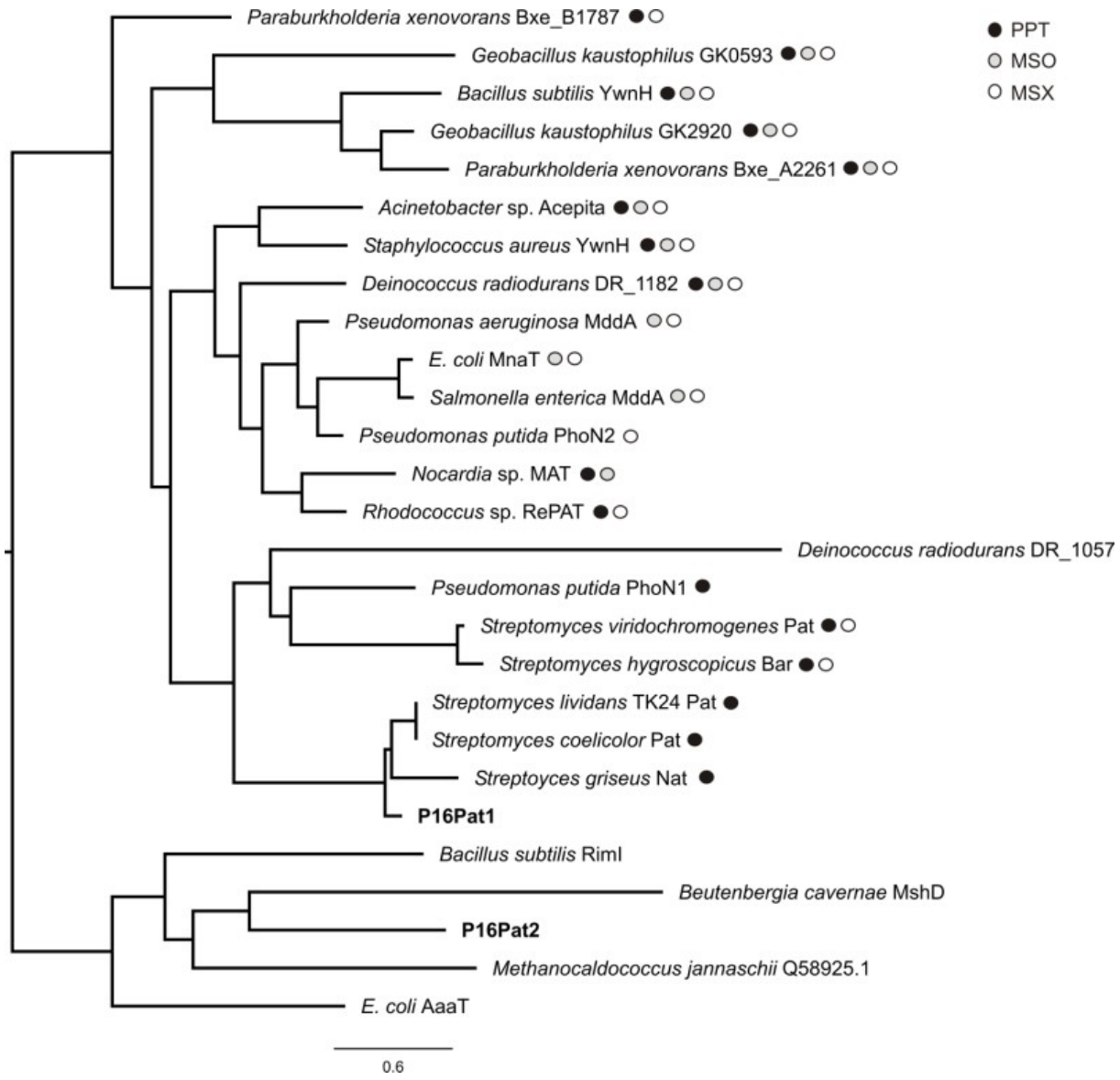

Figure 99. Phylogenetic tree of annotated acetyltransferases and the putative PPT N-acetyltransferases of *S. mirabilis*. Circles indicate known substrates of these enzymes regarding phosphinothricin (PPT) and the two oxidized methionine compounds methionine sulfone (MSO) and methionine sulfoximine (MSX).

transfer. However, in contrast to Pat and Bar, PhoN1 shows no activity on MSX (Paez-Espino et al., 2015).

The enzymes that clustered with P16Pat2 were all members of the GNAT acetyltransferase superfamily acetylating a variety of substrates. They are not as well investigated as the PPT N-acetyltransferases, but all of them serve detoxification purposes by acetylating either antibiotic compounds and nonhydrolyzable aminoacyl adenylates (*E. coli* YhhY and Rim proteins) or a precursor of mycotiol, a compound that protects cells from oxidative stress (mycothiol synthase MshD) (Kazakov et al., 2014; Koledin et al., 2002; Rawat et al., 2002).

Amino acid sequence alignment

To further examine whether the substrate spectrum could be inferred from the primary structure of the proteins, the amino acid sequences of P16Pat1 and P16Pat2 were aligned with homologous N-acetyltransferases (Figure 100).

Despite their different substrate spectra, the alignment showed coinciding residues in several positions in the acetyltransferases, which were probably essential for acetylation function and stability of the enzyme. For instance, residues E99, Y103, G112, L117, A135, N141 and S114 of P16Pat1, which are involved in binding of acetyl-CoA in *Rhodococcus* sp. RePAT (Wu et al., 2014), were almost strictly conserved in all considered acetyltransferases, with several substitutions in P16Pat2 (E99Q, Y103A, A118L, S144A).

For the MSO and MSX acetylating MddA of *P. aeruginosa* (PaMddA), residues shaping the substrate binding sites (R75, E85, H86, S87, V88, T89) (Davies et al., 2007) were all conserved in P16Pat1, but not P16Pat2. However PaMddA I30, W31 and F77, which are important for the interaction with the substrate, were substituted in all considered *Streptomyces* sp. acetyltransferases. These sites might determine the substrate spectrum, as F77 of MddA was exclusively conserved in PhoN2, which also

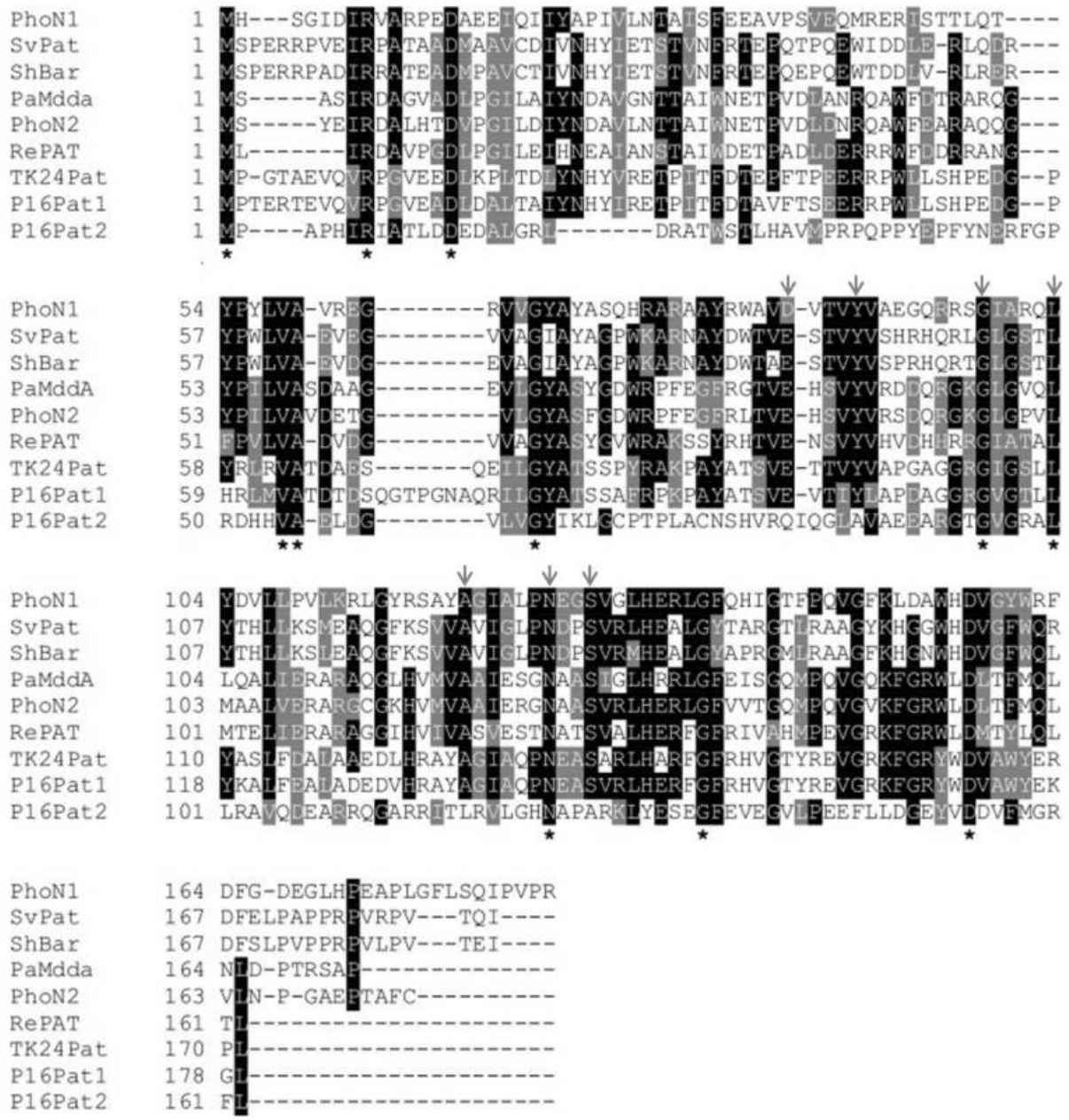

Figure 100. Alignment of known PPT N-acetyltransferases with the two putative homologous enzymes of *S. mirabilis*. Residues matching the consensus sequence generated by comparing all sequences are shaded in black, while similar amino acids are shaded grey. Asterisks indicate residues which were identical in all sequences. Arrows mark residues known to be essential for substrate specificity and acetyl-CoA binding.

does not acetylate PPT, while in the other proteins, this position was occupied by lysine or arginine residues (K91 in P16Pat1).

Single-site exchanges in PhoN1, the *P. putida* enzyme exclusively acting on PPT, were shown to broaden the substrate spectrum (Paez-Espino et al., 2015). Interestingly, two of these exchanges (D85E, S32T) correlated with residues in P16Pat1 (E99, T35). In the mutated PhoN1 a decrease of PPT acetylation activity and increased activity on MSX was observed (Paez-Espino et al., 2015). Especially E99 might be important for the interaction with methionine derivatives, as all other enzymes with characterized substrate spectrum, that act on these substrates, show a glutamic acid residue in this position.

As PPT acetyltransferases were shown to form dimers (Davies et al., 2007; Wu et al., 2014), several residues are involved in subunit interaction. In P16Pat1 these residues were potentially R89, E99, H131, Y169. They were in consensus with the corresponding residues in RePAT and SeMddA, in which these residues enable interaction of the monomers, e.g. by establishing salt bridges (Davies et al., 2007; Wu et al., 2014)

Taken together, for P16Pat1 residues that were important for acetyl-CoA binding were well conserved and also in positions that were expected to be involved in binding of PPT and other substrates a consensus showed with several indicators for a broader substrate spectrum of this enzyme than only PPT. P16Pat2, on the other hand, showed less congruence with the PPT N-acetyltransferases, especially in predicted substrate binding sites. An activity on glutamate analogues was thus unlikely.

Deletion of *P16pat1* and overexpression in *S. lividans* TK24

From the examination of the primary protein structure, no definite conclusion regarding the substrate specificity of both *S. mirabilis* acetyltransferases could be drawn. Therefore, *in vivo* tests were conducted to further investigate the role of these enzymes.

In a directed knock-out approach, *P16pat1* was replaced in the wild type by a resistance cassette containing apramycin as selectable marker. The resulting deletion strain was named Δ*pat1*. Additionally, the knock-out transformant was complemented by re-introducing the native gene on an integrating vector for substantiating the role of P16Pat1, yielding strain Δ*pat1* pSEThphpat (abbr.: hphpat). *P16pat1* was also cloned into vector pUWL201 and transformed in *S. lividans* TK24, yielding strains TK24 pUWLpat1 and the empty vector control TK24 pUWL201.

When the knock-out and complementation transformants were tested for their bialaphos and PPT resistance in CSA liquid culture, Δ*pat1* showed a clear reduction of tolerance to both substances. While the WT tolerated >14 µg/ml bialaphos and >165 mM PPT in CSA, the deletion strain only grew at concentrations upto 7 µg/ml and 27.8 mM, respectively.

The generally stronger inhibitory effect of bialaphos as compared to PPT has already been observed and might be ascribed to different uptake mechanisms. The phosphinothricin tripeptide is transported into the cell *via* oligopeptide transporters, while PPT, like MSXd, is taken up by other systems, like methionine transporters (Diddens et al., 1976).

In agar and disc diffusion assays the response of all transformants was further tested, also with regard to the influence of different media types. Therefore, three media were used: TSB as complex medium and CSA and AM as less complex and minimal media.

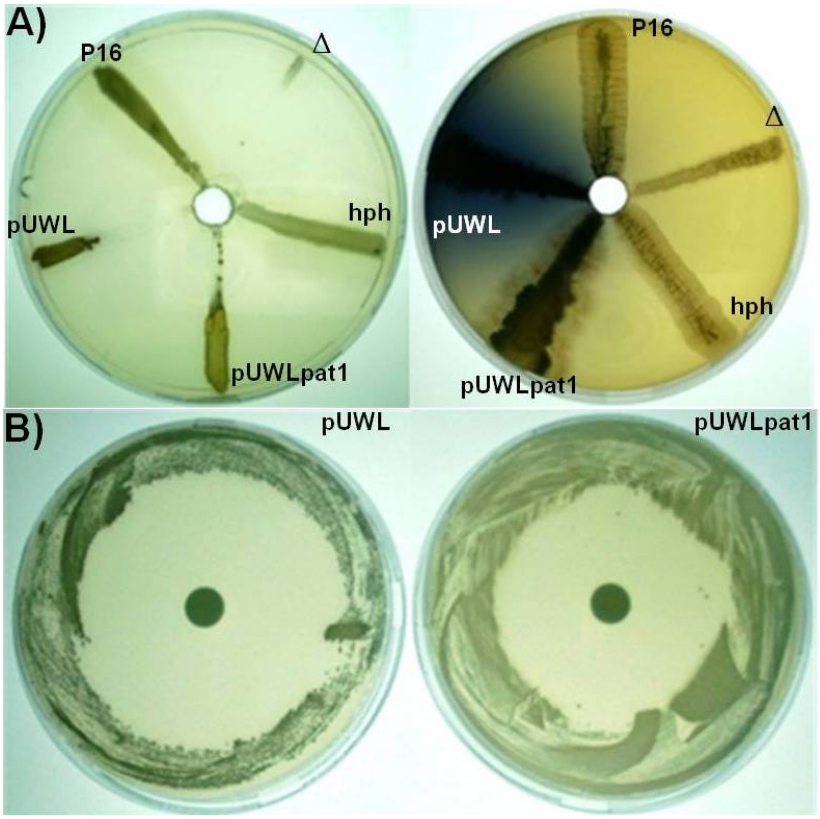

Figure 101. A) Agar diffusion assay on CSA (left) and TSB medium (right) testing bialaphos sensitivity of *S. mirabilis* WT (P16), *P16pat1* deletion strain (Δ), complemented deletion strain (hph) and *S. lividans* TK24 carrying either the empty pUWL201 (pUWL) or the vector with *P16pat1* inserted (pUWLpat1).
B) Disc diffusion assay on AM medium for comparing the bialaphos sensitivity of TK24 pUWL201 (pUWL) and TK24 pUWLP16pat1 (pUWLpat1).

In the agar diffusion assay with PPT (Figure 101 A), the influence of the medium composition became clearly visible. While on CSA medium growth of Δ*pat1* was inhibited by PPT, no such effect could be seen on TSB, which was probably due to the availability of glutamine in the complex medium that compensated for the inactivation of the glutamine synthetase. On CSA, where only traces of glutamine should be available in the medium, the deletion strain only grew half as wide to the PPT source in the centre as the WT, which was not affected by PPT.

A similar observation was made by Hentchel & Escalante-Semerena (2015), who found that on minimal medium low concentrations of MSO or MSX inhibited growth of a *Sa. enterica* strain impaired in MddA production completely, while in complex medium higher concentrations were necessary to elicit an effect.

The complemented transformant grew as well as the WT (Figure 101 A) which confirmed the importance of *P16pat1* for PPT resistance. This was also substantiated by the enhanced growth of the *S. lividans* P16Pat1-overexpressing strain, which grew better than the empty vector control.

To test whether the growth defect of the deletion strain was due to insufficient glutamine supply, the WT, Δ*pat1* and hphpat were tested for their PPT tolerance in liquid CSA medium with and without glutamine supplementation (Figure 102). Without glutamine the WT and hphpat grew simi-

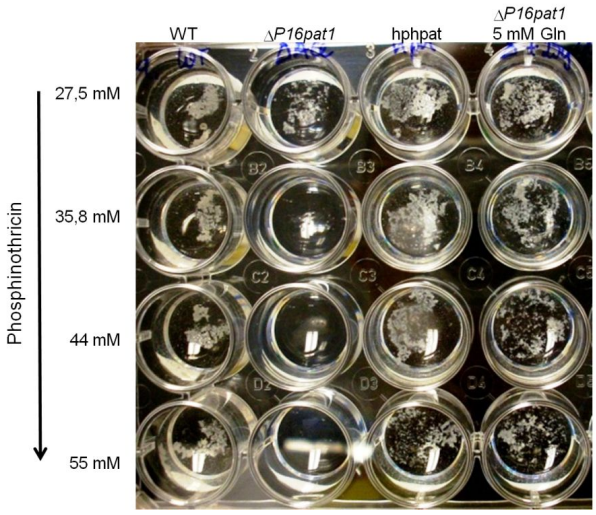

Figure 102. Growth of *S. mirabilis* wildtype (WT), *P16pat1* deletion strain and complementation mutant (hphpat) in liquid CSA medium with increasing PPT concentrations. In the last column, glutamine was added to the medium, inoculated with the knock-out strain.

larly well at all tested PPT concentrations (upto 55 mM), while the Δ*pat1* only tolerated upto 37 mM. However, when glutamine (5 mM) was added to the medium, the deletion strain grew at higher PPT concentrations, comparable to the WT. This proved that the loss of *P16pat1* could be compensated extracellularly by providing glutamine in the medium, leading to the conclusion that inhibition of glutamine synthesis was the major reason for growth reduction in Δ*pat1*.

This was in accordance with other studies that found that the inhibitory action of bialaphos, as well as other glutamate analogues, could be abolished by glutamine supplementation (Bayer et al., 1972; Hentchel & Escalante-Semerena, 2015).

In disc diffusion assays, where the test substance was directly added on a filter disc on a lawn of spores, the difference between CSA and AM medium was apparent (Figure 103). While on CSA only the deletion strain was inhibited by bialaphos, on AM also the WT and complemented transformant showed a zone without growth around the disc, although with a smaller diameter than for Δ*pat1*. In contrast to the tests in CSA liquid culture, this effect could not be compensated by addition of glutamine to the medium (data not shown). The reduced bialaphos resistance of the WT strain on AM medium, could therefore not only be attributed to the lack of glutamine in the medium, but also to other compounds that are known to inhibit the glutamine synthetase, e.g. asparagine and iron, which were two components of AM medium (Evstigneeva et al., 2003; Levine et al., 1981; Rebello & Strauss, 1969). This additional pressure on the glutamine synthase enhanced the inhibitory effect of bialaphos.

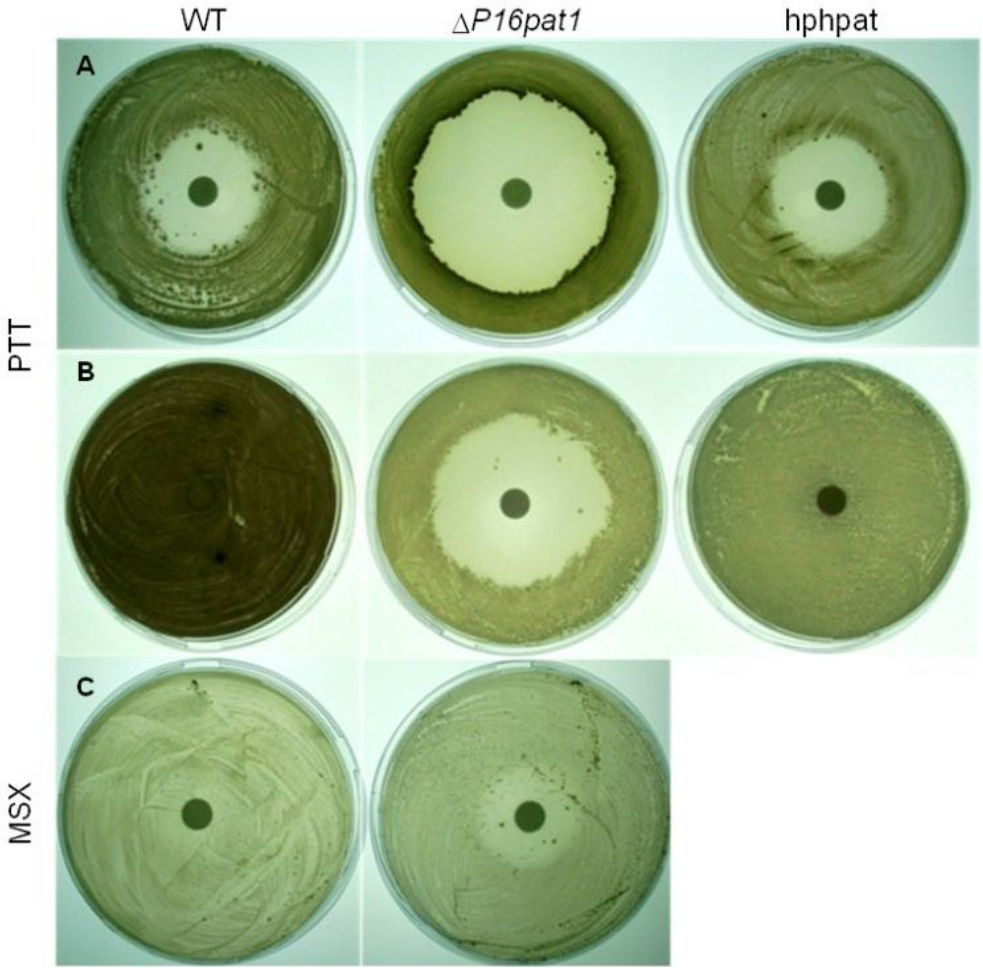

Figure 103. Disc diffusion assays on AM medium (A,C) and CSA medium (B) comparing the sensitivity of *S. mirabilis* (WT), *P16pat1* deletion strain (Δ*P16pat1*) and the complemented deletion strain (hphpat) to methionine analogues.

Like in the agar diffusion test, *S. lividans* benefitted in the disc diffusion assay from the overproduction of P16Pat1, being able to tolerate higher bialaphos concentrations. This beneficial effect in heterologous overexpression of a Pat enzyme has already been shown for *S. coelicolor* Pat, that enabled growth of a PPT-sensitive *Streptomyces* strain at >1 mg/ml bialaphos when harbouring a multicopy plasmid with *pat* (Bedford et al., 1991).

The computational analysis suggested that P16Pat1 might also act on other glutamate analogues. This was again tested in a disc diffusion assay. For hydroxylysine, MSO and MSXd no effect was observed on any medium, but a slight growth reduction of Δ*pat1* was caused by MSX (Figure 103 C), although to a lesser extent than by PPT. It might be that *S. mirabilis* possesses other enzymes for the detoxification of these compounds or the inhibitory concentrations were not reached in the experiments.

Determination of *Streptomyces* sp. Pat substrate spectrum using overexpression in *E. coli*

For excluding the interference of other *Streptomyces sp.* acetyltransferases that might have an overlapping substrate spectrum with P16Pat1, and also for testing the activity of the second putative PPT N-acetyltransferase, P16Pat2, overexpression experiments in *E. coli* DH5α were conducted.

Similar experimental setups have already been used to proof the activity of *bar* and *pat* gene products of the bialaphos producer strains *S. hygroscopicus* and *S. viridochromogenes*, as well as from other bacteria, e.g. *P. putida* (Paez-Espino et al., 2015; Strauch et al., 1988; Thompson et al., 1987).

Both *S. mirabilis* enzymes and the empty vector control were tested regarding their response to bialaphos and different glutamate analogues in M9 minimal medium. Overexpression of P16Pat1 enabled growth at elevated concentrations of bialaphos, MSO and MSX (Figure 104). The level of bialaphos resistance conferred by P16Pat1 corresponded to that of the *S. hygroscopicus* Bar protein (Thompson et al., 1987). Due to the reversibility of inhibition by MSO, the control strain and the P16Pat2 expressing strain also showed growth after 18 hours in the MSO treatment. In contrast, MSX completely abolished growth of these strains, as its binding to the glutamine synthase is irreversible (Ronzio et al., 1969).

However, no difference in was observed with hydroxylysine and MSXd addition, as these substances had no inhibitory effect on *E. coli* (Figure 104). Under the given testing conditions no inhibitory concentration of MSXd could be reached. This was due to differences in glutamine synthase inhibition level by the different methionine compounds with MSX having the strongest effect, followed by MSO, while MSXd only exhibits low-level inhibition (Ronzio et al., 1969). Furthermore, enzymatic activities are sometimes only detectable at high substrate concentrations, if the substance in question is a poor substrate. The N-acetyltransferase Acepita of *Acinetobacter* sp. was first shown to exclusively act on MSO and MSX. Later, in a follow-up study also acetylation of PPT has been detected, although at a low level (Davies et al., 2009; VanDrisse et al., 2016).

Another factor, that may have prevented the detection of enzyme activity were the testing conditions. Enzyme activity is often adapted to the conditions of the environmental habitat where the organism has been isolated. For example, the PPT N-acetyltransferase of the deep-sea bacterium *Rhodococcus* sp. exhibits higher activity at low temperatures (Wu et al., 2014). However, being soil-

dwelling organisms, *Streptomyces* sp. most likely harbor enzymes, where this effect should be negligible at the testing temperature of 37 °C.

Nevertheless, it could not be excluded that P16Pat1 also acted on other oxidized methionine compounds, like MSXd. For a thorough determination of the substrate spectrum of P16Pat1 *in vitro* tests should be conducted, in which also reactions with poor substrates could be detected, although these reactions do not necessarily have to be relevant *in vivo*.

The activity of P16Pat1 on MSO and MSX and its close relationship to PPT N-acetyltransferases of several less-well investigated *Streptomyces sp.* PPT N-acetyltransferases (Figure 99) lead to the hypothesis, that these might also have a broader substrate spectrum than recognized upto now. To test this, the *pat* gene of *S. lividans* TK24 (TK24Pat) was tested in *E. coli* overexpression experiments, analogous to the *S. mirabilis* genes.

In contrast to P16Pat1, TK24Pat only enabled growth with bialaphos (Figure 104), but not upon addi-

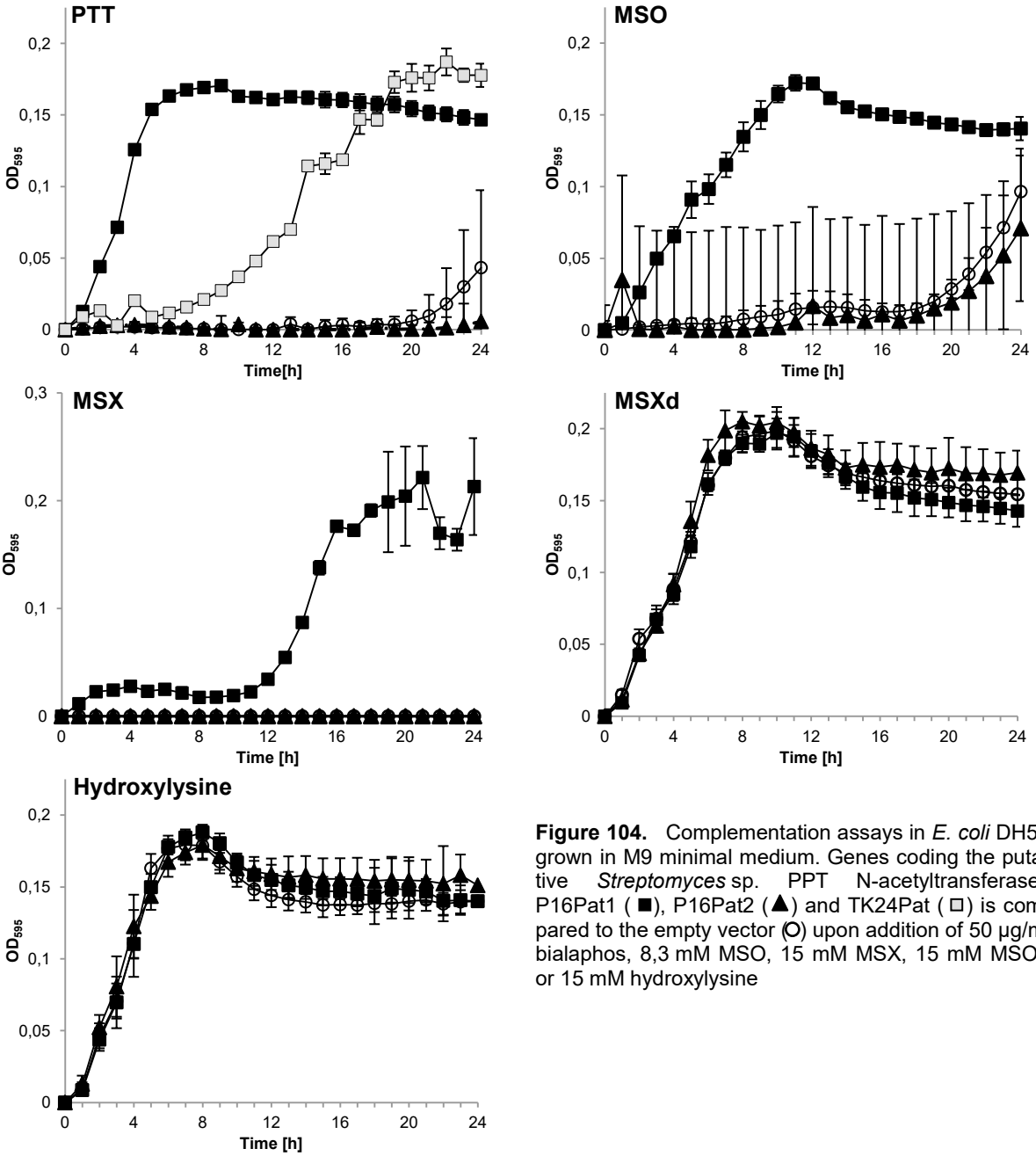

Figure 104. Complementation assays in *E. coli* DH5α grown in M9 minimal medium. Genes coding the putative *Streptomyces* sp. PPT N-acetyltransferases P16Pat1 (■), P16Pat2 (▲) and TK24Pat (□) is compared to the empty vector (○) upon addition of 50 µg/ml bialaphos, 8,3 mM MSO, 15 mM MSX, 15 mM MSOd or 15 mM hydroxylysine

tion of MSX or MSO (data not shown), despite 77 % amino acid sequence identity to P16Pat1. The activity of TK24Pat was lower, resulting in a longer lag phase in the treatment with bialaphos. MSO and MSX either did not serve as substrate for the enzyme or the activity on these compounds was too low for detection in this experimental set-up.

Differing substrate spectra of PPT N-acetyltransferases despite high sequence similarity, has already been observed for *S. hygroscopicus* Bar and *S. viridochromogenes* Pat, which share 87 % amino acid identity. Bar can use MSX and hydroxylysine as substrates, while the later cannot be acetylated by Pat (Thompson et al., 1987; Vinnemeier et al., 1995). Apparently, few exchanges of amnio acid residues are enough to alter the activity of these enzymes.

The poor activity of TK24Pat was in agreement with findings of Bedford et al. (1991) for *S. coelicolor* Bar, which could only confer a high level of PTT resistance, when the coding gene was delivered on a multicopy plasmid. Despite the high similarity of P16Pat1 and this Bar protein, the former exhibited a high activity.

Overexpression of P16Pat2 had no beneficial effect on *E. coli* growth in any treatment (Figure 104), which was in accordance with the conclusions drawn from the amino acid sequence comparison and phylogenetic classification above.

Conclusion

S. mirabilis P16B-1 was not a producer of bialaphos, but harboured a PPT N-acetyltransferase, designated P16Pat1, that was solely responsible for the detoxification of the conversion product phosphinothricin. Growth inhibition by bialaphos was mainly due to glutamine depletion, which inhibits the glutamine synthase, as growth of a *P16pat1* knock-out strain was enabled by addition of glutamine. Besides PPT, P16Pat1 also acted on the oxidized methionine compounds MSX and MSO. The activity on the later substances might be of greater ecologic importance for the strain, as amino acid modification is one result of protein damage due to oxidative stress (Cabiscol et al., 2000), which a bacterium probably faces more often than the antibiotic bialaphos. Thus, P16Pat1 might act as agent against side-effects of environmental stresses.

It could not be excluded, that *S. mirabilis* also harboured additional enzymes for the detoxification of these compounds, as the inhibition of the *P16pat1* deletion strain was low. Additionally, other substances, which were not tested in this study, might also serve as substrates. To the best of our knowledge, this is the first report on a *Streptomyces* sp. PPT N-acetyltransferase acting on methionine sulfone. So far, only the acetylation of MSX has been tested and confirmed for *S. viridochromogenes* Pat and *S. hygroscopicus* Bar (Thompson et al., 1987; Vinnemeier et al., 1995). However, other related compounds were not tested. Therefore, it is highly likely that the substrate spectrum of some *Streptomyces* sp. PPT N-acetylases is broader than realized upto now, as seen for P16Pat1.

Regarding the high sequence homology among PPT N-acetyltransferases, horizontal gene transfer was often hypothesized as the source for these genes (Paez-Espino et al., 2015; Wohlleben et al., 1988). In *P. putida* MSX acetylating PhoN2 was identified as endogenous protein, while *phoN1*, whose product acts on PPT, has probably been acquired recently by gene transfer. This might also be the case for *P16pat1*, as its GC content was comparably low and horizontal gene transfer is often observed in soil habitats (Heuer & Smalla, 2007).

The role of P16Pat2 in *S. mirabilis* remained obscure. It was characterized as a member of the GNAT acetyltransferases that might be involved directly or indirectly in stress response, by either acetylating toxic compounds or being involved in the synthesis of agents against stressors. As the sequence identity to characterized enzymes was low, a further search for putative substrates of this enzyme was not feasible in the framework of this project.

From an application-oriented point of view, several bacterial PPT N-acetyltransferases have already been introduced in plants, like tobacco and tomato, where they confer high-level resistance against PPT and PTT which can then be used as non-selective herbicides (Block et al., 1987; Cui et al., 2016; Wohlleben et al., 1988; Yun et al., 2009). The genes are stabily inherited and have no adverse evect on plant growth and performance (Cui et al., 2016). However, closer examinations of the transcriptome and metabolome of these transgenic plants revealed pleiotropic effects in gene expression and unintended activities of the enzymes (Abdeen & Miki, 2009; Christ et al., 2017). Thus, *S. hygroscopicus* Bar was found to also act on endogenous plant amino acids due to its promiscuity resulting in increased levels of acetyl-aminoadipate and acetyl-tryptophan (Christ et al., 2017). P16Pat1 showed a substrate spectrum and activity level comparable to that of ShBar, however the sequence similarity was higher to the less promiscuous TK24Pat, which has not been used for plant transformation, as far as the author knows. Some residues that were found important for substrate positioning and affinity in ShBar (Christ et al., 2017) were exchanged in P16Pat1, wherefore the latter might have a lower affinity to plant amino acids. As its activity on PPT is higher than that of TK24Pat, it might be interesting to test P16Pat1 *in planta* for creating a resistance system that is more selective than ShBar, preventing unintended acetylation of amino acids.

Lastly, this study proofed that the product of SMI5667, P16Pat2, which was annotated as putative PPT acetyltransferase did not act on phosphinothricin, wherefore the annotation should be corrected.

As P16Pat1 and P16Pat2 exhibited different substrate spectra, the maintenance of both acetyltransferase-coding genes in *S. mirabilis* was not redundant

4. Discussion

Cytoplasmatic metal ions can inactivate enzymes e.g. by displacing metal cofactors from the active site and disrupting the structure of nucleic acids and phospholipid membranes, thereby negatively affecting cell growth and viability (Ma et al., 2009c; Macomber & Hausinger, 2011; Nies, 1999). If present in excess, even essential metals would become toxic. Hence, bacteria have evolved various strategies for regulating metal homeostasis on different cellular levels, protecting themselves from these harmful effects. On the one hand, metal homeostasis relies on metal chaperones and membrane transporters that mediate metal influx and efflux. On the other hand, homeostasis is regulated on the transcriptional level by metal-specific regulatory proteins and even on the RNA level by small noncoding RNAs (Chandrangsu et al., 2017).

In the present study, merely the first two levels of homeostasis were considered and it was shown that metal resistance in *Streptomyces* sp. is a multi-gene phenomenon, in which plasmids can play a significant role. To what extend a particular component of the metal homeostasis system impacts the equilibrium depends on several factors. Regarding metal transporters, it is known that they exhibit different affinities and capacities. This applies for major essential metals like sodium with NhaA and NhaB, but also for heavy metals like Ni^{2+}, for which transporters with high and low capacity are known (Liesegang et al., 1993; Schmidt et al., 1991). In the present study, the considered Ni^{2+} transporter, P16NreB and the *Streptomyces* sp. HoxN proteins, were assumed to exhibit low transport efficiency, but a high specificity, which impeded the determination of transport activity in case of the streptomycete HoxN transporters. P16NhaA1, in contrast, was a high capacity transporter whose loss significantly increased Li^+ sensitivity, especially at alkaline conditions.

The hypothesis of Amoroso et al. (2000), that the high Ni^{2+} resistance observed in *Streptomyces* sp. isolates from the former uranium mining site, was due to active metal efflux, could be substantiated by the presented results. However, in the present study, several aspects of *Streptomyces* sp. stress response have been addressed. The prevailing acidic conditions in the contaminated soil necessitate the ability to maintain a stable proton gradient across the cell membrane which is the prerequisite for the functioning of other transport systems, like metal efflux transporters. Being a member of the MFS family, P16NreB can be assumed to exhibit a metal/H^+ antiporter function. Thus, NhaA transporters also provide the basis for resistance systems to other metals, besides being means of tolerance to high Li^+ and Na^+ concentrations themselves.

A stable intracellular proton concentration is also required for important enzyme functioning, like the cytochrome c oxidase. Being a cuproenzyme, CcO is an example for the essential role heavy metals can play in the cell and that changes in copper homeostasis would change cellular processes. In *Streptomyces* sp., copper is additionally responsible for switching between developmental stages. However, this element is especially known for its high potential of generating oxidative stress, one main reason for heavy metal toxicity. Thus, the cell depends on mechanisms for coping with this induced secondary stress, besides removing the actual metal ion from the cytoplasm. In the present study, the hydrolase E13YjjG was shown to potentially fulfil this role by detoxifying oxidized nucleotides.

Gadd (1992) pointed out that there should be a differentiation between the terms “resistance” and “tolerance” when considering means of bacterial survival in contaminated habitats. While the former refers to detoxification mechanisms directed against the present contaminant, the latter comprises intrinsic properties and cellular modifications enabling survival in the habitat. Following this view, E13YjjG could be accounted a mean of tolerance, while P16NreB directly promoted metal resistance.
The streptomycete life cycle is often considered an adaption to environmental conditions, especially for surviving adverse periods as spores (Flardh & Buttner, 2009). Thus, the protective cellulose-like layer around the hyphae possibly was a measure of tolerance against compounds like antibiotics, as seen in section 3.7. Likewise, the modulation of cell wall properties controlled by sigma factors could promote the adaption to changing environmental conditions. However, the cellulose layer, which was beneficial for adaption to the general soil environment, did prove disadvantageous regarding heavy metal exposure. Hence, it was no mean of tolerance to this stressor.
Besides abiotic factors in soil, one can assume that the investigated strains were also challenged with biotic factors in their original habitat, being members of a complex community of microorganisms, which competed for the scarce resources. Hence, they had to evolve strategies for protection against adversary activities. From the investigated genes in this study, *P16melC2* and *P16pat1* most probably served this purpose by degrading antibiotic and phenolic compounds produced by other organisms.
In this section the presented results and considerations will be put in a larger context and potential factors influencing the outcome of the experiments will be discussed with regard to different aspects.

4.1 Methodological considerations

In this study several molecular biological techniques were applied. By using random and targeted gene mutagenesis as well as protein overexpression in different heterologous species the characteristics of different proteins and their influence on the host were determined. The author believes that random transposon mutagenesis is a promising approach for discovering novel resistance mechanisms in the streptomycete strains. However, from the problems encountered in the first application of this method, several conclusions can be drawn, as to what has to be considered: firstly, transformants should be tested for the presence of the native plasmids, since plasmid loss can potentially exert a stronger impact on metal resistance than the actual transposon integration. However, plasmid-free transformants of *S. mirabilis* could be compared to the cured *S. mirabilis* strain 489_3 in order to identify chromosomal encoded resistance determinants. Secondly, when using thiostrepton responsive regulators, the described method should be modified by maybe adding the antibiotic at an earlier time point, as the likeliness of an early transposition event is high anyway. The transformants should always be checked by Southern Blot analysis right after bringing the transposon-carrying vector into the streptomycete.
With the help of this technique surely new genes and linkages could be discovered. For example, Marrero et al. (2007) applied transposon mutagenesis for the identification of heavy metal resistance genes in *Serratia marcescens* and found that mutants with reduced Ni^{2+} resistance showed insertion sites in genes not primarily connected to heavy metal resistance but global cell processes, e.g. *gidA*

and *rplC*, encoding a global regulator and ribosomal subunit. Thus, metal resistance apparently comprises numerous factors acting in concert, which could be hardly predicted bioinformatically.

Besides the candidate genes determined by random transposon mutagenesis, *in silico* approaches were used for identification of suitable target genes for gene deletions, on the basis of known resistance determinant sequences. Of course, this bioinformatic approach can give an idea on the function of proteins (Bertini & Cavallaro, 2010). However, proteins for metal resistance often belong to common families, like the major facilitator family in case of P16NreB, which makes them hard to predict *in silico*. Also, transcriptional repressors do not necessarily exhibit any known metal-sensing motif, as is the case for KmtR of *M. tuberculosis* (Campbell et al., 2007) or proteins that show a high sequence similarity can still function differently, like the NhaA transporters of *E. coli* and *H. pylori* or CopA of *L. lactis* and *Ent. hirae* (Padan et al., 2004; Solioz et al., 2010). Thus, a bioinformatic analysis provides first hints on the role of a protein, which then has to be confirmed by practical approaches, as was the case in this study.

Here, protein functions were exclusively studied *in vivo*, although *in vitro* studies might offer valuable clues on e.g. binding properties or enzymatic activities. However results from *in vitro* experiments are not necessarily of relevance within the cell, as the testing conditions often do not correspond to the intracellular situation. The formaldehyde-responsive regulator FrmR of *Salmonella enterica*, for example, was found to respond *in vitro* also to metals, but is *in vivo* out-competed by native metal sensors. Likewise, the Ni^{2+} chaperone SlyD can bind other metals like Cu^{2+} and Zn^{2+} in *in vitro* tests, but this binding was found to be too weak in the cytoplasm for buffering these metal concentrations efficiently enough for conferring metal resistance (Kaluarachchi et al., 2011; Osman et al., 2015). However, in future investigations of the studied proteins, *in vitro* tests would help confirming their suggested role in the streptomcete's stress resistance and might explain some observations made in this study.

An effect, which proved important when investigating the impact of metal resistance systems in heterologous hosts, was the strong dependence on the genetic background. Of course, this is of utmost importance regarding the transferability of the endogenous *Streptomyces* sp. plasmids and their capability of conferring metal resistance in other bacteria. The efficient expression of proteins and interaction between chromosomal and plasmid-encoded determinants may vary even between members of the same genus (Liesegang et al., 1993), as exemplified here by the negative impact that pII had on the tolerance of oxidative stress by *S. lividans* TK24, while *S. mirabilis* benefitted from pII regarding oxidative stress resistance. Likewise, the deletion of *P16nreB* resulted in a higher Ni^{2+} resistance reduction in *S. mirabilis*, whereas the Ni^{2+} sensitivity in *S. lividans* TK24 did not increase as strongly compared to a *S. lividans* TK24 carrying the intact pII. A similar influence of the genetic background on metal resistance reduction caused by a deletion was observed for different *Cupriavidus necator* strains carrying the same mutation in a plasmidal heavy metal resistance locus (Liesegang et al., 1993).

Moreover, plasmid-encoded resistance determinants are not necessarily expressed to the same degree in every host. The *Hafnia alvei* plasmid pEJH501 coding a nickel resistance determinant conferred the same resistance level in *E. coli* and *Se. macescens*, while when transferred to *Klebsiella oxytoca*, the conferred resistance level was lower, due to ineffective protein expression (Park et al., 2003). Even in an *E coli* system, the choice of host impacts the results: the capability of copper resistance genes to confer resistance to different *E. coli* strains depended on the genetic background, growth conditions and medium type, e.g. no difference in resistance was observed in minimal medium,

but in complex (Staehlin et al., 2016). Thus, when investigating the role of a protein in its hosts, also heterologous expression can be of limited validity or applicability to other organisms.
Of course, gene deletion *in vivo* can lead to unwanted side effects, like changing the expression of co-transcribed genes or other nearby operons. Sometimes, promoters can be located within operons, enabling the separate regulation of specific genes (Foster et al., 2012), wherefore replacement by a resistance cassette would also change the transcription of other genes. This might account for the change of Ni^{2+} resistance of Δ*yjjG*, which was probably a polar effect rather than the result of loss of E13YjjG function.
The essentiality of some genes can even prevent their deletion. Here, deletion of the NiSOD encoding *sodN* genes of both investigated *Streptomyces* sp. strains was not successful. In literature, several similar cases have been reported, e.g. for genes encoding the K^+/H^+ antiporter Sha4 and DivIVA of *S. coelicolor* (Flärdh, 2003; Song, 2013), leading to the conclusion that essential genes which are required for cell survival cannot be deleted. Thus, NiSOD apparently was essential for both strains and its loss could not be compensated by other SOD proteins, like FeSOD.

4.2 Inherent factors influencing heavy metal resistance

Crossregulation
The results presented in the previous sections suggested interrelations between resistance systems for particular metals, e.g. Ni^{2+} and Cu^{2+}, but especially for systems coping with heavy metals and oxidative stress. Deletion of components of the copper resistome, P16CopY and P16CopZ, decreased Ni^{2+} resistance. When the *S. mirabilis* plasmid pII was transferred to the heavy metal sensitive *S. lividans* TK24, the increase of heavy metal resistance in the latter was more pronounced as compared to the difference between *S. mirabilis* P16 WT and the cured P16 489_3. It could be assumed that this was the result of crosstalk between different resistance systems, either for different metals or by plasmid- and chromosome-encoded determinants.
There are several examples for metal resistance operons being under the control of more than one transcriptional regulator. Thus, the transcription of resistance determinants can be delicately regulated in response to different signals. The operon *nikABCDE* of *E. coli* is negatively regulated by the Ni^{2+} responsive NikR, but also by the two-component system NarLX, which responds to nitrate, repressing *nikABCDE* transcription at elevated nitrate concentrations (Chivers & Sauer, 2000; Rowe et al., 2005). Additionally, the fumarate and nitrate reduction regulatory protein Fnr was shown to enable transcription of this operon in dependence on oxygen concentration (De Pina et al., 1999).
Likewise, the Ni^{2+} homeostasis operon, *nrs*, of *Synechocystis* sp. is associated with a two-component signal transduction system, termed NrsRS, responding to Ni^{2+} and Co^{2+} (Lopez-Maury et al., 2002), but also regulated by InsR, a CsoR-like metalloregulator, whose binding site is located within the operon for independent repression of *nreD* transcription (Foster et al., 2012). Thereby, *nrs* transcription can take place in a constitutive and an inducible manner.
Hence, it was highly likely that such a crossregulation would also influence the transcription of genes encoded on plasmid pII and that a crosstalk between chromosomal regulators and plasmidal genes occurred. Investigations of the transcriptome might help substantiating this hypothesis.

The two given examples show that a system, which was not investigated here, but can be expected to be of great importance, are two-component signal transduction systems, which often regulate metal trafficking proteins (Singh et al., 2014). These might impact the results of this study, as intracellular cross-talk between two-component signal transduction systems and cytoplasmatic metalloregulators has been observed also for copper homeostasis operons (Gudipaty et al., 2012; Outten et al., 2001) and loss of a component, e.g. *P16copY*, might thereby impact other systems, as metal homeostasis systems can be closely connected. The latter fact can be exemplified by the copper and iron trafficking system in *Saccharomyces* sp.: The copper chaperone Atx1 delivers Cu(I) to the copper-transporting ATPase Ccc2p and Fet3p, an oxidase involved in uptake of Fe^{3+}. Thus, deletion of *atx1* results in iron-deficiency in the cell. Conversely, the transcription of *atx1* can be activated also by an iron-sensing regulator (Lin et al., 1997). In *Pseudomonas stutzeri* the Cu^{2+} and Zn^{2+} responsive regulators CopRS and CzcR share genomic targets due to conserved promoter sequences resulting in an interplay of both homeostasis systems (Garber et al., 2018). A similar crossregulation might cause the change of Ni^{2+} resistance in the *Streptomyces* sp. *cop* deletion strains and might account for the significantly reduced Ni^{2+} content in the biomass of these strains as compared to the WT.

Regarding intracellular Ni^{2+}, there are at least two sensors known in *Streptomyces* sp.: Nur and SrnQ (Ahn et al., 2006; Kim et al., 2003). For further investigations of the metal resistome of the streptomycete strains, it would be interesting to investigate their role in heavy metal response.

Heavy metal systems do not solely interact on the transcriptional level. They can be additionally influenced by the presence of other metal ions. When transporters transport several metals, high concentrations of one element can abolish transport of the other, as is the case for NhlF (Degen et al., 1999) or Nic1p (Eitinger et al., 2000), where Ni^{2+} uptake is inhibited by Co^{2+}. This might lead to false conclusions, as was the case for NixA. The Ni^{2+} transporting activity of NixA is inhibited by Co^{2+}, Cu^{2+} and Zn^{2+}, which lead to the hypothesis that these ions were transported as well. Only in a latter study, Fischer et al. (2016) showed that NixA was exclusively transporting Ni^{2+}. On the other hand, the strictly Ni^{2+} transporting HoxN is not affected by Co^{2+} (Degen et al., 1999). Thus, for making reliable statements on the substrate spectrum of the here investigated transporters, further studies are required.

Protein mismetallation

The ability of a metal sensor to respond to metals is determined by its binding affinity and metal-ligand coordination geometry (Foster et al., 2012; Ma et al., 2009c). Therefore, metal binding proteins are not necessarily specific for one single metal, but due to global metal binding motifs are able to bind several different metals, e.g. ZinT of *E. coli* binds Zn^{2+}, Ni^{2+}, Cd^{2+} due to its His-rich metal-binding centre (Kershaw et al., 2007).

Particularly members of the vast CsoR family are known to often bind not only their cognate substrate, but also other ions, to which other family members actually respond. The *Synechocystis* sp. Ni^{2+} sensor InrS is responsible for the repression of the predicted Ni^{2} efflux pump NrsD, but still can bind Cu(I) *in vitro* (Foster et al., 2012). The CsoR Cu(I) sensor of *Bacillus substilis* can bind Ni^{2+}, Co^{2+} and Zn^{2+}, although no allosteric response is evoked and the regulator is left inactive (Ma et al., 2009a). Thus, metal sensors also influence each other in their responses by scavenging metals from the cytosol which could otherwise lead to mismetallation of other sensors, whereby the binding constant is one main determinant for regulating the succession of metal binding (Foster et al., 2012). Porto et al.

(2015) hypothesized that the non-allosteric metal binding of CsoR members might play a role in metal sequestration for intracellular stress reduction, which would be in accordance with the reduced nickel resistance in the *Streptomyces* sp. *cop* deletion strains. However, the CopZ overexpressing *S. lividans* TK24 strain also was more sensitive to Ni^{2+}, contradicting a buffering effect of this chaperone.
Whether mismetallation has an actual consequence *in vivo* is hard to substantiate. The Ni^{2+} chaperone SlyD was shown to bind Cu(I), Co^{2+} and Zn^{2+} as well, with a much higher affinity for Cu(I) *in vitro*. Nevertheless, *in vivo* this protein was highly specific for Ni^{2+} and copper binding was neglectable (Kaluarachchi et al., 2011).

Compensation by other systems and secondary effects
Often, several systems participate in maintaining the homeostasis of a particular metal in the cell. In *C. metallidurans*, the role model of a heavy metal resistant organism, metal uptake systems display a low, overlapping selectivity, wherefore deletion of one importer might have no visible effect because the loss can be compensated by other transporters (Herzberg et al., 2016; Kirsten et al., 2011). The existence of multiple metal export and import systems with overlapping activities complicates the study of the role of a single transporter. In the present study, this effect was most pronounced when studying the HoxN transporters. Ni^{2+} uptake cannot be solely mediated by these transporters, but also by unspecific transport. Thus, the phenotypic changes caused by *hoxN* deletion were subtle which underlined the complicated interplay between metal uptake systems in the metal transportome.
By having several transport system for one metal at their disposal cells can regulate metal fluxes more reliably. The successive activation of resistance systems, for example, helps maintaining homeostasis when one system is saturated (Outten et al., 2001). P16NreB probably is involved in the first line of defence against elevated intracellular Ni^{2+} concentrations with low capacity, as the introduction of an additional *P16nreB* copy in *S. mirabilis* did not result in a high increase in Ni^{2+} resistance.
The phenotypic changes caused by deletion of metal resistance genes often exceed the change in resistance, as metal stress has numerous implications in the cell and many yet unknown effects can be expected. Thus, phenotype descriptions in this study were certainly not exhaustive and secondary effects have to be expected. In *M. tuberculosis csoR* deletion increased the resistance to Cu(I), as was observed for *P16copY*, but in medium without copper addition, the bacterium showed an hypoxia-type stress response and the dormancy survival regulon (DosR) was induced (Marcus et al., 2016). Djoko et al. (2017) revealed a link between copper stress and glutamine metabolism and consequently acid stress in *E. coli*, as result of close association of respective genes on the chromosome. Thus, removal of components of the copper resistome can be expected to influence metabolism and induce other stress responses also in streptomycetes.

4.3 Heavy metals and oxidative stress

Aerobic life requires the ability to cope with reactive oxygen species, which are constantly formed in the cell as metabolic byproduct. This stress can be increased, when the cells are additionally challenged with exogenous oxidants, like heavy metals, wherefore they have to be able to minimize lethal effects by direct mechanisms, but also to correct sustained damage. Environmental oxidizing agents threaten genome stability and can induce genetic mutations, which in eukaryotes are involved in can-

cer development and senescence (Brierley & Martin, 2013; Cadet & Wagner, 2013; Kasprzak, 2011; Rai, 2010) – one reason why environmental heavy metal pollution is of general importance.
Oxidative DNA damage comprises base damage, cross-linking between DNA and amino acids, strand scission and depurination (Kasprzak, 2011). Additionally, heavy metals can inhibit DNA repair systems. Oxidized bases were found to accumulate in organisms exposed to heavy metals (Hirano & Tamae, 2010). Ni^{2+}, for example, induces the formation of 8-oxoguanine. In *E. coli* the nucleotidase MutT is responsible for the detoxification of this compound (Maki & Sekiguchi, 1992), while the HAD family hydrolase YjjG is specific for dUMP and several noncanonical pyrimidine derivatives (Titz et al., 2007; Weiss, 2007). The *S. acidiscabies* hydrolase E13YjjG conferred tolerance to 5-Fd and 5-Fu, analogously to the *E. coli* enzyme. However, it cannot be excluded that this hydrolase could also use 8-oxoguanine as substrate. Thus, E13YjjG is an indirect protector from heavy metal stress. It is not a first line heavy metal defence mechanism, but might be of importance for protecting cellular processes by maintaining the integrity of the nucleotide pool, thus preventing damage caused by oxidative stress, inflicted by heavy metals. By comparing the level of DNA damage caused by oxidative stress in the *S. acidiscabies* WT and Δ*yjjG* the importance of E13YjjG could be substantiated. Often, combinations of chromatographic and mass spectrometric techniques are applied for this purpose (Dizdaroglu et al., 2002).
An interesting finding in this study was the fact that the presence of pIl in the heterologous host *S. lividans* TK24 increased the strains sensitivity to oxidative stress, while *S. mirabilis* benefitted from pIl regarding this stressor. Apparently, regulatory determinants encoded on the plasmid interfered with the stress response system of *S. lividans* TK24. From the literature, several connections between transcriptional regulation of metal homeostasis and oxidative stress response are known. Either, regulators are redox-responsive themselves or they are indirectly responsible for oxidative stress response by regulating expression of specific enzymes, like SOD (Ahn et al., 2006; Torres et al., 2014). If pIl would encode a transcriptional repressor that would negatively affect the transcription of genes encoding oxidative stress response determinants in *S. lividans* TK24, the sensitivity to this stressor would increase. However, this suggestion needs further confirmation.

4.4 Exogenous factors influencing heavy metal resistance

The functioning of biotic systems is strongly impacted by external, abiotic conditions. In case of bacteria, the cultivation conditions play a vital role when aiming at comparing different phenotypic traits. The media composition may change gene expression, wherefore direct comparison of, for example, metal resistance levels between studies should always be regarded with caution. The pH is another factor of high importance, as many biological processes work optimally only in a certain pH range and it directly influences the bioavailability and speciation of metals. The drastically increased sensitivity of *S. mirabilis* to Li^{+} at alkaline pH illustrated this correlation, even for essential metals. Some metal efflux transporters are assumed to work in a metal/H^{+} antiporter mode, like NreB (Nies, 2003; Pini et al., 2014). Thus, changes of internal pH and thereby proton gradients would impact their capacity to alleviate metal stress. Whether P16NreB functions in this pH-dependent manner has to be determined in further studies but might also help explaining the difference of resistance level on certain media. To

the authors knowledge, the actual transport function of NreB-like transporters has not been investigated thoroughly yet. However, the interdependence of nickel resistance systems and pH in *Streptomyces* sp. has been observed in a *Streptomyces aureofaciens* strain isolated from metal contaminated riparian sediment with a markedly increased resistance at pH 6 compared to pH 7 (Van Nostrand et al., 2007), which could hardly be explained by a higher Ni^{2+} availability (Pumpel et al., 2003).

Effects of heavy metals and general media composition have to be carefully differentiated in *Streptomyces* sp., as the latter has a major influence on the streptomycete life cycle and metabolism (Flardh & Buttner, 2009; Fujimoto et al., 2016). Besides the provided carbon source, the availability of inorganic phosphate apparently plays an important role in *Streptomyces* sp. development and possibly also in metal resistance, as polyphosphate has metal sequestering properties (Aiking et al., 1984; Diaz et al., 2005; Worrall & Vijgenboom, 2010). In *S. coelicolor* a putative CsoR protein is not part of a *cop*-like locus, but clusters with genes potentially participating in transport of inorganic phosphate, which is why a transcriptional connection between phosphate and copper resistance can be assumed (Worrall & Vijgenboom, 2010).

The reason why an emphasis is put on the connection between metal resistance and media composition is the observation, that *S. mirabilis* exhibits especially high Ni^{2+} resistance on minimal medium, which is unexpected, as in complex medium heavy metals are potentially less bioavailable due to interactions with present compounds, wherefore other strains, like *S. lividans* TK24, are more resistant on complex media. This phenomenon in *S. mirabilis* is apparently specific to Ni^{2+}, since to copper the strain was more resistant on complex TSB as compared to AM. Furthermore, it might be connected particularly to plasmid pII, as the loss of this plasmid reversed the effect, rendering the strain more sensitive to $NiSO_4$ on AM agar as compared to TSB agar. Thus, it can be assumed that Ni^{2+} transport activity promoted by plasmid-encoded determinants would depend on compounds provided in the medium or that transcription of resistance determinants was regulated in dependence of media composition. The above mentioned nitrate-responsive regulation system NarLX, which controls the *nik* operon (Rowe et al., 2005) is one example for nutritional compounds governing expression of metal homeostasis systems.

On the *S. mirabilis* plasmid pII two ORFs near *P16nreB* were predicted to encode the transcriptional regulators NmtR and KmtR. These have been found in *M. tuberculosis* to both sense Ni^{2+} and Co^{2+}, but work in a medium-dependent manner. While KmtR-dependent repression was alleviated independently from metal addition in complex medium, NmtR remained bound under the same conditions and was only released in minimal medium or medium supplemented with Ni^{2+} or Co^{2+}. It was hypothesised that this was due to a higher affinity of KmtR to Ni^{2+} and Co^{2+} compared to NmtR (Campbell et al., 2007; Cavet et al., 2002). Hence, if highly efficient resistance determinants encoded on the *S. mirabilis* plasmid and/or chromosome were under control of the plasmid-encoded NmtR and the regulatory mechanisms were similar to that of the *M. tuberculosis* regulator, these resistance systems could be more efficiently transcribed when the strain was grown on minimal medium. These two regulator genes are suitable candidates for further investigations in this direction.

As stated above, the cultivation conditions impact *Streptomyces* sp. development. Their membrane lipid composition exhibits a high level of plasticity depending on the given phase (liquid or solid), medium composition and life stage, enabling their adaption to e.g. nutrient availability, pH and osmotic pressure (Poralla et al., 2000; Sandoval-Calderon et al., 2015). The impact of the cell envelope com-

position on the metal resistance of *S. mirabilis* was confirmed by deletion of *P16cslA* and *P16sfECF*. However, surprisingly, the resistance to Ni^{2+} increased in the deletion strains. To the author's knowledge, the sequestering effect of the cellulose-like cover of *Streptomyces* sp. hyphae for heavy metals has not been determined yet. This might help explaining the strong increase in Ni^{2+} resistance in Δ*cslA*. Likewise, the change of cell envelope composition in dependence on the media, might contribute to the higher resistance on minimal medium, if these changes reduce the entrance of Ni^{2+} in the cell.

Lastly, also the production of melanin by *S. mirabilis*, which depends on the availability of several compounds, as shown in section 3.2., was shown to negatively influence heavy metal resistance on complex medium. The phenolic intermediates formed during melanin synthesis are more toxic and might exert stress on the bacterial cell (Graham et al., 1978; Yang & Chen, 2009), which interferes with metal resistances. Furthermore, there are additional costs for tyrosinase synthesis and maturation, which Schmidt et al. (2009) assumed the main reason for the reduced Ni^{2+} resistance of *S. mirabilis* on TSB. Possibly, both explanations contribute to the higher Ni^{2+} sensitivity, but there have to be additional factors, as deletion of *P16melC2* did not increase Ni^{2+} resistance on TSB to the same level as on minimal medium.

4.5 *Streptomyces* sp. development with regard to heavy metals

The complex life cycle of streptomycetes involves several stages which necessitate the adaption of the hyphael cover, e.g. for crossing the liquid-air interface and enable aerial growth, which results in the formation of persistent spores. The involvement of the cellulose-like fibres of *Streptomyces* sp. in the heavy metal resistance of these bacteria has not been investigates, yet. However, the results presented in this study indicate, that they might impact growth under metal stress negatively. Nevertheless, heavy metals are also required for proper development of *Streptomyces* sp. Especially copper was shown to contribute to the switch between vegetative and reproductive growth (Petrus et al., 2016)(Kieser Hopwood 91). The cuproenzyme GlxA, an oxidase which is closely connected to CslA regarding gene localization and function, and the copper chaperone Sco, which delivers Cu(I) to CcO and GlxA, are required for morphogenesis (Chaplin et al., 2015; Liman et al., 2013; Petrus et al., 2016). The essentiality of copper might explain the presence of several genes encoding Cu(I)-dependent transcriptional regulators, CopZ-like proteins and further Cu(I) homeostasis systems in the genome of *S. mirabilis*, as the homeostasis has to be carefully regulated for optimal ion supply.

The *in silico* study of the *S. mirabilis* genome revealed that this strain lacked the *ram* cluster, which was in accordance with the inability to form aerial hyphae on complex media, as the necessary SapB protein that would reduce the surface tension and thereby facilitate erection of hyphae (Kodani et al., 2004), was absent. To the author's knowledge there are no reports on naturally SapB-deficient *Streptomyces* sp. strains. Possibly, the *sapB*-dependent developmental pathway is redundant for survival in soil, where the vegetative growth phase can be expected to last only a few days (Wellington et al., 1990) and humidity constantly changes. However, it was hypothesised that SapB could also play a role in later developmental stage, as the protein is constantly secreted in at a low level also by aerial hyphae (de Jong et al., 2012). Whether the lack of SapB in *S. mirabilis* contributes to the strain's

heavy metal resistance, e.g. by saving production costs, or whether its re-introduction could further increase resistance, remains to be determined.

4.6 Ecological relevance

When investigating environmental isolates under laboratory conditions, the question, in how far phenotypic traits are of actual relevance in the habitat, remains elusive. In case of the here investigated strains there was a connection between the possession of several heavy metal resistance systems and the high metal concentration in the original habitat as a mean of adaption. Nevertheless, some of the investigated genes would rather support the strains' survival within the microbial soil community or are means of adaption to the changing regimes in the soil, like the possession of several NhaA-type transporters that was in accordance with findings for *S. coelicolor* (Kim et al., 2011), a heavy metal sensitive bacterium.

The location where *S. mirabilis* P16B-1 was isolated was characterised by a low pH, which increased the metal mobility. In the soluble metal fraction, especially Ni^{2+}, Cd^{2+}, Co^{2+}, Mn^{2+} and Zn^{2+} were enriched. Copper was not as highly concentrated, but still elevated compared to the control soil (Schmidt et al., 2009; Schmidt et al., 2005). Nevertheless, the present study concentrated on nickel and copper, since the toxicity of heavy metals varies and being highly cytotoxic but still essential for *Streptomyces* sp. life, copper is an important element. However, further studies of Cd^{2+} resistance, in particular, could help to study the adaption of *S. mirabilis* to these conditions more thoroughly. The high heavy metal resistance of the strains was in accordance with the conventional hypothesis that metal contamination supports the acquisition of heavy metal resistance genes by certain community members, increasing their fitness (Sandaa et al., 2001).

Plasmids are considered to be one mean of adaption, because they often can be comparably easily acquired *via* horizontal gene transfer and carry beneficial phenotypic traits. The latter fact was substantiated for the endogenous plasmids of both *Streptomyces* sp. strains. The presented results confirmed the hypothesis of Schmidt et al. (2009) that at least one plasmid was involved in the heavy metal resistome of *S. mirabilis* P16B-1. In particular, the large endogenous plasmid pII conferred high Ni^{2+} resistance. Plasmids conferring metal resistance are well known from other species, like *Enterobacteria* sp., *Cupriavidus* sp. and *Sinorhizobium* sp., some of which were shown to be transferrable, as was the case for pII (Lee et al., 2006; Pini et al., 2014; Schmidt & Schlegel, 1994). However, even the cured *S. mirabilis* strain 489_3 still exhibited higher Ni^{2+} resistance than heavy metal sensitive *Streptomyces* sp. suggesting additional metal resistance determinants encoded on the chromosome, possibly as a result of adaption to the high heavy metal contamination in its original habitat. A similar task sharing of chromosomally and plasmid-encoded factors in metal resistance has been observed in species from other contaminated sites, e.g. *Cupriavidus metallidurans* CH34 and *Hafnia alvei* (Mergeay et al., 1985; Park et al., 2003). Resistance determinants found in the latter two organisms mostly belonged to protein families ubiquitously distributed in all organisms, which complicates their prediction *in silico*.

Whether the endogenous streptomycete plasmids could be passed to other soil community members, is hardly predictable. Since they carry heavy metal resistance genes, their acquisition could be beneficial for other organisms and makes the transfer more likely, as gene functions is one important factor

influencing plasmid transfer (Nakamura et al., 2004). Furthermore, at least one of the resistance genes of pII, *P16nreB* and possibly also *P16copZ*, was shown to be transcribed even in distantly related organisms, which is the prerequisite for their functioning in a wide variety of hosts.

Under laboratory conditions the transfer of pII to *S. lividans* and *Kribbella* sp. has been observed, but stable maintenance in the latter apparently was hampered. Several factors influence this transfer, which might be less likely met in nature. For conjugation between *Streptomyces* sp., actively growing mycelium and direct cell contact is required (Thoma et al., 2016). Furthermore, not all organisms can participate in this transfer equally, as plasmid spreading within community is also highly dependent on donor efficiency. Efficient donors may significantly accelerate transfer, while organisms without donor capacities would be a “dead end”. These donor abilities may even vary between species of the same genus (Dionisio et al., 2002). In another study, members of the Actinomycetales showed an increased permissiveness for plasmids under heavy metal stress, while the permissiveness of other community members decreased under metal stress (Klumper et al., 2017). Thus, the transfer of pII should be studied with members of the present soil community from its habitat for assessing the spreading potential of this plasmid.

Nevertheless, heavy metal contamination of soil is a stress, that has the potential to accelerate bacterial evolution and gene transfer (Gillings & Stokes, 2012), which was emphasised in the present study by the high genetic congruence to other heavy metal resistant organisms, in particular to *Streptomyces* sp. CdTB01, a strain which was isolated from heavy metal contaminated soil in China (Zhou et al., 2016).

4.7 Evolution of plasmid-encoded heavy metal resistance genes

Tracing the evolutionary history of genes encoded on the streptomycete plasmids might help determining their origin and former hosts. The *nre* resistance determinant, for instance, is found in many different organisms and was considered to easily spread among community members *via* horizontal gene transfer (Pini et al., 2014) which was in accordance with the potential of *P16nreB* to be transcribed even in *E. coli*. Likewise, the combination of resistance genes in clusters, like the close genomic location of *cop* genes on pII, could be a consequence of a linkage between chromosomal and plasmidal resistance genes, which thereby can be transferred together with improved resistance robustness (Staehlin et al., 2016). Regarding the high sequence identity between the plasmid-encoded P16CopY and chromosomal P16cCsoR2 and other *Streptomyces* sp. CsoR proteins, it is highly likely, that this was originally a genuine chromosomally encoded *Streptomyces* sp. protein that was mobilised on a plasmid.

Tracking the development of copper resistance islands has been achieved in other studies. Staehlin et al. (2016) analyzed the emergence and evolution of a “Copper Homeostasis and Silver Resistance Island” in Enterobacteria and found that the diversification of this cluster corresponded to anhropogenic activity connected to copper utilization. It is tempting to speculate, to what extend the mining activities in the Ronneburg area influenced the evolution of the present microbial community. Possibly, a similar analysis would help determining in how far horizontal gene transfer influenced the acquisition of resistance genes by *S. mirabilis*.

However, the present study indicates an adaption, or possibly co-evolution, between the large *S. mirabilis* plasmid and the strain's chromosome. This showed in differential consequences of pIl presence in the native host *S. mirabilis* and the heterologous host *S. lividans* TK24. In the latter, the plasmid negatively affected oxidative stress response and increased copper accumulation, while in the former plasmid-encoded determinants helped coping with this kind of stress.
A more extensive bioinformatic study of pIl structure might reveal its evolutionary origin and the developmental fate of the plasmid. For future investigations on this topic, it might be interesting to concentrate on transposon sequences and regions with comparably low GC content, as this is often viewed as an indicator for recently acquired genes (Huang et al., 2003). But also plasmid-encoded spore-associated proteins and genes targeted by developmental regulators give hints on plasmid evolution within the host, as found for the *S. coelicolor* plasmid SCP1 (Bentley et al., 2004).

4.8 Practical implications

Numerous studies underline the prevalence and importance of actinobacteria in metal contaminated habitats (Amoroso et al., 1998; El Baz et al., 2015; Remenár et al., 2014; Van Nostrand et al., 2007). It appears self-evident that their capabilities could be exploited for remediation purposes, since metal contamination already poses problems and will continue to be an urgent threat to the environment with mankind requiring rare elements for the production of technical devices which necessitates the intensive exploitation of more and more rock material and creates polluted habitats along the way. This is not only a challenge for the microbial community, but will sooner or later also become a problem for the ever growing human population.
The application of metal resistant bacteria, like *C. metallidurans* CH34, in the clean-up of contaminated waste water or the bioremediation potential of *Enterobacter* sp. has been determined (Diels et al., 1995; Lancaster et al., 2014; Naik et al., 2012; Sinha et al., 2013). Likewise, the strains used in the present study were investigated for their plant growth promoting activity, which could support phytoremediation of metal contaminated sites (Dimkpa et al., 2008; Schütze et al., 2015; Schütze et al., 2014). These studies showed that both strains promoted growth of *Sorghum bicolor* or other plants, as well as their production of compounds potentially promoting plant survival under metal stress.
However, Nies (2000) pointed out that when heavy metal resistance of a cell was mainly based on metal efflux, the organism would be less suitable for biosorption and bioremediation use. As the results of the present study indicate that efflux processes constitute one main mechanism for resistance in *S. mirabilis* the strain might be of limited use for direct application in the field with the aim of metal removal.
However, there are other ways for the practical application of heavy metal resistance systems in bioremediation approaches, as given by Lodewyckx et al. (2001). The authors transformed endophytic strains of *Burkholderia* sp. and *Herbaspirillum* sp. with the *ncc-nre* resistance determinants of *C. metallidurans*, which resulted in an increased removal of Ni^{2+} from liquid culture through sequestration and precipitation. However, successful application *in planta* depended on the bacterial strain and plant. Thus, these systems have to be carefully evaluated before they could be applied in clean-up setups.

Resistance determinants could also be used as selection marker in molecular applications, as has been shown for the *C. necator nre* determinant, which proved a suitable marker for the construction of mini-Tn5 transposons that could be transferred to members of different subclasses of Proteobacteria (Taghavi et al., 2001).

Being *Streptomyces* sp. strains, *S. mirabilis* P16B-1 and *S. acidiscabies* E13 could also prove to carry other useful traits for industrial applications besides metal resistance determinants. Of course, antibiotic synthesis clusters or other secondary metabolites might be interesting. However, from the here investigated proteins, the tyrosinase is a candidate for practical application, as these enzymes are used for treatment of wastewater by removing phenolic compounds, as well as in medical applications and other industrial areas (Do et al., 2017; Faccio et al., 2012; Roy et al., 2014).

4.9 Conclusion

The present study of two heavy metal resistant *Streptomyces* sp. strains isolated from contaminated soil proved that their resistance machinery comprises several components and lines of defence that were substrate-specific but nevertheless influenced the cell's reaction to other stressors. Thus, the study confirmed assumptions of other authors, who predicted the resistome of both strains to be composed of several co-operating factors (Haferburg et al., 2008; Schmidt et al., 2007).

In particular, the resistome of *S. mirabilis* is a complex system, as the two endogenous plasmids seem to harbour determinants that increase resistance, like metal efflux transporter, but also act in a contrary way, e.g. *via* transcriptional repressors or the tyrosinase, wherefore the effect of a single system can hardly be distinguished.

For further investigating the properties of the plasmids, they should be studied individually in a heterologous host, like *S. lividans* TK24, while the cured *S. mirabilis* strain 489_3 could serve for investigation of chromosomally encoded resistance determinants. By introducing the plasmids individually back in 489_3, putative interactions between chromosomally and plasmidal resistance determinants could be studied. Here, the re-introduction of plasmid fragments in 489_3 was a first step in this direction.

At least the large endogenous *S. mirabilis* plasmid was shown to be transferrable and confer heavy metal resistance, especially to Ni^{2+}. The transfer could be of ecological impact, since it also took place under sub-natural conditions in soil microcosms. Thereby it was shown that resistance determinants may spread in a natural community of streptomycetes, which might also be of importance for the practical application, as the spread of genetic modifications could hardly be controlled in the environment

The fact that the cured *S. mirabilis* strain was still more Ni^{2+} resistant than the metal-sensitive *S. lividans* TK24 proved the existence of additional chromosomal resistance determinants in the former. By using new and improved prediction methods and the described random transposon mutagenesis approach, it is highly likely that other, possibly yet unknown determinants are going to be identified, as unknown metal transport systems exist, even in well-investigated species like *E. coli* (Rowe et al., 2005).

Summary

Intensive mining activities are often accompanied by environmental heavy metal pollution, which poses not only a threat to human health but also challenges to the indigenous microbial community.
In the present study, two *Streptomyces* sp. strains, *S. mirabilis* P16B-1 and *S. acidiscabies* E13, isolated from a former uranium mining site located near Ronneburg (Thuringia, Germany) which stand out by their high metal resistance, were investigated with regard to the underlying genetic resistance determinants with the aim of assessing their potential for supporting bioremediation approaches.
After establishing a transformation system for *Streptomyces* sp. which was based on plasmid transfer by conjugation with *E. coli*, the streptomycetes were transformed by random transposon mutagenesis with Tn5 and mariner family transposons yielding mutants with reduced Ni^{2+} resistance. The integration sites were identified and served as targets for further investigation using PCR-targeted gene replacement for confirming their roles in the metal resistome.
From genome sequencing it was known that the highly Ni^{2+} resistant *S. mirabilis* P16B-1 carried two endogenous plasmids. Here, it was demonstrated that the larger of which, plasmid pII, was shown to play a major role in conferring Ni^{2+} resistance and to be transferrable to *S. lividans* on plates and in soil microcosms, while the tyrosinase-encoding gene *melC2* located on the smaller plasmid had a slightly negative effect on the strain's nickel resistance but increased the resistance to phenolic compounds. The reduced Ni^{2+} resistance of the *S. mirabilis* transposon transformants was mostly attributed to the loss of plasmid pII in the course of the transformation procedure. It was shown that an NreB-like transporter encoded on this plasmid contributed to Ni^{2+} resistance and that the gene could also be transcribed in *E. coli*, implying a wide host range for this determinant.
Additionally, several components of the *cop* and *cus* copper homeostasis systems were identified *in silico* on plasmid pII. Deletion of *P16copY* and *P16copZ*, encoding a transcriptional repressor and chaperone, respectively, impacted copper homeostasis and indicated interactions between plasmid-encoded determinants and the host chromosome, which were species-specific, as no similar effects were observed for *S. lividans* carrying pII.
S. acidiscabies E13 also harboured one endogenous plasmid, but no transfer to other species was observed. However, it was also involved in stress response, since a plasmid-encoded hydrolase was shown to protect the strain from the antimetabolites 5-Fu and 5-Fd.
These findings underlined the importance of plasmids within a community for coping with different environmental stressors. The transferability of pII to other *Streptomyces* sp. in soil microcosms proved its potential to spread within a soil habitat potentially enabling survival of other, more sensitive community members.
Further genes impacting metal homeostasis and environmental stress response were investigated, which also influence the strain's ability to survive in a soil habitat. Deletion of HoxN-like Ni^{2+} transporters in both strains disturbed Ni^{2+} homeostasis, possibly by reducing Ni^{2+} uptake, but no definite conclusion could be drawn due to the low activity of this type of transporter. In *S. mirabilis*, the $Li^+(Na^+)/H^+$ antiporter P16NhaA1 was vitally important for survival under Li^+ stress and a phosphinothricin N-acetyltransferase also acted on oxidized methionine compounds, which could be generated as by-product of heavy metal stress, thus it could contribute to coping with metal stress.

Also the composition of the extracellular matrix around the streptomycete hyphae and cell membrane composition impact metal resistance. Unexpectedly, reduction of the attachment of glucan fibres to the hyphae of *S. mirabilis* by loss of CslA function increased Ni^{2+} resistance, possibly by changing expression of other EPS compounds or reducing accumulation of metals in near vicinity of the hyphae at the glucan fibres.

Taken together, by demonstrating the applicability of molecular transformation methods of heavy metal resistant *Streptomyces* sp. strains this study provided the basis for further investigations of the metal resistome. Furthermore, the results indicated that metal resistance of both investigated strains was a result of multiple genetic determinants, whose contribution to the overall survival in contaminated soil has to be assessed more thoroughly.

Zusammenfassung

Schwermetallbelastungen von Böden sind eine häufige Folge von Bergbauaktivitäten und stellen nicht nur eine Bedrohung für die menschliche Gesundheit dar, sondern sind auch eine Herausforderung für die dort vorhandene mikrobielle Gemeinschaft.

In der vorliegenden Studie wurden zwei *Streptomyces* sp.-Stämme, *S. mirabilis* P16B-1 und *S. acidiscabies* E13 untersucht, die von einem ehemaligen Uranbergbaugebiet nahe Ronneburg (Thüringen, Deutschland) stammen und sich vor allem durch ihre hohe Schwermetallresistenz auszeichnen. Ziel war es herauszufinden, welche genetischen Grundlagen für diese Resistenz verantwortlich sind und Einsatz der Streptomyceten zur Unterstützung von Bioremediationsvorhaben zu evaluieren.

Dazu wurde zunächst ein Transformationssystem für *Streptomyces* sp. etabliert, das auf dem Plasmidtransfer durch Konjugation mit *E. coli* basierte. Die Streptomyceten konnten so mittels Transposonmutagenese mit Transposons der Tn5- und mariner-Familien transformiert werden und es wurden mehrere Mutanten mit verringerter Ni^{2+}-Resistenz isoliert. Die Transposonintegrationsstellen wurden identifiziert und die entsprechenden Gene dienten anschließend als Ziele für eine gerichtete Deletion mittels gezieltem Gen-Targeting, um ihre Beteiligung an der Metallresistenzmaschinerie der Stämme zu belegen.

Durch die Sequenzierung der Genome war bereits bekannt, dass der Ni^{2+}-resistente *S. mirabilis* zwei endogene Plasmide trägt. Hier konnte nachgewiesen werden, dass das größere der beiden, Plasmid pII, einen Hauptanteil zur Ni^{2+}-Resistenz dieses Stammes beiträgt und auch an andere Spezies, wie *S. lividans*, weitergegeben werden kann, sowohl auf Nähragarplatten als auch in Bodenmikrokosmen. Das Tyrosinase-kodierende Gen *melC2*, hingegen, das auf dem kleineren Plasmid lag, beeinflusste die Ni^{2+}-Resistenz leicht negativ, erhöhte jedoch die Resistenz des Stammes gegen phenolische Verbindungen.

Die Verringerung der Ni^{2+}-Resistenz bei den Transposonmutanten wurde überwiegend im Verlust von Plasmid pII im Laufe der Transformationsprozedur verursacht. Es konnte gezeigt werden, dass ein Transporter des NreB-Typs, der auf pII kodiert war, einen Beitrag zur Ni^{2+}-Resistenz leistet und das

dazugehörige Gen auch in *E. coli* transkribiert werden kann, was für ein weites Wirtsspektrum dieses Mechanismus spricht.

Weiterhin wurden auf pII mehrere Komponenten der *cop*- und *cus*-Systeme für Kupferhomöostase *in silico* identifiziert. Gen-Deletion von *P16copY* und *P16copZ*, die einen Transkiptionsrepressor bzw. ein Kupferchaperon kodieren, beeinflusste nicht nur die Kupferhomöostase in *S. mirabilis*, sondern gab Hinweise auf eine Interaktion zwischen Plasmid-kodierten Faktoren und dem Chromosom, die Spezies-spezifisch waren, da keine ähnlichen Effekte bei einem pII-tragenden *S. lividans* beobachtet wurden.

S. acidiscabies E13 trug auch ein endogenes Plasmid, bei dem jedoch kein Transfer zu anderen Spezies gezeigt werden konnte. Allerdings trug auch dieses Plasmid zur Stress-Reaktion des Bakteriums bei, da gezeigt werden konnte, dass eine Plasmid-kodierte Hydrolase den Stamm vor den Antimetaboliten 5-Fd und 5-Fu schützt.

Diese Ergebnisse belegten die Wichtigkeit endogener Plasmide in der Reaktion der Streptomyceten auf unterschiedliche Umweltstressoren. Insbesondere Plasmid pII könnte potentiell an andere *Streptomyces* sp. innerhalb einer Community weitergegeben werden und so das Überleben auch weniger resistenter Bakterien ermöglichen.

Es wurden weiterhin andere Gene untersucht, die ebenfalls die Metallhomöostase und Stressreaktion der Stämme und so deren Überlebensfähigkeit im Boden beeinflussen. Deletion von Genen, die HoxN-Typ Nickeltransporter kodierten, störte die Nickelhomöostase beider Stämme, vermutlich durch eine Reduzierung der Nickelaufnahme. Aufgrund der niedrigen Transportaktivität dieser Transporter konnten jedoch keine endgültigen Schlüsse über ihre Funktionalität gezogen werden. Für den *S. mirabilis* $Li^+(Na^+)/H^+$-Antiporter P16NhaA1 konnte nachgewiesen werden, dass er essentiell für das Überleben unter hohen Li+-Konzentrationen ist, und die Phosphinothricin-N-acetyltransferase P16Pat1 konnte oxidierte Methioninverbindungen als Substrat nutzen, wie sie auch als Nebeneffekt bei Schwermetallstress entstehen können, weshalb das Enzym indirekt bei der Stressreaktion auf Metallbelastung helfen könnte.

Die Zusammensetzung der extrazellulären Matrix um die Hyphe der Streptomyceten und die Zusammensetzung der Zellmembran beeinflussen ebenfalls die Schwermetallresistenz. Überraschenderweise führte die Reduktion der Anhaftung der Glucan-Fasern an die Hyphe von *S. mirabilis* durch Deletion von *cslA* zu einer Erhöhung der Nickelresistenz. Dies wurde möglicherweise durch eine veränderte Exprimierung anderer EPS-Verbindungen oder durch die Reduzierung der Metallakkumulation an den Fasern nahe der Hyphe verursacht.

Alles in allem konnte diese Studie die Grundlage für weitere Untersuchungen der Schwermetallresistenzmaschinerie der Stämme liefern, indem mehrere Transformationsmethoden etabliert wurden. Die erzielten Ergebnisse belegen dass die Schwermetallresistenz beider untersuchter Stämme das Ergebnis mehrerer genetischer Komponenten war, deren Beitrag zum Überleben in kontaminierten Bodenhabitaten weiter untersucht werden muss.

References

Abdeen, A. & Miki, B. (2009): The pleiotropic effects of the *bar* gene and glufosinate on the *Arabidopsis* transcriptome. *Plant Biotechnology Journal,* **7** (3), 266-282.

Ahn, B. E., Cha, J., Lee, E. J., Han, A. R., Thompson, C. J. & Roe, J. H. (2006): Nur, a nickel-responsive regulator of the Fur family, regulates superoxide dismutases and nickel transport in *Streptomyces coelicolor*. *Molecular Microbiology,* **59** (6), 1848-1858.

Aiking, H., Stijnman, A., van Garderen, C., van Heerikhuizen, H. & van 't Riet, J. (1984): Inorganic phosphate accumulation and cadmium detoxification in *Klebsiella aerogenes* NCTC 418 growing in continuous culture. *Applied and Environmental Microbiology,* **47** (2), 374-377.

Akiyama, M., Maki, H., Sekiguchi, M. & Horiuchi, T. (1989): A specific role of MutT protein: to prevent dG:dA mispairing in DNA replication. *Proceedings of the National Academy of Sciences of the United States of America,* **86** (11), 3949-3952.

Alhadeff, R., Ganoth, A., Krugliak, M. & Arkin, I. T. (2011): Promiscuous binding in a selective protein: the bacterial Na^+/H^+ antiporter. *PLoS ONE,* **6** (10), e25182.

Alhadeff, R. & Warshel, A. (2015): Simulating the function of sodium/proton antiporters. *Proceedings of the National Academy of Sciences USA,* **112** (40), 12378-12383.

Allegrini, S., Scaloni, A., Ferrara, L., Pesi, R., Pinna, P., Sgarrella, F., Camici, M., Eriksson, S. & Tozzi, M. G. (2001): Bovine cytosolic 5'-nucleotidase acts through the formation of an aspartate 52-phosphoenzyme intermediate. *The Journal of Biological Chemistry,* **276** (36), 33526-33532.

Allen, K. N. & Dunaway-Mariano, D. (2004): Phosphoryl group transfer: evolution of a catalytic scaffold. *Trends in Biochemical Sciences,* **29** (9), 495-503.

Altimira, F., Yanez, C., Bravo, G., Gonzalez, M., Rojas, L. A. & Seeger, M. (2012): Characterization of copper-resistant bacteria and bacterial communities from copper-polluted agricultural soils of central Chile. *BMC Microbiology,* **12**, 193.

Altschul, S. F., Gish, W., Miller, W., Myers, E. W. & Lipman, D. J. (1990): Basic local alignment search tool. *Journal of Molecular Biology,* **215** (3), 403-410.

Amann, E., Ochs, B. & Abel, K.-J. (1988): Tightly regulated tac promoter vectors useful for the expression of unfused and fused proteins in Escherichia coli. *Gene,* **69** (2), 301-315.

Aminov, R. I. (2011): Horizontal gene exchange in environmental microbiota. *Frontiers in Microbiology,* **2**, 158.

Amoroso, M. J., Castro, G. R., Carlino, F. J., Romero, N. C., Hill, R. T. & Oliver, G. (1998): Screening of heavy metal-tolerant actinomycetes isolated from the Sali River. *The Journal of General and Applied Microbiology,* **44** (2), 129-132.

Amoroso, M. J., Schubert, D., Mitscherlich, P., Schumann, P. & Kothe, E. (2000): Evidence for high affinity nickel transporter genes in heavy metal resistant *Streptomyces* spec. *Journal of Basic Microbiology,* **40** (5-6), 295-301.

An, Q., Robins, P., Lindahl, T. & Barnes, D. E. (2007): 5-Fluorouracil incorporated into DNA is excised by the Smug1 DNA glycosylase to reduce drug cytotoxicity. *Cancer Research,* **67** (3), 940-945.

Anderl, J. N., Franklin, M. J. & Stewart, P. S. (2000): Role of antibiotic penetration limitation in *Klebsiella pneumoniae* biofilm resistance to ampicillin and ciprofloxacin. *Antimicrobial Agents and Chemotherapy,* **44** (7), 1818-1824.

Arciola, C. R., Campoccia, D., Gamberini, S., Cervellati, M., Donati, E. & Montanaro, L. (2002): Detection of slime production by means of an optimised Congo red agar plate test based on a colourimetric scale in *Staphylococcus epidermidis* clinical isolates genotyped for *ica* locus. *Biomaterials,* **23** (21), 4233-4239.

Arguello, J. M., Eren, E. & Gonzalez-Guerrero, M. (2007): The structure and function of heavy metal transport P1B-ATPases. *Biometals,* **20** (3-4), 233-248.

Arguello, J. M., Raimunda, D. & Padilla-Benavides, T. (2013): Mechanisms of copper homeostasis in bacteria. *Frontiers in Cellular and Infection Microbiology,* **3**, 73.

Arkin, I. T., Xu, H., Jensen, M. O., Arbely, E., Bennett, E. R., Bowers, K. J., Chow, E., Dror, R. O., Eastwood, M. P., Flitman-Tene, R., Gregersen, B. A., Klepeis, J. L., Kolossvary, I., Shan, Y. & Shaw, D. E. (2007): Mechanism of Na^+/H^+ antiporting. *Science,* **317** (5839), 799-803.

Arnesano, F., Banci, L., Bertini, I., Ciofi-Baffoni, S., Molteni, E., Huffman, D. L. & O'Halloran, T. V. (2002): Metallochaperones and metal-transporting ATPases: a comparative analysis of sequences and structures. *Genome Research,* **12** (2), 255-271.

Arnesano, F., Banci, L., Bertini, I., Huffman, D. L. & O'Halloran, T. V. (2001): Solution structure of the Cu(I) and apo forms of the yeast metallochaperone, Atx1. *Biochemistry,* **40** (6), 1528-1539.

Attila, C., Ueda, A. & Wood, T. K. (2009): 5-Fluorouracil reduces biofilm formation in *Escherichia coli* K-12 through global regulator AriR as an antivirulence compound. *Applied Microbiology and Biotechnology,* **82** (3), 525-533.

Bacon, D. F. & Treffers, H. P. (1961): Spontaneous and mutator-induced reversions of an *Escherichia coli* auxotroph. I. Prototrophic types and their growth characteristics. *Journal of Bacteriology,* **81**, 786-793.

Baker, B. J. & Banfield, J. F. (2003): Microbial communities in acid mine drainage. *FEMS Microbiology Ecology,* **44** (2), 139-152.

Baker, J., Sengupta, M., Jayaswal, R. K. & Morrissey, J. A. (2011): The *Staphylococcus aureus* CsoR regulates both chromosomal and plasmid-encoded copper resistance mechanisms. *Environmental Microbiology,* **13** (9), 2495-2507.

Banks, D., Younger, P. L., Arnesen, R.-T., Iversen, E. R. & Banks, S. B. (1997): Mine-water chemistry: the good, the bad and the ugly. *Environmental Geology,* **32** (3), 157–174.

Bao, K. & Cohen, S. N. (2001): Terminal proteins essential for the replication of linear plasmids and chromosomes in *Streptomyces*. *Genes & Development,* **15** (12), 1518-1527.

Bayer, E., Gugel, K., Hägele, K., Hagenmaier, H., Jessipow, S., König, W. & Zähner, H. (1972): Stoffwechselprodukte von Mikroorganismen. Phosphinothricin und Phosphinothricyl-alanyl-alanin. *Helvetica Chimica Acta,* **55**, 224-239.

Bazire, A. & Dufour, A. (2014): The *Pseudomonas aeruginosa rhlG* and *rhlAB* genes are inversely regulated and RhlG is not required for rhamnolipid synthesis. *BMC Microbiology,* **14**, 160.

Beausejour, J. & Beaulieu, C. (2004): Characterization of *Streptomyces scabies* mutants deficient in melanin biosynthesis. *Canadian Journal of Microbiology,* **50** (9), 705-709.

Bedford, D. J., Lewis, C. G. & Buttner, M. J. (1991): Characterization of a gene conferring bialaphos resistance in *Streptomyces coelicolor* A3(2). *Gene,* **104** (1), 39-45.

Beites, T., Pires, S. D., Santos, C. L., Osorio, H., Moradas-Ferreira, P. & Mendes, M. V. (2011): Crosstalk between ROS homeostasis and secondary metabolism in *S. natalensis* ATCC 27448: modulation of pimaricin production by intracellular ROS. *PLoS ONE,* **6** (11), e27472.

Bentley, S. D., Brown, S., Murphy, L. D., Harris, D. E., Quail, M. A., Parkhill, J., Barrell, B. G., McCormick, J. R., Santamaria, R. I., Losick, R., Yamasaki, M., Kinashi, H., Chen, C. W., Chandra, G., Jakimowicz, D., Kieser, H. M., Kieser, T. & Chater, K. F. (2004): SCP1, a 356 023 bp linear plasmid adapted to the ecology and developmental biology of its host, *Streptomyces coelicolor* A3(2). *Molecular Microbiology,* **51** (6), 1615-1628.

Bernan, V., Filpula, D., Herber, W., Bibb, M. & Katz, E. (1985): The nucleotide sequence of the tyrosinase gene from *Streptomyces antibioticus* and characterization of the gene product. *Gene,* **37** (1-3), 101-110.

Bertini, I. & Cavallaro, G. (2010): Bioinformatics in bioinorganic chemistry. *Metallomics,* **2** (1), 39-51.

Bertram, J., Stratz, M. & Durre, P. (1991): Natural transfer of conjugative transposon Tn916 between gram-positive and gram-negative bacteria. *Journal of Bacteriology,* **173** (2), 443-448.

Betancourt, A. M., Bernan, V., Herber, W. & Katz, E. (1992): Analysis of tyrosinase synthesis in *Streptomyces antibioticus*. *Journal of General Microbiology,* **138**, 787-794.

Bhatnagar, S. K. & Bessman, M. J. (1988): Studies on the mutator gene, *mutT* of *Escherichia coli*. Molecular cloning of the gene, purification of the gene product, and identification of a novel nucleoside triphosphatase. *The Journal of Biological Chemistry,* **263** (18), 8953-8957.

Bhatt, A., Kieser, H. M., Melton, R. E. & Kieser, T. (2001): Plasmid transfer from *Streptomyces* to *Mycobacterium smegmatis* by spontaneous transformation. *Molecular Microbiology,* **43** (1), 135-146.

Bhattacharya, A., Sood, P. & Citovsky, V. (2010): The roles of plant phenolics in defence and communication during *Agrobacterium* and *Rhizobium* infection. *Molecular Plant Pathology,* **11** (5), 705-719.

Bibb, M. J. & Cohen, S. N. (1982): Gene expression in *Streptomyces*: construction and application of promoter-probe plasmid vectors in *Streptomyces lividans*. *Molecular & General Genetics,* **187** (2), 265-277.

Bibb, M. J., Domonkos, A., Chandra, G. & Buttner, M. J. (2012): Expression of the chaplin and rodlin hydrophobic sheath proteins in *Streptomyces venezuelae* is controlled by sigma(BldN) and a cognate anti-sigma factor, RsbN. *Molecular Microbiology,* **84** (6), 1033-1049.

Bibb, M. J., Freeman, R. F. & Hopwood, D. A. (1977): Physical and genetical characterisation of a second sex factor, SCP2, for *Streptomyces coelicolor* A3(2). *Molecular & General Genetics,* **154**, 155-166.

Bibb, M. J. & Hopwood, D. A. (1981): Genetic studies of the fertility plasmid SCP2 and its SCP2* variants in *Streptomyces coelicolor* A3(2). *Microbiology,* **126** (2), 427-442.

Bibb, M. J., Janssen, G. R. & Ward, J. M. (1985): Cloning and analysis of the promoter region of the erythromycin resistance gene (*ermE*) of *Streptomyces erythraeus*. *Gene,* **38** (1-3), 215-226.

Bibb, M. J., Molle, V. & Buttner, M. J. (2000): ςBldN , an extracytoplasmic function RNA polymerase sigma factor required for aerial mycelium formation in *Streptomyces coelicolor* A3(2). *Journal of Bacteriology,* **182** (16), 4606-4616.

Bibb, M. J., Ward, J. M. & Hopwood, D. A. (1978): Transformation of plasmid DNA into *Streptomyces* at high frequency. *Nature,* **274**, 398-400.

Bibb, M. J., Ward, J. M., Kieser, T., Cohen, S. N. & Hopwood, D. A. (1981): Excision of chromosomal DNA sequences from *Streptomyces coelicolor* forms a novel family of plasmids detectable in *Streptomyces lividans*. *Molecular & General Genetics,* **184** (2), 230-240.

Bierman, M., Logan, R., O'Brien, K., Seno, E. T., Nagaraja-Rao, R. & Schoner, B. E. (1992): Plasmid cloning vectors for the conjugal transfer of DNA from *Escherichia coli* to *Streptomyces* spp. *Gene,* **116**, 43-49.

Billini, M., Stamatakis, K. & Sophianopoulou, V. (2008): Two members of a network of putative Na^+/H^+ antiporters are involved in salt and pH tolerance of the freshwater cyanobacterium *Synechococcus elongatus*. *Journal of Bacteriology,* **190** (19), 6318-6329.

Bilyk, B. & Luzhetskyy, A. (2014): Unusual site-specific DNA integration into the highly active pseudo-*attB* of the *Streptomyces albus* J1074 genome. *Applied Microbiology and Biotechnology,* **98** (11), 5095-5104.

Bilyk, B., Weber, S., Myronovskyi, M., Bilyk, O., Petzke, L. & Luzhetskyy, A. (2013): *In vivo* random mutagenesis of streptomycetes using *mariner*-based transposon *Himar1*. *Applied Microbiology and Biotechnology,* **97** (1), 351-359.

Bishop, A., Fielding, S., Dyson, P. & Herron, P. (2004): Systematic insertional mutagenesis of a streptomycete genome: a link between osmoadaptation and antibiotic production. *Genome Research,* **14** (5), 893-900.

Blanton, R. L., Fuller, D., Iranfar, N., Grimson, M. J. & Loomis, W. F. (2000): The cellulose synthase gene of *Dictyostelium*. *Proceedings of the National Academy of Sciences USA,* **97** (5), 2391-2396.

Block, M. D., Botterman, J., Vandewiele, M., Dockx, J., Thoen, C., Gosselé, V., Movva, N. R., Thompson, C., Montagu, M. V. & Leemans, J. (1987): Engineering herbicide resistance in plants by expression of a detoxifying enzyme. *The EMBO Journal,* **6** (9), 2513-2518.

Blodgett, J. A., Zhang, J. K. & Metcalf, W. W. (2005): Molecular cloning, sequence analysis, and heterologous expression of the phosphinothricin tripeptide biosynthetic gene cluster from *Streptomyces viridochromogenes* DSM 40736. *Antimicrobial Agents and Chemotherapy,* **49** (1), 230-240.

Blount, B. C. & Ames, B. N. (1994): Analysis of uracil in DNA by gas chromatography-mass spectrometry. *Analytical Biochemistry,* **219** (2), 195-200.

Blundell, K. L., Wilson, M. T., Svistunenko, D. A., Vijgenboom, E. & Worrall, J. A. (2013): Morphological development and cytochrome c oxidase activity in *Streptomyces lividans* are dependent on the action of a copper bound Sco protein. *Open Biology,* **3** (1), 120163.

Bordeleau, E., Ghinet, M. G. & Burrus, V. (2012): Diversity of integrating conjugative elements in actinobacteria: Coexistence of two mechanistically different DNA-translocation systems. *Mobile Genetic Elements,* **2** (2), 119-124.

Brett, C. L., Donowitz, M. & Rao, R. (2005): Evolutionary origins of eukaryotic sodium/proton exchangers. *American Journal of Physiology-Cell Physiology,* **288** (2), C223-C239.

Brierley, D. J. & Martin, S. A. (2013): Oxidative stress and the DNA mismatch repair pathway. *Antioxidants & Redox Signaling,* **18** (18), 2420-2428.

Cabiscol, E., Tamarit, J. & Ros, J. (2000): Oxidative stress in bacteria and protein damage by reactive oxygen species. *International Microbiology,* **3** (1), 3-8.

Cadet, J. & Wagner, J. R. (2013): DNA base damage by reactive oxygen species, oxidizing agents, and UV radiation. *Cold Spring Harbor Perspectives in Biology,* **5** (2).

Campbell, D. R., Chapman, K. E., Waldron, K. J., Tottey, S., Kendall, S., Cavallaro, G., Andreini, C., Hinds, J., Stoker, N. G., Robinson, N. J. & Cavet, J. S. (2007): Mycobacterial cells have dual nickel-cobalt sensors: sequence relationships and metal sites of metal-responsive repressors are not congruent. *The Journal of Biological Chemistry,* **282** (44), 32298-32310.

Capstick, D. S., Willey, J. M., Buttner, M. J. & Elliot, M. A. (2007): SapB and the chaplins: connections between morphogenetic proteins in *Streptomyces coelicolor*. *Molecular Microbiology,* **64** (3), 602-613.

Casali, N. & Riley, L. W. (2007): A phylogenomic analysis of the *Actinomycetales mce* operons. *BMC Genomics,* **8**, 60.

Casali, N., White, A. M. & Riley, L. W. (2006): Regulation of the *Mycobacterium tuberculosis mce1* operon. *Journal of Bacteriology,* **188** (2), 441-449.

Cavet, J. S., Meng, W., Pennella, M. A., Appelhoff, R. J., Giedroc, D. P. & Robinson, N. J. (2002): A nickel-cobalt-sensing ArsR-SmtB family repressor. Contributions of cytosol and effector binding sites to metal selectivity. *The Journal of Biological Chemistry,* **277** (41), 38441-38448.

Chandrangsu, P., Rensing, C. & Helmann, J. D. (2017): Metal homeostasis and resistance in bacteria. *Nature Reviews. Microbiology,* **15** (6), 338-350.

Chang, F. M., Coyne, H. J., Cubillas, C., Vinuesa, P., Fang, X., Ma, Z., Ma, D., Helmann, J. D., Garcia-de los Santos, A., Wang, Y. X., Dann, C. E., 3rd & Giedroc, D. P. (2014): Cu(I)-mediated allosteric switching in a copper-sensing operon repressor (CsoR). *The Journal of Biological Chemistry,* **289** (27), 19204-19217.

Chaplin, A. K., Petrus, M. L., Mangiameli, G., Hough, M. A., Svistunenko, D. A., Nicholls, P., Claessen, D., Vijgenboom, E. & Worrall, J. A. (2015): GlxA is a new structural member of the radical copper oxidase family and is required for glycan deposition at hyphal tips and morphogenesis of *Streptomyces lividans*. *The Biochemical Journal,* **469** (3), 433-444.

Chater, K. F. (1993): Genetics of differentiation in *Streptomyces*. *Annual Review of Microbiology,* **47**, 685-713.

Chater, K. F. (1998): Taking a genetic scalpel to the *Streptomyces* colony. *Microbiology,* **144** (6), 1465-1478.

Chater, K. F., Biro, S., Lee, K. J., Palmer, T. & Schrempf, H. (2010): The complex extracellular biology of *Streptomyces*. *FEMS Microbiology Reviews,* **34** (2), 171-198.

Chater, K. F. & Kinashi, H. (2007): *Streptomyces* linear plasmids: their discovery, functions, interactions with other replicons, and evolutionary significance. -In Meinhardt, F. & Klassen, R. (Eds.): *Microbial Linear Plasmids.* Springer Berlin Heidelberg, Berlin, Heidelberg, pp 1-31.

Chen, C. W. (1996): Complications and implications of linear bacterial chromosomes. *Trends in Genetics,* **12** (5), 192-196.

Chen, C. W., Huang, C. H., Lee, H. H., Tsai, H. H. & Kirby, R. (2002): Once the circle has been broken: dynamics and evolution of *Streptomyces* chromosomes. *Trends in Genetics,* **18** (10), 522-529.

Chen, C. W., Yu, T. W., Lin, Y. S., Kieser, H. M. & Hopwood, D. A. (1993a): The conjugative plasmid SLP2 of *Streptomyces lividans* is a 50 kb linear molecule. *Molecular Microbiology,* **7** (6), 925-932.

Chen, J. S., Reddy, V., Chen, J. H., Shlykov, M. A., Zheng, W. H., Cho, J., Yen, M. R. & Saier, M. H., Jr. (2011): Phylogenetic characterization of transport protein superfamilies: superiority of SuperfamilyTree programs over those based on multiple alignments. *Journal of Molecular Microbiology and Biotechnology,* **21** (3-4), 83-96.

Chen, L. Y., Chen, M. Y., Leu, W. M., Tsai, T. Y. & Lee, Y. H. (1993b): Mutational study of *Streptomyces* tyrosinase *trans*-activator MelC1. MelC1 is likely a chaperone for apotyrosinase. *The Journal of Biological Chemistry,* **268** (25), 18710-18716.

Cheng, J., Guffanti, A. A. & Krulwich, T. A. (1994): The chromosomal tetracycline resistance locus of *Bacillus subtilis* encodes a Na^+/H^+ antiporter that is physiologically important at elevated pH. *The Journal of Biological Chemistry,* **269** (44), 27365-27371.

Chillappagari, S., Miethke, M., Trip, H., Kuipers, O. P. & Marahiel, M. A. (2009): Copper acquisition is mediated by YcnJ and regulated by YcnK and CsoR in *Bacillus subtilis*. *Journal of Bacteriology,* **191** (7), 2362-2370.

Chivers, P. T. & Sauer, R. T. (2000): Regulation of high affinity nickel uptake in bacteria. Ni^{2+}-dependent interaction of NikR with wild-type and mutant operator sites. *The Journal of Biological Chemistry,* **275** (26), 19735-19741.

Cho, Y. H., Lee, E. J., Ahn, B. E. & Roe, J. H. (2001): SigB, an RNA polymerase sigma factor required for osmoprotection and proper differentiation of *Streptomyces coelicolor*. *Molecular Microbiology,* **42** (1), 205-214.

Choulet, F., Aigle, B., Gallois, A., Mangenot, S., Gerbaud, C., Truong, C., Francou, F. X., Fourrier, C., Guerineau, M., Decaris, B., Barbe, V., Pernodet, J. L. & Leblond, P. (2006): Evolution of the terminal regions of the *Streptomyces* linear chromosome. *Molecular Biology and Evolution,* **23** (12), 2361-2369.

Christ, B., Hochstrasser, R., Guyer, L., Francisco, R., Aubry, S., Hortensteiner, S. & Weng, J. K. (2017): Non-specific activities of the major herbicide-resistance gene *bar*. *Nature Plants,* **3** (12), 937-945.

Claessen, D., de Jong, W., Dijkhuizen, L. & Wosten, H. A. (2006): Regulation of *Streptomyces* development: reach for the sky! *Trends in Microbiology,* **14** (7), 313-319.

Claessen, D., Rink, R., de Jong, W., Siebring, J., de Vreugd, P., Boersma, F. G. H., Dijkhuizen, L. & Wösten, H. A. B. (2003): A novel class of secreted hydrophobic proteins is involved in aerial hyphae formation in *Streptomyces coelicolo*r by forming amyloid-like fibrils. *Genes & Development,* **17** (14), 1714-1726.

Clark, L. C., Seipke, R. F., Prieto, P., Willemse, J., van Wezel, G. P., Hutchings, M. I. & Hoskisson, P. A. (2013): Mammalian cell entry genes in *Streptomyces* may provide clues to the evolution of bacterial virulence. *Scientific Reports,* **3**, 1109.

Coates, C. J., Jasinskiene, N., Miyashiro, L. & James, A. A. (1998): *Mariner* transposition and transformation of the yellow fever mosquito, *Aedes aegypti*. *Proceedings of the National Academy of Sciences of the United States of America,* **95** (7), 3748–3751.

Cobine, P., Wickramasinghe, W. A., Harrison, M. D., Weber, T., Solioz, M. & Dameron, C. T. (1999): The *Enterococcus hirae* copper chaperone CopZ delivers copper(I) to the CopY repressor. *FEBS Letters,* **445** (1), 27-30.

Cobine, P. A., George, G. N., Jones, C. E., Wickramasinghe, W. A., Solioz, M. & Dameron, C. T. (2002): Copper transfer from the Cu(I) chaperone, CopZ, to the repressor, Zn(II)CopY: metal coordination environments and protein interactions. *Biochemistry,* **41** (18), 5822-5829.

Collet, J. F., Stroobant, V. & Van Schaftingen, E. (1999): Mechanistic studies of phosphoserine phosphatase, an enzyme related to P-type ATPases. *The Journal of Biological Chemistry,* **274** (48), 33985-33990.

Colvin, J. R. & Witter, D. E. (1983): Congo red and calcofluor white inhibition of *Acetobacter xylinum* cell growth and of bacterial cellulose microfibril formation: Isolation and properties of a transient, extracellular glucan related to cellulose. *Protoplasma,* **116** (1), 34-40.

Comba, S., Sabatini, M., Menendez-Bravo, S., Arabolaza, A. & Gramajo, H. (2014): Engineering a *Streptomyces coelicolor* biosynthesis pathway into *Escherichia coli* for high yield triglyceride production. *Biotechnology for Biofuels,* **7** (1), 172.

Combes, P., Till, R., Bee, S. & Smith, M. C. M. (2002): The *Streptomyces* genome contains multiple pseudo-*attB* sites for the phiC31-encoded site-specific recombination system. *Journal of Bacteriology,* **184** (20), 5746-5752.

Corbett, D., Schuler, S., Glenn, S., Andrew, P. W., Cavet, J. S. & Roberts, I. S. (2011): The combined actions of the copper-responsive repressor CsoR and copper-metallochaperone CopZ modulate CopA-mediated

copper efflux in the intracellular pathogen *Listeria monocytogenes*. *Molecular Microbiology,* **81** (2), 457-472.

Courvalin, P. (1994): Transfer of antibiotic resistance genes between gram-positive and gram-negative bacteria. *Antimicrobial Agents and Chemotherapy,* **38** (7), 1447-1451.

Crameri, R., Ettlinger, L., Hutter, R., Lerch, K., Suter, M. A. & Vetterli, J. A. (1982): Secretion of tyrosinase in *Streptomyces glaucescens*. *Journal of General Microbiology,* **128** (2), 371-379.

Cruz-Morales, P., Vijgenboom, E., Iruegas-Bocardo, F., Girard, G., Yanez-Guerra, L. A., Ramos-Aboites, H. E., Pernodet, J. L., Anne, J., van Wezel, G. P. & Barona-Gomez, F. (2013): The genome sequence of *Streptomyces lividans* 66 reveals a novel tRNA-dependent peptide biosynthetic system within a metal-related genomic island. *Genome Biology and Evolution,* **5** (6), 1165-1175.

Cui, J., Gizzi, A. & Stivers, J. T. (2019): Deoxyuridine in DNA has an inhibitory and promutagenic effect on RNA transcription by diverse RNA polymerases. *Nucleic Acids Research*.

Cui, Y., Liu, Z., Li, Y., Zhou, F., Chen, H. & Lin, Y. (2016): Application of a novel phosphinothricin N-acetyltransferase (RePAT) gene in developing glufosinate-resistant rice. *Scientific Reports,* **6**, 21259.

Cullum, J., Altenbuchner, J., Flett, F. & Piendl, W. (1986): DNA amplification and genetic instability in *Streptomyces*. *Biotechnology and Genetic Engineering Reviews,* **4** (1), 59-78.

Cvetkovic, A., Menon, A. L., Thorgersen, M. P., Scott, J. W., Poole, F. L., 2nd, Jenney, F. E., Jr., Lancaster, W. A., Praissman, J. L., Shanmukh, S., Vaccaro, B. J., Trauger, S. A., Kalisiak, E., Apon, J. V., Siuzdak, G., Yannone, S. M., Tainer, J. A. & Adams, M. W. (2010): Microbial metalloproteomes are largely uncharacterized. *Nature,* **466** (7307), 779-782.

Datsenko, K. A. & Wanner, B. L. (2000): One-step inactivation of chromosomal genes in *Escherichia coli* K-12 using PCR products. *Proceedings of the National Academy of Sciences USA,* **97** (12), 6640-6645.

Davies, A. M., Tata, R., Beavil, R. L., Sutton, B. J. & Brown, P. R. (2007): l-Methionine sulfoximine, but not phosphinothricin, is a substrate for an acetyltransferase (gene *PA4866*) from *Pseudomonas aeruginosa*: structural and functional studies. *Biochemistry,* **46** (7), 1829-1839.

Davies, A. M., Tata, R., Snape, A., Sutton, B. J. & Brown, P. R. (2009): Structure and substrate specificity of acetyltransferase ACIAD1637 from *Acinetobacter baylyi* ADP1. *Biochimie,* **91** (4), 484-489.

de Jong, W., Vijgenboom, E., Dijkhuizen, L., Wosten, H. A. & Claessen, D. (2012): SapB and the rodlins are required for development of *Streptomyces coelicolor* in high osmolarity media. *FEMS Microbiology Letters,* **329** (2), 154-159.

de Jong, W., Wosten, H. A., Dijkhuizen, L. & Claessen, D. (2009): Attachment of *Streptomyces coelicolor* is mediated by amyloidal fimbriae that are anchored to the cell surface via cellulose. *Molecular Microbiology,* **73** (6), 1128-1140.

De Pina, K., Desjardin, V., Mandrand-Berthelot, M. A., Giordano, G. & Wu, L. F. (1999): Isolation and characterization of the *nikR* gene encoding a nickel-responsive regulator in *Escherichia coli*. *Journal of Bacteriology,* **181** (2), 670-674.

De Rore, H., Top, E., Houwen, F., Mergeay, M. & Verstraete, W. (1994): Evolution of heavy metal resistant transconjugants in a soil environment with a concomitant selective pressure. *FEMS Microbiology Ecology,* **14** (3), 263-274.

Degen, O. & Eitinger, T. (2002): Substrate specificity of nickel/cobalt permeases: Insights from mutants altered in transmembrane domains I and II. *Journal of Bacteriology,* **184** (13), 3569-3577.

Degen, O., Kobayashi, M., Shimizu, S. & Eitinger, T. (1999): Selective transport of divalent cations by transition metal permeases: the *Alcaligenes eutrophus* HoxN and the *Rhodococcus rhodochrous* NhlF. *Archives of Microbiology,* **171** (3), 139-145.

Deguchi, Y., Yamato, I. & Anraku, Y. (1990): Nucleotide sequence of *gltS*, the Na^+/glutamate symport carrier gene of *Escherichia coli* B. *The Journal of Biological Chemistry,* **265** (35), 21704-21708.

Dell'Amico, E., Mazzocchi, M., Cavalca, L., Allievi, L. & Andreoni, V. (2008): Assessment of bacterial community structure in a long-term copper-polluted ex-vineyard soil. *Microbiological Research,* **163** (6), 671-683.

della-Cioppa, G., Garger, S. J., Sverlow, G. G., Turpen, T. H. & Grill, L. K. (1990): Melanin production in *Escherichia coli* from a cloned tyrosinase gene. *Biotechnology (N Y),* **8** (7), 634-638.

Demaurex, N. & Grinstein, S. (1994): Na^+/H^+ antiport: modulation by ATP and role in cell volume regulation. *Journal of Experimental Biology,* **196** (1), 389-404.

Diaz, M., Esteban, A., Fernandez-Abalos, J. M. & Santamaria, R. I. (2005): The high-affinity phosphate-binding protein PstS is accumulated under high fructose concentrations and mutation of the corresponding gene affects differentiation in *Streptomyces lividans*. *Microbiology,* **151** (Pt 8), 2583-2592.

Dib, J. R., Wagenknecht, M., Hill, R. T., Farias, M. E. & Meinhardt, F. (2010): First report of linear megaplasmids in the genus *Micrococcus*. *Plasmid,* **63** (1), 40-45.

Diddens, H., Zahner, H., Kraas, E., Gohring, W. & Jung, G. (1976): On the transport of tripeptide antibiotics in bacteria. *European Journal of Biochemistry,* **66** (1), 11-23.

Diels, L., Dong, Q., van der Lelie, D., Baeyens, W. & Mergeay, M. (1995): The *czc* operon of *Alcaligenes eutrophus* CH34: from resistance mechanism to the removal of heavy metals. *Journal of Industrial Microbiology,* **14** (2), 142-153.

Dimkpa, C., Svatos, A., Merten, D., Buchel, G. & Kothe, E. (2008): Hydroxamate siderophores produced by *Streptomyces acidiscabies* E13 bind nickel and promote growth in cowpea (*Vigna unguiculata* L.) under nickel stress. *Canadian Journal of Microbiology,* **54** (3), 163-172.

Dionisio, F., Matic, I., Radman, M., Rodrigues, O. R. & Taddei, F. (2002): Plasmids spread very fast in heterogeneous bacterial communities. *Genetics,* **162** (4), 1525-1532.

Dizdaroglu, M., Jaruga, P., Birincioglu, M. & Rodriguez, H. (2002): Free radical-induced damage to DNA: mechanisms and measurement. *Free Radical Biology & Medicine,* **32** (11), 1102-1115.

Djoko, K. Y., Phan, M. D., Peters, K. M., Walker, M. J., Schembri, M. A. & McEwan, A. G. (2017): Interplay between tolerance mechanisms to copper and acid stress in *Escherichia coli*. *Proceedings of the National Academy of Sciences USA,* **114** (26), 6818-6823.

Dmitrieva, N. I. & Burg, M. B. (2005): Hypertonic stress response. *Mutation Research,* **569** (1-2), 65-74.

Do, H., Kang, E., Yang, B., Cha, H. J. & Choi, Y. S. (2017): A tyrosinase, mTyr-CNK, that is functionally available as a monophenol monooxygenase. *Scientific Reports,* **7** (1), 17267.

Doumith, M., Weingarten, P., Wehmeier, U. F., Salah-Bey, K., Benhamou, B., Capdevila, C., Michel, J. M., Piepersberg, W. & Raynal, M. C. (2000): Analysis of genes involved in 6-deoxyhexose biosynthesis and transfer in *Saccharopolyspora erythraea*. *Molecular & General Genetics,* **264** (4), 477-485.

Drees, S. L., Beyer, D. F., Lenders-Lomscher, C. & Lubben, M. (2015): Distinct functions of serial metal-binding domains in the *Escherichia coli* P1-B -ATPase CopA. *Molecular Microbiology,* **97** (3), 423-438.

Du, L., Liu, R. H., Ying, L. & Zhao, G. R. (2012): An efficient intergeneric conjugation of DNA from *Escherichia coli* to mycelia of the lincomycin-producer *Streptomyces lincolnensis*. *International Journal of Molecular Sciences,* **13** (4), 4797-4806.

Dupont, C. L., Johnson, D. A., Phillippy, K., Paulsen, I. T., Brahamsha, B. & Palenik, B. (2012): Genetic identification of a high-affinity Ni transporter and the transcriptional response to Ni deprivation in *Synechococcus* sp. strain WH8102. *Applied and Environmental Microbiology,* **78** (22), 7822-7832.

Dwarakanath, S., Chaplin, A. K., Hough, M. A., Rigali, S., Vijgenboom, E. & Worrall, J. A. (2012): Response to copper stress in *Streptomyces lividans* extends beyond genes under direct control of a copper-sensitive operon repressor protein (CsoR). *The Journal of Biological Chemistry,* **287** (21), 17833-17847.

Eitinger, T., Degen, O., Bohnke, U. & Muller, M. (2000): Nic1p, a relative of bacterial transition metal permeases in *Schizosaccharomyces pombe,* provides nickel ion for urease biosynthesis. *The Journal of Biological Chemistry,* **275** (24), 18029-18033.

Eitinger, T. & Friedrich, B. (1991): Cloning, nucleotide sequence, and heterologous expression of a high-affinity nickel transport gene from *Alcaligenes eutrophus*. *The Journal of Biological Chemistry,* **266** (5), 3222-3227.

Eitinger, T. & Mandrand-Berthelot, M. A. (2000): Nickel transport systems in microorganisms. *Archives of Microbiology,* **173** (1), 1-9.

Eitinger, T., Wolfram, L., Degen, O. & Anthon, C. (1997): A Ni^{2+} binding motif is the basis of high affinity transport of the *Alcaligenes eutrophus* nickel permease. *The Journal of Biological Chemistry,* **272** (27), 17139-17144.

El Baz, S., Baz, M., Barakate, M., Hassani, L., El Gharmali, A. & Imziln, B. (2015): Resistance to and accumulation of heavy metals by actinobacteria isolated from abandoned mining areas. *ScientificWorldJournal,* **2015**, 761834.

Elbing, K. & Brent, R. (2002): Media preparation and bacteriological tools. *Current Protocols in Molecular Biology,* **Chapter 1**, Unit 1.1.

Elliot, M. A., Karoonuthaisiri, N., Huang, J., Bibb, M. J., Cohen, S. N., Kao, C. M. & Buttner, M. J. (2003): The chaplins: a family of hydrophobic cell-surface proteins involved in aerial mycelium formation in *Streptomyces coelicolor*. *Genes & Development,* **17** (14), 1727-1740.

Elnahas, M. O., Amin, M. A., Hussein, M. M. D., Shanbhag, V. C., Ali, A. E. & Wall, J. D. (2017): Isolation, characterization and bioactivities of an extracellular polysaccharide produced from *Streptomyces* sp. MOE6. *Molecules,* **22** (9), 1396.

Endo, K., Kamo, K., Hosono, K., Beppu, T. & Ueda, K. (2001): Characterization of mutants defective in melanogenesis and a gene for tyrosinase of *Streptomyces griseus*. *The Journal of Antibiotics,* **54** (10), 789-796.

Evstigneeva, Z. G., Solov'eva, N. A. & Sidel'nikova, L. I. (2003): Methionine sulfoximine and phosphinothricin-glutamine synthetase inhibitors and activators and their herbicidal activity (A review). *Applied Biochemistry and Microbiology,* **39** (6), 613-618.

Faccio, G., Kruus, K., Saloheimo, M. & Thöny-Meyer, L. (2012): Bacterial tyrosinases and their applications. *Process Biochemistry,* **47** (12), 1749-1760.

Feil, H., Feil, W. S., Chain, P., Larimer, F., DiBartolo, G., Copeland, A., Lykidis, A., Trong, S., Nolan, M., Goltsman, E., Thiel, J., Malfatti, S., Loper, J. E., Lapidus, A., Detter, J. C., Land, M., Richardson, P. M., Kyrpides, N. C., Ivanova, N. & Lindow, S. E. (2005): Comparison of the complete genome sequences of *Pseudomonas syringae* pv. *syringae* B728a and pv. *tomato* DC3000. *Proceedings of the National Academy of Sciences USA,* **102** (31), 11064-11069.

Fernández-Calviño, D. & Bååth, E. (2016): Interaction between pH and Cu toxicity on fungal and bacterial performance in soil. *Soil Biology and Biochemistry,* **96**, 20-29.

Ferreira, A. A., Tette, P. A. S., Mendonça, R. C. S., Soares, A. d. S. & Carvalho, M. M. D. (2014): Detection of exopolysaccharide production and biofilm-related genes in *Staphylococcus* spp. isolated from a poultry processing plant. *Food Science and Technology (Campinas),* **34** (4), 710-716.

Festa, R. A., Jones, M. B., Butler-Wu, S., Sinsimer, D., Gerads, R., Bishai, W. R., Peterson, S. N. & Darwin, K. H. (2011): A novel copper-responsive regulon in *Mycobacterium tuberculosis*. *Molecular Microbiology,* **79** (1), 133-148.

Fischer, F., Robbe-Saule, M., Turlin, E., Mancuso, F., Michel, V., Richaud, P., Veyrier, F. J., De Reuse, H. & Vinella, D. (2016): Characterization in *Helicobacter pylori* of a nickel transporter essential for colonization that was acquired during evolution by gastric *Helicobacter* species. *PLOS Pathogens,* **12** (12), e1006018.

Flärdh, K. (2003): Essential role of DivIVA in polar growth and morphogenesis in *Streptomyces coelicolor* A3(2). *Molecular Microbiology,* **49** (6), 1523-1536.

Flardh, K. & Buttner, M. J. (2009): *Streptomyces* morphogenetics: dissecting differentiation in a filamentous bacterium. *Nature Reviews. Microbiology,* **7** (1), 36-49.

Flett, F., Mersinias, V. & Smith, C. P. (1997): High efficiency intergeneric conjugal transfer of plasmid DNA from *Escherichia coli* to methyl DNA-restricting streptomycetes. *FEMS Microbiology Letters,* **155**, 223-229.

Fogarty, R. V. & Tobin, J. M. (1996): Fungal melanins and their interactions with metals. *Enzyme and Microbial Technology,* **19** (4), 311-317.

Forrellad, M. A., McNeil, M., Santangelo Mde, L., Blanco, F. C., Garcia, E., Klepp, L. I., Huff, J., Niederweis, M., Jackson, M. & Bigi, F. (2014): Role of the Mce1 transporter in the lipid homeostasis of *Mycobacterium tuberculosis*. *Tuberculosis (Edinb),* **94** (2), 170-177.

Foster, A. W., Patterson, C. J., Pernil, R., Hess, C. R. & Robinson, N. J. (2012): Cytosolic Ni(II) sensor in cyanobacterium: nickel detection follows nickel affinity across four families of metal sensors. *The Journal of Biological Chemistry,* **287** (15), 12142-12151.

Freeman, D. J., Falkiner, F. R. & Keane, C. T. (1989): New method for detecting slime production by coagulase negative staphylococci. *Journal of Clinical Pathology,* **42** (8), 872-874.

Fu, C., Javedan, S., Moshiri, F. & Maier, R. J. (1994): Bacterial genes involved in incorporation of nickel into a hydrogenase enzyme. *Proceedings of the National Academy of Sciences USA,* **91** (11), 5099-5103.

Fujimoto, M., Chijiwa, M., Nishiyama, T., Takano, H. & Ueda, K. (2016): Developmental defect of cytochrome oxidase mutants of *Streptomyces coelicolor* A3(2). *Microbiology,* **162** (8), 1446-1455.

Fujimoto, M., Yamada, A., Kurosawa, J., Kawata, A., Beppu, T., Takano, H. & Ueda, K. (2012): Pleiotropic role of the Sco1/SenC family copper chaperone in the physiology of *Streptomyces*. *Microbial Biotechnology,* **5** (4), 477-488.

Fulkerson, J. F., Jr., Garner, R. M. & Mobley, H. L. (1998): Conserved residues and motifs in the NixA protein of *Helicobacter pylori* are critical for the high affinity transport of nickel ions. *The Journal of Biological Chemistry,* **273** (1), 235-241.

Fulkerson, J. F., Jr. & Mobley, H. L. (2000): Membrane topology of the NixA nickel transporter of *Helicobacter pylori*: two nickel transport-specific motifs within transmembrane helices II and III. *Journal of Bacteriology,* **182** (6), 1722-1730.

Gaballa, A., Cao, M. & Helmann, J. D. (2003): Two MerR homologues that affect copper induction of the *Bacillus subtilis copZA* operon. *Microbiology,* **149** (Pt 12), 3413-3421.

Gadd, G. M. (1992): Metals and microorganisms: a problem of definition. *FEMS Microbiology Letters,* **100** (1-3), 197-203.

Galili, L., Rothman, A., Kozachkov, L., Rimon, A. & Padan, E. (2002): Trans membrane domain IV is involved in ion transport activity and pH regulation of the NhaA-Na(+)/H(+) antiporter of *Escherichia coli*. *Biochemistry,* **41** (2), 609-617.

Galperin, M. Y., Moroz, O. V., Wilson, K. S. & Murzin, A. G. (2006): House cleaning, a part of good housekeeping. *Molecular Microbiology,* **59** (1), 5-19.

Garber, M. E., Rajeev, L., Kazakov, A. E., Trinh, J., Masuno, D., Thompson, M. G., Kaplan, N., Luk, J., Novichkov, P. S. & Mukhopadhyay, A. (2018): Multiple signaling systems target a core set of transition metal homeostasis genes using similar binding motifs. *Molecular Microbiology,* **107** (6), 704-717.

García-Domínguez, M., Lopez-Maury, L., Florencio, F. J. & Reyes, J. C. (2000): A gene cluster involved in metal homeostasis in the cyanobacterium *Synechocystis* sp. strain PCC 6803. *Journal of Bacteriology,* **182** (6), 1507-1514.

García-Rivera, J. & Casadevall, A. (2001): Melanization of *Cryptococcus neoformans* reduces its susceptibility to the antimicrobial effects of silver nitrate. *Medical Mycology,* **39** (4), 353-357.

Gasteiger, E., Hoogland, C., Gattiker, A., Duvaud, S. e., Wilkins, M. R., Appel, R. D. & Bairoch, A. (2005): Protein identification and analysis tools on the ExPASy server. -In Walker, J. M. (Eds.): *The Proteomics Protocols Handbook*. Humana Press, Totowa, NJ, pp 571-607.

Gerchman, Y., Olami, Y., Rimon, A., Taglicht, D., Schuldiner, S. & Padan, E. (1993): Histidine-226 is part of the pH sensor of NhaA, a Na^+/H^+ antiporter in *Escherichia coli*. *Proceedings of the National Academy of Sciences of the United States of America,* **90** (4), 1212-1216.

Gerchman, Y., Rimon, A. & Padan, E. (1999): A pH-dependent conformational change of NhaA Na(+)/H(+) antiporter of *Escherichia coli* involves loop VIII-IX, plays a role in the pH response of the protein, and is maintained by the pure protein in dodecyl maltoside. *The Journal of Biological Chemistry,* **274** (35), 24617-24624.

Gerchman, Y., Rimon, A., Venturi, M. & Padan, E. (2001): Oligomerization of NhaA, the Na^+/H^+ antiporter of *Escherichia coli* in the membrane and its functional and structural consequences. *Biochemistry,* **40** (11), 3403-3412.

Gerdes, S. Y., Scholle, M. D., Campbell, J. W., Balázsi, G., Ravasz, E., Daugherty, M. D., Somera, A. L., Kyrpides, N. C., Anderson, I., Gelfand, M. S., Bhattacharya, A., Kapatral, V., D'Souza, M., Baev, M. V., Grechkin, Y., Mseeh, F., Fonstein, M. Y., Overbeek, R., Barabási, A. L., Oltvai, Z. N. & Osterman, A. L. (2003): Experimental determination and system level analysis of essential genes in *Escherichia coli* MG1655. *Journal of Bacteriology,* **185** (19), 5673-5684.

Geslin, C., Llanos, J., Prieur, D. & Jeanthon, C. (2001): The manganese and iron superoxide dismutases protect *Escherichia coli* from heavy metal toxicity. *Research in Microbiology,* **152** (10), 901-905.

Ghinet, M. G., Bordeleau, E., Beaudin, J., Brzezinski, R., Roy, S. & Burrus, V. (2011): Uncovering the prevalence and diversity of integrating conjugative elements in actinobacteria. *PLoS ONE,* **6** (11), e27846.

Gil, R., Sabater-Munoz, B., Latorre, A., Silva, F. J. & Moya, A. (2002): Extreme genome reduction in *Buchnera* spp.: toward the minimal genome needed for symbiotic life. *Proceedings of the National Academy of Sciences USA,* **99** (7), 4454-4458.

Gill, H. S. & Eisenberg, D. (2001): The crystal structure of phosphinothricin in the active site of glutamine synthetase illuminates the mechanism of enzymatic inhibition. *Biochemistry,* **40** (7), 1903-1912.

Gillings, M. R. & Stokes, H. W. (2012): Are humans increasing bacterial evolvability? *Trends in Ecology & Evolution,* **27** (6), 346-352.

Goessweiner-Mohr, N., Arends, K., Keller, W. & Grohmann, E. (2014): Conjugation in gram-positive bacteria. *Microbiology Spectrum,* **2** (4), Plas-0004-2013.

Gonzalez-Guerrero, M. & Arguello, J. M. (2008): Mechanism of Cu^+-transporting ATPases: soluble Cu^+ chaperones directly transfer Cu^+ to transmembrane transport sites. *Proceedings of the National Academy of Sciences USA,* **105** (16), 5992-5997.

Gonzalez-Guerrero, M., Raimunda, D., Cheng, X. & Arguello, J. M. (2010): Distinct functional roles of homologous Cu^+ efflux ATPases in *Pseudomonas aeruginosa*. *Molecular Microbiology,* **78** (5), 1246-1258.

Goulian, M., Bleile, B. & Tseng, B. Y. (1980): Methotrexate-induced misincorporation of uracil into DNA. *Proceedings of the National Academy of Sciences USA,* **77** (4), 1956-1960.

Graham, D. G., Tiffany, S. M. & Vogel, F. S. (1978): The toxicity of melanin precursors. *Journal of Investigative Dermatologyl,* **70** (2), 113-116.

Grass, G., Fan, B., Rosen, B. P., Lemke, K., Schlegel, H. G. & Rensing, C. (2001): NreB from *Achromobacter xylosoxidans* 31A Is a nickel-induced transporter conferring nickel resistance. *Journal of Bacteriology,* **183** (9), 2803-2807.

Grass, G., Franke, S., Taudte, N., Nies, D. H., Kucharski, L. M., Maguire, M. E. & Rensing, C. (2005): The metal permease ZupT from *Escherichia coli* is a transporter with a broad substrate spectrum. *Journal of Bacteriology,* **187** (5), 1604-1611.

Grass, G., Große, C. & Nies, D. H. (2000): Regulation of the *cnr* cobalt and nickel resistance determinant from *Ralstonia* sp. strain CH34. *Journal of Bacteriology,* **182** (5), 1390-1398.

Green, B., Bouchier, C., Fairhead, C., Craig, N. L. & Cormack, B. P. (2012): Insertion site preference of Mu, Tn5, and Tn7 transposons. *Mobile DNA,* **3** (1), 3.

Grégoire, D. S. & Poulain, A. J. (2016): A physiological role for HgII during phototrophic growth. *Nature Geoscience,* **9**, 121-125.

Gregory, K. F. & Huang, J. C. (1964): Tyrosinase inheritance in *Streptomyces scabies* I. Genetic recombination. *Journal of Bacteriology,* **87**, 1281-1286.

Grinstein, S., Woodside, M., Sardet, C., Pouyssegur, J. & Rotin, D. (1992): Activation of the Na^+/H^+ antiporter during cell volume regulation. Evidence for a phosphorylation-independent mechanism. *The Journal of Biological Chemistry,* **267** (33), 23823-23828.

Grohmann, E., Muth, G. & Espinosa, M. (2003): Conjugative plasmid transfer in gram-positive bacteria. *Microbiology and Molecular Biology Reviews,* **67** (2), 277-301.

Groth, A. C., Olivares, E. C., Thyagarajan, B. & Calos, M. P. (2000): A phage integrase directs efficient site-specific integration in human cells. *Proceedings of the National Academy of Sciences USA,* **97** (11), 5995-6000.

Gudipaty, S. A., Larsen, A. S., Rensing, C. & McEvoy, M. M. (2012): Regulation of Cu(I)/Ag(I) efflux genes in *Escherichia coli* by the sensor kinase CusS. *FEMS Microbiology Letters,* **330** (1), 30-37.

Guerra, A. J. & Giedroc, D. P. (2012): Metal site occupancy and allosteric switching in bacterial metal sensor proteins. *Archives of Biochemistry and Biophysics,* **519** (2), 210-222.

Guffanti, A. A., Cohn, D. E., Kaback, H. R. & Krulwich, T. A. (1981): Relationship between the Na^+/H^+ antiporter and Na^+/substrate symport in *Bacillus alcalophilus*. *Proceedings of the National Academy of Sciences USA,* **78** (3), 1481-1484.

Gupta, A. & Lutsenko, S. (2009): Human copper transporters: mechanism, role in human diseases and therapeutic potential. *Future Medicinal Chemistry,* **1** (6), 1125-1142.

Gust, B., Challis, G. L., Fowler, K., Kieser, T. & Chater, K. F. (2003): PCR-targeted *Streptomyces* gene replacement identifies a protein domain needed for biosynthesis of the sesquiterpene soil odor geosmin. *Proceedings of the National Academy of Sciences USA,* **100** (4), 1541-1546.

Ha, H. S., Hwang, Y. I. & Choi, S. U. (2008): Application of conjugation using phiC31 *att/int* system for *Actinoplanes teichomyceticus*, a producer of teicoplanin. *Biotechnology Letters,* **30** (7), 1233-1238.

Haferburg, G., Kloess, G., Schmitz, W. & Kothe, E. (2008): "Ni-struvite" - a new biomineral formed by a nickel resistant *Streptomyces acidiscabies*. *Chemosphere,* **72** (3), 517-523.

Haferburg, G. & Kothe, E. (2007): Microbes and metals: interactions in the environment. *Journal of Basic Microbiology,* **47** (6), 453-467.

Haghdoost, S., Sjölander, L., Czene, S. & Harms-Ringdahl, M. (2006): The nucleotide pool is a significant target for oxidative stress. *Free Radical Biology and Medicine,* **41** (4), 620-626.

Hall, T. A. (1999): BioEdit: a user-friendly biological sequence alignment editor and analysis program for Windows 95/98/NT. *Nucleic Acids Symposium Series,* **41**, 95-98.

Hanahan, D. (1983): Studies on transformation of *Escherichia coli* with plasmids. *Journal of Molecular Biology,* **166** (4), 557-580.

Harada, H., Shibuya, K. & Hiraoka, M. (2006): Combinations of antimetabolites and ionizing radiation. -In Brown, J. M., Mehta, M. P. & Nieder, C. (Eds.): *Multimodal Concepts for Integration of Cytotoxic Drugs.* Springer Berlin Heidelberg, Berlin, Heidelberg, pp 19-34.

Hayakawa, T., Tanaka, T., Sakaguchi, K., Otake, N. & Yonehara, H. (1979): A linear plasmid-like DNA in *Streptomyces* sp. producing lankacidin group antibiotics. *The Journal of General and Applied Microbiology,* **25** (4), 255-260.

Hebbeln, P. & Eitinger, T. (2004): Heterologous production and characterization of bacterial nickel/cobalt permeases. *FEMS Microbiology Letters,* **230** (1), 129-135.

Helmann, J. D. & Chamberlin, M. J. (1988): Structure and function of bacterial sigma factors. *Annual Review of Biochemistry,* **57**, 839-872.

Hempel, A. M., Wang, S. B., Letek, M., Gil, J. A. & Flardh, K. (2008): Assemblies of DivIVA mark sites for hyphal branching and can establish new zones of cell wall growth in *Streptomyces coelicolor*. *Journal of Bacteriology,* **190** (22), 7579-7583.

Hentchel, K. L. & Escalante-Semerena, J. C. (2015): In *Salmonella enterica*, the Gcn5-related acetyltransferase MddA (formerly YncA) acetylates methionine sulfoximine and methionine sulfone, blocking their toxic effects. *Journal of Bacteriology,* **197** (2), 314-325.

Herron, P. R., Hughes, G., Chandra, G., Fielding, S. & Dyson, P. J. (2004): Transposon Express, a software application to report the identity of insertions obtained by comprehensive transposon mutagenesis of sequenced genomes: analysis of the preference for *in vitro* Tn5 transposition into GC-rich DNA. *Nucleic Acids Research,* **32** (14), e113.

Herth, W. & Schnepf, E. (1980): The fluorochrome, calcofluor white, binds oriented to structural polysaccharide fibrils. *Protoplasma,* **105** (1), 129-133.

Herzberg, M., Bauer, L., Kirsten, A. & Nies, D. H. (2016): Interplay between seven secondary metal uptake systems is required for full metal resistance of *Cupriavidus metallidurans*. *Metallomics,* **8** (3), 313-326.

Heuer, H., Fox, R. E. & Top, E. M. (2007): Frequent conjugative transfer accelerates adaptation of a broad-host-range plasmid to an unfavorable *Pseudomonas putida* host. *FEMS Microbiology Ecology,* **59** (3), 738-748.

Heuer, H. & Smalla, K. (2007): Horizontal gene transfer between bacteria. *Environmental Biosafety Research,* **6** (1-2), 3-13.

Hintermann, G., Zatchej, M. & Hutter, R. (1985): Cloning and expression of the genetically unstable tyrosinase structural gene from *Streptomyces glaucescens*. *Molecular & General Genetics,* **200** (3), 422-432.

Hirano, T. & Tamae, K. (2010): Heavy metal-induced oxidative DNA damage in earthworms: a review. *Applied and Environmental Soil Science,* **2010**, 1-7.

Hizi, A., Kamath-Loeb, A. S., Rose, K. D. & Loeb, L. A. (1997): Mutagenesis by human immunodeficiency virus reverse transcriptase: incorporation of O6-methyldeoxyguanosine triphosphate. *Mutation Research,* **374** (1), 41-50.

Holmes, N. A., Walshaw, J., Leggett, R. M., Thibessard, A., Dalton, K. A., Gillespie, M. D., Hemmings, A. M., Gust, B. & Kelemen, G. H. (2013): Coiled-coil protein Scy is a key component of a multiprotein assembly controlling polarized growth in *Streptomyces*. *Proceedings of the National Academy of Sciences USA,* **110** (5), E397-406.

Hopwood, D. A., Kieser, T., Wright, H. M. & Bibb, M. J. (1983): Plasmids, recombination and chromosome mapping in *Streptomyces lividans* 66. *Journal of General Microbiology,* **129**, 2257-2269.

Horbal, L., Fedorenko, V., Bechthold, A. & Luzhetskyy, A. (2013): A transposon-based strategy to identify the regulatory gene network responsible for landomycin E biosynthesis. *FEMS Microbiology Letters,* **342** (2), 138-146.

Hosted, T. J., Wang, T. & Horan, A. C. (2004): Characterization of the *Streptomyces lavendulae* IMRU 3455 linear plasmid pSLV45. *Microbiology,* **150** (6), 1819-1827.

Hu, Z., Hopwood, D. A. & Khosla, C. (2000): Directed transfer of large DNA fragments between *Streptomyces* species. *Applied and Environmental Microbiology,* **66** (5), 2274–2277.

Huang, C. H., Chen, C. Y., Tsai, H. H., Chen, C., Lin, Y. S. & Chen, C. W. (2003): Linear plasmid SLP2 of *Streptomyces lividans* is a composite replicon. *Molecular Microbiology,* **47** (6), 1563-1576.

Huber, M., Hintermann, G. & Lerch, K. (1985): Primary structure of tyrosinase from *Streptomyces glaucescens*. *Biochemistry,* **24** (22), 6038-6044.

Hunte, C., Screpanti, E., Venturi, M., Rimon, A., Padan, E. & Michel, H. (2005): Structure of a Na^+/H^+ antiporter and insights into mechanism of action and regulation by pH. *Nature,* **435** (7046), 1197-1202.

Hutnik, N., Wierzbowska, B., Piotrowski, K. & Matynia, A. (2013): Effect of copper (II) ions on quality of struvite produced in continuous reaction crystallization process at the magnesium ions excess. *Advances in Chemical Engineering and Science,* **03** (04), 1-6.

Ignatova-Ivanova, T. (2017): Exopolysaccharides from bacteria with novel application. -In Metodiev, K. (Eds.): *Immunotherapy - Myths, Reality, Ideas, Future.* IntechOpen, pp 345-354.

Ikeda, K., Masujima, T., Suzuki, K. & Sugiyama, M. (1996): Cloning and sequence analysis of the highly expressed melanin-synthesizing gene operon from *Streptomyces castaneoglobisporus*. *Applied Microbiology and Biotechnology,* **45** (1-2), 80-85.

Imlay, J. A. (2008): Cellular defenses against superoxide and hydrogen peroxide. *Annual Review of Biochemistry,* **77**, 755-776.

Inaba, K., Kuroda, T., Shimamoto, T., Kayahara, T., Tsuda, M. & Tsuchiya, T. (1994): Lithium toxicity and $Na^+(Li^+)/H^+$ antiporter in *Escherichia coli*. *Biological and Pharmaceutical Bulletin,* **17** (3), 395-398.

Inoue, H., Noumi, T., Tsuchiya, T. & Kanazawa, H. (1995): Essential aspartic acid residues, Asp-133, Asp-163 and Asp-164, in the transmembrane helices of a Na^+/H^+ antiporter (NhaA) from *Escherichia coli*. *FEBS Letters,* **363** (3), 264-268.

Inoue, H., Sakurai, T., Ujike, S., Tsuchiya, T., Murakami, H. & Kanazawa, H. (1999): Expression of functional Na^+/H^+ antiporters of *Helicobacter pylori* in antiporter-deficient *Echerichia coli* mutants. *FEBS Letters,* **443** (1), 11-16.

Inoue, H., Tsuboi, Y. & Kanazawa, H. (2001): Chimeric Na(+)/H(+) antiporters constructed from NhaA of *Helicobacter pylori* and *Escherichia coli*: implications for domains of NhaA for pH sensing. *Journal of Biochemistry,* **129** (4), 569-576.

Irnich, S. & Cullum, J. (1993): Random insertion of Tn4560 in *Streptomyces lividans* and *Streptomyces avermitilis*. *Biotechnology Letters,* **15** (9), 895-900.

Ivey, D. M., Guffanti, A. A., Zemsky, J., Pinner, E., Karpel, R., Padan, E., Schuldiner, S. & Krulwich, T. A. (1993): Cloning and characterization of a putative Ca^{2+}/H^+ antiporter gene from *Escherichia coli* upon functional complementation of Na^+/H^+ antiporter-deficient strains by the overexpressed gene. *The Journal of Biological Chemistry,* **268** (15), 11296-11303.

Izano, E. A., Sadovskaya, I., Vinogradov, E., Mulks, M. H., Velliyagounder, K., Ragunath, C., Kher, W. B., Ramasubbu, N., Jabbouri, S., Perry, M. B. & Kaplan, J. B. (2007): Poly-N-acetylglucosamine mediates biofilm formation and antibiotic resistance in *Actinobacillus pleuropneumoniae*. *Microbial Pathogenesis,* **43** (1), 1-9.

Izano, E. A., Sadovskaya, I., Wang, H., Vinogradov, E., Ragunath, C., Ramasubbu, N., Jabbouri, S., Perry, M. B. & Kaplan, J. B. (2008): Poly-N-acetylglucosamine mediates biofilm formation and detergent resistance in *Aggregatibacter actinomycetemcomitans*. *Microbial Pathogenesis,* **44** (1), 52-60.

Jardetzky, O. (1966): Simple allosteric model for membrane pumps. *Nature,* **211** (5052), 969-970.

Jones, G. H. (1985): Regulation of phenoxazinone synthase expression in *Streptomyces antibioticus*. *Journal of Bacteriology,* **163** (3), 1215-1221.

Kall, L., Krogh, A. & Sonnhammer, E. L. (2007): Advantages of combined transmembrane topology and signal peptide prediction--the Phobius web server. *Nucleic Acids Research,* **35** (Web Server issue), W429-432.

Kaluarachchi, H., Siebel, J. F., Kaluarachchi-Duffy, S., Krecisz, S., Sutherland, D. E., Stillman, M. J. & Zamble, D. B. (2011): Metal selectivity of the *Escherichia coli* nickel metallochaperone, SlyD. *Biochemistry,* **50** (49), 10666-10677.

Kamiya, H. (2003): Mutagenic potentials of damaged nucleic acids produced by reactive oxygen/nitrogen species: approaches using synthetic oligonucleotides and nucleotides: survey and summary. *Nucleic Acids Research,* **31** (2), 517-531.

Kang, J. G., Hahn, M. Y., Ishihama, A. & Roe, J. H. (1997): Identification of sigma factors for growth phase-related promoter selectivity of RNA polymerases from *Streptomyces coelicolor* A3(2). *Nucleic Acids Research,* **25** (13), 2566-2573.

Kapoor, V., Li, X., Elk, M., Chandran, K., Impellitteri, C. A. & Santo Domingo, J. W. (2015): Impact of heavy metals on transcriptional and physiological activity of nitrifying bacteria. *Environmental Science & Technology,* **49** (22), 13454-13462.

Kasprzak, K. S. (2011): Role of oxidative damage in metal-induced carcinogenesis. -In Banfalvi, G. (Eds.): *Cellular Effects of Heavy Metals.* Springer, Heidelberg, pp 237-259.

Kataoka, M., Seki, T. & Yoshida, T. (1991): Five genes involved in self-transmission of pSN22, a *Streptomyces* plasmid. *Journal of Bacteriology,* **173** (13), 4220-4228.

Katoh, K., Rozewicki, J. & Yamada, K. D. (2017): MAFFT online service: multiple sequence alignment, interactive sequence choice and visualization. *Brief Bioinform*.

Kazakov, T., Kuznedelov, K., Semenova, E., Mukhamedyarov, D., Datsenko, K. A., Metlitskaya, A., Vondenhoff, G. H., Tikhonov, A., Agarwal, V., Nair, S., Van Aerschot, A. & Severinov, K. (2014): The RimL transacetylase provides resistance to translation inhibitor microcin C. *Journal of Bacteriology,* **196** (19), 3377-3385.

Keen, C. L., Mendelovitz, S., Cohen, G., Aharonowitz, Y. & Roy, K. L. (1988): Isolation and characterization of a linear DNA plasmid from *Streptomyces clavuligerus*. *Molecular & General Genetics,* **212** (1), 172-176.

Keijser, B. J., van Wezel, G. P., Canters, G. W., Kieser, T. & Vijgenboom, E. (2000): The *ram*-dependence of *Streptomyces lividans* differentiation is bypassed by copper. *Journal of Molecular Microbiology and Biotechnology,* **2** (4), 565-574.

Kelemen, G. H., Brown, G. L., Kormanec, J., Potuckova, L., Chater, K. F. & Buttner, M. J. (1996): The positions of the sigma-factor genes, *whiG* and *sigF*, in the hierarchy controlling the development of spore chains in the aerial hyphae of *Streptomyces coelicolor* A3(2). *Molecular Microbiology,* **21** (3), 593-603.

Kendall, K. J. & Cohen, S. N. (1988): Complete nucleotide sequence of the *Streptomyces lividans* plasmid pIJ101 and correlation of the sequence with genetic properties. *Journal of Bacteriology,* **170** (10), 4634-4651.

Kendall, S. L., Burgess, P., Balhana, R., Withers, M., Ten Bokum, A., Lott, J. S., Gao, C., Uhia-Castro, I. & Stoker, N. G. (2010): Cholesterol utilization in mycobacteria is controlled by two TetR-type transcriptional regulators: *kstR* and *kstR2*. *Microbiology,* **156** (Pt 5), 1362-1371.

Kershaw, C. J., Brown, N. L. & Hobman, J. L. (2007): Zinc dependence of *zinT* (*yodA*) mutants and binding of zinc, cadmium and mercury by ZinT. *Biochemical and Biophysical Research Communications,* **364** (1), 66-71.

Kieser, T., Foundation, J. I., Bibb, M. J., Buttner, M. J., Chater, K. F. & Hopwood, D. A. (2000): Practical *Streptomyces* genetics. John Innes Foundation, Norwich, UK, pp 613.

Kieser, T., Hopwood, D. A., Wright, H. M. & Thompson, C. J. (1982): pIJ101, a multi-copy broad host-range *Streptomyces* plasmid: functional analysis and development of DNA cloning vectors. *Molecular & General Genetics,* **185** (2), 223-228.

Kihlken, M. A., Leech, A. P. & Le Brun, N. E. (2002): Copper-mediated dimerization of CopZ, a predicted copper chaperone from *Bacillus subtilis*. *The Biochemical Journal,* **368** (Pt 3), 729-739.

Kim, E. J., Chung, H. J., Suh, B., Hah, Y. C. & Roe, J. H. (1998): Transcriptional and post-transcriptional regulation by nickel of *sodN* gene encoding nickel-containing superoxide dismutase from *Streptomyces coelicolor* Müller. *Molecular Microbiology,* **27** (1), 187-195.

Kim, H. M., Ahn, B. E., Lee, J. H. & Roe, J. H. (2015): Regulation of a nickel-cobalt efflux system and nickel homeostasis in a soil actinobacterium *Streptomyces coelicolor*. *Metallomics,* **7** (4), 702-709.

Kim, J.-S., Kang, S.-O. & Lee, J. K. (2003): The protein complex composed of nickel-binding SrnQ and DNA binding motif-bearing SrnR of *Streptomyces griseus* represses *sodF* transcription in the presence of nickel. *Journal of Biological Chemistry,* **278** (20), 18455-18463.

Kim, M. K., Ha, H. S. & Choi, S. U. (2008a): Conjugal transfer using the bacteriophage phiC31 *att/int* system and properties of the *attB* site in *Streptomyces ambofaciens*. *Biotechnology Letters,* **30** (4), 695-699.

Kim, Y. J., Moon, M. H., Lee, J. S., Hong, S.-K. & Chang, Y. K. (2011): Roles of putative sodium-hydrogen antiporter (*sha*) genes in *S. coelicolor* A3(2) culture with pH variation. *Journal of Microbiology and Biotechnology,* **21** (9), 979-987.

Kim, Y. J., Song, J. Y., Hong, S. K., Smith, C. P. & Chang, Y. K. (2008b): Effects of pH shock on the secretion system in *Streptomyces coelicolor* A3(2). *Journal of Microbiology and Biotechnology,* **18** (4), 658-662.

Kinashi, H., Mori, E., Hatani, A. & Nimi, O. (1994): Isolation and characterization of linear plasmids from lankacidin-producing *Streptomyces* species. *The Journal of Antibiotics,* **47** (12), 1447-1455.

Kirsten, A., Herzberg, M., Voigt, A., Seravalli, J., Grass, G., Scherer, J. & Nies, D. H. (2011): Contributions of five secondary metal uptake systems to metal homeostasis of *Cupriavidus metallidurans* CH34. *Journal of Bacteriology,* **193** (18), 4652-4663.

Kitani, S., Bibb, M. J., Nihira, T. & Yamada, Y. (2000): Conjugal transfer of plasmid DNA from *Escherichia coli* to *Streptomyces lavendulae* FRI-5. *Journal of Microbiology and Biotechnology,* **10** (4), 535-538.

Klepp, L. I., Forrellad, M. A., Osella, A. V., Blanco, F. C., Stella, E. J., Bianco, M. V., Santangelo Mde, L., Sassetti, C., Jackson, M., Cataldi, A. A., Bigi, F. & Morbidoni, H. R. (2012): Impact of the deletion of the six *mce* operons in *Mycobacterium smegmatis*. *Microbes and Infection,* **14** (7-8), 590-599.

Klumper, U., Dechesne, A., Riber, L., Brandt, K. K., Gulay, A., Sorensen, S. J. & Smets, B. F. (2017): Metal stressors consistently modulate bacterial conjugal plasmid uptake potential in a phylogenetically conserved manner. *ISME Journal,* **11** (1), 152-165.

Kodani, S., Hudson, M. E., Durrant, M. C., Buttner, M. J., Nodwell, J. R. & Willey, J. M. (2004): The SapB morphogen is a lantibiotic-like peptide derived from the product of the developmental gene *ramS* in *Streptomyces coelicolor*. *Proceedings of the National Academy of Sciences USA,* **101** (31), 11448-11453.

Kojic, M., Topisirovic, L. & Vasiljevic, B. (1991): Efficient transformation of *Micromonospora melanosporea* protoplasts by *Streptomyces* plasmid. *Current Microbiology,* **23** (6), 343-345.

Koledin, T., Newton, G. L. & Fahey, R. C. (2002): Identification of the mycothiol synthase gene (*mshD*) encoding the acetyltransferase producing mycothiol in actinomycetes. *Archives of Microbiology,* **178** (5), 331-337.

Komeda, H., Kobayashi, M. & Shimizu, S. (1997): A novel transporter involved in cobalt uptake. *Proceedings of the National Academy of Sciences USA,* **94** (1), 36-41.

Kondo, Y., Shomura, T., Ogawa, Y., Tsuruoka, T., Watanabe, H., Totukawa, K., Suzuki, T., Moriyama, C., Yoshida, J., Inouye, S. & Niida, T. (1973): Studies on a new antibiotic SF-/293. 1. Isolation and physico-chemical and biological characterization of SF-1293 substances. *Scientific Reports of Meiji Seika Kaisha,* **13**, 34-41.

Koonin, E. V. & Tatusov, R. L. (1994): Computer analysis of bacterial haloacid dehalogenases defines a large superfamily of hydrolases with diverse specificity. Application of an iterative approach to database search. *Journal of Molecular Biology,* **244** (1), 125-132.

Kosono, S., Ohashi, Y., Kawamura, F., Kitada, M. & Kudo, T. (2000): Function of a principal Na(+)/H(+) antiporter, ShaA, is required for initiation of sporulation in *Bacillus subtilis*. *Journal of Bacteriology,* **182** (4), 898-904.

Kothe, E., Bergmann, H. & Büchel, G. (2005): Molecular mechanisms in bio-geo-interactions: From a case study to general mechanisms. *Chemie der Erde - Geochemistry,* **65**, 7-27.

Kouzminova, E. A. & Kuzminov, A. (2004): Chromosomal fragmentation in dUTPase-deficient mutants of *Escherichia coli* and its recombinational repair. *Molecular Microbiology,* **51** (5), 1279-1295.

Kragh-Hansen, U., le Maire, M. & Moller, J. V. (1998): The mechanism of detergent solubilization of liposomes and protein-containing membranes. *Biophysical Journal,* **75** (6), 2932-2946.

Krulwich, T. A., Sachs, G. & Padan, E. (2011): Molecular aspects of bacterial pH sensing and homeostasis. *Nature Reviews. Microbiology,* **9** (5), 330-343.

Kuchar, J. & Hausinger, R. P. (2004): Biosynthesis of metal sites. *Chemical Reviews,* **104** (2), 509-525.

Kuhstoss, S., Richardson, M. A. & Rao, R. N. (1991): Plasmid cloning vectors that integrate site-specifically in *Streptomyces* spp. *Gene,* **97**, 143-146.

Kuroda, T., Mizushima, T. & Tsuchiya, T. (2005): Physiological roles of three Na^+/H^+ antiporters in the halophilic bacterium *Vibrio parahaemolyticus*. *Microbiology and Immunology,* **49** (8), 711-719.

Kurz, M., Brunig, A. N. & Galinski, E. A. (2006): NhaD type sodium/proton-antiporter of *Halomonas elongata*: a salt stress response mechanism in marine habitats? *Saline Systems,* **2**, 10.

Kuwabara, N., Inoue, H., Tsuboi, Y., Mitsui, K., Matsushita, M. & Kanazawa, H. (2006): Structure−function relationship of the fifth transmembrane domain in the Na^+/H^+ antiporter of *Helicobacter pylori*: Topology and function of the residues, including two consecutive essential aspartate residues. *Biochemistry,* **45** (49), 14834-14842.

Kuznetsova, E., Proudfoot, M., Gonzalez, C. F., Brown, G., Omelchenko, M. V., Borozan, I., Carmel, L., Wolf, Y. I., Mori, H., Savchenko, A. V., Arrowsmith, C. H., Koonin, E. V., Edwards, A. M. & Yakunin, A. F. (2006): Genome-wide analysis of substrate specificities of the *Escherichia coli* haloacid dehalogenase-like phosphatase family. *The Journal of Biological Chemistry,* **281** (47), 36149-36161.

Kyte, J. & Doolittle, R. F. (1982): A simple method for displaying the hydropathic character of a protein. *Journal of Molecular Biology,* **157** (1), 105-132.

Lampe, D. J., Churchill, M. E. & Robertson, H. M. (1996): A purified *mariner* transposase is sufficient to mediate transposition *in vitro*. *The EMBO Journal,* **15** (19), 5470-5479.

Lampe, D. J., Grant, T. E. & Robertson, H. M. (1998): Factors affecting transposition of the *Himar1 mariner* transposon *in vitro*. *Genetics,* **149** (1), 179-187.

Lancaster, W. A., Menon, A. L., Scott, I., Poole, F. L., Vaccaro, B. J., Thorgersen, M. P., Geller, J., Hazen, T. C., Hurt, R. A., Jr., Brown, S. D., Elias, D. A. & Adams, M. W. (2014): Metallomics of two microorganisms relevant to heavy metal bioremediation reveal fundamental differences in metal assimilation and utilization. *Metallomics,* **6** (5), 1004-1013.

Lanoue, A., Burlat, V., Schurr, U. & Röse, U. S. R. (2010): Induced root-secreted phenolic compounds as a belowground plant defense. *Plant signaling & behavior,* **5** (8), 1037-1038.

Le Breton, Y., Mohapatra, N. P. & Haldenwang, W. G. (2006): *In vivo* random mutagenesis of *Bacillus subtilis* by use of TnYLB-1, a *mariner*-based transposon. *Applied and Environmental Microbiology,* **72** (1), 327-333.

Lederberg, J. & Tatum, E. L. (1946): Gene recombination in *Escherichia coli*. *Nature,* **158** (4016), 558.

Lee, E. J., Karoonuthaisiri, N., Kim, H. S., Park, J. H., Cha, C. J., Kao, C. M. & Roe, J. H. (2005): A master regulator sigmaB governs osmotic and oxidative response as well as differentiation *via* a network of sigma factors in *Streptomyces coelicolor*. *Molecular Microbiology,* **57** (5), 1252-1264.

Lee, H. H., Hsu, C. C., Lin, Y. L. & Chen, C. W. (2011): Linear plasmids mobilize linear but not circular chromosomes in *Streptomyces*: support for the 'end first' model of conjugal transfer. *Microbiology,* **157** (9), 2556-2568.

Lee, Y. K., Chang, H. H., Lee, H. J., Park, H., Lee, K. H. & Joe, M. H. (2006): Isolation of a novel plasmid, pNi15, from *Enterobacter* sp. Ni15 containing a nickel resistance gene. *FEMS Microbiology Letters,* **257** (2), 177-181.

Lenarcic, R., Halbedel, S., Visser, L., Shaw, M., Wu, L. J., Errington, J., Marenduzzo, D. & Hamoen, L. W. (2009): Localisation of DivIVA by targeting to negatively curved membranes. *The EMBO Journal,* **28** (15), 2272-2282.

Lentes, C. J., Mir, S. H., Boehm, M., Ganea, C., Fendler, K. & Hunte, C. (2014): Molecular characterization of the Na^+/H^+-antiporter NhaA from *Salmonella* Typhimurium. *PLoS ONE,* **9** (7), e101575.

Lerch, K. & Ettinger, L. (1972): Purification and characterization of a tyrosinase from *Streptomyces glaucescens*. *European Journal of Biochemistry,* **31** (3), 427-437.

Leu, W. M., Chen, L. Y., Liaw, L. L. & Lee, Y. H. (1992): Secretion of the *Streptomyces* tyrosinase is mediated through its *trans*-activator protein, MelC1. *The Journal of Biological Chemistry,* **267** (28), 20108-20113.

Levine, R. L., Oliver, C. N., Fulks, R. M. & Stadtman, E. R. (1981): Turnover of bacterial glutamine synthetase: oxidative inactivation precedes proteolysis. *Proceedings of the National Academy of Sciences USA,* **78** (4), 2120-2124.

Lewinson, O., Padan, E. & Bibi, E. (2004): Alkalitolerance: a biological function for a multidrug transporter in pH homeostasis. *Proceedings of the National Academy of Sciences USA,* **101** (39), 14073-14078.

Li, J., Wang, J. T., Hu, H. W., Ma, Y. B., Zhang, L. M. & He, J. Z. (2016): Copper pollution decreases the resistance of soil microbial community to subsequent dry-rewetting disturbance. *Journal of Environmental Sciences,* **39**, 155-164.

Li, X., Zhou, X. & Deng, Z. (2003): Vector systems allowing efficient autonomous or integrative gene cloning in *Micromonospora* sp. strain 40027. *Applied and Environmental Microbiology,* **69** (6), 3144-3151.

Liesegang, H., Lemke, K., Siddiqui, R. A. & Schlegel, H. G. (1993): Characterization of the inducible nickel and cobalt resistance determinant cnr from pMOL28 of *Alcaligenes eutrophus* CH34. *Journal of Bacteriology,* **175** (3), 767-778.

Lim, C. K. & Cooksey, D. A. (1993): Characterization of chromosomal homologs of the plasmid-borne copper resistance operon of *Pseudomonas syringae*. *Journal of Bacteriology,* **175** (14), 4492-4498.

Liman, R., Facey, P. D., van Keulen, G., Dyson, P. J. & Del Sol, R. (2013): A laterally acquired galactose oxidase-like gene is required for aerial development during osmotic stress in *Streptomyces coelicolor*. *PLoS ONE,* **8** (1), e54112.

Lin, S. J., Pufahl, R. A., Dancis, A., O'Halloran, T. V. & Culotta, V. C. (1997): A role for the *Saccharomyces cerevisiae* ATX1 gene in copper trafficking and iron transport. *The Journal of Biological Chemistry,* **272** (14), 9215-9220.

Lin, Y. S., Kieser, H. M., Hopwood, D. A. & Chen, C. W. (1993): The chromosomal DNA of *Streptomyces lividans* 66 is linear. *Molecular Microbiology,* **10** (5), 923-933.

Linder, T. (2018): Evaluation of the chitin-binding dye Congo red as a selection agent for the isolation, classification, and enumeration of ascomycete yeasts. *Archives of Microbiology,* **200** (4), 671-675.

Liu, J., Xue, Y., Wang, Q., Wei, Y., Swartz, T. H., Hicks, D. B., Ito, M., Ma, Y. & Krulwich, T. A. (2005): The activity profile of the NhaD-type $Na^+(Li^+)/H^+$ antiporter from the soda lake haloalkaliphile *Alkalimonas amylolytica* is adaptive for the extreme environment. *Journal of Bacteriology,* **187** (22), 7589-7595.

Liu, T., Ramesh, A., Ma, Z., Ward, S. K., Zhang, L., George, G. N., Talaat, A. M., Sacchettini, J. C. & Giedroc, D. P. (2007): CsoR is a novel *Mycobacterium tuberculosis* copper-sensing transcriptional regulator. *Nature Chemical Biology,* **3** (1), 60-68.

Lodewyckx, C., Taghavi, S., Mergeay, M., Vangronsveld, J., Clijsters, H. & Lelie, D. v. d. (2001): The effect of recombinant heavy metal-resistant endophytic bacteria on heavy metal uptake by their host plant. *International Journal of Phytoremediation,* **3** (2), 173-187.

Lodge, J. K., Weston-Hafer, K. & Berg, D. E. (1988): Transposon Tn5 target specificity: preference for insertion at G/C pairs. *Genetics,* **120** (3), 645-650.

Longley, D. B., Harkin, D. P. & Johnston, P. G. (2003): 5-fluorouracil: mechanisms of action and clinical strategies. *Nature Reviews Cancer,* **3** (5), 330-338.

Lopez-Maury, L., Garcia-Dominguez, M., Florencio, F. J. & Reyes, J. C. (2002): A two-component signal transduction system involved in nickel sensing in the cyanobacterium *Synechocystis* sp. PCC 6803. *Molecular Microbiology,* **43** (1), 247-256.

Lu, Z. H. & Solioz, M. (2001): Copper-induced proteolysis of the CopZ copper chaperone of *Enterococcus hirae*. *The Journal of Biological Chemistry,* **276** (51), 47822-47827.

Lubben, M., Portmann, R., Kock, G., Stoll, R., Young, M. M. & Solioz, M. (2009): Structural model of the CopA copper ATPase of *Enterococcus hirae* based on chemical cross-linking. *Biometals,* **22** (2), 363-375.

Luzhetskii, A. N., Ostash, B. E. & Fedorenko, V. A. (2001): Intergeneric conjugation *Escherichia coli–Streptomyces globisporus*1912 using integrative plasmid pSET152 and its derivatives. *Russian Journal of Genetics,* **37** (10), 1123-1129.

Luzhetskyy, A., Fedoryshyn, M., Hoffmeister, D., Bechthold, A. & Fedorenko, V. (2002): A gene cloning system for *Streptomyces cyanogenus* S136. *Visnyk of L'viv Univ. Biology Series,* **29**, 62-68.

Ma, Z., Cowart, D. M., Scott, R. A. & Giedroc, D. P. (2009a): Molecular insights into the metal selectivity of the copper(I)-sensing repressor CsoR from *Bacillus subtilis*. *Biochemistry,* **48** (15), 3325-3334.

Ma, Z., Cowart, D. M., Ward, B. P., Arnold, R. J., DiMarchi, R. D., Zhang, L., George, G. N., Scott, R. A. & Giedroc, D. P. (2009b): Unnatural amino acid substitution as a probe of the allosteric coupling pathway in a mycobacterial Cu(I) sensor. *Journal of the American Chemical Society,* **131** (50), 18044-18045.

Ma, Z., Jacobsen, F. E. & Giedroc, D. P. (2009c): Coordination chemistry of bacterial metal transport and sensing. *Chemical Reviews,* **109** (10), 4644-4681.

MacNeil, D. J., Gewain, K. M., Ruby, C. L., Dezeny, G., Gibbons, P. H. & MacNeil, T. (1992): Analysis of *Streptomyces avermitilis* genes required for avermectin biosynthesis utilizing a novel integration vector. *Gene,* **111**, 61-68.

Macomber, L. & Hausinger, R. P. (2011): Mechanisms of nickel toxicity in microorganisms. *Metallomics,* **3** (11), 1153-1162.

Macomber, L. & Imlay, J. A. (2009): The iron-sulfur clusters of dehydratases are primary intracellular targets of copper toxicity. *Proceedings of the National Academy of Sciences USA,* **106** (20), 8344-8349.

Macomber, L., Rensing, C. & Imlay, J. A. (2007): Intracellular copper does not catalyze the formation of oxidative DNA damage in *Escherichia coli*. *Journal of Bacteriology,* **189** (5), 1616-1626.

Maeda, M., Hidaka, M., Nakamura, A., Masaki, H. & Uozumi, T. (1994): Cloning, sequencing, and expression of thermophilic *Bacillus* sp. strain TB-90 urease gene complex in *Escherichia coli*. *Journal of Bacteriology,* **176** (2), 432-442.

Maes, M., Rimon, A., Kozachkov-Magrisso, L., Friedler, A. & Padan, E. (2012): Revealing the ligand binding site of NhaA Na^+/H^+ antiporter and its pH dependence. *The Journal of Biological Chemistry,* **287** (45), 38150-38157.

Mager, T., Rimon, A., Padan, E. & Fendler, K. (2011): Transport mechanism and pH regulation of the Na^+/H^+ antiporter NhaA from *Escherichia coli*: an electrophysiological study. *The Journal of Biological Chemistry,* **286** (26), 23570-23581.

Magnani, D., Barré, O., Gerber, S. D. & Solioz, M. (2008): Characterization of the CopR regulon of *Lactococcus lactis* IL1403. *Journal of Bacteriology,* **190** (2), 536-545.

Mahillon, J. & Chandler, M. (1998): Insertion sequences. *Microbiology and Molecular Biology Reviews,* **62** (3), 725-774.

Maier, T. M., Pechous, R., Casey, M., Zahrt, T. C. & Frank, D. W. (2006): *In vivo Himar1*-based transposon mutagenesis of *Francisella tularensis*. *Applied and Environmental Microbiology,* **72** (3), 1878-1885.

Maki, H. & Sekiguchi, M. (1992): MutT protein specifically hydrolyses a potent mutagenic substrate for DNA synthesis. *Nature,* **355** (6357), 273-275.

Malcolmson, S. J., Young, T. S., Ruby, J. G., Skewes-Cox, P. & Walsh, C. T. (2013): The post-translational modification cascade to the thiopeptide antibiotic berninamycin generates linear forms and altered macrocyclic scaffolds. *Proceedings of the National Academy of Sciences,* **110** (21), S1-S50.

Malinverni, J. C. & Silhavy, T. J. (2009): An ABC transport system that maintains lipid asymmetry in the gram-negative outer membrane. *Proceedings of the National Academy of Sciences USA,* **106** (19), 8009-8014.

Mangiameli, G. (2014): Controlling growth and morphogenesis of the industrial enzyme producer *Streptomyces lividans*. Faculteit der Wiskunde en Natuurwetenschappen. Leiden, Leiden University.

Manivasagan, P., Sivasankar, P., Venkatesan, J., Senthilkumar, K., Sivakumar, K. & Kim, S. K. (2013): Production and characterization of an extracellular polysaccharide from *Streptomyces violaceus* MM72. *International Journal of Biological Macromolecules,* **59**, 29-38.

Mao, X. M., Zhou, Z., Hou, X. P., Guan, W. J. & Li, Y. Q. (2009): Reciprocal regulation between SigK and differentiation programs in *Streptomyces coelicolor*. *Journal of Bacteriology,* **191** (21), 6473-6481.

Marchler-Bauer, A., Derbyshire, M. K., Gonzales, N. R., Lu, S., Chitsaz, F., Geer, L. Y., Geer, R. C., He, J., Gwadz, M., Hurwitz, D. I., Lanczycki, C. J., Lu, F., Marchler, G. H., Song, J. S., Thanki, N., Wang, Z., Yamashita, R. A., Zhang, D., Zheng, C. & Bryant, S. H. (2015): CDD: NCBI's conserved domain database. *Nucleic Acids Research,* **43** (Database issue), D222-226.

Marcos, A. T., Gutierrez, S., Diez, B., Fernandez, F. J., Oguiza, J. A. & Martin, J. F. (1995): Three genes *hrdB*, *hrdD* and *hrdT* of *Streptomyces griseus* IMRU 3570, encoding sigma factor-like proteins, are differentially expressed under specific nutritional conditions. *Gene,* **153** (1), 41-48.

Marcus, S. A., Sidiropoulos, S. W., Steinberg, H. & Talaat, A. M. (2016): CsoR is essential for maintaining copper homeostasis in *Mycobacterium tuberculosis*. *PLoS ONE,* **11** (3), e0151816.

Marrero, J., Auling, G., Coto, O. & Nies, D. H. (2007): High-level resistance to cobalt and nickel but probably no transenvelope efflux: Metal resistance in the Cuban *Serratia marcescens* strain C-1. *Microbial Ecology,* **53** (1), 123-133.

Marsh, P. & Wellington, E. M. H. (1994): Molecular ecology of filamentous actinomycetes in soil. -In O'Gara, F., Dowling, D. N. & Boesten, B. (Eds.): *Molecular ecology of rhizosphere microorganisms.* VCH Verlagsgesellschaft mbH, Weinheim, pp 133-149.

Matoba, Y., Kumagai, T., Yamamoto, A., Yoshitsu, H. & Sugiyama, M. (2006): Crystallographic evidence that the dinuclear copper center of tyrosinase is flexible during catalysis. *The Journal of Biological Chemistry,* **281** (13), 8981-8990.

Matsushima, P., Broughton, M. C., Turner, J. R. & Baltz, R. H. (1994): Conjugal transfer of cosmid DNA from *Escherichia coli* to *Saccharopolyspora spinosa*: effects of chromosomal insertions on macrolide A83543 production. *Gene,* **146** (1), 39-45.

Mazodier, P., Petter, R. & Thompson, C. (1989): Intergeneric conjugation between *Escherichia coli* and *Streptomyces* species. *Journal of Bacteriology,* **171** (6), 3583-3585.

McKenzie, N. L., Thaker, M., Koteva, K., Hughes, D. W., Wright, G. D. & Nodwell, J. R. (2010): Induction of antimicrobial activities in heterologous streptomycetes using alleles of the *Streptomyces coelicolor* gene *absA1*. *The Journal of Antibiotics,* **63** (4), 177-182.

McMahon, H. T. & Boucrot, E. (2015): Membrane curvature at a glance. *Journal of Cell Science,* **128** (6), 1065-1070.

Mengoni, A., Barzanti, R., Gonnelli, C., Gabbrielli, R. & Bazzicalupo, M. (2001): Characterization of nickel-resistant bacteria isolated from serpentine soil. *Environmental Microbiology,* **3** (11), 691-698.

Mergeay, M., Monchy, S., Janssen, P., Houdt, R. V. & Leys, N. (2009): Megaplasmids in *Cupriavidus* genus and metal resistance. -In Schwartz, E. (Eds.): *Microbial Megaplasmids.* Springer Berlin Heidelberg, Berlin, Heidelberg, pp 209-238.

Mergeay, M., Monchy, S., Vallaeys, T., Auquier, V., Benotmane, A., Bertin, P., Taghavi, S., Dunn, J., van der Lelie, D. & Wattiez, R. (2003): *Ralstonia metallidurans*, a bacterium specifically adapted to toxic metals: towards a catalogue of metal-responsive genes. *FEMS Microbiology Reviews,* **27** (2-3), 385-410.

Mergeay, M., Nies, D., Schlegel, H. G., Gerits, J., Charles, P. & Van Gijsegem, F. (1985): *Alcaligenes eutrophus* CH34 is a facultative chemolithotroph with plasmid-bound resistance to heavy metals. *Journal of Bacteriology,* **162** (1), 328-334.

Merkens, H., Kappl, R., Jakob, R. P., Schmid, F. X. & Fetzner, S. (2008): Quercetinase QueD of *Streptomyces* sp. FLA, a monocupin dioxygenase with a preference for nickel and cobalt. *Biochemistry,* **47** (46), 12185-12196.

Merrikh, C. N. & Merrikh, H. (2018): Gene inversion potentiates bacterial evolvability and virulence. *Nature Communications,* **9** (1), 4662.

Metcalf, W. W., Jiang, W. & Wanner, B. L. (1994): Use of the rep technique for allele replacement to construct new *Escherichia coli* hosts for maintenance of R6K gamma origin plasmids at different copy numbers. *Gene,* **138** (1-2), 1-7.

Michaels, M. L., Cruz, C., Grollman, A. P. & Miller, J. H. (1992): Evidence that MutY and MutM combine to prevent mutations by an oxidatively damaged form of guanine in DNA. *Proceedings of the National Academy of Sciences USA,* **89** (15), 7022-7025.

Mills, S. D., Jasalavich, C. A. & Cooksey, D. A. (1993): A two-component regulatory system required for copper-inducible expression of the copper resistance operon of *Pseudomonas syringae*. *Journal of Bacteriology,* **175** (6), 1656-1664.

Mirete, S., de Figueras, C. G. & Gonzalez-Pastor, J. E. (2007): Novel nickel resistance genes from the rhizosphere metagenome of plants adapted to acid mine drainage. *Applied and Environmental Microbiology,* **73** (19), 6001-6011.

Mittova, V., Tal, M., Volokita, M. & Guy, M. (2002): Salt stress induces up-regulation of an efficient chloroplast antioxidant system in the salt-tolerant wild tomato species *Lycopersicon pennellii* but not in the cultivated species. *Physiologia Plantarum,* **115** (3), 393-400.

Mobley, H. L., Garner, R. M. & Bauerfeind, P. (1995): *Helicobacter pylori* nickel-transport gene *nixA*: synthesis of catalytically active urease in *Escherichia coli* independent of growth conditions. *Molecular Microbiology,* **16** (1), 97-109.

Mohn, W. W., van der Geize, R., Stewart, G. R., Okamoto, S., Liu, J., Dijkhuizen, L. & Eltis, L. D. (2008): The actinobacterial *mce4* locus encodes a steroid transporter. *The Journal of Biological Chemistry,* **283** (51), 35368-35374.

Mulrooney, S. B. & Hausinger, R. P. (2003): Nickel uptake and utilization by microorganisms. *FEMS Microbiology Reviews,* **27** (2-3), 239-261.

Murakami, T., Anzai, H., Imai, S., Satoh, A., Nagaoka, K. & Thompson, C. J. (1986): The bialaphos biosynthetic genes of *Streptomyces hygroscopicus*: Molecular cloning and characterization of the gene cluster. *Molecular and General Genetics MGG,* **205** (1), 42-53.

Naik, M. M., Pandey, A. & Dubey, S. K. (2012): Biological characterization of lead-enhanced exopolysaccharide produced by a lead resistant *Enterobacter cloacae* strain P2B. *Biodegradation,* **23** (5), 775-783.

Nakamura, Y., Itoh, T., Matsuda, H. & Gojobori, T. (2004): Biased biological functions of horizontally transferred genes in prokaryotic genomes. *Nat Genet,* **36** (7), 760-766.

Netzker, T., Schroeckh, V., Gregory, M. A., Flak, M., Krespach, M. K., Leadlay, P. F. & Brakhage, A. A. (2016): An efficient method to generate gene deletion mutants of the rapamycin-producing bacterium *Streptomyces iranensis* HM 35. *Applied and Environmental Microbiology,* **82** (12), 3481-3492.

Nies, D. H. (1999): Microbial heavy-metal resistance. *Applied Microbiology and Biotechnology,* **51** (6), 730-750.

Nies, D. H. (2000): Heavy metal-resistant bacteria as extremophiles: molecular physiology and biotechnological use of *Ralstonia* sp. CH34. *Extremophiles,* **4** (2), 77-82.

Nies, D. H. (2003): Efflux-mediated heavy metal resistance in prokaryotes. *FEMS Microbiology Reviews,* **27** (2-3), 313-339.

Nies, D. H. (2016): The biological chemistry of the transition metal "transportome" of *Cupriavidus metallidurans*. *Metallomics,* **8** (5), 481-507.

Nodet, P., Capellano, A. & Fèvre, M. (1990): Morphogenetic effects of Congo red on hyphal growth and cell wall development of the fungus *Saprolegnia monoka*. *Journal of General Microbiology,* **136**, 303-310.

Noumi, T., Inoue, H., Sakurai, T., Tsuchiya, T. & Kanazawa, H. (1997): Identification and characterization of functional residues in a Na^+/H^+ antiporter (NhaA) from *Escherichia coli* by random mutagenesis. *Journal of Biochemistry,* **121** (4), 661-670.

Nozaki, K., Inaba, K., Kuroda, T., Tsuda, M. & Tsuchiya, T. (1996): Cloning and sequencing of the gene for Na^+/H^+ antiporter of *Vibrio parahaemolyticus*. *Biochemical and Biophysical Research Communications,* **222** (3), 774-779.

O'Connell, D. W., Birkinshaw, C. & O'Dwyer, T. F. (2008): Heavy metal adsorbents prepared from the modification of cellulose: a review. *Bioresource Technology,* **99** (15), 6709-6724.

O'Connor, T. J., Kanellis, P. & Nodwell, J. R. (2002): The *ramC* gene is required for morphogenesis in *Streptomyces coelicolor* and expressed in a cell type-specific manner under the direct control of RamR. *Molecular Microbiology,* **45** (1), 45-57.

Ochman, H., Lawrence, J. G. & Groisman, E. A. (2000): Lateral gene transfer and the nature of bacterial innovation. *Nature,* **405** (6784), 299-304.

Oda, Y. (1987): Induction of SOS responses in *Escherichia coli* by 5-fluorouracil. *Mutation Research,* **183** (2), 103-108.

Odermatt, A. & Solioz, M. (1995): Two trans-acting metalloregulatory proteins controlling expression of the copper-ATPases of *Enterococcus hirae*. *The Journal of Biological Chemistry,* **270** (9), 4349-4354.

Odermatt, A., Suter, H., Krapf, R. & Solioz, M. (1993): Primary structure of two P-type ATPases involved in copper homeostasis in *Enterococcus hirae*. *The Journal of Biological Chemistry,* **268** (17), 12775-12779.

Okanishi, M., Ita, T. & Umezawa, H. (1970): Possible control of formation of aerial mycelium and antibiotic production in *Streptomyces* by episomic factors. *The Journal of Antibiotics,* **23** (1), 45-47.

Orsaria, L., Paoletti, L. & Gramajo, H. C. (1998): Characterization of stationary-phase proteins in *Streptomyces coelicolor* A3(2). *FEMS Microbiology Letters,* **162** (2), 275-281.

Osman, D., Piergentili, C., Chen, J., Chakrabarti, B., Foster, A. W., Lurie-Luke, E., Huggins, T. G. & Robinson, N. J. (2015): Generating a metal-responsive transcriptional regulator to test what confers metal sensing in cells. *The Journal of Biological Chemistry,* **290** (32), 19806-19822.

Ostash, B., Makitrinskyy, R., Walker, S. & Fedorenko, V. (2009): Identification and characterization of *Streptomyces ghanaensis* ATCC14672 integration sites for three actinophage-based plasmids. *Plasmid,* **61** (3), 171-175.

Outten, F. W., Huffman, D. L., Hale, J. A. & O'Halloran, T. V. (2001): The independent *cue* and *cus* systems confer copper tolerance during aerobic and anaerobic growth in *Escherichia coli*. *The Journal of Biological Chemistry,* **276** (33), 30670-30677.

Padan, E. (2008): The enlightening encounter between structure and function in the NhaA Na^+/H^+ antiporter. *Trends in Biochemical Sciences,* **33** (9), 435-443.

Padan, E., Bibi, E., Ito, M. & Krulwich, T. A. (2005): Alkaline pH homeostasis in bacteria: new insights. *Biochimica et Biophysica Acta,* **1717** (2), 67-88.

Padan, E., Maisler, N., Taglicht, D., Karpel, R. & Schuldiner, S. (1989): Deletion of *ant* in *Escherichia coli* reveals its function in adaptation to high salinity and an alternative Na^+/H^+ antiporter system(s). *The Journal of Biological Chemistry,* **264** (34), 20297-20302.

Padan, E. & Schuldiner, S. (1986): Intracellular pH regulation in bacterial cells. *Methods in Enzymology,* **125**, 337-352.

Padan, E. & Schuldiner, S. (1994): Molecular physiology of Na^+/H^+ antiporters, key transporters in circulation of Na^+ and H^+ in cells. *Biochimica et Biophysica Acta,* **1185** (2), 129-151.

Padan, E., Tzubery, T., Herz, K., Kozachkov, L., Rimon, A. & Galili, L. (2004): NhaA of *Escherichia coli*, as a model of a pH-regulated Na^+/H^+antiporter. *Biochimica et Biophysica Acta,* **1658** (1-2), 2-13.

Padan, E., Venturi, M., Gerchman, Y. & Dover, N. (2001): Na(+)/H(+) antiporters. *Biochimica et Biophysica Acta,* **1505** (1), 144-157.

Padilla-Benavides, T., McCann, C. J. & Arguello, J. M. (2013): The mechanism of Cu^+ transport ATPases: interaction with Cu^+ chaperones and the role of transient metal-binding sites. *The Journal of Biological Chemistry,* **288** (1), 69-78.

Paez-Espino, A. D., Chavarria, M. & de Lorenzo, V. (2015): The two paralogue *phoN* (phosphinothricin acetyl transferase) genes of *Pseudomonas putida* encode functionally different proteins. *Environmental Microbiology,* **17** (9), 3330-3340.

Paget, M. S. (2015): Bacterial sigma factors and anti-sigma factors: structure, function and distribution. *Biomolecules,* **5** (3), 1245-1265.

Paget, M. S. B., Chamberlin, L., Atrih, A., Foster, S. J. & Buttner, M. J. (1999): Evidence that the extracytoplasmic function sigma factor sigma E is required for normal cell wall structure in *Streptomyces coelicolor* A3(2). *Journal of Bacteriology,* **181** (1), 204-211.

Paget, M. S. B., Hong, H.-J., Bibb, M. J. & Buttner, M. J. (2002): The ECF sigma factors of *Streptomyces coelicolor* A3(2). -In Hodgson, D. A. & Thomas, C. M. (Eds.): *Signals, switches, regulons, and cascades : control of bacterial gene expression.* Cambridge University Press, Cambridge, pp 105-126.

Palumaa, P., Kangur, L., Voronova, A. & Sillard, R. (2004): Metal-binding mechanism of Cox17, a copper chaperone for cytochrome c oxidase. *The Biochemical Journal,* **382** (Pt 1), 307-314.

Pandey, A. K. & Sassetti, C. M. (2008): Mycobacterial persistence requires the utilization of host cholesterol. *Proceedings of the National Academy of Sciences,* **105** (11), 4376-4380.

Pandey, B. P., Lee, N. & Kim, B. G. (2018): Effect of extracellular tyrosinase on the expression level of P450, Fpr, and Fdx and ortho-hydroxylation of daidzein in *Streptomyces avermitilis*. *Applied Biochemistry and Biotechnology,* **184** (3), 1036-1046.

Pandza, S., Biukovic, G., Paravic, A., Dadbin, A., Cullum, J. & Hranueli, D. (1998): Recombination between the linear plasmid pPZG101 and the linear chromosome of *Streptomyces rimosus* can lead to exchange of ends. *Molecular Microbiology,* **28** (6), 1165-1176.

Park, H., Song, B. & Morel, F. M. M. (2007): Diversity of the cadmium-containing carbonic anhydrase in marine diatoms and natural waters. *Environmental Microbiology,* **9** (2), 403-413.

Park, J. E., Schlegel, H. G., Rhie, H. G. & Lee, H. S. (2004): Nucleotide sequence and expression of the *ncr* nickel and cobalt resistance in *Hafnia alvei* 5-5. *International Microbiology,* **7** (1), 27-34.

Park, J. E., Young, K. E., Schlegel, H. G., Rhie, H. G. & Lee, H. S. (2003): Conjugative plasmid mediated inducible nickel resistance in *Hafnia alvei* 5-5. *International Microbiology,* **6** (1), 57-64.

Park, J. S., Lee, S. J., Rhie, H. G. & Lee, H. S. (2008): Characterization of a chromosomal nickel resistance determinant from *Klebsiella oxytoca* CCUG 15788. *Journal of Microbiology and Biotechnology,* **18** (6), 1040-1043.

Park, S. H., Choi, S. S., Kim, Y. J., Chang, Y. K., Sherman, D. H. & Kim, E. S. (2009): Functional expression of SCO7832 stimulates tautomycetin production *via* pathway-specific regulatory gene overexpression in *Streptomyces* sp. CK4412. *Journal of Industrial Microbiology & Biotechnology,* **36** (7), 993-998.

Peng, C., Chai, L.-Y., Tang, C.-J., Min, X.-B., Ali, M., Song, Y.-X. & Qi, W.-M. (2017): Feasibility and enhancement of copper and ammonia removal from wastewater using struvite formation: a comparative research. *Journal of Chemical Technology & Biotechnology,* **92** (2), 325-333.

Pérez-García, I., Rivadeneyra, M. A. & Ramos, C. (1989): The influence of pH on struvite formation by bacteria. *Chemosphere,* **18** (7), 1633-1638.

Petrus, M. L. & Claessen, D. (2014): Pivotal roles for *Streptomyces* cell surface polymers in morphological differentiation, attachment and mycelial architecture. *Antonie Van Leeuwenhoek,* **106** (1), 127-139.

Petrus, M. L., Vijgenboom, E., Chaplin, A. K., Worrall, J. A., van Wezel, G. P. & Claessen, D. (2016): The DyP-type peroxidase DtpA is a Tat-substrate required for GlxA maturation and morphogenesis in *Streptomyces*. *Open Biology,* **6** (1), 150149.

Pettis, G. S. & Cohen, S. N. (1994): Transfer of the plJ101 plasmid in *Streptomyces lividan*s requires a *cis*-acting function dispensable for chromosomal gene transfer. *Molecular Microbiology,* **13** (6), 955-964.

Pettis, G. S. & Cohen, S. N. (2000): Mutational analysis of the *tra* locus of the broad-host-range *Streptomyces* plasmid plJ101. *Journal of Bacteriology,* **182** (16), 4500-4504.

Petzke, L. & Luzhetskyy, A. (2009): In vivo Tn5-based transposon mutagenesis of streptomycetes. *Applied Microbiology and Biotechnology,* **83** (5), 979-986.

Pigac, J. & Schrempf, H. (1995): A simple and rapid method of transformation of *Streptomyces rimosus* R6 and other streptomycetes by electroporation. *Applied and Environmental Microbiology,* **61** (1), 352-356.

Pinero, S., Rivera, J., Romero, D., Cevallos, M. A., Martinez, A., Bolivar, F. & Gosset, G. (2007): Tyrosinase from *Rhizobium etli* is involved in nodulation efficiency and symbiosis-associated stress resistance. *Journal of Molecular Microbiology and Biotechnology,* **13** (1-3), 35-44.

Pini, F., Spini, G., Galardini, M., Bazzicalupo, M., Benedetti, A., Chiancianesi, M., Florio, A., Lagomarsino, A., Migliore, M., Mocali, S. & Mengoni, A. (2014): Molecular phylogeny of the nickel-resistance gene *nreB* and functional role in the nickel sensitive symbiotic nitrogen fixing bacterium *Sinorhizobium meliloti*. *Plant and Soil,* **377** (1), 189-201.

Pinner, E., Kotler, Y., Padan, E. & Schuldiner, S. (1993): Physiological role of *nhaB*, a specific Na^+/H^+ antiporter in *Escherichia coli*. *The Journal of Biological Chemistry,* **268** (3), 1729-1734.

Pinner, E., Padan, E. & Schuldiner, S. (1992): Cloning, sequencing, and expression of the *nhaB* gene, encoding a Na^+/H^+ antiporter in *Escherichia coli*. *The Journal of Biological Chemistry,* **267** (16), 11064-11068.

Poralla, K., Muth, G. & Hartner, T. (2000): Hopanoids are formed during transition from substrate to aerial hyphae in *Streptomyces coelicolor* A3(2). *FEMS Microbiology Letters,* **189** (1), 93-95.

Portmann, R., Magnani, D., Stoyanov, J. V., Schmechel, A., Multhaup, G. & Solioz, M. (2004): Interaction kinetics of the copper-responsive CopY repressor with the *cop* promoter of *Enterococcus hirae*. *JBIC Journal of Biological Inorganic Chemistry,* **9** (4), 396-402.

Porto, T. V., Wilson, M. T. & Worrall, J. A. (2015): Copper and nickel bind *via* two distinct kinetic mechanisms to a CsoR metalloregulator. *Dalton Trans,* **44** (46), 20176-20185.

Pospiech, A. & Neumann, B. (1995): A versatile quick-prep of genomic DNA from gram-positive bacteria. *Trends in Genetics,* **11** (6), 217-218.

Pring, D. R., Levings, C. S., Hu, W. W. & Timothy, D. H. (1977): Unique DNA associated with mitochondria in the "S"-type cytoplasm of male-sterile maize. *Proceedings of the National Academy of Sciences USA,* **74** (7), 2904-2908.

Proudfoot, M., Kuznetsova, E., Brown, G., Rao, N. N., Kitagawa, M., Mori, H., Savchenko, A. & Yakunin, A. F. (2004): General enzymatic screens identify three new nucleotidases in *Escherichia coli.* Biochemical characterization of SurE, YfbR, and YjjG. *The Journal of Biological Chemistry,* **279** (52), 54687-54694.

Pufahl, R. A., Singer, C. P., Peariso, K. L., Lin, S. J., Schmidt, P. J., Fahrni, C. J., Culotta, V. C., Penner-Hahn, J. E. & O'Halloran, T. V. (1997): Metal ion chaperone function of the soluble Cu(I) receptor Atx1. *Science,* **278** (5339), 853-856.

Pumpel, T., Macaskie, L. E., Finlay, J. A., Diels, L. & Tsezos, M. (2003): Nickel removal from nickel plating waste water using a biologically active moving-bed sand filter. *Biometals,* **16** (4), 567-581.

Radchenko, M. V., Waditee, R., Oshimi, S., Fukuhara, M., Takabe, T. & Nakamura, T. (2006): Cloning, functional expression and primary characterization of *Vibrio parahaemolyticus* K^+/H^+ antiporter genes in *Escherichia coli*. *Molecular Microbiology,* **59** (2), 651-663.

Rademacher, C. & Masepohl, B. (2012): Copper-responsive gene regulation in bacteria. *Microbiology,* **158** (Pt 10), 2451-2464.

Radford, D. S., Kihlken, M. A., Borrelly, G. P. M., Harwood, C. R., Brun, N. E. & Cavet, J. S. (2003): CopZ from *Bacillus subtilis* interacts *in vivo* with a copper exporting CPx-type ATPase CopA. *FEMS Microbiology Letters,* **220** (1), 105-112.

Rai, P. (2010): Oxidation in the nucleotide pool, the DNA damage response and cellular senescence: Defective bricks build a defective house. *Mutation Research,* **703** (1), 71-81.

Ramamurthi, K. S. & Losick, R. (2009): Negative membrane curvature as a cue for subcellular localization of a bacterial protein. *Proceedings of the National Academy of Sciences USA,* **106** (32), 13541-13545.

Ramirez, D. C., Mejiba, S. E. & Mason, R. P. (2005): Copper-catalyzed protein oxidation and its modulation by carbon dioxide: enhancement of protein radicals in cells. *The Journal of Biological Chemistry,* **280** (29), 27402-27411.

Ravel, J., Schrempf, H. & Hill, R. T. (1998): Mercury resistance is encoded by transferable giant linear plasmids in two Chesapeake Bay *Streptomyces* strains. *Applied and Environmental Microbiology,* **64** (9), 3383–3388.

Ravel, J., Wellington, E. M. & Hill, R. T. (2000): Interspecific transfer of *Streptomyces* giant linear plasmids in sterile amended soil microcosms. *Applied and Environmental Microbiology,* **66** (2), 529-534.

Rawat, M., Newton, G. L., Ko, M., Martinez, G. J., Fahey, R. C. & Av-Gay, Y. (2002): Mycothiol-deficient *Mycobacterium smegmatis* mutants are hypersensitive to alkylating agents, free radicals, and antibiotics. *Antimicrobial Agents and Chemotherapy,* **46** (11), 3348-3355.

Rebello, J. L. & Strauss, N. (1969): Regulation of synthesis of glutamine synthase in *Bacillus subtilis*. *Journal of Bacteriology,* **98** (2), 683-688.

Reddy, V. S., Shlykov, M. A., Castillo, R., Sun, E. I. & Saier, M. H., Jr. (2012): The major facilitator superfamily (MFS) revisited. *The FEBS Journal,* **279** (11), 2022-2035.

Reichhardt, C., Jacobson, A. N., Maher, M. C., Uang, J., McCrate, O. A., Eckart, M. & Cegelski, L. (2015): Congo red interactions with curli-producing *E. coli* and native curli amyloid fibers. *PLoS ONE,* **10** (10), e0140388.

Reichhardt, C., McCrate, O. A., Zhou, X., Lee, J., Thongsomboon, W. & Cegelski, L. (2016): Influence of the amyloid dye Congo red on curli, cellulose, and the extracellular matrix in *E. coli* during growth and matrix purification. *Analytical and Bioanalytical Chemistry,* **408** (27), 7709-7717.

Remenár, M., Karelová, E., Harichová, J., Zámocký, M., Krčová, K. & Ferianc, P. (2014): Actinobacteria occurrence and their metabolic characteristics in the nickel-contaminated soil sample. *Biologia,* **69** (11), 1453-1463.

Ren, J., Ulvik, A., Refsum, H. & Ueland, P. M. (2002): Uracil in human DNA from subjects with normal and impaired folate status as determined by high-performance liquid chromatography−tandem mass spectrometry. *Analytical Chemistry,* **74** (1), 295-299.

Rensing, C., Fan, B., Sharma, R., Mitra, B. & Rosen, B. P. (2000): CopA: an *Escherichia coli* Cu(I)-translocating P-type ATPase. *Proceedings of the National Academy of Sciences USA,* **97** (2), 652-656.

Rensing, C., Ghosh, M. & Rosen, B. P. (1999): Families of soft-metal-ion-transporting ATPases. *Journal of Bacteriology,* **181** (19), 5891-5897.

Rensing, C. & McDevitt, S. F. (2013): The copper metallome in prokaryotic cells. *Metal Ions in Life Sciences,* **12**, 417-450.

Reuther, J., Gekeler, C., Tiffert, Y., Wohlleben, W. & Muth, G. (2006): Unique conjugation mechanism in mycelial streptomycetes: a DNA-binding ATPase translocates unprocessed plasmid DNA at the hyphal tip. *Molecular Microbiology,* **61** (2), 436-446.

Reyes-Caballero, H., Campanello, G. C. & Giedroc, D. P. (2011): Metalloregulatory proteins: metal selectivity and allosteric switching. *Biophysical Chemistry,* **156** (2-3), 103-114.

Rice, P., Longden, I. & Bleasby, A. (2000): EMBOSS: the European Molecular Biology Open Software Suite. *Trends in Genetics,* **16** (6), 276-277.

Richards, R. G., Sowers, L. C., Laszlo, J. & Sedwick, W. D. (1984): The occurrence and consequences of deoxyuridine in DNA. *Advances in Enzyme Regulation,* **22**, 157-185.

Ridder, I. S. & Dijkstra, B. W. (1999): Identification of the Mg^{2+}-binding site in the P-type ATPase and phosphatase members of the HAD (haloacid dehalogenase) superfamily by structural similarity to the response regulator protein CheY. *The Biochemical Journal,* **339** (2), 223-226.

Riley, P. A. (1997): Melanin. *The International Journal of Biochemistry & Cell Biology,* **29** (11), 1235-1239.

Rimon, A., Gerchman, Y., Kariv, Z. & Padan, E. (1998): A point mutation (G338S) and its suppressor mutations affect both the pH response of the NhaA-Na^+/H^+ antiporter as well as the growth phenotype of *Escherichia coli*. *Journal of Biological Chemistry,* **273** (41), 26470-26476.

Rimon, A., Gerchman, Y., Olami, Y., Schuldiner, S. & Padan, E. (1995): Replacements of histidine 226 of NhaA-Na^+/H^+ antiporter of *Escherichia coli.* Cysteine (H226C) or serine (H226S) retain both normal activity and pH sensitivity, aspartate (H226D) shifts the pH profile toward basic pH, and alanine (H226A) inactivates the carrier at all pH values. *The Journal of Biological Chemistry,* **270** (45), 26813-26817.

Rivadeneyra, A., Gonzalez-Martinez, A., Gonzalez-Lopez, J., Martin-Ramos, D., Martinez-Toledo, M. V. & Rivadeneyra, M. A. (2014): Precipitation of phosphate minerals by microorganisms isolated from a fixed-biofilm reactor used for the treatment of domestic wastewater. *International Journal of Environmental Research and Public Health,* **11** (4), 3689-3704.

Rivadeneyra, M. A., Pérez-García, I. & Ramos-Cormenzana, A. (1992): Influence of ammonium ion on bacterial struvite production. *Geomicrobiology Journal,* **10** (2), 125-137.

Roberts, A. W. & Bushoven, J. T. (2007): The cellulose synthase (*CESA*) gene superfamily of the moss *Physcomitrella patens*. *Plant Molecular Biology,* **63** (2), 207-219.

Robinson, A. E., Lowe, J. E., Koh, E. I. & Henderson, J. P. (2018): Uropathogenic enterobacteria use the yersiniabactin metallophore system to acquire nickel. *The Journal of Biological Chemistry,* **293** (39), 14953-14961.

Robinson, N. J. & Winge, D. R. (2010): Copper metallochaperones. *Annual Review of Biochemistry,* **79**, 537-562.

Rodrigue, A., Effantin, G. & Mandrand-Berthelot, M. A. (2005): Identification of *rcnA* (*yohM*), a nickel and cobalt resistance gene in *Escherichia coli*. *Journal of Bacteriology,* **187** (8), 2912-2916.

Roncero, C. & Duran, A. (1985): Effect of Calcofluor white and Congo red on fungal cell wall morphogenesis: *in vivo* activation of chitin polymerization. *Journal of Bacteriology,* **163** (3), 1180-1185.

Ronzio, R. A., Rowe, W. B. & Meister, A. (1969): Mechanism of inhibition of glutamine synthetase by methionine sulfoximine. *Biochemistry,* **8** (3), 1066-1075.

Ross, S. M. (1994): Retention, transformation and mobility of toxic metals in soils. -In Ross, S. M. (Eds.): *Toxic metals in soil-plant systems.* John Wiley and Sons, Chichester, pp 63-152.

Rothman, A., Padan, E. & Schuldiner, S. (1996): Topological analysis of NhaA, a Na^+/H^+ antiporter from *Escherichia coli*. *Journal of Biological Chemistry,* **271** (50), 32288-32292.

Rowe, J. L., Starnes, G. L. & Chivers, P. T. (2005): Complex transcriptional control links NikABCDE-dependent nickel transport with hydrogenase expression in *Escherichia coli*. *Journal of Bacteriology,* **187** (18), 6317-6323.

Roy, S., Das, I., Munjal, M., Karthik, L., Kumar, G., Kumar, S. & Rao, K. V. B. (2014): Isolation and characterization of tyrosinase produced by marine actinobacteria and its application in the removal of phenol from aqueous environment. *Frontiers in Biology,* **9** (4), 306-316.

Rubin, E. J., Akerley, B. J., Novik, V. N., Lampe, D. J., Husson, R. N. & Mekalanos, J. J. (1999): *In vivo* transposition of *mariner*-based elements in enteric bacteria and mycobacteria. *Proceedings of the National Academy of Sciences USA,* **96** (4), 1645-1650.

Ruckert, C., Albersmeier, A., Busche, T., Jaenicke, S., Winkler, A., Friethjonsson, O. H., Hreggviethsson, G. O., Lambert, C., Badcock, D., Bernaerts, K., Anne, J., Economou, A. & Kalinowski, J. (2015): Complete genome sequence of *Streptomyces lividans* TK24. *Journal of Biotechnology,* **199**, 21-22.

Ryan, R., Ryan, D. & Dowling, D. (2005): Multiple metal resistant transferable phenotypes in bacteria as indicators of soil contamination with heavy metals. *Journal of Soils and Sediments,* **5** (2), 95-100.

Saier, M. H., Jr., Eng, B. H., Fard, S., Garg, J., Haggerty, D. A., Hutchinson, W. J., Jack, D. L., Lai, E. C., Liu, H. J., Nusinew, D. P., Omar, A. M., Pao, S. S., Paulsen, I. T., Quan, J. A., Sliwinski, M., Tseng, T. T., Wachi, S. & Young, G. B. (1999): Phylogenetic characterization of novel transport protein families revealed by genome analyses. *Biochimica et Biophysica Acta,* **1422** (1), 1-56.

Saier, M. H., Jr., Reddy, V. S., Tsu, B. V., Ahmed, M. S., Li, C. & Moreno-Hagelsieb, G. (2016): The Transporter Classification Database (TCDB): recent advances. *Nucleic Acids Research,* **44** (D1), D372-D379.

Sambrook, J. (2001): Molecular cloning : a laboratory manual. Third edition. Cold Spring Harbor, N.Y. : Cold Spring Harbor Laboratory Press, pp 2100.

Sandaa, R., Torsvik, V. V., Enger, Daae, F. L., Castberg, T. & Hahn, D. (1999): Analysis of bacterial communities in heavy metal-contaminated soils at different levels of resolution. *FEMS Microbiology Ecology,* **30** (3), 237-251.

Sandaa, R. A., Torsvik, V. & Enger, Ø. (2001): Influence of long-term heavy-metal contamination on microbial communities in soil. *Soil Biology and Biochemistry,* **33** (3), 287-295.

Sandoval-Calderon, M., Guan, Z. & Sohlenkamp, C. (2017): Knowns and unknowns of membrane lipid synthesis in streptomycetes. *Biochimie,* **141**, 21-29.

Sandoval-Calderon, M., Nguyen, D. D., Kapono, C. A., Herron, P., Dorrestein, P. C. & Sohlenkamp, C. (2015): Plasticity of *Streptomyces coelicolor* membrane composition under different growth conditions and during development. *Frontiers in Microbiology,* **6**, 1465.

Santangelo, M. P., Blanco, F. C., Bianco, M. V., Klepp, L. I., Zabal, O., Cataldi, A. A. & Bigi, F. (2008): Study of the role of Mce3R on the transcription of *mce* genes of *Mycobacterium tuberculosis*. *BMC Microbiology,* **8**, 38.

Santi, D. V., McHenry, C. S. & Sommer, H. (1974): Mechanism of interaction of thymidylate synthetase with 5-fluorodeoxyuridylate. *Biochemistry,* **13** (3), 471-481.

Saxena, D., Ben-Dov, E., Manasherob, R., Barak, Z., Boussiba, S. & Zaritsky, A. (2002): A UV tolerant mutant of *Bacillus thuringiensis* subsp. *kurstaki* producing melanin. *Current Microbiology,* **44** (1), 25-30.

Saxena, I. M., Brown, R. M., Jr. & Dandekar, T. (2001): Structure-function characterization of cellulose synthase: relationship to other glycosyltransferases. *Phytochemistry,* **57** (7), 1135-1148.

Saxena, I. M., Brown, R. M., Jr., Fevre, M., Geremia, R. A. & Henrissat, B. (1995): Multidomain architecture of beta-glycosyl transferases: implications for mechanism of action. *Journal of Bacteriology,* **177** (6), 1419-1424.

Sazinsky, M. H., LeMoine, B., Orofino, M., Davydov, R., Bencze, K. Z., Stemmler, T. L., Hoffman, B. M., Arguello, J. M. & Rosenzweig, A. C. (2007): Characterization and structure of a Zn^{2+} and [2Fe-2S]-containing copper chaperone from *Archaeoglobus fulgidus*. *The Journal of Biological Chemistry,* **282** (35), 25950-25959.

Schmidt, A., Haferburg, G. & Kothe, E. (2007): Superoxide dismutases of heavy metal resistant streptomycetes. *Journal of Basic Microbiology,* **47** (1), 56-62.

Schmidt, A., Haferburg, G., Schmidt, A., Lischke, U., Merten, D., Ghergel, F., Büchel, G. & Kothe, E. (2009): Heavy metal resistance to the extreme: *Streptomyces* strains from a former uranium mining area. *Chemie der Erde - Geochemistry,* **69**, 35-44.

Schmidt, A., Haferburg, G., Sineriz, M., Merten, D., Büchel, G. & Kothe, E. (2005): Heavy metal resistance mechanisms in actinobacteria for survival in AMD contaminated soils. *Chemie der Erde - Geochemistry,* **65**, 131-144.

Schmidt, A., Hagen, M., Schütze, E., Schmidt, A. & Kothe, E. (2010): *In silico* prediction of potential metallothioneins and metallohistins in actinobacteria. *Journal of Basic Microbiology,* **50** (6), 562-569.

Schmidt, T. & Schlegel, H. G. (1989): Nickel and cobalt resistance of various bacteria isolated from soil and highly polluted domestic and industrial wastes. *Microbiology Letters,* **62** (5), 315–328.

Schmidt, T. & Schlegel, H. G. (1994): Combined nickel-cobalt-cadmium resistance encoded by the *ncc* locus of *Alcaligenes xylosoxidans* 31A. *Journal of Bacteriology,* **176** (22), 7045-7054.

Schmidt, T., Stoppel, R. D. & Schlegel, H. G. (1991): High-level nickel resistance in *Alcaligenes xylosoxydans* 31A and *Alcaligenes eutrophus* KTO2. *Applied and Environmental Microbiology,* **57** (11), 3301-3309.

Schrempf, H. (1983): Deletion and amplification of DNA sequences in melanin-negative variants of *Streptomyces reticuli*. *Molecular & General Genetics,* **189** (3), 501-505.

Schütze, E., Ahmed, E., Voit, A., Klose, M., Greyer, M., Svatos, A., Merten, D., Roth, M., Holmstrom, S. J. & Kothe, E. (2015): Siderophore production by streptomycetes - stability and alteration of ferrihydroxamates in heavy metal-contaminated soil. *Environmental Science Pollution Research,* **22** (24), 19376-19383.

Schütze, E., Klose, M., Merten, D., Nietzsche, S., Senftleben, D., Roth, M. & Kothe, E. (2014): Growth of streptomycetes in soil and their impact on bioremediation. *Journal of Hazardous Materials,* **267**, 128-135.

Schütze, E., Weist, A., Klose, M., Wach, T., Schumann, M., Nietzsche, S., Merten, D., Baumert, J., Majzlan, J. & Kothe, E. (2013): Taking nature into lab: biomineralization by heavy metal resistant streptomycetes in soil. *Biogeosciences Discussions,* **10** (2), 2345-2375.

Sebbane, F., Mandrand-Berthelot, M. A. & Simonet, M. (2002): Genes encoding specific nickel transport systems flank the chromosomal urease locus of pathogenic *Yersiniae*. *Journal of Bacteriology,* **184** (20), 5706-5713.

Seifried, A., Schultz, J. & Gohla, A. (2013): Human HAD phosphatases: structure, mechanism, and roles in health and disease. *The FEBS Journal,* **280** (2), 549-571.

Selim, M. S., Amer, S. K., Mohamed, S. S., Mounier, M. M. & Rifaat, H. M. (2018): Production and characterisation of exopolysaccharide from *Streptomyces carpaticus* isolated from marine sediments in Egypt and its effect on breast and colon cell lines. *Journal of Genetic Engineering and Biotechnology,* **16** (1), 23-28.

Sensfuss, C. & Schlegel, H. G. (1988): Plasmid pMOL28-encoded resistance to nickel is due to specific efflux. *FEMS Microbiology Letters,* **55** (3), 295-298.

Servin-Gonzalez, L., Sampieri, A. I., Cabello, J., Galvan, L., Juarez, V. & Castro, C. (1995): Sequence and functional analysis of the *Streptomyces phaeochromogenes* plasmid pJV1 reveals a modular organization of *Streptomyces* plasmids that replicate by rolling circle. *Microbiology,* **141**, 2499-2510.

Sevin, D. C., Fuhrer, T., Zamboni, N. & Sauer, U. (2017): Nontargeted *in vitro* metabolomics for high-throughput identification of novel enzymes in *Escherichia coli*. *Nature Methods,* **14** (2), 187-194.

Shi, X., Festa, R. A., Ioerger, T. R., Butler-Wu, S., Sacchettini, J. C., Darwin, K. H. & Samanovic, M. I. (2014): The copper-responsive RicR regulon contributes to *Mycobacterium tuberculosis* virulence. *MBio,* **5** (1), e00876-00813.

Shimamoto, T., Inaba, K., Thelen, P., Ishikawa, T., Goldberg, E. B., Tsuda, M. & Tsuchiya, T. (1994): The NhaB Na^+/H^+ antiporter is essential for intracellular pH regulation under alkaline conditions in *Escherichia coli*. *Journal of Biochemistry,* **116** (2), 285-290.

Shivani, Y., Subhash, Y., Sasikala, C. & Ramana, C. V. (2016): Description of 'Candidatus *Marispirochaeta associata*' and reclassification of *Spirochaeta bajacaliforniensis, Spirochaeta smaragdinae* and *Spirochaeta sinaica* to a new genus *Sediminispirochaeta* gen. nov. as *Sediminispirochaeta bajacaliforniensis* comb. nov., *Sediminispirochaeta smaragdinae* comb. nov. and *Sediminispirochaeta sinaica* comb. nov. *International Journal of Systematic and Evolutionary Microbiology,* **66** (12), 5485-5492.

Sies, H. (1997): Oxidative stress: oxidants and antioxidants. *Experimental Physiology,* **82** (2), 291-295.

Silver, S. & Misra, T. K. (1988): Plasmid-mediated heavy metal resistances. *Annual Review of Microbiology,* **42**, 717-743.

Silver, S. & Walderhaug, M. (1992): Gene regulation of plasmid- and chromosome-determined inorganic ion transport in bacteria. *Microbiological Reviews,* **56** (1), 195-228.

Silvestro, D. & Michalak, I. (2012): raxmlGUI: a graphical front-end for RAxML. *Organisms Diversity & Evolution,* **12** (4), 335-337.

Simoes, F., Vale, P., Stephenson, T. & Soares, A. (2018): The role of pH on the biological struvite production in digested sludge dewatering liquors. *Scientific Reports,* **8** (1), 7225.

Singh, K., Senadheera, D. B. & Cvitkovitch, D. G. (2014): An intimate link: two-component signal transduction systems and metal transport systems in bacteria. *Future Microbiology,* **9** (11), 1283-1293.

Sinha, A., Kumar, S. & Khare, S. K. (2013): Biochemical basis of mercury remediation and bioaccumulation by *Enterobacter* sp. EMB21. *Applied Biochemistry and Biotechnology,* **169** (1), 256-267.

Sioud, S., Aigle, B., Karray-Rebai, I., Smaoui, S., Bejar, S. & Mellouli, L. (2009): Integrative gene cloning and expression system for *Streptomyces* sp. US 24 and *Streptomyces* sp. TN 58 bioactive molecule producing strains. *Journal of Biomedicine & Biotechnology,* **2009**, 464986.

Smaldone, G. T. & Helmann, J. D. (2007): CsoR regulates the copper efflux operon *copZA* in *Bacillus subtilis*. *Microbiology,* **153** (Pt 12), 4123-4128.

Soderholm, N., Javadi, A., Flores, I. S., Flardh, K. & Sandblad, L. (2018): Affinity to cellulose is a shared property among coiled-coil domains of intermediate filaments and prokaryotic intermediate filament-like proteins. *Scientific Reports,* **8** (1), 16524.

Solioz, M., Abicht, H. K., Mermod, M. & Mancini, S. (2010): Response of gram-positive bacteria to copper stress. *JBIC Journal of Biological Inorganic Chemistry,* **15** (1), 3-14.

Song, D., Coughlin, J., Ju, J., Zhou, X., Shen, B., Zhao, C. & Deng, Z. (2008): Alternative method for site-directed mutagenesis of complex polyketide synthase in *Streptomyces albus* JA3453. *Acta Biochimica et Biophysica Sinica,* **40** (4), 319-326.

Song, J. Y. (2013): Heterologous expression of a putative K^+/H^+ antiporter of *S. coelicolor* A3(2) enhances K^+, acidic-pH shock tolerances, and geldanamycin secretion. *Journal of Microbiology and Biotechnology,* **23** (2), 149-155.

Sparks, D. L. (2005): Toxic metals in the environment: The role of surfaces. *Elements,* **1** (4), 193-197.

Spatz, K., Kohn, H. & Redenbach, M. (2002): Characterization of the *Streptomyces violaceoruber* SANK95570 plasmids pSV1 and pSV2. *FEMS Microbiology Letters,* **213** (1), 87-92.

Staehlin, B. M., Gibbons, J. G., Rokas, A., O'Halloran, T. V. & Slot, J. C. (2016): Evolution of a heavy metal homeostasis/resistance island reflects increasing copper stress in Enterobacteria. *Genome Biology and Evolution,* **8** (3), 811-826.

Stahler, F. N., Odenbreit, S., Haas, R., Wilrich, J., Van Vliet, A. H., Kusters, J. G., Kist, M. & Bereswill, S. (2006): The novel *Helicobacter pylori* CznABC metal efflux pump is required for cadmium, zinc, and nickel resistance, urease modulation, and gastric colonization. *Infection and Immunity,* **74** (7), 3845-3852.

Stamatakis, A. (2014): RAxML version 8: a tool for phylogenetic analysis and post-analysis of large phylogenies. *Bioinformatics,* **30** (9), 1312-1313.

Stegmann, E., Pelzer, S., Wilken, K. & Wohlleben, W. (2001): Development of three different gene cloning systems for genetic investigation of the new species *Amycolatopsis japonicum* MG417-CF17, the ethylenediaminedisuccinic acid producer. *Journal of Biotechnology,* **92** (2), 195-204.

Stinchi, S., Azimonti, S., Donadio, S. & Sosio, M. (2003): A gene transfer system for the glycopeptide producer *Nonomuraea* sp. ATCC39727. *FEMS Microbiology Letters,* **225** (1), 53-57.

Stoppel, R.-D. & Schlegel, H. G. (1995): Nickel-resistant bacteria from anthropogenically nickel-polluted and naturally nickel-percolated ecosystems. *Applied and Environmental Microbiology,* **61** (6), 2276-2285.

Stoppel, R. D., Meyer, M. & Schlegel, H. G. (1995): The nickel resistance determinant cloned from the enterobacterium *Klebsiella oxytoca*: conjugational transfer, expression, regulation and DNA homologies to various nickel-resistant bacteria. *Biometals,* **8** (1), 70-79.

Strauch, E., Wohlleben, W. & Puhler, A. (1988): Cloning of a phosphinothricin N-acetyltransferase gene from *Streptomyces viridochromogenes* Tu494 and its expression in *Streptomyces lividans* and *Escherichia coli*. *Gene,* **63** (1), 65-74.

Strausak, D. & Solioz, M. (1997): CopY is a copper-inducible repressor of the *Enterococcus hirae* copper ATPases. *The Journal of Biological Chemistry,* **272** (14), 8932-8936.

Straw, M. L., Chaplin, A. K., Hough, M. A., Paps, J., Bavro, V. N., Wilson, M. T., Vijgenboom, E. & Worrall, J. A. R. (2018): A cytosolic copper storage protein provides a second level of copper tolerance in *Streptomyces lividans*. *Metallomics,* **10** (1), 180-193.

Strohl, W. R. (1992): Compilation and analysis of DNA sequences associated with apparent streptomycete promoters. *Nucleic Acids Research,* **20** (5), 961-974.

Sun, F. H., Luo, D., Shu, D., Zhong, J. & Tan, H. (2014): Development of an intergeneric conjugal transfer system for xinaomycins-producing *Streptomyces noursei* Xinao-4. *International Journal of Molecular Sciences,* **15** (7), 12217-12230.

Suzuki, H. (2011): Improvement of transformation efficiency by strategic circumvention of restriction barriers in *Streptomyces griseus*. *Journal of Microbiology and Biotechnology,* **21** (7), 675-678.

Tabillion, R. & Kaltwasser, H. (1977): Energieabhängige ^{63}Ni-Aufnahme bei *Alcaligenes eutrophus* Stamm H1 und H16. *Archives of Microbiology,* **113** (1), 145-151.

Taghavi, S., Delanghe, H., Lodewyckx, C., Mergeay, M. & van der Lelie, D. (2001): Nickel-resistance-based minitransposons: new tools for genetic manipulation of environmental bacteria. *Applied and Environmental Microbiology,* **67** (2), 1015-1019.

Taglicht, D., Padan, E. & Schuldiner, S. (1991): Overproduction and purification of a functional Na^+/H^+ antiporter coded by *nhaA* (*ant*) from *Escherichia coli*. *The Journal of Biological Chemistry,* **266** (17), 11289-11294.

Taglicht, D., Padan, E. & Schuldiner, S. (1993): Proton-sodium stoichiometry of NhaA, an electrogenic antiporter from *Escherichia coli*. *The Journal of Biological Chemistry,* **268** (8), 5382-5387.

Tan, B. G., Vijgenboom, E. & Worrall, J. A. (2014): Conformational and thermodynamic hallmarks of DNA operator site specificity in the copper sensitive operon repressor from *Streptomyces lividans*. *Nucleic Acids Research,* **42** (2), 1326-1340.

Teixeira, E. C., Franco de Oliveira, J. C., Marques Novo, M. T. & Bertolini, M. C. (2008): The copper resistance operon *copAB* from *Xanthomonas axonopodis* pathovar *citri*: gene inactivation results in copper sensitivity. *Microbiology,* **154** (Pt 2), 402-412.

The-UniProt-Consortium (2017): UniProt: the universal protein knowledgebase. *Nucleic Acids Research,* **45** (D1), D158-d169.

Thelen, P., Tsuchiya, T. & Goldberg, E. B. (1991): Characterization and mapping of a major Na^+/H^+ antiporter gene of *Escherichia coli*. *Journal of Bacteriology,* **173** (20), 6553-6557.

Thoma, L. & Muth, G. (2012): Conjugative DNA transfer in *Streptomyces* by TraB: is one protein enough? *FEMS Microbiology Letters,* **337** (2), 81-88.

Thoma, L. & Muth, G. (2015): The conjugative DNA-transfer apparatus of *Streptomyces*. *International Journal of Medical Microbiology,* **305** (2), 224-229.

Thoma, L., Vollmer, B. & Muth, G. (2016): Fluorescence microscopy of *Streptomyces* conjugation suggests DNA-transfer at the lateral walls and reveals the spreading of the plasmid in the recipient mycelium. *Environmental Microbiology,* **18** (2), 598-608.

Thompson, C. J., Movva, N. R., Tizard, R., Crameri, R., Davies, J. E., Lauwereys, M. & Botterman, J. (1987): Characterization of the herbicide-resistance gene *bar* from *Streptomyces hygroscopicus*. *The EMBO Journal,* **6** (9), 2519-2523.

Thong, S., Ercan, B., Torta, F., Fong, Z. Y., Wong, H. Y., Wenk, M. R. & Chng, S. S. (2016): Defining key roles for auxiliary proteins in an ABC transporter that maintains bacterial outer membrane lipid asymmetry. *Elife,* **5**.

Tian, J., Wu, N., Li, J., Liu, Y., Guo, J., Yao, B. & Fan, Y. (2007): Nickel-resistant determinant from *Leptospirillum ferriphilum*. *Applied and Environmental Microbiology,* **73** (7), 2364-2368.

Tiffert, Y., Gotz, B., Reuther, J., Wohlleben, W. & Muth, G. (2007): Conjugative DNA transfer in *Streptomyces:* SpdB2 involved in the intramycelial spreading of plasmid pSVH1 is an oligomeric integral membrane protein that binds to dsDNA. *Microbiology,* **153** (Pt 9), 2976-2983.

Tillotson, R. D., Wosten, H. A., Richter, M. & Willey, J. M. (1998): A surface active protein involved in aerial hyphae formation in the filamentous fungus *Schizophillum commune* restores the capacity of a bald mutant of the filamentous bacterium *Streptomyces coelicolor* to erect aerial structures. *Molecular Microbiology,* **30** (3), 595-602.

Titz, B., Häuser, R., Engelbrecher, A. & Uetz, P. (2007): The *Escherichia coli* protein YjjG is a house-cleaning nucleotidase *in vivo*. *FEMS Microbiology Letters,* **270** (1), 49–57.

Toledo, A. V., Franco, M. E. E., Yanil Lopez, S. M., Troncozo, M. I., Saparrat, M. C. N. & Balatti, P. A. (2017): Melanins in fungi: Types, localization and putative biological roles. *Physiological and Molecular Plant Pathology,* **99**, 2-6.

Torres, M. J., Argandoña, M., Vargas, C., Bedmar, E. J., Fischer, H.-M., Mesa, S. & Delgado, M. J. (2014): The global response regulator RegR controls expression of denitrification genes in *Bradyrhizobium japonicum*. *PLoS ONE,* **9** (6), e99011-e99011.

Tottey, S., Rondet, S. A., Borrelly, G. P., Robinson, P. J., Rich, P. R. & Robinson, N. J. (2002): A copper metallochaperone for photosynthesis and respiration reveals metal-specific targets, interaction with an importer, and alternative sites for copper acquisition. *The Journal of Biological Chemistry,* **277** (7), 5490-5497.

Tran, N. T., Den Hengst, C. D., Gomez-Escribano, J. P. & Buttner, M. J. (2011): Identification and characterization of CdgB, a diguanylate cyclase involved in developmental processes in *Streptomyces coelicolor*. *Journal of Bacteriology,* **193** (12), 3100-3108.

Tsai, Y. P. & Chen, H. T. (2011): Influence of sludge retention time on tolerance of copper toxicity for polyphosphate accumulating organisms linked to polyhydroxyalkanoates metabolism and phosphate removal. *Bioresource Technology,* **102** (23), 11043-11047.

Tsuboi, Y., Inoue, H., Nakamura, N. & Kanazawa, H. (2003): Identification of membrane domains of the Na^+/H^+ antiporter (NhaA) protein from *Helicobacter pylori* required for ion transport and pH sensing. *The Journal of Biological Chemistry,* **278** (24), 21467-21473.

Tusnady, G. E. & Simon, I. (1998): Principles governing amino acid composition of integral membrane proteins: application to topology prediction. *Journal of Molecular Biology,* **283** (2), 489-506.

Tzubery, T., Rimon, A. & Padan, E. (2004): Mutation E252C increases drastically the K_m value for Na^+ and causes an alkaline shift of the pH dependence of NhaA Na^+/H^+ antiporter of *Escherichia coli*. *The Journal of Biological Chemistry,* **279** (5), 3265-3272.

Ueda, K., Oinuma, K. I., Ikeda, G., Hosono, K., Ohnishi, Y., Horinouchi, S. & Beppu, T. (2002): AmfS, an extracellular peptidic morphogen in *Streptomyces griseus*. *Journal of Bacteriology,* **184** (5), 1488-1492.

Ueda, K., Tomaru, Y., Endoh, K. & Beppu, T. (1997): Stimulatory effect of copper on antibiotic production and morphological differentiation in *Streptomyces tanashiensis*. *The Journal of Antibiotics,* **50** (8), 693-695.

Umeda, K., Shiota, S., Futai, M. & Tsuchiya, T. (1984): Inhibitory effect of Li^+ on cell growth and pyruvate kinase activity of *Escherichia coli*. *Journal of Bacteriology,* **160** (2), 812-814.

Valls, M. & de Lorenzo, V. (2002): Exploiting the genetic and biochemical capacities of bacteria for the remediation of heavy metal pollution. *FEMS Microbiology Reviews,* **26** (4), 327-338.

van Dissel, D., Claessen, D., Roth, M. & van Wezel, G. P. (2015): A novel locus for mycelial aggregation forms a gateway to improved *Streptomyces* cell factories. *Microbial Cell Factories,* **14**, 44.

van Dissel, D., Willemse, J., Zacchetti, B., Claessen, D., Pier, G. B. & van Wezel, G. P. (2018): Production of poly-beta-1,6-N-acetylglucosamine by MatAB is required for hyphal aggregation and hydrophilic surface adhesion by *Streptomyces*. *Microbial Cell,* **5** (6), 269-279.

Van Houdt, R., Monsieurs, P., Mijnendonckx, K., Provoost, A., Janssen, A., Mergeay, M. & Leys, N. (2012): Variation in genomic islands contribute to genome plasticity in *Cupriavidus metallidurans*. *BMC Genomics,* **13**, 111.

van Keulen, G., Jonkers, H. M., Claessen, D., Dijkhuizen, L. & Wosten, H. A. B. (2003): Differentiation and anaerobiosis in standing liquid cultures of *Streptomyces coelicolor*. *Journal of Bacteriology,* **185** (4), 1455-1458.

Van Nostrand, J. D., Khijniak, T. V., Gentry, T. J., Novak, M. T., Sowder, A. G., Zhou, J. Z., Bertsch, P. M. & Morris, P. J. (2007): Isolation and characterization of four gram-positive nickel-tolerant microorganisms from contaminated sediments. *Microbial Ecology,* **53** (4), 670-682.

VanDrisse, C. M., Hentchel, K. L. & Escalante-Semerena, J. C. (2016): Phosphinothricin acetyltransferases identified using *in vivo, in vitro*, and bioinformatic analyses. *Applied and Environmental Microbiology,* **82** (24), 7041-7051.

Ventura, M., Canchaya, C., Tauch, A., Chandra, G., Fitzgerald, G. F., Chater, K. F. & van Sinderen, D. (2007): Genomics of Actinobacteria: tracing the evolutionary history of an ancient phylum. *Microbiology and Molecular Biology Reviews,* **71** (3), 495-548.

Vinnemeier, J., Dröge-Laser, W., Pistorius, E. K. & Broer, I. (1995): Purification and partial characterization of the *Streptomyces viridochromogenes* TÜ494 phosphinothricin-N-acetyltransferase mediating resistance to the herbicide phosphinothricin in transgenic plants. *Zeitschrift für Naturforschung C,* **50** (11-12), 796-805.

Vithanage, M., Rajapaksha, A. U., Oze, C., Rajakaruna, N. & Dissanayake, C. B. (2014): Metal release from serpentine soils in Sri Lanka. *Environmental Monitoring and Assessment,* **186** (6), 3415-3429.

Voeykova, T., Emelyanova, L., Tabakov, V. & Mkrtumyan, N. (1998): Transfer of plasmid pTO1 from *Escherichia coli* to various representatives of the order *Actinomycetales* by intergeneric conjugation. *FEMS Microbiology Letters,* **162** (1), 47-52.

Vogelmann, J., Ammelburg, M., Finger, C., Guezguez, J., Linke, D., Flotenmeyer, M., Stierhof, Y. D., Wohlleben, W. & Muth, G. (2011): Conjugal plasmid transfer in *Streptomyces* resembles bacterial chromosome segregation by FtsK/SpoIIIE. *The EMBO Journal,* **30** (11), 2246-2254.

Volff, J. N. & Altenbuchner, J. (2000): A new beginning with new ends: linearisation of circular chromosomes during bacterial evolution. *FEMS Microbiology Letters,* **186** (2), 143-150.

von Heijne, G. (1992): Membrane protein structure prediction. Hydrophobicity analysis and the positive-inside rule. *Journal of Molecular Biology,* **225** (2), 487-494.

von Rozycki, T. & Nies, D. H. (2009): *Cupriavidus metallidurans*: evolution of a metal-resistant bacterium. *Antonie Van Leeuwenhoek,* **96** (2), 115-139.

Wackett, L. P., Dodge, A. G. & Ellis, L. B. M. (2004): Microbial genomics and the periodic table. *Applied and Environmental Microbiology,* **70** (2), 647-655.

Wang, J. & Pettis, G. S. (2010): The *tra* locus of streptomycete plasmid pIJ101 mediates efficient transfer of a circular but not a linear version of the same replicon. *Microbiology,* **156** (9), 2723-2733.

Wang, L.-y., Li, S.-t. & Li, Y. (2003): Identification and characterization of a new exopolysaccharide biosynthesis gene cluster from *Streptomyces*. *FEMS Microbiology Letters,* **220** (1), 21-27.

Wang, L., Yu, Y., He, X., Zhou, X., Deng, Z., Chater, K. F. & Tao, M. (2007): Role of an FtsK-like protein in genetic stability in *Streptomyces coelicolor* A3(2). *Journal of Bacteriology,* **189** (6), 2310-2318.

Wang, X. K. & Jin, J. L. (2014): Crucial factor for increasing the conjugation frequency in *Streptomyces netropsis* SD-07 and other strains. *FEMS Microbiology Letters,* **357** (1), 99-103.

Waqas, M. (2018): Investigation of conjugational transfer of plasmids from *Streptomyces* strains to bacteria isolated from a heavy metal contaminated site. Institute for Microbiology. Jena, Friedrich Schiller University Jena.

Warren, R., Hsiao, W. W., Kudo, H., Myhre, M., Dosanjh, M., Petrescu, A., Kobayashi, H., Shimizu, S., Miyauchi, K., Masai, E., Yang, G., Stott, J. M., Schein, J. E., Shin, H., Khattra, J., Smailus, D., Butterfield, Y. S., Siddiqui, A., Holt, R., Marra, M. A., Jones, S. J., Mohn, W. W., Brinkman, F. S., Fukuda, M., Davies, J. & Eltis, L. D. (2004): Functional characterization of a catabolic plasmid from polychlorinated- biphenyl-degrading *Rhodococcus* sp. strain RHA1. *Journal of Bacteriology,* **186** (22), 7783-7795.

Weaden, J. & Dyson, P. (1998): Transposon mutagenesis with IS6100 in the avermectin-producer *Streptomyces avermitilis*. *Microbiology,* **144** (7), 1963-1970.

Wehmeier, U. F. (1995): New multifunctional *Escherichia coli-Streptomyces* shuttle vectors allowing blue-white screening on XGal plates. *Gene,* **165** (1), 149-150.

Weiss, B. (2007): YjjG, a dUMP phosphatase, is critical for thymine utilization by *Escherichia coli* K-12. *Journal of Bacteriology,* **189** (5), 2186-2189.

Wellington, E. M., Cresswell, N. & Saunders, V. A. (1990): Growth and survival of streptomycete inoculants and extent of plasmid transfer in sterile and nonsterile soil. *Applied and Environmental Microbiology,* **56** (5), 1413-1419.

West, I. C. & Mitchell, P. (1974): Proton/sodium ion antiport in *Escherichia coli*. *Biochemical Journal,* **144** (1), 87-90.

Westpheling, J., Ranes, M. & Losick, R. (1985): RNA polymerase heterogeneity in *Streptomyces coelicolor*. *Nature,* **313** (5997), 22-27.

Wheatley, R. M. & Poole, P. S. (2018): Mechanisms of bacterial attachment to roots. *FEMS Microbiology Reviews,* **42** (4), 448-461.

Willey, J., Santamaria, R., Guijarro, J., Geistlich, M. & Losick, R. (1991): Extracellular complementation of a developmental mutation implicates a small sporulation protein in aerial mycelium formation by *S. coelicolor*. *Cell,* **65** (4), 641-650.

Wimmer, R., Herrmann, T., Solioz, M. & Wuthrich, K. (1999): NMR structure and metal interactions of the CopZ copper chaperone. *The Journal of Biological Chemistry,* **274** (32), 22597-22603.

Wohlleben, W., Arnold, W., Broer, I., Hillemann, D., Strauch, E. & Puhler, A. (1988): Nucleotide sequence of the phosphinothricin N-acetyltransferase gene from *Streptomyces viridochromogenes* Tu494 and its expression in *Nicotiana tabacum*. *Gene,* **70** (1), 25-37.

Wolfram, L. & Bauerfeind, P. (2002): Conserved low-affinity nickel-binding amino acids are essential for the function of the nickel permease NixA of *Helicobacter pylori*. *Journal of Bacteriology,* **184** (5), 1438-1443.

Wolfram, L., Friedrich, B. & Eitinger, T. (1995): The *Alcaligenes eutrophus* protein HoxN mediates nickel transport in *Escherichia coli*. *Journal of Bacteriology,* **177** (7), 1840-1843.

Wolfram, L., Haas, E. & Bauerfeind, P. (2006): Nickel represses the synthesis of the nickel permease NixA of *Helicobacter pylori*. *Journal of Bacteriology,* **188** (4), 1245-1250.

Worrall, J. A. & Vijgenboom, E. (2010): Copper mining in *Streptomyces*: enzymes, natural products and development. *Natural Product Reports,* **27** (5), 742-756.

Wu, G., Yuan, M., Wei, L., Zhang, Y., Lin, Y., Zhang, L. & Liu, Z. (2014): Characterization of a novel cold-adapted phosphinothricin N-acetyltransferase from the marine bacterium *Rhodococcus* sp. strain YM12. *Journal of Molecular Catalysis B: Enzymatic,* **104**, 23-28.

Xia, W., Li, H., Sze, K. H. & Sun, H. (2009): Structure of a nickel chaperone, HypA, from *Helicobacter pylori* reveals two distinct metal binding sites. *Journal of the American Chemical Society,* **131** (29), 10031-10040.

Xu, H., Chater, K. F., Deng, Z. & Tao, M. (2008): A cellulose synthase-like protein involved in hyphal tip growth and morphological differentiation in *Streptomyces*. *Journal of Bacteriology,* **190** (14), 4971-4978.

Xu, M., Zhu, Y., Zhang, R., Shen, M., Jiang, W., Zhao, G. & Qin, Z. (2006): Characterization of the genetic components of *Streptomyces lividans* linear plasmid SLP2 for replication in circular and linear modes. *Journal of Bacteriology,* **188** (19), 6851-6857.

Yamasaki, M. & Kinashi, H. (2004): Two chimeric chromosomes of *Streptomyces coelicolor* A3(2) generated by single crossover of the wild-type chromosome and linear plasmid SCP1. *Journal of Bacteriology,* **186** (19), 6553-6559.

Yang, H. Y. & Chen, C. W. (2009): Extracellular and intracellular polyphenol oxidases cause opposite effects on sensitivity of *Streptomyces* to phenolics: a case of double-edged sword. *PLoS ONE,* **4** (10), e7462.

Yang, Y., Kurokawa, T., Takahama, Y., Nindita, Y., Mochizuki, S., Arakawa, K., Endo, S. & Kinashi, H. (2011): pSLA2-M of *Streptomyces rochei* is a composite linear plasmid characterized by self-defense genes and homology with pSLA2-L. *Bioscience, Biotechnology, and Biochemistry,* **75** (6), 1147-1153.

Yoshida, Y., Furuta, S. & Niki, E. (1993): Effects of metal chelating agents on the oxidation of lipids induced by copper and iron. *Biochimica et Biophysica Acta,* **1210** (1), 81-88.

Youn, H. D., Kim, E. J., Roe, J. H., Hah, Y. C. & Kang, S. O. (1996): A novel nickel-containing superoxide dismutase from *Streptomyces* spp. *The Biochemical Journal,* **318** (3), 889-896.

Yun, C. S., Hasegawa, H., Nanamiya, H., Terakawa, T. & Tozawa, Y. (2009): Novel bacterial N-acetyltransferase gene for herbicide detoxification in land plants and selection maker in plant transformation. *Bioscience, Biotechnology, and Biochemistry,* **73** (5), 1000-1006.

Zhang, J. & Inouye, M. (2002): MazG, a nucleoside triphosphate pyrophosphohydrolase, interacts with Era, an essential GTPase in *Escherichia coli*. *Journal of Bacteriology,* **184** (19), 5323-5329.

Zhang, R., Zeng, A., Fang, P. & Qin, Z. (2008): Characterization of replication and conjugation of *Streptomyces* circular plasmids pFP1 and pFP11 and their ability to propagate in linear mode with artificially attached telomeres. *Applied and Environmental Microbiology,* **74** (11), 3368-3376.

Zhang, Y., Rodionov, D. A., Gelfand, M. S. & Gladyshev, V. N. (2009): Comparative genomic analyses of nickel, cobalt and vitamin B12 utilization. *BMC Genomics,* **10**, 78.

Zhao, Z., Zhou, Z., Li, L., Xian, X., Ke, X., Chen, M. & Zhang, Y. (2014): A copper-responsive gene cluster is required for copper homeostasis and contributes to oxidative resistance in *Deinococcus radiodurans* R1. *Molecular BioSystems,* **10** (10), 2607-2616.

Zhou, G., Yang, H., Zhou, H., Wang, C., Fu, F., Yu, Y., Lu, X. & Tian, Y. (2016): Complete genome sequence of the *Streptomyces* sp. strain CdTB01, a bacterium tolerant to cadmium. *Journal of Biotechnology,* **229**, 42-43.

Zuo, Z., Liu, Y., Zhang, Y., Wang, C. & Heng, C. (2012): Mutation of the *Streptomyces clavuligerus* by traditional and molecular breeding to increase the biosynthesis of clavulanic acid. *African Journal of Microbiology Research,* **6** (13), 3144-3153.

Abbreviations

aa	Amino acid
A. dest	Destilled water
appr.	Approximately
CcO	Cytchrome c oxidase
COG	Cluster of Orthologous Groups
CR	Congo Red
CTAB	Cetrimonium bromide
Δ	Deletion
DIG	Digoxigenin
DMSO	Dimethyl sulfoxide
DNA	Deoxyribonucleic acid
dNTP	Nucleoside triphosphate
EDTA	Ethylenediaminetetraacetic acid
EPS	Exopolysaccharides
EVC	Empty vector control
5-Fu	5-fluorouracil
5-Fd	5-fluorouridine
HAD	Haloacid dehydrogenase
ICP-MS	Inductively Coupled Plasma - Mass Spectrometry
IPGT	Isopropyl β-D-1-thiogalactopyranoside
kb	Kilo basepair
MSO	Methionine sulfone
MSX	Methionine sulfoximine
MSXd	Methionine sulfoxide
NTA	Nitrilotriacetic acid
OD	Optical density
ORF	Open reading frame
PCR	Polymerase chain reaction
Pfam	Protein families
PNAG	Poly-β-1,6-N-acetylglucosamine
PPT	Phosphinothricin
PTT	Phosphinothricyl-alanyl-alanine
ROS	Reactive oxygen species
SDS	Sodium dodecyl sulfate
SOD	Superoxide dismutase
TAE	Tris-acetate-EDTA
TMD	Trans membrane domains
TMPD	N,N,N',N'-tetramethyl-p-phenylenediamine
Tn	Transposon
UV	Ultraviolet
w/o	Without
WT	Wildtype

Supplemental Material

S1 - DNA isolation from streptomycetes (Pospiech & Neumann, 1995, modified)

Material:

- SET buffer:
  - 75 mM NaCl
  - 25 mM EDTA (pH 8)
  - 20 mM Tris-HCl (pH 7,5)
- 10 mM EDTA (pH 8)
- Lysozyme solution: 50 mg/ml
- Proteinase K solution: 20 mg/ml
- 20 % SDS
- 5 M NaCl
- CTAB: 10 % CTAB, dissolved in 0,7 M NaCl
- 70 % Ethanol (4°C), chloroform/isoamyl alcohol, isopropanol

Steps:

- Take mycelium from liquid culture → centrifuge (13000 rpm, 15 min) → discard supernatant
- Add 1 ml 10 mM EDTA, vortex → centrifuge (13000 rpm, 15 min) → discard supernatant
- Resuspend pellet in 500 µl SET buffer and add 10 µl lysozyme solution → incubate 30 min at 37°C, invert regularly
- Centrifuge (13000 rpm, 5 min) → discard supernatant
- Resuspend in 500 µl 10 mM EDTA, → centrifuge (13000 rpm, 5 min) → discard supernatant
- Resuspend in 500 µl SET buffer, add 14 µl proteinase K solution and 30 µl SDS → mix by inverting several times
- Incubate 1 h at 55°C, invert every 10 min
- + 200 µl 5 M NaCl, invert
- + 130 µl CTAB, invert → 10 min 55°C, then 5 min 37°C
- + 500 µl chloroform/isoamyl alcohol, invert → 30 min at 20°C, invert every 5 min
- Centrifuge: 15 min, 13000 rpm, 20°C
- Transfer aqueous (upper) phase in new tube
- Add 0,6 vol. isoproanol, invert → incubate 30 min at RT (or at -20°C over night if DNA concentration is low)
- Centrifuge: 15 min, 13000 rpm, 4°C
- Discard supernatant
- + 500 µl 70 % ethanol → immediately remove ethanol, close the tube and centrifuge a couple of seconds
- Remove rest of ethanol → let DNA pellet dry
- Dilute DNA in 50 µl pure water
- Incubate 10 min at 65°C

S2 - Southern Blot and hybridisation

Material

- Nylon membrane
- DNA isolated from streptomycetes isolates
- DIG-labeled probe
- Positive control

Solutions

20× SSC
3 M NaCl
0.3 M sodium citrate, pH 7-8

Denaturation sol.
0,5 M NaOH
1,5 M NaCl

Neutralisation sol.
0.5 M Tris/HCl pH 7.5
3 M NaCl

Standard hybridisation buffer
5× SSC
1 % blocking reagent
0.02 % SDS

2× wash buffer
2× SSC
0.1 % SDS

0.5× wash buffer
0.5× SSC
0.1 % SDS

Detection buffer
10 mM NaCl
10 mM Tris/HCl pH 9.5

Detection wash buffer
0.1 M maleic acid pH 7.5
0.15 M NaCl
0.3 % Tween 20

Blocking solution
0.1 M maleic acid pH 7.5
0.15 M NaCl
1 % blocking reagent

Procedure

1) Restriction of genomic DNA and gel electrophoresis
- Digest 10 µg DNA with restriction enzyme:
  - → Prepare on ice: 10 µg DNA + 10 µl 10x buffer + 5 µl enzyme → fill up to 100 µl with pure water
  - → Centrifuge for a couple of seconds
  - → Incubate over night at 37 °C
- Precipitate DNA by addition of 1/10 Vol sodium acetate (3M) (→ mix well) and 2 Vol ice cold 96 % ethanol
- Mix by vortexing
- Centrifuge for 15 min, 13000 rpm, 4°C
- Discard supernatant, dry
- Solve pellet in 15 µl pure water, add 4 µl loading dye, mix (with pipette)
- Electrophoresis in 0.8 % agarose gel (use also 5 µl marker λ*Pst* I and positive control)
- 1 to 2 hours at 100 V for good separation over whole length of gel
- Ethidium bromide staining for 15 min
- Documentation of the gel under UV light

2) Depurination of the DNA
- Incubate gel for 10 min in 250 mM HCl (by shaking)

3) Denaturation, neutralisation and blotting
- Wash gel 2 x 10 min in denaturation solution
- Short rinsing in *A. dest*.
- Wash gel 2 x 10 min in neutralisation solution
- Cut membranes and Whatman paper (6 paper per membrane) in the same size as the gel
- Transfer the DNA onto the membrane over night by blotting using 20x SSC

Next day:

4) Fixation of DNA on the 2 membranes
- Remove clingfilm and papers carefully from membrane
- 3 min incubation of the membrane with UV light

5) Pre-hybridisation and hybridisation
- Put the membrane in hybridisation tube

- Add standard hybridisation buffer (20 ml/100 cm^2 surface of the membrane)
- Pre-hybridisation for 2 h at 68 °C rolling in the hybridisation oven
- Discard pre-hybridisation buffer
- Pour hybridization mixture (DIG-labelled denatured probe in 5 ml standard hybridisation buffer) in the tube
- Hybridization at 68 °C over night
- Remove the probe (reusable, store at -20 °C)
- Wash 2 x 5 min in 2x SSC wash buffer at room temperature (RT) rolling in the hybridisation oven
- Wash 2 x 15 min in 0.5x SSC at 68 °C rolling in the hybridisation oven

6) Detection
- Equilibrate in detection wash buffer (2 min)
- Incubation in blocking solution at RT for at least 30 min
- Incubation with alkaline phosphatase coupled anti-DIG antibody (1:10000 in blocking solution) for 30 min at RT
- 2 x 15 min in detection wash buffer at RT
- 2 min equilibration in detection buffer (not detection wash buffer!)
- Put the membrane on clingfilm with a few drops of CDP Star solution (amount depending on the size of the membrane)
- Cover membrane without bubbles in clingfilm
- Incubate 5 min at RT
- Detection of the chemo-luminescence on X-ray film in photographic lab, under red light
- Exposition at RT for 5 to 15 min depending on the intensity of the signal
- Bath in developer for 2 min, wash in water, bath in fixation solution for 2 min
- Rinse under tab water, dry at RT

S3 - Targeted gene replacement in *Streptomyces* sp., including conjugation

1. Cosmid construction

- Backbone: pKOSi (Netzker et al 2014)
- Amplification of DNA fragment that contains the gene of interest plus approx. 2000 bp upstream and downstream
  - Best results for streptomycetes: nested PCR, GLX Star polymerase, 2-step PCR in right PCR machine
  - If no amplificate with above mentioned conditions: try Phusion polymerase with GC buffer and addition of 7,5% DMSO + 10% betaine in PCR mixture
  - Nested primers have to have restriction enzyme cutting sites at 5' end (starting with 6 random bases for optimal performance of enzyme)
  - If nested amplificate shows several bands: clean-up by gel extraction; otherwise: clean-up with PCR purification kit → elution in 40 µl H_2O
- Digestion of pKOSi and PCR product with appropriate restriction enzymes in 50 µl end volume each
  - Use approx. 4 µg of vector and entire 40 µl PCR product
  - For vector digest: add 1 µl alkaline phosphatase (Fast-AP)
  - Example:
    40 µl PCR product
    1 µl enzyme A
    1 µl enzyme B
    5 µl 10x buffer
    3 µl H_2O
  - Time: at least 4 hours; best: overnight → incubation temperature depends on enzyme (usually 37°C)
- Clean-up of digest using PCR purification kit → elution in 20 µl H_2O each → measure concentration
- Ligation of digested vector and PCR product using T4 ligase
  - Choose amount of DNA according to the formula:

$$\text{PCR product needed [ng]} = \frac{\text{insert lenght [bp] x amount of vector [ng]}}{\text{vector lenght [bp]}} \text{ x } 5$$

    → Use 200-400 ng DNA altogether
  - Mixture:
    XX µl PCR product
    XX µl vector
    1 µl T4
    2.5 µl T4 buffer
    → add up water to 25 µl end volume
  - Ligate for approx. 4h at room temperature or 14°C over night
  - Stop ligation: 65°C 10 min
- Transformation of *E. coli* with 1.5 µl of ligation mixture (approx. 55 µl *E. coli*)
  - Use *E. coli* DH5α or *E. coli* TransforMax, for example
  - Plate on StdI containing 25 µg/ml kanamycin
  - Choose successful transformants e.g. by colony PCR or isolation from random colonies → liquid over night culture → plasmid isolation with Plasmid Purification Kit → test insertion of PCR product by digesting approx. 500 ng plasmid with same restriction enzymes as used before in 20 µl end-volume
- Transformation of *E. coli* BW25113 pIJ790
  - IMPORTANT: pIJ790 is temperature sensitive and will be lost at incubation temperatures above 30°C!
  - Transform this strain with 1.5 µl plasmid solution → incubate 1h at 30°C after transformation
  - Plate on StdI containing 25 µg/ml kanamycin and chloramphenicol → incubate at 28°C over night
  - Select transformants → liquid culture (28°C) → plasmid isolation with kit for testing successful transformation

2. **Resistance cassette amplification**
   - Template: plasmid pIJ773
   - Primers:
     - The 5' end of the primers have to be complementary to DNA upstream and downstream the target gene (39 bp each)
     - 3' end of primers are complementary to sequences on template plasmid
       - Upstream: ATTCCGGGGATCCGTCGACC
       - Downstream: TGTAGGCTGGAGCTGCTTC
   - PCR conditions: GLX Star polymerase, 2 step PCR, 2:30 min elongation
   - Purification of product with gel extraction → 2 consecutive times!!! → last step: elution in 20 µl H_2O → measure concentration

3. **Knock-out on plasmid**
   - Prepare over night culture of *E. coli* BW25113 pIJ790 pKOSiXXX in SOB medium
   - Preparation of electrocompetent cells:
     - Next morning: prepare 20 ml SOB liquid culture + 250 µl L-arabinose (1 M stock solution, filtered) + 50 µl kanamycin (10 mg/ml stock solution) + 16 µl chloramphenicol (36 ml/ml stock solution)
     - → incubate at 28°C on shaker until OD_{600} of approx. 0.6 is reached
     - Wash 3 times with ice cold 10% glycerine (centrifuge 10 min at 4°C, 130000 rpm) →resuspend in 60 µl 10% glycerine
   - Electroporation of entire 60 µl electrocompetent cells with 200-300 ng resistance cassette → revive cells one hour at 37°C
   - Plate on StdI containing 25 µg/ml kanamycin + 25 µg/ml chloramphenicol → 37°C over night
   - Colony PCR with transformants
     - Primers for apramycin resistance gene on resistance cassette:
       ApraF: GGTCCACAGCTCCTTCCGTA
       ApraR: TTATGAGCTCAGCCAATCGAC
     - DreamTaq, green buffer, 3 step PCR with annealing at 60°C for 10s and elongation at 72°C for 1 min
     - Prepare liquid culture of transformants that show a band → over night
     - Plasmid isolation with kit → gel electrophoresis → successful insertion transformants often now contain 2 kinds of plasmid: the cosmid without knock-out and plasmid with integrated resistance cassette
   - Transformation of *E. coli* ET12567 pUZ8002 with 1.5 µl of isolated knock-out plasmid (also if it is a mixture of cosmid with and without knock out → native cosmids will get lost during transformant selection)
   - → plating on StdI + apramycin + kanamycin + chloramphenicol (each 25 µg/ml) over night
   - Preparation of overnight liquid cultures of transformants
   - Plasmid isolation with kit → transformants now should only contain cosmid with knocked-out gene (to make sure: additional PCR with primers for resistance cassette as above)

4. **Conjugation**

DAY 1
   - *E. coli* pre-culture: inoculate 10 ml StdI (+ apramycin + kanamycin + chloramphenicol (each 25 µg/ml)) with E. coli ET12567 pUZ8002 pKOSIXXX-knock-out and incubate on shaker (150 rpm), 37°C over night

DAY 2
   - *E.coli*:
     - Inoculate 20 ml StdI (+ same antibiotics as pre-culture) with 1 ml E. coli-over night culture → incubate at 37°C at 150 rpm, ca. 1.5-3 h until OD_{595} = 0.5-0.7
     - → centrifuge the culture (11.000 rpm, 10 min, 4°C)
     - Wash 2 times with 2xTY (centrifuge as before)
     - Resuspend pellet in 250 µl 2xTY
   - *Streptomyces*:
     - Resuspend few spores in 250 µl 2xTY
     - Heat shock: 10 min 50°C → let cool down for 5-10 min
   - → mix *E. coli* and *Streptomyces* suspensions and plate whole mixture on MS medium containing 10 mM $MgCl_2$ → incubate over night at 28°C

DAY 3

- Cover plates with 1 ml sterile tab water containing 60 µl nalidixic acid (stock: 10 mg/ml) + 20 µl apramycin (stock 25 mg/ml) per plate → leave open until dry
- Incubate at 28°C until streptomycete colonies become visible
- After about 1 week: isolation of transformants by picking single colonies on CSA plates containing 25 µg/ml apramycin + 25 µg/ml nalidixic acid
- When transformants are properly grown (approx. after 3-5 days): picking some colonies on CSA (without antibiotics) → incubation at 37 °C for 2 days and then at 28°C until properly grown

5. Transformant purification

- When transformants from 37°C plate are properly grown and show spore production: preparation of spore suspension of one transformant → dilution series (usually until 10^{-4})
- Plate last 2 dilution steps on CSA + apramycin
- Singulation of grown transformants on CSA + apramycin
- Colony PCR with grown transformants:
    - Resuspend some mycelium in 40 µl pure water
    - 20 min 99°C, 450 rpm
    - Freeze over night at -20°C
    - PCR:
        - Primers: up- and downstream of knocked-out gene
        - GLX Star polymerase, 2-step PCR with appropriate elongation time (depending on target gene length)
    - If transformants show only one band in expected length of resistance cassette: probably clean knock-out → prepare liquid culture in TSB + 25 µg/ml apramycin
    - If transformants show 2 bands: not clean → repeat dilution series and singulation step

6. Confirmation of knock-out

- DNA isolation, e.g. by salting-out procedure
- PCR with primers and conditions as *Streptomyces* colony PCR before
- Southern Blot
    - Probe: approx. 800 bp DNA fragment directly upstream target gene
    - Restriction enzyme choice: if possible, choose restriction enzymes that cut one time in the target gene and create fragments not larger than 4000 bp and do not cut in the probe or between probe and target gene
        - Alternatively: enzyme that cuts in restriction cassette but not in wildtype gene

S4 – Primers used in the study

Table S4-1. Primers used for *aac(3)IV* detection and sequencing of rescue plasmids generated from Streptomyces sp. transposon transformants

Primer name	Sequence	Purpose
ApraF	GGTCCACAGCTCCTTCCGTA	Amplification of aac(3)IV fragment
ApraR	TTATGAGCTCAGCCAATCGAC	
pMODf	CCAACGACTACGCACTAGCCAAC	Sequencing of rescue plasmids
pMODr	GAGCCAATATGCGAGAACACCCGAGAA	

Table S4-2. Primers used for targeted gene replacement in *S. mirabils* P16B-1.

Target abbreviation	Primer name	Sequence	Purpose
tetR	n2TetRCon_for	ACACCTCCAGCACCACCTTCCCC	Primary Cosmid PCR
	n2TetRCon_rev	CGACGTACGTGCCGACCGGC	Primary Cosmid PCR
	TetR-CosmF	GTTACTTCTAGAGTCAAGGGCAGGGCGGCGGC	Secondary cosmid PCR
	TetR-CosmR	AATGATGGATCCGGTGGCGGGCGATCTCGTCC	Secondary cosmid PCR
	TetR downstr	CAGTAGCCCTCTCTGCCGGTCGCTCAACCCCA GGGGTTATGTAGGCTGGAGCTGCTTC	resistance cassette
	TetR upstr	TCGAAGGAGGTGCCGGGGCGTGCGTAGGCTC GGGGCATGATTCCGGGGATCCGTCGACC	resistance cassette
	TetR-ko-ctr_F	GCCGCCGAACTCCTTCACCT	deletion control
	TetR-ko-ctr_R	GGGGTCGGTAGACGTCACTCGA	deletion control
	TetR-ko-SB-F	GGCCCCGCCGAGCATCTTGC	probe Southern Blot
	TetR-ko-SB-R	CCCCGAGGTCCTGGTTCCCGTG	probe Southern Blot
Lipo	nLipoConF	CGTCCTGCTGGCCACCGCGC	Primary Cosmid PCR
	nLipoConR	GCGCCGCGTCATCTGCACCG	Primary Cosmid PCR
	LipoCosmF	AATAATAAGCTTTGCAGGCGGCGGCGTGAGCG	Secondary cosmid PCR
	LipoCosmR	AATAATGATATCCTCGACTCCCCGGCAAGCGTC	Secondary cosmid PCR
	Lipo-ko-F	CGGGTTAGTGATGTGACGGAATCGTGCGTGTC CATGACCATTCCGGGGATCCGTCGACC	resistance cassette
	Lipo-ko-R	ACCGGGCCCGGGTCTCAGTTCGAGTCCGCGTT CTCCAGATGTAGGCTGGAGCTGCTTC	resistance cassette
	Lipo-ko-ctr-F	GTCAAGGGCAAGAAGGGCTG	deletion control
	Lipo-ko-ctr-R	CCAGGGCATGTCGTTCAGTG	deletion control
	Lipo-ko-SB-F	CCTGGTCGAGGACACCTGGC	probe Southern Blot
	Lipo-ko-SB-R	CGCGGAAGAGCAGGTCGTTC	probe Southern Blot
Antip	nAntiportConF	AGCGGTTCCTCGACACGTAC	Primary Cosmid PCR
	nAntiportConR	TGCGTCACTGTAGTCGTGCG	Primary Cosmid PCR
	AntiportCosmF	AATAATAAGCTTGGGACGGGGCGAAGAAGGAC	Secondary cosmid PCR
	AntiportCosmR	AATAATGATATCGGTAGGACAGGCGTTCCCGT	Secondary cosmid PCR
	Antipor-koF	GCCGTCAGCAAGCAGCCGTAACGACCCGGAGG TCCCGCCATTCCGGGGATCCGTCGACC	resistance cassette
	Antipor-koR	CGGTCCTGACTGTCCGGTTCTGACCATCCGGTT CTGCTCTGTAGGCTGGAGCTGCTTC	resistance cassette
	Antipo-ko-ctrF	GGGAAGTCTGGTCGGCGGTG	deletion control
	Antipo-ko-ctrR	GGGCTGATCTCTACGGTCTGGCTG	deletion control
	Antip-ko-SB_F	GCGGAGAACCGGGAGCTGGGG	probe Southern Blot
	Antip-ko-SB_R	ATGGGCGCCCGCGTGGACGT	probe Southern Blot
AceTra	nAcTrCon_F	GTCCACCCCCTGCCAACCGC	Primary Cosmid PCR
	nAcTrCon_R	CCTTGCGTCGCTCCGTGAGC	Primary Cosmid PCR
	AcTrCosm_F	AATATTTCTAGACCAACCGCCAACCCGCCAACC G	Secondary cosmid PCR
	AcTrCosm_R	AATAATCCTAGGGCGGACCTCGTCAAAACCCC	Secondary cosmid PCR
	AcTr_ko_F	CCGCTAGAGGCCCTTCTCGTACCAGGCCACAT CCCAGTAATTCCGGGGATCCGTCGACC	resistance cassette
	AcTr_ko_R	CGCCCCCCTCTTTTTCTGATCATGCAGTACCCT GTGCCGTGTAGGCTGGAGCTGCTTC	resistance cassette
	AcTr_ko-contF	CTCCTGGTCGGTCGAGTTCG	deletion control
	AcTr_ko-contR	CAGCTCGACTTCCTTGGCGG	deletion control
	AcTr-ko-SB-F	CGCAAGGGAGCACGCATGGC	probe Southern Blot
	AcTr-ko-SB-R	TGTCGCCGTCGTCGTCCACC	probe Southern Blot
GlyTra	nGlyTraConF	TCACGGCACCTTGACCCACT	Primary Cosmid PCR
	nGlyTraConR	GCCGAAATGTCCCTGCCCTT	Primary Cosmid PCR

	GlyTraCosmF	AATAATAAGCTTGGGCCGCGAGTCCCGGTAGA GGTACG	Secondary cosmid PCR
	GlyTraCosmR	AGTTTTTCTAGATCCGTGCCGCGCCAGCCCTG	Secondary cosmid PCR
	Glytra-ko-F	ACGGGCACCGTCTTTCATTTCTTACGTCCCCCA AGGGAATCTGTAGGCTGGAGCTGCTTC	resistance cassette
	Glytra-ko-R	TCCGTTGTGTGGAGGATGTGGTGATGCCGACC TGCCAGCATTCCGGGGATCCGTCGACC	resistance cassette
	Glytra-ko-ctr-F	GTTGTCCTGGTTGTTGCCCG	deletion control
	Glytra-ko-ctr-R	TTCGTACACGCGTCCCAATT	deletion control
	GlyTra-ko-SB-F	GGGGTAGGTCGGGAACTGGC	probe Southern Blot
	GlyTra-ko-SB-R	CGGGCACTGGGACATCATCC	probe Southern Blot
PutProt	nPutProtConF	AGAAGACCGGCAAGAAGACC	Primary Cosmid PCR
	nPutProtConR	CAGCACGATCAGACACATGA	Primary Cosmid PCR
	PutProtCosmF	AATTTATCTAGAGGTCTGCTCGGCACCAACTG	Secondary cosmid PCR
	PutProtCosmR	AATTTACTCGAGACGCGATGGTCAGGTTCTGC	Secondary cosmid PCR
	PutProt-ko_F	GTCGTGAGCCCTGTACGTCGCTGTTCGCGAAC CGCTTGCTGTAGGCTGGAGCTGCTTC	resistance cassette
	PutProt-ko_R	ACGCTCAGTTGTCCGGCGAGCGCAGCACCCGT AGGTGGCATTCCGGGGATCCGTCGACC	resistance cassette
	PutProt-ko-ctrF	GCTCGATTCCGTATCCCTCC	deletion control
	PutProt-ko-ctrR	GACGGGAAAATGGTCGTGTC	deletion control
	PutProt-ko-SB_F	CATCGACGCACCGGTCCCGG	probe Southern Blot
	PutProt-ko-SB_R	ACGTTCGCCGGGCTTCCTGC	probe Southern Blot
sodN	sodNconF	TTGGTATCATGATGGGACTCGCCTTCCATCTC	Primary Cosmid PCR
	sodNconR	TTGGTATCATGAAGTTGAAGATCGTGTCGGGC	Primary Cosmid PCR
	nSodConF	TTATTAAAGCTTGCGTGGACCGCCTCGGCCTCT	Secondary cosmid PCR
	nSodConR	TTATTAGGATCCGGACTTCGCGGGCACCGTCG	Secondary cosmid PCR
	P16-sod-k.o.R	GGAGAAACCGAACAGGTCGCGGGCCGAGCCGT ATGACCATGTAGGCTGGAGCTGCTTC	resistance cassette
	P16-sod-k.o.F	ATCACGAGGAAGGACAGCTCAATGCTCTCCCG CCTGTTTATTCCGGGGATCCGTCGACC	resistance cassette
	sod-ko-contr.F	ACCTCCCCGGTCCATCCTCC	deletion control
	sod-ko-contr.R	GTCATGGACGCCGTGTTCGG	deletion control
	P16sod-ko-SB-F	TCCATCTCACCGCGTACGGC	probe Southern Blot
	P16sod-ko-SB-R	GGTGGAGGATGGACCGGGGA	probe Southern Blot
tipA	nP16-tipCon-F	GGGGTAGCGGTCCGCGTTCC	Primary Cosmid PCR
	nP16-tipCon-R	GCTGCCCTACACGACCGCCG	Primary Cosmid PCR
	P16-tipCosm-F	AATTTTTCTAGAGCGTTCCGCCGCATCCAGCG	Secondary cosmid PCR
	P16-tipCosm-R	AATTTCTCGAGTCCCAGGGTCGGCCACTTACTT CG	Secondary cosmid PCR
	P16tip-ko-F	CGTGAGGGCTGATGGTGGGACGCGTACGGAG GAAGGAGCATTCCGGGGATCCGTCGACC	resistance cassette
	P16tip-ko-R	CACCCGCAGTGGAGAGTGCCCCTTACCGTCTT GCCGTCATGTAGGCTGGAGCTGCTTC	resistance cassette
	P16tipA-ko-ctr-F	CACGGCCACACCCTAAGCGG	deletion control
	P16tipA-ko-ctr-R	GGAGGTGTGCGCCTACGGCA	deletion control
	P16tip-ko-SBF	GGGTGTCCGAGCCGGGAGAA	probe Southern Blot
	P16tip-ko-SBR	CTCGTCCTGCTGGGCGTCAG	probe Southern Blot
P_{tipA}	P16-Ptip-ko-F	CCCGAAGGGAGCGCTTCGGTACCCCGGGAATT CCGGCTTATTCCGGGGATCCGTCGACC	resistance cassette
	P16-Ptip-ko-R	GAGTAGCCCACTTCCGCTCCTTCCTCCGTACGC GTCCCATGTAGGCTGGAGCTGCTTC	resistance cassette
SigFak	nSigFakConF	GGCGAGCGTGGTGAAGGAGG	Primary Cosmid PCR
	nSigFakConR	CCGCGAGTTCCACCGACGAG	Primary Cosmid PCR
	SigFakCosmF	AATAATAAGCTTGATCAGCAGGGCGGTGACGA	Secondary cosmid PCR
	SigFakCosmR	AATAATGGATCCAAGGCGTCATGGGGAAGGGC	Secondary cosmid PCR
	SigFak-koF	CGGCAGTGCTTTTTCCGGTTTTTCCGGCGGTTC TACGGCATTCCGGGGATCCGTCGACC	resistance cassette
	SigFak-koR	GGACCGGCGGGTGAGCGCAAAGGGGCCCTCA TGGCGACGTGTAGGCTGGAGCTGCTTC	resistance cassette
	SigFak-ko-ctr_F	CGGGTTTCCGGCGGCTCGAC	deletion control
	SigFak-ko-ctr_R	CCCCTCCACAACCGCGGCTACC	deletion control
	SigFak-ko-SB-F	CCCGATCGGCCCCTGCATCC	probe Southern Blot
	SigFak-ko-SB-R	AAACCCGGCCGCAAGACCCC	probe Southern Blot
hoxN	nP16-hoxCon_F	CGATGTAGGGGTCCCACTCG	Primary Cosmid PCR

	nP16-hoxCon_R	TGCGAGCCAGGTCCAGACAG	Primary Cosmid PCR
	P16-hoxCosm_F	AATAGAAAGCTTGTCGAAGACCACGTGGCGGG	Secondary cosmid PCR
	P16-hoxCosm_R	AATAAAGGATCCCAGGTCCAGACAGCCGAGCTG	Secondary cosmid PCR
	P16hox-ko-R	TCGGCGACGAGGTGAGAACGGCTGCTGCCCGGCGAGAGCTGTAGGCTGGAGCTGCTTC	resistance cassette
	P16hox-ko-F	GTGCGCCCTCCAGCCGAACTCACGCGTCACCCGCTGTCAATTCCGGGGATCCGTCGACC	resistance cassette
	P16hox-ko-ctr_F	GGCCTGCTCGTCGGAGTCAGCG	deletion control
	P16hox-ko-ctr_R	CAAGGCGGACAGGGCGGGG	deletion control
	P16hox-ko-SB-F	GGGCCGCGACCAGATCCAGC	probe Southern Blot
	P16hox-ko-SB-R	GTGCACGGTCTGAGCCCACCC	probe Southern Blot
nreB	nNreBCon_F	GCGGTACCCCGAAGGTCCCC	Primary Cosmid PCR
	nNreBCon_R	TCCCCCATCAAGACCCACGG	Primary Cosmid PCR
	nreBCosm_F	AATTATTCTAGACCCGGCCTCGATCACGCTGC	Secondary cosmid PCR
	nreBCosm_R	AATTAACTCGAGGAGAAGGCCCAGGCTCTCGC	Secondary cosmid PCR
	nreB-ko_F	GAGGCTCTCCACTGTACCTACATGTGCGCACCTGCGCACATTCCGGGGATCCGTCGACC	resistance cassette
	nreB-ko_R	CCGGCGCGTACGGCACCTCCCCCTCGGCGGCCTGAACCTTGTAGGCTGGAGCTGCTTC	resistance cassette
	nreB-ko-ctr-F	CGTGCCGACCAGGGCGATGA	deletion control
	nreB-ko-ctr-R	GCACCTGACCGGCGTACCGC	deletion control
	nreB-ko-SB-F	CGCTCAGCATCACCACACGG	probe Southern Blot
	nreB-ko-SB-R	ACAGTGGCCCTCGGCTTGCT	probe Southern Blot
copY	nCupRes_Con_F	CCGTCTGCGCCTGGCCGAGC	Primary Cosmid PCR
	nCupRes_Con_R	CGGGACAGCGGTGTGGAGGACG	Primary Cosmid PCR
	CupRes_Cosm_F	AATATAAAGCTTCGGGCGCCCACCAGTTGGCC	Secondary cosmid PCR
	CupRes_Cosm_R	AATATGGGATCCGTCCGGTCAGCCGCAACGCC	Secondary cosmid PCR
	CopY-ko-F	ATTCCGGGGGTCGGCGTGACGGATGCCAAGTCGTGGTTCATTCCGGGGATCCGTCGACC	resistance cassette
	CopY-ko-R	GTACCGAGGTGTCGGGAGACGCGGGTGCAGGATCAGGTGTGTAGGCTGGAGCTGCTTC	resistance cassette
	CopY-ko-SB-F	GAGGCCGGGTGAGGTGCTGG	probe Southern Blot
	CopY-ko-SB-R	CGACAGCGCGAACGCAGGGC	probe Southern Blot
	CopY-ko-ctr-F	GGACGTCGTGGCAACAATGACC	deletion control
	CopY-ko-ctr-R	CCGGTGTTCCTCGTGGTTCC	deletion control
copZ	CuP2-ko-R	CCCGGTCAGTGGGCGTGGGCCGAAGCGCGGCCGGAGAGGTGTAGGCTGGAGCTGCTTC	resistance cassette
	CuP2-ko-F	CTCCGTATAGCGGCAGCTGCTTGCGTAGCGTCGGCCTCCATTCCGGGGATCCGTCGACC	resistance cassette
	Cup2-ko-SB-F	CACCCGCGTCCTGAGAATCG	probe Southern Blot
	Cup2-ko-SB-R	TCTCCTTCGCCCGTCACGCT	probe Southern Blot
	CuP2-ko-ctr-F	TGTTGACGCCCCGGAGCAGG	deletion control
	CuP2-ko-ctr-R	TTCGCCGTGCGCCAGTAAGG	deletion control
phoxN	nP16pHoxNCon_F	TACGATCCCGAGACCTCACG	Primary Cosmid PCR
	nP16pHoxNCon_R	ATGTCGGCCACGGTCTTGAC	Primary Cosmid PCR
	P16pHoxNCosm_F	TAAAATAAGCTTCTCAACCGGCGTTTCTGGACC	Secondary cosmid PCR
	P16pHoxNCosm_R	AATAATCTCGAGGCGGTGCAGGATGTCGGCCAC	Secondary cosmid PCR
	phox-ko_F	CTGCCAGGGACCACGCCGAGCCCCGCCGAGCGAGGAAGCATTCCGGGGATCCGTCGACC	resistance cassette
	phox-ko_R	TACTCATGGGCTGCTTCCCTCGGGGCGATCTCGGCCATGTGTAGGCTGGAGCTGCTTC	resistance cassette
	P16phox-ko-ctr_F	GCCCCGCCGAGCGAGGAAGC	deletion control
	P16phox-ko-ctr_R	GGCACCAGCCGGACACCGCC	deletion control
p(II)-ko	K.o.-P16pII-F	GCGTATGGACATCGGTGCGTCATCCTGCCCTGCCGTATGATTCCGGGGATCCGTCGACC	resistance cassette
	K.o.-P16pII-R	GGACGGTGTGGACCAGCGGTGACCGCAAGCGTGGCCTCATGTAGGCTGGAGCTGCTTC	resistance cassette
	K.o.-P16p12-CF	GCCGAACGCTGACCAGCCGC	deletion control
	K.o.-P16p12-CR	CCAGCCTGCCGGACGGTGTG	deletion control
melC2	n_pI-TyrCon-F	GGTCGGCTGAATTGTTCGCAGGG	Primary Cosmid PCR
	n_pI-TyrCon-R	TATGACGAGGGCGGCGGCAC	Primary Cosmid PCR
	pI-TyrCosm-F	AATTTTCTCGAGCCGGAGGGCCAGCGAACTGG	Secondary cosmid PCR
	pI-TyrCosm-R	AATTTTTCTAGAGCAGCGTGGGTATCGGGGCACCG	Secondary cosmid PCR

	pI-Tyr-ko-F	CAGCACATCGTGGAGTCCCGCACATGACCGTA CGCAAGAATTCCGGGGATCCGTCGACC	resistance cassette
	pI-Tyr-ko-R	CCGGACCTGTGAACGCGCCGTCAGACGGTGTC GAAGGTGTGTAGGCTGGAGCTGCTTC	resistance cassette
	Tyr-ko-ctr-F	ACGCCCGTCACGTCTGGGGT	deletion control
	Tyr-ko-ctr-R	CGACGGCAGCTGGATCAGCG	deletion control
	Tyr-ko-SB-F	TCATGTCGTCGTGCGCTGTC	probe Southern Blot
	Tyr-ko-SB-R	AGAGGTGGCCGTCCAGGAAC	probe Southern Blot

Table S4-3. Primers used for targeted gene replacement in *S. acidiscabies* E13.

Target abbre-viation	Primer name	Sequence	Purpose
Phos	n2PhosCosm_for	CATCTGCTGCTCGACCTGTCCGAGG	Primary Cosmid PCR
	n2PhosCosm_rev	TCGCGATGCCCTGGCGGTTG	Primary Cosmid PCR
	PhosCosmF	AATTATTCTAGAGCATCAACGCACTCCTGAAGG	Secondary cosmid PCR
	PhosCosmR	AGTCAAGGATCCACGGTCTTCATGAGGTGCTG	Secondary cosmid PCR
	K.o.-PhosF	GCATCGTACTAGTCGAAGAATGGCGTATCCGAC ATCGTGATTCCGGGGATCCGTCGACC	resistance cassette
	K.o.-PhosR	GCGCCCGACCGCTCGGCCAGCGCGAGGCCCG CGGCCCTATGTAGGCTGGAGCTGCTTC	resistance cassette
	Phos-ko-ctr_F	GGAGGAAGTCACGGTTTCAC	deletion control
	Phos-ko-ctr_R	ACGTGTTCGTCTCCTTCGTC	deletion control
	Phos-ko-SB-F	CACGTGGGCGAGGGGACCTC	probe Southern Blot
	Phos-ko-SB-R	GGACCGGCATACGAGGGACCC	probe Southern Blot
hoxN	nE13hoxNCon_F	TGACCCCGGCACTCCGTCGC	Primary Cosmid PCR
	nE13hoxNCon_R	GACGTCGATCCGGCCGCTCG	Primary Cosmid PCR
	E13hoxNCosm_F	AATTTAGGATCCAGTCCGACGACGACCGCGAG	Secondary cosmid PCR
	E13hoxNCosm_R	AATAATAAGCTTGAGGCGGATCGCGGAGGCGG	Secondary cosmid PCR
	E13hox-ko-F	TCGACATCTGACCTCGGCTTTACTGCGCCCTAG TAGCACTGTAGGCTGGAGCTGCTTC	resistance cassette
	E13hox-ko-R	GCGAAGGCGCCCTACTCGACGCGCTGCTCGGC CGGTTGTATTCCGGGGATCCGTCGACC	resistance cassette
	E13hox-ko-SB-F	GAGGGCGACGGCGACGGACA	probe Southern Blot
	E13hox-ko-SB-R	CCTGGGGATGCGGCACGCCT	probe Southern Blot
	E13hox-ko-ctr-F	GGTTCGTCCCGGGCGGGTAC	deletion control
	E13hox-ko-ctr-R	CCCCGCACAGCCGTTCGCCT	deletion control
sodN	nsodN_E13_CosF	AGGCCTCCCGGCGGTTCTCC	Primary Cosmid PCR
	nsodN_E13_CosR	CCTCGGCGATGGTGAGCAGTGC	Primary Cosmid PCR
	sodN_E13_CosF	TTATTATCTAGAAGGGCGTCGCAGTCGGTCGT	Secondary cosmid PCR
	sodN_E13_CosR	TTATTAAAGCTTCGCACGCCAGGTCAAGGACGC	Secondary cosmid PCR
	E13-sod-k.o.R	GGGTCAGGCCTGCTTGGTCTCCCAGAAGATCTT GTCGATTGTAGGCTGGAGCTGCTTC	resistance cassette
	E13-sod-k.o.F	TCAATGCTCTCCCGCCTGTTTGCCCCCAAGGTG AAGGTCATTCCGGGGATCCGTCGACC	resistance cassette
	E13sodN-ko-ctrF	GAACTCGACAGCGTGCCCAC	deletion control
	E13sodN-ko-ctrR	CACCAGTCCCAGTCTCACCCTG	deletion control
	E13sodN-ko-SB-F	GGGGAGGTGCCGGTGATGCCGG	probe Southern Blot
	E13sodN-ko-SB-R	AGCAACGCGTCGGCGGCCCG	probe Southern Blot
tipA	nE13-tipCon-F	CCATCACCAGGTTGGGCCGCG	Primary Cosmid PCR
	nE13-tipCon-R	CCTCGGTTCGGAGATCTCGCG	Primary Cosmid PCR
	E13-tipCosm-F	AAATATTCTAGAGGGGTAGCGGTCGGCGTTGC G	Secondary cosmid PCR
	E13-tipCosm-R	AAATTTCTCGAGTCTTCCTGCGGCTGCCGGGC	Secondary cosmid PCR
	E13tip-ko-F	GTGGCGTGAGGACCCATCGTGAAGCGCGTACC GAGGAAGATTCCGGGGATCCGTCGACC	resistance cassette
	E13tip-ko-R	GGCCGCCATGGACGGACGCCCCTTACTCCTTT GTCTACGTGTAGGCTGGAGCTGCTTC	resistance cassette
	E13tipA-ko-ctr-F	CGGTCACGGGCTCACCCTAA	deletion control
	E13tipA-ko-ctr-R	CATGGACGGACGCCCCTTACT	deletion control
	E13tip-ko-SB-F	TTCACCACGGTCATCAGCGC	probe Southern Blot
	E13tip-ko-SB-R	GCCGAACAGCTCAAGGACGT	probe Southern Blot
P_{tipA}	E13-Ptip-ko-F	GCCGCCCGGGGGCGTCCCGGGCCGGACGACG GGCCGGGAATTCCGGGGATCCGTCGACC	resistance cassette
	E13-Ptip-ko-R	AGTAGCTCAACGTCCGCTCCTTCCTCGGTACGC	resistance cassette

		GCTTCATGTAGGCTGGAGCTGCTTC	
$P_{tipA(alt)}$	E13-P(alt)tip-ko-F	CGGCGGGGGAGAGGCCGCCCGGGGGCGTCCC GGGCCGGAATTCCGGGGATCCGTCGACC	resistance cassette
	E13-P(alt)tip-ko-R	TCCTTCCTCGGTACGCGCTTCACGATGGGTCCT CACGCCTGTAGGCTGGAGCTGCTTC	resistance cassette
yjjG	nE13_HydrolCon_F	TTGGCCCGGTTCTTCGTCCA	Primary Cosmid PCR
	nE13_HydrolCon_R	GCACGCGAGAGGTGGAGTTCC	Primary Cosmid PCR
	E13_HydrolCon_F	TTATTAAAGCTTCAGCGGTGGGACGAGTACAT	Secondary cosmid PCR
	E13_HydrolCon_F	TTAGTAGGATCCTCACACAGCCAGGTTTCCGG	Secondary cosmid PCR
	E13_Hydrol-k.o.2F	GTGCTACTCCGTCTCGTTGAGCAGGATGGTGAT GGCGTCATTCCGGGGATCCGTCGACC	resistance cassette
	E13_Hydrol-k.o.2R	AAGTGATCTGTCGTAGGGCGCCCTCAAGGACTT GACGGCTGTAGGCTGGAGCTGCTTC	resistance cassette
	E13Hyd-ko-ctr_F	CGGGCGGGCAGAGGCTGATG	deletion control
	E13Hyd-ko-ctr_R	GTCTCCCACCGGGCCACCTGA	deletion control
	Hydrol-ko-SB-F	CGCCGATCGAGTCCTTGCTG	probe Southern Blot
	Hydrol-ko-SB-R	GGGCGCTGAAGGTGAGCTCTT	probe Southern Blot

Table S4-3. Primers used for genetic complementation of streptomycete strains.

Primer name	Sequence	Purpose	Plasmid name
hphMFS-F	AATTATTCTAGAGGCCCGTCCCGGC GCGTACGTCG	P16nreB for pSEThph	pSEThphMFS
hphMFS-R	AATATTGCGGCCGCTTCACGGCGT GTCTCCACCA	P16nreB for pSEThph	
nAceTraF	AATAATGCGGCCGCCACCCCCGTA CCGAGCACTT	P16pat1 for pSEThph	pSEThphpat1
nAceTraR	AATAATGGATCCGGCGTCGAGCAG CGGCGTAC	P16pat1 for pSEThph	
Antip2F	TTATTATCTAGAGGGCGGGCTCTCA CAGGTCC	P16nhaA1 for pSEThph	pSEThphnhaA1
Antip2R	TTATTAGCGGCCGCGGTTCTGCTCA GATCATGCC	P16nhaA1 for pSEThph	
Ecol.nhaA-F	AATTTTCGATCGTCCTACACTATAAT CTGATTTTAACG	E. coli nhaA for pSEThph	pSEThphEcnhaA
Ecol.nhaA-R	AATAGTGCGGCCGCTTGTAATTGAT ATGAGACAT	E. coli nhaA for pSEThph	
GlytraF	TCACTCATTAATCCAGCGCGAGCAC CACCGCC	P16cslA for pSEThph	pSEThphcslA
GlytraR	TTATTAGCGGCCGCAGTGACCCCAT CTTCGTACAC	P16cslA for pSEThph	
SigFak_for	TTATTACGCGCGCGAGGCGGATTTT TTTCGGGGG	P16sfECF for pSEThph	pSEThphSfECF
SigFak_rev	TTATTAGGATCCCCACGGCAACGG CGACGGGCGG	P16sfECF for pSEThph	
E13_Hydrol_F	TTATTACGCGCGCGCTACTCCGTCT CGTTGAGCA	E13yjjG for pSEThph	pSEThphyjjG
E13_Hydrol_R	TTATTTGGATCCTTGACCGGTGTCA GTCCTGCTGAGG	E13yjjG for pSEThph	
P16hoxN-F	AATTTATCTAGACGACCGCGCCCAG GCAGCAGG	P16hoxN for pSEThph	pSEThphP16hox
P16hoxN-R	AATAAAGCGGCCGCACATCAGGGT GCTGCCCAAG	P16hoxN for pSEThph	
E13hox-SET-F	AAATTATCTAGAGTGTGGAAATGTA CGGGCGAAGGCGCC	E13hoxN for pSEThph	pSEThphE13hox
E13hox-SET-F	AATAATGCGGCCGCGATCCTGGTC GACATCTGAC	E13hoxN for pSEThph	
phox-pSET-R	TAGTTTTCTAGACTCAACCGGCGTT TCTGGACC	P16phoxN for pSEThph	pSEThphP16phox
phox-pSET-F	AATAATGCGGCCGCGCGGTGCAGG ATGTCGGCCAC	P16phoxN for pSEThph	
CuP2Cosm-pSET-F	AATATACGCGCGCGATCACGGCCG GGACGAGGAT	copY-copZ carrying fragment of P16pII for pSEThph	pSEThphCuP2Cosm
CuP2Cosm-pSET-R	AATATACGCGCGCGGCCGCATGAG CTGGTCACTC	copY-copZ carrying fragment of P16pII for pSEThph	
nreBCosm-pSET-F	AATTACCGCGCGCGTAGACCCGGC CTCGATCACG	P16nreB carrying fragment of P16pII for pSEThph	pSEThphnreBCosm
nreBCosm-	AATTACCGCGCGCGTCGCCGAGAA	P16nreB carrying fragment	

pSET-R	CGTAGAGCTC	of P16pII for pSEThph	
phox-pSET-R	TAGTTTTCTAGACTCAACCGGCGTTTCTGGACC	P16phoxN carrying fragment of P16pII for pSET152	pSETphoxCosm
phox-pSET-F	AATAATGCGGCCGCGCGGTGCAGGATGTCGGCCAC	P16phoxN carrying fragment of P16pII for pSET152	
P16tipA-F	AATAAATCTAGAGCGGCAACACCGACCACCACGG	P16tipA for pSEThph	pSEThphP16tipA
P16tipA-R	AATAAAGCGGCCGCAGAATCCGGTAAGGGGCACC	P16tipA for pSEThph	
E13tipA-F	AATAAATCTAGAGAGCCGCTTCGTCGGTCACG	E13tipA for pSEThph	pSEThphE13tipA
E13tipA-R	AATAAAGGATCCAGGAGTAGCGCGAACGGCCC	E13tipA for pSEThph	

Table S4-4. Primers used for construction of pTrc99A derivatives.

Primer name	Sequence	Purpose	Plasmid name
Antip_pTrc_F	TTATTATCTAGAAGGGCGGGCTCTCACAGGTCC	P16 nhaA1 for pTrc99A	pTrcnhaA1
Antip_pTrc_R	TTATTACTGCAGGGTTCTGCTCAGATCATGCC	P16 nhaA1 for pTrc99A	
nhaA2-pTr-F	TTTTTTAAGCTTGATCTGTTCGAGGGCGCCCG	P16 nhaA2 for pTrc99A	pTrcnhaA2
nhaA2-pTr-R	AATATTTCTAGATCCTTCCCCGGCATCGTTTCG	P16 nhaA2 for pTrc99A	
AcTr-pTrc_F	AATAGTGGATCCGTGGGAGGTCGGATGCCAACG	P16pat1 for pTrc99A	pTrcP16pat1
AcTr-pTrc_R	AATAATAAGCTTACGGGTTCTGGCTGGGGCTG	P16pat1 for pTrc99A	
Actr2-pTrc-F	AATAAAGGATCCAAAACGGGCCGGGACTCCGC	P16pat2 for pTrc99A	pTrcP16pat2
Actr2-pTrc-R	AATAAAAAGCTTCGGGCGACCTGATCACCTCGT	P16pat2 for pTrc99A	
TK24pat2F	TATTGTGGATCCGTTATGCCGGGAACTGCCGA	TK24pat for pTrc99A	pTrcTK24pat
TK24pat2F	AATAAAAAGCTTCGACGGGTTCTGGATGGGCC	TK24pat for pTrc99A	
E13hox-pTrc-F	AATAATAAGCTTAAATGTACGGGCGAAGGCGC	E13hoxN for pTrc99A	pTrcE13hox
E13hox-pTrc-R	AATAATGGATCCTGACCTCGGCTTTACTGCGC	E13hoxN for pTrc99A	
P16phox-pTrc-F	AATTTAAAGCTTATCCTGCCAGGGACCACGCC	P16phoxN for pTrc99A	pTrcphox
P16phox-pTrc-R	AATTTATCTAGACGCATGTAACTCCTCAGCGCA	P16phoxN for pTrc99A	
MFS-pTrc-F	AATAAAGGATCCTGCGGTCGGCGGGTCAATTC	P16nreB for pTrc99A	pTrcMFS
MFS-pTrc-R	AATAAAAAGCTTCCCGCCCGACATCCTCGACC	P16nreB for pTrc99A	
hox-pTrc-F	AAATACAAGCTTTCCTGCCAGGGACCACGCCGAGC	P16hoxN for pTrc99A	pTrcP16hox
hox-pTrc-R	AATTATTCTAGAGGCACCAGCCGGACACCGCC	P16hoxN for pTrc99A	
Hyd-pTrcF	AATATTAAGCTTCTCCGTCTCGTTGAGCAGGA	E13yjjG for pTrc99A	pTrcyjjG
Hyd-pTrcR	AATAATGGATCCGCGTGTCGAGTGGCGATGCG	E13yjjG for pTrc99A	
A3(2)sodNF	ATTAATGCGGCCGCCACTGCGACCTGCCCTGCGGCGTGTA	S. coelicolor A3(2) sodN for pSET152	pSETsod
A3(2)sodNR	ATTAATTCTAGACGGGCCCCTTCGGGCTGCCCTGCGGC	S. coelicolor A3(2) sodN for pSET152	

Table S4-5. Primers used for construction of streptomycete overexpression plasmids.

Primer name	Sequence	Purpose	Plasmid name
Acetra_OvExF	AATAATAAGCTTGTGGGAGGTCGGATGCCAACG	P16pat1 for pUWL201	pUWLpat1
Acetra_OvExR	AATAATGGATCCACGGGTTCTGGCTGGGGCTG	P16pat1 for pUWL201	
Antip_OvEx_F	AATAGTAAGCTTGTGGCCACGCCCAGTGCCAA	P16nhaA1 for pUWL201	pUWLP16nhaA1
Antip_OvEx_R	AATAAACTGCAGGCTCAGATCATGCCGGACCGTCGT	P16nhaA1 for pUWL201	
CuP2-OvEx_F	AATAATGGATCCCCCGATGGGCGTGTCCCTGT	P16copZ for pUWL201	pUWLCopZ
CuP2-OvEx_R	AATAATAAGCTTCGGATGGCTGGGCGACTTTTCGGC	P16copZ for pUWL201	
pP16-MFS-OvEx-F	AATATAGGATCCCTGGATACGTGCCGGAGGAC	P16nnreB for pUWL201	pUWLMFS
pP16-MFS-OvEx-R	AATAACAAGCTTAGGCCGAACGGAGCGATCGA	P16nnreB for pUWL201	

S5 – Electronic supplementary material

Number	File name	Content
eS1	Primers.xlsx	Primers used in this study
eS2	Accession numbers tree.xlsx	Accession numbers of sequences used for phylogenetic tree generation
eS3	Accession numbers aa sequence allignments.xlsx	Acession numbers for sequences used for protein sequence alignments
eS4	Chemicals.xlsx	Chemicals used in this study
eS5	Investigated genes.xlsx	Sequences of genes and proteins of *S. mirabilis* and *S. acidiscabies* investigated in this study
eS6	Rescue plasmid sequences.xlsx	Sequencing results of rescue plasmids generated from *Streptomyces* sp. transposon transformants
eS7	E. coli growth curves.xlsx	Raw data *E. coli* growth tests
eS8	Biomass metal content.xlsx	Raw data biomass metal analysis
eS9	Urease and attachment test.xlsx	Raw data urease activity test and mycelium attachment assay

Acknowledgment

I want to thank Prof. Dr. Kothe and Prof. Dr. Brakhage for giving me the opportunity to work on this project, for their guidance and for granting me the freedom of developing and realizing my own project and experiments. I know that this autonomy in work was a unique opportunity one rarely finds in professional life and I always appreciated it.
Furthermore, my thanks go to Dr. Katrin Krause who encouraged me not to give up when I was disappointed and helped me to look deeper in the single subjects!

I am grateful for the advices of Dr. Tina Netzker and Dr. Volker Schroeckh from the HKI who helped me especially during the initial phase of this project for getting started and provided important plasmids, protocols and hints in how to continue. For their help in the chemical and mineralogical analysis of my samples I also want to acknowledge Dr. Dirk Merten and Prof. Dr. Falko Langenhorst from the Institute of Geology.

Of course, I want to thank the entire Microbial Communication group and all colleagues who supported me during this time and created a positive working atmosphere. Insbesondere möchte ich Christin Reichmann und Petra Mitscherlich danken, die stets für mich und die anderen da waren und gemeinsam mit Katrin nicht zu unterschätzende Konstanten in der AG sind. Lieben Dank für eure Unterstützung.
Und selbstverständlich darf ich die ganze Bürogemeinschaft der ersten Etage nicht vergessen, inkl. Mable, die leider auch mal meine schlechte Laune und Frustration ertragen mussten. Ich danke euch für die lustige und zum Teil aufschlussreiche gemeinsame Zeit.

Und last but not least, danke ich meinen Eltern, die mich stets in meinem Weg unterstützten und mir ein sorgenfreies Studium ermöglichten, sowie ein Heim, in das ich stets zurückkehren kann. Mein Schwesterchen soll natürlich nicht unerwähnt bleiben - you have a bright future ahead of you!
An dieser Stelle dürfen selbstverständlich auch meine Freunde nicht fehlen, die die ganze Zeit hinter mir standen, mich unterstützt haben und nun vermutlich genau so froh sind wie ich, dass die Arbeit endlich fertig ist. Vor allem Jenny und Jenny, sowie Martha! Ihr habt meine Hochs und Tiefs miterlebt und hattet immer ein offenes Ohr. Danke dafür!

Eigenständigkeitserklärung

I hereby declare that this dissertation “Genetic modification of heavy metal resistant *Streptomyces* sp. strains” is an original work. I vouch that the content of this dissertation has not, in part or whole, been accepted for the award of any degree in any University or Institution.

Ich erkläre, dass ich die Dissertation “ Genetic modification of heavy metal resistant *Streptomyces* sp. strains” selbständig und nur mit der darin angegebenen Hilfe verfasst habe. Die Dissertation wurde in keiner anderen Fakultät oder Universität eingereicht.

Hanka Brangsch